QC
851
.G73
v.3

Air Ministry
Meteorological Research Committee
MRP 452-551 (non-inclusive)

MRP No.	Title	Author
452	The Size Distribution of Raindrops - Part II.	A.C. Best
453	The Size Distribution of Raindrops.	R.F. Jones
455	Report on Some Synoptic Studies of Atmospheric Dynamics.	J.S. Sawyer
458	The Heights and Temperatures at the Tops of Radar Echoes Associated with Various Cloud Systems.	R.F. Jones
462	Relation Between the Standard Deviation of Temperature at Constant Pressure and at Constant Height.	A.F. Crossley
469	Empirical Formulae for the Terminal Velocity of Water Drops Falling Through the Atmosphere.	A.C. Best
472	The Size of Cloud Particles in Strato-cumulus Cloud.	R. Frith
481 AD 223135	Development of Marine Meteorological Instruments.	O.M. Ashford
482	Detection of Icing Conditions by Radar.	R.F. Jones
483	A Note on M.R.P. 472 - the Size Distribution of Cloud Particles in Strato-cumulus Cloud.	A.C. Best
484	The Relation Between the Radar Echoes from Cumulus and Cu Nb Clouds and the Turbulence Within Those Clouds.	R.F. Jones
486 AD 223160	The Humidity of the Lower Stratosphere - the Results of High Level Ascents by Aircraft of the Meteorological Research Flight.	H.C. Shellard
489	Condensation Trails from Jet Aircraft.	J.K. Bannon
491	Some Experiments on Heat Transfer Near the Ground.	N.E. Rider G.D. Robinson
496	The Terminal Velocity and Rate of Dispersion of 'Window' in Radar Wind Measurements.	A.C. Best
498	Some Further Considerations of the Measurement and Indirect Evaluation of Natural Evaporation.	F. Pasquill
499	The Wilson Cloud Chamber as a Hygrometer.	H.P. Palmer

MRP No.	Title	Author
502	Index of M.R.P.'s Approved for General Distribution.	
503	An Approximate Measurement of the Aerodynamic Drag of Grassland.	F. Pasquill
504	Methods of Comparison of Height Measurements by Radio Sonde and Radar.	D.N. Harrison
517	Advective Temperature Change in the 1,000 - 700 m.b. and 700 - 500 m.b. Layers.	J.M. Craddock
518	Changes of Air Temperature - Comments on M.R.P. 517.	A.H.R. Goldie
526	The Warming of Cold Air Masses Over the Sea.	J.M. Craddock
527 AD 080757	Variation With Altitude of the Speed Correction Coefficients of Aircraft Thermometers.	H.C. Shellard
528	Frost Point Hygrometer for Use on the Ground.	D.D. Clark
535	The Horizontal Dimensions of Cumulo-nimbus Clouds at Various Heights.	R.F. Jones
538	The Size of Cloud Droplets.	A.C. Best
539	M.R.C. Research Programme 1950/51.	
542	An Ultra-rapid Aircraft Thermometer.	D.R. Grant
546	Temperature and Humidity Gradients in the First Hundred Metres at Rye.	A.C. Best E. Knighting K. Stormonth R.H. Pedlow N.E. Rider
547	A Study of the Transfer of Heat and Water Vapour Above a Surface of Short Grass.	G.D. Robinson
551	Index of M.R.P.'s Approved for General Distribution.	

AIR WEATHER SERVICE
TECHNICAL REFERENCE FILES

M.R.P. 502
18th August, 1949.

R 5544

AIR MINISTRY

METEOROLOGICAL RESEARCH COMMITTEE.

INDEX OF M.R.Ps. APPROVED FOR GENERAL DISTRIBUTION.
(Appendix No. 6 of M.R.P. 200).

M.R.P.	TITLE	AUTHOR
451	Index of M.R.Ps. approved for General Distribution.	
452	The Size Distribution of Raindrops - Part II.	A.C. Best
453	The Size Distribution of Raindrops.	R.F. Jones
455	Report on some Synoptic Studies of Atmospheric Dynamics.	J.S. Sawyer
458	The Heights and Temperatures at the tops of Radar Echoes associated with various Cloud Systems.	R.F. Jones
462	Relation between the Standard Deviation of temperature at Constant Pressure and at Constant Height.	A.F. Crossley
469	Empirical Formulae for the Terminal Velocity of Water Drops falling through the Atmosphere.	A.C. Best
472	The Size of Cloud Particles in Strato-Cumulus Cloud.	R. Frith
477	The Uncertainty of Radar Wind Smoothing on Ocean Weather Ships.	D.N. Harrison
481	Development of Marine Meteorological Instruments.	O.M. Ashford

/482

G. 248023/DS/10/49/280.

Incl #9

542	An Ultra-Rapid Aircraft Thermometer.	D.R. Grant
546	Temperature and Humidity Gradients in the first hundred metres at Rye.	A.C. Best E. Knighting K. Stormonth R.H. Pedlow N.E. Rider
547	A study of the transfer of heat and water vapour above a surface of short grass.	G.D. Robinson

M.R.P.	TITLE	AUTHOR
482	Detection of Icing Conditions by Radar (Note by Met. Office from information supplied by R.F. Jones)	
483	A Note on M.R.P.472 - the Size Distribution of Cloud Particles in Strato-Cumulus Cloud.	A.C. Best
484	The Relation between the Radar Echoes from Cumulus and Cu Nb clouds and the turbulence within those clouds.	R.F. Jones
486 ✓	The Humidity of the Lower Stratosphere - the results of high level ascents by aircraft of the Meteorological Research Flight.	H.C. Shellard
489		
491	Some Experiments on Heat Transfer near the Ground.	(N.E. Rider (G.D. Robinson
496	The terminal Velocity and Rate of Dispersion of 'Window' in Radar wind measurements.	A.C. Best
498	Some further considerations of the measurement and indirect evaluation of natural evaporation.	F. Pasquill
499	The Wilson Cloud Chamber as a Hygrometer.	H.P. Palmer

G.248023/DS/10/49/280.

To recipients of M.R.P. 601.

Will you please amend the previous "Index of M.R.Ps. approved for General Distribution" (M.R.P.551) to read Appendix No.7 of M.R.P.200.

~~Yours faithfully, M.R.P.551~~

A.C. Best

M.O.15

31st May, 1951.

G.291650/JDG/5/51/170

510	Meteorological Aspects of Turbulence affecting Aircraft at High Altitudes.	J.K. Bannon
517	Advective Temperature Change in the 1,000 - 700 m.b. and 700 - 500 m.b. layers	J.M. Craddock
518	Changes of Air Temperature - Comments on M.R.P. 517.	A.H.R. Goldie
526	The Warming of Cold Air Masses over the Sea.	J.M. Craddock
527	Variation with Altitude of the Speed Correction Coefficients of Aircraft Thermometers.	H.C. Shellard
528	Frost Point Hygrometer for Use on the Ground.	D.D. Clark
535	The Horizontal Dimensions of Cumulo-Nimbus Clouds at Various Heights.	R.F. Jones
538	Size of Cloud Droplets.	A.C. Best
539	M.R.C. Research Programme 1950/51.	
542	An Ultra-Rapid Aircraft Thermometer.	D.R. Grant
546	Temperature and Humidity Gradients in the first hundred metres at Rye.	A.C. Best E. Knighting K. Stormonth R.H. Pedlow N.E. Rider
547	A study of the transfer of heat and water vapour above a surface of short grass.	G.D. Robinson

G.269269/DC/6/50/100

This report has not yet been published and is to be treated CONFIDENTIALLY. Its contents must not be quoted.

SEP 26 19

M.R.P.551
28th April, 1950.

AIR MINISTRY

METEOROLOGICAL RESEARCH COMMITTEE

INDEX OF M.R.Ps. APPROVED FOR GENERAL DISTRIBUTION

(Appendix No.7 of M.R.P.200)

M.R.P.	TITLE	AUTHOR
502	Index of M.R.Ps. approved for General Distribution.	
503	An Approximate Measurement of the Aerodynamic Drag of Grassland.	F. Pasquill
504	Methods of Comparison of Height Measurements by Radio Sonde and Radar.	D.N. Harrison
510	Meteorological Aspects of Turbulence affecting Aircraft at High Altitudes.	J.K. Bannon
517	Advective Temperature Change in the 1,000 - 700 m.b. and 700 - 500 m.b. layers	J.M. Craddock
518	Changes of Air Temperature - Comments on M.R.P. 517.	A.H.R. Goldie
526	The Warming of Cold Air Masses over the Sea.	J.M. Craddock
527	Variation with Altitude of the Speed Correction Coefficients of Aircraft Thermometers.	H.C. Shellard
528	Frost Point Hygrometer for Use on the Ground.	D.D. Clark
535	The Horizontal Dimensions of Cumulo-Nimbus Clouds at Various Heights.	R.F. Jones
538	Size of Cloud Droplets.	A.C. Best
539	M.R.C. Research Programme 1950/51.	
542	An Ultra-Rapid Aircraft Thermometer.	D.R. Grant
546	Temperature and Humidity Gradients in the first hundred metres at Rye.	A.C. Best E. Knighting K. Stormonth R.H. Pedlow N.E. Rider
547	A study of the transfer of heat and water vapour above a surface of short grass.	G.D. Robinson

G.269269/DC/6/50/100

AIR WEATHER SERVICE
TECHNICAL REFERENCE FILES
NOV 17 1952

M.R.P. 452.
S.C. III/17.
7th December, 1948.

AIR MINISTRY

METEOROLOGICAL RESEARCH COMMITTEE.

The Size Distribution of Rain Drops - Part II.

by

AT1-172-128

A.C. BEST.

1. Introduction. Since M.R.P. 352 (1) was written some additional data on the size distribution of raindrops have become available. The purpose of this report is to review this additional data and to compare it with the data used in M.R.P. 352. The interest in drop size distribution is mainly concerned with the raindrops while they are still in the air and the following paragraphs are accordingly restricted to this aspect of the subject. In particular the empirical formula for representing the drop size distribution in the air, given in section 13 of M.R.P. 352, is re-examined.

2. Some Empirical Formulae. In M.R.P. 352 it was shown that, with reasonable accuracy, the drop size distribution in rain can be represented by the equation

$$1 - F = \exp\left\{ - \left(\frac{d}{a}\right)^n \right\} \quad \ldots\ldots\ldots\ldots\ldots\ldots\ldots\ldots (1)$$

where F = fraction of water in the air comprised by drops having diameter less than 'd'

and 'a' and 'n' are constants for a particular rate of rainfall. The constant 'n' showed no consistent variation with rate of rainfall but the constant 'a' was given by

$$a = A I^p \quad \ldots\ldots\ldots\ldots\ldots\ldots\ldots\ldots\ldots\ldots (2)$$

where I is the intensity of rainfall and 'A' and 'p' are constants. It was also shown that

$$W = C I^r \quad \ldots\ldots\ldots\ldots\ldots\ldots\ldots\ldots\ldots\ldots (3)$$

$$D_{50} = (0.69)^{1/n} a \quad \ldots\ldots\ldots\ldots\ldots\ldots\ldots\ldots (4)$$

where W = amount of liquid water in unit volume of space

D_{50} = a diameter such that 50% of the water in the air is comprised of drops with diameter less than D_{50}.

and C and r are constants.

A parameter of importance in the investigation of radar responses from clouds or precipitation is

$$Z = \sum d^6 \quad \ldots\ldots\ldots\ldots\ldots\ldots\ldots\ldots\ldots\ldots (5)$$

where d is the diameter of the water drop contributing to the radar response and the summation is taken over all the drops in unit volume. Now if equation (1) is valid it is easily shown that

$$Z = \sum d^6 = \frac{6Wa^3}{\pi} \Gamma\left(\frac{n+3}{n}\right) \quad \ldots\ldots\ldots\ldots\ldots\ldots (6)$$

/where

where Γ is the ordinary Gamma function. Substituting for a and W from equations 2 and 3 we get

$$Z = 1.91\ C\ A^3\ I^{r+3p}\ \Gamma\left(\frac{n+3}{n}\right) \quad \ldots\ldots\ldots\ldots\ldots\ldots\ldots(7)$$

It is convenient to write this in the form

$$Z = Z_o\ I^{r+3p} \quad \ldots\ldots\ldots\ldots\ldots\ldots\ldots\ldots\ldots\ldots\ldots(8)$$

where Z_o is a constant which is independent of the rate of rainfall.

It can also be shown from equation (1) that

$$\frac{D_{75} - D_{25}}{D_{50}} = \frac{1.38^{1/n} - 0.29^{1/n}}{0.69^{1/n}} \quad \ldots\ldots\ldots\ldots\ldots(9)$$

where the definitions of D_{75} and D_{25} are analogous to that of D_{50}.

3. The New Data. The data which have become available since the writing of M.R.P. 352 are in four parts. These are described below.

(a) Indian data. Kelkar (2) has published a brief account of the measurement of drop size distribution in rain by means of the filter paper method - except that smooth paper was used instead of filter paper. He gives a table showing the average percentage precipitation in raindrops grouped according to diameter, the table being subdivided for drizzle, light showers, moderate showers, heavy showers and very heavy showers. Using the terminal velocities quoted in M.R.P. 352 Kelkar's data have been used to plot log log (1/(1-F)) against log d for each category of precipitation except drizzle (for which the number of points was too small). The results are shown in fig 1 and the deduced values of a and n are as follows

	Number of drops	a	n
Light showers	3211	1.266	2.54
Moderate showers	2310	1.607	4.32
Heavy showers	366	1.959	6.10
Very heavy showers	2415	3.516	2.05
		Mean	3.75

Clearly there is a big variation in n and, as will be seen later, the mean value of n is in excess of the mean value obtained from the work of other investigators. This is not unexpected since Kelkar describes all his precipitation as showers. The significant feature of these results is not that they show a variation in n but rather that with such a small number of drops the plots in fig. 1 do approximate to straight lines so well.

Unfortunately Kelkar does not give the data from which the rate of rainfall can be estimated. However a comparison of the values of a quoted above with the values of a corresponding to various rates of rainfall given in table 3 in section 5 below suggests that the rates of rainfall were

Light showers	1mm/hr.
Moderate showers	2.5 mm/hr.
Heavy showers	6 mm/hr.
Very heavy showers	25 to 30 mm/hr.

These precipitation rates seem to fit the descriptions reasonably well.

(b) Canadian data. Marshall, Langille and Palmer (3) have published a description of some work carried out in Canada the primary purpose of which was to relate the radar response from precipitation to the size distribution of raindrops in the precipitation.

In a subsequent paper (4) Marshall and Palmer have revised some of their conclusions presented in the earlier paper. They state that, from their measurement of raindrop sizes the following formulae can be obtained

$$W = 72\ I^{0.88} \text{ mm}^3/\text{cubic metre} \quad \ldots\ldots\ldots\ldots\ldots\ldots(10)$$

$$Z = 220\ I^{1.60} \text{ mm}^6/\text{cubic metre} \quad \ldots\ldots\ldots\ldots\ldots\ldots(11)$$

where W, Z and I are as defined for equations 2, 3, and 5 and I is measured in mm/hour.

Marshall and Palmer (4) also state that, except at small diameters, the drop size distribution in rain can be represented by

$$N_d = N_o\ e^{-bd} \quad \ldots\ldots\ldots\ldots\ldots\ldots\ldots\ldots\ldots\ldots(12)$$

where $N_d\ \Delta d$ is the number of drops per unit volume having diameter between d and $d+\Delta d$. With the centimetre as the unit of length.

$$N_o = 0.08 \text{ cm}^{-4} \quad \ldots\ldots\ldots\ldots\ldots\ldots\ldots\ldots\ldots\ldots(13)$$

$$b = 41\ I^{-0.21} \text{ cm}^{-1} \quad \ldots\ldots\ldots\ldots\ldots\ldots\ldots\ldots\ldots\ldots(14)$$

In the paper two small scale graphs are given, one showing the experimental points upon which equation 12 is based and the other comparing curves based upon equation 12 with experimental distribution curves for the three values 1 mm/hour, 5 mm/hour and 25 mm/hour of I. In view of the success in M.R.P. 352 of equations 1, 2 and 3 in representing drop size distribution in rain it seemed desirable to test those equations on the Canadian data. Unfortunately the small scale plot of the experimental data in Marshall and Palmer's paper is scarcely adequate to permit the determination of the original experimental values. Accordingly the following indirect methods were adopted.

If equations 1, 2 and 3 can represent the Canadian data then we see from a comparison of equations 3 and 10 and of equations 8 and 11 that

$$C = 72 \quad \ldots\ldots\ldots\ldots\ldots\ldots\ldots\ldots\ldots\ldots\ldots\ldots\ldots\ldots\ldots\ldots(15)$$

$$r = 0.88 \quad \ldots\ldots\ldots\ldots\ldots\ldots\ldots\ldots\ldots\ldots\ldots\ldots\ldots\ldots\ldots\ldots(16)$$

$$r + 3p = 1.60 \text{ and so } p = 0.24 \quad \ldots\ldots\ldots\ldots\ldots\ldots\ldots\ldots\ldots\ldots(17)$$

Now from equations 12 and 14 it is easily shown that the fraction of liquid water in the air composed of drops with diameter exceeding d is given by

$$e^{-bd}\left\{\frac{b^3d^3}{6} + \frac{b^2d^2}{2} + bd + 1\right\} \quad \ldots\ldots\ldots(18)$$

where b is given by equation 14. In the notation of M.R.P. 352 expression 18 is represented by F where

$$1 - F = \exp\left\{-\left(\frac{d}{a}\right)^n\right\} \quad \ldots\ldots\ldots\ldots\ldots\ldots\ldots\ldots(1)$$

$$a = A\ I^p \quad \ldots\ldots\ldots\ldots\ldots\ldots\ldots\ldots\ldots\ldots\ldots\ldots(2)$$

and $p = 0.24$ from equation 17.

Thus we can evaluate expression 18 for selected values of I and d and treat these computed values as experimental observations for the purpose of determining n and A. This has been done. The selected values of I and d were

I = 1 mm/hr.	d = 1, 1.5, 2 mm
I = 5 mm/hr.	d = 1.5, 2, 2.5 mm
I = 25 mm/hr.	d = 2, 2.5, 3 mm

The resulting nine values of (1 - F) were used to determine A and n by the method of least squares, the results being

$$A = 1 \quad (19)$$
$$n = 1.849 \quad (20)$$

These values of A and n are comparable with those put forward in M.R.P. 352 but that does not of itself justify the application of equations 1 and 2 to the Canadian data. However the following table compares the value of expression 18 (i.e. values based on equations 12 and 14) with values based on equations 1 and 2 using values of p, A and n from 17, 19 and 20.

I mm/hr.	d mm	Value of F From Exp. 18	From Eqtn 1
1	1	0.414	0.368
	1.5	0.138	0.120
	2.0	0.037	0.027
5	1.5	0.362	0.355
	2.0	0.165	0.171
	2.5	0.067	0.070
25	2.0	0.401	0.422
	2.5	0.236	0.271
	3.0	0.130	0.161

Reference to the figure in Marshall and Palmer's paper shows that equation 12 overestimates the number of raindrops at the smaller diameters, the experimental curve reaching the line representing equation 12 at 1mm for I = 1 mm/hr., 1.45 mm for I = 5 mm/hr. and 1.7 mm for I =25 mm/hr. Thus it seems reasonable to assume that equations 1, 2 and 3 can adequately represent the Canadian data. A further check is provided by inserting the values of C, A and n in equation 7. This gives Z_o = 199 compared with the value of 220 in equation 11 as quoted by Marshall and Palmer.

(c) Hilo data. Anderson (5) has described some measurements of drop size distribution in rain near Hilo, Hawaii. These measurements were made in connection with a study of the attenuation of 1.25 cm radiation through rain. Anderson gives his results in the form of a graph showing experimental values of D_{50} plotted against I. A mean curve is drawn through the experimental points. Against each plotted point on the figure is also written the value of $(D_{75} - D_{25})/2$. The data provided by Anderson is inadequate to test whether his results can be represented by equation 1. If however we assume that this form of equation is applicable it is possible to deduce approximate values for the constants involved as follows.

From each of the experimental points plotted in the figure in Anderson's paper the value of I and of D_{50} was read and the value of $(D_{75} - D_{25})/2$ noted. These sets of values were then grouped according to the value of I and mean values obtained for I, D_{50} and $(D_{75} - D_{25})/2$. Then the value of n was obtained using equation 9 and hence the value of a using equation 4. The results of these computations were as follows

Range of I mm/hr.	No. of points	Mean I mm/hr.	D_{50} mm	$(D_{75} - D_{25})/2$ mm	n	a mm
2	1	2.0	0.95	0.11	4.9	1.024
3 - 5	2	3.5	1.17	0.23	3.9	1.287
5 - 10	17	9.2	1.57	0.28	4.4	1.706
10 - 20	16	16.2	1.87	0.29	5.1	2.01
20 - 30	10	25.5	1.95	0.33	4.7	2.11
30 - 50	10	37.5	2.19	0.44	3.9	2.41
					mean 4.48	

/Having

Having obtained n and a for certain values of I we can now obtain W from the equation

$$I = 0.0036\, W \sum V(F_{d_2} - F_{d_1}) \quad \ldots\ldots\ldots\ldots\ldots\ldots(21)$$

where the numerical coefficient is appropriate to the units employed, V is the terminal velocity of drops having diameter $(d_1 + d_2)/2$ and the summation is taken from F = 0 to F = 1. For this purpose the range of F was divided into 20 groups. Since Anderson had used values of the terminal velocities of drops as quoted in Physics of the Air by Humphreys these same terminal velocities were used in this part of the work. The results were as follows

I mm/hr.	2.0	3.5	9.2	16.2	25.5	37.5
W mm^3/m^3	151	232	510	815	1260	1756

Having obtained a and W for various values of I the best straight lines were fitted by the method of least squares to the logarithms of these quantities yielding the results

$$A = 0.881 \qquad p = 0.283 \qquad C = 82 \qquad r = 0.838$$

where the symbols have the same significance as in equations 2 and 3. As a check on this part of the work values of D_{50} were read from Anderson's mean curve for various values of I. By the method of least squares it was found that these could be represented by

$$D_{50} = 0.788\, I^{0.3}$$

From equations 2 and 4 we see (using a mean value of 4.48 for n) that this corresponds to

$$A = 0.857 \qquad p = 0.300$$

in reasonably good agreement with the values above. Now from equation 7 we see that, substituting for A, C, r, and p and putting n = 4.48

$$Z = 1.91 \; 82 \; 0.881^3 \; I^{1.687} \; \Gamma(1.67)$$

$$= 96.7 \; I^{1.687}$$

Wexler (6) however has stated that Anderson's data yields the result

$$Z = 208\, I^{1.53}$$

Wexler does not state whether he had access to Anderson's original data but the inadequacy of the data in Anderson's published paper suggests that this is so. We must conclude then that either equation 1, the basis of the present treatment, does not adequately represent Anderson's data or that Wexler and Anderson have interpreted the results differently.

It will be noticed that the mean value obtained for n is very different from that obtained from other data (with the exception of Kelkar's data). Anderson states that his measurements were made in orographic rain and it is possible that the results differ from those of other workers on that account.

(d) East Hill data. During the past twelve months or so the relation between the radar echoes obtained from clouds and precipitation and the characteristics of the clouds and precipitation has been investigated at East Hill by Mr. R.F. Jones. In the course of this work a number of drop size distributions in rain have been measured, some at East Hill itself and a greater number at three neighbouring Meteorological Office stations within 'radar range' of East Hill which were co-operating in this work. The method employed in these experiments was identical with the filter paper method

employed at Shoeburyness and Ynyslas and described in M.R.P.352. Only one filter paper was exposed at a time in these later experiments. The volume of data collected can be assessed from the following table

Number of rain periods	18
Number of papers used	149
Number of drops measured	163317

The measured drops were grouped within the diameter ranges 0 to 0.5 mm, 0.5 to 1.0 mm, etc.

In a few cases (34 papers) the number of drops in the smallest size group (diameter 0.0 to 0.5 mm) were not counted as these very small drops contribute very little to the radar echo. It was desirable to make some allowance for this when examining the size distribution and the following procedure was adopted. From the 115 papers on which the smallest drops were counted it was found that the volume of water reaching the ground comprised by drops having diameter less than 0.5 mm was as follows

Rate of rainfall (mm/hr)	0 - 1	1 - 2	2 - 3	3 - 5	5 - 10
Volume of water reaching ground comprised by drops with diameter less than 0.5 mm	5%	3%	2%	1.5%	1.5%

and a correction was made to the 34 papers based upon these figures.

The East Hill data has been analysed to test the validity of equation 1. To do this log log $(1/(1 - F))$ has been plotted against log d in fig. 1, d being measured in mm, for various rates of rainfall. It can be seen that, except for the highest rate of rainfall, the plots give reasonably good straight lines over a wide range of values of F, thus justifying the form of equation 1. The number of papers contributing to each plot in fig. 1 was as follows

Rate of rainfall (mm/hr.)	0.39	1.46	2.47	3.17	7.02	25.12
Number of papers	70	50	10	6	10	3
Total duration of exposure (secs)	3049	1227	158	60	57	8.4

In view of the linearity of the lines obtained from other sets of similar data it is considered that the departure from linearity of the line corresponding to the highest rate of rainfall in this set is not significant and is probably due to the small amount of data. Since the present method of analysis is applicable only when log log $(1/(1 - F))$ is a linear function of log d the data corresponding to the highest rate of rainfall at East Hill will not be considered further.

The concentration of liquid water in the air for various rates of rainfall was also computed as described in section 12 of M.R.P.352.

The values obtained from the East Hill data for n, a and W are as follows,

Table 1.
From East Hill Data.

I mm/hr.	n	a mm.	W mm^3/m^3
0.41	2.00	1.13	31
1.42	2.35	1.38	91
2.45	2.11	1.73	137
3.69	1.77	2.07	183
7.44	1.70	2.38	353
Mean	1.99		

/Fitting

Fitting equations 1, 2 and 3 to these data by the method of least squares yields the following values for the various parameters

$$A = 1.38 \quad p = 0.269 \quad C = 65 \quad r = 0.829$$

4. Comparison of Existing Data. Equations 1, 2 and 3 have been fitted to each set of data in M.R.P. 352 separately by the method of least squares and the various parameters evaluated. The values of Z_o have also been determined from equation 7. The results, together with those obtained from the new data in the preceding paragraphs are tabulated in table 2 below.

Table 2.
Values of Parameters in Drop Size Distribution.

	n	A	p	C	r	Z_o	r+3p
Ynyslas	2.49	1.18	0.203	74	0.845	257	1.454
Shoeburyness	2.29	1.56	0.209	59	0.816	505	1.443
Lenard	2.59	1.42	0.272	61	0.840	360	1.656
Laws, Parsons	2.29	1.25	0.199	72	0.867	317	1.464
Canada	1.85	1.00	0.240	72	0.880	199	1.600
East Hill	1.99	1.38	0.269	65	0.829	436	1.636
Hilo	4.48	0.88	0.283	82	0.838	97	1.687
India	3.75						
Mean values excluding Hilo and India	2.25	1.30	0.232	67	0.846	346	1.542

There are a number of points to be noted in connection with the numerical values in this table.

(a) These numerical values are appropriate when d is measured in mm, W in mm^3/m^3 and Z in mm^6/m^3 .

(b) In order that the table shall be self consistent the value 199 for C from the Canadian data, i.e. the value obtained above, has been preferred to the more accurate value of 220 obtained directly by the authors of that work. The difference however is small.

(c) The mean values of C, A and n given in table 2 lead to a value of 335 for Z_o if substituted in equation 7. Naturally this is very close to the average of the values for Z_o obtained from each set of data separately.

(d) The validity of table 2 is of course dependent upon the applicability of equations 1, 2, and 3. Of these perhaps equation 1 is the most important. The evidence in support of the form of equation 1 comprises the linearity of the lines in fig. 5 of M.R.P.352, of the lines in fig. 1 of the present note and the agreement between the two ways of computing F as shown in the table of para. 3(b) above.

(e) The values in table 2 are appropriate only in the region where the terminal velocities of the drops are as quoted in M.R.P.352, i.e. near the surface. At greater heights the terminal velocities will be smaller and the values of W must be increased accordingly.

Equations 1, 2 and 3 should give a reasonably close representation of the average distribution of liquid water in the air near the ground during precipitation, if the mean values of the parameters in table 2 are inserted in the equations, for about 80% of the water, i.e. excluding the 20% of the water comprised by the smallest and the largest drops. It is probable however that the mean values of the parameters will not be appropriate either in purely orographic rain or in rain which is essentially of the showery type.

5. Numerical Application of the Formulae. Using the mean values of n, A, p, C, and r given at the foot of table 2 the distribution of liquid water and of number of drops according to drop diameter have been computed from equations 1, 2 and 3 for various rates of rainfall. The values of a and of W were also computed. The results of these computations are given in tables 3 and 4. The tabulated values are given to a higher degree of accuracy than is justified by the experimental data upon which the values of the parameters are based in order to illustrate the variations predicted by the formulae. For completeness the amount of liquid water and the number of drops comprised by drops with diameter less than 0.25 mm have also been tabulated though it is not suggested that the formulae are applicable to such small drops.

Table 3.

Values of a and of W.

I. mm/hr.	a mm.	W mm^3/m^3
0.5	1.107	37
1.0	1.300	67
2.5	1.608	145
5.0	1.888	261
10.0	2.218	470
25.0	2.743	1020

Table 4.

Distribution of liquid water and of number of drops.

I mm/hr.	0.50	1.00	2.50	5.00	10.0	25.0	0.50	1.00	2.50	5.0	10.0	25.0
Drop Diameter mm.	Liquid water mm^3/m^3						Number of drops per cubic metre					
0.00-0.25	1.3	1.6	2.2	2.7	3.4	4.6	1250	1585	2136	2685	3369	4538
0.25-0.50	4.4	5.7	7.9	10.1	12.7	17.3	160	208	287	364	461	625
0.50-0.75	6.9	9.5	13.8	17.9	23.1	31.8	54	74	108	140	180	248
0.75-1.00	7.7	11.6	18.3	24.8	32.9	46.4	22	33	52	71	94	132
1.00-1.25	6.8	11.7	20.6	29.7	41.0	59.9	9	16	28	40	55	80
1.25-1.50	4.8	10.0	20.6	31.9	46.5	71.3	3.55	7	15	23	34	52
1.50-1.75	2.9	7.3	18.4	31.5	49.0	79.8	1.27	3.27	8	14	22	35
1.75-2.00	1.40	4.7	14.9	28.7	48.6	84.9	0.41	1.37	4.33	8	14	25
2.00-2.25	0.57	2.64	11.1	24.5	45.5	86.5	0.11	0.53	2.20	4.87	9	17
2.25-2.50	0.20	1.30	7.5	19.4	41.4	84.6	0.03	0.19	1.07	2.76	6	12
2.50-2.75	0.05	0.56	4.6	14.4	34.1	79.9	0.01	0.06	0.49	1.52	3.60	8
2.75-3.00	0.01	0.21	2.64	10.1	27.5	73.0	0.001	0.02	0.21	0.81	2.21	6
3.00-3.25		0.07	1.37	6.6	21.1	64.3		0.004	0.09	0.41	1.32	4.03
3.25-3.50		0.02	0.65	4.0	15.4	55.0		0.001	0.03	0.20	0.77	2.74
3.50-3.75		0.01	0.28	2.42	10.8	45.6			0.01	0.10	0.43	1.83
3.75-4.00			0.11	1.25	7.2	36.6			0.004	0.04	0.24	1.20
4.00-4.25			0.04	0.63	4.6	28.5			0.001	0.02	0.13	0.77
4.25-4.50			0.01	0.30	2.80	21.6				0.01	0.06	0.49
4.50-4.75				0.13	1.63	15.8				0.003	0.03	0.31
4.75-5.00				0.06	0.90	11.2				0.001	0.015	0.19
5.00-5.25				0.02	0.48	7.8					0.007	0.11
5.25-5.50				0.01	0.24	5.2					0.003	0.06
5.50-5.75					0.12	3.37					0.001	0.04
5.75-6.00					0.05	2.13					0.001	0.02
6.00-6.25					0.02	1.30						0.011
5.25-6.50					0.01	0.77						0.006
6.50-6.75						0.44						0.003
6.75-7.00						0.25						0.001
7.00-7.25						0.13						

6. Deviations from the formulae. In order to assess the closeness with which the formulae fit the observational data the following procedure was adopted.

The value 2.25 obtained above for n is the mean of the average values obtained from each set of data. Each set of data however provided several experimental values of n, these values being tabulated in table 5 of M.R.P.352 and in table 1 of the present report. Accordingly the root mean square of $(n - 2.25)$ was computed using the values of n from these two tables (excluding the values obtained from Niederdorfer and from Defant) and from the Canadian data. Since the method of treatment of the Canadian data yielded only the average value of n, viz 1.85, this value was included five times in order to give weight to that data similar to that given to the other observations. The standard deviation of n computed in this way was 0.41.

A different procedure was adopted with regard to the parameter a. This quantity varies with I, the rate of precipitation, and the rate of precipitation is tabulated in table 5 of M.R.P. 352 and table 1 of the present report for each observed value of a. Values of a were computed from equation 2 using $A = 1.30$ and $p = 0.232$ for each value of I in these tables. Denoting the computed value of a by a_f the root mean square of the quantity $(a_f - a)/a_f$ was computed. Again special steps were necessary to give adequate weight to the Canadian data. Five 'observational values' of a were computed for the Canadian data using equation 2 and the values 1.0 and 0.24 for A and p, these being the values of these parameters computed solely from this data, the observational values being computed for values 1, 5, 10, 15 and 25 mm/hr of I. The percentage standard deviation of a computed in this way from all the data (again excluding Niederdorfer and Defant) was 18.3%.

The procedure adopted with regard to the standard deviation of W was similar to that for a and the result was 13.5%.

These standard deviations do not represent the standard deviations of single measurements of drop size distribution from that predicted by equations 1, 2 and 3. These would depend upon the size of the filter paper used, the duration of exposure and various other factors. The figures quoted above can be used only to indicate the closeness with which the experimental data, treated in the way described in M.R.P. 352 and the present report, fit the formulae deduced.

7. Effect of variation in the numerical values of the parameters. If we regard the parameter a as determining the scale upon which the drop diameters are measured we see that the drop size distribution is the same for all rates of rainfall. This is of assistance in appreciating the effect of variations in a upon the drop size distribution. If we have two distributions in which the parameter a has values in the ratio k to 1 the fraction of liquid water comprised by drops with diameter between d_1 and d_2 in the distribution with parameter a will be comprised by drops with diameter between kd_1 and kd_2 in the distribution with parameter ka. The ratio of the number of drops between d_1 and d_2 in the 'a' distribution to the number of drops between kd_1 and kd_2 in the 'ka' distribution will be k^3.

The effect of variations in W is self evident.

It is clear that an increase in the value of n will decrease the spread of the distribution. In order to illustrate the magnitude of this effect the drop size distribution for $I = 5$ mm/hr has been recomputed using the same values of a and W but with $n = 4$. The results are given in table 5 and may be compared with the corresponding columns of table 4.

/Table 5.

Table 5.

Distribution of liquid water and of drops for I = 5 mm/hr, a = 1.888 mm, W = 261 mm^3/m^3 and n = 4.

Drop Diameter mm.	Liquid water mm^3/m^3	No of Drops.
0.00-0.25	0.08	79
0.25-0.50	1.2	43
0.50-0.75	5.1	40
0.75-1.00	13.3	38
1.00-1.25	25.9	35
1.25-1.50	40.2	30
1.50-1.75	50.5	22
1.75-2.00	50.8	15
2.00-2.25	39.5	7.9
2.25-2.50	22.7	3.2
2.50-2.75	9.2	0.97
2.75-3.00	2.5	0.20
3.00-3.25	0.41	0.03
3.25-3.50	0.04	0.002

It can be seen that the effect of increasing n from 2.25 to 4.0 has been to transfer the diameter at which the maximum concentration of liquid water occurs from between 1.25 and 1.50 mm to between 1.75 and 2.00 mm and to increase the maximum concentration from 32 mm^3/m^3/0.25 mm diameter to 50.8 mm^3/m^3/0.25 mm diameter. Actually if the predominant diameter is computed on the lines indicated in paragraph 14(ii) of M.R.P.352 we find that the predominant diameters are 1.454 and 1.757 mm in the two cases. To a large extent the effect of the change in n is reduced if we consider a larger range of diameters embracing the predominant diameter. Thus if we consider the drops having diameters between 0.75 mm and 2.5 mm we find that the amounts of liquid water are 191 mm^3/m^3 and 243 mm^3/m^3 for n = 2.25 and 4.0 respectively and the effect of the variation in n on the number of drops is even less marked, the numbers being 163.6 and 151.1 $/m^3$ for n = 2.25 and n = 4.0 respectively.

8. Summary. The available experimental evidence relating to the drop size distribution in rain has been reviewed and it is shown that, on the average

$$1 - F = \exp\left\{ - \left(\frac{d}{a}\right)^{2.25} \right\}$$

$$a = 1.30\, I^{0.232}$$

$$W = 67\, I^{0.846}$$

where F = fraction of liquid water in the air comprised by drops having diameter less than 'd' mm.
I = rate of rainfall in mm/hr.
W = amount of liquid water in the air in mm^3/m^3.

these formulae are probably valid for approximately the 80% of the liquid water which excludes the smallest and the largest drops. The numerical values of the constants may need adjustment if the rain is specifically showery in nature or is of orographic origin.

The distribution of drops and liquid water has been computed on the basis of the above formulae for selected rates of rainfall.

Finally the effect of varying the values of the numerical constants is considered.

/References

References.

1. The size distribution of raindrops. A.C. Best, M.R.P. 352.

2. Size of raindrops. V.N. Kelkar, Proc. Ind. Acad. of Sciences, Vol XXII 1945.

3. Measurement of rainfall by radar. J.S. Marshall, R.C. Langille, and W. McK. Palmer, Journal of Met., Vol 4, No. 6, Dec. 1947.

4. The distribution of raindrops with size. J.S. Marshall and W. McK. Palmer, Journal of Met., Vol 5, No. 4, Aug. 1948.

5. Drop size distribution measurements in orographic rain. Lloyd J. Anderson. Bull. Amer. Met. Soc., Vol 29, No. 7, Sept. 1948.

6. Rain intensities by radar. R. Wexler, Journal of met., Vol 5, No. 4 Aug. 1948.

G. 217598/D.S./12/48.

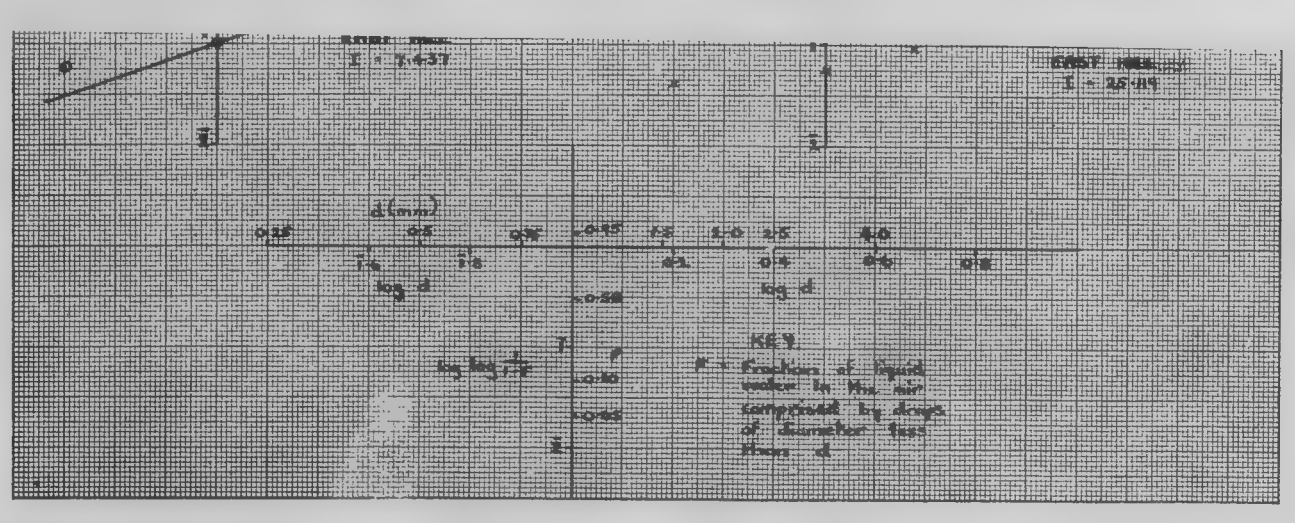

FIG. 1.

DISTRIBUTION BY DROP SIZE OF WATER IN THE AIR. M.R.P. 452.

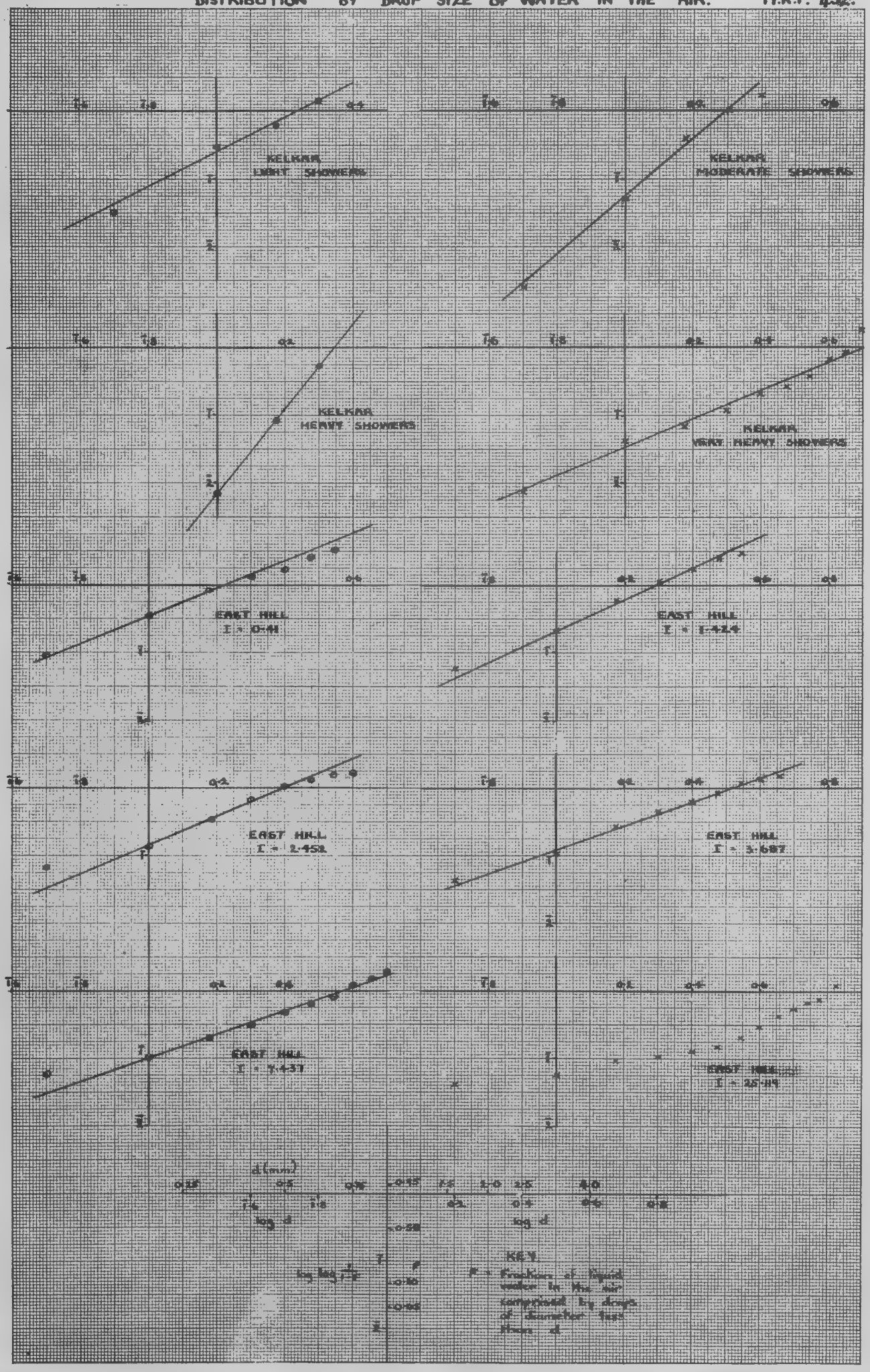

...treated. Its contents must not be quoted.

M.R.P. 453
S.C.III/18
7th December, 1948

AIR MINISTRY

METEOROLOGICAL RESEARCH COMMITTEE

The Size Distribution of Raindrops

by
R.F. Jones

AIR WEATHER SERVICE
TECHNICAL REFERENCE FILES

1. Introduction

In a previous paper (1) the writer has given an analysis of 147 cases of drop size distributions obtained by the filter paper method from four stations in the Midlands of England. The distributions were there used to obtain calculated values of the radar signal intensity function, ΣND^6, and rate of rainfall.

The same distributions can be used to calculate the volume distributions of raindrops in the air for various rates of rainfall.

Best (2) concentrated on the volume of water comprised by the raindrops but in this note the distribution of the actual number of raindrops of different sizes is considered.

2. Data available and presentation of results.

147 drop size distributions from four stations - Abingdon, Bassingbourn, Cranfield and East Hill - are available relating to rates of rainfall from 0.02 to 33 mm/hr; 117 of the cases refer to rates of rainfall in the range from 0 to 2 mm/hr.

The drop size distributions were measured in terms of the number of drops reaching the ground having diameters in the ranges 0 - 0.5 mm, 0.5 - 1.0 mm, 1.0 - 1.5 mm etc., with the exception that for some of the higher rates of rainfall the drops in the range 0 - 0.5 mm were not counted since, although large in number, their contribution to the rate of rainfall was very small. Numbers of drops in the range 0 - 0.5 mm diameter are not therefore considered in this note.

Mean drop size distributions at the ground were determined for various ranges of rates of rainfall and converted into the volume distribution expressed as number of drops per cubic metre. For rates of rainfall greater than 3 mm/hr the observations were too scattered to allow of the formation of reasonable mean values for a narrow interval of rainfall rates except for a series of four readings for which the rainfall rates fell between 7.68 and 7.94 mm/hr. (obtained on three different dates at East Hill). The 16 readings between 3 mm/hr. and 10 mm/hr. were however used to obtain a mean volume distribution for this interval. Only four readings were available for rainfall rates above 10 mm/hr. and these have not been used.

The volume distributions of drops obtained in this manner are shown in Table I.

Graphs showing log N against D, where N is the number of raindrops per cu.m. of diameter D - .25 to D + .25 mm, were plotted for various rates of rainfall and are shown in Fig. I.

3. The volume distribution of raindrops.

Examination of the graphs in Fig. I shows that, except for the smallest drops (i.e. drops of diameter less than about 1.25 mm), the curves obey, though not always very closely, an equation of the form:

$$N = k', 10^{-a'D} \qquad \text{(i)}$$

where N is the number of drops per m^3 in the $\frac{1}{2}$ mm range D - 0.25 to D + 0.25 mm and D is in mm.

It can be seen that k' is sensibly constant for all rates of rainfall R and a ' is a constant for a particular value of R but varies with R.

The mean value of k' is given by:

$$\log k' = 3.65 \qquad \text{(ii)}$$

The slope of the curves in Fig. I gives the value of a' for the various rates of rainfall R. Since the curves indicate the probability of k' being a constant for all R the curves were re-drawn to pass through the common point log N = 3.65 when D = 0 and the values of a' obtained from these curves.

To find the relation between a' and R, log a' was plotted against log R as shown in Fig. II. As will be seen the points so obtained lie reasonably close to a straight line the equation of which, by the method of least squares, is

$$\log a' = 0.24 - 0.21 \log R$$

$$\text{i.e.} \quad a' = \frac{1.74}{R^{0.21}} \qquad \text{(iii)}$$

We can express (i) in the form

$$N = k' . e^{-aD} \qquad \text{(iv)}$$

where $a = \log_e 10 . a' = 2.3\, a'$

$$= \frac{4.00}{R^{0.21}} \quad \text{from (iii)} \qquad \text{(v)}$$

Suppose now $N_D = k . e^{-aD}$ (vi)

where $N_D \delta D$ is the number of drops in the range D to $D + \delta D$ mm.

The number of drops, N, in the range D - 0.25 to D + 0.25 mm. is then given by

$$N = \int_{D-0.25}^{D+0.25} k . e^{-aD}\, dD$$

$$= \frac{2k}{a} \sinh (0.25a) . e^{-aD}$$

But from (iv) $N = k' . e^{-aD}$

Hence $$k = \frac{ak'}{2\sinh(0.25a)}$$

$$= \frac{2k'}{R^{0.21} \sinh(R^{-0.21})} \quad \text{from (v)} \qquad \text{(vii)}$$

/4.

4. The values of $\sum ND^6$ and $\sum ND^3$

If we assume a volume distribution of the form (vi) then

$$\sum N_D D^6 \delta D = \sum k. \; e^{-aD} D^6 \delta D$$

$$= \int_0^\infty k.e^{-aD} D^6 \, dD$$

Strictly the limits of integration should be from 0 to D_{max}, where D_{max} is the maximum possible diameter of a raindrop (approx. 6.5 mms), but it can be shown that $\int_{6.5}^{\infty} k.e^{-aD} D^6 \, dD$ is quite negligible for all rates of rainfall being considered here ($R \leqslant 10$ mm/hr).

Since a is a constant for a particular value of R we find

$$\sum N_D D^6 \delta D = \int_0^\infty k.e^{-aD} D^6 \, dD$$

$$= \frac{720\,k}{a^7}$$

$$= 392.6 \; \frac{R^{1.26}}{\sinh (R^{-0.21})} \quad \text{from (ii), (v) and (vii)}$$

The values of this function are shown plotted in Fig. III for values of R from 0.1 to 10 mm/hr. It will be seen that for these values of R the function can be represented to a high degree of accuracy by the expression

$$\sum ND^6 = 323 \; R^{1.53} \quad \text{.....(viii)}$$

Similarly $\sum N_D D^3 \delta D = \frac{6k}{a^4}$ (the contribution to the integral for $D > 6.5$ being again negligibly small).

Thus $\frac{\pi}{6} \sum N D^3 \delta D$ = volume of water in the form of raindrops per cu. m. of air

$$= W$$

$$= \frac{109.6 \; R^{0.63}}{\sinh (R^{-0.21})}$$

The values of this function are also plotted in Fig. III for values of R from 0.1 to 10 mm/hr and it will be seen that the function can be represented to a high degree of accuracy by the expression

$$W = 93.3 \; R^{0.88} \quad \text{(ix)}$$

5. Comparison with other workers

(i) A.C. Best[2]

Best concentrated on the volume of water comprised by the raindrops rather than the actual numbers of such drops. He has shown (Table II, p.7) that the mean value of $\sum ND^6$ by using all the data available (except Hilo and India) is given by

$$\sum ND^6 = 346\ R^{1.542}$$

which is in remarkably close agreement with the expression (viii) above. The East Hill data alone however by his methods gave

$$\sum ND^6 = 436\ R^{1.636}$$

illustrating how the constants in this equation depend on the method of smoothing of the actual readings (see also Section 5 (iv) below). The form of relationship

$$1 - F = \exp\left[-\left(\frac{D}{a_1}\right)^n\right]$$

found by Best to represent the drop size distribution in rain leads to

$$N \equiv \frac{6}{\pi}\ \frac{C}{A^n}\ R^{r-np}\ n\ D^{n-4}\ \exp\left[-\frac{DR^{-p}}{A}\right]^n \delta D$$

in which C, A, r, p, and n are empirical constants. This expression for N is more complicated than that in section 3.

Best also obtained the mean value (Table II, p.7)

$$W = 67\ R^{0.846}$$

($W = 65\ R^{0.829}$ using the East Hill data alone) which, as regards the index of R, is in fair agreement with (ix) above.

As mentioned in Section 3 para.1 however the equation $N = k', 10^{-a'D}$ for the number of drops is not valid for the observed numbers of drops of diameters less than 1.25 mm and examination of the curves of Fig. I shows that for these smaller drops the equation overestimates the number compared with observations. The expressions for $\sum ND^6$ and W (equations (viii) and (ix)) therefore will be overestimates of the values which would be obtained using the observed numbers of smaller drops and this overestimation is likely to be greater for W than for $\sum ND^6$. Comparison with the mean values of Best suggests that the overestimation for $\sum ND^6$ is negligible due to the dependence on the sixth power of the diameter but is more serious for W where the cube only of the diameter is involved.

(ii) Marshall and Palmer (3)

These writers have used distributions obtained at Ottawa to perform similar deductions to the above and have obtained values of k and a (after a change of units) given by

$$\log k = 3.90$$

$$a = \frac{4.1}{R^{0.21}}$$

/The

The value of a is in remarkably close agreement with the value obtained above but they do not indicate any dependence of k upon R.

Their values of a and k lead to

$$\sum ND^6 = 296\ R^{1.47}$$
$$\text{and } W = 89\ R^{0.84}$$

The same writers obtained experimentally

$$\sum ND^6 = 220\ R^{1.60}$$
$$\text{and } W = 72\ R^{0.88}$$

(iii) R. Wexler[4]

Using data of Laws and Parsons this writer obtained

$$\sum ND^6 = 320\ R^{1.44}$$
$$\text{and } W = 68\ R^{0.88}$$

(iv) R.F. Jones

The data used above was also used by the writer to obtain the value of $\sum ND^6$ directly.

The mean value of $\sum ND^6$ for all values of R used (from 0.02 to 33.0 mm/hr) was shown to be

$$\sum ND^6 = 339\ R^{1.74}$$

which compares with $323\ R^{1.53}$ of equation (viii) above and $436\ R^{1.636}$ as obtained by Best (2) using the same data. For values of R in the range from 0 to 2 mm/hr only, however, the expression $\sum ND^6 = 353\ R^{1.29}$ was obtained, while for the range of R from 2 to 8 mm/hr the expression became $\sum ND^6 = 78\ R^{2.82}$.

6. Conclusion and Summary

Drop size distribution curves based on experiment lead to an expression for the drop size distributions of drops of diameter 1.25 mm or greater for rates of rainfall between 0 and 10 mm/hr in the form

$$N_D = k.\ e^{-aD}$$

where $N_D\,\delta D$ is the number of drops per cu. m. in the range D to D + δD of the diameter D mm. k and a are constants for a particular rate of rainfall R but vary with R according to the expressions

$$a = \frac{4.00}{R^{0.21}}$$

$$k = \frac{8934}{R^{0.21}\sinh(R^{-0.21})}$$

The considerable smoothing of the drop size distributions so introduced leads to results in good agreement with those of other workers also using "smoothed" readings.

/In

In the particular case of theoretical radar echo intensity (proportional to ΣND^6 the use of the unsmoothed readings directly (see para.5(ii) and (iv) above) did not give such close agreement suggesting a more complex drop size distribution than the one obtained above. It is noteworthy that although separate drop size distributions obtained in Canada and England gave remarkably similar smoothed results the determinations of ΣND^6 from the same distributions were markedly different (see para.5(ii) and (iv)).

7. References

1. Jones R.F.; The relation between radar echo intensity and rate of rainfall. J.M.R.P. 99, Air Ministry, London, 1948.

2. Best A.C.; The size distribution of raindrops - Part II. M.R.P. 452, Met. Off. London, 1947.

3. Marshall J.S. and Palmer W.Mc.K.; The distribution of raindrops with size. J.Met., Milton Mass., Vol.5, No.4., August 1948, p.165.

4. Wexler R.; Rain intensities by radar. J.Met., Milton Mass., Vol.5 No.4., August 1948., p.171.

G.224889/D.S./5/49/40.

TABLE I

Volume Distribution N in numbers of drops per m^3 in specified ranges of diameter for various rates of rainfall R

Number of drops per cubic metre

Range of R (mm/hr)	No. of readings	Mean R (mm/hr)	Raindrop diameters in mms									
			0.5-1.0	1.0-1.5	1.5-2.0	2.0-2.5	2.5-3.0	3.0-3.5	3.5-4.0	4.0-4.5	4.5-5.0	5.0-5.5
0.00 - 0.25	13	0.14	33.1	3.35	.117							
0.25 - 0.75	47	0.51	78.6	14.68	1.345	.116	.0161	.0026	.0012			
0.75 - 1.25	29	1.02	92.0	32.00	4.42	.531	.0769	.0065	.0028			
1.25 - 1.75	24	1.48	156.0	39.20	6.75	.964	.1084	.0196				
1.75 - 2.25	12	1.92	126.4	47.30	10.62	1.85	.266	.0261				
2.00 - 3.00	10	2.46	97.9	44.5	13.71	3.008	.762	.111	.05	.0072		
3.02 - 9.64	16	6.06	180.2	83.7	24.64	7.94	3.00	.764	.56	.162	.106	.017
7.68 - 7.94	4	7.81	258.6	156.3	32.4	16.2	3.564					

G.217,590(a)/L.W/12/48.

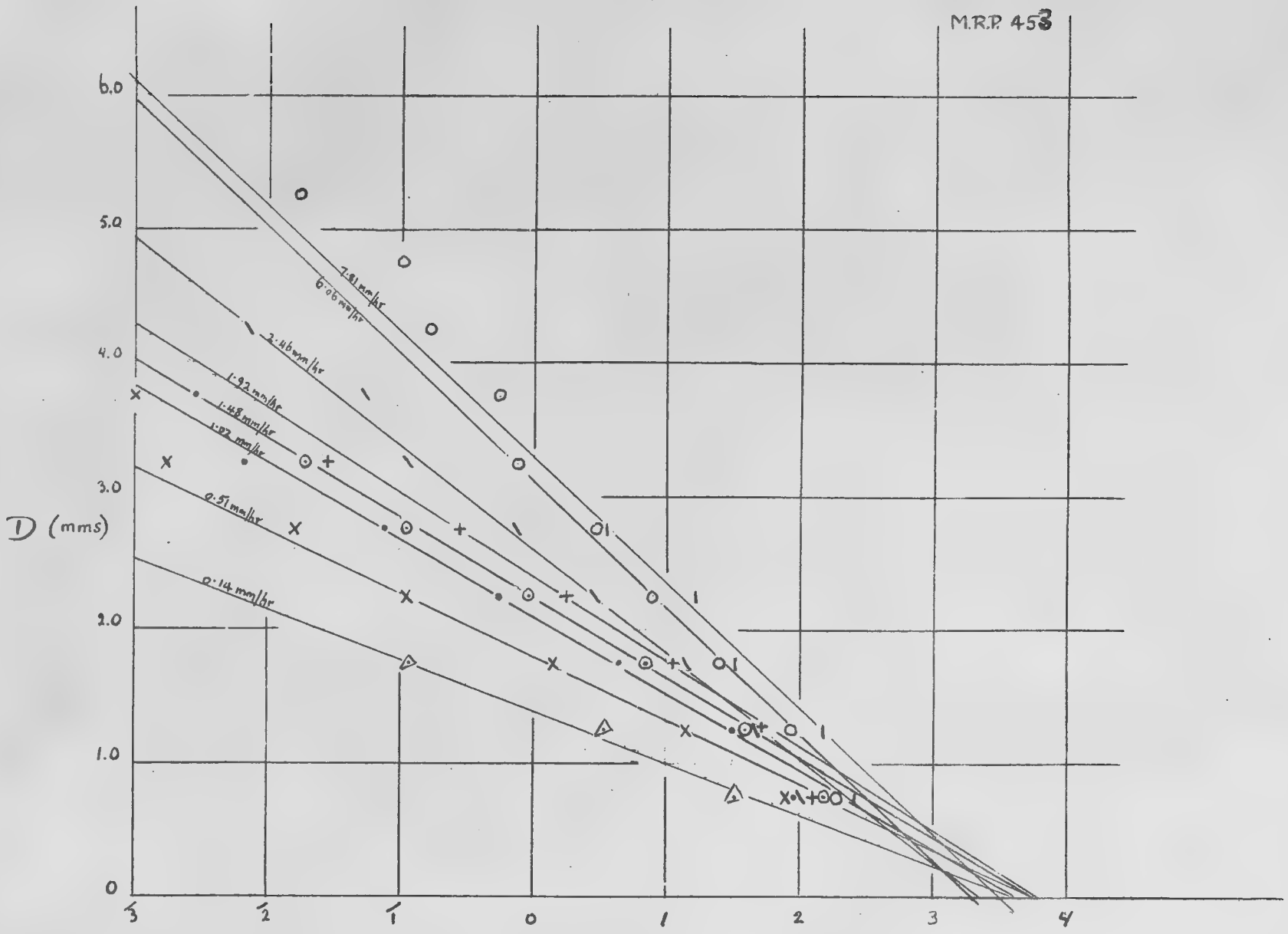

x 0.51 mm/hr. + 1.92 mm/hr
• 1.02 mm/hr \ 2.46 mm/hr
⊙ 1.48 mm/hr 1 7.81 mm/hr
△ 0.14 mm/hr O 6.06 mm/hr.

FIG I. CURVES OF LOG N AGAINST D FOR VARIOUS RATES OF RAINFALL. N IS NO. OF DROPS PER M^3 OF DIAMETER D − 0·25 TO D + 0·25 MMS.

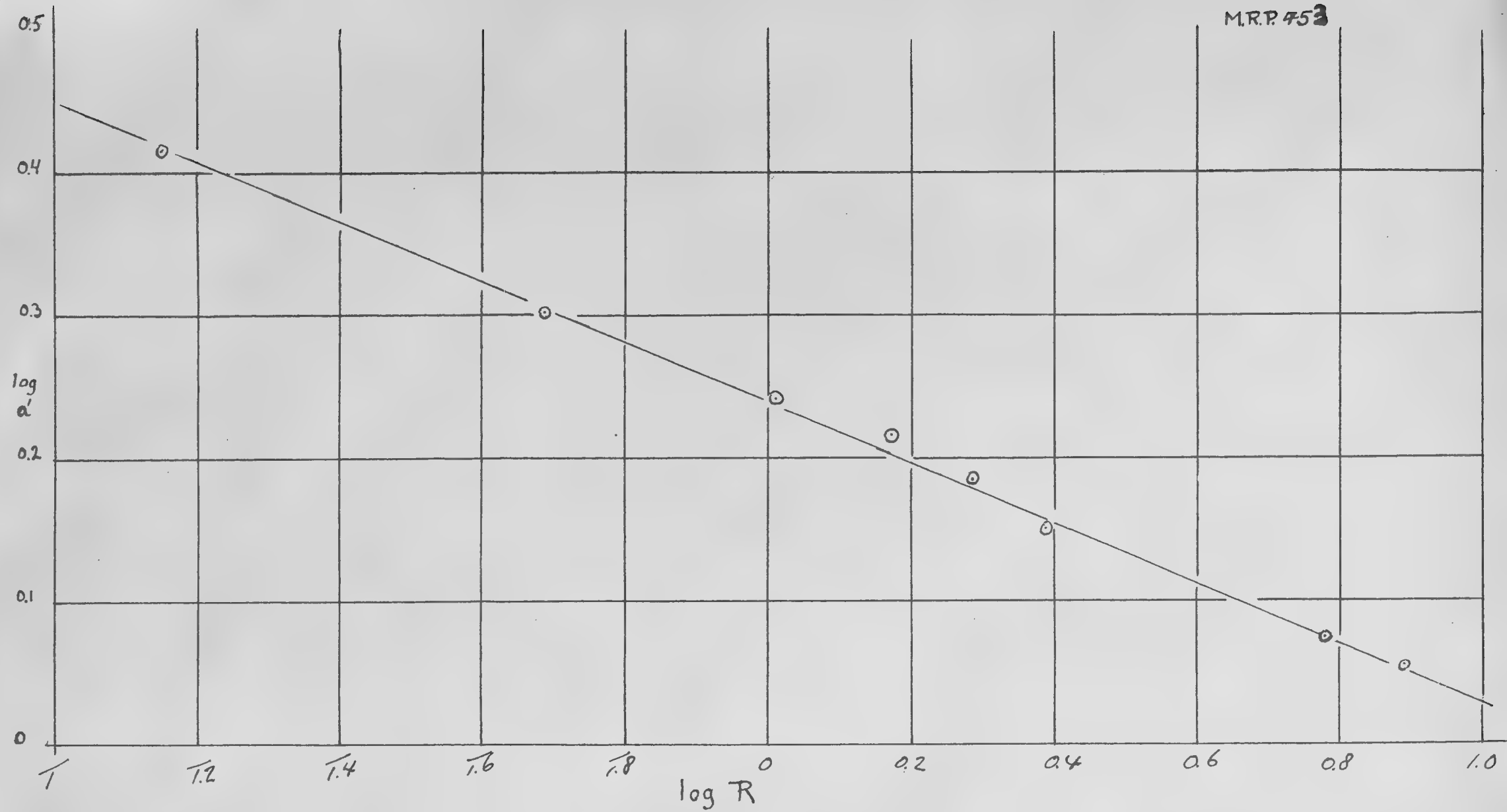

Fig II LOG a' against LOG R. a' is the slope of the curves in Fig I which have the equation $N = \kappa' . 10^{-a'D}$. R is in mm/hr

(Curves in Fig I were adjusted to give $\log \kappa' = 3.65$ for all values of R)

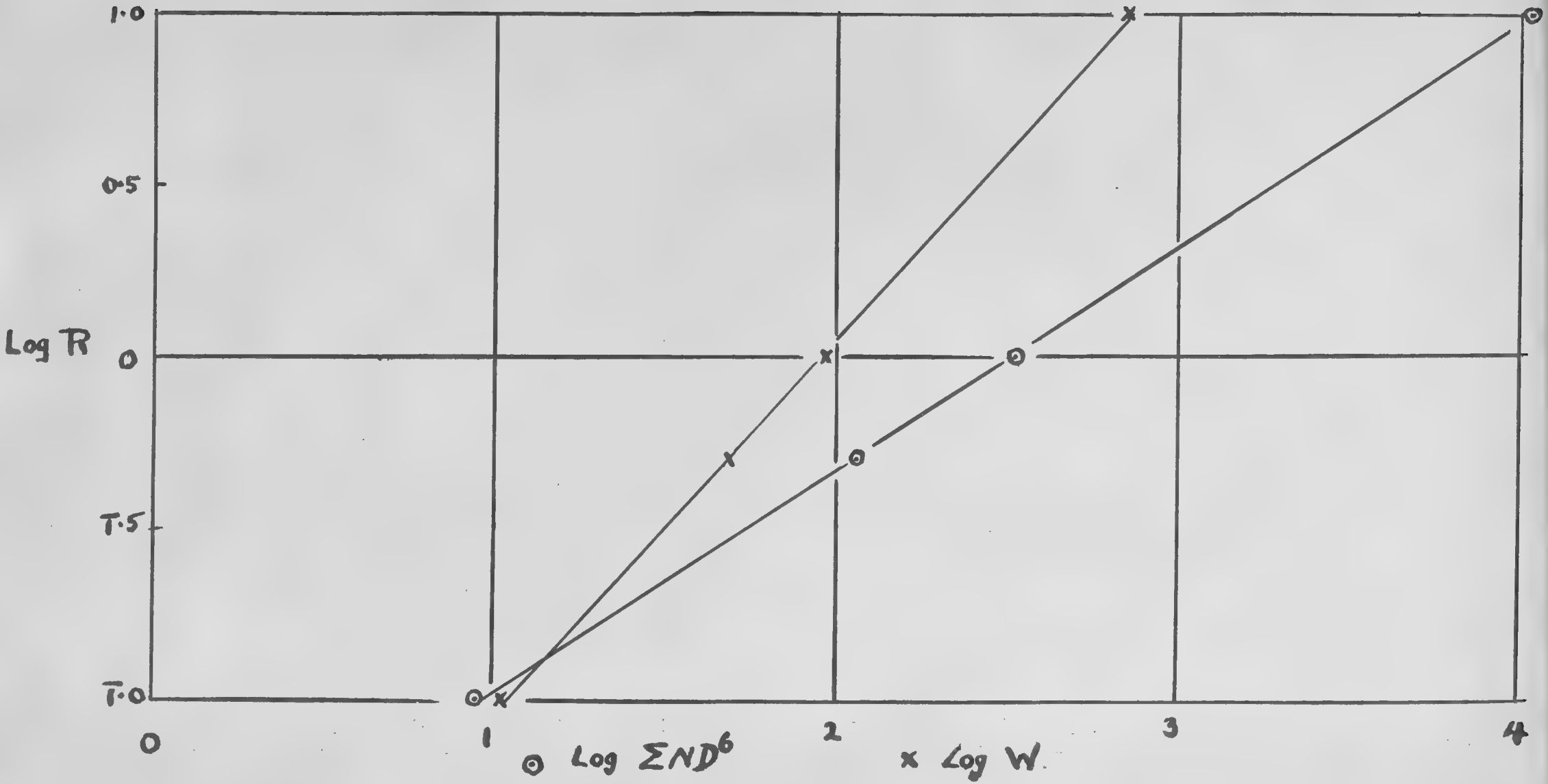

FIG III CURVES OF LOG ΣND^6 AND LOG W AGAINST LOG R.

R is rate of rainfall in mm/hr. N = No. of drops per m^3 of diameter D mm. W = volume of water in form of raindrops per m^3.

M.R.P. 455
SC.II/26
29.12.48.

AIR MINISTRY

METEOROLOGICAL RESEARCH COMMITTEE

Report on some synoptic studies of atmospheric dynamics

by

J.S. Sawyer

555750

Introduction

This note summarises the results of studies of the distribution and changes of the vertical component of vorticity in two synoptic situations. Some general conclusions are given.

In recent theoretical papers (Rossby (1); Sutcliffe (2) etc.) much use has been made of the vertical component of the vorticity vector in atmospheric motion and its theoretical relationship with the horizontal divergence of the motion, the so-called "vorticity equation". The results are broadly justified by their success in explaining observed phenomena in a qualitative manner; quantitative verification is made difficult by the uncertainty of many of the atmospheric variables involved e.g. the wind and temperature at levels in the free atmosphere.

However, the synoptic studies here described were undertaken in order to ascertain how far quantitative treatment of vorticity in the atmosphere could be carried out, and whether the changes in vorticity, as far as these could be estimated on a field basis, led to fields of convergence and divergence in harmony with those to be expected on general synoptic grounds. For this purpose charts of the vertical component of vorticity were drawn, the convergence and divergence of the motion were deduced on the basis of the vorticity equation, and vertical velocities deduced from the convergence on the basis of the "continuity relation"; the distribution of both convergence and vertical motion were compared with those usually attributed to the type of synoptic situation studied, areas of upward motion were also compared with the rain areas and vertical speeds with those estimated on a thermodynamic basis.

Because of the uncertainties of the details in the pressure and contour patterns, the available charts and their changes required much smoothing in order to obtain any sort of continuity. This process must be to some extent arbitrary and subjective, and it is not thought that a detailed report, unless it were to deal with every relevant observation, would be of any value. It is, however, considered that a summary of the provisional conclusions will be of wide interest, because, for the purposes of dynamical synoptics, the subject is of fundamental importance. In brief, the vorticity equation is substantiated in that it leads to a distribution of convergence and divergence on the occasions studied which is in accord with accepted synoptic models.

In order to produce vorticity charts over a wide area from available data, it is necessary to assume that the geostrophic relation is a satisfactory approximation for the purpose. Consequently the broad agreement of the deduced convergence patterns with expectation, can be regarded as partial justification of the use of vorticity based on geostrophic motion, as well as supporting the validity of the relation between vorticity and divergence as a synoptic tool.

Method

The method adopted can be summarised as follows:-

(1) Charts of the vertical component of vorticity (ζ) relative to the earth are drawn. These are based on measurements of $\nabla^2 h$ on constant pressure charts of the 1000, 700, 500 and 300 mb charts (h = height of the isobaric surface); the geostrophic wind relation is thus assumed. A vorticity chart is constructed separately for the individual levels and for a series of synoptic hours.

555750 1

Jul 1
N73431

(2) Charts of the logarithm of the absolute vorticity, $\log_e(\zeta + f)$ - where f = coriolis parameter - are deduced from the charts of ζ by graphical methods.

(3) Charts of $\frac{D}{Dt}\log_e(\zeta + f)$ are constructed indicating the rate of change following the air motion on the assumption of geostrophic flow. If the "vorticity equation"

$$\mathrm{div}_2 V = -\frac{1}{\zeta + f}\frac{D}{Dt}(\zeta + f)$$

is satisfied, these charts are essentially charts of the two dimensional divergence.

The charts of $\frac{D}{Dt}\log_e(\zeta + f)$ are constructed for an interval between two synoptic hours t_1 and t_2 by displacing the isopleths of the chart of $\log_e(\zeta + f)$ at time t, to a position appropriate to the epoch $\frac{t_1+t_2}{2}$ on the basis of geostrophic motion - the technique is similar to that used in synoptic practice for the displacement of a front. The isopleths appropriate to time t_2 are similarly displaced in the reverse direction to be appropriate to the epoch $\frac{t_1+t_2}{2}$. Finally isopleths of $\frac{D}{Dt}\log_e(\zeta + f)$ are obtained by graphical subtraction of the two sets of curves; the final chart can be interpreted as a divergence chart if the "vorticity equation" is assumed true.

(4) By ignoring the surface pressure tendency and the contour of the ground, rough charts of $\frac{Dp}{Dt}$ are constructed for the standard level; this is done by graphical addition of the appropriately weighted divergence at levels below. These charts display the essential features of the field of vertical motion. (Part of the charts for the 700 mb level are shown in Figs. 1 and 2 for the two occasions studied).

The method is essentially one of analysis of the synoptic situation; it is not of direct forecasting value.

Results

The technique was applied to two synoptic situations including an active polar air depression and a "wave depression" with an open warm sector. The main results are summarised below.

Most of the broad features of the divergence charts show a reversal between the 1000 mb and 300 mb levels; convergence at 1000 mb level corresponds with divergence at 300 mb: divergence at 1000 mb with convergence at 300 mb.

Convergence in the lower troposphere is clearly indicated in advance of depressions with corresponding divergence at the 300 mb level; in the rear of depressions the divergence is near the ground and the convergence aloft.

Divergence at the lower levels and convergence aloft was deduced near the main ridges of high pressure.

The upward velocity as deduced at the 700 mb level showed maxima in advance of the depressions exceeding 10cm/sec; this value is of the same order as that deduced by Bannon (3) from the observed rates of rainfall in a number of depressions. In the two cases studied the main rain areas agreed in general with the regions for which substantial upward motion was deduced, i.e. exceeding about 4cm/sec at the 700 mb level.

The charts of vertical motion show rates of subsidence approaching 10cm/sec in small areas associated with the ridges of high pressure but not necessarily coinciding with the ridge line. Rapid subsidence is also indicated in the rear of the depressions. These velocities are greater than

55750

those usually attributed to subsiding air (4), but the charts suggest that the areas of intense subsidence are of limited extent, and air soon passes through them. The total descent is not therefore necessarily as great as might be suggested, and does not necessarily conflict with thermodynamical considerations.

Agreement between vertical speeds deduced from the vorticity charts and those based on thermodynamical considerations following Grahams method (5) was not close; however where rates of subsidence or ascent were large there was general agreement as to sign and magnitude. Moreover there is substantial evidence that non-adiabatic processes play a significant role in temperature changes even over a few hours so that methods based on the conservation of potential temperature are not likely to be accurate.

Conclusions

Despite the substantial errors inherent in the technique employed, the broadly convincing nature of the results regarding divergence and vertical motion suggests that the general form of the field of vertical motion is determined uniquely by the principal features of the pressure field and the changes taking place in them. It also suggests that considerations of vorticity based on the assumption of geostrophic flow are a valid basis for deductions regarding the general distribution of cyclonic and anticyclonic development in the atmosphere (e.g. Sutcliffe (2)); and further that the pressure field is determined by a good synoptic network sufficiently closely for such methods to be applied.

It must however be added that the technique as at present employed is long and laborious; the results too are very crude. Its results are not likely to be sufficiently accurate to establish beyond doubt the distribution of vertical motion in typical synoptic types; however, it should prove a useful if cumbersome tool in directing attention to the factors in atmospheric dynamics which particularly merit attention in specified synoptic situations.

If some rapid and practical technique of drawing vorticity charts could be devised, there is little doubt that their routine use in synoptic work would prove of value. It may be remarked that the use, in this way, of vorticity change following the air motion, is a natural extension of the recognised synoptic technique in which isallobaric "highs" and "lows" are associated with divergence and convergence.

References

(1) Rossby, C.G.; Planetary flow patterns in the atmosphere, Quart. J.R. Met., Soc., London, 66 Suppt., 1940, p.68.

(2) Sutcliffe, R.C.; A contribution to the problem of development. Quart. J.R. Met., Soc., London, 73, 1947, p.370.

(3) Bannon, J.K.; The estimation of large scale vertical currents from the rate of rainfall. Quart. J.R. Met., Soc., London, 74, 1948, p.57.

(4) Pettersen, S.; Sheppard, P.A., Priestley, C.H.B., and Johannessen, K.R.; An investigation of subsidence in the free atmosphere. Quart. J.R. Met., Soc., London, 73, 1947, p.43.

(5) Graham, R.C.; The estimation of vertical motion in the atmosphere. Quart. J.R. Met., Soc., 73, 1947, p.407.

555750

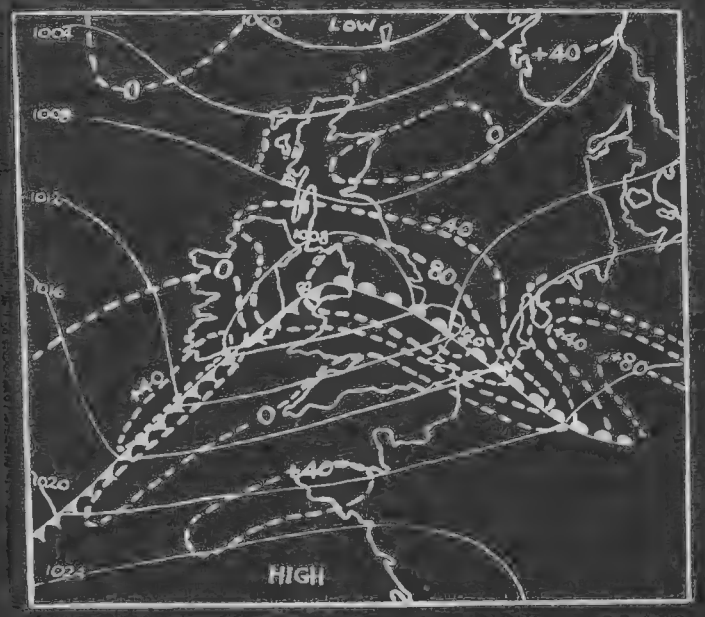

Fig. 1. Isopleths of $\frac{Dp}{Dt}$ at 700 mb. level and synoptic situation 1800 G.M.T. March 17th, 1948.

Note. $\frac{Dp}{Dt}$ is the rate of change of pressure on a moving element of the atmosphere. Positive signs indicate subsidence and negative signs ascent.

Units - $mb/sec \times 10^{-4}$; approximately 40 mb/sec $\times 10^{-4} = 4.5$ cm/sec

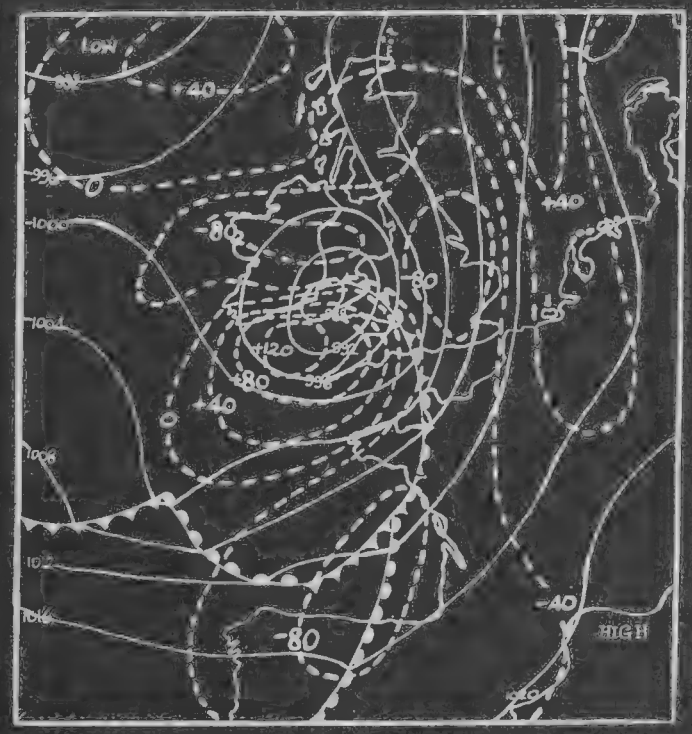

Fig. 2. Isopleths of $\frac{Dp}{Dt}$ at 700 mb level and synoptic situation 0001 G.M.T. 30th March, 1948.

555750

This re[illegible] treated
CONT[illegible] its
contents must not be quoted.

M.R.P.458

S.C.III/19

5th January, 1949.

AIR MINISTRY

METEOROLOGICAL RESEARCH COMMITTEE

The Heights and Temperatures at the Tops of Radar Echoes Associated with Various Cloud Systems.

by R.F. JONES.

1. Introduction.

AIR WEATHER SERVICE
TECHNICAL REFERENCE FILES

Since 13th March, 1947 weather echoes have been observed regularly from the Meteorological Radar Station at East Hill using an A.M.E.S. Type 21 radar equipment which consists of a Type 13 Height-Range indicator and a Type 14 Plan Position Indicator (P.P.I.) operating on a wave length of 10 cm.

A large number of readings and photographs of weather echoes have been made showing the horizontal and vertical extent of these echoes in many different weather situations together with, on some occasions, measurements of the intensities of the echoes received.

Other workers in Canada and U.S.A. have been similarly engaged at different times but, as far as the writer is aware, little has been done in correlating the vertical extent of the weather echoes received with the upper air data provided by a regular sequence of radiosonde ascents at a reasonably close network of stations.

The present paper gives the results of the analysis of a large number of Height-Range photographs and written observations made during the period 13th March, 1947 to October 4th, 1948. Similar data are still being acquired in conjunction with the investigation of other aspects of the radar-meteorological problems.

2. The Equipment.

The equipment used for height-range measurements is the standard equipment known as A.M.E.S. Type 13 operating on a wave length of 10 cm. and using a pulse of 2 microseconds duration. A common transmitting and receiving aerial is used which is made up of two sections of a parabolic metal cylinder cut in the focal plane, each section being 20 ft. high and $18\frac{1}{2}$ in. horizontally separated by a 1 in. thick panel. This gives beam widths (measured to half power) of $7\frac{1}{2}$ degrees in the horizontal and $1\frac{1}{2}$ degrees in the vertical plane. The aerial is mounted with the long dimension vertical and is made to sweep continuously about a horizontal axis from -1° to 19°, one complete up and down movement taking 10 seconds, while it can be turned to any required azimuth by remote control from the Operations Room.

The presentation on the display tube gives range and height of the echo observed directly. A simple switching device enables the same tube to be used to give the intensity of the echo examined. This intensity was usually measured with the aerial sweeping and hence gives the maximum intensity in the vertical column comprising the echo at a given range. The aerial can be stopped at any desired elevation but for the purposes of this paper only intensities with the aerial sweeping are used.

Photographs of the display tube were taken as required on 35 mm. film and the developed film subsequently analysed under a microfilm reader.

The principle on which photographs were taken was to endeavour to take a photograph of any interesting echo which was observed. "Interesting" in this connection would not only involve the photographing of the most intense echoes but also echoes of unusual shapes, echoes being investigated by an

/aircraft

aircraft under our control and, on some occasions, the following of one particular echo in its changes with time. On many days there were echoes on many bearings while a particular echo might extend through several degrees of azimuth and it was, of course, impossible to photograph all echoes at all stages of their existence. In general, however, a photograph or written record would be available for the most noteworthy echoes, including those extending to the greatest height, of a particular day during the time of operation of the radar (usually to about 1730 clock time).

In taking a photograph one particular echo or part of an echo was usually in view and therefore brought directly into the radar beam but this would not preclude the appearance on the photograph of echoes at different ranges which were possibly not directly in the beam (which has a horizontal width of $7\frac{1}{2}$ degrees).

3. Preparation of the readings for analysis.

For the purposes of this paper the ranges at which observations were made (which had usually a maximum value of 75 miles) were split up into the ranges from 11 - 20, 21 - 30, 31 - 40, 41 - 50, 51 - 60 and 61 - 75 miles. Readings were not considered for ranges of less than 11 miles since the maximum angle of the aerial sweep (19 degrees) did not permit measurements of the highest tops on all occasions at such short ranges.

The readings from the photographs - of which some 1200 were analysed for this paper - and written records were arranged to show the maximum tops of weather echoes observed within these ranges and the maximum top for each day (or each type of weather if more than one type occurred on one day) for each range was extracted. A close analysis of the weather situation for these days was made and a decision made as to which radiosonde ascent (usually at Larkhill or Downham for 0600, 1200 or 1800 GMT up to and including 31st December 1947 and for 0900 or 1500 GMT after that date) gave the most likely upper air conditions for the locality of the weather echo under examination. On some occasions, particularly with quickly moving fronts, it was not possible to get a representative upper air ascent but on most occasions it is considered that a reasonable approximation to the actual conditions has been obtained.

Having decided on the representative upper air ascent for each weather echo the temperature of the air at the height of the maximum tops of the weather echoes was determined for each of the ranges mentioned.

Finally the temperatures themselves were split up into ranges so that the number of occurrences of tops within a certain range of temperatures at specified ranges of distance was obtained.

The result of this analysis is shown in Table I; the number of different weather situations involved is 164.

On some occasions, however, a particular weather phenomenon would not affect equally all ranges, e.g. in thunderstorm conditions an active storm may be viewed at 40 - 50 miles, say, while at 10 - 20 miles only a degenerate storm may be seen with the result that the top of the storm at 40 - 50 miles appears higher than the one at 10 - 20 miles. Similarly in frontal conditions, if the front had already passed the station before observations commenced higher tops might be seen on the longer ranges than on the shorter. On another occasion the distant echo might be fully in the radar beam while the most intense part of a nearby echo might not be on exactly the same bearing giving again an apparently higher top at the longer range. When allowance is made for the fall off of echo intensity with range R (inversely proportional to R^2 if the echo fills the radar beam and to R^4 if the echo fails to fill the beam) it seems virtually certain that an echo with a high top at long range would have given a top at least as high (and possibly higher) at shorter ranges, so that the typical top for the weather situation in question may not have been directly measured at all ranges. For this reason a second table, Table II, has been constructed which shows the minimum temperature of the top of a weather echo in a particular weather situation irrespective of the range (greater than 10 miles). The range at which this top was noted is shown in the Table (as is

the date also) and it may be regarded as certain that, if all the echoes had been observed at the range 11 -20 miles, the temperatures of the tops of the echoes would have been at least as low as those shown in Table II, with the great probability that in the more extreme cases (e.g. 30th July 1947 and 21st August 1947 when the only echo was at 61 - 75 miles) the temperature would have been considerably less than that shown.

The number of occurrences, out of the total of 164, when this minimum temperature fell within various ranges of temperature is shown in Table III.

It is of considerable interest to determine whether the occurrences of tops within a particular range of temperatures have any similar weather features and for this reason the occasions within each range have been examined and the types of weather associated with them have been listed. This analysis is given in Table IV with detail which is thought to be of considerable interest.

Finally those occasions when it was thought probable that the echo viewed came from a thunderstorm were separated from the occasions when it was almost certain that no thunderstorms were present. These occasions, with remarks, are listed in Table V. On some of these occasions signal intensity readings were also made as well as on occasions when thunderstorms were unlikely to be present. A comparison of such occasions during periods when the performance of the equipment was known, by special tests, to have been particularly uniform is given in Table VI. To enable a comparison to be made of intensities measured at different ranges a column is included giving the intensity to be expected if all measurements were made at a constant range of 20 miles. This value is obtained as follows:-

Suppose at range R the volume giving the weather echo entirely fills the radar beam then the power received at the aerial is proportional to $1/R^2$. (If the echo does not fill the beam the proportionality is as $1/R^4$). The received signal intensity is measured as a signal to noise ratio (S/N) and although this does not measure the actual power received the relative power of two signals is proportional to $(S/N)^2 - 1$. The relative power reading therefore to allow for change in range from R to 20 miles is given by

$$((S/N)^2 - 1)\frac{R^2}{20^2}$$

if the echo fills the beam and

$$((S/N)^2 - 1)\frac{R^4}{20^4}$$

if the echo does not. As it is impossible to say whether the echo did in fact fill the beam although, except at the longer ranges, it is almost certain to have done so, the value

$$((S/N)^2 - 1)\frac{R^2}{20^2}$$

is assumed as the correction factor in all cases while a note may be made that at the long ranges this value may be too small by a further factor of $R^2/20^2$.

It should be further noted as mentioned above, (Section 2) that the signal to noise ratio in these cases is measured with the aerial sweeping and hence is proportional to the maximum signal intensity from the volume comprising the weather echo.

4. Discussion of points arising from the analysis.

A. The temperature at the top of the echo in relation to the vertical currents within the echo.

An examination of Table IV brings out the probability of a close relationship between the temperature at the top of the echo and the vertical currents likely to be experienced within the echo.

/Vertical

Vertical currents are generally assumed, with considerable justification, to be large in cumulonimbus cloud and particularly in thunderstorm clouds and to be small, or at any rate if strong of very limited extent, in the layer type of clouds. It can be immediately seen - and Table V brings out the point more clearly - that the thunderstorm conditions are associated with low echo top temperatures and conversely that the higher temperatures at the echo top are associated with the layer clouds.

Thus when the temperature at the echo top is below - 40°F, 19 out of 21 occasions were almost certainly associated with thunderstorms while the remaining two were associated with conditions which gave heavy squally showers locally and may well have been thunderstorms at the time of observation. In the range from - 30°F to -39°F, five occasions out of eight gave thunderstorms but the ranges at which they were viewed were in all cases greater than 21 miles and, with one exception, lower echo top temperatures, sufficient to put them in the range below - 40°F, may have been found if it had been possible to view them at shorter range. The exception mentioned (H.6 of Table IV) was at - 39°F and as this was the tropopause temperature at that time echo top temperatures below - 39°F could not have occurred. The remaining occasions of probable thunderstorms which gave echo tops in the ranges higher than - 30°F were all viewed at ranges greater than 30 miles or the observations were incomplete for various reasons as detailed in Table V with one very important exception. On this occasion (D.27 of Table IV) thunder was reported by two stations at a time when a Spitfire aircraft under our control was making turbulence investigations in the neighbourhood. Reports from the pilot of this aircraft, independently confirmed by other pilots and indirectly from the theoretical cloud top from upper air ascents, placed the cloud top very close to the observed echo top, the temperature of which was 07°F. On this one occasion, therefore, echo top temperatures below -30°F would appear to have been impossible but on all the remaining 41 occasions when thunder was likely to have occurred there are plausible reasons for assuming that, if the particular echo had been viewed in the 11 - 20 miles range, the echo top temperature may well have been lower than -30°F and probably lower than -40°F.

There seem strong grounds, therefore, for assuming that if an echo top is observed at a range of 11 - 20 miles, in this area with this equipment, with a temperature at or below about -39°F then the echo will be from a thunderstorm while the converse that a thunderstorm, if viewed at 11 - 20 miles, will give an echo extending higher than the -39°F isotherm will very probably be true although exceptionally a much lower height may be observed. Deductions of thunderstorms on the basis of echo tops extending above the -39°F isotherm have been rather strikingly confirmed on one or two occasions when thunder had not been expected.

Conversely, of the 50 occasions (Sections A and B of Table IV) when the temperature at the echo top was above 17°F, 36 occasions may be listed as belonging to layer type characteristics of cloud, including in this category weak or slow moving or quasi-stationary fronts. Of the remaining 14 occasions, six (B2, B15, B23, B24, B32, B33) all with temperatures at the echo top less than 32°F, are associated with convection limited by isothermal or stable layers at or near the echo top temperature or convection dying out ahead of a warm front; four (A3, B9, B10, B37) may be dismissed because of the greater range at which they were viewed and the remaining four refer to two occlusions and two warm fronts.

It is noteworthy that there is an apparent minimum in Table III in occurrence of echo top temperatures in the range from 10°F to 17°F and this point will be returned to later (Section 4C). This minimum is also visible in the occurrences of echo tops in the various ranges up to 50 miles as will be seen in Table I. Of the 10 occasions when the minimum echo top temperature irrespective of range fell in the temperature range 10°F to 17°F (Section C of Table IV), seven were connected with inversions or isothermal layers at the echo top heights, indicating limited cloud development, and the other three occasions were associated with layer cloud.

/Considering

Considering next the range from 09°F to -09°F (Sections D and E of Table IV) we find that of 57 occasions, 8 (D7, D21, D23, D27, E19, E21, E25, E29) have already been discussed under the thunderstorm occasions. Of the remaining 49 occasions, 35 are associated with fronts or troughs, the cold fronts and troughs (which are frequently almost indistinguishable from cold fronts) with one exception having echo top temperatures of 00°F or lower. This exception, when the echo top temperature was 09°F, was associated with a cold front which the P.P.I. display showed to consist of three narrow parallel belts of precipitation suggesting that the front really consisted of three separate stages of cold air and was therefore presumably not as active as a normal cold front. Warm front phenomena were, in general, associated with echo top temperatures of 00°F or higher and as might perhaps be expected, echoes associated with occlusions were more or less evenly distributed through the whole range from 09°F to -09°F. The 14 other occasions in this range which remain to be accounted for contain nine occasions of either limited convection or decaying cumulonimbus activity, two occasions of snow in a cold easterly current, two occasions of warm air instability and one occasion (E27) which is dealt with later under section 4B when discussing the echo intensities from thunderstorms.

Finally in the range from -10°F to -29°F (Sections F and G of Table IV) we have 18 occasions of which 8 (F1, F6, F7, G2, G4, G8, G9, G10) have been discussed under the thunderstorm occasions. Of the remaining 10 occasions, four refer to cumulonimbus, two to cold fronts, two to occlusions and one each to unstable medium cloud and a warm front. As the majority of echoes associated with frontal occasions have temperatures at their tops in a higher range of temperatures than this, it can be assumed that the occasions here encountered were occasions of particularly active fronts in which, due to instability in the warm air, cumulonimbus clouds were probably embedded in the frontal cloud system.

We can, therefore, construct a rough table showing the temperatures to be expected at the top of weather echoes viewed with this equipment in this area at 11 - 20 miles for various types of weather. This is shown in Table VII below:-

Table VII

Types of weather associated with ranges of echo top temperatures when viewed at 11 - 20 miles.

<table>
<tr><th>Temperature</th><th colspan="3">Weather Type</th></tr>
<tr><td>Lower than -40°F
-40°F</td><td colspan="3">Thunderstorms.</td></tr>
<tr><td>-30°F
-20°F
-10°F</td><td colspan="3">Particularly active fronts probably containing cumulonimbus embedded in the frontal cloud system but probably without thunder.
Cumulonimbus clouds probably without thunder.</td></tr>
<tr><td>00°F</td><td>Unstable medium cloud. Normal cold fronts and troughs.</td><td>Most occlusions.</td><td rowspan="3">Convection limited by stable layers at or near the echo top temp., decaying Cb activity with approach of frontal conditions.</td></tr>
<tr><td>09°F</td><td>Normal warm fronts.</td><td>Snow showers</td></tr>
<tr><td>18°F</td><td colspan="2"></td></tr>
<tr><td>32°F
Higher than 32°F</td><td colspan="2">Layer type clouds including weak and slow moving or quasi-stationary fronts.</td></tr>
</table>

This table indicates that in general terms it is almost certainly correct to say that the temperature at the top of the weather echo gives a good indication of the strength of the vertical currents within the weather echo.

Absolute values of the vertical currents cannot, of course, be inferred but it is hoped to deal more rigorously with this point at a later date as a result of cumulonimbus investigations which are now proceeding.

B. The echo intensities from thunderstorms.

An examination of Table VI shows that not only is the temperature at the top of a thunderstorm echo (when allowance is made for range) probably much lower than for other echoes, except in the one exceptional case already referred to (D27 of Table IV), but also, with this same exception, that the maximum signal intensity is probably much greater than that from most other weather echoes. In Table VIB there are only three occasions when thunderstorms were probably not present which give echo intensities comparable with those from some thunderstorms. Two of these occasions (for 25/8/48 and 4/5/48) were associated with particularly active fronts while the third occasion on 22/7/48 (E27 of Table IV) was viewed at a range of 48 miles to the northwest. On this latter occasion, although no thunder was reported from the Midlands and South of the country, thunder was reported in South Yorkshire and Lancashire and this echo may therefore have come from an isolated storm of short duration.

The conclusion seems justified that not only does the weather echo from a thunderstorm usually extend to a lower temperature than other weather echoes but also that the intensity of the received echo is usually much greater. In exceptional conditions a very strong echo may be received from non-thunderstorm precipitation and very exceptionally (D27 of Table IV, 4/10/48) a thunderstorm may give an echo indistinguishable from that from many other echoes not associated with thunderstorm conditions.

If we accept the theoretical deduction that the echo intensity is proportional to ΣND^6, where N is the number of drops of diameter D per unit volume, we see that the increased echo intensity can be explained either by a great increase in the number of drops per unit volume or by a much smaller proportionate increase in the diameter of the drops or by a combination of the two effects. It seems likely that the spectacular increase in signal intensity in changing from an ordinary shower to a thunderstorm is due to an increase in the size of the drops since, with the stronger vertical currents, the life of a waterdrop within the cloud will be appreciably longer and give greater opportunity for the growth of the drop.

Some light is thrown, therefore, on the physical properties which distinguish a thunderstorm from other cumulonimbus clouds namely that for a thunderstorm the vertical currents and raindrop size must be greater than in an ordinary cumulonimbus. This may lend support to the "breaking drop" theory of separation of electrical charge within a thunderstorm.

It may also be significant that the temperature at the top of the thunderstorm echo is usually below about $-40^{\circ}F$ and therefore in the region where a sudden increase in the number of ice particles is likely to take place, as observed by Findeisen and Schulz (8). This suggests that a contributory factor to the generation of a thunderstorm may be the introduction of a number of supercooled raindrops into a volume containing large numbers of ice crystals.

C. Types of weather echo and their probable explanation.

Not only, as shown in Table VII of Section 4A, does the echo top temperature indicate a type of weather likely to be associated with the echo but the echoes themselves, as viewed on the height-range display tube, have certain outstanding characteristics of form or structure.

/Let

Let us consider first the occasions when the echo top temperature is greater than 17°F, The responses on these occasions which, as shown in Table VII, are associated with "Layer type clouds including weak and slow moving or quasi-stationary fronts" are usually in the form of a band of echo (see Photograph (i)) of varying thickness but rarely giving responses down to ground level and sometimes associated with a brighter band near the freezing level.

Ryde(1) (p 186, 1st para) has shown theoretically that if snow falls as dispersed ice crystals each having a mass less than about 1 to 2 mg. the echo would be less than from rain having the same precipitation rate. It is therefore possible to visualise an occasion of precipitation when the echo is not visible as long as the ice crystals forming the precipitation are discrete and small but becomes visible when something occurs either to increase the size of the ice crystals or to aggregate them into snowflakes or to melt them into raindrops.

The fact that the responses with echo top temperatures above 17°F rarely extend to ground level would indicate that the response from the raindrops was itself too small to be seen by this radar. So it is unlikely that the echo up to 18°F can be due to discrete ice particles and the inference is that the precipitation was made visible only by the aggregation of the ice crystals to form snowflakes, with an enhancement of this echo at the freezing level due to the melting process as explained by Ryde (1) (p 188), leading to what is commonly known as the "Bright Band" effect. On some occasions indeed it is probable that only the enhanced echo due to the Bright Band effect was visible.

It can be assumed therefore that in the case of responses with echo top temperatures above 17°F the response is due to snowflakes composed of a number of crystals or to melting snowflakes giving the Bright Band effect. The aggregation of snow crystals to produce snowflakes is generally agreed to take place when the snow crystals are made wet through collision with numbers of small supercooled water droplets, the latent heat of fusion liberated being sufficient to keep the surface at any rate of the crystal at or near 32°F. This can only take place (a) if the crystal collides with a sufficient number of supercooled water droplets and (b) if the temperature is high enough so that the loss of heat to the surrounding atmosphere is compensated by the gain of heat from the latent heat of fusion liberated by the supercooled water droplets on freezing. It is suggested that with low vertical current speeds conditions (a) and (b) above are satisfied at temperatures greater than 17°F but that for lower temperatures the ice particles, although growing by collision and condensation in the atmosphere which is supersaturated relative to ice, remain dry so that aggregation to form snowflakes is impossible. A paper by Nakaya and Terada (2) indicates that the normal size of individual ice crystal encountered has a terminal velocity of the order of 1/3 to 1 metre/sec. so that it may be noted that should the vertical current exceed about 1 metre/sec. no ice crystals can fall past the 18°F isotherm. The explanation of radar echo given above therefore can only apply to vertical currents of less than about 1 metre/sec. and probably less than 1/3 metre/sec.

We come now to echoes with top temperatures less than 10°F. As Table VII shows these can be divided into two sections, the one including normal fronts and high level instability and the other cumulonimbus (including in this category particularly active fronts). The normal frontal cases are in the higher part of the range i.e. with temperatures at the top of the echo from 09°F to -10°F and with the cold fronts in the 00°F to -10°F part of this range. These frontal cases were often associated with a Bright Band indicating the presence of melting snowflakes or ice crystals and hence it would be reasonable to expect a similar explanation to that for echoes with top temperatures above 17°F to apply. If this is so we must assume that (a) aggregation to snowflakes occurs at temperatures as low as -10°F in occasions of stronger vertical currents and that (b) although the vertical currents are stronger they are still less than about 1 metre/sec. Examining (b) more closely, the slope of a warm front is usually taken as between 1 in 100 and 1 in 150. (Met. Glossary (3) p 206). The ascent of warm air overriding cold air is the agency producing the rain and the weather echo. If the difference in components of the horizontal velocity of the air at right angles to the front in the warm and cold air is 40 mph (which would certainly be an extreme case) the rate of ascent of the warm air (Brunt(4) p.353)

for a slope of 1 in 100 would be 0.4 mph which is equivalent to about. 0.6 ft/sec and well within the limit set by (b). In a cold front with a slope of about 1 in 50 the rate of ascent would be greater but still well within the limit set by (b). Bannon,(5) by considering the rate of rainfall, also concludes that in active depressions over the North Atlantic the rate of ascent of the air is generally of the order of 10 - 20 cm/sec, so that upward velocities of less than 1 metre/sec. can be generally said to be associated with all normal frontal cases. Occasionally, however, latent instability in the warm air or other effects may cause the rate of ascent to be increased and this would explain the occasional absence of the Bright Band and the appearance at times of columns within the echo containing a Bright Band (see photograph (iii)).

Echoes of the frontal type, therefore, can be explained in the same way as the layer type echoes with top temperatures above 17°F if we can assume that the greater vertical currents (but still less than 1 metre/sec) leads to aggregation of the ice crystals to snowflakes at a greater height (i.e. lower temperature). This might occur since the greater vertical current would slow down the rate of fall of the ice crystal giving it greater chance of growth and may also make available a greater number of supercooled water droplets.

This explanation, however, makes it difficult to account for the apparent low frequency of echo tops in the temperature range of 17°F to 10°F. The foregoing explanation would imply that aggregation to snowflakes is uncommon at temperatures from 17°F to 10°F which itself implies that ice crystals falling from above either pick up enough supercooled water to make aggregation possible before reaching the 10°F isotherm or, having failed to aggregate by that time, they must for some reason wait until reaching at least the 18°F isotherm before doing so.

An alternative explanation was therefore sought to account for the low frequency of echo tops in the 10°F to 17°F region and a possibility was found in an alternative explanation of the echoes with tops above the 10°F isotherm.

The fact that a Bright Band is still observed with such echoes indicates almost certainly that the change of state from ice to water is taking place at or near the freezing level and therefore the probable explanation of echoes showing a Bright Band and extending above the freezing level must still require the echoes to come from the ice phase. The only alternative to ice crystal aggregation is that the echoes come from the ice crystals themselves. As already mentioned Ryde (1)(p186) has indicated that "when snow falls as dispersed crystals, each having a mass of about 1 to 2 mg, we should expect that the echo intensity would not be very different from that produced by rain at the same precipitation rate". With the stronger vertical currents, still less than about 1 metre/sec however, (Ryde (1) P 184 last line), and greater vertical extent of cloud in frontal cases than in the other layer type cases giving echo tops below the 17°F isotherm, the ice crystals descend slower and traverse a greater depth of cloud and so are much more likely to reach the 1 - 2 mg. mass required to give an echo on their own account. The echoes with tops above the 10°F isotherm and showing a Bright Band near the freezing level may therefore be explained as due to large ice crystals of the order of 1 - 2 mg. mass in sufficient numbers to give an echo on their own account in the top at least of the echo, although they may, of course, aggregate to snowflakes in the same way as smaller crystals when falling below the 17°F isotherm. (see photograph (ii)).

We therefore have two types of Bright Band echoes:-

(i) In very weak vertical currents, probably less than 1/3 metre/sec, and also probably limited thickness of cloud, echoes the tops of which are below the 17°F isotherm due to the aggregation and subsequent melting of small ice crystals which are not big enough to give an echo on their own account.

/(ii)

(ii) In stronger vertical currents, but still less than about 1 metre/sec, usually associated with frontal systems and probably great depth of cloud, echoes the tops of which are above the 10°F isotherm due to the ice crystals themselves, the ice crystals having grown to the requisite size due to their small rate of fall through a considerable depth of cloud.

The low frequency of echo tops (associated with a Bright Band) in the range 10°F to 17°F is ascribed to a low frequency of occurrence of cloud and vertical current conditions intermediate between (i) and (ii).

Finally we encounter the cumulus and cumulonimbus type of echo with temperatures at the top usually below -10°F, although, on occasions of convection cloud the vertical development of which has been limited by the presence of a stable layer, cumulus and cumulonimbus type echoes have been observed with temperatures at all values from 30.5°F downwards including the majority of the cases in the layer of minimum frequency from 10°F to 17°F.

The outstanding characteristic of this echo type is its appearance as a strong vertical column of echo (see photograph (v)) with clear cut vertical edges and no indication of any Bright Band phenomena. The strongest part of the echo is <u>not</u> in the form of a horizontal band but appears as a vertical column with the absolute maximum intensity at some point or at a series of points at different heights within this column, The conclusion seems inescapable that we are dealing with a completely different type of echo formation, while the absence of any sign of Bright Band leads to a suggestion that there is no enhancement of the echo due to melting at the freezing level because there is nothing there to melt! i.e. the echo seen on this equipment from a cumulonimbus cloud comes from liquid water drops at all heights. As support for this idea may be quoted an occasion (on 20th April, 1948) when the Spitfire aircraft investigating cumulonimbus clouds reported icing from 26,000 feet (temperature -39°F) to 18,000 feet (temperature -7°F) which to use the pilot's own words "seemed to be formed by very small water droplets which spread out on the windscreen in the form of very small transparent oval patches. Its thickness was negligible ..... At 10,000 feet to 8,000 feet there was rain .....". The temperature at 10,000 feet according to upper air ascents was 22°F and at 8,000 feet, 30°F.

Disregarding for the moment the absence of the Bright Band, the only alternative to the above hypothesis would be that at some stage the echo came from hail instead of water drops since the existence of snowflakes in the large vertical currents of a cumulonimbus seems impossible. As shown by Hooper and Kippax[6] large snowflakes have a terminal velocity of about 2 metres/sec. - a value which is almost certainly exceeded in the upward velocity of the most moderate cumulonimbus clouds (Goldie)[7]. The echo intensity from hailstones however (Ryde [1] p 183) is only 0.18 of that from raindrops of the same diameter for a wavelength of 10 cm (which is our radar wavelength) so that to explain the radar echo at some height above the freezing level solely in terms of hailstones would imply hailstones of greater diameter than the raindrops in the normal raindrop distribution which gives an echo and also the same number per cubic metre. The infrequency with which hail is reported even when the freezing level is near the surface would suggest that hail is not an essential component of shower type precipitation.

When account is taken also of the absence of a Bright Band the suggestion is made therefore that cumulonimbus echoes are principally (and perhaps often entirely) due to supercooled waterdrops of <u>raindrop size</u> and, on the basis of some measurements which have been made, probably larger than 1.0 - 1.5mm diameter. To explain the fact that such echoes usually extend to temperatures below -10°F requires a theory to explain how liquid water drops of such a size can arrive at such a height. Findeisen and Schulz in a paper summarised by Best [8] have shown that condensation on nuclei will occur almost exclusively as supercooled water droplets in cumulus clouds down to a temperature of -20°F and that even at temperatures of -40°F the number of ice crystals produced "does not yet approach the number of water drops formed in the same space". The existence of supercooled water therefore at temperatures below -10°F (the echo top temperatures for most cumulonimbus clouds) cannot be called in question but its existence in raindrop size is not so readily explained.

If all drops of raindrop size originate around an ice crystal as required by the Bergeron-Findeisen theory it is difficult to see why the drop should be liquid at temperatures below -10°F and the argument against hail has already been given above. The alternative would appear to be the growth to raindrop size without the assistance of an ice crystal by condensation and coalescence as supercooled water. In addition the presence of cumulus and cumulonimbus type echoes (i.e. column type echoes without a Bright Band) with echo top temperatures as high as 30.5°F suggests also that in the limited convection occurrences which yield such high values of the echo top temperatures still without a Bright Band, growth to raindrop size is taking place by coalescence and condensation as supercooled water since, as mentioned above, Findeisen and Schulz have shown ice crystals to be extremely infrequent at such temperatures. According to Findeisen, quoted by Simpson (9), (Table VII p 130) growth by condensation alone would take an impossibly long time but Simpson (9) (pp 131 - 132) gives the argument in favour of growth to raindrop size by coalescence and condensation without the aid of ice crystals in strong vertical currents and it is suggested that the radar evidence may lend some support to this view.

Since to produce a radar echo the drops must almost certainly be greater than 1.0 - 1.5 mm diameter, and hence have a terminal velocity of the order of 5 metres/sec, and since in many cumulonimbus clouds the vertical current must frequently exceed this value (7), drops of this size must frequently be carried upwards in the vertical current until either they have grown to a size which will permit them to fall down through the current or the current itself decreases to 5 metres/sec or less. The top of the echo may therefore be associated with a decrease of the vertical current speed to about 5 metres/sec and we see why the echo top temperatures decrease with increasing vertical speed within the cloud.

In some cases the vertical current speed over a considerable interval of height may exceed the terminal velocity of the largest raindrop which can exist without disruption (9.6 metres/sec) and in this case there would be no raindrops in this interval unless they were formed while travelling upwards in the vertical current or already formed below these heights. For there to be a continuous radar echo growth to raindrop size must take place in the ascending current unless large hailstones falling down provide the echo. Typical thunderstorm echoes (photographs (v) - (xiv)) give no indication of any hollow core which would be necessary on any other explanation and the presence of large hailstones, while sometimes occurring, is not an invariable feature of the thunderstorm.

To the two differing types of Bright Band weather echoes we must therefore add, with strong vertical currents, possibly greater than 5 metres/sec, a third entirely different echo, namely the cumulonimbus echo due to waterdrops alone.

We now have some evidence of two different methods of formation of rain:-

(i) With small vertical current speeds less than about 1 metre/sec such as occur in layer and frontal clouds, the formation of rain from the melting of large ice crystals or snowflakes formed from an aggregate of crystals at or about the freezing level and leading to the Bright Band phenomena.

(ii) The formation of rain without the assistance of ice crystals in strong vertical currents by growth and coalescence as supercooled waterdrops.

Examples have been observed when a Bright Band has been seen close to a shower type of echo (see photographs (x) - (xv)) and this can be explained if we regard the Bright Band as evidence of a reduction in the vertical current as may occur for instance in a degenerate cumulonimbus cloud.

D. Radar echoes and the icing of aircraft

A corollary of the ideas suggested in Section 4C above is that the presence of a weather echo above the freezing level is an indication of either

(i) the presence of snowflakes formed by the sticking together of wet snow crystals;

/(ii)

or (ii) the presence of very large ice crystals;

or (iii) the presence of supercooled water drops of raindrop size.

Conditions (i) and (iii) are very favourable conditions for rapid ice accretion on an aircraft while although condition (ii), if the ice crystals are dry, is not a likely cause of ice accretion this condition may occur in combination with either of the other two.

The introduction of an aircraft therefore into a weather echo above the freezing level would almost certainly lead to the formation of ice on the aircraft. It is hoped to investigate this aspect further in cooperation with aircraft but it may be mentioned that Spitfire aircraft investigating cumulonimbus type echoes frequently report icing of varying severity when flying in the echoes well above the freezing level.

It is clear from Section 4C that supercooled water drops can be present without giving a weather echo, if they are smaller than a certain limiting size, so that absence of a weather echo would not indicate absence of icing risk. It seems highly probable, however, that flight through a weather echo above the freezing level would give a grave risk of severe icing and it may well be that the worst icing conditions are associated with weather echoes.

In this connection attention is drawn to a table due to Bigg (10) which is summarised in Table VIII below, in which it is seen that there is a marked drop in occurrences of ice formation from the range 22°F to 18°F to the range 17°F to 13°F from a frequency of 43 out of 217 cases in the first range to 13 in the second range followed by an increase to 15 in the range from 12°F to 08°F. It should be noted, however, as pointed out by Simpson, (12) that the numbers in the Table have no very strict meaning since the number of flights within each group of temperatures was not the same. The general appearance of the Table would have suggested a further fall in frequency for the range 12°F to 08°F but in fact a small rise in frequency occurs. The significant fall in cases of ice accretion occurs at a temperature of 18°F, which corresponds exactly with the fall in frequency of echo top temperatures, while the small rise in frequency for the range 12°F to 08°F (where a fall in frequency would have been expected) corresponds to a rise in frequency of echo top temperatures below 10°F and may also be significant.

Table VIII

Frequency of Ice Formation in Cloud with respect to Temperature.(10)

Temperature	Above 32 F	32°F - 28°F	27°F - 23°F	22°F - 18°F	17°F - 13°F	12°F - 08°F	07°F - 03°F	02°F - -2°F	Below -02°F	Total
Occurrence of ice formation	0	56	78	43	13	15	3	4	5	217

It would appear probable therefore that the risk of severe ice formation in conditions where the vertical currents are small i.e. in many cases of layer cloud, is low when the temperature is below 18°F but that in cumulonimbus clouds, where the vertical currents are strong, icing may be severe even when the temperature is as low as -30°F, while in thunderstorms the risk may still be great at temperatures well below -40°F and indeed on some occasions right down to the tropopause temperature.

E. Radar echoes and turbulence.

Investigations are now proceeding in an endeavour to find any correlation between radar echoes and turbulence and will no doubt be the subject of a report in due course.

/Without

Without in any way prejudging the results of these investigations it may be noted that, on the evidence of this paper, if the echo top temperature is a guide to the vertical currents within the echo, rapid fluctuations of the echo top, either in space or time, would be expected to be reflected in the turbulence within the cloud, if turbulence is related, as seems reasonable, to variations of the vertical current in the horizontal plane. Turbulence would therefore be expected to be most marked near isolated columns of echo or at the sharp edge of a considerable column of echo e.g. at the sharp edge of a cumulonimbus echo (see photograph (iv)), while within an echo with a more or less level top little turbulence may be encountered. Isolated columns and sharp vertical edges are, in general, characteristics of the cumulonimbus echo and it is well known that the cumulonimbus cloud is regarded as the most turbulent. Some cumulonimbus echoes, however, have quite a level top but with very well marked vertical edges and it would be expected, if the foregoing is true, that turbulence would be much more marked at the edge of such an echo than in the centre of it.

It cannot be too strongly emphasised however that the radar echo is due to precipitation and that any correlation with turbulence is incidental to this; i.e. although the existence of an echo may give some indication of turbulence to be expected the corollary that areas of marked turbulence will necessarily give a radar echo is by no means justified unless it can be shown that precipitation and turbulence are closely related.

5. Photographs of the height-range tube illustrating some of the points mentioned in Section 4

Photograph (i) Illustrating Sections A and B of Table IV.

This is a typical layer cloud type of echo associated with an occlusion. Note the level top extending over a considerable range. The freezing level was at 4,200 feet and at 5,500 feet the temperature was 26°F.

In accordance with the theory of Section 4, this echo is typical of those associated with small vertical currents in which the echo is received from snowflakes and melting snowflakes and has a top below the 17°F isotherm.

Photograph (ii) Illustrating Section D of Table IV.

This is again a layer type of echo associated with precipitation from medium cloud in an Easterly current, a depression being situated in the English Channel. Note again the level top extending over a considerable range at 15,000 feet. The temperature at this height, however, is 03°F. There is a tendency for a Bright Band associated with the freezing level at 4,000 feet.

The echo above the 18°F isotherm in this case is interpreted as coming from large individual ice crystals which have grown to the necessary size during their slow fall through a considerable depth of cloud, against a stronger vertical current than exists in photograph (i) above. Below the 18°F isotherm the ice crystals aggregate and melt to give the Bright Band effect.

Photograph (iii) Illustrating another feature of Section D of Table IV.

This layer type of echo was associated with a quickly moving warm front. Note the Bright Band associated with the freezing level at 4,000 feet. At shorter ranges, however, there is an upper band of responses with a top at 06°F, while between this band and the Bright Band there is a considerable diminution in echo.

The upper band of responses visible on the shorter ranges is thought to be due to the growth of the ice crystals in this layer to a size sufficient to give an echo on their own account. The echo received is probably weak and disappears as the range increases. The lack of echo between the upper response and the Bright Band is a puzzling feature but may be due to the ice crystals falling from this saturated (or possibly supersaturated relative to ice) layer into layer which is unsaturated and there is therefore a certain amount of evaporation leading to a decrease in size of the ice crystals and a diminution of the echo. The echo increases again near the freezing level as the ice

crystals aggregate and melt. The upper band of responses may therefore indicate the lower limit of the altostratus sheet associated with the warm front, the air beneath this sheet not yet having become saturated by the evaporation into it of the precipitation falling from above.

Photograph (iv) Illustrating Section E of Table IV.

These weather echoes are associated with a cold front. Note the solid block of echo with a level top at 15,000 feet and column type echoes closer in which merge with the solid block. The top of the highest column is at -04°F while the top of the solid block is at 21°F indicating isolated stronger vertical currents within the frontal layer type of clouds.

Photograph (v) Illustrating Sections F and G of Table IV.

This is a typical cumulonimbus echo with a top at -21°F. Note the clear cut vertical edges indicating a "solid" type of vertical current. The persistence of form of an echo of this type suggests that, although the vertical current is strong, it is not subject to violent changes in value i.e. although a strong vertical current is indicated the turbulence well within the echo may not be at all severe while the turbulence at the edges (see Section 4E) of the echo may be much worse.

Photograph (vi)

This is also a cumulonimbus echo but note the diffuse echo at the side of the main column. This echo was investigated by a Spitfire aircraft (the aircraft can be seen at 15,000 feet at 28 miles range) and the diffuse echo is undoubtedly associated with the anvil of the cumulonimbus. Note how the anvil echo leads to a Bright Band in the neighbourhood of the freezing level which was at 5,000 feet indicating the ice structure of the anvil.

Photograph (vii) Illustrating Sections H, I and J of Table IV.

This is a typical thunderstorm echo. Note the similarity to ordinary cumulonimbus echoes (photograph (v)) although on a much larger scale.

Photograph (viii)

This is also a thunderstorm echo, note the tendency for the echo column (and hence probably the vertical currents) to diverge near the top. The nearer column of echo was very probably a strongly developing new cumulonimbus at the edge of the main thunderstorm mass. Development of this character has often been noticed by the pilots investigating cumulonimbus clouds.

Photograph (ix)

This is an unusually narrow thunderstorm echo which was received from a very isolated storm. Development of this storm took place in conditions of exceptionally high surface temperatures (over 90°F) with little other cloud development for many miles around.

Photographs (x) - (xv)

This is a series of six photographs taken during the thunderstorms of 27th June 1947 and referred to by Douglas and Lewis (11).

Note the tendency for a Bright Band to appear in the neighbourhood of the freezing level as the main storm moves away indicating, it is thought, degeneracy and a decrease in strength of the vertical currents.

Photograph (xvi)

These are echoes associated with an occlusion. Note the marked inclination to the vertical of the echo above the Bright Band at 7,000 feet. The mean wind below 7000 feet was 190 degrees 20 knots and the mean wind in the layer from 7,000 to 14,000 feet about 220 degrees, 25 knots. The echo at 7,000 feet at 12 miles appears to link to the echo at 14,000 feet at 18 miles and if this

/difference

difference of 6 miles in 7,000 feet is due to the difference in wind between 7,000 and 14,000 feet (which has a mean value of about 5 kts) then the inference is that the precipitation giving the echo takes approximately 1 hour to fall from 14,000 to 7,000 feet giving an approximate speed of fall of 2 ft/sec. The actual value of the up-current in the layer from 7,000 to 14,000 feet is not known so that it can only be stated that the terminal velocity of the particles comprising the precipitation was at least 2 ft/sec although (Bannon (5)) it is unlikely appreciably to exceed this value. This value is within the values of terminal velocities usually ascribed to individual ice crystals of 1/3 to 1 metre/sec (2).

6. Summary

Evidence has been produced to support the belief that temperatures at the tops of weather echoes are an indication of the relative strengths of the vertical currents within the echoes.

Two types of weather echo are indicated according to whether the vertical currents are strong or weak giving support to a theory of two different methods of producing waterdrops of raindrop size in the atmosphere.

Photographic examples of the two different echo types are given together with some photographs showing the two types existing simultaneously.

Related phenomena such as the absolute magnitude of the vertical currents, icing of aircraft and turbulence are briefly mentioned but will be probably dealt with in greater detail in subsequent papers.

7. List of References

1. Ryde, J.W.: The attenuation and radar echoes produced at centimetre wave-lengths by various meteorological phenomena. Meteorological Factors in Radio Wave Propagation - Report of a Conference held on 8th April 1946 at The Royal Institution, London by Phys. Soc. and R. Met. Soc., Phys. Soc. Report, London, p.169.

2. Nakaya U. and Terada T.; Simultaneous observations on the mass, falling velocity and form of individual snow crystals Series II. Journal of Faculty of Science, Hokkaido Imperial Univ., Vol I, No. 7.

3. Meteorological Office; The Meteorological Glossary. London, 1939.

4. Brunt, D.; Physical and Dynamical Meteorology. Cambridge, 1939.

5. Bannon J.K.; The estimation of large scale vertical currents from the rate of rainfall. M.R.P. No. 353, Air Ministry, Meteorological Research Committee, London, 1947.

6. Hooper, J.E.N. and Kippax A.A.; Interim report on measurements of radar echo intensities from rain and snow. T.R.E. Report No. T 2082, 1947.

7. Goldie, A.H.R.; Report on existing information relating to gustiness. M.R.P. No. 155, Air Ministry, Met. Research Committee. London.

8. Best A.C. (Summary by); Experimental investigations into the formation of ice particles in the atmosphere - Findeisen and Schulz. M.R.P. No. 361, Air Ministry, Met. Research Committee, London, 1947.

9. Simpson, G.C.; On the formation of cloud and rain. Quart. J.R. Met. Soc., London, 67, 1941, p.99.

10. Bigg, W.H.; Ice formation in clouds in Great Britain. Prof. Notes Met. Off., London. No. 81, 1937.

11. Douglas C.K.M. and Lewis L.F.; Thunderstorm of June 27, 1947. Met. Mag., London, 76, 1947, p.179.

12. Simpson G.C.; Ice accretion on aircraft. Prof. Notes Met. Off., London, No. 82, 1942.

/Table I

tuations

TABLE I

Number of Occurrences of Echo Top Temperatures within certain Intervals of Temperature at Various Ranges.

ange

Temperature Interval (°F)	Range (miles) 11 - 20	21 - 30	31 - 40	41 - 50	51 - 60	61 - 75
Over 40	3	0	0	0	0	0
40 - 32	11	13	8	6	1	1
31 - 18	33	37	17	16	9	3
17 - 10	16	10	8	4	4	3
09 - 01	26	16	9	6	2	1
00 - -09	21	19	19	11	5	0
-10 - -19	11	9	4	2	1	0
-20 - -29	3	5	5	2	1	0
-30 - -39	5	7	4	1	0	0
-40 - -49	7	3	4	3	3	0
Below -49	3	6	3	4	2	1
TOTAL	139	125	81	55	28	9

1-20
1-50
1-20
1-20
1-20
1-20
1-20
1-20
1-20, 31-40
1-20
1-20
1-20
1-30
1-20
-30
-20
-30
-20
-20
-20
-20
-30
-20
-30
-20
-20
-20, 31-40
-30

G.217950/I.S./1/49

18/7/47	-41	30,000	51-60	8/4/48	-39	20,500	41-50
28/7/47	-24	29,500	31-40	17/4/48	-08	18,000	11-20
30/7/47	27	15,000	61-75	19/4/48	-64	34,000	41-60
19/8/47	-18	25,000	51-60	20/4/48	-57	31,000	11-20
21/8/47	34	11,000	61-75	21/4/48	-07	21,000	31-40
22/8/47	-02	21,500	11-20	22/4/48	39	5,000	11-20
8/9/47	06	17,500	41-50	28/4/48	09	15,000	11-20
12/9/47	35	11,500	21-40	29/4/48	10	12,000	21-30
16/9/47	-04	22,000	21-30	30/4/48	-23	17,000	21-30
18/9/47	18	15,000	11-20	3/5/48	-05	14,500	31-40
19/9/47	03	20,000	21-30	4/5/48	-13	20,000	11-20
23/9/47	-21	20,000	21-30	"	24	9,000	11-30
29/9/47	44	7,000	11-20	10/5/48	17	14,000	11-20
8/10/47	29	9,500	11-20	11/5/48	-07	19,500	31-40
10/10/47	39	6,000	11-30	"	-25	23,500	31-40
14/10/47	15	15,000	11-20	12/5/48	15	13,000	11-20
22/10/47	-03	18,500	11-20	24/5/48	-03	13,000	11-20
"	01	17,000	11-20	25/5/48	11	11,500	11-30
"	24	9,000	11-30	26/5/48	-36	22,000	21-30
24/10/47	25	9,000	31-50	28/5/48	13	11,000	11-20
3/11/47	-28	20,000	41-50	29/5/48	-15	20,000	11-20
12/11/47	29	9,000	11-20	31/5/48	-19	21,000	21-30

TABLE II

Minimum Echo Top Temperature and corresponding height for Various Weather Situations irrespective of range.

Date	Temp (°F)	Maximum echo height (feet)	Range
13/3/47	09	15,000	11-20, 31-40
21/3/47	-07.5	20,000	31-40, 41-50
24/3/47	38	2,000	11-20
"	20	5,000	11-20
27/3/47	34	5,000	21-30
28/3/47	29	7,000	21-30
22/4/47	-05	17,500	11-20
"	-47	27,000	21-30, 31-40
23/4/47	30.5	5,000	11-20, 31-40
"	06	15,000	11-20
24/4/47	04	15,000	11-20
29/4/47	Below -32	Above 25,000	11-20
30/4/47	30	5,000	11-20
2/5/47	28	4,500	11-20
6/5/47	-09	18,000	31-40
8/5/47	-07	20,000	11-20, 21-30
12/5/47	24	10,000	11-20
13/5/47	-42	30,000	11-20
16/5/47	-11	17,500	41-50
4/6/47	-53	33,000	21-30
5/6/47	26	10,000	11-20, 21-50
6/6/47	-25	20,000	11-20
17/6/47	21	15,000	21-30
18/6/47	20	15,000	21-30
20/6/47	-05	20,000	31-40
23/6/47	08	21,000	11-20
27/6/47	-61	44,000	41-75
30/6/47	-03	19,000	21-30
1/7/47	29	10,000	11-20
2/7/47	-04	21,000	21-30
4/7/47	09	18,500	11-20
7/7/47	22	12,000	21-30
8/7/47	-16	19,000	21-30
9/7/47	-35	25,000	21-30
10/7/47	01	17,500	11-20
14/7/47	-67	38,500	31-40
16/7/47	-30	29,000	21-30
18/7/47	-41	30,000	51-60
28/7/47	-24	29,500	31-40
30/7/47	27	15,000	61-75
19/8/47	-18	25,000	51-60
21/8/47	34	11,000	61-75
22/8/47	-02	21,500	11-20
8/9/47	06	17,500	41-50
12/9/47	35	11,500	21-40
16/9/47	-04	22,000	21-30
18/9/47	18	15,000	11-20
19/9/47	03	20,000	21-30
23/9/47	-21	20,000	21-30
29/9/47	44	7,000	11-20
8/10/47	29	9,500	11-20
10/10/47	39	6,000	11-30
14/10/47	15	15,000	11-20
22/10/47	-03	18,500	11-20
"	01	17,000	11-20
"	24	9,000	11-30
24/10/47	25	9,000	31-50
3/11/47	-28	20,000	41-50
12/11/47	29	9,000	11-20
14/11/47	35	3,000	11-20
20/11/47	27	12,000	41-50
22/11/47	16	17,000	11-20
27/11/47	23	5,000	11-20
28/11/47	17	7,000	11-20
5/12/47	30	5,000	11-20
6/12/47	03	12,500	11-20
18/12/47	30	4,500	11-20
30/12/47	05	8,000	11-20
1/1/48	34	8,000	11-20, 31-40
6/1/48	09	11,500	11-20
7/1/48	06	12,500	11-20
9/1/48	18	10,000	11-20
12/1/48	-05	17,000	11-30
20/1/48	00	10,000	11-20
23/1/48	04	12,000	11-30
24/1/48	-45	22,000	11-20
28/1/48	-08	13,000	21-30
"	-23	18,000	11-20
29/1/48	-28	20,000	11-20
"	-04	13,000	11-20
30/1/48	24	10,000	11-20
3/2/48	06	12,500	11-20
5/2/48	29	5,500	21-30
"	21	10,500	11-20
6/2/48	-42	22,000	41-50
13/2/48	32	7,000	21-30
19/2/48	06	7,000	21-30
20/2/48	-04	7,500	11-20
15/3/48	16	12,000	11-20
16/3/48	23	8,000	11-20
17/3/48	-03	16,000	11-30
31/3/48	00	19,000	11-20
1/4/48	-43	22,000	11-30
2/4/48	08	12,000	11-20
3/4/48	-35	20,000	11-20
5/4/48	-34	18,000	11-20, 31-40
6/4/48	04	12,000	21-30
8/4/48	-39	20,500	41-50
17/4/48	-08	18,000	11-20
19/4/48	-64	34,000	41-60
20/4/48	-57	31,000	11-20
21/4/48	-07	21,000	31-40
22/4/48	39	5,000	11-20
28/4/48	09	15,000	11-20
29/4/48	10	12,000	21-30
30/4/48	-23	17,000	21-30
3/5/48	-05	14,500	31-40
4/5/48	-13	20,000	11-20
"	24	9,000	11-30
10/5/48	17	14,000	11-20
11/5/48	-07	19,500	31-40
"	-25	23,500	31-40
12/5/48	15	13,000	11-20
24/5/48	-03	13,000	11-20
25/5/48	11	11,500	11-30
26/5/48	-36	22,000	21-30
28/5/48	13	11,000	11-20
29/5/48	-15	20,000	11-20
31/5/48	-19	21,000	21-30

Date	Temp (°F)	Maximum echo height (feet)	Range
1/6/48	-40	26,000	11-40
2/6/48	-50	30,000	21-30
3/6/48	-29	21,000	21-30
8/6/48	-02	21,000	11-40
9/6/48	15	19,000	21-30
"	-07	25,000	41-50
10/6/48	-49	33,000	11-20
14/6/48	-65	40,000	21-30
17/6/48	-50	30,000	11-20
"	09	15,000	21-30
18/6/48	04	15,500	11-20
21/6/48	25	10,000	11-20
22/6/48	-08	19,000	11-30
25/6/48	34	10,000	41-60
28/6/48	-47	26,000	11-20
29/6/48	18	10,000	11-20
30/6/48	31	6,500	11-20
12/7/48	00	20,000	31-40
13/7/48	-11	20,000	11-20
14/7/48	29	9,000	11-20
16/7/48	18	11,000	11-30
22/7/48	00	18,000	41-50
24/7/48	26	11,500	11-20
28/7/48	-70	41,500	31-40
29/7/48	-61 (approx)	38,000	85-120
30/7/48	-68	41,000	31-50
3/8/48	34	10,000	11-20
5/8/48	30	10,000	11-30
"	03	19,000	41-50
6/8/48	-22	25,000	31-40
7/8/48	18	14,000	11-20
9/8/48	30	10,000	61-75
10/8/48	29	7,000	11-20
11/8/48	-37	28,000	21-30
"	20	14,000	11-20
13/8/48	-01	19,000	21-30
17/8/48	-07	20,000	11-20
19/8/48	06	17,000	51-60
20/8/48	06	15,000	11-20
23/8/48	08	15,500	21-50
25/8/48	-17	25,000	11-20
3/9/48	-46	30,000	11-20, 41-50
10/9/48	-04	22,000	21-30
1/10/48	09	20,000	11-20
4/10/48	07	12,000	21-30

TABLE III

Number of occurrences of minimum echo top temperatures within certain intervals of temperature. (See Table II).

Temperature Interval (°F)	Number of occasions.
Over 32	11
32 - 18	39
17 - 10	10
09 - 01	27
00 - -09	30
-10 - -19	8
-20 - -29	10
-30 - -39	8
-40 - -49	10
Below -49	11
TOTAL	164

G.217950/I.S./1/49

1.	28/3/47	29	7,000	21-30	Warm air, layer cloud.
2.	23/4/47	30.5	5,000	11-20 31-40	Convection dying out ahead of warm front.
3.	30/4/47	30	5,000	11-20	Layer cloud from NE.
4.	2/5/47	28	4,500	11-20	Layer cloud from ENE.
5.	12/5/47	24	10,000	11-20	Layer cloud from ENE.
6.	5/6/47	26	10,000	11-50	Upper warm front.
7.	17/6/47	21	15,000	21-30	Slow moving or quasi-stationary front.
8.	1/7/47	29	10,000	11-20	Weak occlusion dying out.
9.	7/7/47	22	12,000	21-30	Cold front. If the range had been 11-20 miles it is probable that this would have fallen in a lower temp. range.

TABLE IV

Type of weather associated with echo top temperatures.

A. Echo top temperatures over 32°F. No. of occasions 11.

No.	Date	Temp. (°F)	Height of echo top (feet)	Range (miles)	Type of air and Remarks.
1.	24/3/47	38	2,000	11-20	Rear view of weak cold front. Considerable layer cloud behind front.
2.	27/3/47	34	5,000	21-30	Warm air, possibly weak quasi-stationary front.
3.	21/8/47	34	11,000	61-75	Thundery conditions extreme South. If viewed at shorter range temp. of top would certainly have been much lower.
4.	12/9/47	35	11,500	21-30 31-40	Quasi-stationary front.
5.	29/9/47	44	7,000	11-20	Weak cold front possibly with waves.
6.	10/10/47	39	6,000	11-30	Weak quasi-stationary front.
7.	14/11/47	35	3,000	11-20	Slight rain associated with wave on cold front to south.
8.	1/1/48	34	8,000	11-20 31-40	Quickly moving weak warm front.
9.	22/4/48	39	5,000	11-20	Weak occlusion.
10.	25/6/48	34	10,000	41-60	Weak slow moving warm front.
11.	3/8/48	34	10,000	11-20	Layer cloud from NE.

B. Echo top temperatures 18 - 32°F. No. of occasions 39.

No.	Date	Temp. (°F)	Height of echo top (feet)	Range (miles)	Type of air and Remarks
1.	28/3/47	29	7,000	21-30	Warm air, layer cloud.
2.	23/4/47	30.5	5,000	11-20 31-40	Convection dying out ahead of warm front.
3.	30/4/47	30	5,000	11-20	Layer cloud from NE.
4.	2/5/47	28	4,500	11-20	Layer cloud from ENE.
5.	12/5/47	24	10,000	11-20	Layer cloud from ENE.
6.	5/6/47	26	10,000	11-50	Upper warm front.
7.	17/6/47	21	15,000	21-30	Slow moving or quasi-stationary front.
8.	1/7/47	29	10,000	11-20	Weak occlusion dying out.
9.	7/7/47	22	12,000	21-30	Cold front. If the range had been 11-20 miles it is probable that this would have fallen in a lower temp. range.

No.	Date	Temp. (°F)	Height of echo top (feet)	Range (miles)	Type of air and Remarks
10.	30/7/47	27	15,000	61-75	Thundery conditions but if the range had been 11-20 mls the temp. would certainly have been much lower.
11.	24/3/47	20	5,000	11-20	10/10 Sc and St with sleet.
12.	18/6/47	20	15,000	21-30	Slow moving cold front.
13.	18/9/47	18	15,000	11-20	Warm front.
14.	8/10/47	29	9,500	11-20	Warm sector layer cloud.
15.	22/10/47	24	9,000	11-20 21-30	Cold air immediately after passage of cold front. i.e. limited depth of cold air.
16.	24/10/47	25	9,000	31-50	Weak warm front moving West.
17.	12/11/47	29	9,000	11-20	Weak cold front with very narrow belt of pptn.
18.	20/11/47	27	12,000	41-50	Warm sector.
19.	27/11/47	23	5,000	11-20	Layer cloud from NE.
20.	5/12/47	30	5,000	11-20	Occlusion.
21.	18/12/47	30	4,500	11-20	Layer cloud from NE.
22.	9/1/48	18	10,000	11-20	Occlusion.
23.	30/1/48	24	10,000	11-20	Line of cumulonimbus. Isothermal layer at 18°F
24.	5/2/48	29	5,500	21-30	Convection dying out ahead of warm front.
25.	5/2/48	21	10,500	11-20	Warm front
26.	13/2/48	32	7,000	21-30	Weak warm front.
27.	16/3/48	23	8,000	11-20	Weak secondary cold front.
28.	4/5/48	24	9,000	11-30	Slow moving occlusion.
29.	21/6/48	25	10,000	11-20	Weak occlusion.
30.	29/6/48	18	10,000	11-20	Convection layering out into 10/10 cloud from NE.
31.	30/6/48	31	6,500	11-20	Layer cloud from NE.
32.	14/7/48	29	9,000	11-20	Limited convection. Isothermal layer at 29°F leading to formation of layer cloud.
33.	16/7/48	18	11,000	11-30	Limited convection leading to layer cloud. Isothermal layer at 18°F.
34.	24/7/48	26	11,500	11-20	Local rain from layer cloud well ahead of surface occlusion. Upper warm front?

No.	Date	Temp. (°F)	Height of echo top (feet)	Range (miles)	Type of air and Remarks
35.	5/8/48	30	10,000	11-30	Weak warm front.
36.	7/8/48	18	14,000	11-20	Layer cloud behind occlusion.
37.	9/8/48	30	10,000	61-75	Cold front. Temp. of top would certainly have been lower at shorter range. Thunder at Manston.
38.	10/8/48	29	7,000	11-20	Layer cloud with strong inversion above.
39.	11/8/48	20	14,000	11-20	Layer cloud behind occlusion.

C. Echo top temperatures 10 - 17°F No. of occasions 10

No.	Date	Temp. (°F)	Height of echo top (feet)	Range (miles)	Type of air and Remarks.
1.	14/10/47	15	15,000	11-20	Weak secondary cold front.
2.	22/11/47	16	17,000	11-20	Warm sector.
3.	28/11/47	17	7,000	11-20	Layer cloud from NE.
4.	15/3/48	16	12,000	11-20	Warm sector. Isothermal layer developed later at this height with temp. 22°F.
5.	29/4/48	10	12,000	21-30	Convection limited by inversion at this height.
6.	10/5/48	17	14,000	11-20	Convection cloud. Isothermal layer developed later at this height.
7.	12/5/48	15	13,000	11-20	Slow moving weak cold front. Inversion developed at this height from 15 to 19°F.
8.	25/5/48	11	11,500	11-30	Limited convection. Inversion 11 - 14°F at this height.
9.	28/5/48	13	11,000	11-20	Limited convection. Isothermal layer at this height.
10.	9/6/48	15	19,000	21-30	Limited convection. Isothermal layer at this height.

D. Echo top temperatures 01 - 09°F. No. of occasions 27

No.	Date	Temp. (°F)	Height of echo top (feet)	Range (miles)	Type of air and Remarks
1.	13/3/47	09	15,000	11-20 31-40	Instability in warm air.
2.	23/4/47	06	15,000	11-20	Rapidly moving warm front.
3.	24/4/47	04	15,000	11-20	Cumulonimbus anvil.

No.	Date	Temp. (°F)	Height of echo top (feet)	Range (miles)	Type of air and Remarks
4.	23/6/47	08	21,000	11-20	Weak warm front with unstable medium cloud.
5.	4/7/47	09	18,500	11-20	Weak occlusion.
6.	10/7/47	01	17,500	11-20	Warm front or occlusion.
7.	8/9/47	06	17,500	41-50	Cold front. Temp. of top probably lower at shorter range. Thunder at Felixstowe.
8.	19/9/47	03	20,000	21-30	Warm front.
9.	22/10/47	01	17,000	11-20	Cloud system in rear of cold front.
10.	6/12/47	03	12,500	11-20	Polar trough.
11.	30/12/47	05	8,000	11-20	Polar trough.
12.	6/1/48	09	11,500	11-20	Occlusion.
13.	7/1/48	06	12,500	11-20	Occlusion.
14.	23/1/48	04	12,000	11-30	Medium cloud associated with occlusion to South.
15.	3/2/48	06	12,500	11-20	Convection immediately following wave on cold front. Limited depth cold air.
16.	19/2/48	06	7,000	21-30	Intermittent snow from 10/10 cloud in cold E'ly.
17.	2/4/48	08	12,000	11-20	Occlusion moving quickly.
18.	6/4/48	04	12,000	21-30	Occlusion.
19.	28/4/48	09	15,000	11-20	Cold fronts. on P.P.I. appeared as 3 parallel lines of echo.
20.	17/6/48	09	15,000	21-30	Convection after passage of occlusion. Limited cold air.
21.	18/6/48	04	15,500	11-20	Convection cloud. a.m. observation. Thunder in p.m.
22.	5/8/48	03	19,000	41-50	Occlusion.
23.	19/8/48	06	17,000	51-60	Convection cloud. Thunder reported from this area. If viewed at shorter range temp. probably much lower.
24.	20/8/48	06	15,000	11-20	Occlusion, isothermal layer at this height.
25.	23/8/48	08	15,500	21-50	Convection cloud layering out under inversion at this height.
26.	1/10/48	09	20,000	11-20	Warm front.
27.	4/10/48	07	12,000	21-30	Possibly occlusion. Thunder was associated with this echo although cloud top known not to have appreciably exceeded this height.

E. Echo top temperatures -09 - 00°F. No. of occasions 30.

No.	Date	Temp. (°F)	Height of echo top (feet)	Range (miles)	Type of air and Remarks
1.	21/3/47	-07.5	20,000	31-50	Cold front.
2.	22/4/47	-05	17,500	11-20	Cold front.
3.	6/5/47	-09	18,000	31-40	Medium cloud instability.
4.	8/5/47	-07	20,000	11-30	Trough or cold front.
5.	20/6/47	-05	20,000	31-40	Weak warm front with medium cloud instability. (Base of echo, 15,000 ft)
6.	30/6/47	-03	19,000	21-30	Slow moving occlusion.
7.	2/7/47	-04	21,000	21-30	Warm front.
8.	22/8/47	-02	21,500	11-20	Blown off top of cumulonimbus cloud.
9.	16/9/47	-04	22,000	21-30	Cold front.
10.	22/10/47	-03	18,500	11-20	Cloud system ahead of cold front and deepening depression.
11.	12/1/48	-05	17,000	11-30	Occlusion.
12.	20/1/48	00	10,000	11-20	Weak trough.
13.	28/1/48	-08	13,000	21-30	Decaying cumulonimbus ahead of occlusion.
14.	29/1/48	-04	13,000	11-20	Back bent occlusion.
15.	20/2/48	-04	7,500	11-20	Snow showers in cold E'ly.
16.	17/3/48	-03	16,000	11-30	Unstable medium cloud ahead of warm front.
17.	31/3/48	00	19,000	11-20	Rapidly moving warm front or occlusion.
18.	17/4/48	-08	18,000	11-20	Trough associated with depression B. of Biscay.
19.	21/4/48	-07	21,000	31-40	Thundery low B. of Biscay. Probably relics of thunder activity. At shorter ranges temp. may have been lower. Thunder at Defford, not elsewhere.
20.	3/5/48	-05	14,500	31-40	Convection dying out ahead of warm front.
21.	11/5/48	-07	19,500	31-40	Probably remains of thundery activity. If viewed at shorter range temp. may have been lower. Thunder at Lympne, not elsewhere.
22.	24/5/48	-03	13,000	11-20	Convection in weak NW current.
23.	8/6/48	-02	21,000	11-40	Thick cloud well ahead of surface cold front - may be remains of thundery activity.

No.	Date	Temp. (°F)	Height of echo top (feet)	Range (miles)	Type of air and Remarks
4.	23/6/47	08	21,000	11-20	Weak warm front with unstable medium cloud.
5.	4/7/47	09	18,500	11-20	Weak occlusion.
6.	10/7/47	01	17,500	11-20	Warm front or occlusion.
7.	8/9/47	06	17,500	41-50	Cold front. Temp. of top probably lower at shorter range. Thunder at Felixstowe.
8.	19/9/47	03	20,000	21-30	Warm front.
9.	22/10/47	01	17,000	11-20	Cloud system in rear of cold front.
10.	6/12/47	03	12,500	11-20	Polar trough.
11.	30/12/47	05	8,000	11-20	Polar trough.
12.	6/1/48	09	11,500	11-20	Occlusion.
13.	7/1/48	06	12,500	11-20	Occlusion.
14.	23/1/48	04	12,000	11-30	Medium cloud associated with occlusion to South.
15.	3/2/48	06	12,500	11-20	Convection immediately following wave on cold front. Limited depth cold air.
16.	19/2/48	06	7,000	21-30	Intermittent snow from 10/10 cloud in cold E'ly.
17.	2/4/48	08	12,000	11-20	Occlusion moving quickly.
18.	6/4/48	04	12,000	21-30	Occlusion.
19.	28/4/48	09	15,000	11-20	Cold fronts. on P.P.I. appeared as 3 parallel lines of echo.
20.	17/6/48	09	15,000	21-30	Convection after passage of occlusion. Limited cold air.
21.	18/6/48	04	15,500	11-20	Convection cloud. a.m. observation. Thunder in p.m.
22.	5/8/48	03	19,000	41-50	Occlusion.
23.	19/8/48	06	17,000	51-60	Convection cloud. Thunder reported from this area. If viewed at shorter range temp. probably much lower.
24.	20/8/48	06	15,000	11-20	Occlusion, isothermal layer at this height.
25.	23/8/48	08	15,500	21-50	Convection cloud layering out under inversion at this height.
26.	1/10/48	09	20,000	11-20	Warm front.
27.	4/10/48	07	12,000	21-30	Possibly occlusion. Thunder was associated with this echo although cloud top known not to have appreciably exceeded this height.

E. Echo top temperatures -09 - 00°F. No. of occasions 30.

No.	Date	Temp. (°F)	Height of echo top (feet)	Range (miles)	Type of air and Remarks
1.	21/3/47	-07.5	20,000	31-50	Cold front.
2.	22/4/47	-05	17,500	11-20	Cold front.
3.	6/5/47	-09	18,000	31-40	Medium cloud instability.
4.	8/5/47	-07	20,000	11-30	Trough or cold front.
5.	20/6/47	-05	20,000	31-40	Weak warm front with medium cloud instability. (Base of echo, 15,000 ft)
6.	30/6/47	-03	19,000	21-30	Slow moving occlusion.
7.	2/7/47	-04	21,000	21-30	Warm front.
8.	22/8/47	-02	21,500	11-20	Blown off top of cumulonimbus cloud.
9.	16/9/47	-04	22,000	21-30	Cold front.
10.	22/10/47	-03	18,500	11-20	Cloud system ahead of cold front and deepening depression.
11.	12/1/48	-05	17,000	11-30	Occlusion.
12.	20/1/48	00	10,000	11-20	Weak trough.
13.	28/1/48	-08	13,000	21-30	Decaying cumulonimbus ahead of occlusion.
14.	29/1/48	-04	13,000	11-20	Back bent occlusion.
15.	20/2/48	-04	7,500	11-20	Snow showers in cold E'ly.
16.	17/3/48	-03	16,000	11-30	Unstable medium cloud ahead of warm front.
17.	31/3/48	00	19,000	11-20	Rapidly moving warm front or occlusion.
18.	17/4/48	-08	18,000	11-20	Trough associated with depression B. of Biscay.
19.	21/4/48	-07	21,000	31-40	Thundery low B. of Biscay. Probably relics of thunder activity. At shorter ranges temp. may have been lower. Thunder at Defford, not elsewhere.
20.	3/5/48	-05	14,500	31-40	Convection dying out ahead of warm front.
21.	11/5/48	-07	19,500	31-40	Probably remains of thundery activity. If viewed at shorter range temp. may have been lower. Thunder at Lympne, not elsewhere.
22.	24/5/48	-03	13,000	11-20	Convection in weak NW current.
23.	8/6/48	-02	21,000	11-40	Thick cloud well ahead of surface cold front - may be remains of thundery activity.

No.	Date	Temp. (°F)	Height of echo top (feet)	Range (miles)	Type of air and Remarks
24.	9/6/48	-07	25,000	41-50	Frontal cloud associated with wave in Channel.
25.	22/6/48	-08	19,000	11-30	Convection limited by isothermal layer but observations incomplete. Thunder reported.
26.	12/7/48	00	20,000	31-40	Occlusion.
27.	22/7/48	00	18,000	41-50	Showers in W'ly current. If viewed at shorter range temp. may have been lower. Thunder reported further North.
28.	13/8/48	-01	19,000	21-30	Polar trough
29.	17/8/48	-07	20,000	11-20	Polar trough possibly with cold front. Thunder at Gorleston but nowhere else.
30.	10/9/48	-04	22,000	21-30	Occlusion.

F. Echo top temperatures -19 - -10°F No. of occasions 8.

No.	Date	Temp (°F)	Height of echo top (feet)	Range (miles)	Type of air and Remarks
1.	16/5/47	-11	17,500	41-50	Thundery showers. At closer range temp. would probably have been lower. Thunder reported S of this area.
2.	8/7/47	-16	19,000	21-30	Convection cloud. This was a.m.; thunder in p.m.
3.	19/8/47	-18	25,000	51-60	Probably thundery although no actual reports. At closer range temp. probably lower.
4.	4/5/48	-13	20,000	11-20	Warm front.
5.	29/5/48	-15	20,000	11-20	Medium cloud in E'ly current associated with depression English Channel.
6.	31/5/48	-19	21,000	21-30	Cold front or cold occlusion. Thunder reported but obs. concentrated on one bearing and may have missed highest tops.
7.	13/7/48	-11	20,000	11-20	Cold air. Thunder reported but observations mainly concentrated on Spitfire flight. No report of thunder by pilot.
8.	25/8/48	-17	25,000	11-20	Cold front.

/G.

G. Echo top temperatures -29 - -20°F No. of occasions 10

No.	Date	Temp. (°F)	Height of echo top (feet)	Range (miles)	Type of air and Remarks
1.	6/6/47	-25	20,000	11-20	Polar trough or secondary cold front.
2.	28/7/47	-24	29,500	31-40	Thundery trough. Thunder reported. At shorter range temp. probably lower.
3.	23/9/47	-21	20,000	21-30	Cold air.
4.	3/11/47	-28	20,000	41-50	Cold air. Thunder reported. At shorter range temp. would probably have been lower.
5.	28/1/48	-23	18,000	11-20	Occlusion
6.	29/1/48	-28	20,000	11-20	Occlusion
7.	30/4/48	-23	17,000	21-30	Cold air.
8.	11/5/48	-25	23,500	31-40	Cold air. Thunder reported. At shorter range temp. would probably have been lower.
9.	3/6/48	-29	21,000	21-30	Cold air. Thunder reported but observations concentrated on Spitfire flight. No report of thunder by pilot.
10.	6/8/48	-22	25,000	31-40	Occlusion. Thunder reported. At shorter range temp. would probably have been lower.

H. Echo top temperatures -39 - -30°F. No. of occasions 8.

No.	Date	Temp. (°F)	Height of echo top (feet)	Range (miles)	Type of air and Remarks.
1.	29/4/47	Below -32	25,000 above	11-20	Unstable medium cloud well ahead of surface warm front.
2.	9/7/47	-35	25,000	21-40	Cold air. Thunder reported. At shorter range temp. may have been lower.
3.	16/7/47	-30	29,000	21-30	Occlusion. Thunder reported. At shorter range temp. may have been lower.
4.	3/4/48	-35	20,000	11-20	Cold air, No thunder reported.
5.	5/4/48	-34	18,000	11-20 31-40	Cold air. No thunder reported.
6.	8/4/48	-39	20,500	41-50	Cold air. Thunder reported. This was tropopause temp.
7.	26/5/48	-36	22,000	21-30	Widespread thundery activity. Thunder reported. At shorter range temp. may have been lower.
8.	11/8/48	-37	28,000	21-30	Occlusion close to centre of deepening depression. Thunder reported. At shorter range temp. may have been lower.

I. Echo top temperatures -49 - -40°F No. of occasions 10

No.	Date	Temp. (°F)	Height of echo top (feet)	Range (miles)	Type of air and Remarks
1.	22/4/47	-47	27,000	21-40	Cold air. No reports of thunder but heavy squally showers locally.
2.	13/5/47	-42	30,000	11-20	Thundery medium cloud. Heavy thundery shower noted locally. Thunder in early morning far to SW.
3.	18/7/47	-41	30,000	51-60	Warm front moving West. Thunder reported.
4.	24/1/48	-45	22,000	11-20	Depression English Channel. Thunder reported.
5.	6/2/48	-42	22,000	41-50	Cold air. Thunder reported.
6.	1/4/48	-43	22,000	11-30	Cold air. Thunder reported. This was tropopause temp.
7.	1/6/48	-40	26,000	11-40	Polar trough. Thunder reported. This was tropopause temp.
8.	10/6/48	-49	33,000	11-20	Thunderstorms moving North from France.
9.	28/6/48	-47	26,000	11-20	Polar trough. Thunder reported.
10.	3/9/48	-46	30,000	11-20 41-50	Close to centre of depression. Thunder reported. This was tropopause temp.

J. Echo top temperatures below -49°F No. of occasions 11.

No.	Date	Temp. (°F)	Height of echo top (feet)	Range (miles)	Type of air and Remarks
1.	4/6/47	-53	33,000	21-30	Thundery medium cloud. Thunder reported.
2.	27/6/47	-61	44,000	41-75	Thunderstorms from France
3.	14/7/47	-67	38,500	31-40	Stagnant air thunderstorms
4.	19/4/48	-64	34,000	41-60	Stagnant air thunderstorms
5.	20/4/48	-57	31,000	11-20	Thunderstorms in trough from South.
6.	2/6/48	-50	30,000	21-30	Point of occlusion at centre of depression. Thunder reported.
7.	14/6/48	-65	40,000	21-30	Thunderstorms from France
8.	17/6/48	-50	30,000	11-20	Centre of depression. Thunder reported.
9.	28/7/48	-70	41,500	31-40	Isolated cumulonimbus with very high surface temps. Thunder reported.
10.	29/7/48	-61	38,000	85-120	Cold front thunderstorms. "Cloudburst" at Cardiff was one of echoes picked up.
11.	30/7/48	-68	41,000	31-50	Cold front thunderstorms.

Note The majority of the above temps. were tropopause temps.

/TABLE V

TABLE V

The occasions in the various temperature ranges when thunderstorms were probably viewed.

Temperature Interval (°F)	Frequency	Remarks
Over 32	1 out of 11	This was observed at 61-75 miles and only report of thunder was "thunder heard" at Portland Bill.
32 - 18	1 out of 39	This was at 61-75 miles range, thunder being reported at Manston.
17 - 10	Nil out of 10	
09 - 01	4 out of 27	1 at 51-60 miles, 1 at 41-50, 1 may have missed highest tops as obs. only made in morning, and 1 case when top was known not to have been at a lower temp.
00 - -09	4 out of 30	On 3 occasions thunder only reported at one distant station (more than 50 miles away) and on remaining occasion obs. were incomplete.
-10 - -19	3 out of 8	1 at 41-50 miles, on the other two occasions obs. were concentrated on one area due to other work and may have missed highest tops.
-20 - -29	5 out of 10	1 at 41-50 miles, 3 at 31-40, lat 21-30 but on this occasion obs. concentrated on one area due to other work and almost certainly missed actual storms.
-30 - -39	5 out of 8	1 at 41-50 miles and remainder at 21 - 30 miles.
-40 - -49	8 out of 10	The remaining two occasions gave heavy squally showers locally and may have been thunderstorms at the time of observation.
Below -49	11 out of 11	

/TABLE VI

TABLE VI

Signal intensities on thunderstorm occasions compared with occasions when thunderstorms probably not present.

A. Thunderstorm Occasions

Date	Minimum echo temperature (°F)	Height of echo top (feet)	Range (miles)	S/N ratio	Relative power at 20 miles	Remarks
1/6/48	-40	26,000	21	50:1	2755	
10/6/48	-49	33,000	15	40:1	899	
14/6/48	-65	40,000	23	130:1	22350	
28/7/48	-70	41,500	43	17:1	1332	
30/7/48	-68	41,000	45	14:1	987	
3/9/48	-46	30.000	19	60:1	3247	
4/10/48	07	12,000	21	17:1	317	Very isolated thunder. Reading may not have been taken at the exact position of the storm.

B. Thunderstorms probably not present.

Date	Minimum echo temperature (°F)	Height of echo top (feet)	Range (miles)	S/N ratio	Relative power at 20 miles	Remarks
30/4/48	-23	17,000	26½	6:1	60	Convection cloud.
29/1/48	-28	20,000	22½	9:1	101	Occlusion
25/8/48	-17	25,000	12	90:1	2916	Cold front, line squall conditions.
29/5/48	-15	20,000	28	16:1	500	Medium cloud.
4/5/48	-13	20,000	20	45:1	2024	Warm front
13/8/48	-01	19,000	29	3:1	17	Polar trough
22/7/48	00	18,000	48	14:1	1122	See Section 4B, para 1.
8/6/48	-02	21,000	12	7:1	16	Thick upper cloud
3/5/48	-05	14,500	38	6:1	126	Convection dying out.
17/4/48	-08	18,000	34½	12½:1	461	Trough.
29/1/48	-04	13,000	22	9:1	97	Back bent occlusion
9/6/48	15	19,000	15½	5:1	14	Limited convection
28/5/48	13	11,000	15	7½:1	30	Limited convection
7/8/48	18	14,000	19	10:1	90	Layer cloud
16/7/48	18	11,000	12	30:1	323	Limited convection.
4/5/48	24	9,000	21	11:1	132	Slow moving occlusion.

PHOTOGRAPH (i)
29.1.48
1044 G.M.T.
EARING 246°T

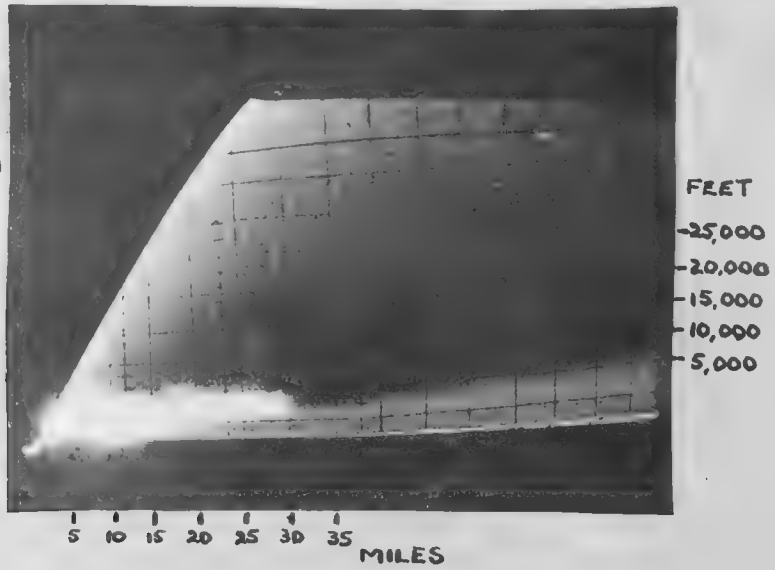

PHOTOGRAPH (ii)
29.5.48.
1003 G.M.T.
BEARING 181°T

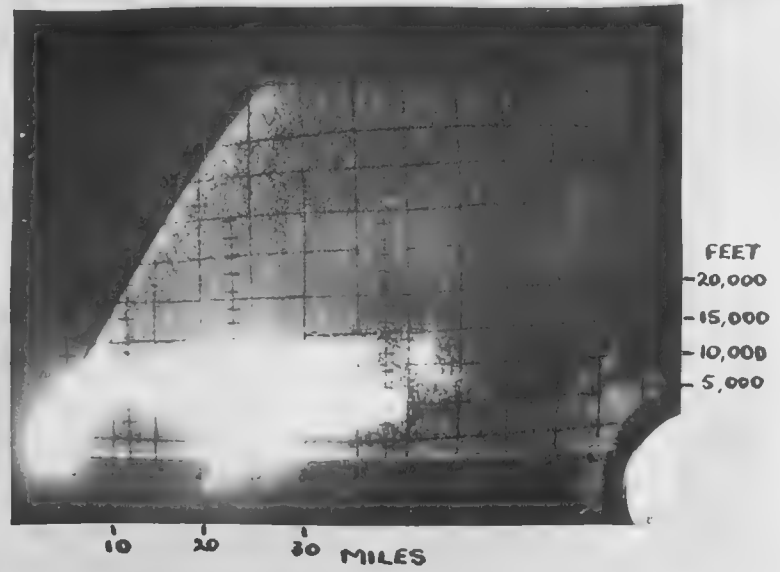

OTOGRAPH (iii)
23.4.47.
0945 G.M.T.
EARING 230°T

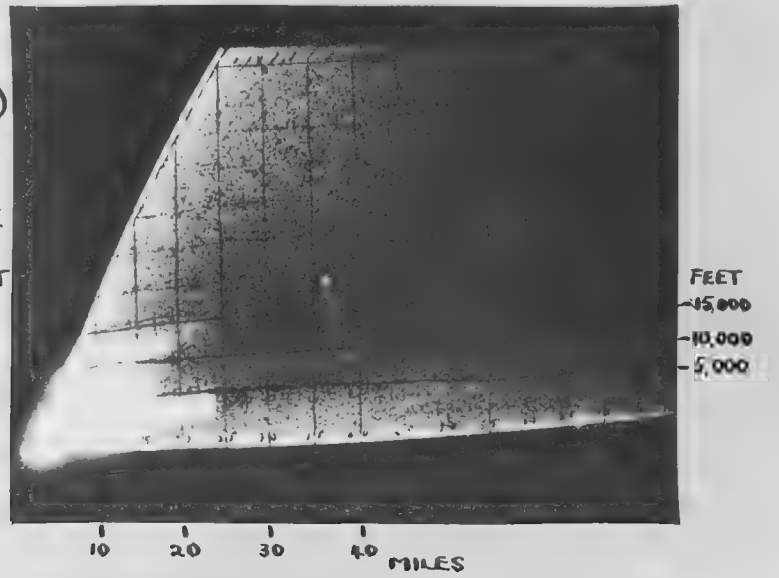

PHOTOGRAPH (iv)
16.9.47.
1044 G.M.T.
BEARING 250°T

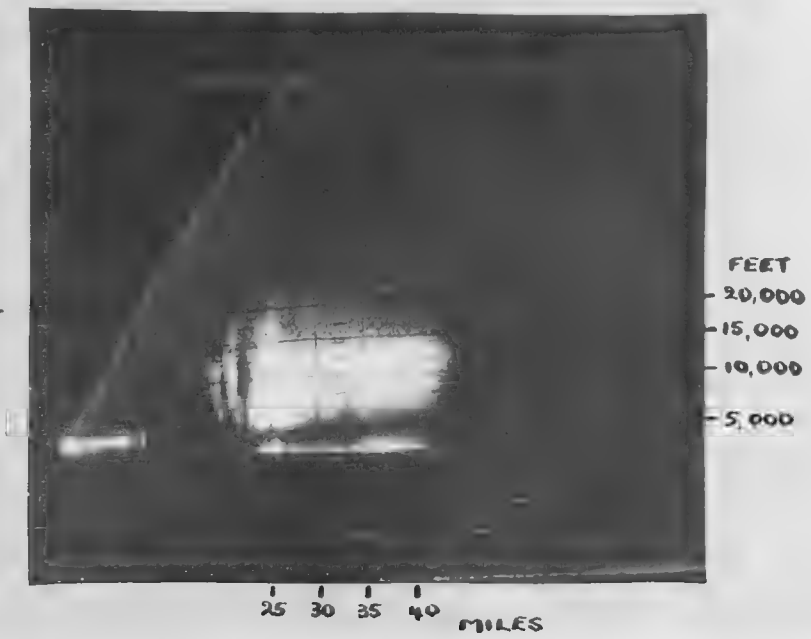

PHOTOGRAPH (v)

23.9.47.

1552 G.M.T.

BEARING 073°T

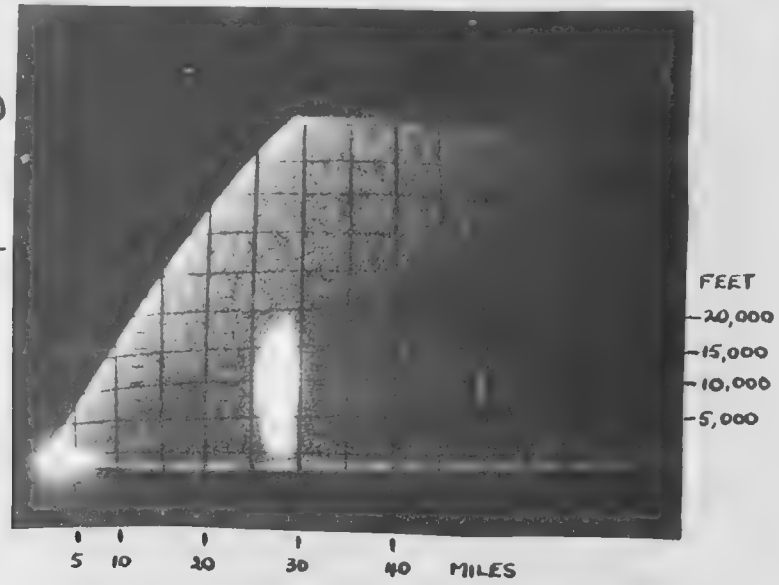

PHOTOGRAPH (vi)

1.6.48

1435 G.M.T.

BEARING 190°T

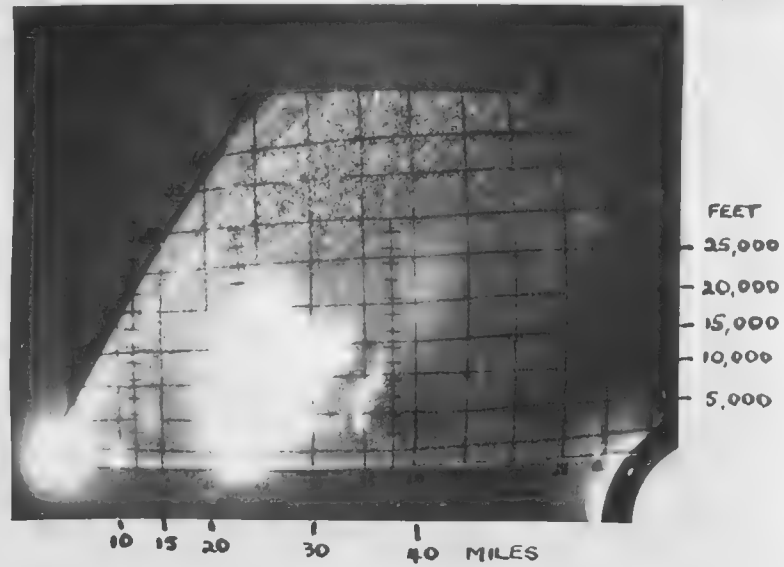

PHOTOGRAPH (vii)

14.7.47

1422 G.M.T.

BEARING 289°T

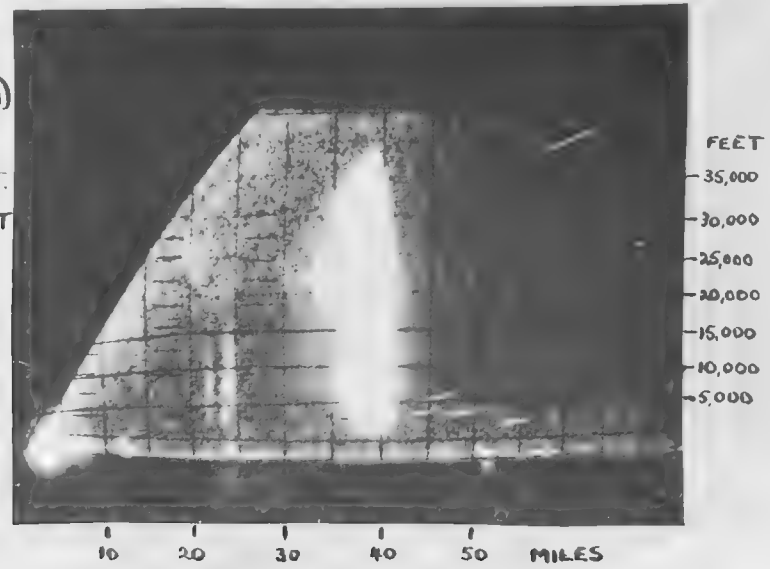

PHOTOGRAPH (viii)

30.7.48

1544 G.M.T.

BEARING 194° T

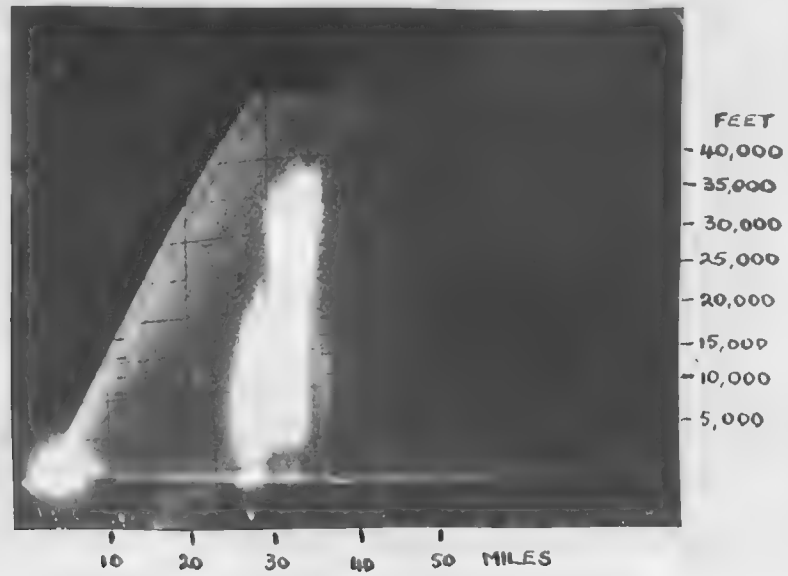

PHOTOGRAPH (ix)
28.7.48.
1605 G.M.T.
BEARING 340°T

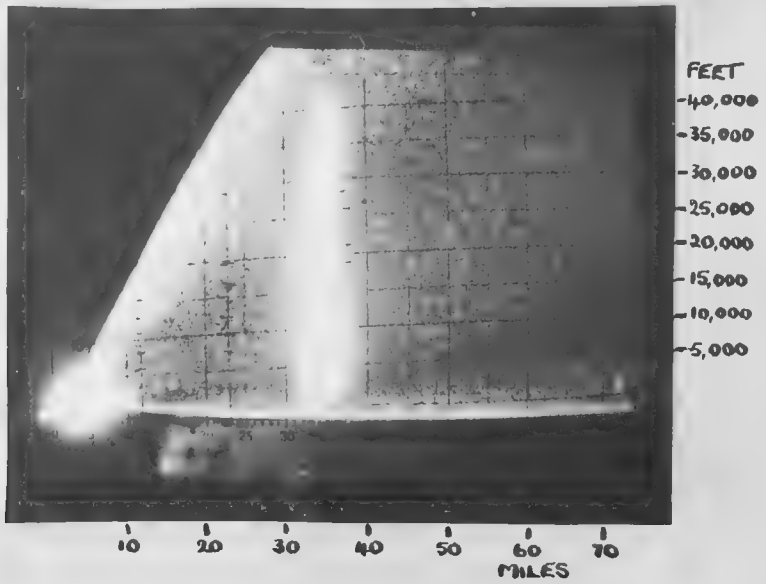

PHOTOGRAPH (x)
27.6.47.
1234 G.M.T.
074°T

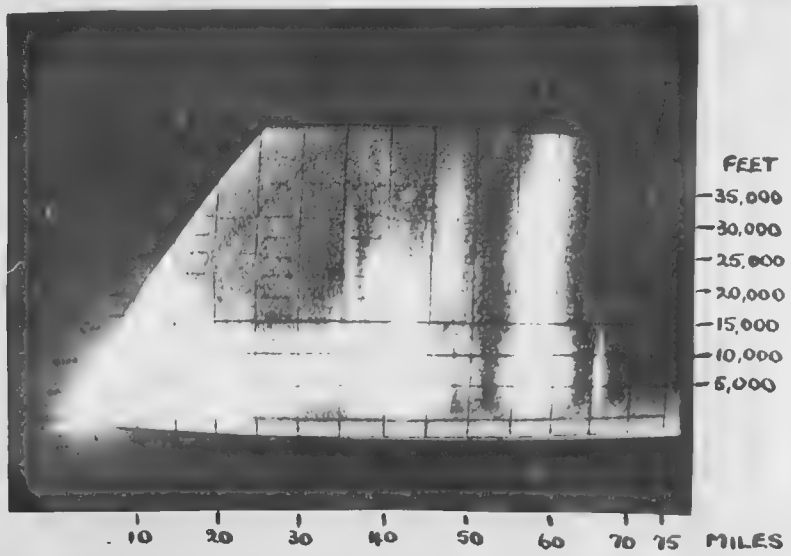

PHOTOGRAPH (xi)
27.6.47.
1244 G.M.T.
BEARING 064°T

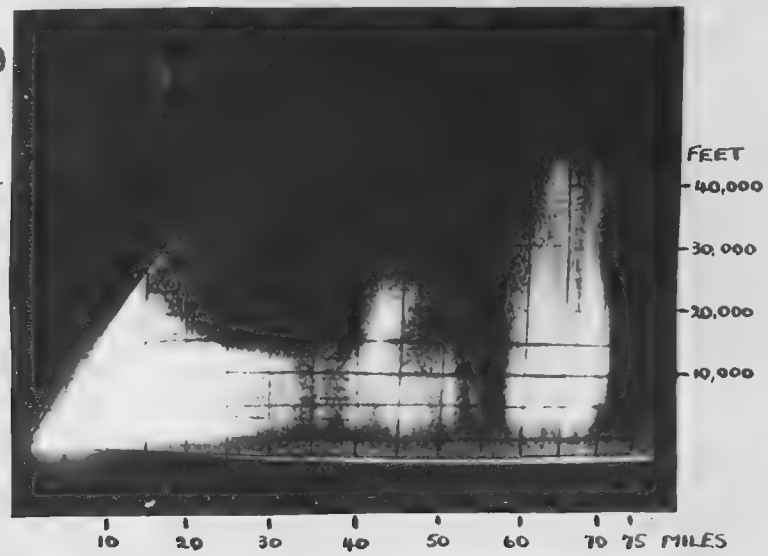

PHOTOGRAPH (xii)
27.6.47.
1252 G.M.T.
BEARING 030°T

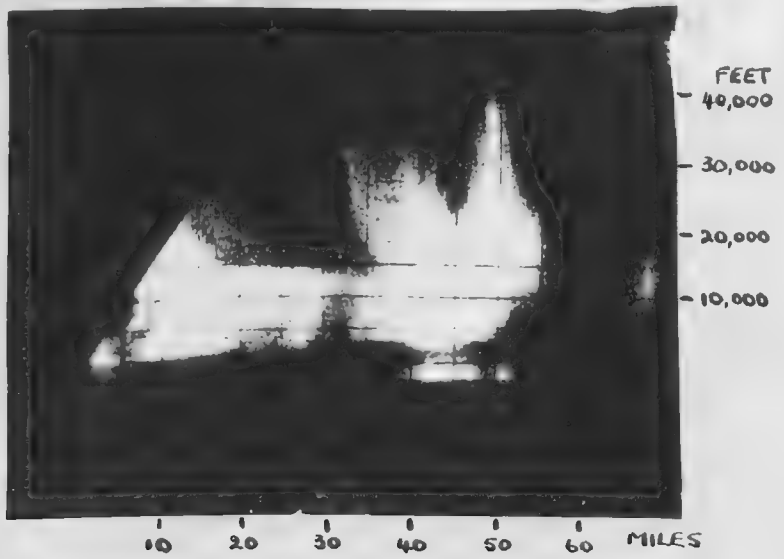

PHOTOGRAPH (xiii)
27.6.47.
1255 G.M.T.
BEARING 050°T

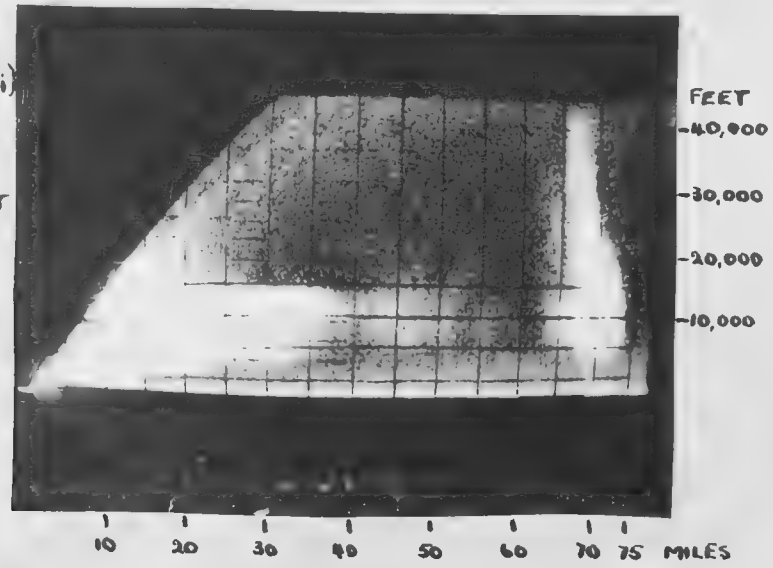

PHOTOGRAPH (xiv)
27.6.47.
1300 G.M.T.
BEARING 055°T

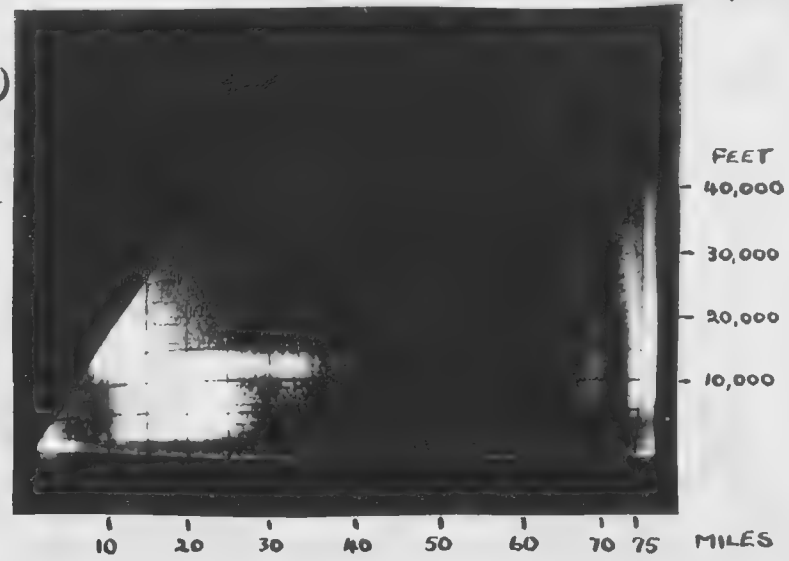

PHOTOGRAPH (xv)
27.6.47.
1304 G.M.T.
BEARING 028°T

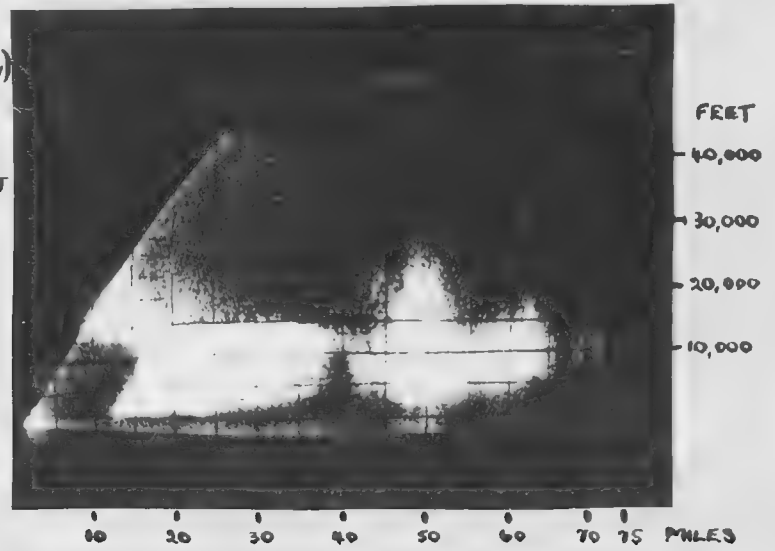

PHOTOGRAPH (xvi)
11.8.48
1004 G.M.T.
BEARING 068°T

... been ... treated ... Its ... be quoted.

M.R.P. 462
S.C.II/29

14th. January, 1949.

AD 223134

AIR MINISTRY.

METEOROLOGICAL RESEARCH COMMITTEE

Relation between the standard deviation of temperature at constant pressure and at constant height.

by
A. F. Crossley

AIR WEATHER SERVICE
TECHNICAL REFERENCE FILES

Introductory Note.

In order to give information to aviators on the frequency of upper air temperatures it is necessary to draw world maps (a) of the mean temperature (b) of the standard deviation of temperature. Since the aviator uses pressure heights the maps should also be pressure height maps. Most data at present published regarding standard deviation of temperature in the upper air is for fixed tape measure heights.

The first thing therefore is to establish the correct relationship between standard deviation at constant pressure height and that at constant tape-measure height. This has been done in the following note.

1. The formal relationship

We consider a set of pairs of observations of temperature, T_p, at a constant pressure p, and temperature, T_h, at a constant height h. On any particular occasion, suppose the pressure p occurs at a height $h + \delta h$, and the height h occurs at pressure $p + \delta p$. Then we can write

$$T_p = T_h + \lambda\,\delta h \qquad \ldots\ldots\ldots\ldots (1)$$

where λ is the average temperature gradient on that occasion between the levels of p and h. Also if

$$\lambda = \bar{\lambda} + \lambda'$$

where a bar is used to denote the mean of a set of observations, then

$$T_p - T_h = \bar{\lambda}\,\delta h + \lambda'\delta h$$

and

$$\bar{T}_p - \bar{T}_h = \bar{\lambda}\,\overline{\delta h} + \overline{\lambda'\delta h}$$

It is assumed for the present that $\overline{\delta h}$ is zero (see appendix). Now λ' the variation of the local temperature gradient from its mean value, is not necessarily small in comparison with $\bar{\lambda}$. It may however be taken that (except in the lowest layers influenced by surface inversions) the numerically larger values of λ' are greatly outnumbered by the smaller values, so that $\overline{\lambda'\delta h}$ can be regarded as a small term of the second order; and generally λ' will be regarded as of first order wherever it occurs under a bar. We accordingly write

$$\bar{T}_p = \bar{T}_h = \bar{T}$$

Further, on the individual occasion we write

$$T_p = \overline{T} + T'_p \quad , \quad T_h = \overline{T} + T'_h \qquad \ldots\ldots\ldots (3)$$

Now since the height h is associated with pressure $p + \delta p$, we can write

$$T_p - T_h = -\frac{\partial T_p}{\partial p}\delta p = -\left(\frac{\partial \overline{T}}{\partial p}\delta p + \frac{\partial T'_p}{\partial p}\delta p\right) \qquad \ldots\ldots (4)$$

Comparing with (2), we see that $-\frac{\partial \overline{T}}{\partial p}\delta p$ and $\overline{\lambda}\,\delta h$ are identical, so that the remaining terms on the right are also identical. Consequently it is legitimate to regard $\partial T'_p/\partial p$, like λ', as a first order term whenever it occurs under a bar.

We now write from (3) and (4)

$$T'_p = T'_h - \frac{\partial T_p}{\partial p}\delta p$$

whence

$$T'^2_p = T'^2_h - 2\,T'_h\frac{\partial T_p}{\partial p}\delta p + \left(\frac{\partial T_p}{\partial p}\right)^2(\delta p)^2$$

The standard deviations of temperature at constant pressure and at constant height are given respectively by

$$p\sigma^2_T = \overline{T'^2_p} \quad , \quad h\sigma^2_T = \overline{T'^2_h}$$

so that by taking means of both sides of the preceding equation we obtain

$$p\sigma^2_T = h\sigma^2_T - 2\,\overline{T'_h\frac{\partial T_p}{\partial p}\delta p} + \overline{\left(\frac{\partial T_p}{\partial p}\right)^2(\delta p)^2}$$

We can now replace $\partial T_p/\partial p$ by its mean value $\partial \overline{T}/\partial p$, since this involves only neglect of small terms of third and higher orders; consequently

$$p\sigma^2_T = h\sigma^2_T - 2\frac{\partial \overline{T}}{\partial p}\overline{T'_h\,\delta p} + \left(\frac{\partial \overline{T}}{\partial p}\right)^2\overline{(\delta p)^2}$$

Also,

$$\overline{T'_h\,\delta p} = {}_hr_{pT}\cdot {}_h\sigma_p\cdot {}_h\sigma_T,$$

where ${}_hr_{pT}$ is the correlation coefficient between pressure and temperature at height h, and this is known to be positive; while the standard deviation of pressure at height h is given by

$${}_h\sigma^2_p = \overline{(\delta p)^2}$$

Therefore

$$p\sigma^2_T = h\sigma^2_T - 2\frac{\partial \overline{T}}{\partial p}\cdot {}_hr_{pT}\cdot {}_h\sigma_p\cdot {}_h\sigma_T + \left(\frac{\partial \overline{T}}{\partial p}\right)^2\cdot {}_h\sigma^2_p \qquad \ldots\ldots (5)$$

which is the required relationship, expressing the standard deviation of temperature at constant pressure in terms of functions referring to a fixed height. With a transformation of the coefficient $\partial \overline{T}/\partial p$, it may also be written

/ $p\sigma^2_T$

$$ {}_p\sigma_T^2 = {}_h\sigma_T^2 + \frac{2\bar{\lambda}}{g\bar{\rho}} \cdot {}_h r_{pT} \cdot {}_h\sigma_p \cdot {}_h\sigma_T + \left(\frac{\bar{\lambda}}{g\bar{\rho}}\right)^2 \cdot {}_h\sigma_p^2 \quad \ldots\ldots (6) $$

2. Comparison of the two standard deviations

The value of $\partial\bar{T}/\partial p$ in the I.C.A.N. atmosphere is instanced by the following figures :-

Pressure (mb)	700	500	300
$\frac{\partial\bar{T}}{\partial p}$ (°C/mb)	.073	.097	.142

From the figures given below it is seen that since ${}_h\sigma_p$ is comparable with ${}_h\sigma_T$ and the coefficient $(\partial\bar{T}/\partial p)^2$ is relatively small; it follows that in the troposphere

$$ {}_p\sigma_T < {}_h\sigma_T $$

In the stratosphere, where $\partial\bar{T}/\partial p$ is zero, the two standard deviations are equal.

As an illustration, we use the following figures for Agra for December - February quoted by Miss Carruthers.*

p	${}_h\sigma_T$	${}_h\sigma_p$	${}_h r_{pT}$	$\frac{\partial\bar{T}}{\partial p}$	${}_p\sigma_T$
mb	°C	mb		°C/mb	°C
475	3.3	4.2	0.79	.0975	3.0
267	4.7	3.9	0.55	.1731	4.4

The values of ${}_p\sigma_T$ as given by the formula (5) are entered in the last column. They indicate that (in this case) the standard deviation of temperature at constant height exceeds that at constant pressure by less than half a degree centigrade.

Figures which were evaluated for Larkhill at 500 mb are as follows, in the same units as above.

	p	${}_h\sigma_T$	${}_h\sigma_p$	${}_h r_{pT}$	$\frac{\partial\bar{T}}{\partial p}$	${}_p\sigma_T$	
						calc.	obs.
July 1947	500	3.9	4.1	0.76	.098	3.6	3.4
Jan. 1947	500	6.1	9.1	0.87	.098	5.3	5.4

In this case the difference between the two standard deviations is just half a degree centigrade.

Since the standard deviations and correlation coefficients appear not to vary greatly with height within the troposphere (cf. Dines, Geop. Mem. No. 13), the largest difference between the two standard deviations

---

*From Beit. Phys. Atm. 23, pp. 238 - 247

of temperature may be expected to occur just below the tropopause, on account of the increase with height of the factor $\partial\overline{T}/\partial p$ or $-\overline{\lambda}/g\overline{\rho}$ (eqns. 5 and 6). A rough calculation based on the figures given above but on a value of $\partial\overline{T}/\partial p$ at 50,000 ft about double that at 300 mb (or three times that at 500 mb) indicates that the extreme difference between ${}_p\sigma_T$ and ${}_h\sigma_T$ amounts to approximately 1°C just below the equatorial tropopause.

Summing up, we see that the excess of the standard deviation of temperature at constant height over that at constant pressure is positive and increases with height up to the tropopause, but is zero in the stratosphere. In the troposphere the difference reaches about 0.5°C at about 35,000 ft, and about 1°C towards the tropopause in equatorial regions.

Appendix

The characteristic and statical equations are

$$p = R\rho T_p \qquad \text{and} \qquad \delta p = -g\rho\,\delta h$$

whence

$$\frac{\delta p}{p} = -\frac{g}{R}\frac{\delta h}{T_p}$$

$$= -\frac{g}{R}\frac{\delta h}{\overline{T}_p + T_p'}$$

or

$$\frac{\delta p}{p} = -\frac{g\,\delta h}{R\,\overline{T}_p}\left(1 - \frac{T_p'}{\overline{T}_p}\right)$$

to the first order in $T_p'/\overline{T}_p$. Taking means of both sides, we obtain

$$\overline{\frac{\delta p}{p}} = -\frac{g}{R\,\overline{T}_p}\left(\overline{\delta h} - \frac{\overline{\delta h\,T_p'}}{\overline{T}_p}\right)$$

Now $\overline{\delta h\,T_p'}$, which is proportional to the correlation coefficient between the height and temperature of a given pressure surface, is known to be different from zero. The above equation therefore shows that $\overline{\delta p}$ and $\overline{\delta h}$ cannot both be zero, in other words the levels to which p and h refer cannot be identical. The difference however is small. If we assume, for example, that $\overline{\delta p}$ is zero, then

$$\overline{\delta h} = \frac{\overline{\delta h\,T_p'}}{\overline{T}_p}$$

and this is seen to be small if only on account of the factor $\overline{T}_p$ in the denominator. This may be confirmed by the values for Larkhill (July, 1947), at 500 mb which give

$$\overline{\delta h\,T_p'} = 800 \text{ ft °A}, \qquad \overline{T}_p = 259°A,$$

whence $\overline{\delta h} = 3.5$ ft

Also $\overline{\lambda} = -0.2°A / 100$ ft

giving $\overline{\lambda}\,\overline{\delta h} = -0.007°A,$

so confirming the equality, for practical purposes, of $\overline{T}_p$ and $\overline{T}_h$, although theoretically they cannot be precisely equal.

Acknowledgement

Acknowledgement is made to Mr J.S. Sawyer, M.A. for a suggestion which led to a shortening of the algebra.

28th January, 1949.

AIR MINISTRY

METEOROLOGICAL RESEARCH COMMITTEE

Empirical Formulae for the Terminal Velocity of Water Drops falling through the Atmosphere

by

A.C. Best

AIR WEATHER SERVICE TECHNICAL REFERENCE FILES

1. Introduction. It is sometimes convenient to have an explicit formula for the terminal velocity of water drops falling through the atmosphere. It is even more convenient if the structure of the formula is sufficiently simple for it to be amenable to mathematical manipulation. Stokes law leads to such a formula, viz.

$$V = \frac{g(\sigma - \rho)\, d^2}{18\, \mu} \qquad \ldots\ldots\ldots\ldots\ldots\ldots\ldots\ldots (1)$$

where V is the terminal velocity of the drop in cm/sec

σ is the density of the drop (unity for water)
ρ is the air density
d is the drop diameter (cm)
μ is the coefficient of viscosity of air.

Unfortunately equation 1 is valid only for very small drops (diameter less than about 0.005 cms).

Schmidt (1) has proposed the following formula

$$V = r^2/(0.00787 + 0.159\, r^{3/2}) \qquad \ldots\ldots\ldots\ldots (2)$$

where V is the terminal velocity in metres/sec and r is the drop radius in mm. Schmidt did not explicitly state the limits of size over which equation 2 is to be used but he apparently regarded it as applicable only to average sized raindrops. Certainly it does not agree with the experimental measurements quoted by Sutton (2) outside the range of diameters 0.5 to 1.5 mm.

Sutton (2) quotes a formula for Re, Reynold's number, which he says is valid only when the drops fall as rigid spheres. Even with this limitation the formula is too complicated to be useful for other than purely arithmetical processes.

In meteorology the terminal velocity of a water drop is determined by the diameter of the drop (or of the sphere of equal volume if the drop is deformed), and by the density and viscosity of the atmosphere. The density and viscosity of the atmosphere vary independently but for many purposes it is adequate to know the terminal velocity of a drop of water falling through a standard atmosphere. In the following paragraphs we shall assume that the drop is falling through the I.C.A.N. standard atmosphere. The values in Table I conform to the specifications of this atmosphere.

Table I.

I.C.A.N. Standard Atmosphere

Height metres	Density gm/cc	Temp. °C	Coefft. Viscosity c.g.s.
0	12.251 10^{-4}	15.0	1.79 10^{-4}
1000	11.11 "	8.5	1.76 "
2058	10.00 "	1.62	1.72 "
3000	9.105 "	-4.5	1.69 "
4220	8.00 "	-12.46	1.65 "
5500	6.97 "	-20.75	1.61 "
6860	6.00 "	-29.58	1.56 "

/The

The values for the coefficient of viscosity were obtained from Sutherland's formula using $c = 117$ and assuming μ_o to be $1.715.10^{-4}$ (see Kaye and Laby - Tables of Physical Constants.) Having adopted this standard atmosphere the air density and viscosity are now to be regarded as a function of height and an explicit formula for the terminal velocity of a water drop should thus contain only two independent variables, viz., the drop diameter d and the height z.

The purpose of this note is to ~~prepare~~ propose three formulae covering three different ranges of drop size, for the terminal velocity of a water drop in the standard atmosphere as defined.

The formulae are

$$0.3 < d < 6.0 \qquad V = 932.2\, e^{0.0405z}\left(1 - e^{-(d/1.77)^{1.147}}\right) \quad \ldots\ldots(3)$$

$$0.05 < d < 0.3 \qquad V = 190.7\, e^{0.0290z}\left(1 - e^{-(d/0.316)^{1.754}}\right) \quad \ldots\ldots(4)$$

$$d < 0.05 \qquad V = 3041\, e^{0.0191z}\, d^2 \quad \ldots\ldots\ldots\ldots\ldots\ldots(5)$$

where d is the drop diameter in mm and z is the height in km. Of these three formulae equation 5 of course is a simple adaptation of equation 1.

It may be of interest that the form of equations 3 and 4 was suggested by the similarity in shape between a graph showing terminal velocity as a function of drop diameter and a graph showing the cumulative volume of liquid water in the air (in the form of raindrops) as a function of drop diameter when the writer was preparing M.R.P. 452.

2. The Experimental Data Available.

(a) Large drops. Experimental measurements of the terminal velocities of water drops falling in air have been published by Lenard (3), Schmidt (1), Flower (4), Laws (5) and Sutton (2). The first three of these investigations used methods which were undoubtedly inferior in accuracy to the methods described in (2) and (5) and will not be discussed here.

Law's method depended upon photographing the falling drop with a still camera. Interposed between camera and drop was a disc rotated by a synchronous motor: a sector was cut out of the disc and thus a number of short straight lines appeared on the negative due to the image of the falling drop being received intermittently on the negative. The velocity was computed from the separation of these lines and a knowledge of the speed of rotation of the disc. The method described by Sutton employed six sharp edged horizontal beams of light through which the drop fell in succession. The passage of the drop was recorded photograpically by an Einthoven fibre galvanometer operated by photo-electric cells which were actuated by the passage of the drop through the beams of light. A time base was provided by a second fibre of the galvanometer recording the vibrations of a valve maintained elinvar fork. These two methods appear to be of comparable accuracy and in fact give very similar results, Laws' values being approximately 2½% greater than Sutton's values for drop diameters exceeding about 1.5 mm. Moreover both Laws' and Sutton's values differ markedly from those of Lenard, Schmidt and Flower.

It seems safe to assume that the results of Laws and of Sutton are both very nearly correct and, other things being equal, it would be necessary to choose between them. However Sutton quotes terminal velocities over a range of air densities whereas Laws worked only at the surface value of air density. Accordingly Sutton's values of the terminal velocity will be used over the ranges of drop diameter and air density covered by his results.

/As

As mentioned above terminal velocity is affected both by air density and by viscosity. Sutton quotes his results in two tables. The first gives the terminal velocity of drops of various sizes falling through an atmosphere at 20°C and 750 mm Hg. The second gives terminal velocities at various air densities for each of several differently sized drops. In the second table the air densities were not the same for each drop size. Sutton does not explicitly state the value of μ but he does say that the air temperature throughout was between 17°C and 21°C. Accordingly it has been assumed that coefficient of viscosity was $1.81.10^{-4}$ c.g.s., corresponding to 19°C.

For each drop size the terminal velocity has been plotted against air density and from the resulting curve the terminal velocity read for specified air densities. Combining these results with Sutton's first table (for air at 20°C and 750 mm Hg we have $\rho = 11.888.10^{-4}$ gm/cc) we get Table 2.

Table 2.

Terminal velocity of water drops falling through air of density ρ and viscosity $1.81.\ 10^{-4}$ poise.

ρ (gm/cc)x10^4	6	6.97	8	9.105	10	11.11	11.888	12	12.251
d(cm)					V(cm/sec)				
0.069							278		
0.077							318		
0.079							314		
0.229							697		
0.338	1059	1014	971	929	895	852	827	824	816
0.407	1102	1055	1011	970	940	901	876	872	866
0.442	1135	1085	1040	994	960	921	899	892	885
0.493	1147	1102	1058	1012	978	934	902	900	890
0.542	1171	1125	1076	1026	986	944	918	914	907
0.595	1200	1142	1086	1032	991	948	919	915	906
0.624	1201		1081		988		909	908	900
0.637							914		
0.667							917		
0.725							916		

The gaps in this table at small values of d result from gaps in the data of M.R.P. 40. The gaps at large diameters have been left because, as will appear later, equation 3 is not applicable at these large diameters.

The figures in Table 2 will be used as the basic data in support of equation 3.

(b) Small drops. It is clear that below a certain size drops of water will fall as rigid spheres. Without yet considering what the critical size may be we shall now examine the data available relating to the terminal velocity of rigid spheres falling through air.

It is customary to define the drag coefficient C of a sphere moving through a fluid of density ρ by the equation

$$D = C\rho V^2 \pi d^2/8 \quad \ldots\ldots\ldots\ldots\ldots\ldots\ldots\ldots\ldots\ldots (6)$$

where D is the force in the direction of motion of the sphere which resists that motion. C is a function only of Reynolds' Number Re. A lot of experimental work has been done to determine the relation between C and Re and this work has been reviewed by Davies (6) who has shown that C and Re are related by the following empirical equations.

$\mathrm{Re} < 4.$ $\quad \mathrm{Re} = \frac{C\,\mathrm{Re}^2}{24} - 2.3363.\ 10^{-4}(C\,\mathrm{Re}^2)^2 + 2.0154.\ 10^{-6}(C\,\mathrm{Re}^2)^3$

$$- 6.9105.\ 10^{-9}(C\,\mathrm{Re}^2)^4 \quad \ldots\ldots\ldots\ldots\ldots\ldots (7)$$

$3 < \mathrm{Re} < 10{,}000.$ $\quad \log \mathrm{Re} = -1.29536 + 9.86.\ 10^{-1}(\log C\,\mathrm{Re}^2)$

$$- 4.6677\ 10^{-2}(\log C\,\mathrm{Re}^2)^2 + 1.1235\ 10^{-3}(\log C\,\mathrm{Re}^2)^3 \ \ldots (8)$$

These two equations are in good agreement over the common range of Re. As Davies has pointed out, the convenience of these equations arises from the fact that, if we equate the right hand side of equation 6 to the gravitational force acting on the sphere immersed in the fluid we find that $C\,Re^2$ is independent of V. In fact if we put g = 981 and assume the sphere has unit density we can show that

$$C\,Re^2 = 1308\,\rho d^3/\mu^2 \quad \ldots\ldots\ldots\ldots\ldots\ldots\ldots\ldots(9)$$

Thus equations 7 and 8 provide a simple - though laborious - way of computing the terminal velocity of a rigid sphere falling through a fluid of density ρ and viscosity μ. We shall use values computed from these equations as the basic data for the terminal velocity of drops up to a critical diameter not so far determined.

3. Variation of terminal velocity of water drops with diameter

(a) Large drops. Table 3 shows the terminal velocity of drops computed from the formula

$$V = 942.9(1 - e^{-(d/1.77)^{1.147}}) \quad \ldots\ldots\ldots\ldots\ldots\ldots\ldots(10)$$

where V is in cm/sec and d is measured in m.m. The last two columns show respectively the experimental values from M.R.P. 40 for $\rho = 11.888.10^{-4}$, $\mu = 1.81.10^{-4}$ and also the values computed from equation 8 for the same density and viscosity.

Table 3.

Terminal Velocity of water drops at $\rho = 11.888.10^{-4}$, $\mu = 1.81.10^{-4}$

d mm	Eqtn.10	Table 2 cm/sec.	Eqtn.8
0.3	115.4	-	114.1
0.5	197.2	-	201.6
0.69	271.4	278	-
0.77	301.3	318	-
0.79	308.6	314	-
1.00	382.0	-	391.2
1.75	591.5	-	613.1
2.29	696.9	697	-
3.38	827.5	827	-
4.07	872.8	876	-
4.42	888.7	899	-
4.93	905.9	902	-
5.42	917.4	918	-
5.95	925.9	919	-
6.24	929.4	909	-
6.37	930.7	914	-
6.67	933.2	917	-
7.25	936.8	916	-

These values have been plotted in Fig.1. It is clear from Fig.1 that equation 10 adequately represents Sutton's results for diameters 0.69 to 5.95 m.m and the position of the points computed from equation 8 relative to Sutton's experimental points strongly suggests that the drops fall as rigid spheres up to a diameter of about 1 m.m. In this connection we may recall that in M.R.P. 330 (7) it was shown that falling water drops depart visibly from a spherical shape when d exceeds a value of about 1.75 m.m. This is confirmed by the position of the 1.75 m.m. point computed from equation 8 in Fig.1.

(b) Small drops. Table 4 shows the terminal velocity of drops computed from equation 4 (with z = 0) and from equations 7 or 8 as appropriate, for $\rho = 12.251\ 10^{-4}$, $\mu = 1.79\ 10^{-4}$. In view of Fig.1 we may regard equations 7 and 8 as applicable to water drops having diameter less than 1 m m. The reason for the choice of values of ρ and μ different from those used in Table 3 will appear later.

/Table 4.

Table 4.

Terminal velocity of water drops at
$\rho = 12.251\ 10^{-4}$, $\mu = 1.79\ 10^{-4}$

d m.m	Eqtn. 4	Eqtns.7/8
	cm/sec.	
0.03	3.04	2.72
0.04	5.01	4.79
0.05	7.37	7.36
0.10	23.73	24.96
0.15	45.2	46.8
0.20	68.9	68.8
0.25	92.4	91.3
0.30	114.2	113.7

The values in Table 4 have been plotted in Fig.2. It is clear that equation 4 adequately represents the terminal velocities of water drops with a diameter range 0.05 to 0.3 m.m. falling through air with $\rho = 12.251\ 10^{-4}$ and $\mu = 1.79\ 10^{-4}$.

(c) Very small drops. If in equation 1, we put $\sigma = 1$, $\rho = 12.251.10^{-4}$, $\mu = 1.79.10^{-4}$, $g = 981$, we get

$$V = 3041\ d^2 \quad \ldots\ldots\ldots\ldots\ldots\ldots\ldots\ldots (11)$$

where V is in cm/sec and d in m.m. Table 5 shows the terminal velocity of drops computed from equations 7 and 11. It appears that the error involved in using Stokes' law to compute the terminal velocity of water drops is about 3.3% for a diameter of 0.05 m.m. and decreases rapidly as the diameter decreases, becoming less than 1% for a diameter of 0.03 m.m.

Table 5.

Terminal velocity of water drops at
$\rho = 12.251\ 10^{-4}$, $\mu = 1.79\ 10^{-4}$

d m.m.	Eqtn.11	Eqtn.7	Eqtn.11 / Eqtn.7
	cm/sec		
0.03	2.74	2.72	1.0063
0.04	4.87	4.79	1.0165
0.05	7.60	7.36	1.0330
0.10	30.41	24.96	1.2183

(d) Reduction of equation (10) to standard surface conditions. Equation 10 refers to values of ρ and μ which do not occur together in Table 1. Since all the values of terminal velocity in Table 2 refer to $\mu = 1.81\ 10^{-4}$ and it will be necessary below to consider corrections for this it is convenient to describe here the method of making these corrections.

Let $V(\rho,\mu)$ denote the terminal velocity in air of density ρ and with viscosity corresponding to that density from Table 1.

Let $V(\rho,\mu) / V(\rho, 1.81\ 10^{-4})$ be denoted by r. Then it has been assumed that the ratio r is the same for rigid spheres and for water drops of the same size. From equation 8, r was computed for rigid spheres for each air density in Table 1 and for the three diameters, 0.3, 2.5 and 5.0 m m. The ratio r was then plotted against diameter for each value of ρ. Using this family of curves of viscosity correction the terminal velocity of a water drop falling through the I.C.A.N. atmosphere can be computed if the velocity is known for the same air density and a viscosity $1.81\ 10^{-4}$. This "viscosity correction" was very small for the size of drop covered by Sutton's experimental results. The numerical values will be considered in paragraph 4 below.

/To

To reduce equation 10 to standard I.C.A.N. surface conditions the following procedure was adopted. From Table 2 the ratio V (11.888. 1.81)/ V(12.251. 1.81) was computed for each diameter from 3.38 m m to 5.95 m m. These ratios were then divided by the value of r, corresponding to the same diameter, obtained from the viscosity correction curve for $\rho = 12.251. 10^{-4}$. The results gave V(11.888, 1.81)/V(12.251, 1.79) for drops having diameter from 3.38 to 5.95 m m. In order to extend the correction to smaller sizes the value of V(11.888, 1.81)/V(12.251, 1.79) was computed directly from equation 8 for values 0.3 and 1.0 m m of d. The results of these computations are shown in Table 6.

Table 6.

Values of V(11.888, 1.81)/V(12.251, 1.79) for water drops.

d (m m)	0.3	1.0	3.38	4.07	4.42	4.93	5.42	5.95
Ratio	1.0033	1.0091	1.0128	1.0111	1.0155	1.0133	1.0120	1.0143

The mean value of the ratios in Table 6 is 1.0114 and it is clear that departures from this mean are very small. Accordingly this value has been adopted for the whole range of d from 0.3 to 5.95. Then dividing the coefficient of the right hand side of equation 10 by 1.0114 we obtain for the terminal velocity of drops with diameter between 0.3 and 5.95 m m at $\rho = 12.251. 10^{-4}$, $\mu = 1.79.10^{-4}$.

$$V = 932.2(1 - e^{-(d/1.77)^{1.147}}) \quad \ldots\ldots\ldots\ldots (12)$$

(e) Junction of formula for large and small drops. It is clear from Tables 4 and 5 that the variation of terminal velocity with diameter changes smoothly from equation 4 to Stokes Law (equation 11) at d = 0.05 m m and we must now consider the junction between equations 4 and 12 at d = 0.3 m m. For this purpose figure 3 has been constructed. The curve in this figure has been computed in two parts. That part corresponding to drops with diameter exceeding 0.3 m m is based upon equation 4 (with z = 0). The part corresponding to the smaller drops is based upon equation 12, it is clear that the curve is continuous at d = 0.3 m m both with regard to V and also with regard to $\partial V/\partial d$.

4. Variation of terminal velocity of water drops with height

(a) Large drops. The figures in Table 2 have been used to compute the ratio of the velocity at other densities to the velocity at $\rho = 12.251. 10^{-4}$, the viscosity being $1.81. 10^{-4}$ in both cases. The viscosity correction curves mentioned in paragraph 3(d) were then used to convert these ratios to the ratios

$$V/V_o = \frac{\text{velocity at I.C.A.N. density and viscosity at height z}}{\text{velocity at surface I.C.A.N. density and viscosity}}$$

for each height and diameter.

To supplement the range of diameters covered the ratios V/V_o were also computed directly for drops having diameter 0.3 and 1.0 m m from equation 8 (i.e. treating these two sized drops as rigid spheres). The results are given in Table 7.

/Table 7.

Table 7.

Ratio of terminal velocity at height z in I.C.A.N. atmosphere to velocity at surface - V/V_o.

Diam. (m m) / Height (km)	0.3	1.0	3.38	4.07	4.42	4.93	5.42	5.95	Mean
				Ratio V/V_o					
0	1.000	1.000	1.000	1.000	1.000	1.000	1.000	1.000	1.000
1.000	1.035	1.042	1.046	1.041	1.042	1.050	1.041	1.046	1.043
2.058	1.076	1.090	1.098	1.087	1.087	1.100	1.088	1.095	1.090
3.000	1.113	1.134	1.142	1.123	1.126	1.139	1.132	1.140	1.131
4.220	1.164	1.197	1.197	1.174	1.180	1.193	1.188	1.201	1.187
5.500	1.222	1.268	1.253	1.226	1.232	1.244	1.244	1.263	1.244
6.860	1.279	1.351	1.314	1.284	1.292	1.297	1.296	1.328	1.305

The last column of Table 7 shows the ratio V/V_o meaned over the whole range of diameters. Examination of the table shows that little error is incurred in using these mean values for all sizes of drop in the range 0.3 to 5.95 m m diameter. In Fig. 4 the logarithms of the mean values of V/V_o have been plotted against z. The curve shows that over the height range to 6 km we may put

$$V = V_o\, e^{0.0405z} \qquad \ldots\ldots\ldots\ldots\ldots\ldots\ldots\ldots (13)$$

for drops having diameter between 0.3 and 5.95 m m. Combining equations (12) and (13) we then have

$$V = 932.2\, e^{0.0405z}\left(1 - e^{-(d/1.77)^{1.147}}\right) \qquad \ldots\ldots (14)$$

for the terminal velocity of a drop of d(m m) diameter at height z km in the I.C.A.N. atmosphere provided d lies between 0.3 and 6.0 m m and z is less than 6 km.

We referred above to the "viscosity correction" necessary to convert the ratio of the velocities at two different densities but both at $\mu = 1.81\ 10^{-4}$ to the ratio of the velocities at the same densities with the appropriate viscosity from Table 1 in each case. Since this correction is the only step involving an assumption in this work it is desirable to indicate the magnitude of the correction. Table 8 gives a few sample values of $V(\rho,\mu)/V(\rho,1.81)$ where $V(\rho,\mu)$ is the terminal velocity (of a rigid sphere) at the density and viscosity corresponding to height z in the I.C.A.N. atmosphere and $V(\rho,1.81)$ is the velocity at the same density but with $\mu = 1.81\ 10^{-4}$.

Table 8.

Ratio $V(\rho,\mu)/V(\rho,1.81)$

Diameter (m m) / Height (k m)	3.38	5.95
	Ratio	
1.000	1.002	1.000
6.000	1.013	1.003

In applying these ratios to produce Table 7 allowance was also made for $V(12.251, 1.81)/V(12.251, 1.79)$ though it was significant only in the case of the 3.38 m m drops.

(b) Small Drops. The ratio V/V_o for drops having diameter 0.05 to 0.3 m m has been computed from equations 7 and 8. The results are given in Table 9.

/Table 9

Table 9

Ratio of terminal velocity at height z in I.C.A.N. atmosphere to velocity at surface - V/V_o.

Diameter (m m) / Height (k m)	0.05	0.10	0.15	0.3 ~~0.25~~	Mean
		Ratio V/V_o			
0	1.000	1.000	1.000	1.000	1.000
1.000	1.019	1.025	1.030	1.035	1.027
2.058	1.045	1.057	1.067	1.076	1.061
3.000	1.065	1.083	1.099	1.113	1.090
4.220	1.093	1.120	1.144	1.164	1.130
5.500	1.123	1.160	1.197	1.222	1.175
6.860	1.161	1.209	1.258	1.279	1.227

The variation of V/V_o with diameter is more systematic, and larger, here than in Table 7. Nevertheless, provided the height range is restricted to about 6 k m it seems that we may use the mean values without serious error. These have been plotted in Fig. 4 and show that up to about 6 k m we may write

$$V = V_o e^{0.029z} \quad \ldots\ldots\ldots\ldots\ldots\ldots\ldots\ldots (15)$$

for drops with diameter between 0.05 and 0.3 m m. This result together with paragraph 3(b) justifies equation 4.

(c) Very Small Drops. It is apparent from equation (1) that for drops which obey Stokes law the variation of V with height is given by the variation of $(1 - \rho)/\mu$. The ratios of this quantity to the surface value for the heights mentioned in Table 1 are given in Table 10 and plotted in Fig. 4.

Table 10.

Ratio V/V_o in I.C.A.N. atmosphere for Stokes law drops

Height (k m)	0	1.0	2.058	3.0	4.220	5.500	6.860
Ratio V/V_o	1.000	1.017	1.041	1.059	1.085	1.112	1.148

For these very small drops we see that

$$V = V_o e^{0.0191z} \quad \ldots\ldots\ldots\ldots\ldots\ldots\ldots\ldots (16)$$

and remembering equation 11 we see that equation 5 is thus justified.

5. Estimate of Errors involved in use of formulae

(a) Large drops. It is difficult to estimate from Table 3 the error involved in the use of equation 10 because the experimental values derived from Table 2 are themselves liable to error. However inspection of the table suggests that within the diameter range 0.3 to 5.95 m m equation 10 is accurate to within 2%. Conversion of equation 10 to equation 14 involves the errors in using the mean values in Table 7 and the errors in the appropriate curve of figure 4. (The errors involved in using the mean value from Table 6 have not been added because they are small and in any case compensate to a small extent the errors from Table 7). The former appear unlikely to exceed another 2% up to 6 k m and the latter are probably less than 1%. Thus we may expect equation 3 to be accurate to 5% over the diameter range 0.3 to 6.0 m m and at heights up to 6 k m, and to be more accurate over a substantial range of the variables.

(b) Small drops. Table 4 indicates that, at the surface equation 4 (with $z = 0$) has an error not exceeding 1.5%. From Table 9 the error in the height term may amount to 5% at 6 k m and figure 4 probably introduces another 0.5% error so that the total error in equation 4 may be 7% in extreme cases.

/(c)

(c) Very Small Drops. From Table 5 we see that the error in Stokes law is 3.3% at d = 0.05 m m and falls off rapidly as d decreases. It seems unlikely that figure 4 will introduce any additional error exceeding 0.5%.

6. Comparative importance of air density and viscosity. The many computations of the terminal velocity of rigid spheres made in the preparation of this note have provided data which illustrate the comparative importance of air density and air viscosity. Although not essential to the main purpose of the work it has been thought to be of sufficient interest to include Figure 5. There are two curves in this figure. One shows the ratio $V(8, 1.81)/V(12.251, 1.81)$ as a function of drop diameter. The other shows $V(8,1.65)/V(8, 1.81)$ as a function of drop diameter. It is clear that for drops greater than about 0.3 m m diameter air density is of prime importance. In the region 0.05 to 0.3 m m diameter density and viscosity are comparable in importance while for smaller drops of course Stokes law applies and air density is of very minor importance.

7. Reynolds Number. Throughout this note drop diameter has been used as a criterion. In many places Reynolds Number would have been more orthodox. However, owing to the small change of velocity with height the use of Reynolds Number would have caused little change in the arguments whereas the use of drop diameter is undoubtedly more convenient to the meteorologist.

8. Summary. The following formulae are suggested for the terminal velocity of a drop of water falling through the I.C.A.N. standard atmosphere

$$0.3 < d < 6.0 \qquad V = 932.2\, e^{0.0405z}\left(1 - e^{-(d/1.77)^{1.147}}\right) \quad \ldots\ldots(3)$$

$$0.05 < d < 0.3 \qquad V = 190.7\, e^{0.0290z}\left(1 - e^{-(d/0.316)^{1.754}}\right) \quad \ldots\ldots(4)$$

$$d < 0.05 \qquad V = 3041\, e^{0.0191z}\, d^2 \quad \ldots\ldots\ldots\ldots\ldots\ldots(5)$$

where d = drop diameter in m m
z = height in k m in the I.C.A.N. atmosphere
V = terminal velocity of drop in cm/sec.

It is shown that equation 3 fits the experimental values quoted in M.R.P.40 and also fits values of the terminal velocity of rigid spheres with diameters from 0.3 to 1.0 m m deduced from formulae due to Davies. It appears that water drops fall as rigid spheres at diameters smaller than 1 m m. Equation 4 fits the terminal velocities of rigid spheres deduced from Davies' formulae. Davies' formulae indicate that Stokes law applies to drops smaller than about 0.04 m m with an accuracy better than 3% and equation 5 is merely Stokes law applied to the I.C.A.N. atmosphere.

The three formulae join up smoothly and it is shown that the error in terminal velocity resulting from the use of these formulae is not likely to exceed 2% at the surface. The possible error increases with height to about 5% at 6 k m in the case of equation 3 and 7% at 6 k m in the case of equation 4. The maximum error in the case of equation 5 occurs at the maximum diameter (0.05 m m) and is not likely to exceed 4% even at 6 k m.

Finally it is shown that for drops of diameter 0.3 to 6.0 m m, air density is more important than air viscosity. For the range 0.05 to 0.3 the two factors are comparable in importance and in the Stokes law region of course viscosity is more important than density.

References

1. Schmidt, W. Met. Zeit. 26 1909
2. Sutton, O.G. M.R.P. 40 1942
3. Lenard, P. Met. Zeit. 21 1904
4. Flower, W.D. Proc. Phys. Soc. 40 Part 4. 1928
5. Laws, O.J. Amer. Geophys. Union Trans. 1941 Part III.
6. Davies, C.N. Proc. Phys. Soc. 57 1945.
7. Best, A.C. M.R.P. 330. 1947.

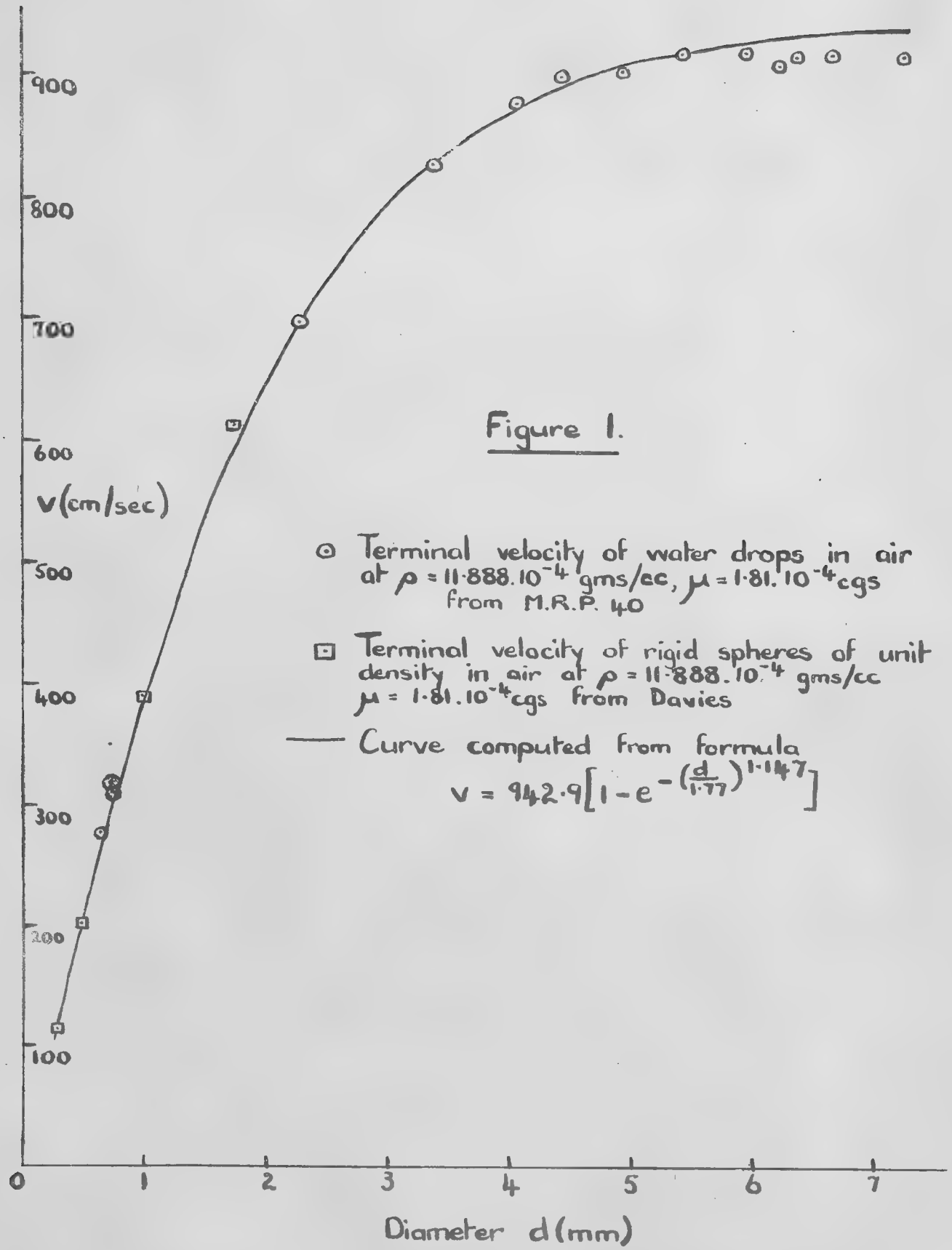

Figure 1.

⊙ Terminal velocity of water drops in air at $\rho = 11{\cdot}888.10^{-4}$ gms/cc, $\mu = 1{\cdot}81.10^{-4}$ cgs from M.R.P. 40

⊡ Terminal velocity of rigid spheres of unit density in air at $\rho = 11{\cdot}888.10^{-4}$ gms/cc $\mu = 1{\cdot}81.10^{-4}$ cgs from Davies

—— Curve computed from formula

$$V = 942{\cdot}9\left[1 - e^{-\left(\frac{d}{1{\cdot}77}\right)^{1{\cdot}147}}\right]$$

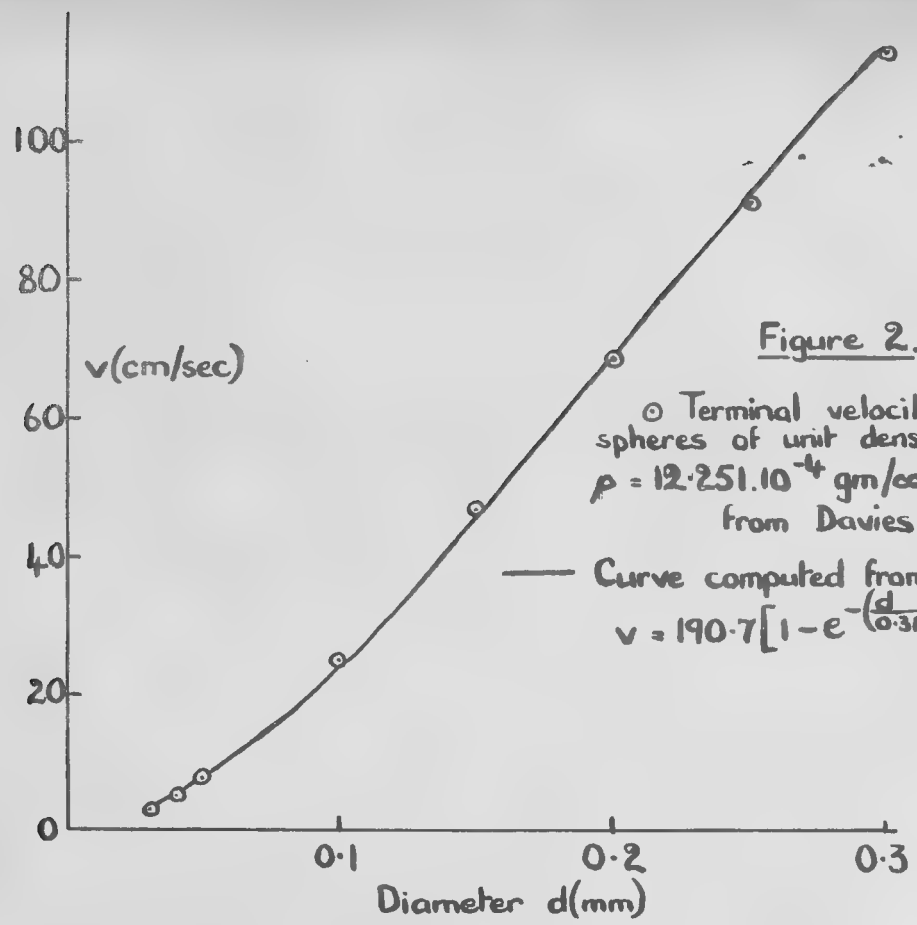

Figure 2.

⊙ Terminal velocity of rigid spheres of unit density in air at $\rho = 12{\cdot}251.10^{-4}$ gm/cc, $\mu = 1{\cdot}79.10^{-4}$ cgs from Davies

—— Curve computed from formula

$$v = 190{\cdot}7\left[1 - e^{-\left(\frac{d}{0{\cdot}316}\right)^{1{\cdot}754}}\right]$$

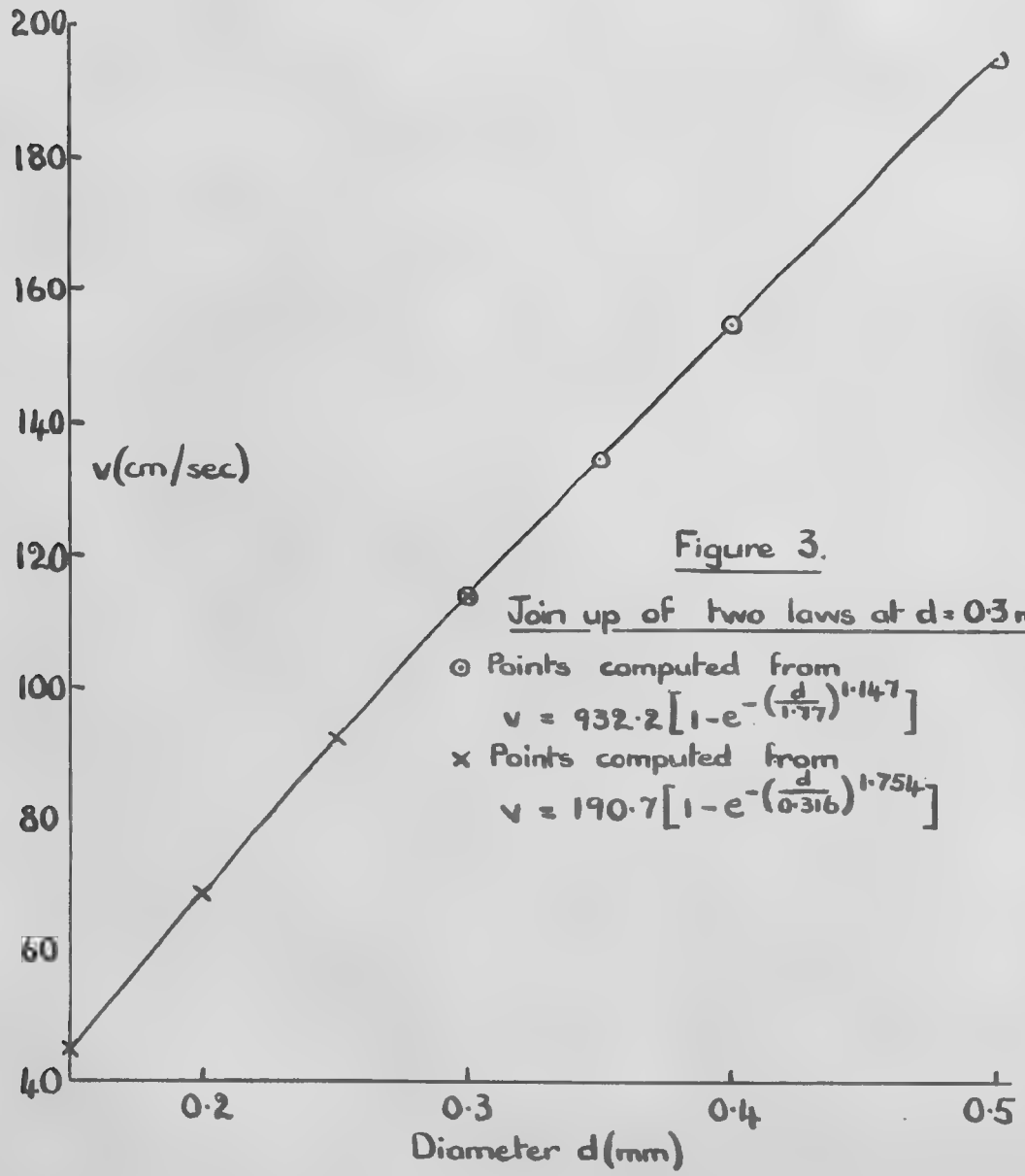

Figure 3.

Join up of two laws at d = 0·3 mm

⊙ Points computed from

$$v = 932{\cdot}2\left[1 - e^{-\left(\frac{d}{1{\cdot}77}\right)^{1{\cdot}147}}\right]$$

× Points computed from

$$v = 190{\cdot}7\left[1 - e^{-\left(\frac{d}{0{\cdot}316}\right)^{1{\cdot}754}}\right]$$

Figure 4.

Variation of terminal velocity with height.

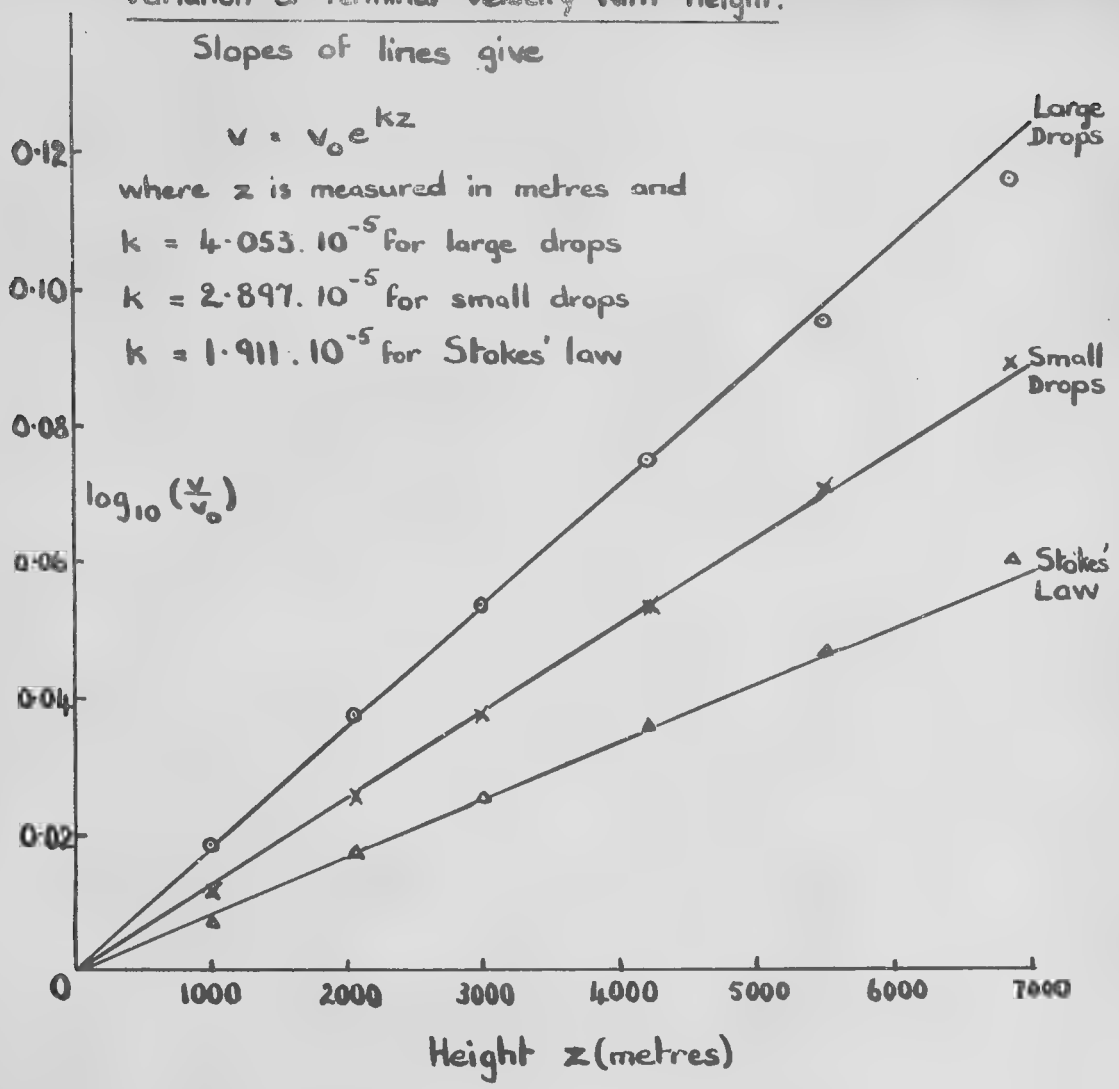

Figure 5.

Variation of relative effects of density and viscosity with drop diameter.

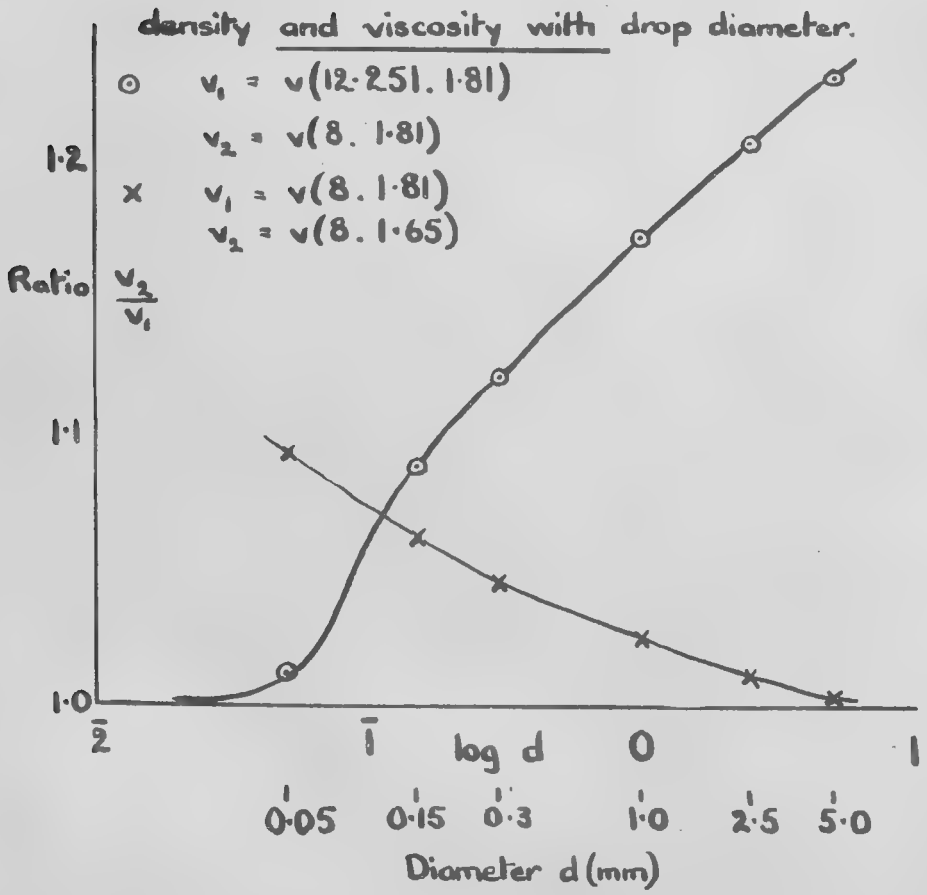

published and is to be treated CONFIDENTIALLY. Its contents must not be quoted.

M.R.P. 472
S.C.III/25
17th February, 1949.

AIR MINISTRY

METEOROLOGICAL RESEARCH COMMITTEE

The Size of Cloud Particles in Strato-cumulus cloud

by R. Frith.

AIR WEATHER SERVICE
TECHNICAL REFERENCE FILES

1. Introduction

Early in 1947 the Meteorological Research Flight was asked to continue the work of Dr. J. Mazur on measuring the size of water particles in natural clouds (M.R.P. 309 refers). We feel that sufficient progress has been made to justify an interim report.

2. Apparatus used

The work discussed in this report has been done using a slightly modified form of the final version of the apparatus used by Mazur. This is not the one described in M.R.P. 309, and the essential features are therefore described here.

Fig.1 represents a cross section of the instrument:-

EF is a microscope slide coated with magnesium oxide. There is a shutter (not shown) arranged to expose each part of the exposure area for 1/100 second. During this time a volume of some 2 to 300 c.c. of air is sampled.

Droplets sufficiently large to be undeviated as the air turns through BE' and DF', will strike the slide between E' and F'. Smaller droplets will be deviated, but all droplets greater than some critical size will strike the plate somewhere between E and F. We have, by analysis of a large number of slides, obtained a picture of the spectrum of drop sizes across the slide; and from this picture we can obtain a rough idea of the percentage catch of droplets smaller than the critical size.

It appears that droplets of diameter greater than 10 μ strike the plate between E' and F'; and that the critical size is about 4.5 μ - i.e., that there is no significant loss of particles of diameter greater than this.

MAY (J. of Sc.Inst. Vol. 22 No. 10) gives data for estimating the impaction efficiency of this type of apparatus. We see from his graphs that if there is just 100% efficiency for particles of diameter 4.5 μ then the efficiencies for diameters 3.5 μ, 2.5 μ, and 1.5 μ are approximately 90%, 50% and 10%. These figures fit in quite well with the spectrum picture obtained by direct counting, and all our results have been adjusted on this basis.

MAY (Porton publication B.D.P. No. 57) has also investigated the relationship between the droplet size and the resultant crater in the Mg O coating. He shows that, for droplets of diameter greater than 20 μ, and for large impingement velocities, the droplet size is about 0.85 of the crater size. There is some uncertainty as to the factor for smaller drops but all available evidence suggests that the same figure of 0.85 is appropriate. We have therefore accepted this figure.

3. Sources of error

Apart from the points discussed in the preceding paragraph, there are other possible sources of error. Among these we may mention:-

(1) The general disturbance of the air flow caused by the presence of the impactor may result in selective sampling.

(2) Turbulence in the throat may deposit droplets on the side walls.

(3) Water from the walls, and from the shutter, may be blown on to the slide, giving rise to spurious craters.

In an attempt to overcome these sources of error a new type of impactor has been designed.

In Fig. 2 OPQR is a rigid frame, across the centre of which is securely held a detachable metal rod of diameter 1/16 in., with a semi-circular cross section. Free to slide in this rigid frame is a shutter ABCD made of thin metal. In one position the section BC covers the wire; in the other position the section AD covers the wire. The shutter is operated by a powerful spring and a trigger release, exposing the rod for 1/100 sec - the time it takes for the space ABCD to cross the wire.

In use the flat side of the rod is coated with Mg O; the shutter is 'wound'; the apparatus held with the flat section of the rod facing into wind (but, of course, covered by the shutter) and the plane of the frame perpendicular to the line of flight. The shutter release is operated and some 2 c.c. of air is sampled - the droplets leaving craters in the Mg.O coating.

With a wire of this diameter there should be a 100% collection efficiency down to at least 2 μ.

In the earliest models many large craters appeared in the Mg O, clearly due to water blown off the shutter. We have not yet completely overcome this trouble.

As we have stated, all the results given in this paper have been obtained using the May - Mazur type of impactor described in paragraph 2.

4. Presentation of results

The slides, after exposure, are examined under a microscope and the craters compared in size with a series of circles - whose diameters increase in multiples of $\sqrt{2}$. For convenience this series of circles is numbered 1, 2, 3 etc.

It is often desirable to present results of such counts graphically, in the form of frequency curves. Custom seems to require that the abscissa of such frequency curves shall be the diameter of the droplets - but we cannot see any justification for this. Indeed since, for most purposes, the real interest lies in the volume of water present, it would seem more reasonable to use the volume of the droplets as the abscissa.

In practice, however, it is much more convenient to use the "size" (1, 2, 3 etc.). This may be regarded as an abscissa of either log diameter, or log surface area, or log volume.

The particular abscissa chosen for the construction of a frequency curve affects its shape, and the position of singular points. This does not really matter provided a consistent system is used throughout. Moreover a double maximum, for example, which appears on a frequency curve, must correspond to a peculiarity of similar nature on any other frequency curve constructed from the same data.

Where frequencies are given in tabular form the tables generally show (a) the number of droplets with diameters between specified values; and (b) the total volume of these drops.

5. Large drops

Sometimes exposed slides show, besides the usual craters with diameters up to 50μ, one or two really large craters (see Plate 1) of diameter 100 to 200 μ. Drops of equivalent size must, of course, exist in some clouds - but two facts make us hesitate to accept the craters which we find as evidence of such drops.

/Firstly:

Firstly: We have seen craters completely outside the exposure area.

Secondly: We have exposed a slide immediately after flying through a large cumulus cloud (in level flight so that the exposure was made in clear air, with no cloud above - but with the impactor still wet as a result of flight through the cloud). Two large craters were found on the slide.

We conclude that the craters are made by spots of water blown from the shutter and walls of the impactor.

There were rarely more than 3 or 4 such craters on any slide. If the craters were, in fact, made by very large particles, these particles would contribute about 0.02 gm per m^3 to the water concentration, compared with a total water content of 0.1 to 0.5 gm per m^3.

The area of the slide normally counted consists of a strip across the centre of the exposed area and it so happens that on no occasion was a large drop found in this area.

6. The variation of water content and droplet sizes in the horizontal in Strato-cumulus.

We decided to use the instrument, in the first place, to investigate the variation of water content, and of droplet size distribution, in the horizontal in Strato-cumulus - this being, from an experimental point of view, the simplest type of cloud.

Three flights have been made. Each flight was in shallow Strato-cumulus (1 to 2,000 ft. thick) and a series of about 12 exposures was made, in each case, over a distance of some 15 miles (5 minutes flying).

Analysis of these exposures shows a wide spread, on any one flight, of both water content and of number of particles. In Fig. 3 we show N (number of particles per c.c.) plotted against W (water content, gm per c.c.). In spite of the scatter it is clear that there is some correlation between N and W - W tending to increase with N. This correlation has been indicated by a regression line on W. We have also drawn a suggested line of best fit, passing through the origin.

We note, in passing, an almost linear relationship between the slope of the line of best fit and (a) the mean number of drops in the samples; (b) the mean mass of water in the samples - as shown in the table below:-

Set No.	Slope	$\overline{N}$	$\overline{W}$
1	0.7	453	628
2	1.6	496	316
3	2.3	538	232

In M.R.P. 309 it was seen that Mazur's data showed no correlation between the number of cloud particles and the liquid water content. We see from the table above that the means of our three sets appear to show an inverse relationship between N and W - whilst the samples in each set, as we have seen, showed a direct relationship. The samples considered in M.R.P. 309 were a heterogeneous collection, made at various heights, in several types of cloud and at many temperatures. It is not surprising that no correlation was found.

It may be remarked in passing that the apparent correlation found, in the same paper, between W and the 'mean volume diameter', D_V, is not real. It is, in fact, a direct consequence of the lack of correlation between N and W!

For, by definition,

$$\frac{\pi}{6}(D_v)^3 = \frac{W}{N}$$

/Therefore

Therefore if W and N are completely independent, there must be a correlation between D_v and W (also, of course, between D_v and N) such that the mean values of D_v and of W would lie about a curve of the form

$$D_v = k\sqrt[3]{W}$$

It is easy to verify that the curve given in Fig. 5 of M.R.P. 309 is of this form.]

7. The scale of the variations

Before discussing possible explanations of the large scatter, we would like to remark upon the dimensions of the problem. In one exposure we collect droplets from a tube 2 square centimetres in section and about 100 cm long. We count only those in a subsidiary tube of cross section about 0.02 sq. cm and about 100 cm long - but repeated tests indicate that such samples are quite representative of the whole tube.

Two exposures made in rapid succession (1 to 2 seconds - 100 to 200 metres apart) generally, but not invariably, give similar results.

The data are not sufficient to form any clear picture of how large a volume our sample really represents, but it seems reasonably safe to assume that it is at least 1,000 cubic metres. In other words we are not dealing with variations between very small samples of cloud, but between fairly large samples, of the order of 10 metre cubes - the size of a very large room.

8. The droplet size distribution

Tables 1, 2 and 3 give full details of the actual counts. For the first set we did not have facilities for high magnification, so that the count does not include droplets of diameter less than 5 μ . For the latter two we were able to measure to 1 μ , the smallest size for which there is a representative catch.

Fig. 4 shows the frequency curves for the means of each set.

The number frequency curves are particularly interesting in showing signs of a double maximum - especially the third set. These maxima occur at

$\leqslant 6\ \mu$	and 11 μ	in the first set
2.5 μ	and 10.5 μ	in the second set
2.5 μ	and 10.5 μ	in the third set.

This double maximum is not present on a frequency curve constructed from the actual catch figures (uncorrected for loss - see para. 2); but it is unlikely that our corrections are seriously in error. (See also appendix, para. 1).

9. The variation in W

Large variations in the water content of the various samples are to be expected - even in samples taken close together, at the same height and in the same cloud. For it is known (see M.R.P. 402) that the atmosphere is far from homogeneous with respect to water content. Variations of water content give rise to variations in cloud density. The variations found on our flights correspond to variations of frost point of about 3 degrees (F), and such variations are common.

It is worth while to study the variations of W in some detail.

Samples with approximately the same water content may have quite different size distributions. (These variations are discussed in the following section). We may assume, however, that, if a sufficiently large number of samples be taken we could, for any specified value of W, construct a representative mean size distribution.

/This

This abstract mean size distribution we shall denote by f - so that $f_{\bar{W}}$ is the size distribution of the mean of a large number of samples, all taken at a fixed level in the cloud, having approximately the same liquid water content $\bar{W}$.

We now assume that $f_{\bar{W}}$, for any fixed $\bar{W}$, is independent of height in the cloud. It is realised that this assumption may be false, but if it is true then we see that by comparing distribution curves $(f_1\ W_1)$ with $(f_2,\ W_2)$ $(W_2 > W_1)$ we can obtain information about the growth of droplets in a cloud.

For every sample with water content W_2 must, at some lower level, have had water content W_1. If an observer had been taking samples at this lower level and had selected and meaned all samples with a water content W_1, he would have obtained a certain distribution curve which, by our assumption, is the same as the (f_1, W_1) actually measured at the higher level.

For example we see at once from fig. 3 that if $W_1 < W_2$ then $N_1 < N_2$, (N being the number of cloud particles).

Langmuir ("Production of rain by chain reaction in cloud at temperature above freezing" G.E.C. report, 3rd February 1948) writes (page 2) "the droplets increased in size and decreased in number after they were formed at the base of the cloud_____" and (page 48) "At higher altitudes (above 150 metres) the concentration (of water droplets) was assumed to remain constant, the moisture released by the expansion being used to increase the size of the droplets."

Thus there appears to be some difference in this respect between the type of clouds we have investigated and the type (orographic cloud in the first case and large cumulus in the second) discussed by Langmuir.

An approximation to mean distribution curves f_1 and f_2 may be obtained in this way. The observations of each set are divided into two groups - of low water content, and of high water content. The mean of the first group is taken as (f_1, W_1); and the mean of the second group as (f_2, W_2).

In Table 4 we show these distributions. We see that

(a) for every size group $N_2 > N_1$ (There are very few exceptions to this statement and the nature of the data justifies some latitude); but

(b) $\%\ N_2 < \%\ N_1$ for the smaller drops, and $\%\ N_2 > \%\ N_1$ for larger drops (see note in (a). We may divide the size range at about 13 μ. Out of 17 groups with diameter less than about 13μ, 14 have $\%\ N_2 < \%\ N_1$; out of 14 groups with diameter greater than about 13 μ, 12 have $\%\ N_2 > \%\ N_1$).

Now when cooling occurs in a cloud, the rate of growth of any particular particle will depend largely upon its size: variations in size will affect the growth in three ways:-

(1) by changing the rate of fall, and therefore the flow of air past the particle;

(2) by changing the surface area;

(3) by changing the radius of curvature, and therefore the saturation vapour pressure over the droplet. Except for very small droplets this is probably relatively unimportant.

The growth of a particle may also be affected by the presence of neighbouring particles. On average, however, we may assume that when a sample of cloud is cooled all particles of diameter d will grow to some diameter d^1; and particles of diameter $> d$ will grow to have diameter $> d^1$. Thus if there are originally N particles of diameter $> d$, there will finally be the same number of particles of size $> d^1$.

/We

We have constructed cumulative number curves for the distributions f_1 and f_2. The above argument enables us to deduce, from these curves, the value of d^1 corresponding to arbitrarily chosen values of d. (Table 5).

The results for the first two cases are remarkably similar. They show an almost uniform ratio v^1/v, but with a clear tendency for the smaller drops to grow relatively more than larger drops.

We are left with the query - is there a real difference between the first two cases and the third? Perhaps further investigations will throw some light on this.

10. The variations in N

There is a wide scatter of N.

Possible causes of this include:-

(1) Variation in the number and type of the condensation nuclei available,

(2) Variations in the rate of cooling, especially at the instant when cloud first forms,

(3) Variations in the age and history of the cloud.

(1) There are so many nuclei always available that it seems unlikely that (1) is very important.

(2) Rapid cooling gives rise to a larger number of droplets than slow cooling.

(3) (i) The effect of the age of the cloud element is complex. Due to slight differences of vapour pressure over droplets of different sizes, there will always be a tendency for smaller drops to evaporate onto larger ones. Except for very small droplets we believe that, in the life of most cloud samples (which is probably of quite a different order to the life of the cloud as a whole), this effect will be slight.

Collisions and consequent coalescence will likewise tend to reduce the number of droplets in a cloud. According to Langmuir's work on collection efficiency, it seems unlikely that, except when the cloud contains quite large drops, this will be of great importance. He suggests, for example, that the collection efficiency of a drop falling through a cloud of particles of diameter 12 μ is zero unless the falling drop has diameter greater than 50 μ.

In cloud there will be a slow sorting of drops due to variations of the rates of fall. The rates of fall, except for large droplets, are so very small that this, also, seems unlikely to have much effect.

(3) (ii) Finally the history of the cloud: a cloud sample is generally in constant up and down motion. It may well be that a complete cycle, entirely within the cloud, may completely change the frequency distribution of droplet sizes, whilst leaving the water content unchanged.

It does not seem possible to separate these various effects. But a study of the combined effects is possible.

If, in Fig. 3 we find the mean of all the samples on the two sides, separately, of the regression line (on W) we shall have two frequency distributions, for each set, with the same water content (approximately) but with different numbers of droplets. These distributions are given in Table 6.

These figures are interesting but it is doubtful whether they furnish a sufficient basis for discussion or for extrapolation. A set of, say, 50 samples - enabling subdivision into, say, five equal water content groups - would be of more value.

/Nevertheless

Nevertheless we have evaluated the Standard Deviation of the two groups of each set. Ideally these Standard Deviations should be constructed against particle volume. However this is impracticable because of the enormous effect on the standard deviations of relatively few drops of larger size. For example the large number group of the first set has a standard deviation of 0.59. But if we had counted just one more drop of size 8, on any slide, the standard deviation would have been 0.69.

We have therefore remained faithful to our base of log (volume). With this base the standard deviations of the various groups are as follows:-

	Large N	Small N
1st set	1.41	1.42
2nd set	2.41	2.51
3rd set	2.08	2.07

The very close agreement in the first and third sets is probably fortuitous. It does appear, however, that there is, in general, no marked difference in the standard deviations of the two groups.

11. Summary

The technique of cloud investigations which we use differs from most others in sampling in detail a small volume of cloud. We have shown the order of the differences which occur from point to point in Strato-cumulus cloud.

Mainly in order to test ideas and methods of analysis - and also to provide a basis for discussion - we have studied in some detail the results of the three series of samples so far obtained - all in Strato-cumulus cloud.

The only firm conclusions which we have been able to draw are:-

(1) That there is a tendency, at a fixed level in any one cloud, for N to increase with W.

(2) That there may be a double maximum in droplet size distribution.

More tentative conclusions are:-

(3) That there is a tendency, when further cooling occurs in a cloud, for the smallest droplets to grow, relatively, faster than somewhat large drops.

(4) That, whatever the cause of samples with the same water content having different numbers of particles, the standard deviation of the frequency distributions (with log (volume) as base) remains fairly constant.

12. Future work

We plan future work on two lines:-

(a) To study in greater detail the variations in Strato-cumulus - by obtaining a much larger number of samples at one level.

(b) To study the variations in Cumulus cloud by obtaining samples (i) at varying heights; and (ii) at various times.

/Appendix

Appendix

1. Double maxima

We have remarked that more or less clearly marked double maxima in the frequency distribution of log (volume) occur in all our Strato-cumulus samples.

These double maxima are puzzling; evidence for them must be examined carefully.

First, as we have remarked, they could arise through a faulty adjustment of the data for lost drops. However we have found that in Alto-cumulus clouds, in which droplet sizes are generally larger than in Strato-cumulus, we frequently find clear double maxima which do not depend upon our adjustment of the data.

For example the following frequency distribution data relate to a sample taken in shallow Alto-cumulus at a temperature just below freezing.

Diam (μ)	1.0 – 1.3	1.3 – 1.9	1.9 – 2.6	2.6 – 3.7	3.7 – 5.2	5.2 – 7.5	7.5 – 10.5	10.5 – 15.0	15.0 – 21.0	21.0 – 30.0
No.	1	8	9	10	9	8	4	35	30	3

These are actual counts, unadjusted.

Secondly we must emphasise that the double maxima cannot merely be a result of using a log (volume) base. For although a frequency curve on a diameter, or volume, base might not, in any specific instance, show a double maximum, it must show a singularity of a similar nature.

Finally it is possible that we are not justified in using a uniform factor 0.85 to reduce crater diameter to drop diameter. It seems unlikely, however, that such an error could result in the appearance of a spurious double maximum.

We believe, therefore, that this is a real, and common, phenomenon in Alto-cumulus and Strato-cumulus types of cloud.

2. Ice crystals

We have never succeeded in obtaining a recognisable impact of an ice crystal.

3. Supercooled water droplets

It is known that in clouds (except perhaps, Cumulus) it is the exception rather than the rule not to find some ice crystals at temperatures below about 20°F. On the other hand we recently exposed some slides in what had been taken to be Cirrus (mainly because a "sun image" had been observed) - yet the slides showed that the cloud was mainly, if not entirely, of water particles. The height was 23,000' and the temperature - 15°F (-29°C). The droplets were about 10 to 15 μ in diameter with a density of 50 to 100 per c.c.

SIZE		1	2	3	4	5	6	7	8		
PARTICLE DIA. (Microns) / SLIDE		5.1 - 7.2	7.2 - 10.0	10.0 - 13.8	13.8 - 20.0	20.8 - 27.5	27.5 - 39.0	39.0 - 55.0	55.0 - 78.0		TOTAL
35	Number	146	118	90	60	35	10	1			460
	Mass (10^{-9} gm)	16	39	73	135	227	180	52			722
36	Number	170	61	86	81	43	10	1			452
	Mass (10^{-9} gm)	19	20	70	182	279	180	52			802
37	Number	224	156	132	89	44	13	0	1		659
	Mass (10^{-9} gm)	25	52	107	198	285	234	0	144		1045
38	Number	263	133	107	66	38	23	2			632
	Mass (10^{-9} gm)	28	44	87	148	247	413	104			1071
39	Number	186	120	94	93	56	15	0			564
	Mass (10^{-9} gm)	21	40	76	209	364	269	0			979
40	Number	130	62	65	64	25	11	0			357
	Mass (10^{-9} gm)	15	21	53	144	162	198	0			593
41	Number	192	87	154	63	19	4	1			520
	Mass (10^{-9} gm)	22	29	124	141	123	72	52			563
42	Number	246	127	165	76	14	8	0			636
	Mass (10^{-9} gm)	28	42	134	171	91	144	0			610
43	Number	192	155	137	119	52	8	2			665
	Mass (10^{-9} gm)	22	51	111	268	338	144	104			1038
44	Number	201	174	102	86	20	4	1			588
	Mass (10^{-9} gm)	22	57	83	193	130	72	52			609
45	Number	173	110	120	58	19	3	2			485
	Mass (10^{-9} gm)	19	36	97	130	123	54	104			563
46	Number	252	162	190	107	32	7	0			750
	Mass (10^{-9} gm)	28	53	154	240	208	126	0			809
Mean per c.c.	Number	158	96	96	64	26	7.8	0.6	0.06		453
	Mass (10^{-9} gm)	18	32	78	144	171	139	34	9.5		625

Table 1. 30th June, 1947.

Strato-cumulus 4,000' - 5,500'. Flight at 4,500', Temp. 43°F.
Volume sampled about 1.25 c.c.

SIZE	1	2	3	4	5	6	7	8	9	10	11	
PARTICLE DIA. (Microns)	1.0 -	1.5 -	2.1 -	3.0 -	4.2 -	6.0 -	8.5 -	12.0 -	17 -	24 -	34 -	Total
SLIDE	1.5	2.1	3.0	4.2	6.0	8.5	12.0	17	24	34	48	
2 Number	40	48	52	32	30	33	59	60	4	1	0	359
Mass (10^{-9} gm)	0.04	0.14	0.42	0.74	2.0	6.1	31	90	17	12	0	159
3 Number	0	54	54	40	25	37	114	100	4	0	0	428
Mass (10^{-9} gm)	0	0.16	0.44	0.93	1.7	6.9	60	150	17	0	0	237
4 Number	10	24	38	27	19	51	52	49	6	1	0	277
Mass (10^{-9} gm)	0.01	0.07	0.31	0.63	1.3	9.5	27	74	25	12	0	150
5 Number	0	6	16	15	17	14	22	6	0	0	0	96
Mass (10^{-9} gm)	0	0.02	0.13	0.35	1.1	2.6	12	9	0	0	0	25
6 Number	60	39	90	65	34	22	80	88	2	0	0	480
Mass (10^{-9} gm)	0.07	0.11	0.73	1.5	2.2	4.1	42	132	8.4	0	0	191
7 Number	0	0	24	14	25	79	158	43	4	0	0	347
Mass (10^{-9} gm)	0	0	0.19	0.33	1.7	15	83	65	17	0	0	182
8 Number	20	51	38	33	43	41	152	16	5	0	0	399
Mass (10^{-9} gm)	0.02	0.15	0.31	0.77	2.8	7.6	80	24	21	0	0	137
9 Number	20	21	66	42	38	92	173	17	2	0	0	471
Mass (10^{-9} gm)	0.02	0.06	0.53	0.98	2.5	17	91	25	8.4	0	0	145
11 Number	20	18	52	28	27	77	134	33	7	0	0	396
Mass (10^{-9} gm)	0.02	0.05	0.42	0.65	1.8	14	70	49	29	0	0	165
12 Number	0	18	38	19	41	66	61	17	3	0	0	263
Mass (10^{-9} gm)	0	0.05	0.31	0.44	2.7	12	32	25	13	0	0	85
13 Number	30	57	164	124	116	94	136	79	9	0	0	809
Mass (10^{-9} gm)	0.03	0.17	1.3	2.9	7.7	17.5	71	118	38	0	0	257
14 Number	20	24	50	49	71	71	221	141	15	0	1	663
Mass (10^{-9} gm)	0.02	0.07	0.41	1.1	4.7	13	116	211	63	0	33	442
15 Number	0	39	78	68	43	43	92	38	5	0	0	406
Mass (10^{-9} gm)	0	0.11	0.63	1.6	2.8	8.0	48	57	21	0	0	139
Mean per c.c. Number	22	40	75	56	53	72	133	69	6.1	0.2	0.1	538
Mass (10^{-9} gm)	0.03	0.12	0.61	1.3	3.5	13.2	77	102	27	2.3	3.2	232

Table 3. 11th July, 1947.

Flight at 6,000' in centre of strato-cumulus layer about 1,000' thick.
Temp 26°F. Volume sampled about 0.77 c.c.

First Set														Total	
Diameter (μ)	5.1 7.2	7.2 10.0	10.0 13.8	13.8 20.0	20.0 27.5	27.5 39	39 55.5	55.5 78							—
frequency N_2	214	131	124	93	44	13	1	0.1						620	
" N_1	181	113	116	68	22	7	1	0						508	
frequency W_2	24	43	101	208	287	228	43	24						958	10^{-9} gm
" W_1	20	37	94	152	143	120	43	0						609	10^{-9} gm
% frequency N_2	34.5	21.2	20.0	15.0	7.1	2.1	0.2	0.02							
" N_1	35.5	22.2	22.8	13.4	4.3	1.4	0.2	0							
% frequency W_2	2.5	4.5	10.5	21.8	30.0	23.8	4.5	2.5							
" W_1	3.3	6.1	15.4	25.0	23.5	19.7	7.1	0							
Second Set															
Diameter (μ)	1 1.5	1.5 2.1	2.1 3.0	3.0 4.2	4.2 6.0	6.0 8.5	8.5 12	12 17	17 24	24 34	34 48	48 68			
frequency N_2	48.5	47	69	44	44	45	45	35	17	7	1.4	0.5		403	
" N_1	51	47	49	40	52	45	48	31	9	2	0.5			375	
frequency W_2	0.07	0.14	0.56	0.88	2.9	6.9	24	52	70	81	48	40		326	10^{-9} gm
" W_1	0.06	0.14	0.39	0.65	3.4	7.9	25	47	38	22	14	0		159	10^{-9} gm
% frequency N_2	12.0	11.5	17.2	11.0	11.0	11.2	11.2	8.7	4.2	1.7	0.3	0.1			
" N_1	13.6	12.6	13.1	10.7	13.9	12.0	12.8	8.3	2.4	0.5	0.1	0			
% frequency W_2	0	0	0.2	0.3	0.9	2.1	7.4	16.0	21.4	24.8	14.7	12.2			
" W_1	0	0.1	0.2	0.4	2.1	5.0	15.8	29.5	23.8	13.8	8.8	0			

Table 4. Frequency distributions corresponding to:-

1. Low Water Content
2. High Water Content

/Third Set

Third Set														Total	
Diameter (μ)	1 1.5	1.5 2.1	2.1 3.0	3.0 4.2	4.2 6.0	6.0 8.5	8.5 12	12 17	17 24	24 34	34 48	48 68			
frequency N_2	24	34	69	50	47	59	129	78	6.4	0.1	0.1			497	
" N_1	13	30	47	34	33	49	87	29	3.6	0.3				325	
frequency W_2	0.03	0.1	0.56	1.16	3.1	10.9	68	116	27	1.7	0.5			230	10^{-9} gm
" W_1	0.01	0.09	0.38	0.79	2.2	9.0	46	43	15	3.4				120	10^{-9} gm
% frequency N_2	4.8	6.8	13.8	10.0	9.4	11.9	26.0	15.6	1.3	0.02	0.02				
" N_1	4.0	9.2	14.5	10.5	10.2	15.1	26.8	8.9	1.1	0.1					
% frequency W_2	0	0.05	0.2	0.5	1.3	4.7	29.5	51	11.7	0.7	0.2				
" W_1	0.01	0.08	0.32	0.66	1.8	7.5	39	36	12.5	2.8					

Table 4. Frequency distributions corresponding to

1. Low water content,
2. High water content.

FIRST SET																				
Original diam.	5.1	5.8	6.6	7.6	8.7	10.0	11.5	13.2	15.1	17.4	20.0	22.9	26.3	μ						
Final diam: / Original diam:	1.41	1.36	1.28	1.24	1.20	1.16	1.18	1.20	1.23	1.19	1.23	1.16	1.15							
Final vol: / Original vol:	2.80	2.52	2.10	1.91	1.73	1.56	1.64	1.73	1.86	1.69	1.86	1.56	1.52							
							Ratio $\frac{W_2}{W_1} = 1.58$													
SECOND SET																				
Original diam.	1.0	1.15	1.33	1.53	1.76	2.03	2.34	2.69	3.11	3.58	4.12	4.74	5.47	6.31	7.26	8.36	9.64	11.09	12.79	14.74	17.00 μ
Final diam: / Original diam:	1.24	1.25	1.26	1.26	1.20	1.15	1.12	1.10	1.07	1.07	1.07	1.10	1.12	1.12	1.13	1.13	1.15	1.17	1.26	1.22	1.33
Final vol: / Original vol:	1.91	1.95	2.00	2.00	1.73	1.52	1.41	1.33	1.23	1.23	1.23	1.33	1.41	1.41	1.44	1.44	1.52	1.60	2.00	1.82	2.35
							Ratio $\frac{W_2}{W_1} = 2.07$													
THIRD SET																				
Original diam.	1.0	1.15	1.33	1.53	1.76	2.03	2.34	2.69	3.11	3.58	4.12	4.74	5.47	6.31	7.26	8.36	9.64	11.09	12.79	14.74	17.00 μ
Final diam: / Original diam:	3.98	3.47	3.20	3.11	2.82	2.69	2.60	2.51	2.43	2.34	2.07	1.86	1.68	1.51	1.40	1.29	1.22	1.20	1.22	1.11	
Final vol: / Original vol:	63.0	41.8	32.8	30.1	22.4	19.5	17.6	15.8	14.3	12.8	8.9	6.4	4.7	3.4	2.7	2.1	1.8	1.7	1.8	1.3	
							Ratio $\frac{W_2}{W_1} = 1.90$													

Table 5. Showing the relative growth of drops of various sizes.

FIRST SET													Total	
Diameter (μ)	5.1	7.2	10.0	13.8	20.0	27.5	39	55.5						
	7.2	10.0	13.8	20.0	27.5	39	55.5	78						
frequency N_1	178	101	94	70	36	12	1	0					492	
" N_2	216	144	146	90	30	7	1	0.1					636	
" V_1	20	33	76	158	234	216	52	0					789	10^{-9} gm
" V_2	24.5	47.5	119	202	196	132	35	24					780	10^{-9} gm
% frequency N_1	36.2	20.4	19.0	14.2	7.3	2.4	0.2	0						
" N_2	34.0	22.7	23.0	14.2	4.7	1.1	0.2	0						
" V_1	2.5	4.2	9.6	20.0	29.6	27.4	6.7	0						
" V_2	3.1	6.1	15.3	26.0	25.2	17.0	4.5	3.1						

SECOND SET														
Diameter (μ)	1	1.5	2.1	3.0	4.2	6.0	8.5	12	17	24	34	48		
	1.5	2.1	3.0	4.2	6.0	8.5	12	17	24	34	48	68		
frequency N_1	35	29	40	25	31	35	40	25	10	5	1	0.3	275	
" N_2	63	63	72	53	61	50	52	40	15	4	0.6	0.1	473	
" V_1	0.04	0.09	0.32	0.58	2.01	6.4	20.9	37	44	59	39	31	240	10^{-9} gm
" V_2	0.07	0.18	0.59	0.95	4.0	8.7	27	60	61	49	19	13	244	10^{-9} gm
% frequency N_1	12.7	10.5	14.5	9.1	11.2	12.7	14.5	9.1	3.6	1.8	0.4	0.1		
" N_2	13.4	13.4	15.2	11.2	12.9	10.6	11.0	8.4	3.2	0.8	0.1	0		
" V_1	0	0	0.1	0.2	0.8	2.7	8.7	15.4	18.2	24.6	16.2	12.9		
" V_2	0	0.1	0.2	0.4	1.6	3.6	11.0	24.6	25.0	20.0	7.7	5.3		

Table 6. Frequency distribution corresponding to:-
1. Low particle number.
2. High particle number.

/THIRD SET

THIRD SET														Total	
Diameter (μ)	1	1.5	2.1	3.0	4.2	6.0	8.5	12	17	24	34				
	1.5	2.1	3.0	4.2	6.0	8.5	12	17	24	34	48				
frequency N_1	10	25	39	28	33	50	98	59	5	0.3	0.1			347	
" N_2	21	35	75	54	49	62	118	41	4.7	0	0			460	
" V_1	0.01	0.07	0.32	0.65	2.2	9.3	52	89	22	3.4	5.0			184	10^{-9} gm
" V_2	0.02	0.10	0.57	1.3	3.2	11.5	62	61	20	0	0			160	10^{-9} gm
% frequency N_1	2.9	7.2	11.2	8.1	9.8	14.4	28.2	17.0	1.4	0.1	0				
" N_2	4.5	7.6	16.2	11.7	10.6	13.4	25.5	8.9	1.0	0	0				
" V_1	0	0	0.2	0.4	1.2	5.1	28.5	48.5	12.0	1.9	2.7				
" V_2	0	0.1	0.4	0.8	2.0	7.2	39.0	38.0	12.5	0	0				

Table 6. Frequency distribution corresponding to

1. Low particle number
2. High particle number.

M.R.P. 472.

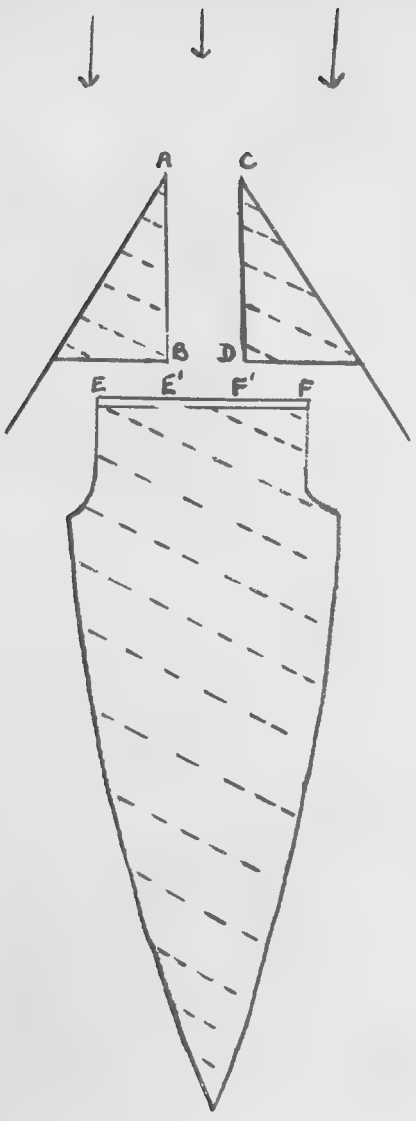

Fig. 1. Cloud droplet impactor. Full scale cross section.

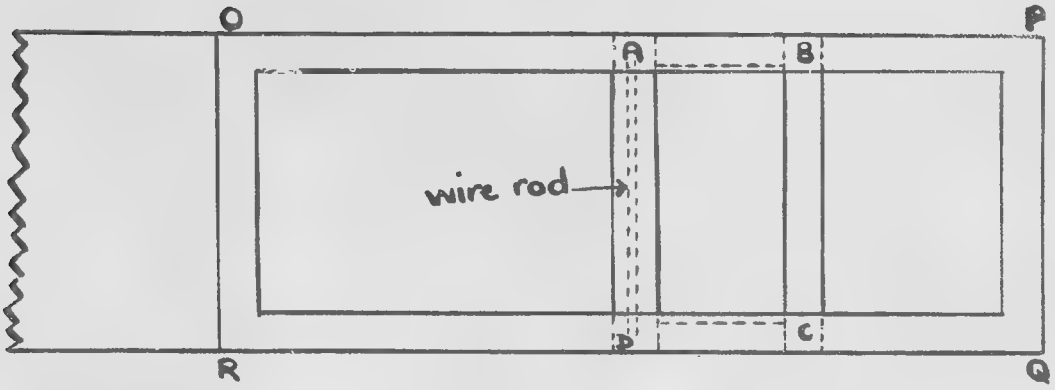

Fig. 2. Wire impactor. Forward view, half scale.

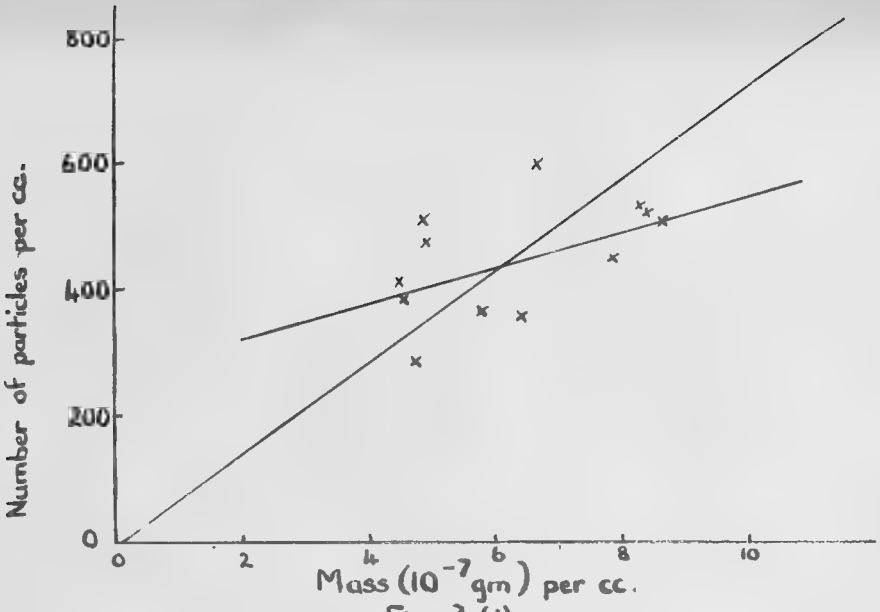

Fig. 3 (i)

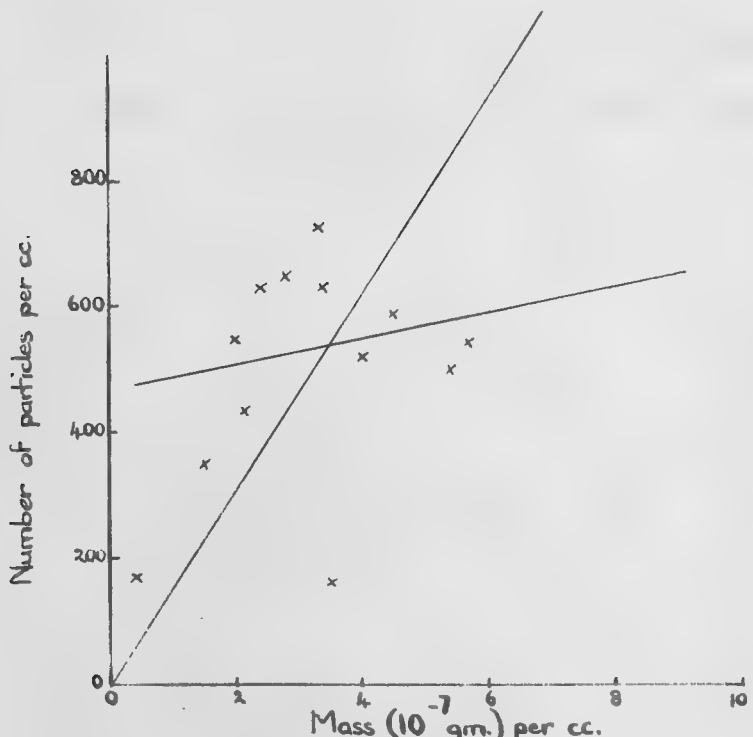

Fig. 3 (ii)

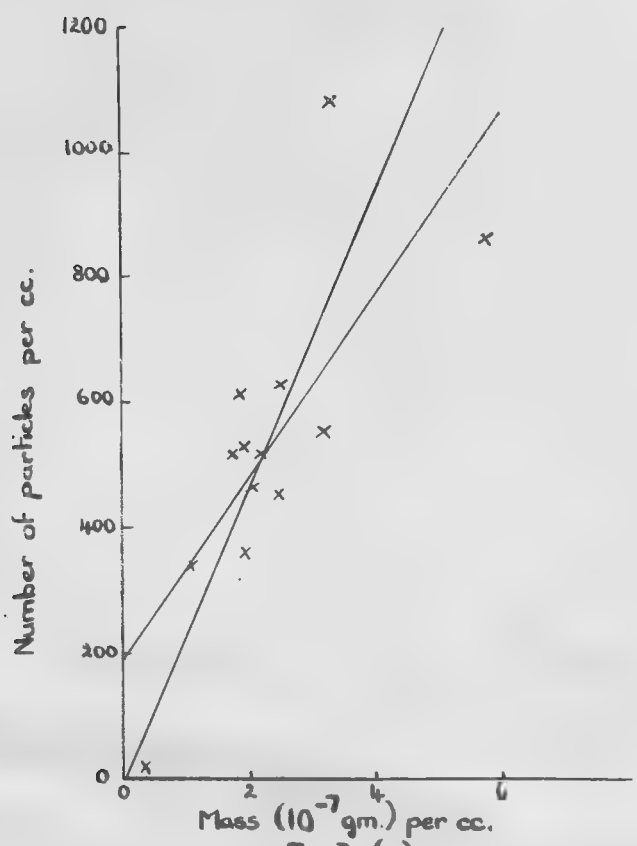

Fig. 3 (iii)

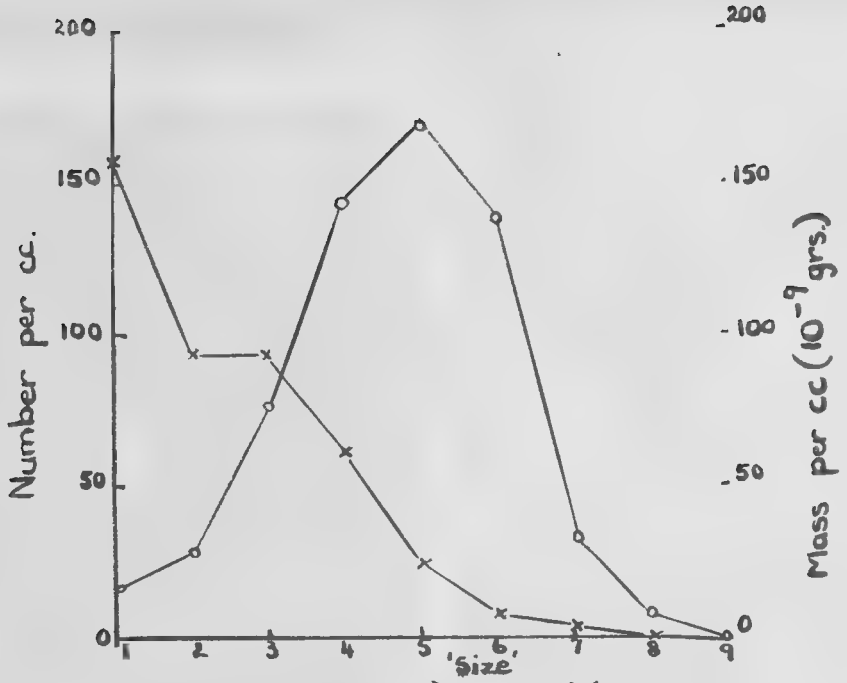

Fig. 4(i) Number (x—x) and Mass (o—o) frequency curves.

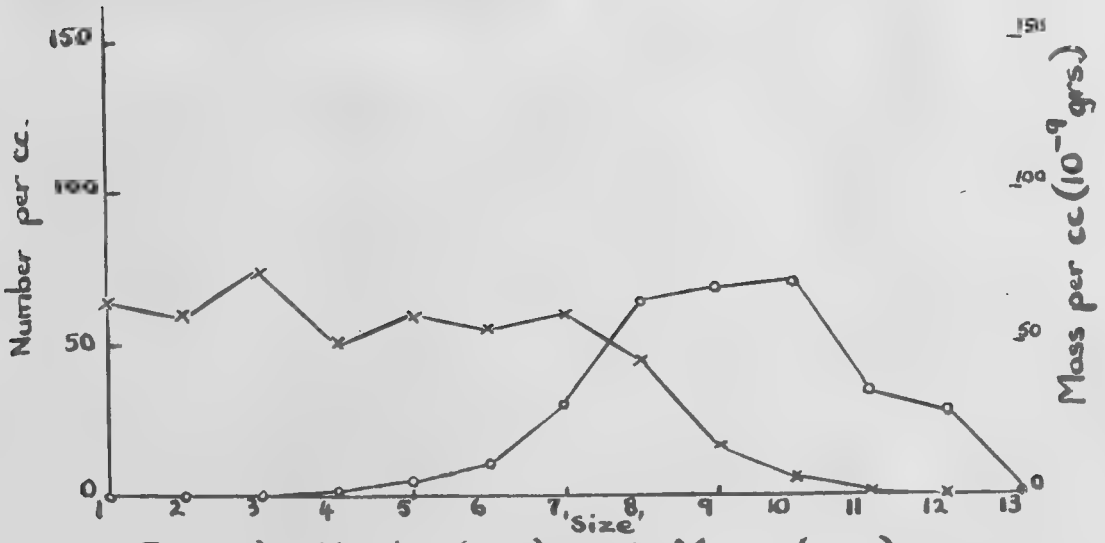

Fig. 4(ii) Number (x—x) and Mass (o—o) frequency curves.

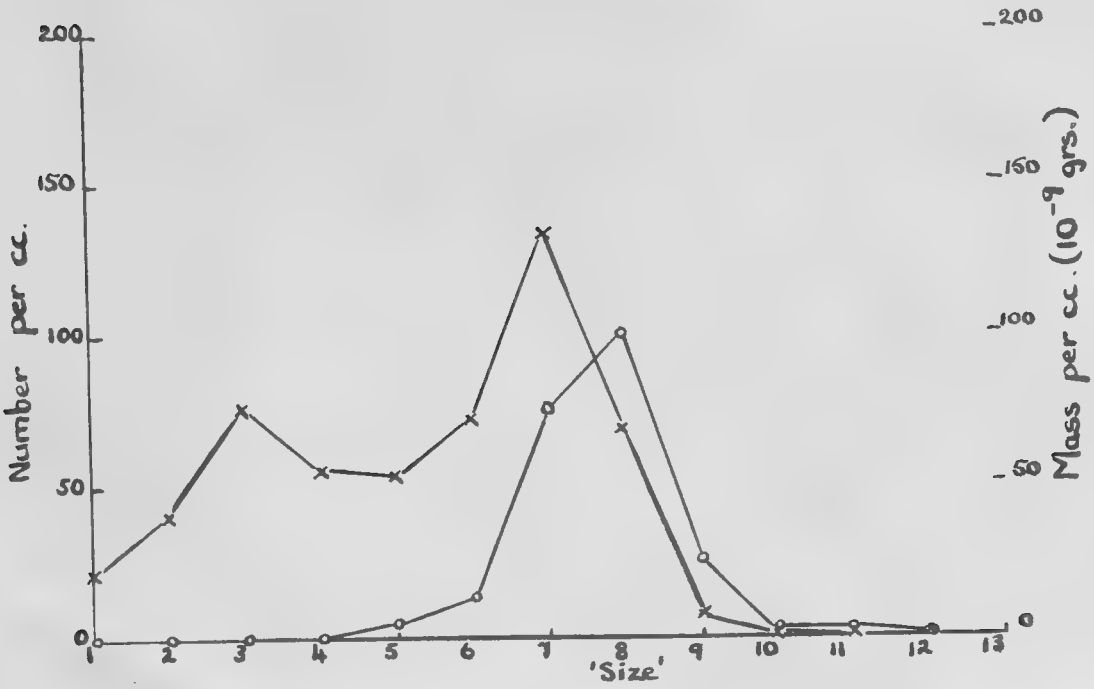

Fig. 4(iii) Number (x—x) and Mass (o—o) frequency curves.

PLATE I

7. It must be emphasized that the figures given here do not represent the total error of wind measurement, but only the differences which can occur in the treatment by different persons of the same set of readings. It is the random errors which give rise to these differences. Observationsl errors which are sufficiently

AIR WEATHER SERVICE
TECHNICAL REFERENCE FILES

8th March, 1949.

AIR MINISTRY

METEOROLOGICAL RESEARCH COMMITTEE

The Uncertainty of Radar Wind Smoothing on Ocean Weather Ships

by

D.N. HARRISON

Summary. Vector differences have been calculated between independent determinations of winds from a given set of radar observations. The mean is 3.7 knots. 50 per cent lie in the range 0-2 knots.

As part of an investigation into the accuracy of radar wind measurements made on the Ocean Weather Ships, an attempt has been made to assess the uncertainty due to the plotting and measuring technique. The uncertainty arises partly from errors of plotting, but chiefly in the smoothing which has to be applied to the trace on account of the scatter due to errors of observation and the comparative coarseness of the readings. The greater the scatter the more scope there is for differences of treatment.

2. Each ship selected from the records 25 typical routine soundings, in which the radar set was working satisfactorily and good heights or ranges were obtained. Both strong and light winds were represented. The radar readings, with the ship's course and speed and data for identifying the pressure levels, but not the wind measurements, were passed to another ship, on which winds were re-computed independently from the data. The re-computation (as, of course, the original computation) was done at sea under normal working conditions by various members of the staff.

3. The vector difference in knots, to the nearest whole number, between each pair of wind values was taken. These differences are a measure of the uncertainty in the plotting and measuring. Excluding three soundings where wrong data appeared to have been used in the re-computation, there are 1963 pairs of wind measurements on 97 ascents. The mean differences for each pressure level and for each pair of ships are shown in Table I. The mean of all is 3.7 knots, but there are marked variations in the mean between different pairs of ships, which probably reflect variations in radar performance, or in the state of the sea during observation and plotting, as well as in the skill of the observers and plotters.

4. The frequency distribution of the vector differences is shown in Table II. The distribution is, of course, far from "normal". The reason is that with a two-dimensional vector the probability of a value r is proportional, not to dr, as in the case of a scalar quantity, but to r.dr. 50 per cent of the values are 0, 1 or 2 knots (i.e. less than 2.5 kt), and 90 per cent lie in the range 0-8 kt (less than 8.5 kt).

5. It was obvious on inspection of the data that a number of very large differences occurred. Many of these have been examined. In a few cases it seems that an error of 90° may have been made in measuring the wind direction, and three such cases have been excluded from Table I, but in the majority no simple explanation suggests itself, and no doubt the cause lies in a genuine difference of treatment by the plotters. In this connection it may be noted that if there is much scatter the smoothing, and therefore the wind measurement, at the extreme end of a trace are subject to increased uncertainty, since the points cannot be related to any following. In one sounding there was a systematic difference of 10° in wind direction, which must have been due to an error of plotting or measuring.

6. Cases where the vector difference was 20 kt or more (amounting to 1.5 per cent of the total) have been examined in relation to the "tolerance" classification allotted in the original report. The tolerances are defined as follows (see M.O.464):- A, 3kt; B, 5kt; C, 10kt; D, greater than 10kt. The analysis is given in Table III. It will be seen that even when class A is reported there may be an uncertainty of at least 20 kt in the wind vector. Every value derived from the last reading of a sounding, which would be expected to be particularly inaccurate, is marked with an asterisk; these are only a small proportion of the total.

7. It must be emphasized that the figures given here do not represent the total error of wind measurement, but only the differences which can occur in the treatment by different persons of the same set of readings. It is the random errors which give rise to these differences. Observationsl errors which are sufficiently systematic to remain after all smoothing has been done are not detected by this method of analysis, but make their contribution to the total error.

/Table I

Table I. Mean Vector Difference (knots)

Original computation by O.W.S. Re-computed by O.W.S.	Recorder Observer	Observer Recorder	Watcher Explorer	Explorer Watcher	Mean	No. of soundings
Pressure level (mb)						
950	3.0	2.5	1.6	2.5	2.4	96
900	3.4	3.0	1.7	1.5	2.4	97
850	3.5	2.8	1.8	1.3	2.4	97
800	2.5	2.6	1.3	2.0	2.1	97
750	3.7	3.1	1.4	1.7	2.5	97
700	3.0	2.8	3.0	1.3	2.5	97
650	4.2	3.6	2.3	2.3	3.1	95
600	3.3	3.4	2.2	2.1	2.8	96
550	3.5	5.4	2.2	1.9	3.2	97
500	3.5	3.4	2.8	2.4	3.0	95
450	4.0	5.8	2.9	2.7	3.9	97
400	4.1	5.4	4.5	2.8	4.2	97
350	4.6	6.6	3.9	2.6	4.4	95
300	5.2	7.4	2.8	2.5	4.4	91
250	8.3	5.9	4.3	3.2	5.3	88
200	6.9	7.2	5.1	2.7	5.2	79
170	4.6	9.4	5.1	3.8	5.3	71
150	4.5	5.7	4.3	2.9	4.1	69
130	7.2	7.8	5.3	4.1	5.4	64
110	4.5	4.2	7.3	4.0	5.4	62
100	7.7	4.0	4.7	3.4	4.6	56
90		1.0	6.5	4.4	5.4	42
80		6.0	6.5	4.0	5.2	37
70			5.5	1.9	3.4	26
60			7.4	2.6	4.7	16
50			2.5	3.0	2.8	5
40			8.0		8.0	1
Mean	4.3	4.5	3.5	2.7	3.7	
No. of obs.	418	413	561	568		1960

Table II. Frequency Distribution of Vector Differences

Vector diff. (kt)	No. of Cases	Percentage	Vector diff. (kt)	No. of Cases	Percentage	Vector diff. (kt)	No. of Cases	Percentage
0	168	8.6	12	21	1.1	24	4	0.2
1	484	24.6	13	21	1.1			
2	362	18.4	14	7	0.4	27	1)	
3	250	12.7	15	8	0.4	32	2)	
4	171	8.7	16	0	0.0	33	2)	
5	117	6.0	17	3	0.2	34	1)	
6	111	5.7	18	3	0.2	35	1)	0.5
7	58	3.0	19	1	0.1	36	1)	
8	43	2.2	20	4	0.2	38	1)	
9	43	2.2	21	2	0.1	44	1)	
10	34	1.7	22	7	0.4			
11	29	1.5	23	2	0.1	Total	1963	100.3

Table III. Analysis of Large Vector Differences (20 kt and greater)

Tolerance Class				
A	B	C	D	Not reported
20	20*	20	44*	22*
22*	20*	21		32
22*	22	21*		33*
22	23	24		38
22	34*	24		
22	36	33		
23		35*		
24				
24				
27				
32				

* last reading of sounding

Its contents must not be quoted.

M.R.P. 481
S.C.I/21
21st March, 1949.

AIR MINISTRY

METEOROLOGICAL RESEARCH COMMITTEE

AD223135

Development of marine meteorological instruments

by

O.M. Ashford

AIR WEATHER SERVICE
TECHNICAL REFERENCE FILES

Introduction

This report summarises the experimental work on meteorological instruments done on board the O.W.S. "Weather Recorder" during the period 30th June - 26th July, 1948. The objects of the trip were to test various new instruments and to assess the accuracy of meteorological instruments used on board the Ocean Weather Ships.

Rainfall

Three different types of raingauge (see Fig. 1) were tried out. The modified standard gauge and the gimbal gauge were mounted on the roof of the balloon shelter and the conical gauge was suspended from aerial insulators above the roof. The conical gauge appeared to be best, largely because it requires no deck space. It is recommended that further tests should be made with the conical gauge in different parts of the ship.

The salinity of the water collected was measured by titration, by an electrical conductivity cell and by specific gravity beads. The beads are the simplest to use and, bearing in mind that the correction for sea spray will in general be small compared with the exposure errors, it is considered that the accuracy of this method, about $\pm$ 4%, is adequate.

Temperature and Humidity

Comparisons were made between the portable screen, clockwork and electric Assmann psychrometers and the hand aspirated psychrometer. It was found that the portable screen even when properly exposed can give rise to serious errors in dry bulb temperature (up to 4°F) and relative humidity and to a lesser extent in dew point (rarely greater than 1°F). Accurate results can be obtained with any of the aspirated psychrometers, but the manually operated model is the best all round instrument for use on ships. The present design suffers from a number of disadvantages and it should be re-designed to make it lighter and safer. It is also desirable to reduce the risk of parallax errors.

Cloud Height

A few tests were made to check the accuracy of visual estimates of cloud height in daylight. On each occasion independent estimates were obtained from as many of the meteorological staff as possible, and these were then compared with the heights computed from the time of disappearance into cloud of the radio-sonde balloon. The visual estimates were often in error by over 100% of the computed height; on one occasion the mean of eight independent estimates was 770 ft. when the computed height was only 400 ft. There is clearly a need for instrumental methods of measuring cloud height at sea both by day and by night.

Visibility

Observations were made with the Loofah visibility meter whenever the visibility was poor, and in every case the reading was greater than the visual observation, the difference being much larger than could be accounted for by errors in the visual estimates. It seemed probable that the air sample inside the Loofah was not representative; to check this, some observations were made with the lid removed from the instrument when the visual estimate of the

/visibility

visibility was $\frac{1}{2}$ mile. The mean readings with the lid on and off were 8 miles and $2\frac{1}{2}$ miles respectively. It is obviously essential to improve the present arrangement, either by mounting the instrument in a better position or by providing forced ventilation. Apart from this question of exposure, the most serious objection to the Loofah is that it makes no allowance for the light scattered by drops of rain or drizzle. In view of the frequency of occurrence of rain and drizzle in the Atlantic, this is bound to be a very serious limitation.

Tests with the Brewer-Beuttell meter, which can only be used at night, were limited to assessing its practical merits. Its handy size and portability are a pleasant contrast to the massive nature of the Loofah, and although the air sample is much smaller than in the Loofah it should be more representative. To set against these advantages is the excessive weakness of the illumination. Even in thick fog the images to be compared were very faint, and it was essential to have the eye in a dark adapted condition. With some practice it was possible to obtain consistent readings, but it is considered that in its present form the instrument is not suitable for routine work. It should be possible to design a better instrument on the same principle.

Temperature and Humidity Gradients

Observations were made of temperature and humidity gradients, when conditions were suitable, with the balanced bridge balloon psychrometer. This instrument consists of two platinum resistance thermometers mounted in a double-walled cylindrical tube through which air is drawn at about 20 ft/sec. by an electrically operated fan. The thermometers are the same as the M.O. aircraft resistance thermometers but with the outer brass casing removed and the wire protected by a coating of insulating lacquer. One thermometer is covered with a close fitting muslin sleeve which is kept wet by 3 or 4 strands of wick from a small water container on the outside of the instrument. The resistance of the thermometers is measured with a balanced bridge indicator with a dial calibrated direct in °F. The temperature can be easily read to the nearest 0.1°F.

The first test on 8th July was carried out from the bridge. The psychrometer was attached to a rope over a pulley mounted at the end of the forward aerial yard arm, and could be lowered over the side to within about a foot of the sea surface or raised to the height of the yard arm. To minimise the effect of the ship, the psychrometer was held about 2 ft. away from the ship's side at all heights from the bridge downwards.

Subsequent measurements were made with the psychrometer attached to a tethered 500 gm. balloon. The balloon was held by two strings, one to the stern of the ship and the other to a wooden or rubber dinghy. With this arrangement the psychrometer could be raised and lowered in air which had not come in contact with any part of the ship - the wind was always on the starboard beam. The maximum height was limited to about 100 ft., the length of the special 4 core cable available with the psychrometer. In the run on 14th July, power was obtained from a dry battery, but on 16th and 22nd July it was supplied from two 6-volt car batteries through a length of 2 core cable, which was a much better arrangement.

During the balloon trials, readings of sea surface temperature and of air temperature and humidity were made from the dinghy. The sea surface temperature was measured with an unprotected mercury-in-glass thermometer which was moved rapidly through the surface layer and read quickly before it could be affected by the air temperature. When the sun was shining, readings were made in the shadow of the dinghy. The air temperature and humidity were measured with a clockwork Assmann, held with the bulbs about 1 ft. above the sea surface.

The ship was stationary during all the gradient measurements. The results of the observations are given in Figure 2, it is not proposed to discuss them here in detail. The chief point is that it has been demonstrated that measurements of temperature and humidity gradients can be obtained at sea from a stationary ship under suitable conditions with the balanced bridge balloon psychrometer. The greater variability of the observation on 8th July is

/partly

partly because the work was carried out from the bridge and partly because of the calm conditions. Observations of sea and air temperatures made from a rubber dinghy in the afternoon showed that both were varying rapidly by as much as 2°F.

Sea and Swell

An Admiralty piezo-electric wave recorder was taken with the object of testing its suitability for routine use on the Weather Ships. In addition it was planned to compare its records with eye observations and if possible with cine-photographs of the waves. The pressure unit was successfully launched and the first record agreed well with visual observations of the waves. Unfortunately a leak developed overnight and the unit was rendered completely unserviceable by sea water: it was not possible to recondition it satisfactorily with the facilities available. An improved model is being made at the Admiralty Research Laboratory.

Atmospheric Pressure

Regular observations were made with two mercury and three aneroid barometers in the wheel house, and with two mercury and three aneroid barometers in the meteorological office. A German hypsometer was used as a portable instrument and was set up in turn in the wheel house and the meteorological office. 36 pairs of readings were made with the hypsometer in the two sites, and the mean difference was 0.92 mb. which is in good agreement with the estimated height difference of 24 ft. On only four occasions did the difference between the sites vary by more than ±0.1 mb. from the mean. This indicates that there is little to choose between the wheel house and the meteorological office as a site for a barometer (apart from pumping effects), and that the hypsometer readings are very consistent.

The German marine hypsometer is described in an unpublished report by Gelbke. It proved to be a most reliable instrument, capable of giving accurate pressure readings in relatively unskilled hands. Two thermometers were available and a series of comparison readings showed a systematic difference of 0.1 mb. Apart from one occasion, the difference between the two thermometers was always within the range of 0.1 ± 0.1 mb. The instrument showed up to best advantage in rough weather. When the mercury and aneroid barometers were "pumping" as much as 2 mb., it was difficult to see any effect at all in the hypsometer; presumably the large lag of the thermometer smooths out any rapid changes.

The readings of the mercury barometers were analysed statistically both by comparison with the hypsometer and by comparing the two pairs of barometers side by side. Assuming that the hypsometer contributes an equal share to the differences in readings between it and the barometer, the probable error of a single barometer reading was found to be 0.13 mb. by the first method and 0.11 mb. by the second. For comparison, the probable error of a mercury barometer at a land station, computed by the second method was 0.12 mb.

Three of the aneroid barometers were made by Wheeler, and the others by various German makers. The probable error of a single reading by comparison with the hypsometer was 0.08 mb. which suggests that for day to day readings, a good aneroid barometer is better on board ship than a mercury barometer. On the other hand, the zero errors of the Wheeler aneroids changed considerably in transit between Harrow and Greenock, and this defect will have to be remedied before they can be considered sufficiently reliable for routine use. On return to Harrow, all the pointers of the Wheeler aneroids were found to be dislodged so it was not possible to make a further zero check.

In addition to the ordinary open-scale barograph in an anti-vibration mounting, an oil-damped barograph was mounted on the table in the meteorological office. The records from the latter were consistently good, the maximum width of the trace being only about 0.3 mb. compared with 2.0 mb. from the ordinary barograph. The damping out of rapid pressure changes applies to genuine changes of the external atmospheric pressure as well as to the local changes due

/to

to the motion of the ship etc. On some quiet days it was obvious that some small genuine changes were only recorded with reduced amplitude by the oil-damped barograph. Likewise, abrupt changes of pressure were appreciably smoothed by the oil damping. Nevertheless there can be no doubt that for normal synoptic work the new barograph is much more suitable than the original type. The traces from both barographs were measured at the time of all the hypsometer readings and the probable error of a single reading was computed by comparing each barograph with the hypsometer and by comparing the barographs with each other. In all three cases the probable error was found to be 0.19 mb.

Sea Surface Temperature

Comparisons between the sea temperature bucket MK.III and other buckets confirmed the greater accuracy of the new model. Apart from one day of light winds and sunshine, the sea surface temperature was very uniform and it was possible to obtain results consistent to within $\pm$ 0.1°F. A thermograph was installed to record the temperature of the water entering the ship's condenser intake. Random differences between the recorded temperature and the sea surface temperature were never greater than 0.5°F.

Wind

Observations with the Elliott cup generator anemometer and a well exposed hand anemometer were compared with visual estimates of wind force. Close agreement was found, the difference rarely exceeding $\frac{1}{2}$ a Beaufort number. Simultaneous hand anemometer measurements were also made in various parts of the ship; in the well exposed situations the readings agreed to within $\pm$ 10%.

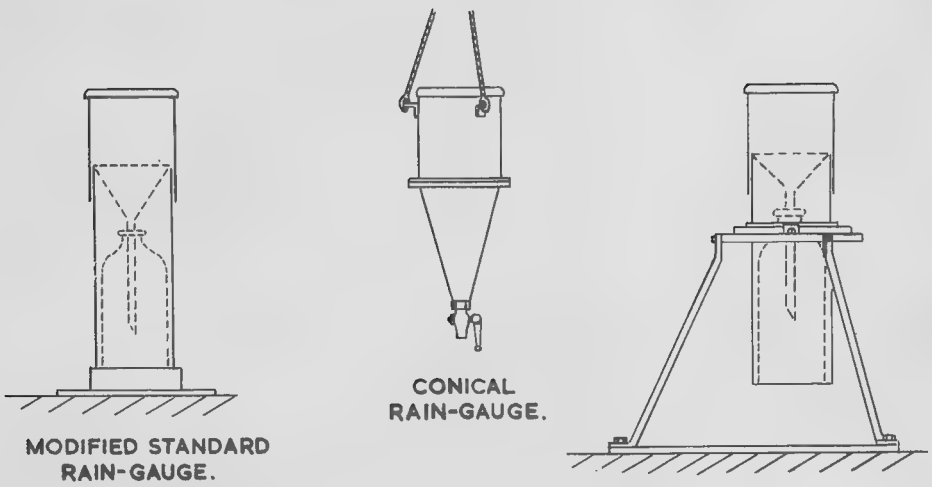

Fig. 1. Different types of raingauges.

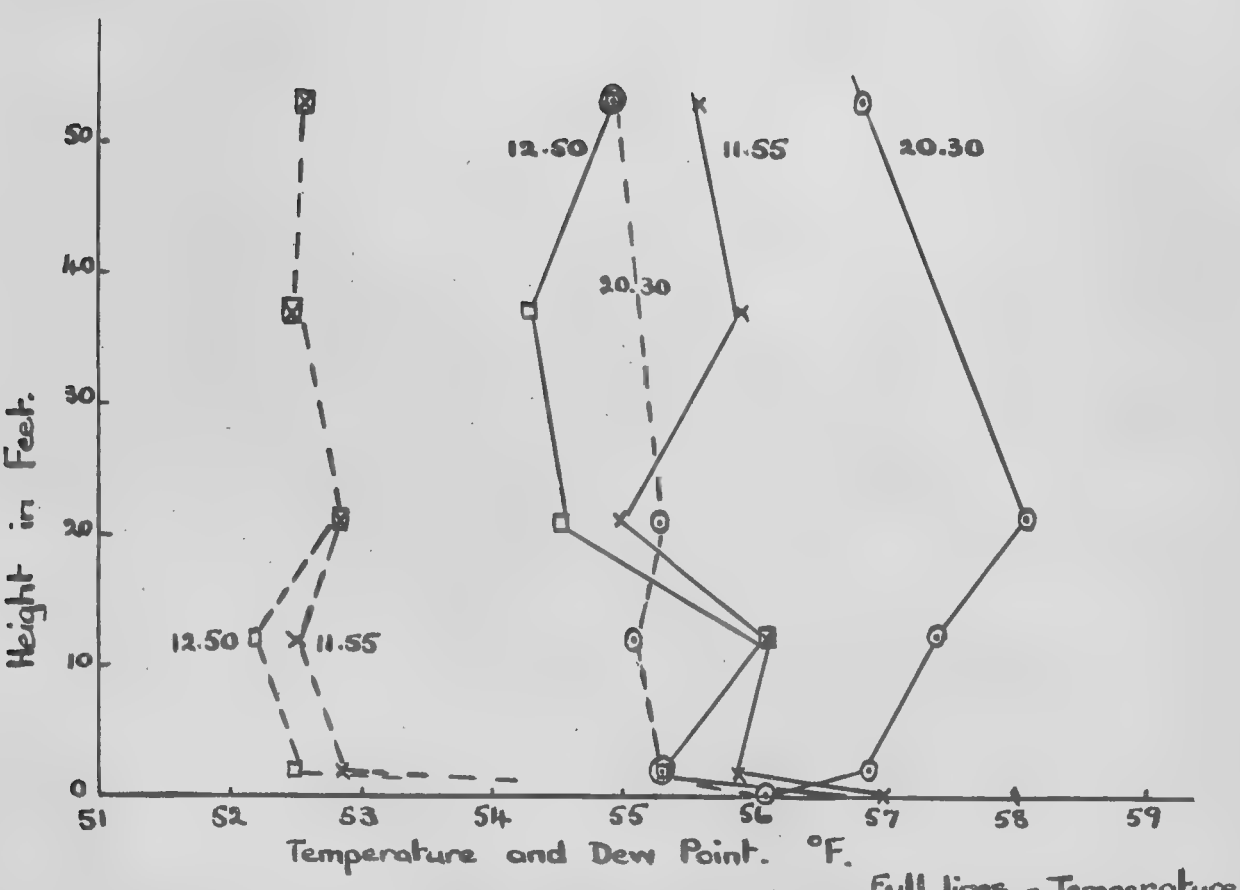

Fig. 2. Observations with balloon psychrometer

(a) Observations made from deck. 8.7.48.

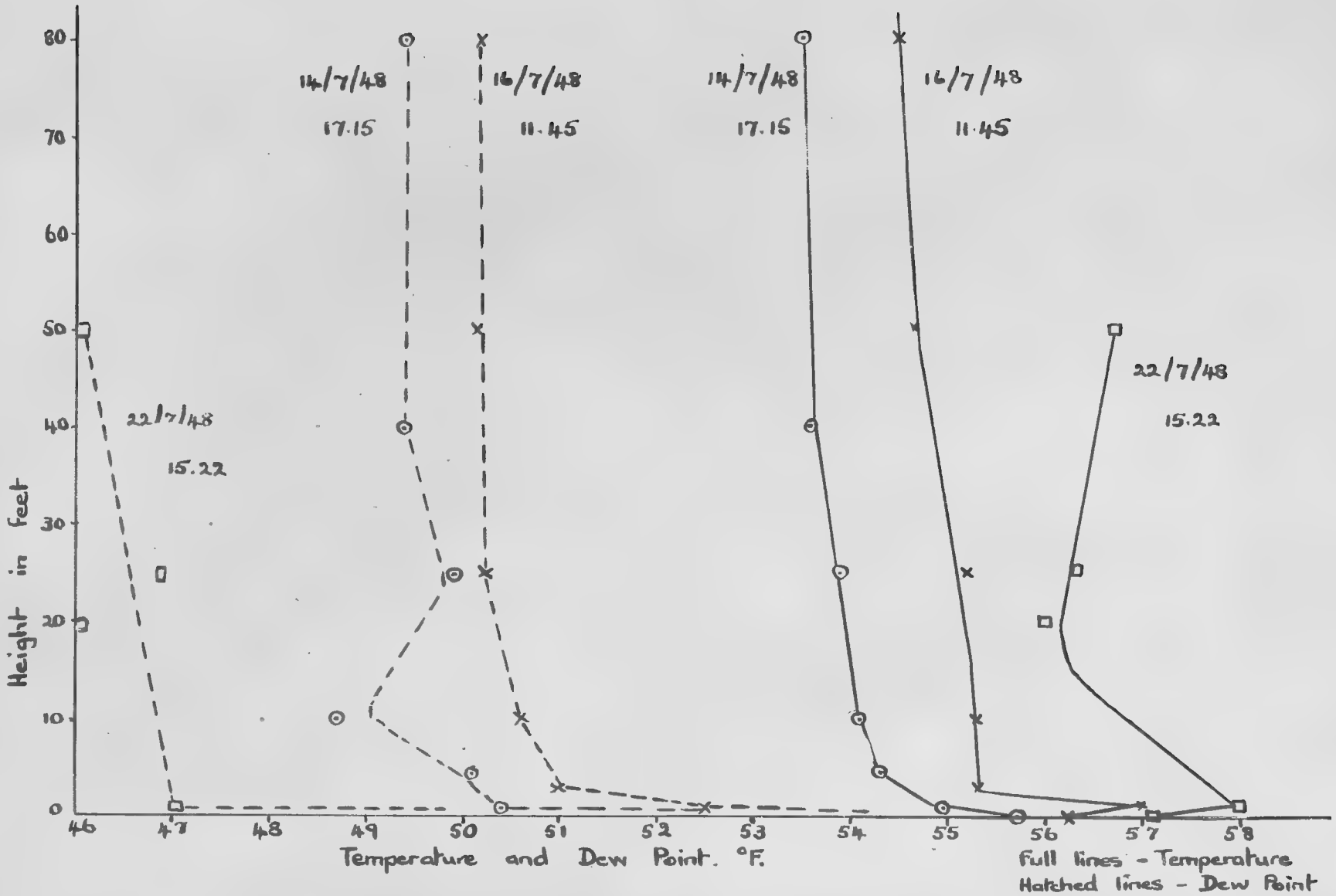

Fig. 2. Observations with balloon psychrometer.
(b) Instrument suspended from balloon.

This report has not yet been published and is to be treated CONFIDENTIAL. Its contents must not be quoted.

M.R.P. 482
S.C.III/27

4th April, 1949

Air Ministry

Meteorological Research Committee

Detection of Icing Conditions by Radar

Note by the Meteorological Office from information supplied by R.F. Jones (East Hill)

AIR WEATHER SERVICE TECHNICAL REFERENCE FILES

A. Introduction

Observations made at the Meteorological Radar Station at East Hill near Dunstable show that it is possible to infer with reasonable confidence the nature of the meteorological conditions producing weather echoes when existing ground equipment is used.

The equipment in question is A.M.E.S. Type 21, consisting of a Type 13 Height Range Indicator and a Type 14 Plan Position Indicator (P.P.I.)

The results of the analysis of a large number of Height Range photographs and other observations made around East Hill during the period March 1947 to October 1948 are given in M.R.P. 458.

The purpose of the present note is to discuss the probable significance of these results in relation to icing and to consider what might possibly be achieved by aircraft radar. At East Hill the Height-Range display has been found to be of most value, whereas aircraft at present carry only the P.P.I. display.

B. Significance of East Hill results in relation to Icing.

In inquiring into the possible application to detection of icing we have to consider specially the echoes received from clouds or parts of clouds above the freezing level. The position can be summarised as follows:-

1. Radar weather echoes originating in parts of a cloud above the freezing level are probably an indication of

(i) snowflakes of large enough size and number, formed by the sticking together of wet ice crystals, or

(ii) very large ice crystals in sufficient numbers, or

(iii) supercooled water drops of raindrop size in sufficient numbers, or

(iv) combinations of (i), (ii) and (iii) above.

2. Conditions (i) and (ii) are most likely to occur in layer type clouds and degenerate cumulus and cumulonimbus clouds and show up on the range-height display as horizontal bands (See photos I or II of M.R.P. 458). Condition (iii) is most likely in active cumulus and cumulonimbus clouds which may or may not be associated with extensive layer clouds; it shows up as a vertical column (See Photos V, VII, VIII).

3. Conditions (i) and (iii) of para. 1 above are favourable conditions for rapid ice accretion on an aircraft entering the weather echo while condition (ii) may not lead to ice accretion, if the ice crystals and the aircraft are dry but, if the aircraft has flown through a part of the cloud containing supercooled water droplets or if the ice crystals are co-existent with supercooled water particles which are not large enough to give a radar echo on their own account, then ice accretion is likely under these conditions also.

Conditions (i) to (iii) of para. 1 therefore may lead to severe ice accretion.

/4.

4. Conditions (i) to (iii) of para. 1 may occur without giving a radar echo if the reflecting particles are (a) not big enough or (b) not in sufficient numbers, so that ice accretion can occur in clouds which do not give a radar echo but it is reasonable to suppose that the most severe icing is likely in the parts of the clouds which give a radar echo extending above the freezing level.

5. The only experience available concerning ice formation in weather echoes comes from reports from Spitfire pilots engaged in the cumulonimbus turbulence investigations i.e. no information is available for layer type clouds.

The reports from the Spitfire pilots are not comprehensive and do not always give the degree of icing nor is it certain that there was definitely no icing when no mention was made of it. A preliminary assessment of the reports available bears out the suggestion of more severe icing inside the echo than elsewhere in the cloud. Other points of interest are:

(i) Complete icing up of the windscreen was reported on two occasions 5 seconds and 15 seconds after entering an echo while on a third occasion icing was so severe immediately after entering the echo that the flight was abandoned (this was the only occasion on which a flight was abandoned due to icing and occurred soon after the series of flights had been started i.e. before the pilot had considerable experience of cumulonimbus flying).

(ii) Moderate icing occurred in snow showers which failed to give a radar echo and some icing was experienced, on occasions, above the echo but with more severe icing in the echo itself.

(iii) A number of runs through an echo above the freezing level produced no mention of icing.

(iv) A noteworthy feature of the reports was the occurrence of rain, with no report of icing, at heights up to 3500 feet above the freezing level as determined by radiosonde ascents. On one occasion at 3400 feet above the freezing level, and after entering the echo, rain washed away ice which had previously formed on the aircraft.

C. Possibilities of aircraft-radar

1. The worst icing conditions could probably be detected and avoided by either a change of course to avoid the weather echo while remaining at the same height or by climbing to pass above the echo although all icing conditions will not thereby be avoided. It is understood that design of equipment, at present, limits the aircraft radar presentation to the PPI display and makes a narrow beam width virtually impossible (beam width is inversely proportional to the aerial aperture). In these conditions there must be some difficulty in deciding whether the echo received does in fact extend up to the line of flight of the aircraft. Tilting the scanner in the vertical plane, however, so that the axis of the main lobe of radiation was inclined at a small angle to the horizontal would probably reduce this difficulty but would still make it impossible to determine the vertical extent of the echo. The use of the PPI presentation therefore would be limited to the avoidance of echoes by change of course rather than change of height. Ability to sweep in the vertical plane would be a great advantage but presumably presents design difficulties.

2. It is doubtful whether, without a height-range display, it is possible to distinguish between supercooled water and ice crystals (with a height-range display the bright band effect would be of assistance) but it is probable that echoes which appear very sharp-edged when viewed with airborne equipment at ranges greater than 2 miles, say, are of the cumulonimbus type and contain supercooled waterdrops while echoes which fade gradually without a marked edge are probably from ice crystals or snow.

3. It would appear, at first sight, that an airborne 3 cm set would be more effective in detecting a weather echo than the 10 cm installation at East Hill, owing to the shorter ranges at which it is possible to work and the gain introduced by the shorter wave length ($1/\lambda^4$). The greater power available at

East Hill, however, combined with the much greater aerial size largely neutralises this effect so that an airborne set of 10 - 15 kw on 3 cm receives the same picture as the East Hill equipment at approximately 1/7.4 of the range if the volume investigated fills the radar beam i.e. what East Hill sees at 15 miles is the same as would be seen by the aircraft at 2 miles. It is justifiable therefore to compare results obtained at East Hill with those likely to be obtained using an airborne set at much shorter ranges. At the very shortest ranges (less than 1 mile, say) it is possible, but not certain, that the airborne set will see a larger echo than the East Hill equipment but it is to be presumed that the aircraft would require to take avoiding action some time before reaching such a short range.

4. The same indication which it is proposed to use to enable an aircraft to avoid severe turbulence will probably be at least as effective in enabling the aircraft to avoid the most severe ice accretion.

5. It would appear that a series of flights could usefully be made by a suitably instrumented aircraft in co-operation with East Hill to investigate more rigorously the relation of weather echoes to icing conditions.

Addendum

Since the above notes were written two further occasions have occurred when the Spitfire aircraft has experienced icing sufficient to cause the abandonment of the flight (see Section B, para. 5(i)).

On one occasion severe icing caused very uneven engine performance accompanied by (or possibly caused by) bad propellor icing and the aircraft made an emergency landing at the nearest available aerodrome.

On the second occasion the aircraft itself was not in jeopardy but the VHF aerial snapped off presumably due to heavy icing; in bad weather the lack of radio contact with the ground may have been very serious.

G. 237932/DS/7/49/120.

This report is not to be published without the consent of the Director of Research and Development (Met.) Air Ministry

METEOROLOGICAL RESEARCH COMMITTEE

A Note on M.R.P.472 - The Size Distribution of Cloud Particles in Strato-Cumulus Cloud - by R. Frith

by

A.C. Best

AIR WEATHER SERVICE
TECHNICAL REFERENCE FILES

1. In M.R.P. 472 Frith gives, in tables 1, 2 and 3, the results of measurements of the size distribution of cloud particles in three different clouds. It seemed worth while examining these figures to see whether the cloud particle size distribution could be represented by an empirical formula similar to that used in M.R.P. 452 for the size distribution of raindrops.

2. Each of the three tables in Frith's paper contains the measurements of samples collected on about a dozen slides. The slides in each table have been divided into three groups according to the total mass of water represented by the particles on the slides. The allocation of the slides to the groups was as follows.

	Table 1	Table 2	Table 3
Group 1	40, 41, 42, 44, 45	2, 6, 7, 8, 11	5, 12
Group 2	35, 36, 46	3, 9, 10, 12	2,4, 6, 7, 8,9,11,15
Group 3	37, 38, 39, 43	4, 5, 13, 14	3, 13, 14

For all the slides of each group from each table the mass of water comprised by particles in the various particle size ranges was totalled. These water masses were then added cumulatively and the cumulative total corresponding to any diameter expressed as a percentage of the total mass of water on all slides in the group (this process is described more fully in M.R.Ps. 352 and 452).

3. Let F denote the fraction of water in the group of samples which corresponds to cloud particles with diameter less than d microns. In fig. 1 $\log \log (1/(1 - F))$ has been plotted against $\log d$. In this figure points corresponding to less than 2% of the total water present, both at small and large diameters, have been omitted. The best straight lines to fit these points have been computed by the method of least squares and are shown in fig. 1. It is clear that, to a close approximation, the drop size distribution in 96% of the liquid water in these clouds can be represented by the formula

$$1 - F = \exp - \left(\frac{d}{a}\right)^n$$

where n and a are constants in any particular group.

4. The values of n and a were obtained from the computation of the line of best fit for each group. These quantities, together with some other data from Frith's tables, are tabulated below.

Table	Group	No. of Slides	n	a	Total Water	Vol. of Air	Water Conc.
				μ	gms x 10^{-9}	cc	gms. 10^{-9}/cc
1	1	5	2.52	24.2	2938	6.25	470
	2	3	2.80	24.8	2333	3.75	622
	3	4	2.50	29.0	4133	5.00	827
2	1	5	3.06	18.1	653	3.85	170
	2	4	2.29	29.4	1001	3.08	325
	3	4	2.34	31.1	1509	3.08	490
3	1	2	3.74	13.3	111	1.54	72
	2	8	4.42	14.2	1269	6.16	206
	3	3	3.83	16.1	936	2.31	405

It appears from this table that there is no systematic variation of n either from cloud to cloud or from group to group. Moreover it is of interest that n is of the same order as was found for raindrops (M.R.P. 452).

The value of "a" however increases with increasing liquid content of the same cloud.

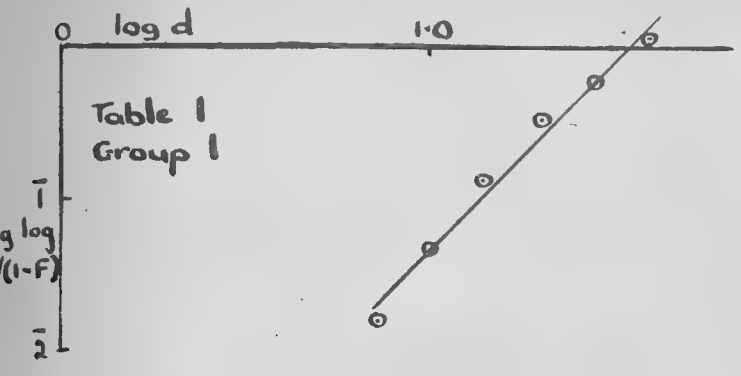
0
log d
1·0
Table 1
Group 1
$\bar{1}$
$\bar{2}$
g log
(1-F)

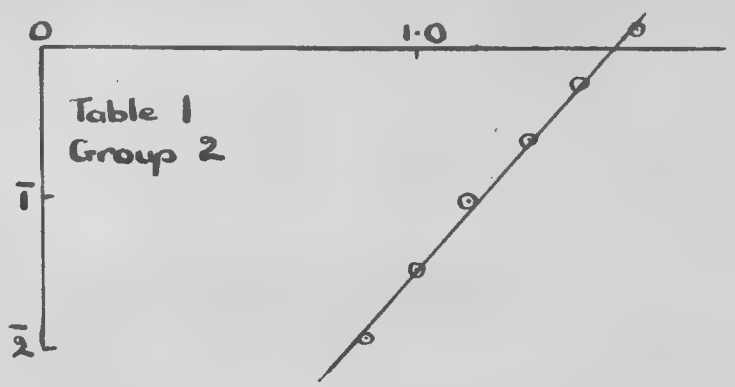
0
1·0
Table 1
Group 2
$\bar{1}$
$\bar{2}$

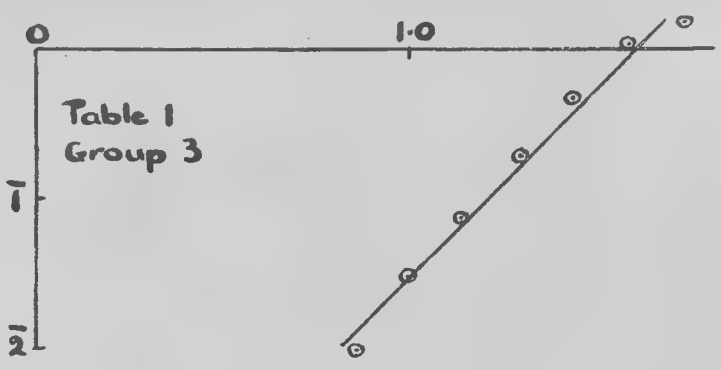
0
1·0
Table 1
Group 3
$\bar{1}$
$\bar{2}$

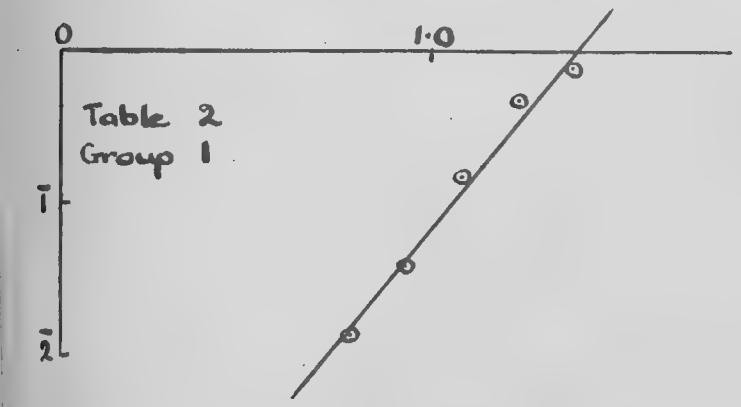
0
1·0
Table 2
Group 1
$\bar{1}$
$\bar{2}$

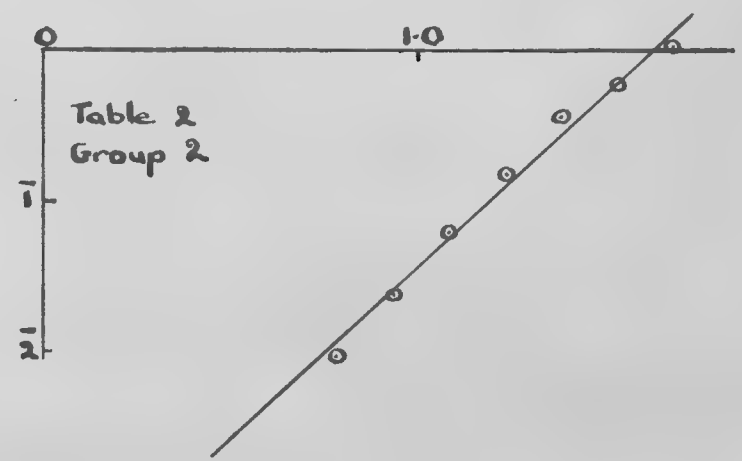
0
1·0
Table 2
Group 2
$\bar{1}$
$\bar{2}$

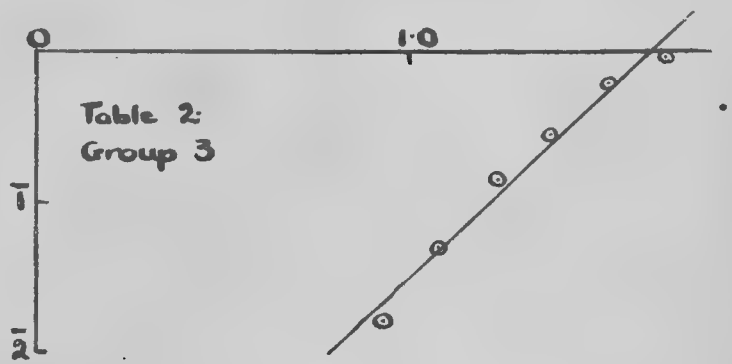
0
1·0
Table 2
Group 3
$\bar{1}$
$\bar{2}$

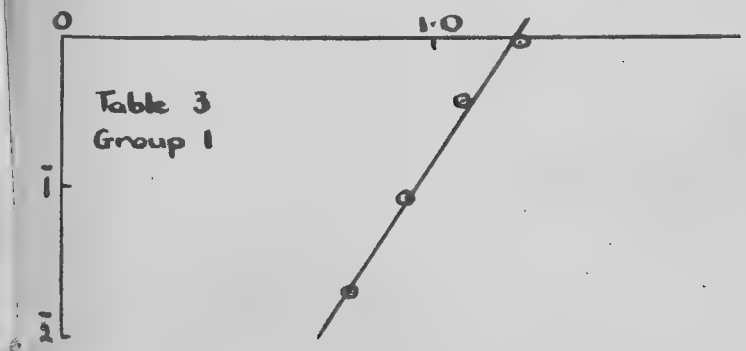
0
1·0
Table 3
Group 1
$\bar{1}$
$\bar{2}$

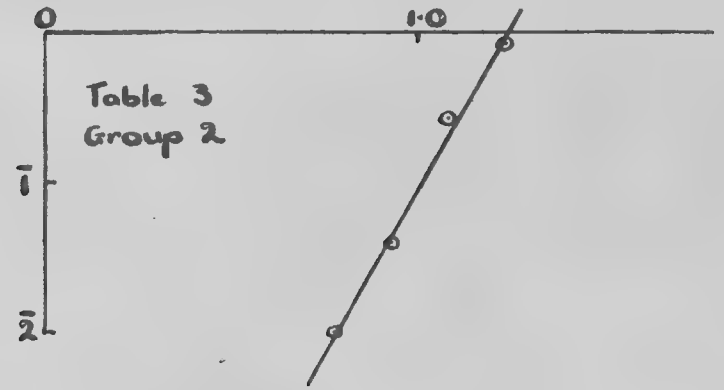
0
1·0
Table 3
Group 2
$\bar{1}$
$\bar{2}$

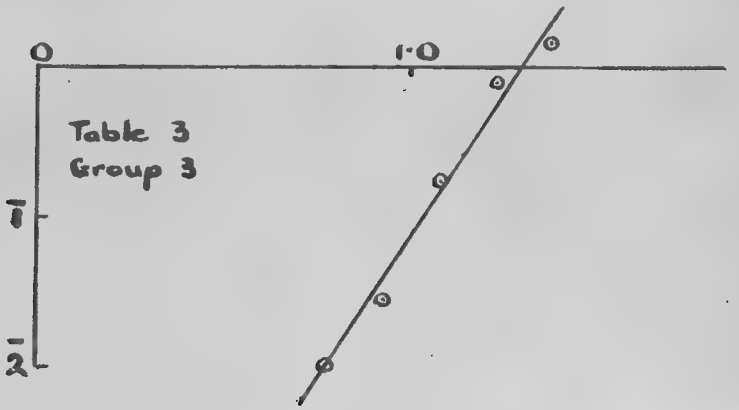
0
1·0
Table 3
Group 3
$\bar{1}$
$\bar{2}$

... quoted.

M.R.P.484
S.C.III/29
14th April, 1949.

AIR MINISTRY

METEOROLOGICAL RESEARCH COMMITTEE

AIR WEATHER SERVICE
TECHNICAL REFERENCE FILES

The Relation between the Radar Echoes from Cumulus and Cumulonimbus Clouds and the Turbulence within those Clouds.

by R.F. Jones.

A report on the first year's operation of the cumulonimbus trials at the Meteorological Office radar station at East Hill in co-operation with aircraft from the Royal Aircraft Establishment at Farnborough.

1. Introduction

The likelihood of the occurrence of severe turbulence within clouds has, in the past, always been related, on the basis of considerable experience, to the visual characteristics of the cloud. On this basis it has been possible to describe the appearance of clouds which are likely to be excessively turbulent and those which would be expected to be relatively smooth. The classification adopted has been in accordance with the recognised meteorological descriptions of cloud types and it has long been recognised that the most turbulent clouds are those of the cumulonimbus and cumulus type. The use of visual characteristics has certain obvious and severe limitations, of which the most marked is the inability to distinguish cloud types in darkness or when the turbulent cloud is obscured from view by intervening layers of cloud. The advent of radar and the discovery that radar echoes can be detected from clouds and precipitation which contain sufficient numbers of drops of great enough size led to the suggestion that the radar characteristics of a cloud may be a useful substitute for the visual ones in the detection of turbulent clouds.

To explore this possibility a series of experiments is being undertaken at the Meteorological Office radar station at East Hill, near Dunstable, and the present report is concerned with the results of the first year's trials.

2. The radar equipment

The radar equipment in use at East Hill is the standard equipment known as A.M.E.S. Type 21, which consists of a Type 13 height-range indicator and a Type 14 plan position indicator (P.P.I.) both operating on a wave length of 10 cm. with a peak power output of 500 kW and a pulse length of 2 microseconds. The aerial of the height-range equipment is mounted to sweep continuously in the vertical plane from -1° to 19°, the complete up and down movement taking 10 seconds, and can be turned to any desired azimuth by remote control from the Operations Room. The aerial, which is a section of a parabolic metal cylinder, gives radar beam widths (measured to half power) of $7\frac{1}{2}$ degrees in the horizontal and $1\frac{1}{2}$ degrees in the vertical plane. The P.P.I. equipment has a similar aerial which is mounted to rotate in the horizontal plane at speeds up to 6 revolutions per minute with beam widths of $1\frac{1}{2}$ degrees in the horizontal and $7\frac{1}{2}$ degrees in the vertical planes.

The displays are such that the Type 13 indicator gives the height and range of an observed echo directly while the P.P.I. gives a bird's eye view of the area surrounding the station and hence the bearing and range of a particular echo. A modification of the Type 13 indicator enables it to be used alternatively as an A-scope giving the intensity of any desired echo.

In operation the P.P.I. equipment is used on continuous rotation and the height-range equipment is turned to the bearing (as indicated by the P.P.I.) of the particular weather echo under examination. An indication of the three-dimensional structure of the weather echo can thus be obtained.

Incl #11

/3.

3. The radar echoes from cumulus and cumulonimbus clouds and discussion of the problem to be investigated

The writer has given elsewhere(1) a description and interpretation of the various types of weather echoes as viewed in the vertical cross-section and has shown how it is possible, after some experience, to distinguish cumulonimbus and cumulus weather echoes from those associated with other cloud formations. The outstanding characteristic of the cumulonimbus type of echo is the appearance of the echo in the form of a strong vertical column with sharply defined vertical edges (see photograph (i)) or in the more extensive formations as, for example, in the thunderstorms which occasionally move north across this country from France, a number of strong columns separated by well marked troughs (photograph (ii). The P.P.I. presentation (photograph (iii)) shows the echoes to be isolated and sharp-edged. Decay of a cumulonimbus is indicated by a tendency for the edges and tops of the echo columns to become less sharply defined and in the later stages there is the appearance of a bright band near the freezing level while the echo loses its well defined column structure (photograph (iv)).

It is important, however, to note that the echo received does not indicate the whole volume of the cloud but only that part of the cloud in which the drop sizes and concentration are great enough to give a detectable signal at the radar receiver. The intensity of the signal received from a volume containing water drops has been shown by Ryde(2) to be proportional to $\sum ND^6$ where N is the number of drops of diameter D per unit volume, so that one single raindrop of diameter 2 mm, say, can give an echo equivalent to that from a million cloud particles of diameter 0.2 mm. The echo from a precipitating cloud, therefore, or from a cloud containing drops of raindrop size suspended in the vertical currents is likely to be enormously greater than that from an ordinary cloud or part of a cloud in which the droplets have not grown above cloud particle size, unless there are some clouds which contain millions of times more cloud particles than a precipitating cloud - which is very unlikely.

With the equipment in use at East Hill experience has shown that the minimum detectable signal is such that it is highly probable that at ranges at which the experiments were performed (over 10 miles) echoes are only received from cumulus and cumulonimbus clouds which are precipitating or which contain raindrops suspended in the vertical current. Clouds or parts of clouds in which the drop size has not reached to raindrop size are not likely to give an echo with this equipment at the ranges used for these experiments.

The radar therefore will indicate the presence of precipitating cumulus and cumulonimbus clouds and hence indicate the general areas where turbulence is likely to be severe but for the maximum use to be made of the radar it is necessary to investigate whether the part of the cloud which gives an echo is the most turbulent part. It is not immediately obvious that large drops in a cloud (and hence a weather echo) and heavy turbulence must be related but, in general terms, it might be reasonable to expect that the largest drops would occur in the strongest up-current, since in such currents the drops will be a longer time within the cloud and hence have a greater chance of growth. Byers and Braham(3), however, have suggested that the precipitation within a cumulonimbus cloud initiates a down-current so that, on this hypothesis, a radar echo might also be associated with a down-current. Turbulence however is presumably related to the way in which the vertical currents change in the horizontal so that passage, for example, from a down-current to an up-current would be expected to give a severe bump, if the edges of the up and down currents were sufficiently clearly defined with only a very narrow zone of transition. The large scale currents themselves may be "solid" currents with little horizontal changes in value and hence relatively small turbulence compared with that encountered at the edges of the current.

The problem to be investigated therefore resolved itself into the question whether the radar echo is the most turbulent portion of the cloud and whether any characteristics of the echo give an indication of the degree of turbulence to be expected and the places within the echo where turbulence is greatest.

/4.

4. The procedure adopted

Arrangements were made with the Royal Aircraft Establishment at Farnborough for Spitfire aircraft from the Aero Flight to participate in the investigation of turbulence in cumulus and cumulonimbus clouds under the general direction of the radar station at East Hill.

As well as with the normal instruments, the Spitfire was equipped with a vertical acceleration recorder with a time base; the recorder could be switched on and off by the pilot and it was possible to get a total of about 20 minutes record on any one sortie. All cloud flying was done at an indicated airspeed of 180 m.p.h. The pilot was briefed to keep his attitude both in pitch and roll as constant as possible when traversing the clouds. Due to the stability characteristics of the aircraft only small corrections were necessary to maintain attitude in pitch but considerably more effort was required to keep the aircraft laterally level.

On any particular sortie the Spitfire aircraft would fly north from Farnborough at a pre-arranged height until identified on the radar display tubes. The rather small echo from a Spitfire made this occasionally a matter of some difficulty and necessitated the great majority of the flights being made within a radius of 40 miles from East Hill. After identification the aircraft was controlled by radio telephone from East Hill and the pilot was given vectors to steer to put him close to a chosen echo. Normally the pilot would be able to recognise the cloud of which the echo was part and he was then given the height to fly through the cloud and the course to steer while in the cloud. This course was chosen so that the aircraft flew either directly towards or directly away from East Hill which meant that the aircraft always investigated the cloud along the line of the radar beam of the height range equipment. A vertical cross-section of the radar weather echo along the line of flight of the aircraft was therefore visible on the height range display tube as well as the echo from the aircraft as long as it was outside the weather echo. The pilot switched on his accelerometer immediately on entering cloud and off again as soon as he was clear of cloud on the other side, the instants of switching on and off being communicated by R/T to East Hill. Readings and photographs of the height range tube were taken at East Hill during the aircraft traverse and particular note made of the instants of entry into and departure from the echo. On some occasions measurements of the intensity of the echo were also made while P.P.I. photographs were taken from time to time.

A number of such flights at different levels would be made through a single echo. If time permitted, other echoes would also be investigated while on some occasions the pilot was directed to an area clear of echo with instructions to make flights through the best developed cumulus he could find. This enabled some comparison to be made of the turbulence in clouds containing an echo with that in clouds which gave no echo at East Hill.

5. The analysis of the accelerometer records

The analysis of the accelerometer records was undertaken by R.A.E. and was normally expressed in the form of a table for each cloud traverse giving the number of gusts encountered of specified magnitude, expressed in terms of the accelerations imparted to the aircraft, up and down gusts being shown separately. These accelerations were given in increments of 0.1g i.e. the ranges 0.1 - 0.2g, 0.2 - 0.3g, 0.3 - 0.4g etc., g being the acceleration due to gravity.

The accelerations measured in this way give an indication of the gradient of the vertical velocity profile at the point where the gust occurs but, as the duration of each gust is likely to vary, only a general indication of the vertical velocity profile could be obtained from a detailed analysis of the points of occurrence of each individual gust.

(By making various assumptions the aerodynamicist is able to convert the acceleration increments into gust velocity increments of the equivalent air speed. An acceleration increment of 0.1g corresponds to an increment, in this report, of 3.6 ft/sec. in equivalent air speed, when this gust velocity is obtained

/"using

"using the standard sharp-edged gust formula with an alleviation factor allowing for the Wagner effect and for an average gust gradient distance of 100 ft.". Throughout this report however the accelerations themselves are used as an indication of gust magnitude and the lower value of each range is used in the graphical illustrations).

On many occasions it was possible to indicate in the analysis sections of the traverses where the turbulence was noticeably greater as regards frequency of gusts or where noticeably smooth patches were encountered and on two occasions (see Section 8(a)) the actual point of occurrence on the traverse of each gust was extracted.

Finally, on a number of those traverses in which gusts greater than ± 0.4g were encountered, the points of occurrence of these especially large gusts were noted.

6. The data available and methods of analysis used

The aircraft first became available in August 1947 and up to and including 4th October, 1948, 26 separate sorties have been made involving 139 traverses of clouds and a total distance flown in cloud of some 700 miles.

For each of these traverses the accelerometer record has been analysed as indicated in Section 5 and for the great majority there are photographs of the height range display tube during the aircraft traverse together with written records of the times of entry into and departure from cloud and echo, times of display tube photographs and comments made by the pilot while in cloud.

Details of the sorties are given in Table I.

In analysing the data two approaches have been made;

(i) a statistical examination of the gust data and (ii) a detailed examination of individual traverses.

These two approaches are dealt with in Sections 7 and 8 below.

7. The statistical analysis of the data

(a) Relation between the vertical extent of the echo and the maximum gusts encountered in the cloud containing the echo.

An analysis would be expected to yield evidence concerning any correlation between the maximum gusts encountered in a cloud containing an echo and any particular characteristic of the echo. One easily discerned characteristic of an echo is its vertical extent and Fig. I shows the result of plotting the maximum up-gust encountered on flights which went through the echo against the height of the echo top above the freezing level. The height of the echo top above the freezing level was chosen in preference to the height above the ground in order to minimize as far as possible differences due to seasonal and air mass effects. Also shown on the line of zero height are the maximum up-gusts encountered in clouds which gave no echo at all.

It will be seen that, although there is a considerable scatter of the observation points, there is a tendency for the maximum up-gust to increase with increase in the height of the echo top above the freezing level, but if the echo extends only some 5,000 feet above the freezing level the gusts encountered are not likely to be any more severe than in clouds which gave no echo at all. The considerable scatter of the points indicates that other factors as well as the vertical extent of the echo must be taken into account.

A similar analysis in respect of down-gusts is shown in Fig.II and we see that only in the very biggest echoes were maximum down-gusts experienced greater than in clouds giving no echo at all and indeed for echoes extending up to about 16,000 feet above the freezing level the maximum down-gust would appear to be independent of the vertical extent of the echo.

/(b)

(b) The appearance of the echo in relation to the maximum gusts encountered in the cloud containing the echo

As mentioned in Section 7(a) above, although the vertical extent of the echo gives a general guide to the severity of the biggest gusts likely to be encountered in the cloud containing the echo, especially in relation to up-gusts, other factors must also be taken into account. Thus an echo of considerable vertical extent may be received from a cloud which is either (a) still growing, (b) at its maximum activity in regard to the vertical currents within it, or (c) in the process of decay but still having sufficiently large, both in size and number, radar-reflecting particles at a considerable height within the cloud. It seems reasonable to suppose that clouds in these three stages, although giving a radar echo extending to the same height, may give maximum gusts differing considerably in magnitude. It is possible that other characteristics of the radar echo may assist in deciding the stage of development which the cloud has reached. The only other characteristic of the echo which can be obtained from the height-range display is the general appearance of the echo with particular reference to the sharpness or otherwise of the edges and tops and the existence of more than one column within the echo. One other characteristic may be obtained by use of the A-scope, namely the intensity of the echo. In this latter connection it has only been possible to measure the intensity of the echo with the aerial sweeping up and down through the echo so that the maximum signal from the whole echo was all that could be measured and not the actual intensity along the line of flight of the aircraft. In addition the difficulty of maintaining contact with the aircraft on the display tube made it impossible on some occasions to take intensity readings.

In Table II is given a general description of the appearance of the echo at the time of the flights through the echo which gave the maximum gusts i.e. the data used for Figs. I and II in Section 7(a) above. Also shown, when available, is the maximum signal strength from the echo adjusted to give the relative received power as if every echo had been viewed at a common range of 20 miles. In order to make comparison easier and to minimize the effect of the vertical extent of the echo - which has been shown in Section 7(a) to exercise a general influence on the up-gust strengths at least - the table is split up to give comparisons between echoes in different ranges of vertical extent of the echo.

It will be seen that in each range of vertical extent the type of echo which gives the greatest up-gusts in the cloud containing the echo is the type which has clear cut edges and tops and sometimes a number of columns and troughs. Conversely relatively smooth conditions are found in clouds containing echoes which have diffuse edges and tops. The correlation of down-gusts with echo appearance is not so well marked and bears out the suggestion of Section 7(a) that, except in the echoes of great vertical extent (more than 16,000 feet above the freezing level), the magnitude of the down-gusts likely to be experienced is not indicated by the presence or otherwise of a weather echo.

In general up-gusts greater than 0.5g occur only in clouds containing echoes showing clear cut edges or more than one column, although one up-gust of 0.6g was encountered in a cloud which gave no echo at all. Clouds which contain echoes with diffuse edges and tops do not give any bigger gusts, up or down, than have been experienced in clouds giving no echoes at all.

With regard to the intensity of the echo it can be seen that the up-gusts of 1.1g and greater occurred in clouds with exceptionally strong echoes but that otherwise there was little correlation between echo intensities and maximum up-gusts. (For example, maximum up-gusts of 0.5g were associated with relative power readings of 355, 40 and 17 while an up-gust of 1.0g was associated with a relative power reading of only 132). The small number of intensity readings, however, does not warrant any firm conclusions.

Thus the appearance of the echo in the vertical cross-section combined with the vertical extent of the echo would appear to give a useful guide to the maximum up-gust likely to be encountered in the cloud containing the echo.

/That

That the appearance of the echo is a useful guide to the activity of the cloud has already been indicated (Section 3, para. 2) and the evidence of Table II supports this idea. The clearly defined and sharp-edged echoes are associated with clouds which are still growing or have only recently reached their maximum activity while a tendency for the edges and tops to become diffuse indicates a decline in activity and decrease in turbulence.

Photographic examples of echoes of large vertical extent with only small up-gusts and of small vertical extent with large up-gusts are given in photographs (iv) and (v) respectively.

(c) Frequency of occurrence of gusts of various magnitudes

A statistical analysis would be expected to yield evidence regarding the frequency with which gusts of a certain magnitude would be encountered when flying through cumulus and cumulonimbus clouds. In the Thunderstorm Project, the Americans(4) (page 4) "arbitrarily decided that for this study only those echoes which extended to at least 25,000 feet would be considered as thunderstorms". 25,000 feet is 9,000 feet above the average freezing level in Florida in summer (page 10). Although there is some reason to believe(1) that the value of 9,000 feet above the freezing level is much too low as a criterion for the vertical extent of a thunderstorm echo it nevertheless seemed worthwhile, for comparison purposes, to separate in this analysis the flights through clouds containing an echo extending more than 9,000 feet above the freezing level from those containing echoes of a less vertical extent and no echoes at all.

In making the analysis the flights were arranged according to the height above or below the freezing level at which the flights took place and the flights in each interval of 2000 feet were then divided into those through clouds containing echoes extending 9,000 feet or more above the freezing level and those through clouds with smaller or no echoes. The numbers of gusts of a certain magnitude, irrespective of sign, were then extracted for each category. Since different distances were flown at different levels the analysis has been expressed in the form of the average number of yards flown in cloud before encountering a gust of specified magnitude. The results of this analysis for the various levels are given in Table III and are shown graphically in Figs. III to XV.

It will be seen that the plotted values for each category of cloud at each level lie reasonably close to smooth curves and where comparison is possible (up to 12,000 feet) there is a significant increase in frequency of the larger gusts when the flights are made through a cloud containing an echo of large vertical extent.

At levels higher than 6,000 feet above the freezing level, however, there appears to be a tendency for the gusts in the ranges 0.1 - 0.2g and 0.2 - 0.3g to be more frequent in the clouds containing the small echoes.

In Fig. XVI is shown the results of plotting the gust frequency for all flights irrespective of height. In this figure a distinction has been drawn between clouds containing an echo extending to less than 9,000 feet above the freezing level and those which gave no echo at all at East Hill. Of the three curves there drawn it is interesting to note that although, as expected, clouds containing big echoes had the greatest frequency, the clouds which gave no echoes at all had a noticeably greater gust frequency than those which gave echoes of relatively small vertical extent (less than 9,000 feet above the freezing level). This suggests that the flights through clouds containing echoes of small vertical extent were probably in many cases through degenerate cumulonimbus clouds with rather weak turbulence while the clouds which failed to give an echo were specially chosen by the pilot as the best developed clouds available in the area free from echo to which he had been sent.

As an indication of the relative magnitudes involved the following values may be quoted from Fig. XVI. Gusts of 0.8 - 0.9g are likely to occur on the average once in 143 miles of cloud flying in clouds containing echoes extending to less than 9,000 feet above the freezing level; once in 59.5 miles of cloud

/flying

flying in well developed cumulus clouds without an echo and once in 20 miles of cloud flying in clouds containing echoes extending more than 9,000 feet above the freezing level.

(d) Variation of gust frequency with height

By using the curves in Figs. III to XV it is possible to obtain smoothed values of the average distances to be flown in clouds containing an echo extending more than 9,000 feet above the freezing level before encountering a gust of specified magnitude. These "smoothed" distances have been plotted in Fig.XVII against the height of flight above the freezing level for the various gust values in terms of g. Also shown on the graph are the distances flown in each of the 2,000 feet height intervals and the number of flights which contributed to that distance.

It is doubtful whether the distances flown at the various heights are sufficient to permit the formulation of definite conclusions but tentative conclusions are listed below.

(i) For gust values 0.1 - 0.2g, 0.2 - 0.3g, 0.3 - 0.4g and 0.4 - 0.5g there appears to be a definite tendency for the gust frequency to decrease slowly with height, this tendency being more marked for the lowest gust values of 0.1 - 0.2g and becoming progressively less marked for higher gust values until the average gust frequency is almost constant with height for values of 0.5 - 0.6g.

(ii) For gust values of 0.6 - 0.7g and greater the scatter of observations is much greater, as may be expected, due to the considerable decrease in frequency with which such gusts were recorded. There appears however the possibility of zones of maximum turbulence in the levels 0 - 2,000, 6,000 - 8,000 and 14,000 - 16,000 feet above the freezing level with a possibility of least turbulence in the zones 2,000 - 6,000 feet and 10,000 - 12,000 feet above the freezing level. Whether any significance can be attached to these zones is, as stated above, very doubtful but it is noteworthy that the 2,000 - 6,000 feet zone of minimum turbulence includes the two levels in which the greatest distances were flown and, furthermore, the 2,000 - 4,000 feet interval which comprised the greatest distance of all levels failed to yield any gusts greater than $\pm$(0.7 - 0.8g) although this value was exceeded at all other height intervals except the relatively short one at 10,000 - 12,000 feet.

(iii) The absolute maximum gust measured (+1.5g) was recorded at 30,000 feet and 19,200 feet above the freezing level although on this sortie flights were also made at 10,000, 15,000, 20,000 and 25,000 feet, while up and down gusts of 1.1g were encountered at 36,000 feet (23,000 feet above the freezing level) on another occasion.

In the report on the Thunderstorm Project(4), a clearly marked zone of maximum turbulence is indicated near the freezing level but, no flights were made at heights greater than 9,000 feet above the freezing level. On the other hand, due to the much lower average height of the freezing level, flights at considerable distances below the freezing level were not possible in the experiments described in the present report, and it may well be that the zone of maximum turbulence noted in America near the freezing level receives greater emphasis from a marked decrease in frequency of gusts at levels below the freezing level. The curves of Fig.XVII give only slight evidence of greater turbulence near the freezing level than is experienced at much greater heights within the cloud.

There remains however the possibility that the relation of the zone of maximum turbulence to the freezing level in the American flights is fortuitous and that the height represents an average height above sea level in the very large cumulonimbus clouds of the tropical regions at which the turbulence may be expected to be greatest. For this reason the data used to obtain Table III and Figs.III to XV have been re-assessed to give the gust frequencies at various height intervals above mean sea level for flights through those clouds

/which

which contained an echo extending 9,000 feet or more above the freezing level. The information so obtained is shown in Table IV and the distribution of gust frequencies with height is shown in Fig.XVIIa which is obtained in a precisely similar way to Fig.XVII except that the height intervals used were 4,000 feet in depth compared with 2,000 feet for Fig.XVII.

Significant features of this graph are listed below.

(i) For a broad range of heights from the 10,000 - 14,000 feet layer to the 18,000 - 22,000 feet layer, (above sea level) which comprises the three layers in which most flights were made and the greatest distances flown, the gust frequencies are sensibly constant.

(ii) There is a progressive decrease in frequency of gusts with descent below the 10,000 - 14,000 feet layer which is most marked for the gusts greater than 0.3g. This suggests that the advice frequently given to pilots to attack cumulonimbus clouds at the lowest possible height is well-founded.

(iii) The number of flights above the 18,000 - 22,000 feet layer was small and may not give representative results but it is noteworthy that, except for the gusts of 0.1 - 0.2g and 0.2 - 0.3g the frequency of gusts is greater in the 22,000 - 26,000 feet layer than in the layers below and remains high at the other higher layers.

On the whole the evidence so far obtained in these flights can only be regarded as inconclusive concerning zones of maximum and minimum turbulence although there is a possibility that the lowest possible flight level, provided this is below 10,000 feet, may give less turbulence than higher in the cloud, while the probability of severe gusts at very great heights on some occasions cannot be overlooked. Through a considerable range of heights above 10,000 feet there is probably little change in turbulence with height in the well developed cumulonimbus clouds which give echoes extending 9,000 feet or more above the freezing level. Comparison with the American results, which were obtained under much more uniform cloud conditions than occur in England, suggests that the height in the cloud at which turbulence will reach a maximum value (at which value it may remain for some further considerable increase in height) is a proportion of the total vertical extent of the cloud - probably rather less than one half. Confirmatory evidence for this hypothesis may be found in the fact that in America the mean maximum radar top of the storms(4) (page 6) was 37,000 feet while in these experiments the value was 25,000 feet.

8. Detailed analyses of particular traverses

The statistical analyses of Section 7 have revealed the fact that the presence of an echo having certain distinctive features within a cumulus or cumulonimbus cloud may be an indication of the degree of turbulence and the maximum gusts likely to be experienced on a flight through the cloud; i.e. some comparison is possible of the turbulence likely to be encountered within different clouds. The analyses do not, however, give any indication of where the zones of maximum turbulence occur within a particular cloud and more especially whether the echo part of the cloud is more turbulent than the part free from echo. To obtain information on this aspect it is necessary to examine individual traverses of a cloud and echo in detail.

(a) The complete gust analysis of two flights through a cloud containing an echo.

The positioning of every individual gust on a flight through an echo is a laborious and lengthy task which cannot be made for every cloud traverse. Such analyses however have been made for two traverses made on the following dates (i) 20th April, 1948 and (ii) 10th June, 1948.

/(i)

(i) Traverse made at 13,000 feet on 20th April, 1948

On this day a cumulonimbus cloud which had been observed from the air to be growing rapidly was investigated by the Spitfire aircraft. The dome of this cloud rose to 32,000 feet and there was an anvil at 27,000 feet. A flight made through the cloud was analysed in detail and compared with the photograph (see photograph (vi)) of the echo on the height range tube at the time of the flight.

The total distance flown in cloud was 16,100 yards and the occurrences of gusts were given in terms of the distance along the track in yards. The analysis is shown in Fig. XVIII where the ordinates are proportional to the magnitude of the gust expressed in terms of the acceleration imparted to the aircraft, measured in g. (Gusts in the range 0.1 - 0.2g are shown with the common value 0.15g, 0.2 - 0.3g as 0.25g etc.). As indicated in Section 5 the duration of each gust is not likely to be the same so that only an approximation to the vertical velocity profile can be obtained by considering each up and down gust as representing an instantaneous increase or decrease in vertical velocity respectively. An examination of Fig.XVIII shows that the arithmetical sum of all the gusts (which is equivalent to assuming that all gusts have the same duration) leads to a large excess of upward velocity, which is unlikely to be real since the accelerometer was switched on and off outside the cloud in conditions which may be presumed to be similar as regards the vertical velocity. A closer examination of the accelerometer record on this occasion revealed that this excess of velocity can probably be accounted for by assuming that, on the average, the negative gusts lasted for a longer time than the positive ones and hence each indiyidual negative gust represented a greater change in vertical velocity than that due to a positive gust of the same magnitude. Roughly this effect can be taken into account by increasing all the negative gusts by a fixed amount sufficient, in the sum, to cancel out the excess upward velocity. The percentage increase applied to each gust therefore decreases as the gust value increases which is equivalent to saying that the large up and down gusts are more nearly of the same duration than the smaller ones. It is not possible to say whether this assumption is justified but it seems likely that an indication of the vertical velocity profile within the cloud may be given by an adjustment of this kind, although the absolute values of the vertical velocity will not be obtained. The vertical velocity profile obtained in this way is shown in Fig. XIX.

Due to failure of the radio telephone and hence lack of exact knowledge of times of switching on and off of the accelerometer it is not possible to make a detailed comparison between this velocity profile and the echo as shown in photograph (vi) but there are undoubted points of similarity between the two; e.g. the ranges of upward velocity at 700 - 2,600, 7,600 - 8,200 and 12,100 - 13,700 yards in Fig. XIX have their counterpart in the three marked columns in the echo, but the narrow upward velocity peak at 5,100 - 5,200 yards has no obvious counterpart, being associated with a part of the echo exhibiting a deep trough. (The flight was made towards the station so that in the photograph the edge of the echo at the greatest range was that first entered by the aircraft).

It will be seen that the maximum upward gust on this traverse occurred at 7,130 yards, probably in the edge of the strong central column of the echo while the maximum downward gust at 3,700 yards probably occurred in the approach to the first trough in the echo. Other large up-gusts occurred at 890, 980, 5,080 and 15,230 yards, the first two being associated with the leading edge of the first column of echo, the third in the deep trough between two columns and the last one probably just beyond the final edge of the echo. A quite well marked down-current would appear to have occurred at this height just beyond the edge of the echo but still in cloud and this is confirmed by the sequence of strong upward gusts experienced by the aircraft just before leaving the cloud.

There appears some reason to believe that the well marked columns in the echo are associated with strong upward currents in which the drop sizes (and hence the echo, the intensity of which is proportional to the sum of the sixth power of the diameter of the drops) are greater than in the neighbouring weaker

/and

and perhaps downward currents. The close proximity of up and down currents would explain the sharp edge which is peculiar to the active cumulonimbus type of echo and may also lead one to expect the greatest turbulence in the edges of the echoes where the vertical current is changing most quickly. (See Section 8(c)).

(ii) Traverse made at 14,000 feet on 10th June, 1948

This flight was through a large mass of cumulonimbus cloud and a detailed analysis as in Section 8(a) (i) above was provided which is shown graphically in Fig. XX. On this occasion the arithmetical sum of all the gusts resulted in a large excess of negative velocity. The up and down gusts of 0.1, 0.2 and 0.3g cancelled each other out almost exactly and the correction applied therefore was to increase all the positive gusts of 0.4g and greater by a fixed amount sufficient in the sum to dispose of the excess negative velocity. The possible vertical velocity profile obtained in this way is shown in Fig. XXI. It must be remembered that the varying durations of each gust make it impossible to determine actual velocities and probably also the relative magnitudes of the vertical velocities in the various peaks and troughs of the velocity profile i.e. the relative heights of the peaks or depths of the troughs may not bear any relation to the relative values of the actual vertical velocities. It is probable however that the existence of marked peaks and troughs in the profile are real and indicate marked up and down currents respectively.

Photograph (ii) shows the appearance of the echo shortly after the aircraft had entered the echo. Detailed readings and additional photographs made it possible to compare this photograph with the velocity profile shown in Fig. XXI. Shown on Fig. XXI are the main features of the echo at the appropriate positions on the velocity profile. It will be seen that the peaks and troughs of the velocity profile bear a close correspondence to the peaks and troughs of the echo although, for the reasons mentioned above, the relative magnitudes are not closely related.

The probability that echo columns are associated with upward currents and marked troughs with downward currents is again demonstrated with pronounced turbulence, either as regards frequency of gusts or magnitude of gusts, in the edges of the columns. It is clear, however, that, while the largest gusts were associated with the echo, the frequency and magnitude of the gusts experienced in the first 3,000 yards in cloud before entry into the echo were comparable with those experienced within the echo (e.g. that part of the traverse from 10,000 to 16,000 yards), while in the patch from 18,000 to 20,000 yards in which the frequency of gusts was very high the pilot reported that he was in a lighter part of the cloud and could see the sun shining.

The detailed analyses of these two traverses explain the statistical evidence of Section 7(b) that the most turbulent clouds are associated with echoes exhibiting sharp edges and tops or a number of columns and troughs, since a sharp edged column of echo is evidence of a well marked up-current and an echo with columns and troughs is evidence of up and down currents in close proximity. This appears to be at variance with the suggestion of Byers and Braham(3) that the precipitation in a thunderstorm cloud initiates a down-current since, under such conditions, it would be expected that the strongest echoes would be associated with a down-current. It is felt however that the evidence here presented and in Section 8(c) below supports the interpretation of a strong column of echo as being associated with a strong upward current.

(b) The occurrence of turbulent patches on traverses relative to the weather echo

As indicated in Section 5, the accelerometer records gave evidence, on occasions, of the occurrence of especially turbulent patches on a run through a cloud. In the analysis of the records the limits of these turbulent patches were indicated whenever they occurred. It was of interest to determine whether these turbulent areas were associated in any way with the part of the cloud containing the weather echo. The detailed analyses of particular flights in

/Section 8(a)

Section 8(a) have indicated that pronounced turbulence is probably associated with the edges of columns of weather echo but also that considerable turbulence could be encountered before entry into the echo. There would appear to be two possibilities;

(i) the presence of a weather echo indicates the part of the cloud where turbulence is likely to be most severe or

(ii) the presence of a weather echo indicates a general increase in the turbulent activity of the whole cloud.

If (i) were true a traverse of a cloud containing an echo would indicate a zone of increased turbulence corresponding to the weather echo while if (ii) were true one would expect consistent turbulence on the whole traverse.

Table V shows how the total number of cloud traverses made (139) was divided between those with consistent turbulence and those which showed division into rough and relatively calm patches, and how those traverses were made relative to the echo in the cloud.

TABLE V

Types of turbulence on traverses through cloud

Position relative to echo:-	Above echo	No echo received from cloud	Through echo	Doubtful	Total
Traverses with consistent turbulence	12	20	44	7	83
Traverses with rough and calm patches	10	3	42	1	56
Totals	22	23	86	8	139

It will be seen that 60% of all traverses gave consistent turbulence but, if those clouds which gave no echo at all are excluded, the chances are about even whether a run through a cloud containing an echo gives consistent turbulence or patches with noticeably rougher conditions. It is noteworthy that nearly all clouds which failed to give an echo were consistently turbulent from entry to departure.

Detailed comparison with photographs was not possible for all those flights through an echo which gave patches of rough and relatively calm conditions but of 22 cases examined the roughest patch of the traverse occurred entirely within the echo on 10 occasions, partly outside and partly inside the echo on 8 occasions and on the remaining 4 occasions entirely outside the echo. Of the 8 occasions when the turbulent patch was partly outside and partly inside the echo the extent of the patch which was clear of echo varied from about 700 to about 7,000 yards, with a mean value of 2,750 yards and on three occasions the part of the patch clear of echo was more extensive than the part within the echo.

In general terms, therefore, it would appear that of a number of flights through cumulonimbus weather echoes in this country about half would show consistent turbulence throughout the cloud while the large majority of flights in the other half would give a noticeably rougher patch on the approach to or inside the echo. On only about a quarter of the total flights, however, would the roughest patch be likely to be encountered entirely within the echo.

/(c)

(c) The places of occurrence of the larger gusts relative to the echo

Having obtained evidence from the complete gust analyses (Section 8(a)) of individual traverses of the probability of the occurrence of large gusts in the edges of strong columns of echo an analysis was made, for those traverses for which detailed readings and photographs were available, of the places of occurrence of the larger gusts relative to the echo. For this purpose the time of occurrence after switching on the accelerometer of each gust of ± 0.4g or greater was obtained and by assessment of readings and photographs its position relative to salient features of the echo was determined. The information obtained in this way is shown in Table VI and the points of interest in the table are summarised below.

(i) 25% of all the larger negative gusts occurred in parts of the clouds completely free of all weather echo whereas the proportion of larger positive gusts was only 17%.

(ii) A significantly greater number of large positive gusts occurred in the leading edge of a column of echo while the reverse was the case in the trailing edge of the echo.

(iii) Narrow columns of echo (i.e. columns in which the leading and trailing edges were so close together that it was impossible to assess exactly where in the column the gust occurred) were associated with a large preponderance of positive gusts.

(iv) Parts of echoes for which the top showed a regular increase or decrease (i.e.free from sudden irregularities) were as likely to give large positive gusts as large negative gusts but the number of gusts in such parts was noticeably less than in the edges of the echo columns.

(v) Of the 7 positive gusts of 0.8g or greater, 6 occurred in the leading edge of a column of echo or in a narrow column of echo, the remaining one (of 0.8g) being in a part of the echo with a steadily increasing top.

(vi) An appreciable number of large gusts with a preponderance of negative gusts occurred in cloud but above the echo, but of the 34 gusts so recorded subsequent analysis showed that at least half occurred above edges or peaks of the echo beneath.

(vii) An appreciable number of large gusts with a preponderance of positive gusts occurred beneath the peak of the echo column but the number of such gusts was noticeably less than those occurring in the edges of the echo.

It is considered that the evidence here produced (particularly sub-sections (ii), (iii), (v) and (vii)) strongly supports the belief that the columns of echo are associated with the occurrence in the cloud of strong upward currents and it was a noticeable feature of the flights that the pilot often reported a substantial bump at the precise moment at which he was observed on the radar tubes to enter a strong column of echo although, of course, being usually already in cloud, he was unaware that he was entering the echo.

(d) The occurrence of large gusts of opposite sign close to each other

The detailed analysis of the larger gusts revealed that, on a number of occasions, a large gust was followed very quickly (frequently within $\frac{1}{2}$ to 3 seconds, equivalent to approximately 50 to 300 yards) by a compensating gust of comparable magnitude but of the opposite sign, while on some occasions three or more large gusts, sometimes but not always of the same sign, would occur within the space of two or three hundred yards. The occurrence of sequences of gusts of this character would appear to suggest the presence of eddies in the zones of transition between the strong up and down currents. Such a situation is shown diagrammatically in Fig. XXII.

/Fig. XXII

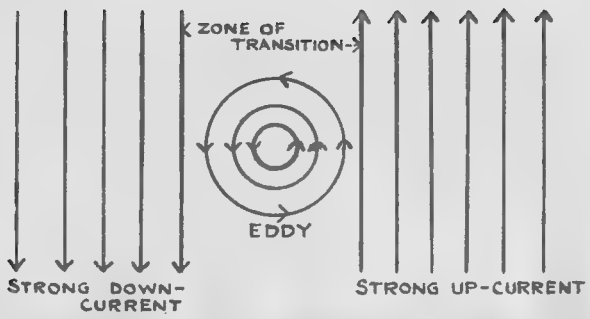

Fig. XXII

The vertical velocity of the air as experienced by the aircraft would then be as shown in Figs. XXIII (a) and (b) according to whether the aircraft went near to or through the centre of the eddy or skirted the eddy respectively.

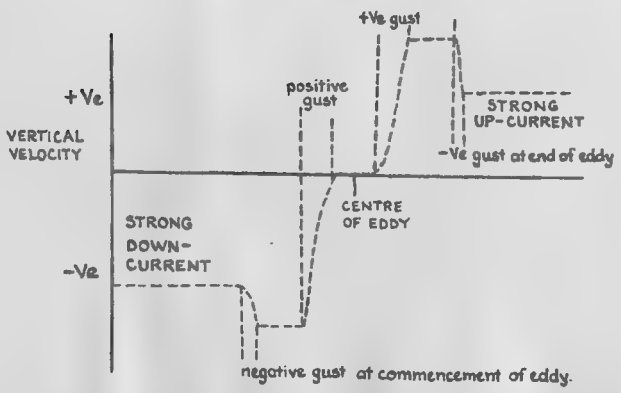

Fig.XXIII (a)

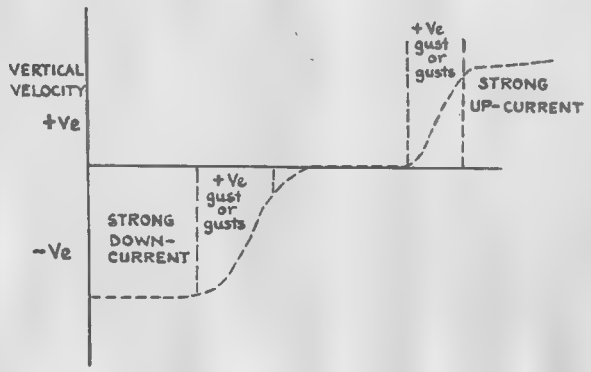

Fig. XXIII (b)

The relative magnitudes of the steady up and down currents and the dimensions of, and speed of the air in, the eddy would determine the magnitude, number and sign of the gusts experienced.

9. Application of the results to the avoidance by an aircraft of severe and unexpected turbulence

As indicated in Section 1 the only possibility, up to the present, of avoiding severe turbulence in clouds has been to rely on the appearance to the pilot of the clouds which experience has shown to be turbulent. This was obviously unsatisfactory while night-flying and even in daylight it is often a matter of difficulty and sometimes impossible to identify a cumulonimbus cloud due to the frequency with which layers of cloud interrupt the line of sight. In particular in frontal belts of cloud it may well be quite impossible to detect hidden cumulonimbus clouds even when flying at a considerable height. That cumulonimbus clouds do occur on occasions in all types of fronts, due to instability in the warm air being lifted, is evidenced by reports of thunder which, although most frequent in cold frontal situations, do occur also with warm fronts and occlusions. It has been shown that the radar will indicate the presence of precipitating cumulus and cumulonimbus clouds and that when viewed in the vertical section an indication of the degree of turbulence likely to be experienced is obtained. Some work has already been done on the use of the PPI display of an airborne 3 cm. set, which shows the projection of a certain

depth of the echo on the horizontal plane at the height of the aircraft, in avoiding turbulence (see, for example, T.C.D.U. Report(5)) but it is suggested that the vertical cross-section will give a clearer indication. In particular in frontal conditions the P.P.I. display is likely to show a large mass of echo some of which may in reality be of only limited vertical extent while an embedded cumulonimbus would be difficult to distinguish from the surrounding echoes. On the height range display however the true nature of the echoes is immediately visible and the column of echo from the hidden cumulonimbus obvious. Photographs (vii) and (viii) illustrate such an occurrence when after smooth flight through a bright band of echo unexpected turbulence was encountered on entering the column of echo.

It must be emphasised however that considerable turbulence may be experienced in clouds which fail to give an echo and that avoidance of the echo alone (see Section 8(b)) when it occurs either by change of course or change of height will not necessarily lead to the avoidance of all serious turbulence although the very biggest bumps are probably associated with the edges of columns of echo of great vertical extent.

10. The suggested structure of active cumulonimbus clouds

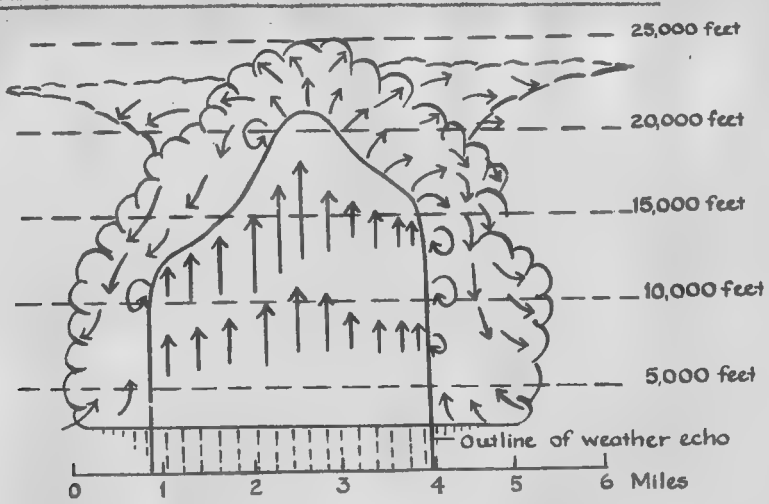

Fig. XXIV.

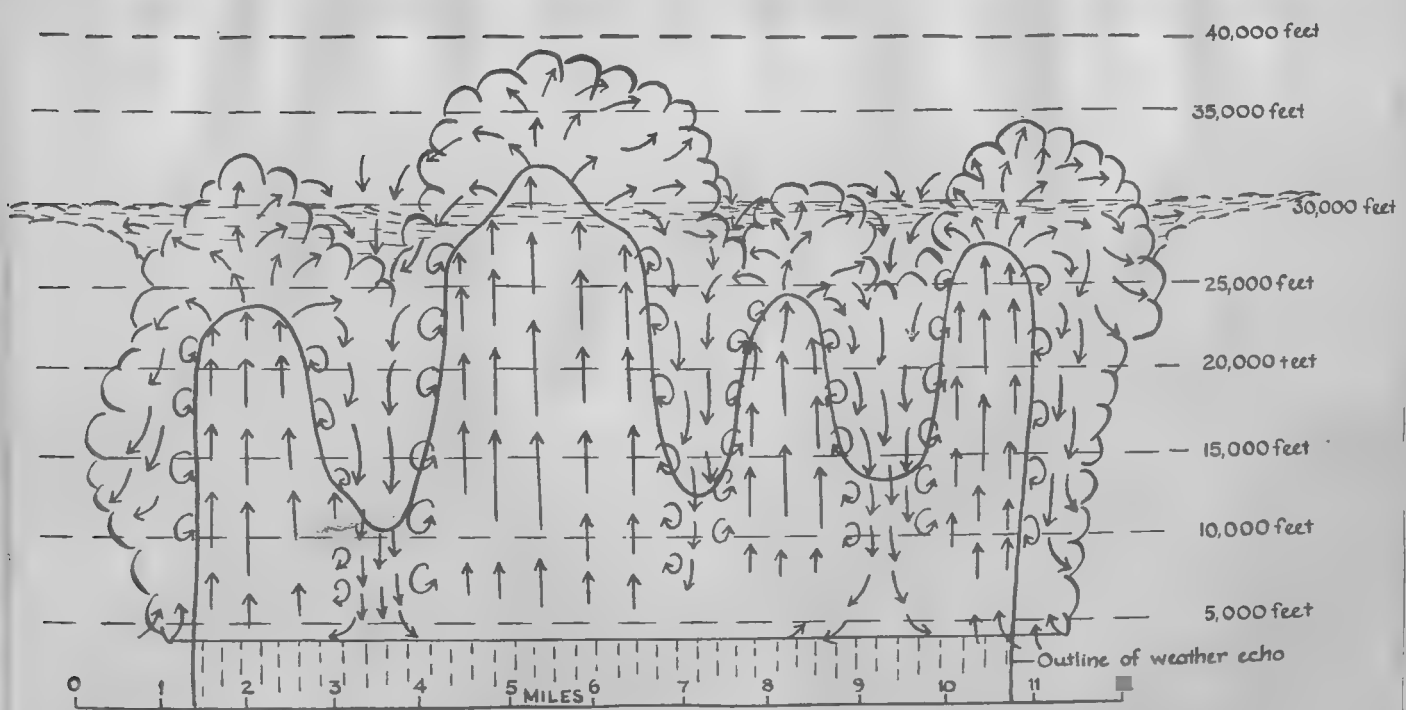

Fig. XXV.

In Figs. XXIV and XXV are given the possible vertical current structure of isolated and extensive active cumulonimbus clouds respectively. The outline of the weather echo is given in each case and it is considered that the structures here shown are consistent with the evidence obtained from the aircraft flights. The actual and relative magnitudes of the vertical currents cannot be inferred and the diagrams are only regarded as schematic.

11. Summary

Evidence has been presented which it is considered permits the formulation of the following tentative conclusions.

(i) Radar can be of great assistance in indicating the presence of turbulent clouds but all turbulent clouds do not give a radar echo. It is probable, however, that in this country very large up and down gusts - of the order of 1g and greater as experienced by a Spitfire aircraft - will always be associated with clouds giving a weather echo.

(ii) The appearance of the weather echo in its vertical cross section is a useful guide to the degree of turbulence likely to be encountered within the cloud containing the echo and provides a useful means of identifying cumulonimbus clouds hidden from view by intervening layers of cloud.

(iii) It is probable that the largest gusts are associated with the edges of strong and sharply defined columns of weather echo.

(iv) The most turbulent part of a cloud traverse is not always entirely within the radar echo, but may extend to some distance on each side of the echo, while many clouds containing a weather echo may give consistent turbulence throughout a traverse.

(v) The evidence supports strongly the belief that well marked columns of echo are associated with strong upward currents and well marked troughs in the echo with downward currents.

(vi) There is no conclusive evidence of flight levels which give maximum turbulence nor is there sufficient evidence to warrant the definition of a level which will give the smoothest possible flight. There is some evidence however to support the belief that the turbulence increases upwards in the cloud until a height of rather less than half (about 0.4) of the total vertical extent of the cloud has been reached whereafter the degree of turbulence probably remains about the same with increasing height.

(vii) The only occasion of damage to the aircraft on these flights was caused by hail which, although very infrequent, presented a serious hazard when it did occur.

12. Acknowledgements

Acknowledgement is made of the ready co-operation of the pilots of the Spitfire aircraft from the Aero Flight, Royal Aircraft Establishment, Farnborough, who have unhesitatingly flown through every cumulonimbus cloud to which they were directed and of the work done by the personnel of the same flight in analysing the accelerometer records.

13. References

1. Jones, R.F.: The height and temperatures at the tops of radar echoes associated with various cloud systems. M.R.P. No. 458, Air Ministry, Meteorological Research Committee, London, 1949.

2. Ryde, J.W.: The attenuation and radar echoes produced at centimetre wave lengths by various meteorological phenomena. Meteorological Factors in Radio Wave Propagation - Report of a conference held on 8th April, 1946 at The Royal Institution, London, by Phys. Soc. and R. Met.Soc., Phys. Soc. Report, London.

/3.

3. Byers and Braham: Thunderstorm structure and circulation. J.Met., Milton, Mass., Vol. 5 No. 3, June 1948.

4. A report on thunderstorm conditions affecting flight operations. Technical Paper No. 7, Thunderstorm Project, Chicago, Ill., Washington April, 1948.

5. Cloud and collision radar warning equipment. Final Report, Transport Command Development Unit, November, 1948.

TABLE I

Details of sorties made by aircraft on cumulonimbus investigations

Sortie No.	Date	Time (GMT)	No. of cloud traverses made	Range (miles)	Remarks
1.	23.9.47.	1430-1530	5	20-30	Isolated cumulonimbus cloud.
2.	20.1.48.	1130-1200	1	20-25	Cu rising out of Sc layer.
3.	29.1.48.	1530-1615	5	15-25	Band of Cu out of Sc layer.
4.	30.1.48.	1500-1615	1	15-20	Band of cumulonimbus. Sortie abandoned due to severe icing on second run.
5.	20.2.48.	1125-1220	6	20-25	Isolated snow showers. No weather echo.
6.	20.4.48.	1400-1530	8	12-25	Large isolated cumulonimbus.
7.	23.4.48.	1330-1430	7	20-30	Isolated Cu clouds. No weather echo.
8.	30.4.48.	1000-1100	7	15-20	Isolated cumulonimbus.
9.	30.4.48.	1400-1500	5	25-30	Isolated Cu.
10.	25.5.48.	1400-1500	5	20-25	Cu rising out of Sc layer.
11.	28.5.48.	1400-1500	2	?	Cu rising out of Sc layer. Aircraft lost on display tubes.
12.	1.6.48.	1400-1500	8	25-35	Cumulonimbus.
13.	2.6.48.	1400-1500	9	15-45	Cumulonimbus.
14.	3.6.48.	1400-1500	7	20-30	Cumulonimbus.
15.	9.6.48.	1500-1600	5	20-25	Cu and cumulonimbus rising out of layer cloud.
16.	10.6.48.	0900-1000	6	10-35	Cumulonimbus.
17.	14.6.48.	1000-1100	7	0-30	Extensive thunderstorms. Ground readings incomplete due to lightning striking power lines.
18.	17.6.48.	1330-1600	7	15-35	Cu.
19.	28.6.48.	1400-1530	7	30-35	Cumulonimbus.
20.	13.7.48.	1345-1500	13	15-30	Cumulonimbus rising out of Sc layer.
21.	29.7.48.	1545-1605	2	about 85	Large cumulonimbus but aircraft too far away to be visible on radar. Weather echo visible.
22.	30.7.48.	1500-1600	3	25-35	Large cumulonimbus.
23.	13.8.48.	1445-1515	4	20-30	Cu.
24.	18.8.48.	1400-1415	2	12-25	Cu flattening out into Sc layer. No echo.
25.	3.9.48.	1430-1515	2	20-25	Cumulus.
26.	4.10.48.	1000-1100	5	10-30	Cu and Sc.

TABLE II

General appearance of echo at time of flights through the echo which gave the maximum gusts.

A. Echoes extending 20,000 - 30,000 feet above freezing level.

Maximum up-gust	Maximum down-gust	Relative power of echo	Description of echo
1.5g	1.3g	22,350	Very strong broad column up to 40,000 feet with sharply defined edges.
1.1g	1.1g	-	Very strong column up to 39,000 feet although viewed at 85 miles.
0.9g	1.0g	563	Well marked peaks and troughs with sharply defined edges.
0.8g	1.0g	-	Single very large column with sharp edges but diffuse top.

B. Echoes extending 12,000 - 16,000 feet above freezing level.

1.1g	0.5g	2,756	Strong and broad column of echo with clear cut edges.
0.9g	0.7g	-	Strong echo with columns and troughs.
0.7g	0.7g	324	Echo with well marked columns and troughs.
0.5g	0.5g	-	Column which was weak and diffuse at height flown through. Edges also rather diffuse and not vertical.
0.5g	0.7g	355	Solid block of echo but with rather diffuse edges and top.
0.4g	0.4g	-	Echo had weak and diffuse top with no obvious columns and showed signs of a bright band.
0.4g	0.7g	-	Narrow and diffuse column of echo.

C. Echoes extending 8,000 - 12,000 feet above freezing level.

0.8g	0.7g	-	Sharp-edged echo with evidence of one strong column and one weak.
0.6g	0.5g	-	Rather weak and diffuse echo but 40-45 miles away.
0.6g	0.4g	53	Narrow column of echo.
0.6g	0.5g	-	Smooth-topped echo with sharp edges.
0.6g	0.4g	123	A broad column with diffuse top followed by narrow more sharply defined column.
0.5g	0.3g	40	Narrow column with sharp edges but rather diffuse top.

D. Echoes extending 4,000 - 8,000 feet above freezing level.

1.0g	0.7g	132	Echo not very strong but with well-marked columns and troughs.
0.8g	0.7g	-	Strong column with clear cut edges and tops.
0.7g	0.3g	73	Single column with clear cut edges but diffuse top.
0.6g	0.8g	318	Half of echo had rather diffuse top and remainder showed two quite strong columns but without clear cut edges.
0.5g	0.5g	17	Column with rather diffuse edges at end of runs and top decreasing during flights.
0.4g	0.3g	4	Rather weak column with diffuse edges at end of runs and top decreasing during flights.
0.3g	0.4g	32	Single narrow column with rounded top.

E. Echoes extending 0 - 4,000 feet above freezing level.

0.5g	0.4g	-	Single column with one sharp edge and diffuse top and other edge.
0.3g	0.4g	15	Echo contained single column in a rather diffuse echo. The column had one sharp edge but top and other edge diffuse.
0.3g	0.3g	-	Diffuse echo with tendency for bright band.

TABLE III

Average distances flown in cloud at different levels above the freezing level before encountering gusts of specified magnitude

(Distances in yards)

A. Clouds containing no echoes and echoes extending to less than 9,000 feet above freezing level.
B. Clouds containing echoes extending to more than 9,000 feet above freezing level.

Height above freezing level (feet)		Gust values														Total distance flown at height shown. (yards)
		± 0.1 to 0.2g	± 0.2 to 0.3g	± 0.3 to 0.4g	± 0.4 to 0.5g	± 0.5 to 0.6g	± 0.6 to 0.7g	± 0.7 to 0.8g	± 0.8 to 0.9g	± 0.9 to 1.0g	± 1.0 to 1.1g	± 1.1 to 1.2g	± 1.2 to 1.3g	± 1.3 to 1.4g	± 1.4 to 1.5g	± 1.5 to 1.6g	
-2,000 to -4,000	A	446	1460	2354	4707	14121	42364	42364	42364	-	42364	-	-	-	-	-	42364
	B	-	-	-	-	-	-	-	-	-	-	-	-	-	-	-	-
0 to -2,000	A	446	891	2465	6446	13967	41900	83800	-	-	-	-	-	-	-	-	83800
	B	408	556	953	2354	4212	13338	20007	-	80030	80030	-	-	-	-	-	80030
0 to 2,000	A	541	831	2820	3948	19738	78955	-	-	-	-	-	-	-	-	-	78955
	B	488	598	1157	2217	2660	7600	10640	17733	53200	53200	-	-	-	-	-	53200
2,000 to 4,000	A	460	880	2641	5856	10361	26938	134688	67344	-	-	-	-	-	-	-	134688
	B	409	591	962	2244	2806	5611	14429	-	-	-	-	-	-	-	-	101000
4,000 to 6,000	A	543	1441	6244	18732	37465	74929	-	-	-	-	-	-	-	-	-	74929
	B	546	845	1038	2582	5619	19104	23880	-	-	-	95520	-	95520	-	-	95520
6,000 to 8,000	A	428	805	1414	2917	15557	23335	46670	-	-	-	-	-	-	-	-	46670
	B	564	903	1374	2107	2633	5267	6320	31600	-	-	-	-	-	-	-	31600
8,000 to 10,000	A	459	486	2429	8500	17000	-	-	17000	-	-	-	-	-	-	-	17000
	B	690	1039	1610	2566	7465	13687	20530	27373	41060	-	-	-	-	-	-	82120
10,000 to 12,000	A	1060	636	2120	12720	2120	12720	12720	-	-	-	-	-	-	-	-	12720
	B	480	932	1052	3262	8155	-	32620	-	-	-	-	-	-	-	-	32620
12,000 to 14,000	B	656	849	1968	3607	6184	21645	21645	21645	43290	43290	-	-	-	-	-	43290
14,000 to 16,000	B	519	1047	1261	1931	2377	5150	6867	-	20600	-	-	-	-	-	-	61800
16,000 to 18,000	B	693	1319	2044	2405	6813	20440	-	20440	-	20440	-	-	-	-	-	40880
18,000 to 20,000	B	805	821	1243	2279	3345	7248	21745	-	-	-	43490	43490	-	-	43490	43490
20,000 to 25,000	B	942	891	1534	2441	3879	5073	65950	-	32975	-	32975	-	-	-	-	65950
All flights at all hts.	A	482	916	2592	5840	13102	37289	96951	121189	-	484756						484756
	B	547	784	1224	2388	3904	8890	16770	67079	73787	147574	184467	737870	737870	-	737870	737870

TABLE IV

Average distances to be flown in clouds containing echoes extending more than 9,000 feet above the freezing level at different levels above mean sea level before encountering gusts of specified magnitude. (Distances in yards).

Height above mean sea level (feet)	Gust values															Total distance flown at height shown (yards)
	± 0.1 to 0.2g	± 0.2 to 0.3g	± 0.3 to 0.4g	± 0.4 to 0.5g	± 0.5 to 0.6g	± 0.6 to 0.7g	± 0.7 to 0.8g	± 0.8 to 0.9g	± 0.9 to 1.0g	± 1.0 to 1.1g	± 1.1 to 1.2g	± 1.2 to 1.3g	± 1.3 to 1.4g	± 1.4 to 1.5g	± 1.5 to 1.6g	
2,000 to 6,000	563	765	1485	4083	16330	24495	48990	24495	48990	-	-	-	-	-	-	48,990
6,000 to 10,000	472	835	1556	4279	5706	22823	68470	-	-	-	-	-	-	-	-	68,470
10,000 to 14,000	477	658	1014	2227	3111	8591	16401	180410	180410	90205	180410	-	-	-	-	180,410
14,000 to 18,000	482	730	1075	2279	4307	10169	13220	132200	-	-	-	-	132200	-	-	132,200
18,000 to 22,000	568	834	1406	2519	4651	10993	15115	24184	40307	120920	-	-	-	-	-	120,920
22,000 to 26,000	607	1165	1205	1653	2451	5076	7897	35535	23690	35535	-	-	-	-	-	71,070
26,000 to 30,000	1156	1079	1156	5393	4045	8090	-	-	8090	-	-	-	-	-	-	16,180
30,000 to 34,000	774	774	1332	1585	2774	5548	16645	-	-	-	33290	33290	-	-	33290	33,290
34,000 to 38,000	895	869	1538	2399	4284	5452	59970	-	-	-	29985	-	-	-	-	59,970

TABLE VI

Places of occurrence of gusts of -0.4g or greater relative to the weather echo

Gust Value	Position of gust									Any other positions	Total
	Clear of all echo (none beneath)	Leading edge of echo column	Beneath or in peak of column	Trailing edge of echo column	Above echo	In part of echo with decreasing top	In part of echo with increasing top	In narrow column of echo	Trough between columns of echo		
-0.4g	23	14	8	15	11	5	1	5	9	1-clear patch between echoes	92
-0.5g	13	4	3	9	3	2	5	1	2	0	42
-0.6g	4	1	2	6	4	1	0	1	1	0	20
-0.7g	1	0	0	4	1	1	1	1	0	0	9
-0.8g	1	0	0	1	0	0	0	0	0	0	2
-0.9g	0	0	0	0	0	0	1	0	0	0	1
-1.0g	0	0	0	0	1	0	0	0	0	0	1
0.4g	13	16	8	8	11	8	2	5	5	1-in weak and diffuse echo	77
0.5g	10	13	7	11	1	1	3	12	1	2-in clear patch between echoes	61
0.6g	5	6	4	1	0	0	1	2	0	0	19
0.7g	1	0	4	1	2	0	0	0	0	0	8
0.8g	0	1	0	0	0	0	1	3	0	0	5
0.9g	0	0	0	0	0	0	0	1	0	0	1
1.0g	0	1	0	0	0	0	0	0	0	0	1
Total -ve gusts	42	19	13	35	20	9	8	8	12	1	167
Total +ve gusts	29	37	23	21	14	9	7	23	6	3	172
Total all gusts	71	56	36	56	34	18	15	31	18	4	339

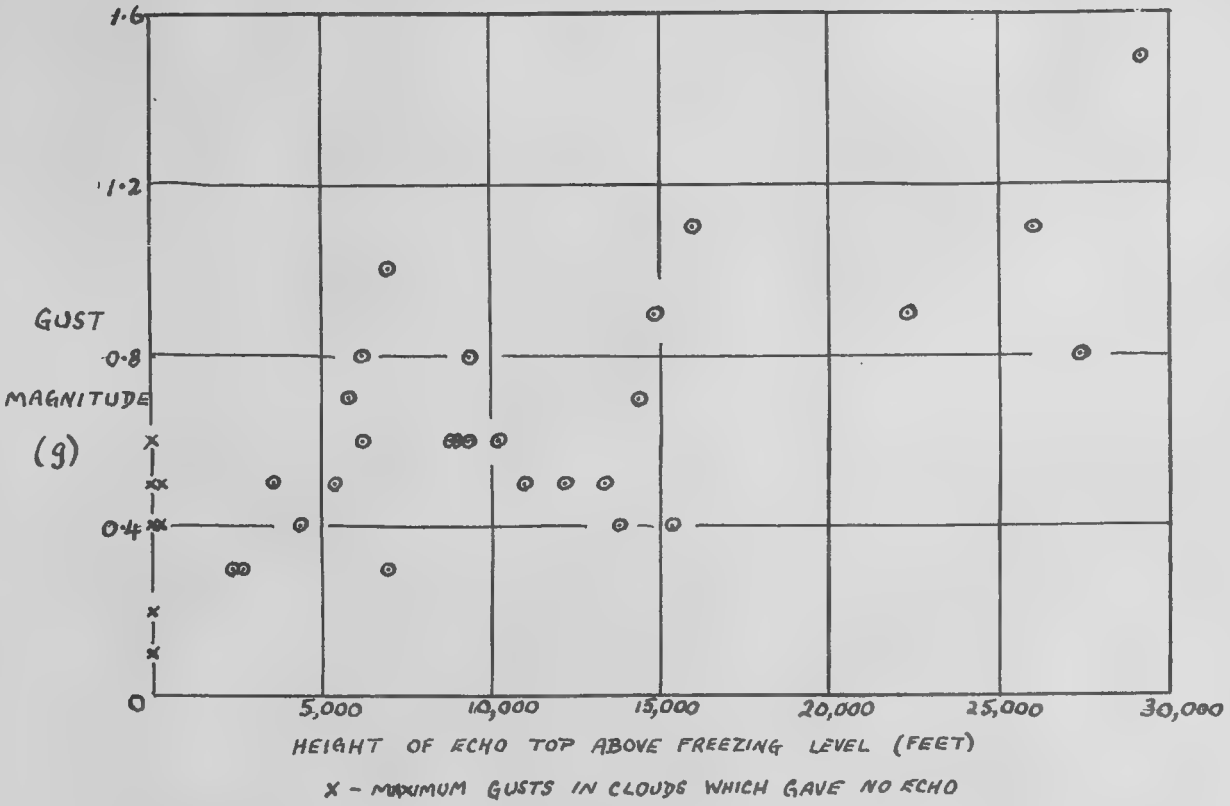

FIG I: VERTICAL EXTENT OF ECHO AND MAXIMUM GUSTS ENCOUNTERED IN CLOUD CONTAINING THE ECHO — UP-GUSTS

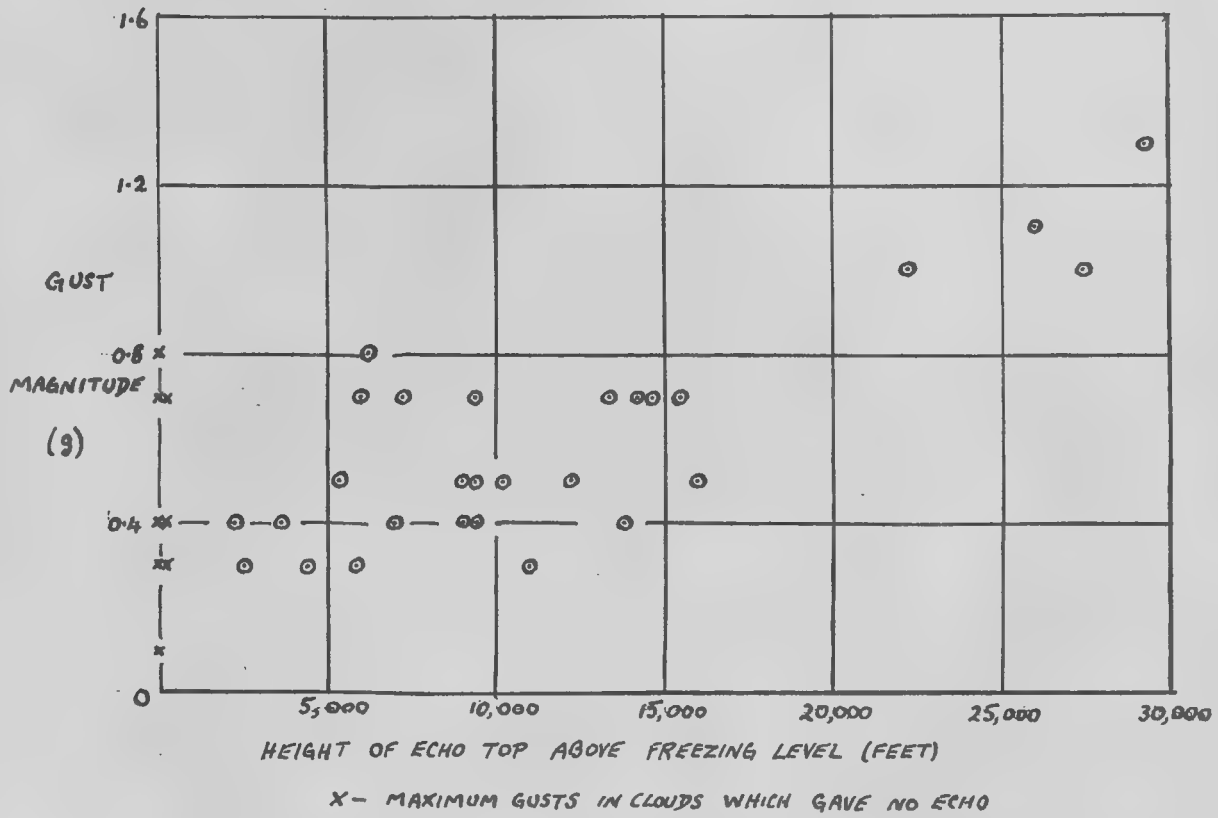

FIG II: VERTICAL EXTENT OF ECHO AND MAXIMUM GUSTS ENCOUNTERED IN CLOUD CONTAINING THE ECHO — DOWN-GUSTS

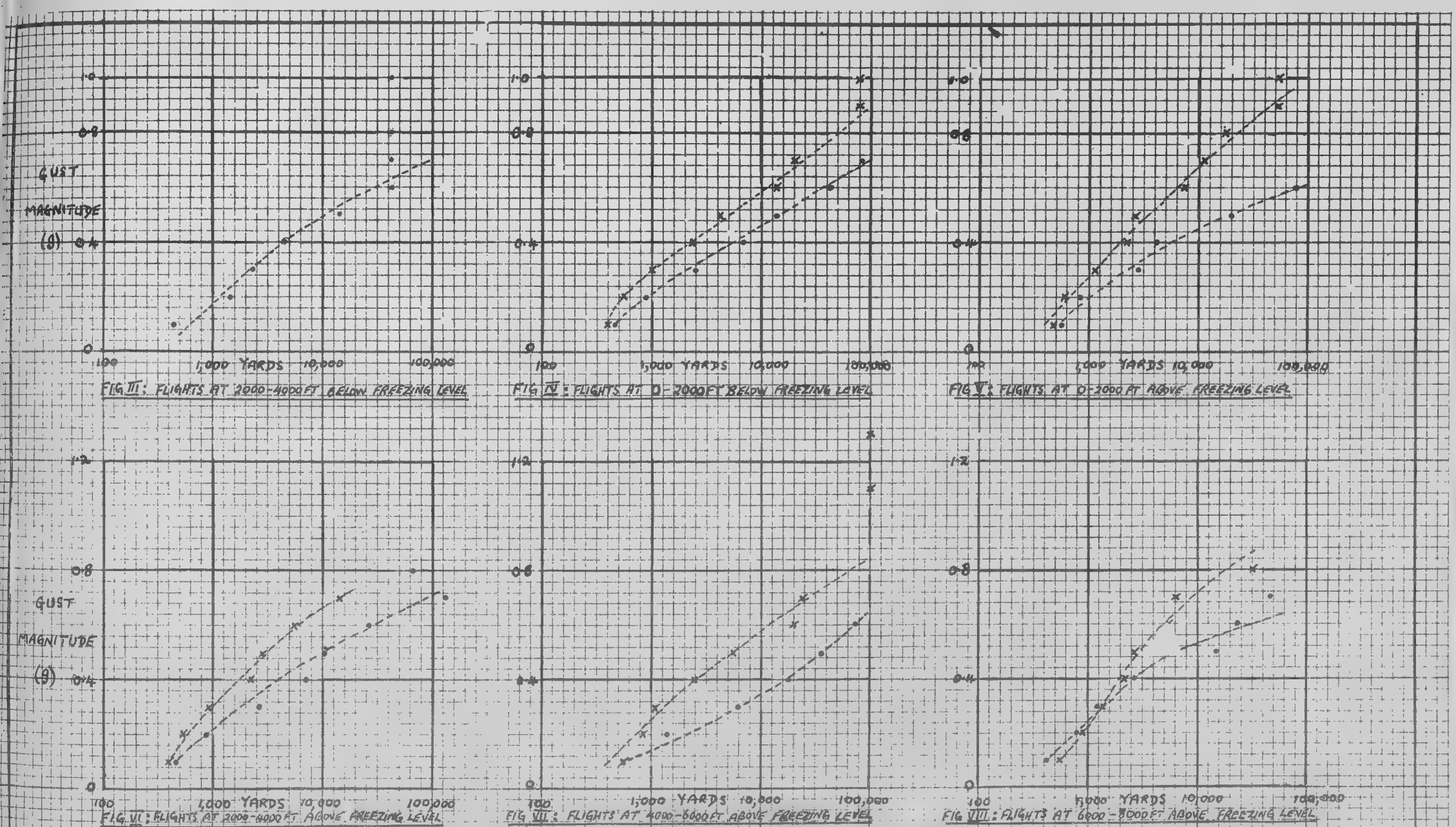

FIG III: FLIGHTS AT 2000-4000 FT BELOW FREEZING LEVEL

FIG IV: FLIGHTS AT 0-2000 FT BELOW FREEZING LEVEL

FIG V: FLIGHTS AT 0-2000 FT ABOVE FREEZING LEVEL

FIG VI: FLIGHTS AT 2000-4000 FT ABOVE FREEZING LEVEL

FIG VII: FLIGHTS AT 4000-6000 FT ABOVE FREEZING LEVEL

FIG VIII: FLIGHTS AT 6000-8000 FT ABOVE FREEZING LEVEL

X - CLOUDS CONTAINING ECHOES EXTENDING 9000 FEET OR MORE ABOVE FREEZING LEVEL. P - CLOUDS CONTAINING SMALLER ECHOES AND NO ECHOES

FIGS III - VIII: DISTANCE FLOWN IN CLOUD BEFORE ENCOUNTERING GUST OF SPECIFIED MAGNITUDE

M.R.P. 484.

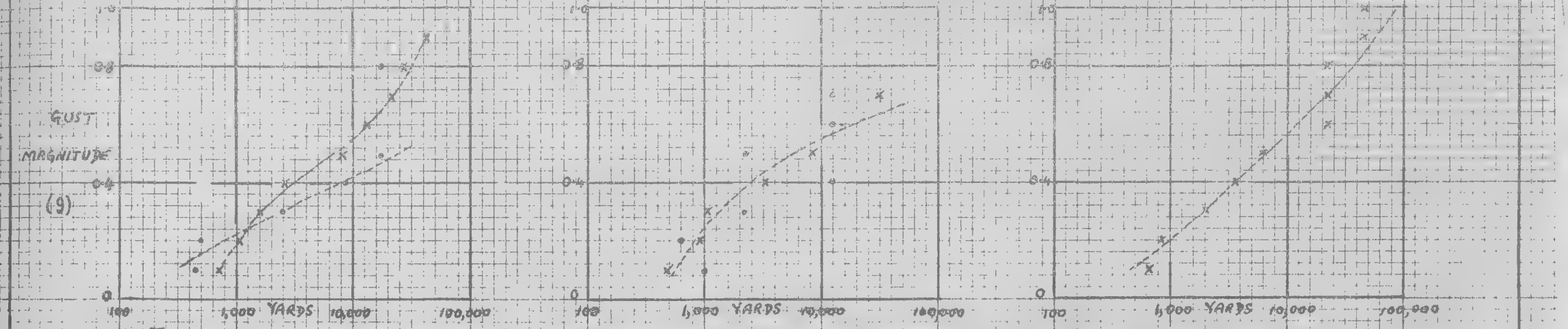

FIG IX: FLIGHTS AT 8000-10,000 FT ABOVE FREEZING LEVEL

FIG X: FLIGHTS AT 10,000-12,000 FT ABOVE FREEZING LEVEL

FIG XI: FLIGHTS AT 12,000-14,000 FT ABOVE FREEZING LEVEL

X = CLOUDS CONTAINING ECHOES EXTENDING 9,000 FT OR MORE ABOVE FREEZING LEVEL • = CLOUDS CONTAINING SMALLER ECHOES AND NO ECHOES

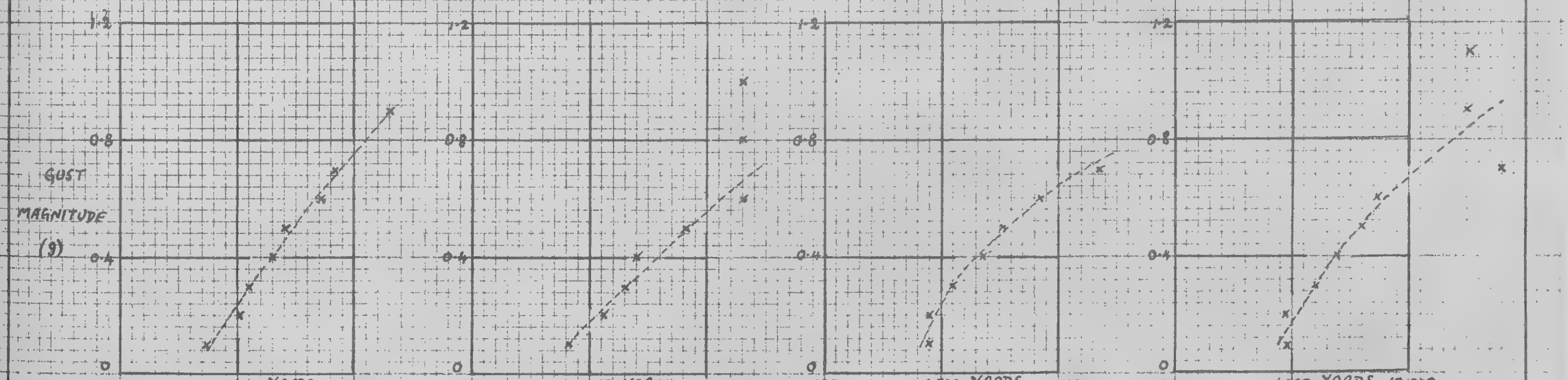

FIG XII: 14,000-16,000 FT ABOVE FREEZING LEVEL

FIG XIII: 16,000-18,000 FT ABOVE FREEZING LEVEL

FIG XIV: 18,000-20,000 FT ABOVE FREEZING LEVEL

FIG XV: 20,000-25,000 FT ABOVE FREEZING LEVEL

FIGS IX - XV: DISTANCE FLOWN IN CLOUD BEFORE ENCOUNTERING GUST OF SPECIFIED MAGNITUDE

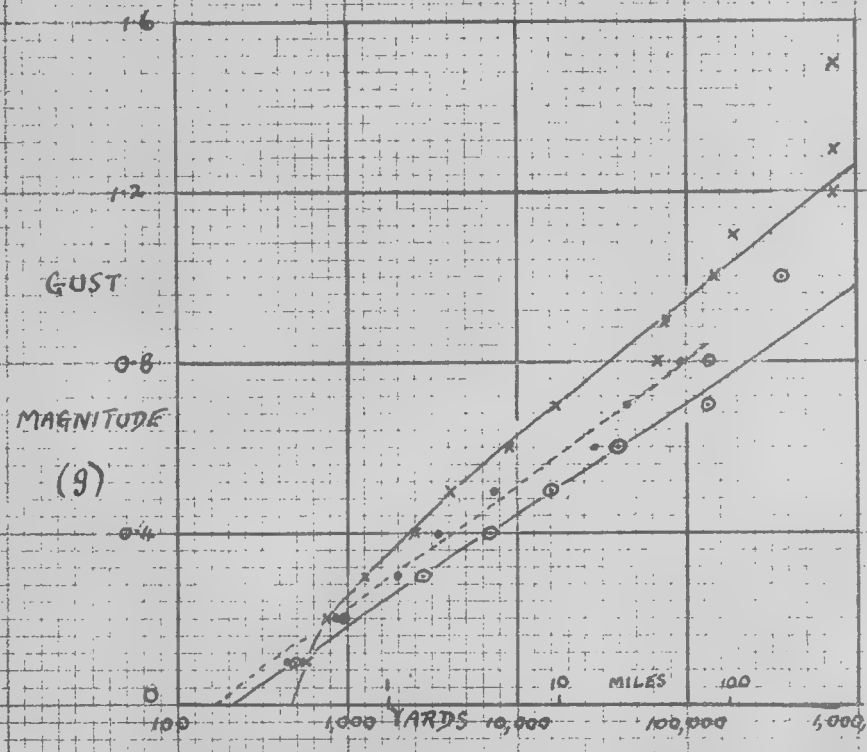

× - CLOUDS CONTAINING ECHOES EXTENDING 9000 FT. OR MORE ABOVE FREEZING LEVEL

⊙ - CLOUDS CONTAINING ECHOES EXTENDING LESS THAN 9000 FT. ABOVE FREEZING LEVEL

• - CLOUDS CONTAINING NO ECHOES

FIG XVI: DISTANCE FLOWN IN CLOUD BEFORE ENCOUNTERING GUST OF SPECIFIED MAGNITUDE. ALL FLIGHTS AT ALL HEIGHTS

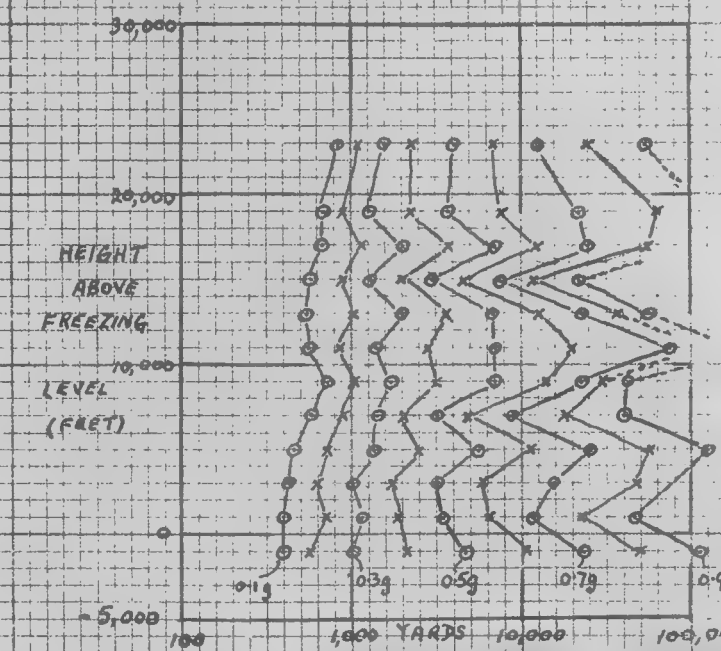

A YARDS	B
65,950	4
43,490	2
40,880	3
61,800	3
43,290	5
32,620	5
82,120	5
31,600	4
95,520	10
101,000	8
53,200	4
80,030	6

COLUMN A: TOTAL DISTANCE FLOWN IN 2000 FT HEIGHT INTERVAL (5000 FT INTERVAL AT 23,000 FT)

COLUMN B: NUMBER OF FLIGHTS IN EACH 2000 FT HEIGHT INTERVAL

CURVES IN ORDER FROM LEFT TO RIGHT REFER TO GUST MAGNITUDES OF 0·1g TO 0·9g RESPECTIVELY

FIG XVII: VARIATION OF GUST FREQUENCY WITH HEIGHT ABOVE FREEZING LEVEL FOR VARIOUS GUST MAGNITUDES

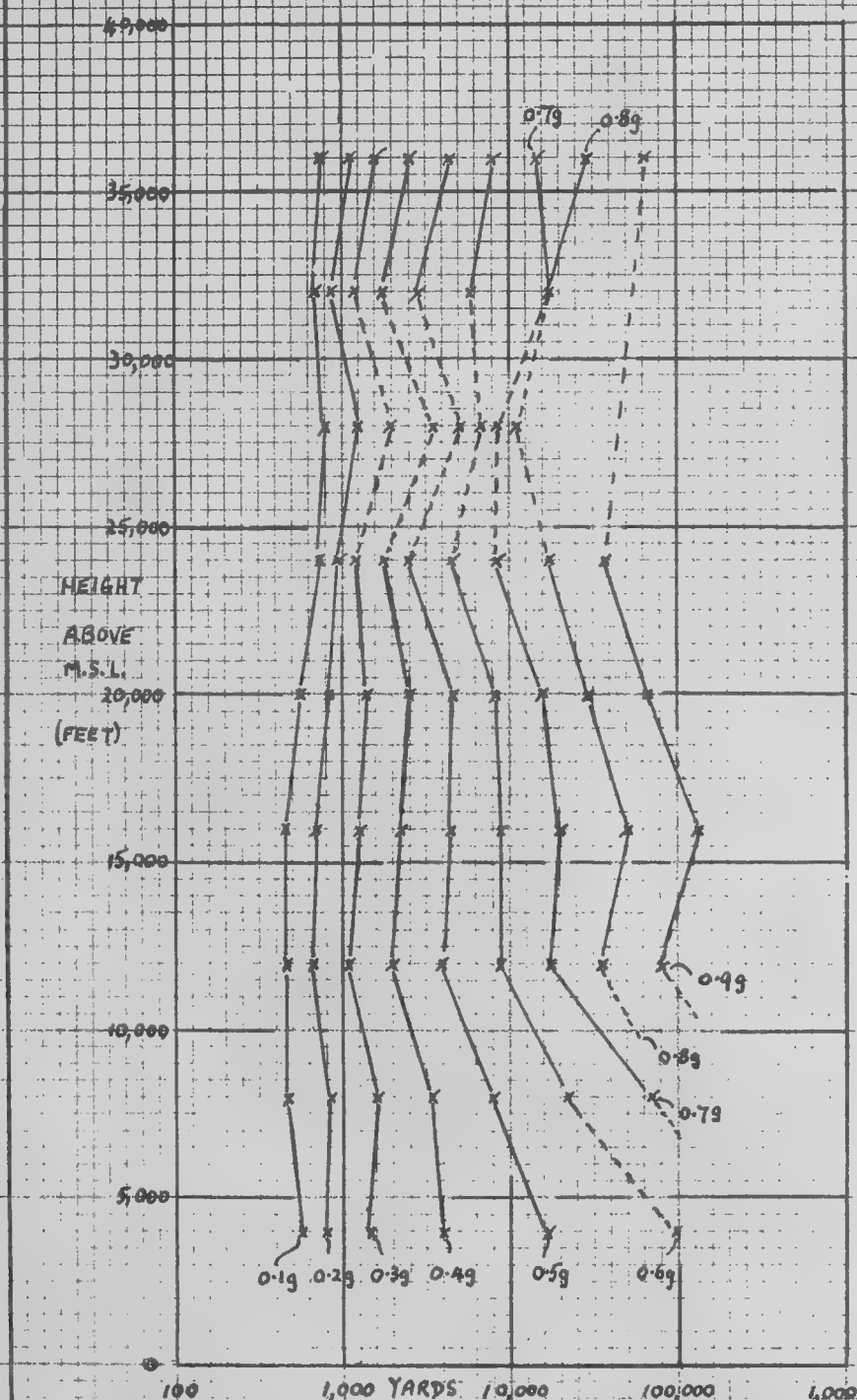

	A	B
	YARDS	
5	9,970	3
4	33,290	1
3	16,180	2
2	71,070	4
1	129,920	10
0	132,200	13
	180,410	15
	68,470	6
	48,990	5

COLUMN A: TOTAL DISTANCE FLOWN IN 4000 FT HEIGHT INTERVAL

COLUMN B: NUMBER OF FLIGHTS IN EACH 4000 FT HEIGHT INTERVAL

FIG XVIIa: VARIATION OF GUST FREQUENCY WITH HEIGHT ABOVE MEAN SEA LEVEL FOR VARIOUS GUST MAGNITUDES

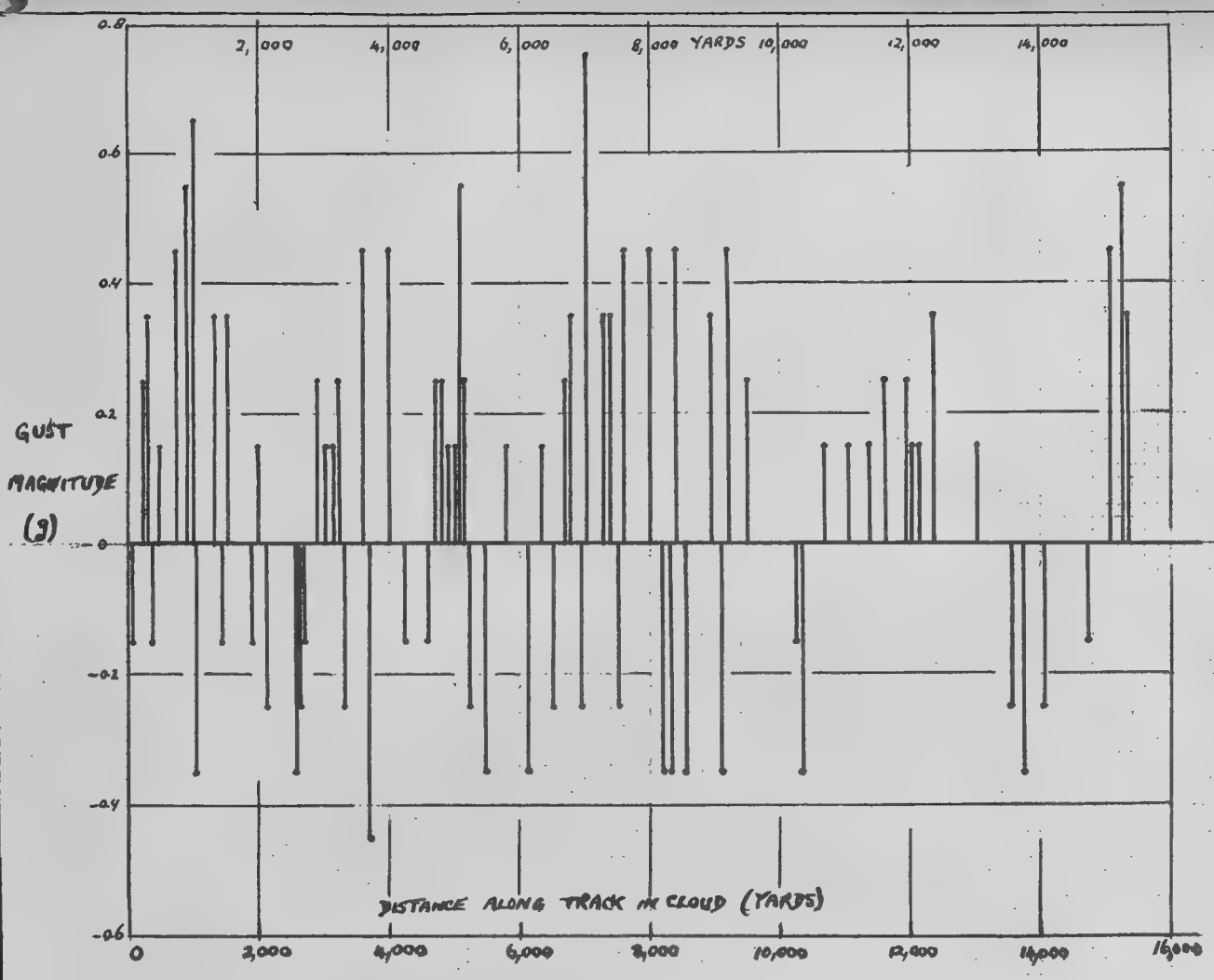

FIG XVIII: FLIGHT AT 13,000 FEET 20TH. APRIL 1948: POINTS OF OCCURRENCE OF GUSTS

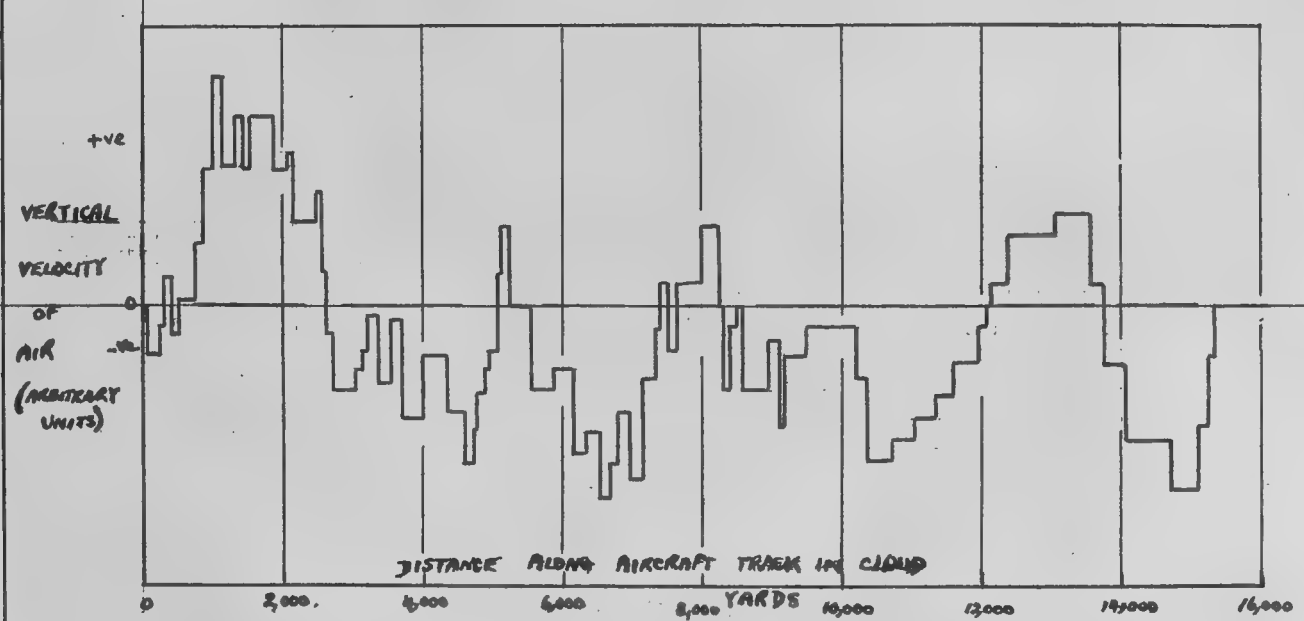

FIG XIX: FLIGHT AT 13,000 FEET 20TH APRIL 1948: POSSIBLE VERTICAL VELOCITY PROFILE OF AIR.
(SEE SECTION 8(a)(i) para 12)

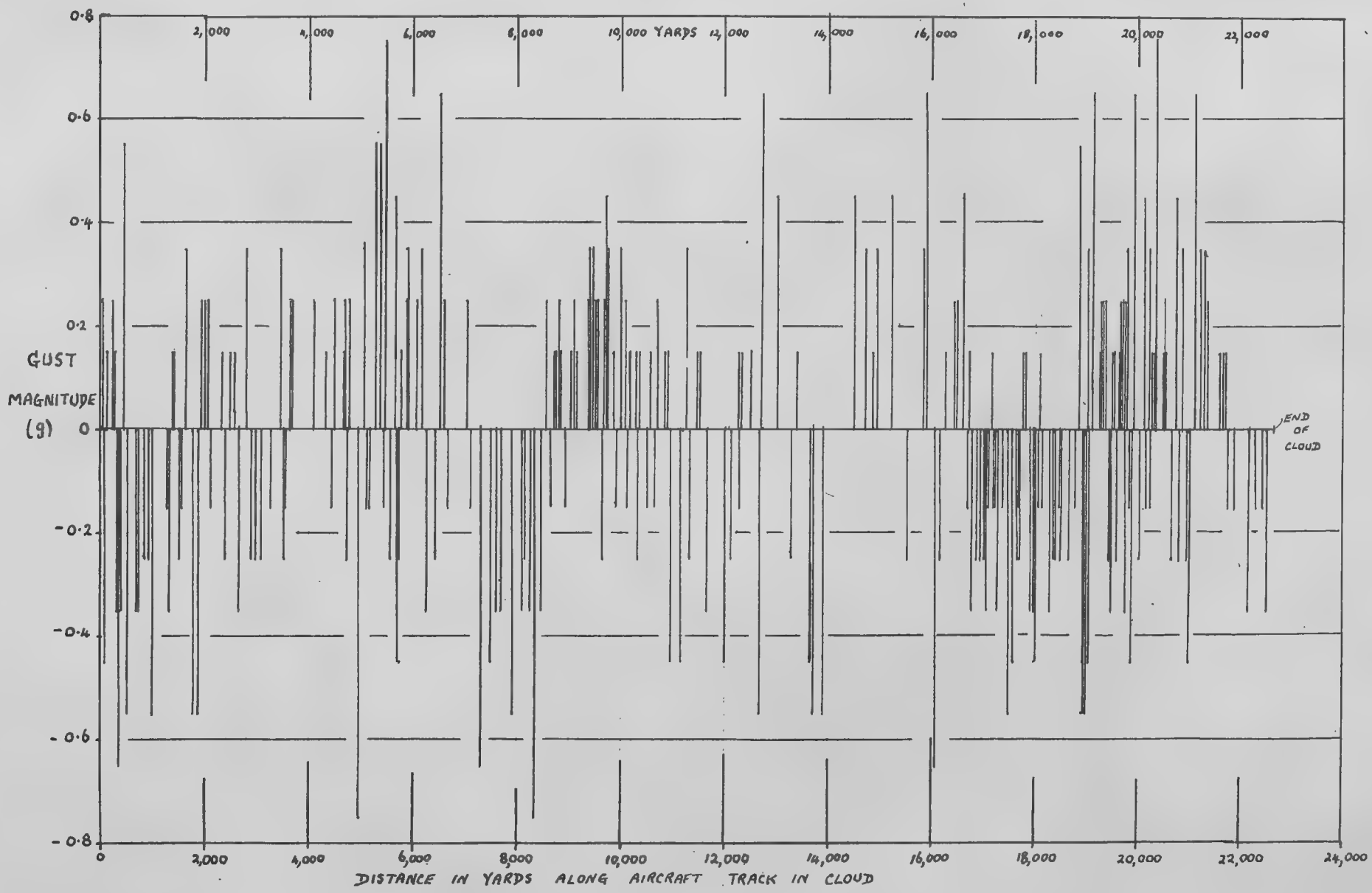

FIG XX: FLIGHT AT 14,000 FT. 10TH JUNE 1948: POINTS OF OCCURRENCE OF GUSTS

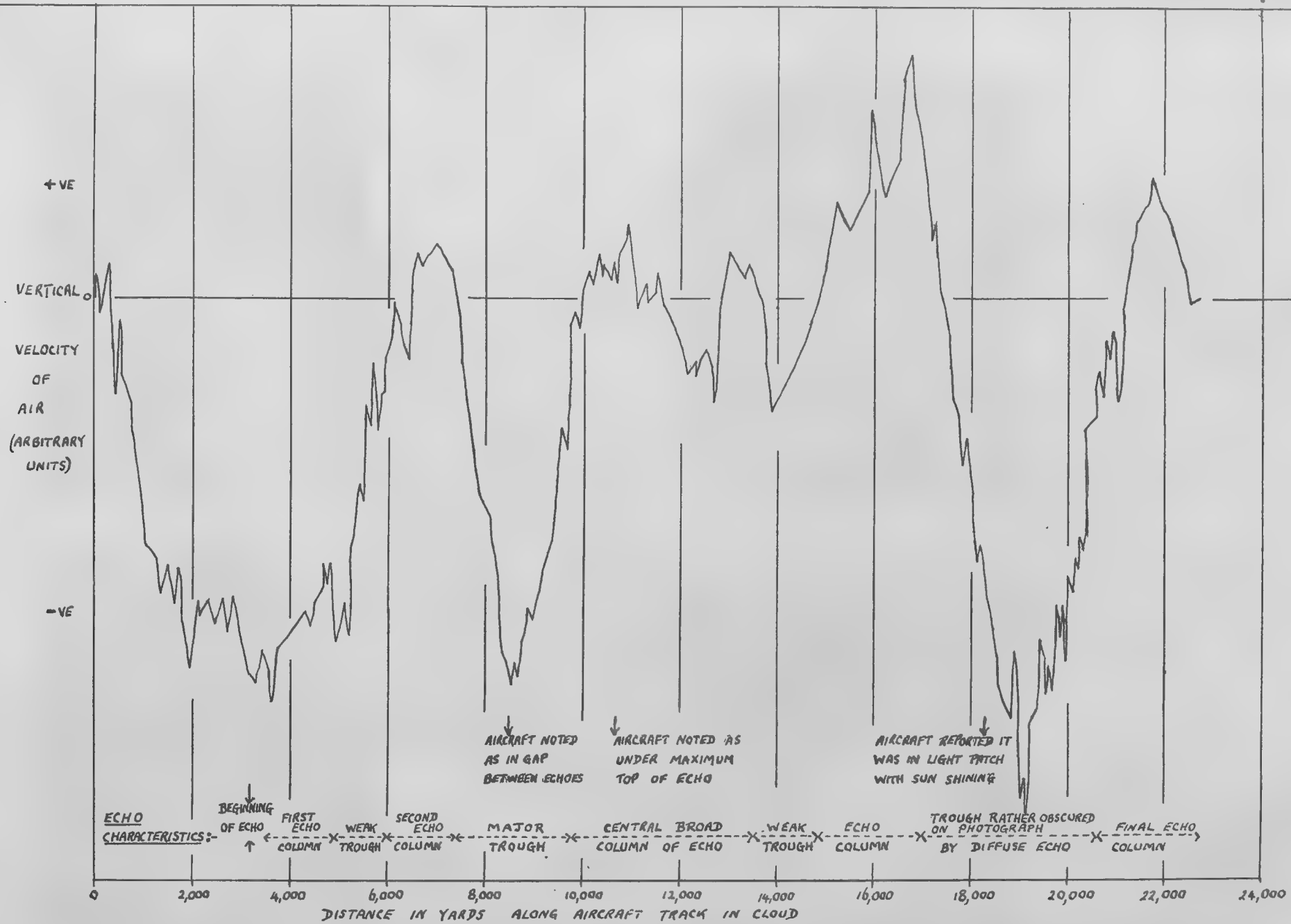

FIG XXI: FLIGHT AT 14,000 FT, 10TH JUNE 1948: POSSIBLE VERTICAL VELOCITY PROFILE OF AIR AND ECHO CHARACTERISTICS (see Section 8(a)(ii), para 1)

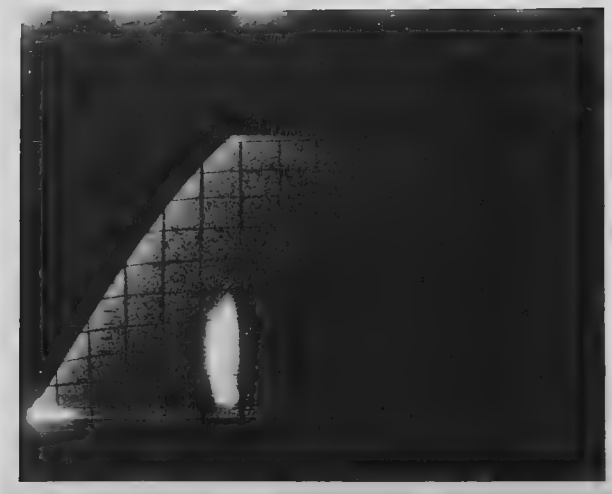

PHOTOGRAPH (i) 23RD SEPTEMBER 1947, 1552 G.M.T.
BEARING 073°T.

TYPICAL WEATHER ECHO FROM ISOLATED ACTIVE CUMULONIMBUS CLOUD. NOTE CLEAR CUT VERTICAL EDGES AND WELL DEFINED TOP.

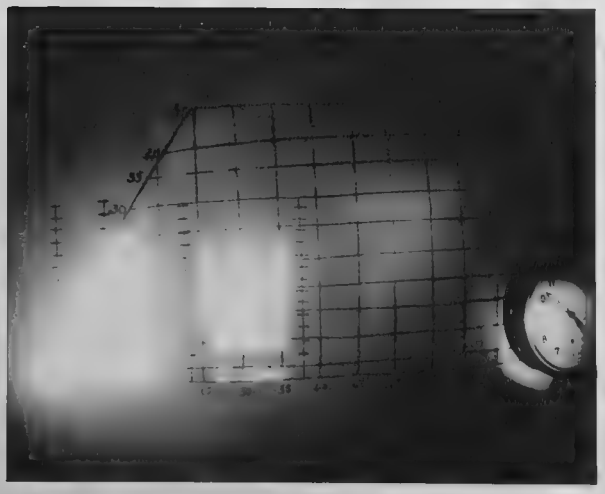

PHOTOGRAPH (ii) 10TH JUNE 1948, 0924 G.M.T.
BEARING 175°T.

TYPICAL WEATHER ECHO FROM EXTENSIVE THUNDERSTORM. NOTE THE APPEARANCE OF COLUMNS AND TROUGHS IN THE ECHO AT 25-35 MILES. THE ECHO FROM 0-20 MILES IS FROM A THUNDERSTORM OVERHEAD AND SURROUNDING THE STATION.
THIS IS THE ECHO INVESTIGATED BY THE SPITFIRE AIRCRAFT AND ANALYSED IN DETAIL (SEE SECTION 8(a)(ii)).

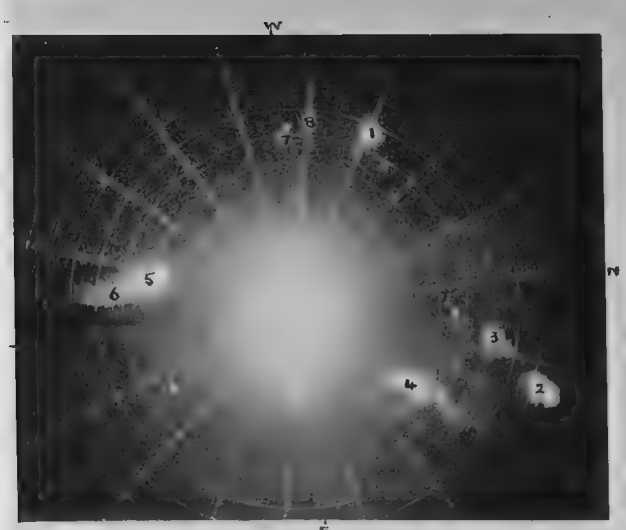

PHOTOGRAPH (iii) 1ST JUNE 1948, 1425 G.M.T.
PPI PHOTOGRAPH OF SHOWER TYPE ECHOES. (ECHOES ARE NUMBERED 1-8 IN PHOTOGRAPH). NOTE ISOLATED NATURE AND SHARP EDGES TO MOST OF ECHOES. THE TENDENCY FOR DIFFUSE EDGES IN ECHOES 4 AND 6 IS A SIGN OF DECAY OF THE CUMULONIMBUS GIVING THE ECHO.

PHOTOGRAPH (iv) 28TH JUNE 1948, 1451 G.M.T.
BEARING 170°T.

ECHO FROM DECAYING CUMULONIMBUS CLOUD. NOTE THE TENDENCY FOR TOP AND SIDES TO BECOME DIFFUSE AND THE APPEARANCE OF A BRIGHT BAND AT ABOUT 5000 FEET (THE FREEZING LEVEL WAS AT 6300 FEET).
THIS ECHO WAS INVESTIGATED BY THE SPITFIRE AIRCRAFT AND IS AN EXAMPLE OF AN ECHO OF LARGE VERTICAL EXTENT WHICH HAD ONLY SMALL UP-GUSTS. (SEE SECTION 7(b)).

X 21604

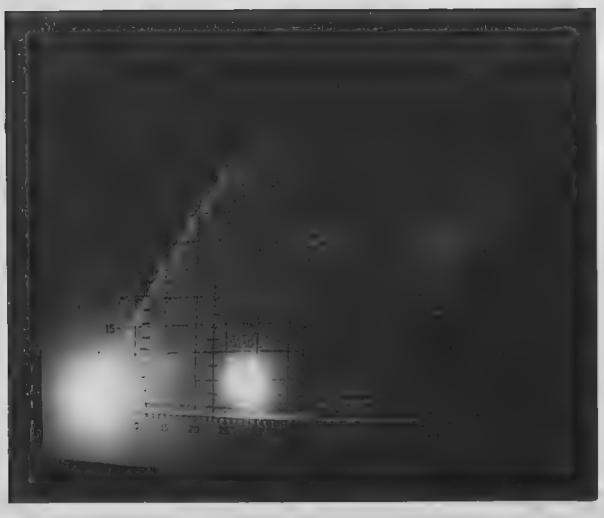

PHOTOGRAPH (v) 17TH JUNE 1948, 1454 G.M.T.
BEARING 090° T.

EXAMPLE OF WEATHER ECHO OF SMALL VERTICAL EXTENT WHICH GAVE LARGE UP-GUSTS (SEE SECTION 7(b)). NOTE THE APPEARANCE OF DISTINCT COLUMNS IN THE ECHO. THE ECHO FROM THE INVESTIGATING AIRCRAFT IS VISIBLE AT 5000 FEET AT 24½ MILES.

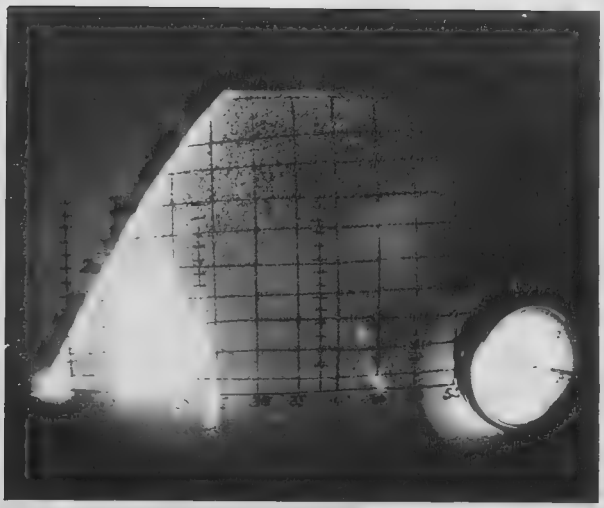

PHOTOGRAPH (vi) 20TH APRIL 1948, 1518 G.M.T.
BEARING 045° T.

THIS IS THE ECHO FOR THE FLIGHT WHICH IS ANALYSED IN DETAIL IN SECTION 8(a)(i). THE FLIGHT WAS MADE TOWARDS THE STATION SO THAT THE ECHO EDGE AT 20 MILES WAS THAT FIRST ENTERED BY THE AIRCRAFT.

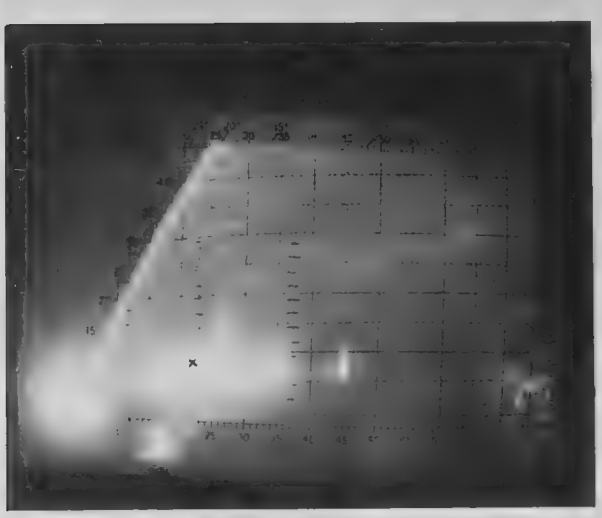

PHOTOGRAPH (vii) 22ND JUNE, 1948. 1127 G.M.T.
BEARING 150° T.

BRIGHT BAND ECHO INVESTIGATED BY METEOROLOGICAL RESEARCH FLIGHT. THE AIRCRAFT (MARKED X) IS AT 22 MILES. FLIGHT IN THIS ECHO WAS "QUITE SMOOTH," BUT SEE PHOTOGRAPH (viii).

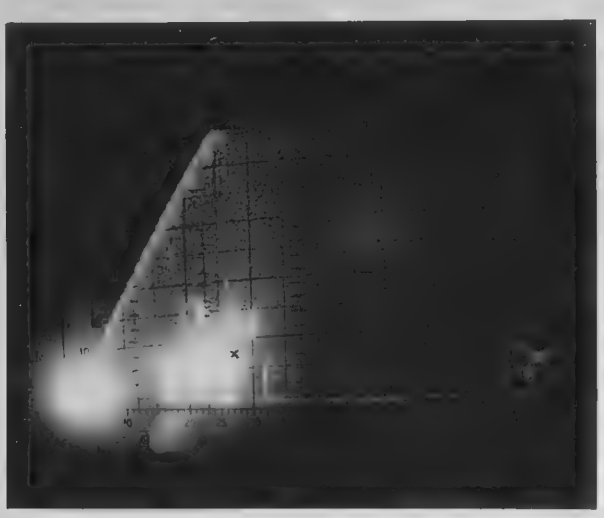

PHOTOGRAPH (viii) 22ND JUNE 1948, 1130 G.M.T.
BEARING 130° T.

THE AIRCRAFT IS NOW AT 27½, HAVING CROSSED THE NARROW ECHO COLUMN AT 25-26½ MILES. UNEXPECTED TURBULENCE WAS EXPERIENCED IMMEDIATELY ON ENTRY INTO THIS COLUMN. (THE FLIGHT WAS NOT MADE ON A COURSE DIRECTLY AWAY FROM THE STATION SO THAT NEITHER PHOTOGRAPH (vii) NOR (viii) GIVES A COMPLETE CROSS-SECTION OF THE WHOLE FLIGHT OF THE AIRCRAFT WHILE IN THE ECHO - PHOTOGRAPH (vii) IS TYPICAL OF THE ECHO UP TO 25 MILES AND PHOTOGRAPH (viii) AFTER 25 MILES RANGE).

This report is not to be published and is to be treated CONFIDENTIALLY. Its contents must not be quoted.

M.R.P. 486 (Revised)
S.C. III/30.
27th September, 1949.

AD 223160

AIR MINISTRY

METEOROLOGICAL RESEARCH COMMITTEE

THE HUMIDITY OF THE LOWER STRATOSPHERE: THE RESULTS OF HIGH LEVEL ASCENTS BY AIRCRAFT OF THE METEOROLOGICAL RESEARCH FLIGHT

by
H.C. Shellard
(Meteorological Office)

AIR WEATHER SERVICE
TECHNICAL REFERENCE FILES

1. Introduction

The results of over 70 high level ascents made in Fortress (1943 - 44) and Mosquito (1945-49) aircraft of the Meteorological Research Flight are summarised in tabular form. Mean values of lower stratosphere and upper troposphere humidity are obtained and the mean lapse rates of frost point and temperature in the neighbourhood of the tropopause are discussed. Significant correlations are shown to exist between height of tropopause and the frost points at several levels, and also between the frost point lapse rate and temperature lapse rate in the lower stratosphere. A high correlation is also found between the frost point at 250 mb and the temperature at 500 mb, the latter being representative of the temperature of the whole column of air in the troposphere.

2. The available data

The ascents dealt with have been made at various times during the past six years and include some made from Boscombe Down in 1943 - 5 as well as more recent ones from Farnborough, the majority of which have been made during 1949. They consist of measurements of temperature and frost point, usually at 1,000 feet intervals, from low level to the aircraft ceiling. Temperatures were measured using M.O. knife type resistance thermometers with balanced bridge indicators. Frost point measurements were made on the early (Fortress) ascents using the M.O. Mk 1 aircraft frost point hygrometer, but on the later (Mosquito) ascents the M.O. pressurised Mk 2a aircraft frost point hygrometer has generally been used. A large number of Mosquito ascents has also been made in which the frost points were measured using the M.O. photo-electic frost point hygrometer, but the results of the majority of these have had to be excluded from this paper as a thermometry error was recently found to have developed in the instrument, thus casting doubt on the accuracy of its previous readings.

Many of the ascents were unfortunately spoiled by instrument failures of one sort or another, whilst on other occasions there has been aircraft trouble causing curtailment of a flight. In the hygrometers perhaps the chief source of trouble has been the mechanism used to cool the thimbles by pumping liquid air.

The ceiling of the Mosquito aircraft employed for these flights varies between 38,000 and 41,000 ft, whilst that of the Fortress used for the ascents of 1943-44 varied from 33,000 to 37,000 ft: nearly three-quarters of the ascents have reached or exceeded the 200 mb level (38,500ft), however.

The results of 64 successful ascents are summarised in Table I; those of another 13 are given in a different form in the subsidiary Table Ia. None of these latter ascents could be included in the main table, ten of them because the tropopause was not reached, one because the tropopause cannot be satisfactorily fixed owing to lack of observations, and the other two because the results are doubtful (these will be referred to again later). It should be mentioned here that the observations are biassed towards low tropopause: the mean height of the tropopause over S. England (from radio-sonde ascents) is about 36,000ft, whilst that given by our ascents is about 34,000ft. The main reason for this is that prior to June 1948 ascents were usually only made when there was considered to be a good prospect of penetrating well into the stratosphere i.e., when the tropopause was low. Since that date ascents have been made regardless of the forecasted tropopause height, but the low

/tropopause

tropopause bias remains for the whole period. In future ascents there will probably be a bias towards high tropopause because of the restrictions on flying imposed by the unsettled weather usually associated with low tropopause.

3. Treatment of the data

Unfortunately the ascents are unevenly distributed throughout the year. Of the 64 listed in Table I, there are in Spring 25, in Summer 12, in Autumn 5, and in Winter 22. They have nevertheless been grouped seasonally in this paper in order to see whether there is any evidence for a seasonal variation of stratosphere humidity. At some later date the number of Summer and Autumn ascents should be greater and it may then be possible to show more conclusively whether such a variation exists.

In the present analysis the seasons have been chosen as indicated below, because the mean tropopause pressure over S. England is a maximum in mid-February and a minimum in mid-August:-

Spring - April, May, June
Summer - July, August, September
Autumn - October, November, December
Winter - January, February, March

The method of treatment has been to extract from each ascent curve, (taking the tropopause as origin) values of temperature and frost point at 25 mb intervals over the range (tropopause pressure, P_c, + 150 mb) to (P_c - 100 mb). The object is to study the transitions from troposphere to stratosphere under different conditions and to enable mean ascent curves relative to the tropopause to be drawn. Values are also given in Table I for the three fixed pressure levels 300, 250 and 200 mb.

The tropopause pressure, P_c, and type, are given in column 3 of the table. It has been found that the current M.O. definitions of type as given in S.D.T.M.107 and in the introduction to the D.W.R. - Upper Air Section, (the two differ slightly) are not sufficiently precise, and for the purpose of this paper the following amended definitions have been adopted.

Type I. There is an abrupt change of lapse rate to inversion, and for no subsequent 3,280 ft (Km) layer does the lapse rate exceed 1.1°F per 1,000 ft (2°C per Km). H_c is the height of the abrupt change.

Type II. There is an abrupt change to a lapse rate of less than 1.1°F per 1,000 ft (2°C per Km), or to isothermal, and for no subsequent 3,280 ft (Km) does the lapse rate exceed 1.1°F per 1,000 ft (2°C per Km). H_c is the height of the abrupt change.

Type III. Where there is no abrupt change of lapse rate H_c is taken as the height of the point at which the lapse rate first becomes less than 1.1°F per 1,000 ft (2°C per Km), provided that it does not exceed this value for any subsequent 3,280 ft (Km) layer.

In addition the following rules have been adopted:-

(i) An abrupt change is defined as one in which the mean lapse rates measured over 1,000 ft layers on either side of the change differ by at least 2°F per 1,000 ft.

(ii) Where there is a double tropopause, i.e. two abrupt changes as defined in (i), the lower one satisfying the type II tropopause definition and the upper one the type I definition given above, then in this paper the tropopause is taken as being at the lower level and is classified as Type II. (Such cases are indicated in the Remarks column in Table I).

Table II is a frequency table, in terms of relative humidity with respect to ice, which conveniently summarises our measurements. The outstanding features are (1) the rapid decrease in relative humidity as the stratosphere is entered and (2) the fact that the relative humidity continues to decrease,

/though

though less rapidly, the further into the stratosphere one goes. Mean values are given for each level. Eight of our ascents have penetrated 100 mb into the stratosphere, the mean relative humidity at that level being 2.2%, and the range, 0.9% to 3.9%. For convenience a table showing relative humidity as a function of temperature and frost point is included as an Appendix.

4. Discussion

(a) General

On examining the ascents the first thing which strikes one perhaps is that there is frequently a sharp fall of frost point on entering the stratosphere. This was remarked upon by Dobson, Brewer and Cwilong[1] in their discussion of some of the early Boscombe Down ascents. This rapid fall of frost point does not always occur, however, and there are many ascents in which the lapse rate of frost point is not materially different above and below the tropopause. Typical examples of ascents of the two types are given in Figs. 1 and 2 respectively.

If all the ascents are separated broadly into these two types it is found that those showing the sharp frost point lapse discontinuity are more often than not associated with a type I tropopause. Conversely those ascents showing no marked frost point lapse discontinuity are more often than not associated with a Type II tropopause. On some of the first type we have also found that the sharp frost point fall does not always coincide with the level of the tropopause as usually defined; it may be a little higher or lower. It is clear from these results that it would be impracticable to replace the rather unsatisfactory definitions of the tropopause, based on temperature lapse changes, by a set of definitions based on changes in the frost point lapse rate.

The other outstanding feature of the ascents is, as has already been mentioned, the dryness of the air in the stratosphere. Frost points nearly always lie within the range -80 to -120°F. We have had two exceptional ascents, however, which indicated conditions of high moisture content in the stratosphere. They occurred on successive days, 19th and 20th January, 1948, and details are given in Table Ia. The first indicated a relative humidity of 26% and the second a relative humidity of 75% at the 200 mb level, which in each case was well into the stratosphere. As the results of these ascents are completely at variance with all otherswe have obtained, and because the humidity measurements were made using the Mk 2a visual hygrometer, whose readings are always subject to a little doubt owing to the possibility of moister pressurised cabin air leaking into the instrument, we have for the present rejected them. It may be that one day we shall obtain similar results again, and meanwhile the possibility remains that very occasionally the air in the lower stratosphere may be nearly saturated.

(b) Mean ascent curves

Table III has been compiled from Table I and gives mean values of temperature and frost point at the various levels. Part A (1) to (7) takes all ascents into account. In Part A (8) to (9) ten ascents of Table I have been omitted because their data are restricted to the troposphere only or the stratosphere only and their inclusion might give misleading results. Part B gives means for 32 selected ascents only, the criterion for selection being that full frost point and temperature data be available from level P_c + 150 mb to level P_c - 50 mb. From Table III mean ascent curves can be plotted. Such curves are given in Figs. 3 to 7 which will now be discussed. As the number of ascents available is so limited, mean curves for each half year rather than each quarter have been plotted, though the quarterly means are given in Table III.

Figure 3 illustrates that there is little seasonal variation in the moisture content of the lower stratosphere. Frost points not far above the tropopause tend to be higher in summer than in winter, but further into the stratosphere there is little difference. No great significance can be attached to the crossing over of the summer and winter frost point curves owing to the very limited number of ascents exceeding the P_c - 50 mb level.

/Due

Due to the relatively high seasonal variation in stratosphere temperature the corresponding relative humidities (entered against the temperature curves of Fig. 3) have higher values in winter than in summer. In the upper troposphere, where the seasonal frost point variation is greater, values of relative humidity are lower in winter than in summer.

The mean curve for the whole year in Fig. 3 gives an average frost point fall of 7.2°F in the 25 mb layer below the tropopause, and a fall of 11.8°F in the 25 mb layer above the tropopause, i.e., there is on the average a marked steepening of the lapse rate as the stratosphere is entered. Turning now to Fig. 4, which gives mean curves for type I and type II tropopauses, we find that the corresponding figures are 7.9 and 13.8 for Type I and 7.0 and 10.6 for Type II. Thus a steep stratospheric frost point lapse rate tends to be associated with Type I tropopause, i.e., with temperature inversion.

Care must be taken in drawing conclusions from the slope of the upper parts of the curves in Figs. 3 and 4. Each point on these curves is the mean of a number of observations, but this number decreases with height. Further, since the aircraft ceiling is limited, the few observations available for the final points on the curves were necessarily made on occasions of low tropopause. To overcome this difficulty to some extent, Part B of Table III was constructed. The corresponding ascent curves are shown in Figs. 5, 6 and 7.

Fig. 5 confirms the result of Fig. 3, that the average summer stratosphere is in its lower layers slightly moister in terms of frost point than the winter one. On the curve for the full year the average frost point lapse is 7.9°F in the 25 mb layer below the tropopause. In the stratosphere the frost point falls 12.2°F in the first and 10.0°F in the second 25 mb layer. The rate of fall of frost point in the stratosphere thus decreases with height and it may be that the frost point eventually becomes constant, though the curves of Fig.5 do not extend sufficiently far upwards to show whether this is so or not. More ascents on occasions of low tropopause, or, preferably, ascents to greater altitudes than 40,000 ft are required.

Fig. 6 indicates perhaps more clearly than Fig. 4 the tendency for a steep frost point lapse rate just above the tropopause to be associated with temperature inversion. When, on the other hand, there is no temperature inversion (Type II tropopause) the discontinuity in frost point lapse rate at the tropopause is quite small. It may well be that this steepening of frost point lapse rate is not specially a characteristic of the tropopause but that it occurs only because there is a temperature inversion, for it is well known that the same effect occurs at subsidence inversions in the troposphere.

In Fig. 7 mean ascent curves are shown for those selected ascents having (a) higher than average and (b) lower than average (for our ascents), tropopauses. The higher mean tropopause is of course colder than the lower one, it also has a lower frost point. The same applies to corresponding levels in the two stratospheres, and it will be noticed that in terms of relative humidity (entered against the temperature curves) there is little between the two. At any fixed pressure level however the air is much drier in terms of frost point if the tropopause is low, and this rule appears to be valid whether the level chosen is in the lower stratosphere or the upper troposphere. There is a slight tendency, not very clear in the figure, for both temperature and frost point discontinuities to be sharper at the high tropopause than the lower one.

(c) Some correlation coefficients.

The results discussed above suggest that there is a correlation between lapse rate of temperature and lapse rate of frost point in the lower stratosphere. Values of temperature fall and of frost point fall in the layer 25 mb thick above the tropopause have been extracted from Table I and correlated. The resulting correlation coefficients are -0.41 from 58 pairs of values if all ascents are considered, and -0.61 from 35 pairs of values if ascents with Type I tropopause only are considered. The probabilities of such correlations arising by random sampling from an uncorrelated population are in both cases less than one in one hundred.

/A

A number of other quantities have also been correlated and the results are set out in the following table:-

Table IV. Some Correlation Coefficients

Temperature at tropopause, T_c	/ Pressure at tropopause, P_c	+ 0.81	64 prs of values
Frost point at tropopause, F_c	/ P_c	+ 0.50	64 "
" " 50mb above t'pause	/ P_c	+ 0.42	37 "
" " at 200mb, F_{200}	/ P_c	- 0.67	48 "
F_{250}	/ P_c	- 0.67	63 "
F_{300}	/ P_c	- 0.62	64 "
F_{200}	/ Temperature at 500 mb, T_{500}	+ 0.62	48 "
F_{250}	/ T_{500}	+ 0.82	63 "
F_{300}	/ T_{500}	+ 0.79	64 "
P_c	/ T_{500}	- 0.61	64 "

The first of these represents a well known fact, the higher the tropopause the colder it is. The correlation between P_c and frost point at the tropopause is moderately significant, but that between P_c and the frost point 50 mb above the tropopause (a level chosen as representative of the stratospheric air) is definitely less so. The three correlations between P_c and frost point at the fixed pressure levels 200, 250 and 300 mb are very significant, These relationships are illustrated in Figs. 8, 9 and 10, which are dot-diagrams showing P_c against frost point at the three levels. In each case the full lines are lines of best fit computed by the method of least squares, whilst the dashed lines are parallel lines enclosing 80% of the observations. They indicate that given P_c the frost points at 200, 250 and 300 mb can be predicted to within 10, $11\frac{1}{2}$ and $13\frac{1}{2}^{\circ}$F respectively, on 80% of occasions. Alternatively given the frost point at either 200, 250 or 300 mb, P_c can be predicted to within 54, 59 or 71 mb, on 80% of occasions. When many more ascents become available it is probable that these figures will be improved, as it may then be possible to construct separate diagrams for each season. All the dots on Fig. 10, for example, which lie outside the dashed lines to the right of the figure are observations made in the summer half year.

These correlations between frost point at 200, 250 and 300 mb and P_c are similar in magnitude to those found by Dines (0.7 approx) and Priestley (0.65)(2) between T_{500} and H_c, and it seems possible, therefore, that the frost point at a fixed level may be associated with the mean temperature of the troposphere through which the moisture may have ascended. Priestley has shown that T_{500} can be taken as representative of the whole column of air in the troposphere, and that it is in fact preferable to T_m (the mean temperature from 1000 mb to 300 mb) for this purpose. Correlation coefficients have therefore been computed for T_{500} and the frost points at 200, 250 and 300 mb and are given in the table above. The last two are remarkably high, and the highest, that of T_{500} and F_{250}, is illustrated in Fig. 11 as a dot-diagram. Here again the line of best fit and lines enclosing 80% of the observations have been drawn in. It follows that given T_{500}, the frost point at 250 mb can be predicted to within $9\frac{1}{2}^{\circ}$F on 80% of occasions. It may be significant that the correlation between frost point and T_{500} is least at 200mb, a level which is predominantly stratospheric. This would suggest that the frost point in the stratosphere is less subject to control by tropospheric processes, or is less of an air mass characteristic, than is the frost point at lower (predominantly tropospheric) levels.

Finally a coefficient of -0.61 between P_c and T_{500}, for our observations, has been computed. This agrees well with Priestley's value of +0.65 between H_c and T_{500}.

5. Conclusions

(1) Frost points in the lower stratosphere (up to 40,000 ft) over S. England are almost invariably low and within the range -80 to -120°F.

/(2)

(2) There is some evidence, not yet conclusive, for a small seasonal variation in the moisture content of the lower stratosphere, frost points being higher in summer than in winter.

(3) There is often an increase in frost point lapse rate at the tropopause. A rapid decrease in frost point above the tropopause is most likely to occur when the temperature lapse changes sharply to inversion, and there appears to be an inverse relation between frost point lapse rate and temperature lapse rate in the lower stratosphere.

(4) Very significant correlations exist between P_c and the moisture content of the atmosphere between 300 and 200 mb, and also between T_{500} and the moisture content of this region. Whilst in the former case there is no very significant variation of the correlation coefficient with height between 300 and 200 mb, in the latter the correlation is definitely least at 200 mb (a predominantly stratospheric level).

(5) Further important results might be obtained by treating each high level ascent synoptically and, in some cases perhaps, deducing the origins of the air masses whose frost points have been measured, by a method of trajectories.

References (1) Proc. Roy. Soc. A. Vol. 185, 1946
(2) S.D.T.M. No. 107, Meteorological Office, Air Ministry.

APPENDIX

Relative Humidity, (with respect to ice), as a function of temperature and frost point.

FROST POINT -°F.	TEMPERATURE -°F.																
	0	5	10	15	20	25	30	35	40	45	50	55	60	65	70	75	80
20	34	45	59	76	100												
25	26	34	44	58	76	100											
30	20	25	33	43	57	75	100										
35	14	19	24	32	41	55	74	100									
40	10	14	18	23	31	40	54	74	100								
45	7	10	13	17	22	30	39	53	73	100							
50	5	7	9	12	16	22	29	39	53	73	100						
55	4	5	7	8	11	15	21	28	38	52	72	100					
60	3	4	5	6	8	11	14	20	27	37	51	72	100				
65	2	3	3	4	6	7	10	14	19	26	36	50	71	100			
70	1	2	2	3	4	5	7	10	13	18	25	35	49	70	100		
75		1	2	2	3	4	5	7	9	13	17	24	34	48	69	100	
80			1	1	2	3	3	5	6	9	12	17	24	34	48	68	100
85					1	2	2	3	4	6	8	11	15	23	32	47	67
90						1	1	2	3	4	5	7	10	15	22	32	45
95								1	2	3	4	5	7	10	15	21	31
100									1	2	2	3	5	7	9	14	19
105			Less than 1 %							1	2	2	3	4	6	9	14
110											1	1	2	3	4	6	9
115													1	2	3	4	6
120														1	2	2	3

TABLE I. TEMPERATURES AND FR… POST-POINTS IN 64 STRATOSPHERE ASCENTS.

DATE	TIME G.M.T.	TROPOPAUSE HEIGHT AND TYPE ft.	Type	150 MB. BELOW TROPOPAUSE F.P. °F	TEMP. °F	125 MB. BELOW TROPOPAUSE F.P. °F	TEMP. °F	100 MB. BELOW TROPOPAUSE F.P. °F	TEMP. °F	75 MB. BELOW TROPOPAUSE F.P. °F	TEMP. °F	50 MB. BELOW TROPOPAUSE F.P. °F	TEMP. °F	25 MB. BELOW TROPOPAUSE F.P. °F	TEMP. °F	AT TROPOPAUSE F.P. °F	TEMP. °F	25 MB. ABOVE TROPOPAUSE F.P. °F	TEMP. °F	50 MB. ABOVE TROPOPAUSE F.P. °F	TEMP. °F	75 MB. ABOVE TROPOPAUSE F.P. °F	TEMP. °F	100 MB. ABOVE TROPOPAUSE F.P. °F	TEMP. °F	300 MB. F.P. °F	TEMP. °F	250 MB. F.P. °F	TEMP. °F	200 MB. F.P. °F	TEMP. °F	LIMIT OF ASCENT. MB.	PLACE (APPROX)	REMARKS.
SPRING																																		
3.5.44	1600	275	II	63	24	65	29	62	35	55	41	61	47	69	53	71	61	95	62							69	53	95	62			235	HUMBER AREA	
5.5.44	1100	400	II	25	10	27	15	30	21	36	26	42	33	48	40	55	47	72	47	89	47	91	51	96	51	96	51					260	S. ENGLAND	
22.4.45	?	250	II	42	21	48	28	56	36	61	42	67	49	73	59	73	69	88	72	102	71	112	70			67	49	73	69	102	71	160	"	
25.4.45	?	275	I	36	24	43	31	46	38	49	45	54	53	64	61	72	70	86	68	103	62	103	57			64	61	86	68	103	57	200	"	
25.5.45	1400	225	I	51	31	43	37	60	45	67	51	68	57	79	60	87	65	101	61	115	61					67	51	79	60	101	61	180	"	
30.5.45	1300	275	I	32	26	39	32	45	39	52	47	61	55	65	61	71	70	100	62	105	56	119	53			65	61	100	62	119	53	200	"	
8.6.45	?	300	I	39	21	45	27	53	33	56	38	59	43	69	48	81	53	92	50	101	47	110	50			81	53	101	47			215	"	
4.4.48	1500	360	II													94	46	98	45	102	45	108	47	109	46	104	44	114	48			215	"	
24.5.48	1500	240	I	64	33	66	38	59	42	55	50	64	57	68	64	76	69	97	59	110	56					61	53	74	66	107	55	180	FARNBORO'—LONDON	
27.5.48	1100	230	I	44	32	54	37	64	44	66	51	66	55	71	63	78	68	86	60	84	54					66	52	72	65	87	59	185	SHAMPTON—LONDON	
29.6.48	1500	285	II	27	20	32	22	39	29	45	33	47	39	54	45	67	52	73	53	88	54	102	45			58	47	73	54	110	43	200	FARNBOROUGH	DOUBLE TROPOPAUSE 240 I
22.4.49	1100	195	I	53	36	56	42	60	49	66	57	75	66	81	72	87	81	102	69							60	48	73	64	86	80	175	"	
25.4.49	1030	250	II	30	28	68	33	68	39	78	44	84	45	94	42	95	50	103	50	103	49					84	45	95	50	103	49	200	"	
26.4.49	1030	250	I	65	29	53	33	61	39	68	44	70	52	87	57	99	61	105	57	108	59					70	52	99	61	108	59	190	FARNBORO'—I.O.W.	
2.5.49	1430	225	I	47	26	50	35	57	43	66	50	74	58	78	65	81	73	99	72							66	50	78	65	99	72	180	FARNBOROUGH	
3.5.49	1100	225	I	52	27	58	35	66	42	68	50	74	57	76	67	83	72	93	73							68	50	76	67	93	73	185	"	
5.5.49	1000	285	II	31	17	37	23	42	30	51	36	57	43	65	49	69	55	76	55	96	55	96	51			67	52	82	57	99	51	195	"	DOUBLE TROPOPAUSE 250 I
18.5.49	1100	260	I	50	25	44	29	46	36	52	43	60	52	67	60	74	66	92	59	103	57					62	55	82	65	108	54	195	"	
13.6.49	1130	195	II	67	32	71	39	77	46	75	53	74	60	78	68	89	74									75	45	73	58	88	74	185	"	
14.6.49	1400	225	II	42	24	51	30	58	37	62	46	67	54	77	61	79	69	92	69							62	46	77	61	92	69	185	"	
15.6.49	1030	225	I	57	26	63	33	69	40	69	48	71	56	77	63	84	69	102	66							69	48	77	63	102	66	185	"	
16.6.49	1030	215	I	53	28	55	35	55	43	63	50	63	58	75	66	90	71	99	67							63	46	66	65	96	70	185	"	
21.6.49	1500	195	II	53	27	57	35	63	43	69	52	72	61	77	71	83	79									62	42	72	59	81	78	185	"	
22.6.49	1030	225	II	43	21	53	29	57	36	57	44	61	50	67	60	73	67	92	71	93	74					57	44	67	60	92	71	180	"	
27.6.49	1030	185	I	30	28	41	36	46	44	56	53	67	60	75	69	85	74									43	39	63	56	79	71	180		
SUMMER																																		
22.8.43	1600	300	I	30	12	36	17	43	23	49	28	55	35	64	42	72	49	84	47							72	49	82	45			230	S. ENGLAND	F.P.'s DOUBTFUL ABOVE 275 MB. TEMPS. BELOW 300 MB. FROM LARKHILL R/S (THERMO U/S).
7.9.43	1500	250	II	57	20	48	26	39	32	34	38	47	46	54	54	67	63	84	62							47	46	67	63			230	"	
19.7.45	1500	280	I	47	12	43	17	46	24	53	31	59	39	62	50	69	57	86	50	95	47	103	48			63	51	87	49	103	49	195	"	
17.8.45	1500	225	I	43	21	47	27	59	35	71	44	70	53	69	60	78	69	104	59							71	44	69	60	104	59	185	"	
5.7.49	0930	300	II	46	14	46	20	47	26	54	32	61	38	67	40	81	44	84	45	86	46	97	48	101	49	81	44	86	46	101	49	195	FARNBOROUGH	
6.7.49	1000	240	II	44	22	43	26	46	32	42	39	56	47	63	55	76	63	83	65	109	58					52	44	70	60	105	58	185	"	DOUBLE TROPOPAUSE 215 I
7.7.49	1100	260	I	32	16	37	24	38	32	45	40	53	49	60	56	80	61	95	59	111	53	112	51			54	52	91	59	112	52	190	"	
8.7.49	1100	250	I	39	20	47	27	56	35	59	42	63	49	67	55	74	61	82	57	94	54					63	49	74	61	94	54	195	"	
14.7.49	1000	250	I	20	19	34	24	46	31	49	39	54	47	61	53	73	59	91	54	101	51					54	47	73	59	101	51	195	"	
15.7.49	1030	260	II	30	17	37	24	38	29	51	36	60	44	62	52	72	58	82	58	102	49					66	47	77	58	106	48	195	"	DOUBLE TROPOPAUSE 240 I
18.7.49	1000	260	I	38	22	41	28	41	36	49	33	54	51	60	59	71	68	94	54	104	49					55	54	79	58	106	48	195	"	
22.7.49	1000	195	II	45	26	44	34	43	42	51	50	62	56	67	66	73	72									41	41	61	55	73	72	185	"	
AUTUMN																																		
22.12.43	1500	300	I	48	22	51	27	53	32	50	38	50	45	62	50	71	60	92	55	106	51	115	46			71	60	105	50			220	S. ENGLAND	
24.12.43	1100	240	I		35	60	42	66	50	68	57	74	63	80	70	87	74	100	72							72	62	84	73			220	S. ENGLAND	
23.10.45	1300	300	I	46	21	58	25	71	29	72	33	73	39	78	48	85	57	86	57	95	51	102	55	109	51	85	57	95	51	109	51	200	"	
8.12.47	1200	345	II	47	25	53	31	62	38	64	44	68	46	76	48	84	55	90	56	95	54	99	52			95	55	100	53			250	FARNBOROUGH	DOUBLE TROPOPAUSE 310 I
19.10.48	1030	330	I	—	—	40	31	42	35	46	40	52	46	58	52	62	58	80	55	97	52	104	50	110	49	84	54	104	50	114	49	200	"	
WINTER																																		
7.2.45	1400	300	I	65	22	67	26	69	32	71	38	72	46	75	52	80	59	91	55	101	55	106	57			80	59	101	55			220	S. ENGLAND.	
9.2.45	1100	260	II	50	30	53	34	63	43	65	50	78	56	75	62	80	66	85	65							82	58	82	65			220	E. ANGLIA	
8.1.48	1430	280	I	62	35	74	39	76	42	72	45	70	51	84	57	93	62	103	59							88	57	103	57			240	SOUTHAMPTON	
22.1.48	1200	315	II													88	57	94	55	97	59	100	52	100	49	91	56	99	52			205	CAMBRIDGE	DOUBLE TROPOPAUSE 270 I
6.2.48	1430	280	II	49	30	55	37	56	45	72	50	82	53	88	57	99	61	101	62	109	57					89	56	100	60			215	FARNBOROUGH	" " 250 I
17.2.48	1600	345	II													60	56	82	59	89	57	93	61	101	59	87	59	97	60			205	SOUTHAMPTON	" " " 260 I
26.2.48	1500	260	II	77	29	82	37	84	44	89	48	89	52	87	55	92	61	107	60	107	63	117	61			87	53	97	59	114	59	185	"	" " " 215 I
27.2.48	1100	285	II													69	68	85	65	92	68	102	70	109	62	66	65	89	66	110	63	190	"	" " " 220 I
21.1.49	1200	240	II	37	26	44	33	50	41	60	48	68	58	76	66	82	75	98	76							63	54	82	73			215	FARNBOROUGH	
28.1.49	1230	205	I	44	36	51	44	63	51	76	58	88	63	97	69	102	72	109	68							65	53	92	64	103	70	185	"	
11.2.49	1200	275	I	31	33	35	38	44	44	55	51	70	55	86	62	88	67	94	67	96	62	104	55			86	62	94	67	104	55	185	"	
15.2.49	1330	195	I	43	35	49	41	56	50	64	60	75	70	81	79	88	88	104	80							56	48	73	68	87	87	175	"	
16.2.49	1200	185	I	57	36	56	45	51	53	67	62	79	71	93	79	97	89									54	48	70	66	95	83	170	"	
17.2.49	1500	250	I									75	59	79	64	84	70	86	68	91	65					75	59	84	70	91	65	185	"	
21.2.49	1500	205	I	43	31	44	40	54	45	59	52	64	60	75	67	84	74	107	64							54	46	66	62	90	73	180	"	
22.2.49	1530	205	II	44	35	52	42	60	50	73	57	80	65	85	77	94	85	105	80							63	52	81	68	92	85	175	"	DOUBLE TROPOPAUSE 190 I
28.2.49	1230	195	I	55	49	61	56	74	64	81	72	90	79	100	87	105	95	112	88							74	63	88	77	103	94	170	"	
1.3.49	1130	225	II	59	37	67	44	75	50	84	57	89	65	98	75	102	85	107	87	110	86					84	57	98	75	107	87	175	"	
2.3.49	1100	205	I	68	43	64	49	78	56	83	63	91	72	97	82	105	92	110	87							78	58	93	74	107	91	170	"	
17.3.49	1500	205	I	56	41	67	50	75	54	76	63	81	70	88	77	93	83	109	76							76	56	83	71	95	82	185	"	
18.3.49	1100	240	II	53	31	70	37	71	44	66	52	73	60	84	68	90	76	97	75	106	72					69	57	85	73	98	77	185	"	DOUBLE TROPOPAUSE 195 I
24.3.49	1230	180	I	66	41	70	48	76	57	85	65	94	73	99	80	102	89									70	50	86	67	101	82	170	"	

TABLE II. FREQUENCY OF RELATIVE HUMIDITY (W.R.T. ICE)

R. HUMIDITY RANGE % / LEVEL	0-0·9	1-2·9	3-4·9	5-9·9	10-14	15-19	20-24	25-29	30-39	40-49	50-59	60-69	70-79	80-89	90-99	⩾100	MEAN R.H. %	TOTAL NO. OF CASES
50 MB. BELOW TROPOPAUSE	0	0	0	3	1	3	5	5	13	9	6	7	5	1	2	0	43·5	60
25 MB. BELOW TROPOPAUSE	0	1	0	2	5	3	4	1	12	7	11	6	3	2	2	1	44·2	60
TROPOPAUSE	0	1	1	7	3	1	4	2	14	10	6	4	6	1	3	1	42·5	64
25 MB. ABOVE TROPOPAUSE	0	4	6	18	8	10	8	4									13·8	58
50 MB. ABOVE TROPOPAUSE	0	16	9	7	2	2	1										5·3	37
75 MB. ABOVE TROPOPAUSE	2	14	2	3													2·7	21
100 MB. ABOVE TROPOPAUSE	1	5	2														2·2	8

TABLE III. MEAN VALUES OF TEMPERATURE AND FROST-POINT. (NUMBER OF ASCENTS GIVEN IN BRACKETS).

CATEGORY		150 MB. BELOW TROPOPAUSE	125 MB. BELOW TROPOPAUSE	100 MB. BELOW TROPOPAUSE	75 MB. BELOW TROPOPAUSE	50 MB. BELOW TROPOPAUSE	25 MB. BELOW TROPOPAUSE	AT TROPOPAUSE	25 MB. ABOVE TROPOPAUSE	50 MB. ABOVE TROPOPAUSE	75 MB. ABOVE TROPOPAUSE	100 MB. ABOVE TROPOPAUSE	300 MB.	250 MB.	200 MB.	MEAN TROPOPAUSE HEIGHT MB.
A. ALL AVAILABLE ASCENTS FOR:—																
(1) YEAR	TEMP. °F	26·9 (58)	33·1 (59)	39·9 (59)	46·6 (59)	53·8 (60)	60·8 (60)	67·0 (6?)	62·9 (58)	56·9 (37)	53·8 (21)	52·0 (8)	51·8 (64)	61·1 (63)	65·2 (48)	253
	F.P. °F	47·6	51·6	56·8	61·8	67·9	74·8	82·0	93·8	99·9	104·5	104·4	69·9	84·0	99·5	
(2) SPRING	TEMP. °F	25·7 (24)	31·8 (24)	38·7 (24)	45·6 (24)	52·5 (24)	59·3 (24)	65·2 (25)	61·2 (22)	56·5 (15)	53·0 (8)	48·5 (2)	49·5 (25)	60·5 (24)	63·6 (21)	250
	F.P. °F	47·3	50·7	55·7	60·1	64·8	72·2	79·8	92·?	100·1	105·1	102·5	68·2	81·1	97·8	
(3) SUMMER	TEMP. °F	18·4 (12)	24·5 (12)	31·4 (12)	37·7 (12)	46·2 (12)	53·5 (12)	60·3 (12)	55·5 (11)	50·9 (8)	49·0 (3)	49·0 (1)	47·3 (12)	56·1 (12)	54·0 (19)	256
	F.P. °F	39·3	41·9	45·2	50·6	57·8	63·0	73·8	88·1	100·3	104·0	101·0	59·9	76·3	100·5	
(4) AUTUMN	TEMP. °F	25·7 (4)	31·2 (5)	36·8 (5)	42·4 (5)	48·0 (5)	53·6 (5)	60·8 (5)	59·0 (5)	52·0 (4)	50·7 (4)	50·0 (2)	57·6 (5)	55·4 (5)	50·0 (2)	303
	F.P. °F	48·0	52·4	58·8	60·0	63·4	70·8	77·8	89·6	98·3	105·0	109·5	81·4	97·6	111·5	
(5) WINTER	TEMP. °F	34·5 (18)	41·2 (18)	48·1 (18)	55·0 (18)	62·0 (19)	69·2 (19)	74·1 (22)	69·8 (20)	64·4 (10)	59·3 (6)	56·7 (3)	55·7 (22)	65·8 (22)	76·9 (15)	243
	F.P. °F	53·3	58·9	65·2	72·1	79·3	86·6	89·8	99·3	99·8	103·7	103·3	74·4	88·3	99·8	
(6) SUMMER HALF-YEAR	TEMP. °F	22·8 (27)	28·9 (28)	35·7 (28)	42·3 (28)	49·8 (28)	57·2 (28)	63·7 (28)	58·3 (24)	53·8 (18)	50·0 (8)	49·7 (3)	48·6 (28)	57·7 (28)	58·6 (25)	249
	F.P. °F	43·3	47·0	51·6	56·0	61·3	67·5	76·7	90·0	99·6	106·1	106·7	63·5	78·2	99·6	
(7) WINTER HALF-YEAR	TEMP. °F	30·5 (31)	37·0 (31)	43·8 (31)	50·5 (31)	57·4 (32)	64·0 (32)	69·5 (36)	66·2 (34)	59·8 (19)	56·2 (13)	53·4 (5)	54·1 (36)	63·9 (35)	72·4 (23)	256
	F.P. °F	51·3	55·8	61·4	67·0	73·7	81·2	86·1	96·6	100·1	103·5	103·0	71·7	88·6	94·6	
(8) TYPE I TROPOPAUSE	TEMP. °F	27·8 (31)	33·8 (32)	40·3 (32)	46·9 (32)	54·6 (33)	61·5 (33)	68·2 (33)	63·0 (33)	54·8 (19)	52·2 (10)	50·0 (2)				249
	F.P. °F	46·8	50·5	57·0	61·8	67·1	74·7	82·6	96·4	101·0	107·8	109·5				
(9) TYPE II TROPOPAUSE	TEMP. °F	24·2 (21)	30·3 (21)	37·1 (21)	43·5 (21)	49·9 (21)	56·4 (21)	63·5 (21)	64·0 (21)	59·6 (14)	54·0 (7)	50·0 (2)				263
	F.P. °F	47·1	51·8	55·6	60·3	67·2	73·2	80·2	90·8	99·6	102·0	98·5				
B. ASCENTS GIVING FULL DATA FROM (TROPOPAUSE − 100) TO (TROPOPAUSE + 50 MB) FOR:—																
(1) YEAR (32)	TEMP. °F			35·8	41·8	48·6	54·8	61·6	59·2	56·7						272
	F.P. °F			53·4	58·3	63·6	70·7	78·6	90·8	100·8						
(2) SUMMER HALF-YEAR (18)	TEMP. °F			34·1	40·1	47·6	54·5	60·9	57·2	53·8						265
	F.P. °F			49·6	53·9	59·5	65·4	75·0	88·6	99·6						
(3) WINTER HALF-YEAR (14)	TEMP. °F			38·0	43·9	49·8	55·4	62·6	61·8	60·5						281
	F.P. °F			58·4	63·8	69·1	77·6	83·5	93·5	102·2						
(4) TYPE I TROPOPAUSE (18)	TEMP. °F			35·9	41·9	49·4	56·2	62·7	57·7	54·3						270
	F.P. °F			52·1	56·3	61·2	68·8	77·3	91·6	101·6						
(5) TYPE II TROPOPAUSE (14)	TEMP. °F			35·6	41·6	47·4	53·2	60·2	61·1	59·8						274
	F.P. °F			55·1	60·7	66·8	73·3	80·5	89·6	99·6						
(6) HIGH TROPOPAUSE (17) (ABOVE 272 MB.)	TEMP. °F			38·2	44·4	51·8	58·4	65·1	62·2	59·9						246
	F.P. °F			56·8	61·0	66·5	73·4	81·5	94·2	103·6						
(7) LOW TROPOPAUSE (15) (BELOW 272 MB.)	TEMP. °F			33·0	38·8	44·9	50·8	57·7	55·8	53·1						302
	F.P. °F			49·7	55·1	60·5	67·8	75·6	86·8	97·5						

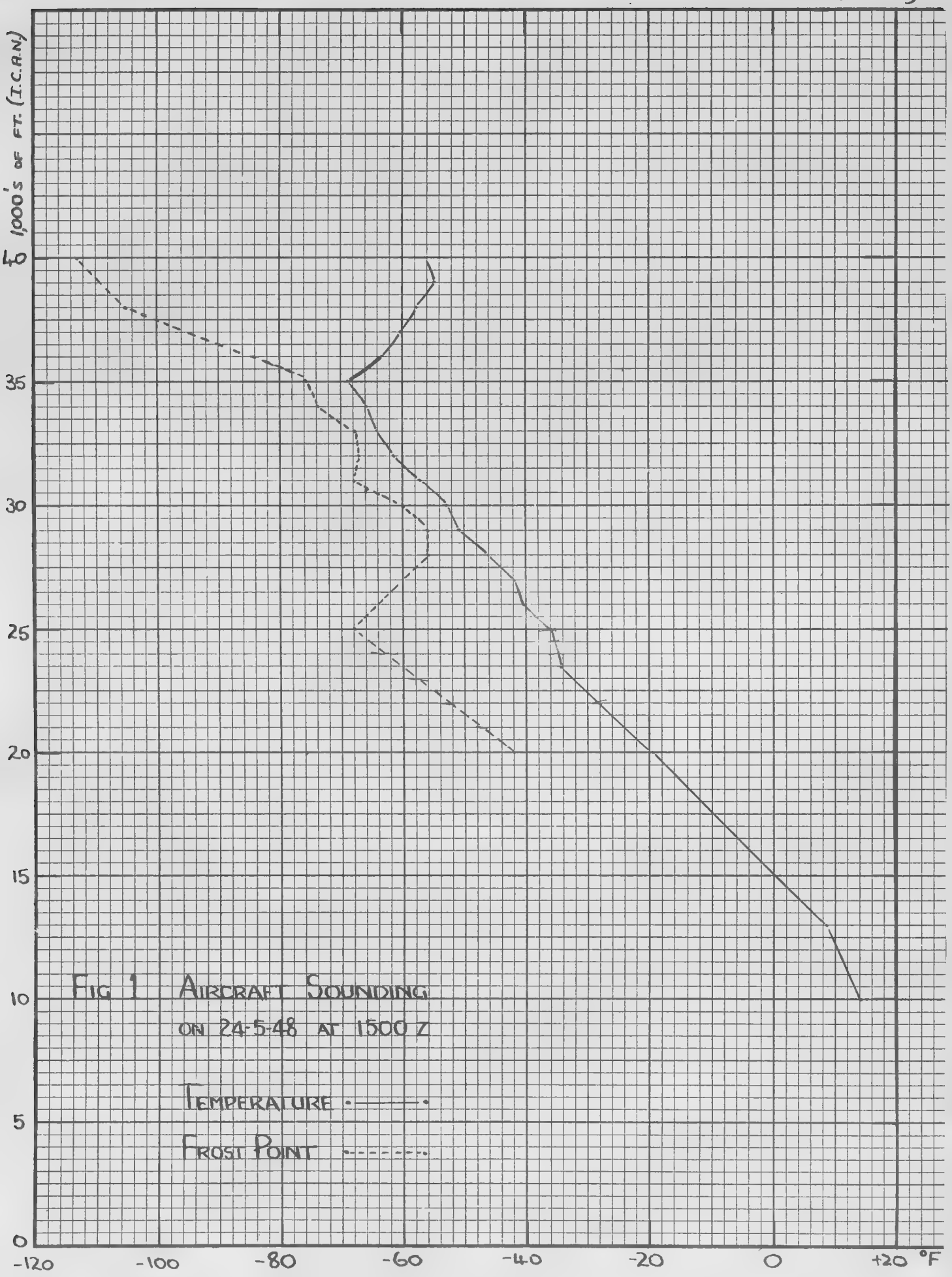

FIG 1 AIRCRAFT SOUNDING ON 24-5-48 AT 1500 Z

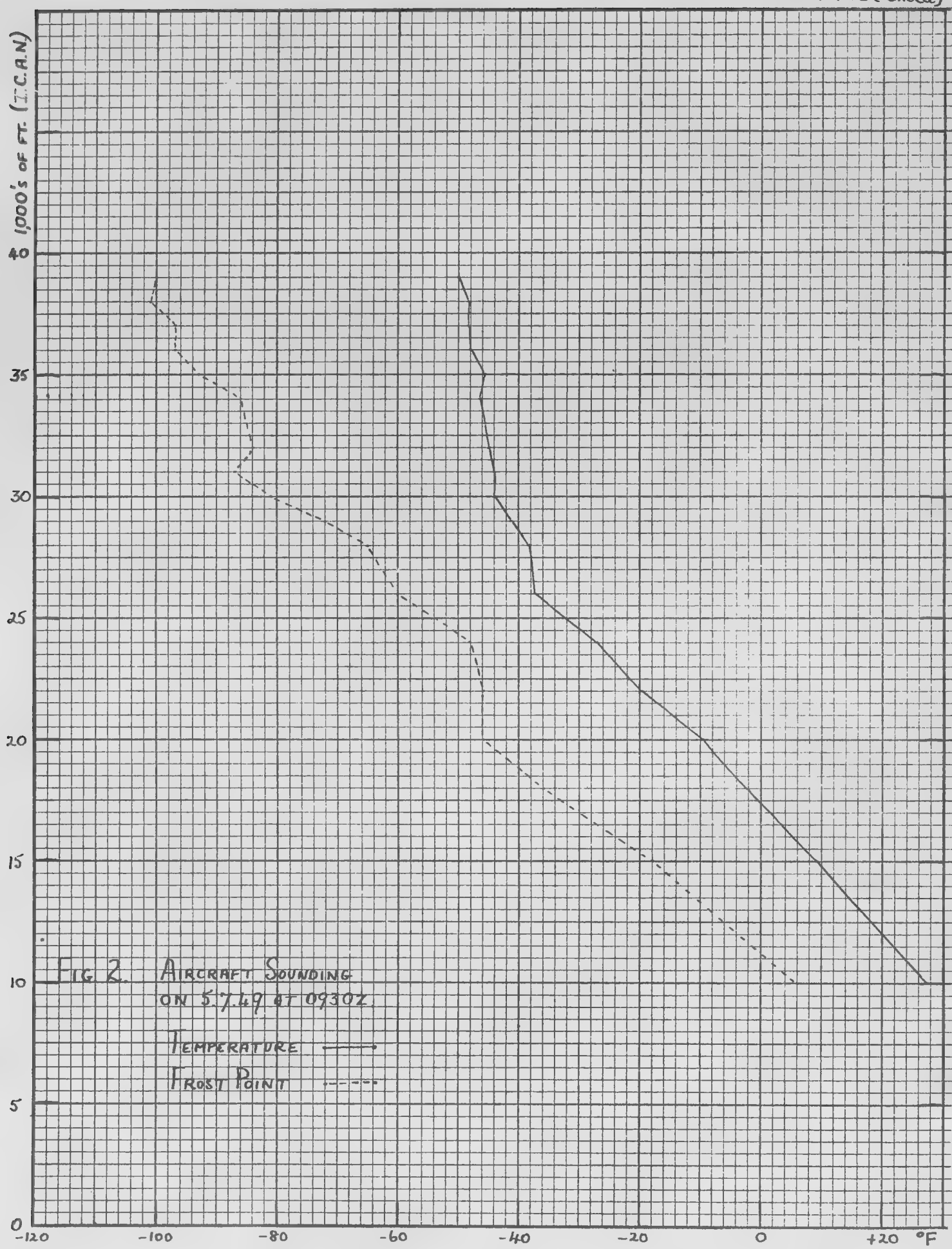

FIG 2. AIRCRAFT SOUNDING ON 5.7.49 AT 0930Z.

TEMPERATURE ——•

FROST POINT ---•

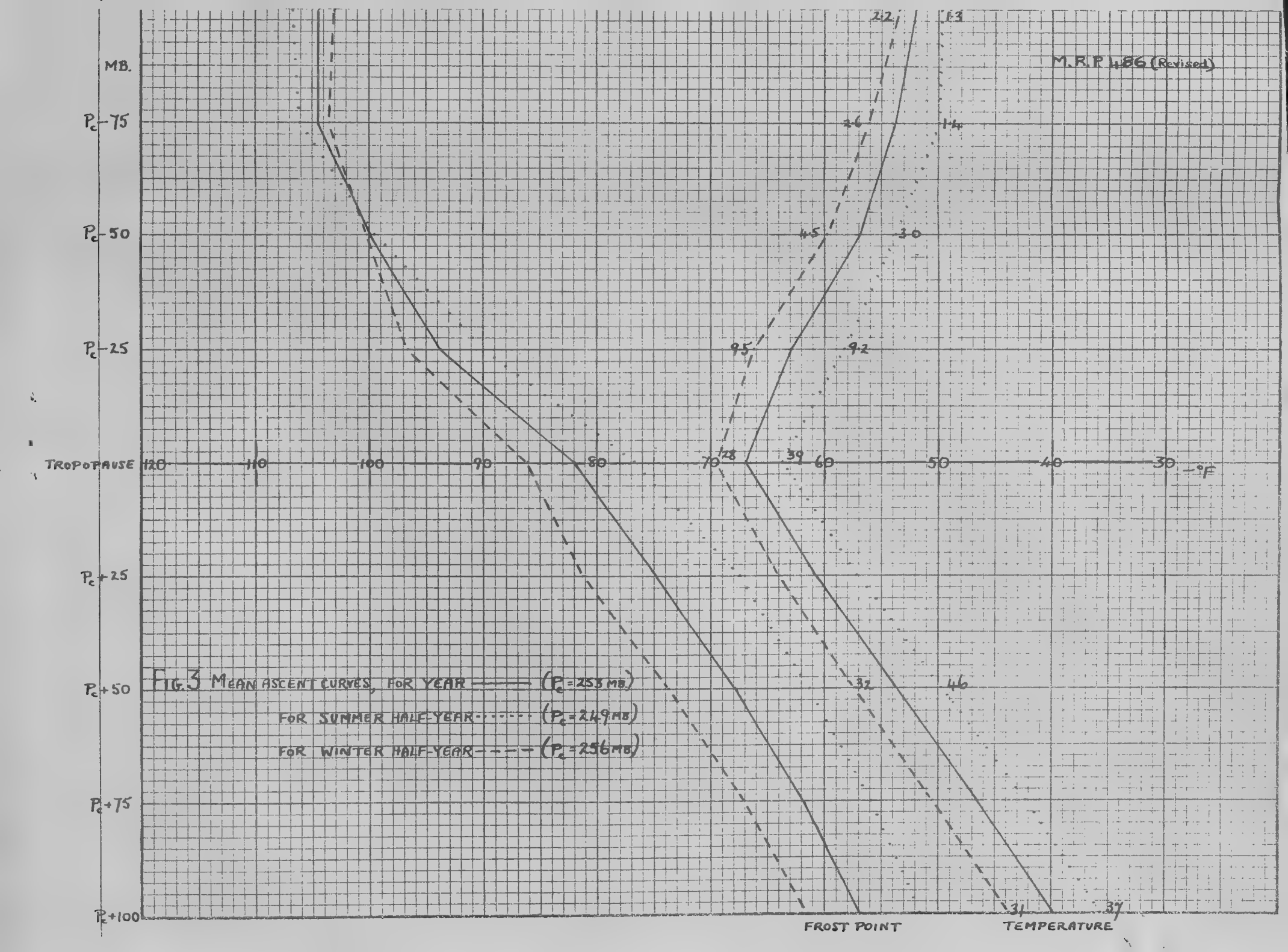
M.R.P 1486 (Revised)
MB.
P_c-75
P_c-50
P_c-25
TROPOPAUSE
P_c+25
P_c+50
P_c+75
P_c+100
120
110
100
90
80
70
60
50
40
30
°F
FROST POINT
TEMPERATURE
FIG. 3 MEAN ASCENT CURVES, FOR YEAR ——— (P_c=253 MB.)
FOR SUMMER HALF-YEAR ····· (P_c=249 MB.)
FOR WINTER HALF-YEAR - - - - (P_c=256 MB.)

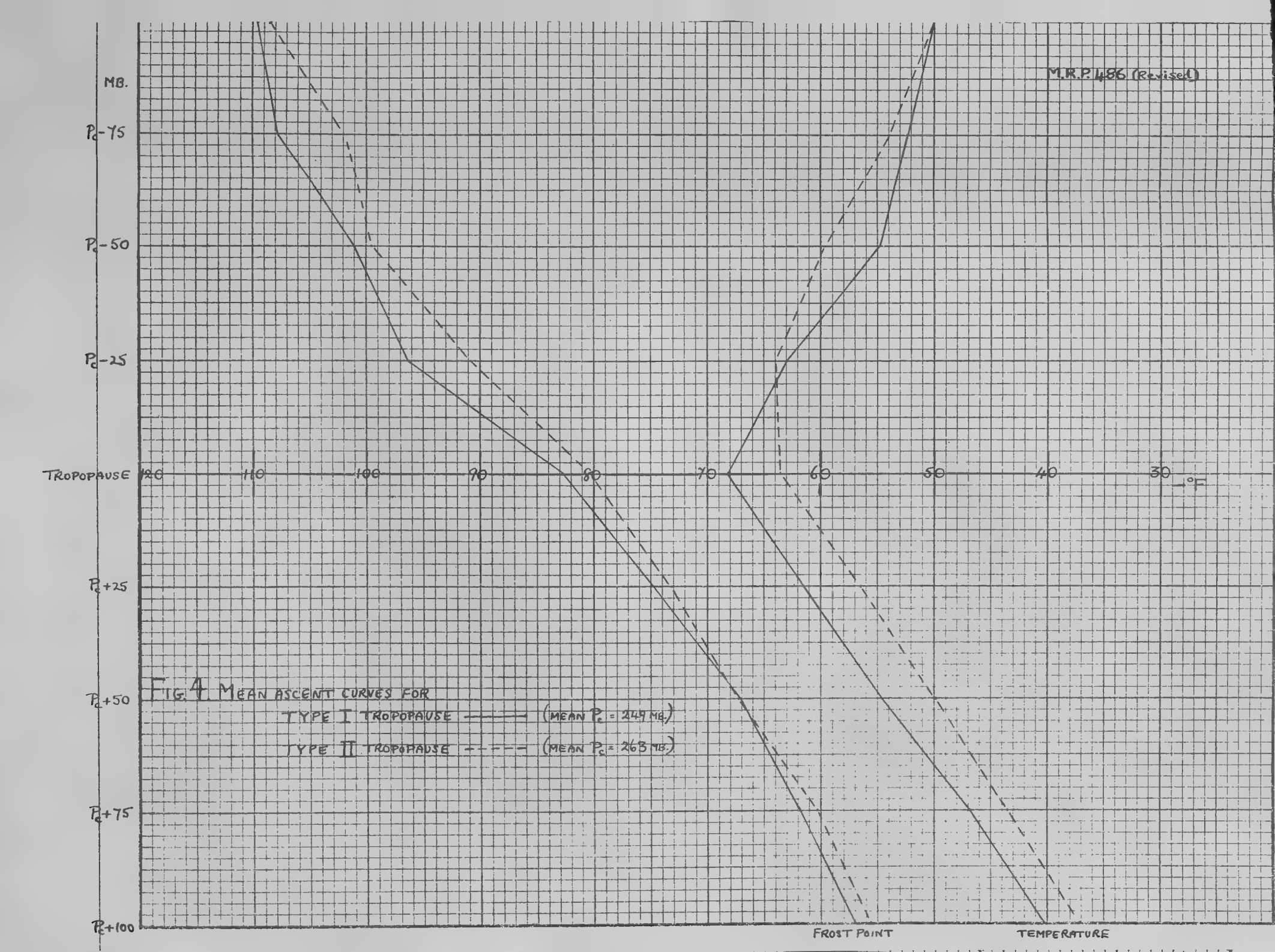
M.R.P. 486 (Revised)
MB.
P_c-75
P_c-50
P_c-25
TROPOPAUSE
P_c+25
P_c+50
P_c+75
P_c+100
120
110
100
90
80
70
60
50
40
30
°F
FROST POINT
TEMPERATURE
FIG. 4 MEAN ASCENT CURVES FOR
TYPE I TROPOPAUSE ——— (MEAN P_c = 249 MB.)
TYPE II TROPOPAUSE - - - - (MEAN P_c = 263 MB.)

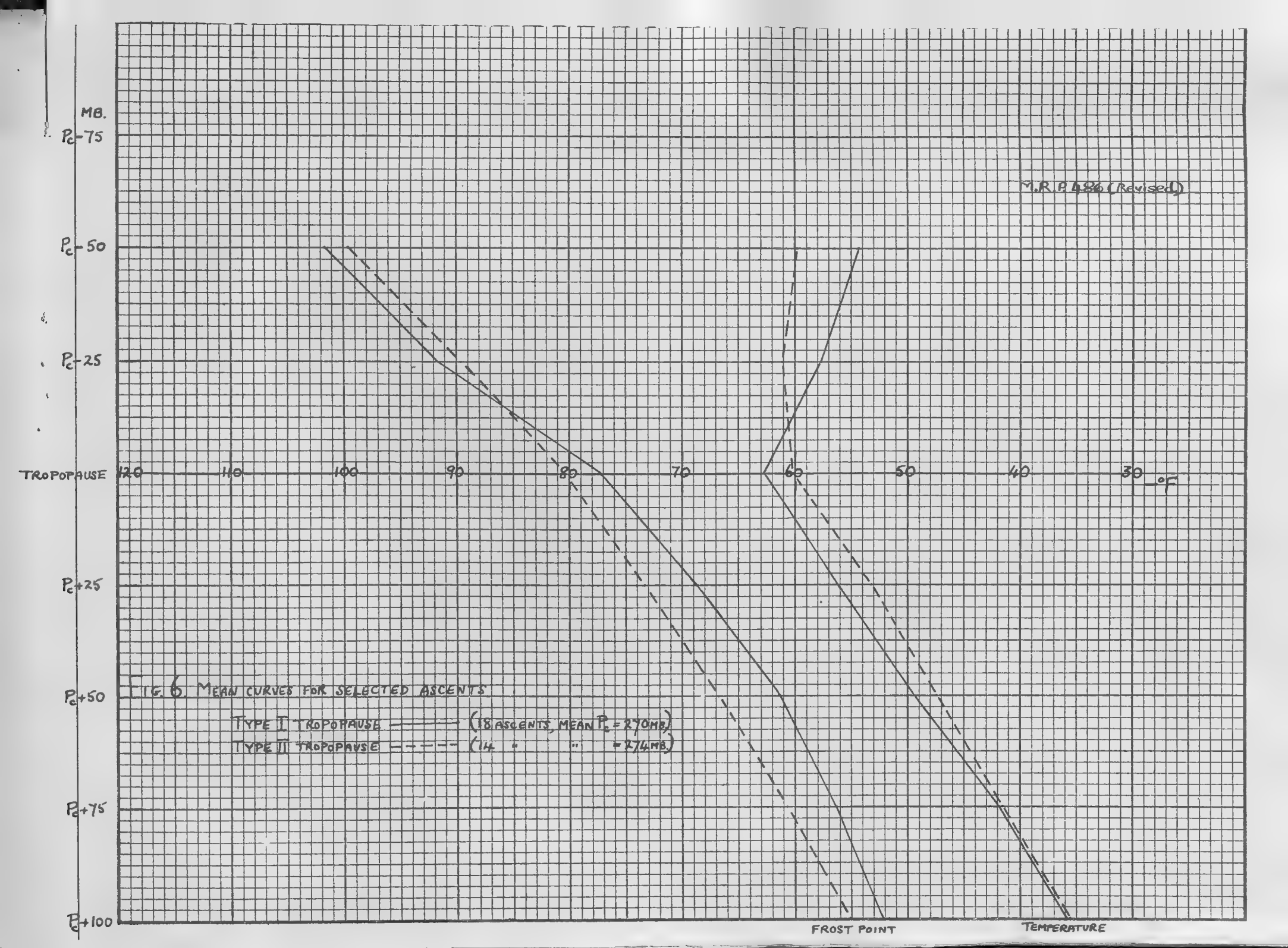

FIG. 6. MEAN CURVES FOR SELECTED ASCENTS

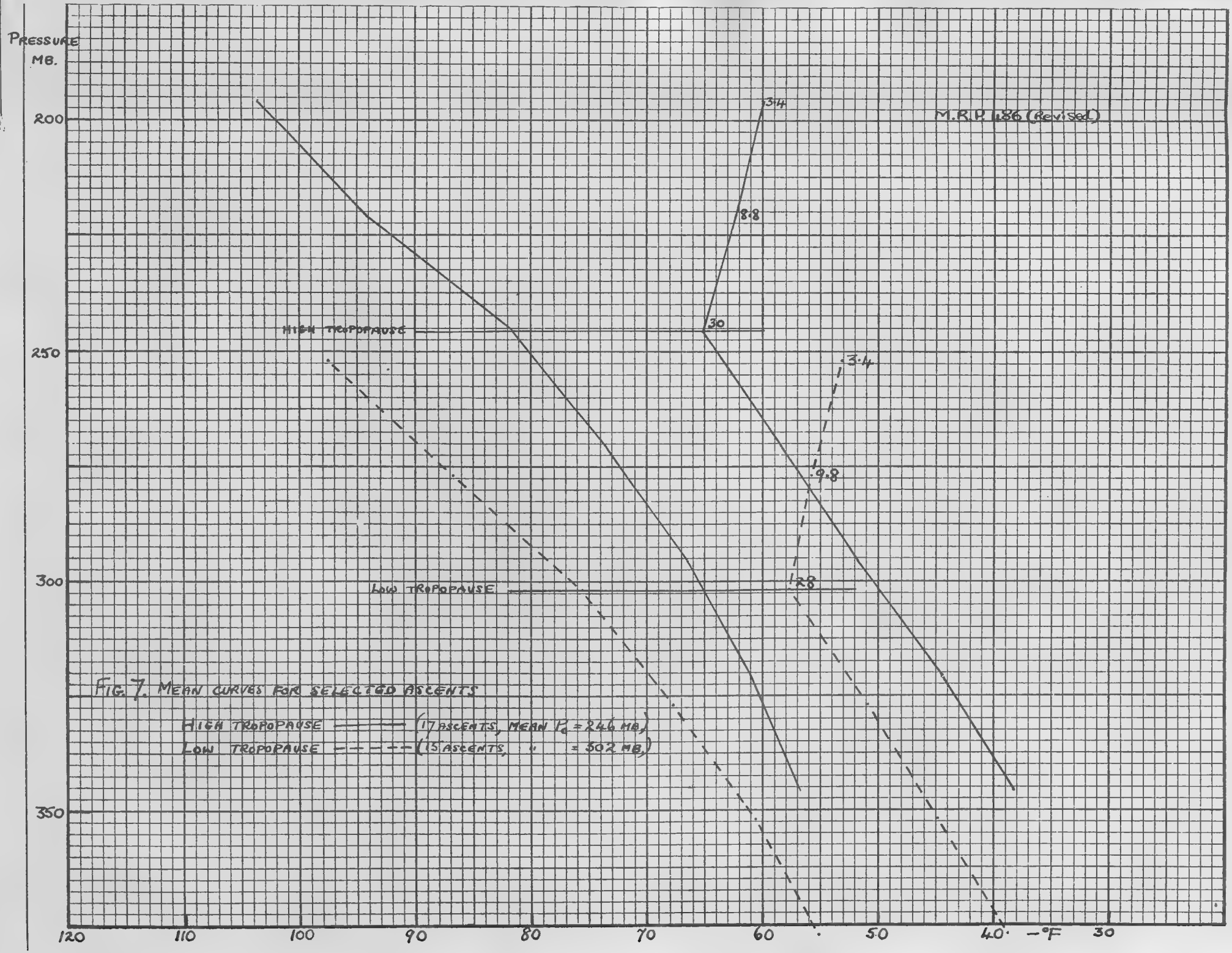

FIG. 7. MEAN CURVES FOR SELECTED ASCENTS

HIGH TROPOPAUSE ——— (17 ASCENTS, MEAN P_t = 246 MB.)

LOW TROPOPAUSE – – – – (15 ASCENTS, " = 302 MB.)

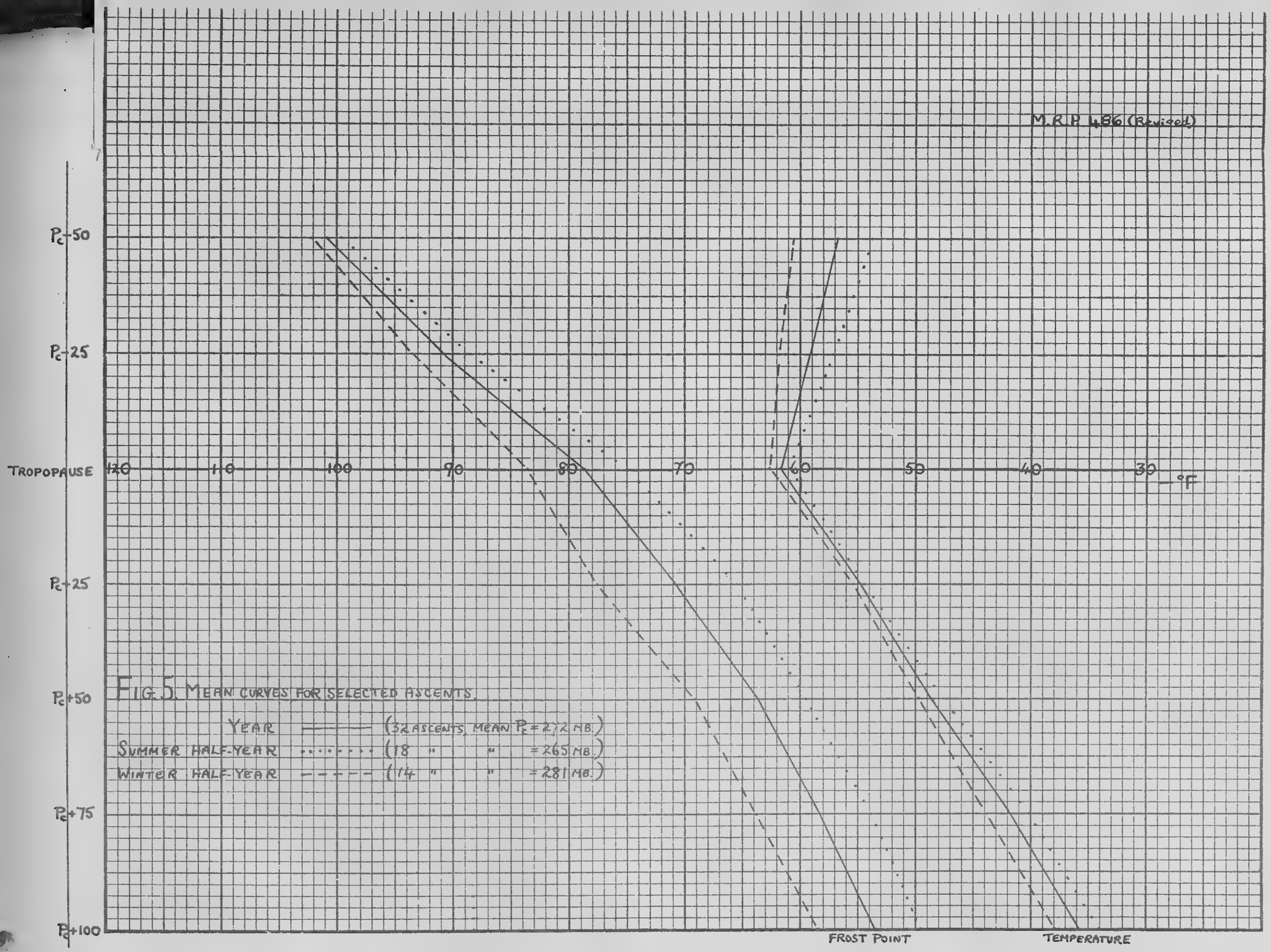

FIG 5. MEAN CURVES FOR SELECTED ASCENTS.

YEAR ——— (32 ASCENTS, MEAN P_c = 272 MB.)
SUMMER HALF-YEAR ····· (18 " " = 265 MB.)
WINTER HALF-YEAR – – – – (14 " " = 281 MB.)

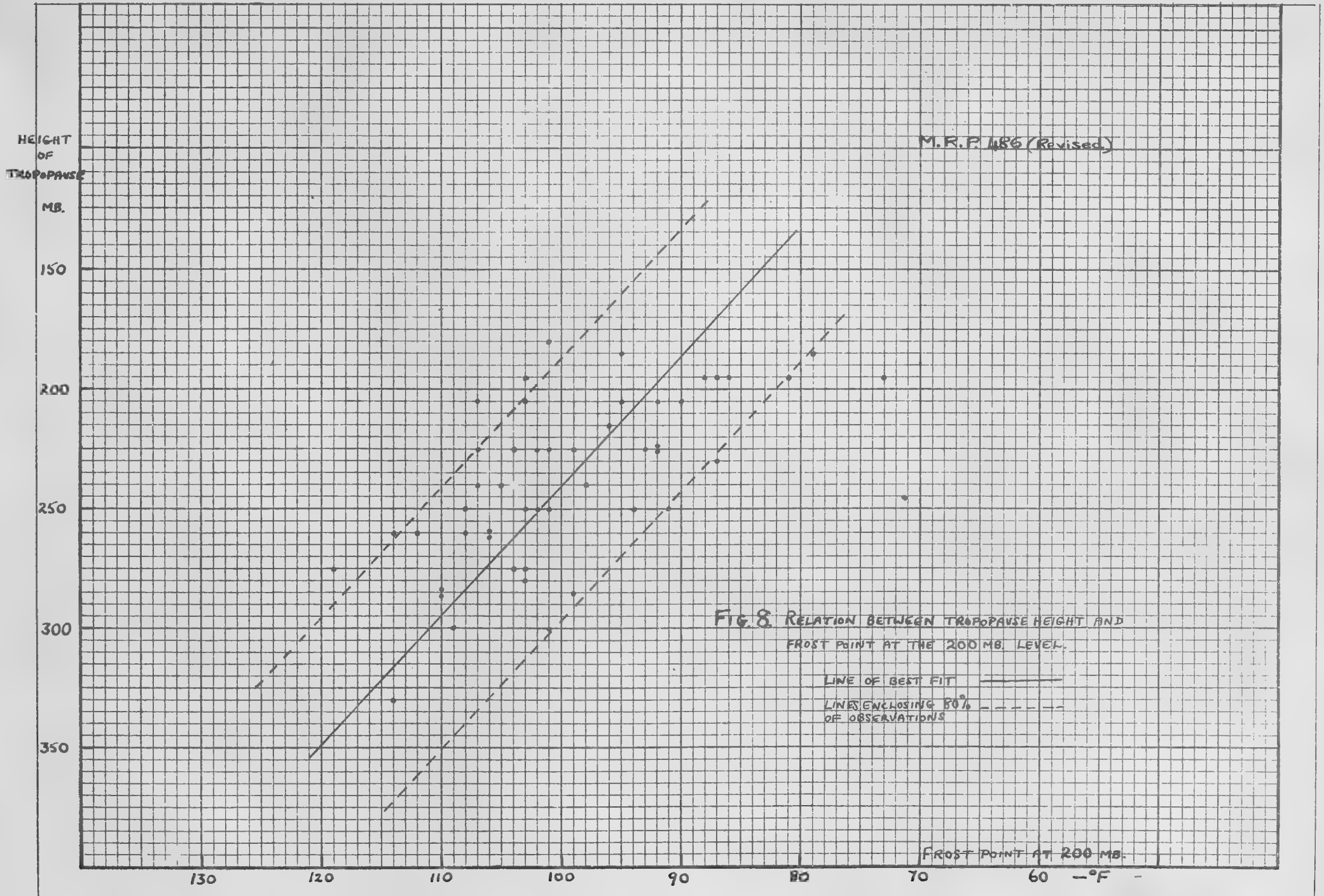

FIG. 8. RELATION BETWEEN TROPOPAUSE HEIGHT AND FROST POINT AT THE 200 MB. LEVEL.

LINE OF BEST FIT ————

LINES ENCLOSING 80% OF OBSERVATIONS – – – – – –

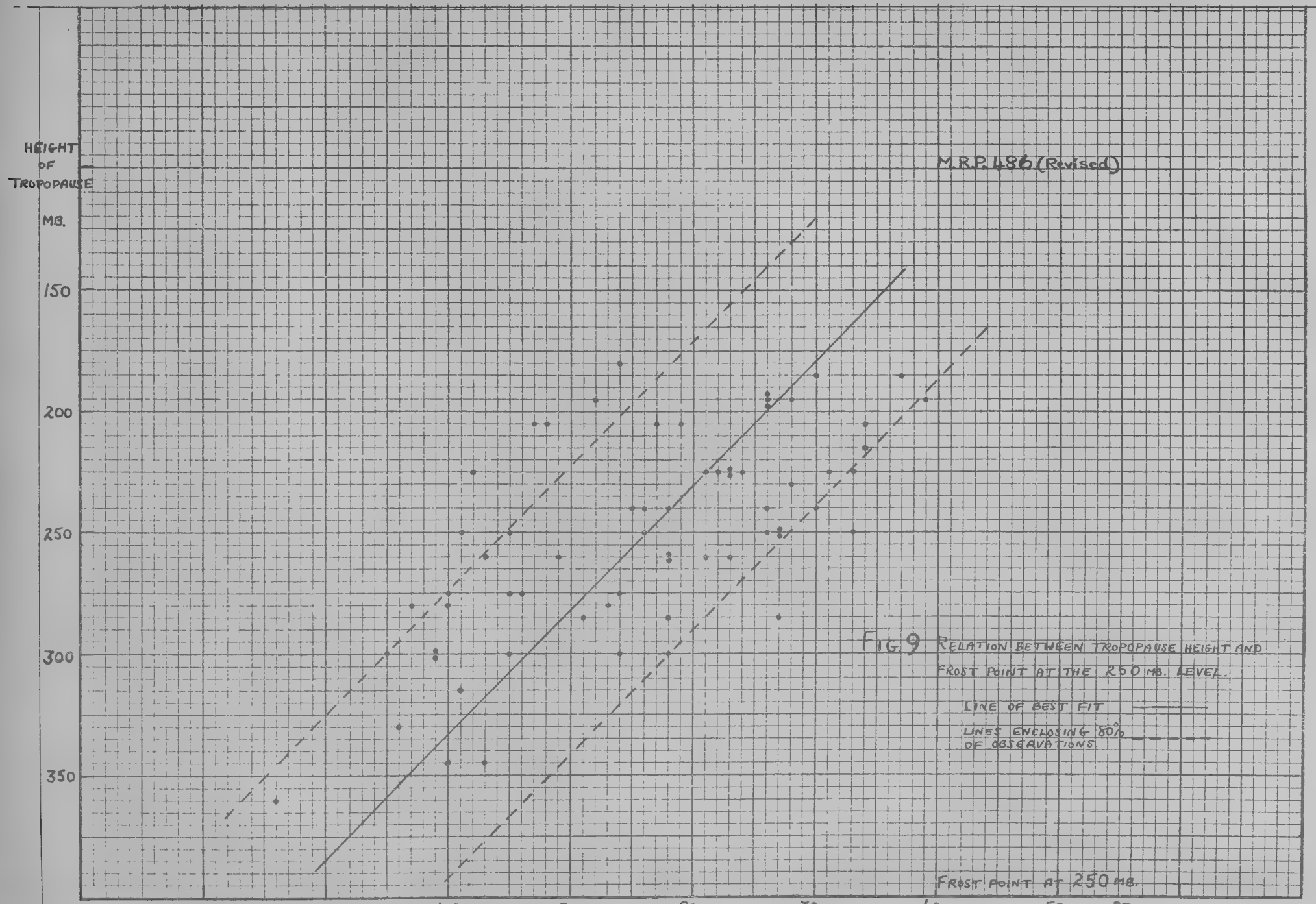
HEIGHT OF TROPOPAUSE
MB.
150
200
250
300
350
120
110
100
90
80
70
60
50
—°F
M.R.P.486 (Revised)
FIG. 9 RELATION BETWEEN TROPOPAUSE HEIGHT AND FROST POINT AT THE 200 MB. LEVEL.
LINE OF BEST FIT
LINES ENCLOSING 80% OF OBSERVATIONS
FROST POINT AT 250 MB.

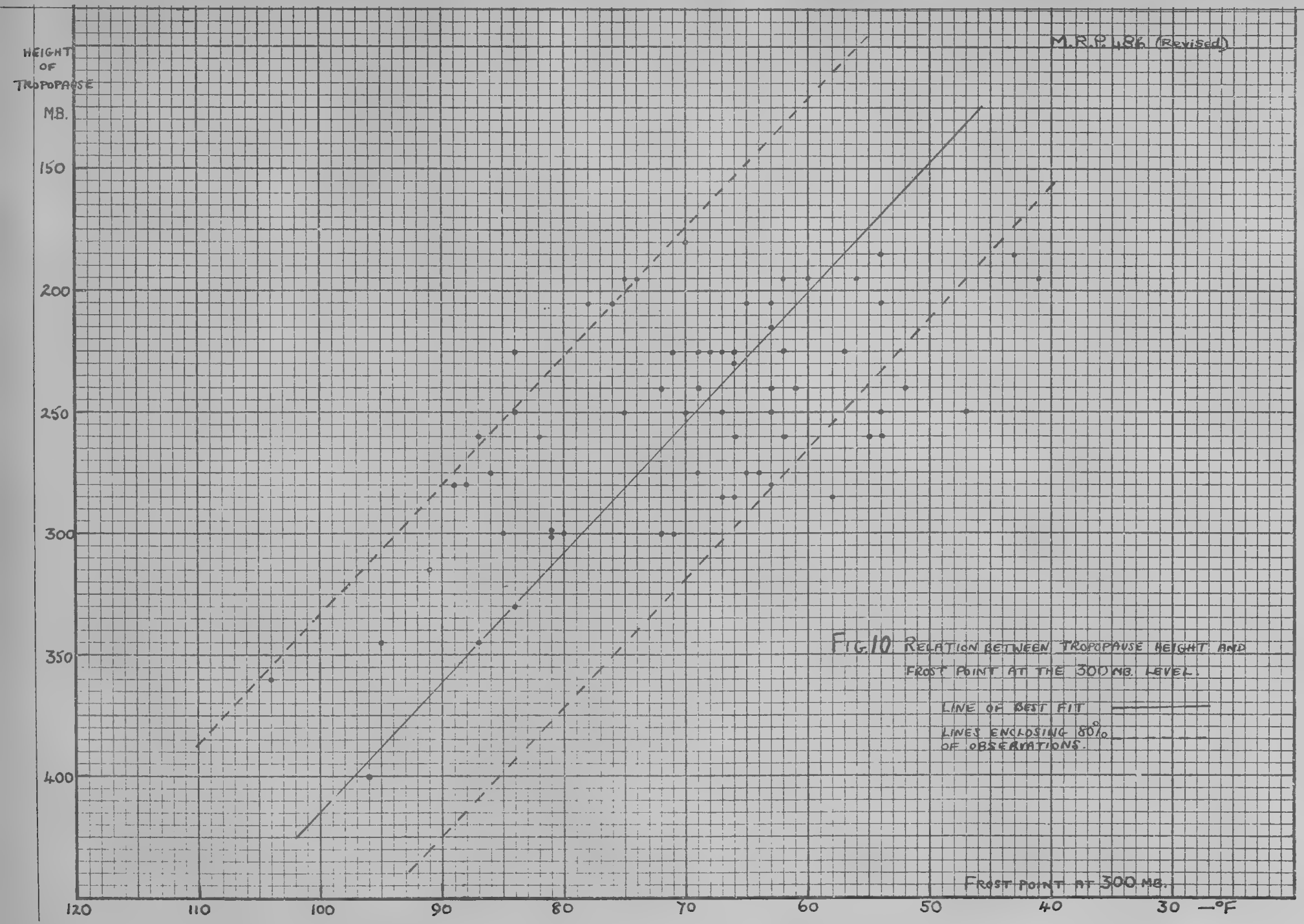

FIG. 10 RELATION BETWEEN TROPOPAUSE HEIGHT AND FROST POINT AT THE 300 MB. LEVEL.

LINE OF BEST FIT ————

LINES ENCLOSING 80% OF OBSERVATIONS. - - - - -

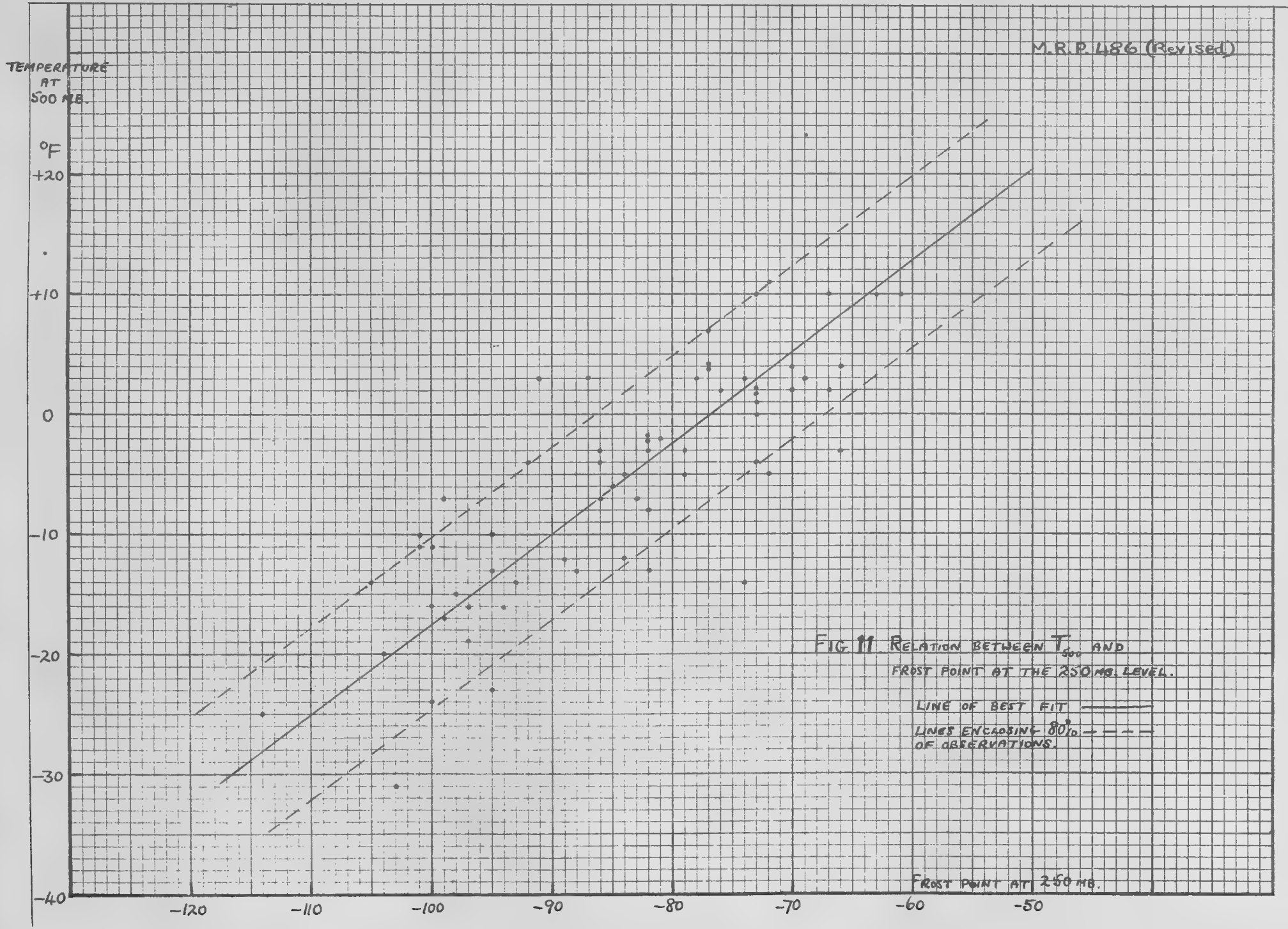

FIG. 11 RELATION BETWEEN T_{500} AND FROST POINT AT THE 250 MB. LEVEL.

LINE OF BEST FIT ————

LINES ENCLOSING 80% OF OBSERVATIONS. — — — —

Addendum to M.R.P. 489

M.R.P. 489
S.C.III/33
12th May, 1949.

AIR MINISTRY

METEOROLOGICAL RESEARCH COMMITTEE

Condensation Trails from Jet Aircraft.

by

J.K. Bannon

AIR WEATHER SERVICE
TECHNICAL REFERENCE FILES

Summary

Immunity temperatures, above which exhaust condensation trails are very unlikely to occur, are evaluated for heights from 20,000 to 50,000 ft. for the Meteor aircraft. From 133 reports from high flying jet aircraft, temperatures are deduced, for the same range of heights, below which trails are almost invariably formed. Approximate estimates of relative humidity deduced from the occurrence of non persistent trails are discussed and examples given for the lower stratosphere.

1. Introduction

The physical factors governing the formation of exhaust trails from aircraft engines are discussed in M.O.479.(1). In that memorandum 'immunity temperatures' (so called Mintra temperatures) are calculated, for the cruising Spitfire, above which condensation trails are very unlikely to form. On the assumption that the cross-section of the trail of the atmosphere affected by the heating and moisture from the engine is 30 sq. metres, temperatures may be calculated, below which the passage of the aircraft will always cause saturation or super-saturation in the trail; i.e. condensation trails are certain below these temperatures. These are the so called Drytra temperatures and are given in S.D.I.S. No.48.

It was observed that jet engined aircraft on occasions did not form exhaust trails until temperatures considerably below the Spitfire Drytra temperatures were reached. Accordingly the engine characteristics, speed, etc. of the Meteor 4 (two Rolls Royce Derwent 5 engines) have been investigated from the point of view of exhaust condensation trail formation.

2. Immunity Temperatures for the Meteor 4

The fuel consumption of the Derwent 5 engine varies greatly with varying engine speeds; the following details have been calculated assuming that the aircraft is flying at the normal cruising speed with the usual engine speed (13,600 revs. per minute). These cruising speeds are also about the safe maximum speeds for this aircraft.

Details of the performance of the aircraft have been obtained from the 'Pilot's Notes' for the aircraft and from the Publication 'Rolls Royce Derwent 5 - Performance', D.S.D. 53, December, 1945: they are as follows, after some slight interpolation.

Table I

Performance of Meteor IV

Height ft.	Engine Revs. per minute	Thrust lb.	Speed (true) knots	Fuel consumption gal. per hour
20,000	13,600	1376	476	289
30,000	"	1084	470	208
40,000	"	792	466	126

The fuel used, kerosene, has density 0.8 gm/cc and a heat of combustion of 9.8×10^3 gm. cal./gm. (Reference (2)). On combustion, 1 gm. of fuel produces 1.45 gm. of water vapour. (Authority - Rolls Royce Laboratory).

From the rate of working of the engine and the total amount of energy available from the combustion of the fuel it is easily calculated that the following proportions of the fuel energy are available as heat in the trail from the engine:-

Table II

Percentage of fuel energy available as heat (P)

20,000 ft.	87 per cent.
30,000 ft.	86 " "
40,000 ft.	84 " "
50,000 ft.	81.5" " (by extrapolation)

If y = fuel consumption (gal./hour)

V = speed of the aircraft (knots)

then F = gm. of fuel used per metre of path, when cruising,

$= 1.96 \frac{y}{V}$ gm./metre.

It is found that y/V is almost exactly a linear function of height between 20,000 and 40,000 ft. and this fact has been used to extrapolate to 50,000 ft. Table III gives values of F for various heights.

Table III

Gms of fuel used per metre of path by Meteor IV cruising.

Height (ft)	F (gm/metre)
20,000	1.19
30,000	0.87
40,000	0.53
50,000	0.20

Using the notation of M.O. 479 let

F = gm. of fuel used per metre of path.

A = cross section (in metres^2) of trail into which exhaust gases pass.

P = percentage of total energy in fuel which goes as heat into the same trail.

k = amount of water vapour produced by combustion of 1 gm. of fuel (= 1.45 for kerosene).

= density of air at temperature T.

D = gm/m^3 of water vapour required for saturation at temperature T.

E = percentage effect of the exhaust vapour on the relative humidity in the atmosphere.

H = percentage effect of the engine heat on the relative humidity in the atmosphere.

Then $$E = \frac{kF}{AD} \times 100$$

and (as in M.O.479), the rise in temperature produced in the trail by the heat dissipated will be:-

$$T = \frac{P}{100} \times 9800 \times \frac{F}{0.24\,A}$$

$$= \frac{P}{100} \times \frac{40800\,Fp_o}{A\rho_o T_o} \times \frac{T}{p}$$

where p_o , T_o , ρ_o are pressure, temperature and density, respectively, at standard conditions, 9800 the calorific value of the fuel and o.24 the specific heat of air at constant pressure.

Also

$$H = T \frac{dD}{dT} \frac{100}{D}$$

Hence

$$E - H = \frac{100F}{AD} \left(k - \frac{P}{100} \times \frac{40800\,p_o}{\rho_o T_o} \frac{T}{p} \frac{dD}{dT} \right) \ldots\ldots\ldots(1)$$

The Mintra temperatures are those which make E - H = 0 and are computed from the term in brackets on the right hand side of Eq. (1). If saturation with respect to ice is considered the criterion for contrail formation then D is the water vapour content for saturation with respect to ice; if saturation with respect to water is required, then D is the vapour content for saturation with respect to water.

Table IV below gives Mintra temperatures at various heights, (those above 40,000 ft. are by extrapolation as indicated above), for the cruising Meteor IV, (a) for saturation with respect to ice and (b) for saturation with respect to water. For temperatures above those given, the 2nd term within the brackets on the right hand side of Eq.(1) is greater than the first, i.e. the water vapour provided by the exhaust is more than offset by the heating due to the engine and E - H is therefore negative; condensation trails should thus be unlikely to form. It should be noted that the derivation of these (Mintra) temperatures is independent of the area of the cross-section of the trail behind the engine.

Table IV

Mintra, Drytra and Justra Temperatures for Meteor IV

Height 1000's of ft.	Mintra temperatures (°F) (a) (ice)	(b) (water)	Relative Humidity per cent 90	80	70	60	50	25	0 (Drytra)
					(J u s t r a *)				
20	-26.5	-31.5	-44	-51	-56	-59.5	-62	-68	-71
25	-30.5	-35.5	-47	-54	-59	-62.5	-65	-70	-73
30	-35	-39	-51	-57	-62	-65	-68	-72.5	-76
35	-38	-44	-55	-61	-65	-68	-71	-76	-80
40	-42	-48	-59	-65	-69.5	-73	-75	-80	-83.5
45	-46	-52	-63	-69	-74	-77	-79	-84	-88
50	-50	-55	-66	-73	-79	-83	-86	-89.5	-94

* See Section 4.

It is seen that the temperatures in Table IV Col.(a) differ little from those given for curve I in Fig. 1 of M.O.479 at 20,000 ft. but that in the region of 40,000 ft. to 50,000 ft. they are about 4°F warmer. In this country the temperature-height curve cuts the Mintra curve below 30,000 ft. on the great majority of occasions, so that the Spitfire Mintra, which is printed on the present edition of the Te-phi-gram (Form 2810A), may be applied to the Meteor aircraft with an error usually less than 1°F. In the tropics the difference will be greater.

M.O.479 states that experimental evidence points to the formation of contrails when saturation with respect to ice is attained in the exhaust trail. Recent evidence from aircraft observations neither confirms nor denies this though, from laboratory experiments, it seems likely that saturation with respect to water is usually required. Fournier d'Albe (3) has found that condensation first occurs when saturation with respect to water is attained. Of the 93 reports of contrails formed by jet aircraft which have been considered (period December 1947 - February 1949), one showed that contrails had formed at a temperature 9°F above the ice Mintra but once formed these trails appeared to spread vertically and horizontally and it is inferred that the atmosphere was super saturated and failed to produce cloud naturally for lack of suitable condensation (or sublimation) nuclei. Of all the other reports of condensation trails formed outside cloud, none were at temperatures above the ice Mintra, 4 were at temperatures above the water Mintra and the remainder were 2°F or more below the water Mintra. Certainly the ice Mintra should be almost infallible as an immunity temperature and its use is recommended in day to day forecasting rather than the water Mintra merely because it is an upper bound and provides a certain margin for error.

Condensation trails are not always composed of ice particles, however. There is one report of an aircraft experiencing icing on re-crossing its own contrail and Dr. Frith of the Meteorological Research Flight says that when condensation trails are formed by a Mosquito, (piston engined, airscrew driven), it is his experience that clear ice almost always forms on the plane just behind the engine, indicating the presence of super-cooled water. (This has been noticed by at least one other observer; Aanensen (4)). On the other hand the condensation trail which formed at a temperature 9°F above the ice Mintra (see above) was later observed from the ground to give a 22° halo with the sun when it must therefore have contained ice crystals. It seems quite likely that many condensation trails are composed of super-cooled water droplets to begin with, gradually changing to ice clouds; this gradual change often occurs in natural clouds at low temperatures. (Ludlam, (5)).

3. Drytra temperatures

From Eq (1) we may derive the following equation:-

$$D\left(1 - \frac{x}{100}\right) \quad \frac{2.84}{A}\,\frac{y}{V}\left(1 - \frac{P}{100} \times 81\,\frac{T}{p}\,\frac{dD}{dT}\right) \qquad \ldots\ldots(2)$$

where x = relative humidity of the surrounding air which, with the moisture provided by the exhaust, will result in saturation in the trail of cross section A m^2.

However, the area A cannot be measured satisfactorily. It may, conceivably, vary with height.

The details of 135 high altitude flights by jet aircraft have been scrutinised, (greatest height attained on any flight was 48,000 ft. but 40,000 ft. was the usual maximum height); the lowest temperatures without trails were as follows:-

Date	Pressure (mb)	Temperature (°F)	Depression of temperature(°F) below Ice Mintra	Region
23.1.48	275	-75	39	Tropopause
11.3.48	200	-77	37	Troposphere
9.11.48	150	-86	41	Stratosphere

These flights were all in the Norfolk area and temperatures were interpolated from the Downham Market radio-sonde observations.

Obviously the air must have been extremely dry on each of these occasions. It is known, (e.g. Dobson, Cwilong and Brewer, (6)), that very low humidities are often found in the stratosphere and sometimes also in the upper troposphere. If we assume that on each of these occasions the relative humidity was 10% with respect to water then, solving equation (2) gives values of A of 51.5, 45.3 and 58.4 m^2 respectively. (It will be seen later, section 5, that there is little difference to the results if some other relative humidity, less than 10% is assumed). These estimated areas have no appearance of varying systematically with height; the second value, 45.3 m^2, was evaluated from an observation in the troposphere and is therefore liable to be too small, (higher humidities are more usual in the troposphere than in the stratosphere).

If we assume that A remains constant with height then we must take the greatest value of A, above, as the most likely to be correct. With this value for A it is possible to calculate, putting $x = 0$ in Eq (2), the temperatures (for particular heights) at which the moisture in the exhaust will saturate the trail with respect to water. These are the so called Drytra temperatures, below which condensation trails should invariably form and they are given in the last column of Table IV. (These Drytra temperatures are 6°F and 11°F lower, at 20,000' and 35,000' respectively, than those given in S.D.I. S.No.48).

4. Atmospheric humidity as deduced from contrails.

On the assumption that condensation trails begin to be formed when the air in the trail reaches saturation with respect to water, (a reasonable assumption; see discussion in section 2), we may use Equation (2), with the value of A determined in section 3, to determine roughly the relative humidity of the air when faint short trails are formed or at the first appearance or disappearance of trails on an ascent or descent. (This method is referred to briefly in the last para. of Addent 5 to S.D.I. S. No.48). The temperatures (which we may call "Justra') corresponding to various humidities at various heights are given in Table IV; the various humidity lines may be plotted on a tephigram and with their aid observations of short trails, (or first appearance or disappearance of trails), together with the known height of the aircraft and the temperature at that level, may be used to read off, immediately, a rough value for the relative humidity.

5. Discussion of possible errors in Drytra and Justra temperatures.

The assumptions made in arriving at these Drytra and Justra temperatures must be kept in mind. They are:-

(a) that the area of a cross section of the trail of air affected by an engine is 58.4 m^2 at a short distance (30-50 yd.) behind the engine. (It is known that the wake of a jet engine, up to 20-30 yd., is a cone of angle 7 to 8°; this is not incompatible with this cross sectional area).

(b) that saturation with respect to water in the trail leads to condensation.

(c) that the aircraft, (Meteor IV with Derwent 5 engines), is flying at cruising speed and with the normal fuel consumption.

Assumption (a) has been discussed above; that the cross section should be constant with height is not obvious from any physical reasoning as the character of the turbulence in the wake may well change with pressure, though it seems unlikely that changes would be great. With the data available, however, it is only possible to assume A constant. Assumption (b) seems reasonable in view of Fournier d'Albe's experiments (3) and the fact that the combustion of rather crude kerosene must maintain a plentiful supply of condensation nuclei. (c) may not be realised exactly in many cases but it is thought that variations in speed, especially below the cruising speed, (and the cruising speed is near the maximum safe speed so that it will seldom be exceeded), should accompany appropriate variations in fuel consumption; the efficiency of the engine is not likely to vary rapidly about the cruising speed. In confirmation of this there have been no reports of condensation trails varying with varying aircraft speeds. Similarly with modern aerodynamically 'clean' aircraft and efficient engines burning the same type of fuel, there is little reason to suppose that the figures calculated for the Meteor should not apply approximately to other jet aircraft.

If the assumptions (a), (b) and (c) are valid, errors in deriving the Drytra and Justra temperatures and hence in estimating relative humidities may arise from errors in calculating A.

In Eq (2) the second term in the brackets on the right hand side is about 0.1 to 0.2 and changes only slowly with temperature; accordingly, if there was an error, T in the estimation of the temperature by which A was calculated, then:-

$$\frac{1}{D}\frac{dD}{dT}\,T + \frac{1}{A}\,A = 0 \text{ approximately.}$$

For $T = 1°F$, at 45,000 ft, $A/A = 0.05$

Errors in x, (x), as calculated from Eq (2) and Justra temperatures, will have errors resulting from errors in the estimation of A, given by:-

$$\frac{x}{100 - x} = \frac{A}{A}$$

Hence an error of 1°F in the temperature observation leading to the estimate of A, will make

$$\frac{x}{100 - x} = 0.05$$

i.e. x varying from 0 at 100% relative humidity
to 5% at 0% " "

It is seen from the figures in Table IV that if the relative humidity assumed in deriving A is less than 1% (as is sometimes observed in the stratosphere) then the error in the Drytra temperature is less than 2°F and the errors in resulting Justra temperatures will lead to errors in x ranging from 10% (for very dry air) downwards.

6. Examples of humidity values deduced from contrail observations.

As an example of the type of information regarding humidity in the upper atmosphere which it is possible to deduce from contrail observations, Table V has been prepared from observations made from jet aircraft during 1948; it gives details of humidity in the lower stratosphere for 23 occasions. When the contrials were persistent it was possible to say that the air must have been very moist. When the trails were short then the humidity has been deduced by the method of section 4, these calculated humidities will be of the nature of lower limits as no account has been taken of the length of the trail except that it was "short", e.g. a trail of 500 yds. will imply a moister atmosphere than one of 200 yds. Where the height is given in the Table as, e.g. 'To 40,000 ft.' it

means that from the tropopause to 40,000 ft. the relative humidity was as stated. Where the height is given as, e.g., 'At 45,000 ft', it means that the deduced humidity applies only to that level.

Table V.

STRATOSPHERE HUMIDITIES
as deduced from Contrail Observations.

Date 1948	Time	Area	Tropopause (height & type)	Height	Relative humidity in stratosphere
24/2	0915	Wash	32,800' I	To 35,000'	60 - 75%
5/3	1045	Wash	34-35,000' II	To 40,000'	50 - 60%
5/3	1430	Wash	37,900' II	To 40,000'	About 50%
16/3	1100	Wash	38,300' I	At 40,000'	25% or more
16/3	1600	Wash	38,000' I	At 40,000'	25% or more
17/3	0950	Wash	37,400' II	At 40,000'	25% or more
17/3	1120	Wash	38,000' I	To 40,000'	Very Moist at times. (Persistent but discontinuous trails)
22/3	1530	Kings Lynn	33,800' II	At 40,000'	80%
				Below 40,000'	Over 50%
23/3	1015	Wash	37,000' II	To 40,000'	25 - 55%
23/3	1415	Wash	39,100' I	At 40,000'	Very moist
24/3	1045	Wash	37,600' II	To 40,000'	Very moist
9/4	1300-1530	Wash	31,200' I	At 34,000'	Very moist
				At 35,000'	Less than 70%
12/4	10-1100	Wash	37,200' I	To 40,000'	Over 60%
12/4	1330	Wash	39,800' I	At 40,000'	Over 40%
3/5	1030	Wash	32,900' II	To 35,000'	Over 70% (Later fell below 60%)
5/5	1030	Wash	33,700' I	At 35,000'	65%, drier below
8/6	1500	Wash	38,600' I	To 40,000'	70 - 80% or more
5/10	1310	10 miles N of Cromer	36,000' II	At 41,000'	70 - 80%
7/10	1245	Norfolk	37,500' I	To 40,500'	50 - 75%
9/11	1510	80 miles W of West Raynham	41,500' I	To 45,000'	Very moist
				Above 45,500'	10%
10/11	1245	West Raynham	43,100' I	To 45,000'	Very moist
				Above 45,000'	Less than 60%
19/11	1030	West Raynham	41,500' II	To 45,500'	Very moist
				45,500' - 46,500'	30 - 40%
22/11	1100	Norfolk	38,000' II	To 44,000'	25% at 38,000' 70% at 44,000'

It is seen that high humidities must occur in the lower stratosphere not infrequently. So far, accurate humidity observations in the stratosphere, (Dobson, Brewer and Cwilong (6)) and more recent observations by the Meteorological Research Flight), have shown relative humidities usually less than 10 per cent; but it must be remembered that the aircraft observations using the frost-point hygrometer have mostly been made the tropopause was well below average height. In the above Table V, 16 out of the 23 cases had a tropopause higher than the average for the time of year.

7. Conclusions.

For forecasting purposes the Mintra temperatures given in M.O. 479 and printed on the tephigram (Form 2810A) should be reasonably correct for jet aircraft over this country; over the tropics they may be 3 to 4°F too low.

Temperatures below which contrails are bound to form (Drytra temperatures) depend on the cross sectional area of the trail of air affected by the engine; it is thought that the Drytra temperatures given in Table IV, having an observational backing, should prove fairly reliable.

G.224940/D.S./5/49/40.

As direct observations of humidity in the upper troposphere and lower stratosphere are so few and at present limited to heights below about 40,000 ft, information gained from a study of condensation trails, though not of first class accuracy, may add considerably to our knowledge. A preliminary scrutiny of recent observations, for example, provides evidence that the lower stratosphere is not infrequently quite moist.

Acknowledgment

Acknowledgment is due to the Meteorological Officer, Central Fighter Establishment, West Raynham, who obtained most of the observations used in this investigation by a careful interrogation of pilots.

References

1.	A.H.R. Goldie	1943	Condensation Trails from Aircraft, M.O.479.
2.	G.W.C. Kaye and T.H. Laby	1941	Tables of Physical and Chemical Constants
3.	E.M. Fournier d'Albe	1948	Nature, Vol. 162, 11 Dec., 1948, pp 921-2.
		1949	Q.J. Roy. Met. Soc., Vol. 75, pp 1-14
4.	C.J.M. Aanensen	1948	Met. Mag., Vol. 77, p.17.
5.	F.H. Ludlam	1948	Q. Journal Roy. Met. Soc., Vol.74, pp 39-56.
6.	G.M.B. Dobson with A.W. Brewer and B.M. Cwilong.	1946	Proc. Roy. Soc., A Vol. 185, pp 144-175.

ISSUED TO H.M. SHIPS AS AN ADDENDUM TO M.M. NO.15.

Issued 16th August, 1949 M.O.O. C.41/1949

METEOROLOGICAL OFFICE ORDERS

SERIES C

Exhaust Condensation Trails formed by Jet Engined Aircraft
(A.971140/48)

A note on Condensation Trails from Jet Aircraft (M.R.P.489) is distributed as an Appendix to this Order.

2. The note discusses exhaust condensation trails from jet engined aircraft. The investigation uses the methods of M.O.479, in which trails from piston engined aircraft are considered. It will be noted that over the United Kingdom the immunity (or Mintra) temperatures for a typical jet aircraft (Meteor) are very similar to those of a typical piston engined aircraft (Spitfire); the Drytra temperatures, below which condensation trails are certain, are probably appreciable lower for the jet aircraft than for the piston engined aircraft.

3. The note also discusses the estimation of atmospheric humidity from observations of condensation trails. Since the results so far obtained (Table V) appear to be at variance with direct measurements of humidity at high levels, further particulars of the occurrence of condensation trails, particularly in the stratosphere, are desired in order that the basis of the deductions recorded in Table V may be confirmed or adjusted. Reports of observations upon condensation trails should, therefore, continue to be sent, through the usual channels, to the Director (M.O.15) as instructed in M.O.O. C.35/1948.

4. In the meantime the values of humidity given in M.R.P.489, as computed from observations of condensation trails, should be regarded as provisional and should not be quoted.

N.K. JOHNSON
Director

Meteorological Office,
Air Ministry, London, W.C.2.

6th August, 1949.

G.241128/HC/8/49/400

31p

This rep... ...ted its contents must not be quoted.

M.R.P. 491
S.C.III/34
18th May, 1949.

AIR MINISTRY

METEOROLOGICAL RESEARCH COMMITTEE

Some experiments on heat transfer near the ground

by

N.E. Rider and G.D. Robinson

AIR WEATHER SERVICE
TECHNICAL REFERENCE FILES

1. SUMMARY

Experiments are described in which temperatures, humidities and winds were measured at heights of 4 to 200 cm above a level surface of short grass, simultaneously with measurements of solar and atmospheric radiation, and of earth temperatures. Paragraphs 3 and 4 discuss the methods of observing and reducing the observations and Paragraph 5 describes the material obtained.

It is shown that the results may be used to indicate directly the constancy or inconstancy with height of the ratio of the eddy diffusivity to the eddy conductivity (paragraphs 6 and 7), and it is concluded that this ratio is usually, but perhaps not always constant. On the assumption of approximate equality of the coefficients, their values, and the fluxes of heat and water vapour, are computed (paragraph 8). The variation with height of the gradients of temperature, humidity, and wind is examined in paragraph 9, and it is concluded that the variation with height of eddy diffusivity and conductivity differs from that of eddy viscosity.

The relative roles of convection and radiation in determining the heat flux and its change with height are examined (paragraph 11), and it is concluded that they are of equal importance.

Finally some consequences of the fluctuations of temperature are discussed with reference to the adequacy of the usual definition of eddy conductivity.

2. INTRODUCTION

A scheme for the investigation of the flux of heat and water vapour was outlined in M.R.P. 378, and the present report deals with some initial experiments on these lines. The results are in some respects disappointing in that they prove some of the projects of M.R.P. 378 to be impracticable, but in spite of this they are considered to show sufficient interesting features to justify a report at the present stage of the work. It has been found impossible to make any unreserved generalisation from the results and much of the interest lies in details peculiar to individual experiments; the report is therefore necessarily discursive.

3. APPARATUS AND EXPERIMENTAL PROCEDURE

(i) Site. The experiments were conducted on a surface of level grass, which was kept mown to an average length of 1-2cm. This was surrounded by a solid fence about 1.5m high which was about 50m away from the site at its nearest point. In certain directions there were huts, buildings and very large trees at distances of 50-100m; in all except one of the present experiments the wind blew from directions clear of these obstacles. It is usually accepted that reproducible profiles representative of a given surface can be obtained up to a height of about 1/100 of the distance of unobstructed flow over the surface; we may therefore expect our results to be of general interest at heights up to about 50cm.

(ii) Dry and Wet bulb temperatures. The thermometer installation was similar to that described by Pasquill (M.R.P. 362), and was subjected to the same laboratory tests. Thermometers were installed at approximately 4, 8, 12, 25,

/50,

50, 100 and 200 cm above the surface. Both the "bulbs" and the housings were smaller than Pasquill's (about $\frac{1}{2}$ linear). The ventilation rate was about 3 m/s, and in these conditions the lag coefficient of the dry bulb was 65 secs, the wet bulb lags being correspondingly less than Pasquill's values. In the first two runs to be discussed the circuits were arranged to record differences between successive thermometers, the top thermometer being referred to a standard. The experimental procedure was to read the seven differential dry bulb circuits, and follow this immediately by reading the corresponding wet bulb circuits. The time required to read a series of dry and wet bulb temperatures was about 2 mins. Surprisingly large fluctuations of temperature were found (see paragraph12) and the circuits were changed so that in the later runs the dry bulb at each height was referred in turn to the standard, and these seven observations were followed immediately by a direct determination of the wet bulb depression at each height. The standard was a copper block of similar size to the thermometer "bulbs", and was immersed in liquid paraffin contained in a large vacuum vessel, which also contained a heavy copper coil to facilitate heat exchange. All circuits were calibrated in the laboratory twice during the series of runs under discussion. The calibrations were consistent with the circuit resistances and the known thermoelectric power of the Cu-Constantan couples used. The sensitivity available was 9.5mm per ^{o}F in the dry bulb circuits and 3.0mm per ^{o}F in the wet bulb depression circuits. The standard temperature was read at short intervals throughout each run, on an M.O. "Inspectors" type thermometer, to 0.02^{o}F. ¤

(iii) Earth temperatures. These were measured by thermocouples at depths of 1, 2, 4, 8, 16 and 32 cm. below the surface. In addition one thermocouple was attached to a copper block about 2mm wide which was half buried and half exposed to the air. The installation was similar to that used by Pasquill (unpublished), but differed in detail of construction. The only differences which required to be mentioned are our use of smaller general dimensions, and of long lengths of 47 S.W.G. copper wire for internal connections, to minimize heat flow within the instrument. The circuits were arranged to give temperature differences between successive junctions, with "surface" and 32cm readings referred to a standard (contained in the same vacuum flask as the air temperature standard). The sensitivity was about 3.5 mm. per ^{o}F. It was often found that the sum of the differences did not agree with the difference between top and bottom temperatures, and in these circumstances the "surface" reading was ignored, as it was liable to comparatively rapid variations. (The reading was not used in the investigation; it appeared to bear little relation to true surface temperature). It was usually possible with the two observers available to obtain only three runs of earth temperatures in the half hour over which experiments extended.

(iv) Solar radiation i.e. total radiation per unit of horizontal surface. This was measured by a Moll-Gorczynski solarimeter recording continuously on a millivoltmeter, and standardised in sunlight against Angstrom pyrheliometer No. 24. Reflected radiation was measured by inverting the solarimeter, but when the incident radiation was very small the reflection coefficient was taken as 17%, a value obtained from a number of experiments on the lawns at Kew.

(v) Long wave ("atmospheric") radiation. This was measured by means of a Linke-Fuessner radiometer directed alternately on sky and ground at $52\frac{1}{2}^{o}$ from the vertical, and surface temperature was checked directly by a grass thermometer (Robinson 1947). In most of the experiments the sky was clear, but, in some, small amounts of high and medium cloud were present, and an attempt was made to take a representative sample of the sky when using the radiometer under these conditions. In daylight it was possible to take three radiometer determinations each on ground and sky during the course of an experiment, at night about 6 determinations on each were made. The grass thermometer was read at frequent intervals during each experiment.

/(vi)

¤ Suitably graduated centigrade thermometers were requested but not supplied.

(vi) Wind. Wind measurements were made with sensitive M.O. type cup anemometers. The number available varied during the period under review, and in some cases no wind profile was obtained. At other times up to eight anemometers were exposed at heights (mid-point of cups) from 5 to 200 cm. For the two lowest heights it was necessary to sink the dial of the anemometer below the surface and to work the controls by means of a spring and cord. For this reason, and because of lack of observers the anemometers were left to record for the 30 minutes of each run, and provided a mean wind for the whole period. It was soon found that the calibrations supplied were mutually inconsistent, and we are indebted to Mr. G.W. Hartley of the Meteorological Office, Harrow, who made wind tunnel calibrations for us, using one of our instruments as a standard. The corrections he supplied were applied retrospectively. In several of the experiments the anemometers were recording speeds below those for which they had been calibrated and at which they were expected to be reliable. The readings, when reduced by extrapolation, produce consistent profiles of the accepted form, but must be treated with caution.

(vii) Evaporation. No attempt was made to measure natural evaporation over the grass surface; we do not consider that the required accuracy could have been approached in most of the experiments. The readings of a recording evaporation tank of standard M.O. pattern (Observers Handbook, M.O. 191, 1946) exposed in surroundings of mown grass about 100m from the experimental site, are available and will be referred to later.

4. REDUCTION OF OBSERVATIONS AND CONSTRUCTION OF PROFILES

(i) Temperature. In the July and October experiments the temperature differences between successive thermometers were obtained, to a nominal accuracy of $0.01^{\circ}F$, on 7 occasions in the 30 mins. occupied by each run. The 200cm temperature was obtained, to a nominal accuracy of $0.02^{\circ}F$, on a similar number of occasions. (The time of each galvanometer reading was noted and graphical interpolation made between the observed standard temperatures). The mean temperature differences over the 30 mins., and the mean 200cm. temperature were obtained from these readings, and hence the mean temperatures at the various heights.[*] In the November experiments an average of 13 determinations of the temperature, nominally accurate to $0.02^{\circ}F.$, at each height were obtained, and the normal method of reduction was to take the mean at each height over the full period. The temperatures were plotted on a linear scale against height, and the best fitting smooth curve drawn by hand, with no mechanical aid, through the points. Tangents were drawn to this curve at the heights of these thermometers, and the slope of the tangents measured. No mechanical aid was used in drawing the tangents. Conversion to centigrade degrees was made after computing the gradients.

The drawing of the profile curves and tangents was a crucial point in the investigation. In general there was a well defined smooth curve through the temperature points, but even so the drawing of the actual curve introduced more uncertainty in the gradients than did the drawing of the tangents to a given curve. The probable errors involved in the procedure were estimated by making several independent determinations on the same data, and the bearing of these errors on the results will be discussed in later sections. Figs. 1, 2 and 3 which contain two of the most doubtful profiles and one of the most definite,

/give

---

[*] In fact the 4cm temperature was also obtained by reference to the standard, and it was found that the sum of the differential measurements differed by as much as 10% ($0.3^{\circ}F$) from the difference of the extreme temperatures. This effect may have been due in some degree to the very large fluctuations of observed temperature (see paragraph 12) coupled with the small number of readings, but we believe it was largely caused by systematic stray thermal e.m.fs. introduced by the use of constantan from different sources in the "standard" circuit. This was suggested by tests, but not established definitely; we have however little hesitation in using the profiles. (If this explanation is correct the gradients will not be affected).

give an indication of the uncertainties involved. The alternative is to fit a curve of known functional form to the points by algebraic methods and to obtain the gradients analytically. Robinson (MRP.377) has shown that Best's (1935) temperature measurements in clear skies in June can be fitted closely by a power law up to 120 cm., and Pasquill (MRP.424) has used a logarithmic law for temperature, humidity, and wind, although he found it necessary to allow one of his three "constants" to vary systematically with height. We took the view that previous work had not established any one form of general temperature-height relation, and we defend our empirical method on these grounds. In particular it is suggested that it is in part begging the question to impose, as Pasquill does, the same functional form on the variation with height of temperature, humidity, and wind when seeking relations between the eddy diffusion coefficients for heat, water vapour, and momentum.

(ii) Humidity. In the July and October experiments the wet bulb temperatures were obtained and meaned for each height in the same way as the dry bulb temperatures. Using mean wet and dry bulb temperatures for each height the dew point was found from Marvin's tables (Psychrometric Tables, etc. by C.F. Marvin. U.S. Weather Bureau, Washington, 1912), * graphical interpolation being necessary. Water content was found from the M.O. Hygrometric Tables (M.O.265 4th Edition p.44), again using graphical interpolation. In reducing the results of the November experiments each reading of the wet bulb depression was associated with the mean of the dry bulb readings taken immediately before and after it, and the dew point and water content computed. The mean, for the 30 minute run, of the water content at each height was then taken, and plotted against height. Profiles and tangents were drawn empirically, as for temperature, conversion to concentration being made after computation of the gradients. It was found that humidity readings generally showed more scatter than temperature readings and a unique profile was correspondingly more difficult to draw. In view of the temperature fluctuations found it is by no means clear that psychrometric methods can be made to give profiles with much more certainty than in these experiments, even if the speed of reading is increased, owing to the different lags of wet and dry bulbs. In ideal conditions of constant temperature and humidity the desirable accuracy (1% or better in concentration) is hardly attainable even with temperatures accurate to 0.02°F, using the tables at present available.

(iii) Wind. A long series of observations, culminating in the work of Deacon (1948) has established a general law of the variation of wind with height near the ground of the form $\partial u/\partial z \propto z^{c}$ The wind observations were therefore plotted against the log of height, or on log-log paper, and the appropriate logarithmic or power law deduced. (All the occasions for which detailed wind observations are available have either neutral stability or inversion conditions). The velocity gradients at the required height were then deduced analytically.

(iv) General validity and reliability of the gradients. The validity of the arguments developed later depends on the assumption of horizontal homogeneity in the mean values of the elements considered. As mentioned in 3(i), a considerable fetch of wind over the surface under consideration is required for this. (See e.g. Deacon, loc cit p.6). No direct evidence was obtained, but the experience of others suggests that our results should be generally valid up to about 50cm. An inflection in the profiles of all elements which was noticed from time to time, usually around 100 cm, may be taken as indirect support for this. Apart from this question of principle, it was in some cases found difficult to draw anything approaching a unique curve below about 10cm and above 70cm (or even 40cm if the inflection mentioned above were present) owing to scatter of the points and the possibility of error in the lowest and highest points. This was particularly true of humidity. We can therefore only claim general validity and reliability for the gradients in the range 10-40cm, extending in some cases to 7-60cm.

/(v)

* These tables are for aspirated (sling) psychrometers, and are in °F.

(v) Rate of change of temperature and humidity. To compute the changes in the fluxes of heat and water it was necessary to measure the rate of change of temperature and humidity. The individual readings at all heights were plotted against time, and a smoothed curve drawn through them. The mean rate of change over the experimental period was computed from the end points of these curves, not from the actual first and last readings. This minimised the possibility of errors due to the fluctuations.

5. OBSERVATIONAL MATERIAL

To the present time nine experiments, eight of them successful, of 30 mins. duration have been made. The material available from these experiments will be discussed in this section.

(i) July 19, 1948. 1400-1430 G.M.T. Wind (by Dines anemometer) W.S.W. 5.7 m/s. There was some cirrus cloud, but not in the region of the sun during the experiment. The temperature profile was well defined, but the wet bulb at 100cm was faulty, and the humidity profile only moderately well defined. Wind observations were made at 25, 50, 100 and 200cm, and therefore were not sufficiently detailed in the region of most interest for velocity gradients to be determined. There was strong insolation and a high surface temperature.

(ii) October 2, 1948, 1055-1125 G.M.T. The wind (S.W. 4.6 m/s) was in this case from a direction in which very large obstacles (trees and a hut) lie within 100m of the site. The temperature profile was moderately well defined, the humidity profile well defined in spite of faulty readings at 100cm. No wind observations were taken on the site. There was some high cloud but the solar radiation record was steady. No observations were taken with the Linke-Fuessner radiometer, and atmospheric radiation was calculated by means of the radiation chart (Robinson 1947). Insolation was strong and surface temperature comparatively high.

(iii) October 19, 1948, 1535-1605 G.M.T. It was impossible to draw any reasonable smooth curve through the humidity points, and the 4 and 7 cm. temperature readings were anomalous. The experiment will not be considered further in the present report.

(iv) November 10, 1948, 1455-1525 G.M.T. The wind was S.S.E. 2.6 m/s. Conditions changed quickly during the run, as the solar radiation decreased to small values. Initially there was a lapse of humidity throughout and a temperature maximum at 100cm. Finally there was a temperature inversion throughout with a very small but definite inversion of humidity. The usual procedure of meaning over 30 mins. was applied, and in addition separate 10 minute means were taken. Over the full period the humidity was constant with height within the limits of error of a poorly defined profile. The temperature profile was well defined. Four anemometer readings were taken between 5 and 45cm, they defined a logarithmic profile with moderate accuracy.

(v) 10 November 1948, 1735-1805 G.M.T. Wind S. 0.9 m/s. There were strong temperature and humidity inversions, with rapid cooling at all levels. The profiles were moderately well defined, and showed a strong inflection about (or below) 50cm. Gradients were not computed above this height. Four wind observations between 5 and 45cm. defined a simple power law type profile reasonably accurately, in spite of the very low wind speeds.

(vi) 11 November 1948, 1400-1430 G.M.T. Wind WSW 1.5 m/s. The sun was shining through high and thin medium cloud so that insolation was varying slowly and was weak. Temperatures at all heights varied systematically with the radiation, the amplitude of the variation being 1.5°F at 4cm and 1°F at 200cm. The means for 30 mins. showed a slight inversion of temperature and a lapse of humidity, the temperature profile being moderately well, and the humidity profile poorly, defined. The wet bulb reading at 100 cm. showed a gross error. Seven wind observations were available between 5 and 200 cm. They showed a logarithmic profile to 50 cm, with unsystematic deviations at 80-200cm.

/(vii)

(vii) 24 November 1948, 1740-1810 G.M.T. Wind E, 2.3 m/s. There was a strong inversion of temperature, with a slow overall cooling during the experiment. The surface temperature was below freezing point. The temperature profile was well defined with an inflection about 100cm, the humidity profile subject to considerable uncertainty. There were five wind observations between 5 and 200 cm, indicating, not very definitely, a logarithmic profile up to 50 cm.

(viii) 26 November, 1948, 1555-1625 G.M.T. Wind ESE 0.7 m/s. Solar radiation was negligible. The observed temperatures and humidities at all heights showed a fairly rapid fall during most of the experiment, followed by a rapid rise in the last few minutes. Both temperature and humidity showed large inversions, and both profiles were well defined. There was a strong inflection in the temperature profile at about 100 cm. Surface temperatures were below the freezing point, and ice was observed to be forming on the grass thermometer. There was much free water on the grass and the ground was saturated. Eight wind observations were made between 5 and 200 cm. The winds were very light, but the results appeared consistent. They were fitted with good accuracy to a simple power law up to 100 cm, above which there was a strong inflection.

(ix) 26 November 1948. 1740 to 1810 G.M.T. Wind E by S 1.0 m/s. The general visibility was poor at the start of this experiment (about 500 yds). After 10 minutes thick ground fog began to form over the site, the top of the layer being exceptionally well defined. The thickness of the layer increased quickly, reaching 100 cm by 1800 and 200 cm by 1810. The profiles of temperature and humidity were computed for the first 10 minutes, that is for the conditions of thin general fog. They were well defined. The ground was saturated with moisture, and a thick coating of ice formed on the grass thermometer. There was evidence of some freezing of the moisture on the grass. In many of the readings of the lower thermometers the wet bulb temperature was higher than the dry bulb, probably owing to the formation of rime on the frozen wet bulbs. In these circumstances saturation with respect to water was assumed in computing the humidities. There is an inflection at about 100 cm in the temperature curve, which is also unique in the present series in having a comparatively small temperature gradient between the surface and 4 cm. Six wind observations were made between 5 and 200 cm; those from 5 to 60 cm can be represented reasonably well by means of a power law. There is an inflection at about 50 cm, above which the wind increases almost linearly with height.

Figs. 1, 2 and 3, illustrate the nature of the curves found, and include cases of good and bad definition of the profiles.

6. METHOD OF EXAMINATION OF RESULTS

(i) Notation. Symbols and units in this report are

Z	height above surface.	cm
T	temperature (°C unless otherwise stated)	
e	water vapour concentration (g. per g. of air)	
F(Z)	Total vertical flux of heat at height Z.	cal.cm^{-2} sec^{-1}
C(Z)	Non-radiative " " " " " " " "	
R(Z)	Radiative " " " " " " " "	
E(Z)	Vertical flux of water vapour at height Z.	g.cm^{-2}sec^{-1}
G(0)	Flux of heat in ground at the surface.	cal. cm^{-2}sec^{-1}
K(Z)	Eddy conductivity, defined by $-\frac{C(z)}{\rho c_p (\partial T/\partial z + \Gamma)_z}$	cm^{2}sec^{-1}

/D(Z)

$D(Z)$ Eddy diffusivity, defined by $-\dfrac{E(z)}{\rho\,(\partial e/\partial z)_z}$ $cm^2 sec^{-1}$

$N(Z)$ Eddy (kinematic) viscosity $cm^2 sec^{-1}$

k, d, ν Molecular (thermometric) conductivity, diffusivity, and (kinematic) viscosity, respectively

$A(Z) = D(z)/K(z)$

$f(z) = \dfrac{\partial e}{\partial z}\Big/\left(\dfrac{\partial T}{\partial z} + \Gamma\right)$

$\phi(z) = f(z)\left\{C(z) - C(0)\right\}$

Fluxes directed away from the surface are considered positive. In the numerical work, necessarily very approximate, ρ and c_p, the density and specific heat at constant pressure of air, are taken as 1.2×10^{-3} g cm^{-3} and 0.25 cals. $deg^{-1}g^{-1}$, respectively. For the latent heat of condensation of water (λ) the value of 600 cals. g^{-1} is used.

(ii) Methods of determination of the fluxes of heat and water vapour. It was desired to determine the fluxes $F(Z)$ $R(Z)$, $C(Z)$ and $E(Z)$, and hence the eddy diffusion coefficients $K(Z)$ and $D(Z)$. The radiative flux $R(Z)$ is calculable by means of the radiation chart (see M.R.P. 377), the other quantities must be determined from this together with the observed values of $R(0)$ and $G(0)$, and the values of the space and time derivatives of T and e obtained from the observations.

We have

$$F(z) - F(0) = -\int_0^z \rho c_p \frac{\partial T}{\partial t}\,dz \qquad \ldots\ldots \quad (1)$$

$$E(z) - E(0) = -\int_0^z \rho \frac{\partial e}{\partial t}\,dz \qquad \ldots\ldots \quad (2)$$

$$C(Z) - C(0) = \Big[F(Z) - F(0)\Big] - \Big[R(Z) - R(0)\Big] \qquad - (3)$$

so that the increases in the fluxes at height Z over their surface values are easily calculated. The values of $C(0)$ and $E(0)$ are then required to complete the solution.

Conservation of energy in the vanishingly thin surface layer gives

$$C(0) + \lambda E(0) = -\Big[R(0) + G(0)\Big] \qquad - (4)$$

which expresses $C(0) + \lambda E(0)$ in terms of measured quantities, but a further relation is required in order to separate the components, and this cannot be obtained without assumptions regarding A, the ratio of the eddy coefficients.

From the definitions we have

$$\frac{E(Z)}{C(Z)} = \frac{A(Z)f(Z)}{c_p} \qquad - (5)$$

It will be seen that the experimental results show the changes of the fluxes with height, $\{F(Z) - F(0)\}$ and $\lambda\{E(Z) - E(0)\}$, to be normally very small compared with the observed values of $C(0) + \lambda E(0)$, and it is a reasonable inference that the individual fluxes $C(Z)$ and $E(Z)$ vary only slowly with height. We may therefore write

$$\frac{E(0)}{C(0)} \doteq \frac{A(Z)f(Z)}{c_p} \qquad - (6)$$

The ratio $f(Z)$ may easily be computed from the observations, and was found to be normally constant; (6) therefore indicates constancy of A. It seems reasonable to suppose that if the ratio $A\{= D(Z)/K(Z)\}$ is invariant with

/height,

height, D(Z) and K(Z) are likely either to be equal or to have the same ratio as the corresponding molecular coefficients, i.e. about 1.2. We therefore have

$$\frac{E(0)}{C(0)} \doteq \frac{f}{c_p} \qquad - (7)$$

and this relation together with (4), is used in paragraph 8 for the reduction of the observations.

The assumption A = 1 is frequently made by workers on this problem, and is justified by reference to the theoretical ("mixing length") derivation of the expressions which we have used to define D and K. We prefer to regard it as a reasonable, though not a necessary, inference from our observations. To recapitulate, these observations show that the changes with height of the fluxes C and λE are normally very small compared with $C(0) + \lambda E(0)$, and that f is normally constant with height within the limits of our experimental error. The first of these implies that, if A(0) is of the order of magnitude unity, then $E(Z)/C(Z) = E(0)/C(0)$, the restriction on A(0) being necessary because we have no direct indication that the sum $C(0) + \lambda E(0)$ in any of our experiments is not overwhelmingly composed of one of its terms. It follows that invariance of f with height implies invariance of A. As was pointed out in M.R.P. 378 it should now be possible to obtain a solution without further assumption. If in (6) we write $f(Z)\,C(Z) = \phi(z) + f(Z)\,C(0)$, and differentiate, remembering $\partial A/\partial z = 0$, we obtain

$$C(0) = \frac{c_p}{A} \frac{\partial E(z)}{\partial z} \Big/ \frac{\partial f(z)}{\partial z} - \frac{\partial \phi(z)}{\partial z} \Big/ \frac{\partial f(z)}{\partial z} \qquad \ldots\ldots (8)$$

the first term being in many cases small compared with the second. This method was tried, but abandoned when it was found that the accuracy attained in measuring the gradients was quite inadequate. We are therefore driven to the further assumption $A \doteq 1$, and can justify this initially only on the intuitive grounds stated above, but finally by its success in providing a reasonable explanation of the observations.

In passing we may note a special case of (5) which is of some interest in discussion of the later experiments. For molecular conduction and diffusion in a saturated atmosphere, if $|\partial T/\partial z| \gg \Gamma$, (5) reduces to

$$\frac{E(z)}{C(z)} = \frac{1}{c_p} \frac{d}{K} \left(\frac{\partial e_{sat}}{\partial T}\right)_z \qquad \ldots\ldots (9)$$

e_{sat} being the saturation concentration of water vapour at temperature T appropriate to the height Z. By using the surface temperature, (9) yields the limiting value of the ratio E(0)/C(0) at a saturated surface, and may provide a useful check on results obtained by other methods.

(iii) Reduction of the wind observations. No great use was made of the wind observations, and little time will be spent discussing them. Reference is made to the work of Sheppard (1947), which shows empirically that in neutral and moderately unstable conditions the wind speed u in the lowest metre is given by the equation

$$u = \frac{1}{0.4} \sqrt{\frac{\tau_o}{\rho}} \log \frac{z + z_o}{z_o} \qquad \ldots\ldots (10)$$

/where

where τ_o is the horizontal shear stress at the earth's surface and z_o a constant. Identifying the shear stress with the vertical flux of momentum, and assuming this to be constant in the steady state, the (kinematic) eddy viscosity N(Z) is defined by

$$N(z) = -\tau_o / \rho \frac{\partial u}{\partial z}$$

and if (10) holds

$$N(z) = (0.4)^2 z^2 \frac{\partial u}{\partial z} \qquad \ldots\ldots\ldots (11)$$

In the present experiments there were some cases of a fairly well defined logarithmic wind profile, and N(Z) was computed from (11) for comparison with the Ks and Ds. In other cases there were insufficient wind data, or the profile was represented better by a simple power law than by the logarithmic law. In these cases no attempt was made to compute N, but its variation with height, complementary to that of $\partial u/\partial z$, was examined.

7. THE RATIO OF THE COEFFICIENTS D AND K

With the possible exception of the run on 26th November, 1948, 1740-1750 G.M.T., which will be discussed later (paragraph 8) it was found that the changes in flux of heat and water in the layer considered were very small compared with the sum of the fluxes, and therefore (6) is almost certainly applicable.

TABLE I

Table I shows the variation of f with height, and it is seen that, with one exception (2 October) f is reasonably constant in the range 7.5cm - 50cm, and that the values at 13.5cm and 25cm, the two points within the region, 10-40cm, where we consider the results both reliable and generally applicable, are certainly equal within the experimental limits except on 2 October. The run on 2 October shows equality of f at 7.5 and 13 cm; it was made in the most unfavourable wind direction, with very large obstacles close upwind of the experimental site, and cannot therefore be regarded as very reliable. We conclude from Table I that in the horizontally homogeneous layer the ratio of the eddy diffusivity to the eddy conductivity is usually constant with height but that there may be exceptional occasions.

8. COMPUTATION OF THE EDDY COEFFICIENTS AND FLUXES

The ratio of the molecular diffusivity to the molecular (thermometric) conductivity is about 1.2 at the temperatures with which we are concerned (Montgomery 1947). It therefore seems reasonable to try this value for the normally constant ratio of the eddy coefficients. For calculations of the type proposed, and in view of the uncertainties of our data, it is sufficient to use a value which is close to 1 and which gives a round figure for the individual terms C(0) and $\lambda E(0)$ when equations (4) and (6) are combined, using the f values observed in the range 10-40 cms. The results of applying this method to the individual runs will now be examined.

TABLE II

19th July, 1400-1430

The results are shown in Table II. In addition to K(Z), values of the change with height of the fluxes F, R and E, are given, as they will be referred to later. The N values, computed from (11) are uncertain, as they are obtained by fitting a logarithmic relation to the winds observed at 25 cm and 50 cm. Sheppard's (1947) results suggest that deviations due to instability should not be too great, but the temperatures and humidities indicate that 50 cm may have been above the horizontally homogeneous layer. Values of the Richardson number

/have

$R_i = \frac{g}{T}(\frac{\partial T}{\partial z} + \Gamma)/(\frac{\partial u}{\partial z})^2$ have been much used as an indication of stability and are added in the table, the velocity gradients being obtained from the logarithmic formula. The derived value of C(0) gives $\lambda E(0) = 5.5 \times 10^{-3}$ cals cm^{-2} sec^{-1}, or $E(0) = 9.2 \times 10^{-6}$ g cm^{-2} sec^{-1}, a rate of evaporation of 0.33mm. hr^{-1}. The rate of evaporation indicated by the recording evaporation tank was 0.35 ± 0.05 mm hr^{-1}. The uncertainties in R(0) and G(0) indicated in this and subsequent tables, are estimates of the largest likely errors, based on the variation of individual readings and on previous experience in other investigations with the solarimeter and radiometer.

TABLE III

2nd October, 1055-1125.

The results are shown in Table III. In this case f was not constant above 13.5 cm, and C(0) was chosen to make A ≒ 1 at the lowest height. The justification for this is that conditions must tend to molecular conduction as the surface is closely approached, so that the limiting value of A at Z = 0 is about 1.2. The simplest assumption is that the variation of A is monotonic, since it shows a steady decrease in the range of height investigated. The chosen value of C(0) leads to a rate of evaporation of 0.18 mm/hr, that observed from the evaporation tank being 0.12 ± 0.05 mm/hr.

TABLES IV AND V

10th November, 1455-1525

When averaged over the full period of the experiment the humidity was found to be constant with height within the limits of error. The humidity gradient, f, and A were therefore indeterminate. Means were taken over the first 10 minutes of the experiment, and the results are given in Table IV. Table V shows the results for the full 30 minutes period, treated by assuming zero flux of humidity, corresponding to the observed zero gradient and it will be noted that K(Z) and N(Z) are of the same order of magnitude. The great difference between the computed Ks for the 10 and 30 minute periods calls for explanation. The possibilities are:-

(a) The difference is real - this seems very unlikely in view of the comparative agreement of K and N for the 30 minute period, and the absence of any very obvious change in wind speeds during the run. The Ks for 1455-1505 are higher than those found on 19th July in unstable conditions and a higher wind. They can be reduced by a factor of about 2 if the observed $C(0) + \lambda E(0)$ is too high by an amount equal to the estimated possible error, but even then the anomaly remains large.

(b) The assumption A ≒ 1 does not hold in this case. On inspection this is found to offer no solution of the difficulty. A large value of $C(0) + \lambda E(0)$ has to be dealt with by small gradients, and if K is decreased D must be increased.

(c) That in these circumstances, of small gradients changing rapidly with height and in time, the fluxes are not proportional to the gradients, and the eddy diffusion coefficients are not determinable from the definitions we have used. This will be further discussed in section 12

There was no detectable change of level in the evaporation tank during the period.

/TABLE VI

TABLE VI

10th November, 1735-1805.

The results are shown in Table VI. This was a straightforward case, and no comment need be made. The high value of the Richardson number is noteworthy. The rate of condensation -E(0) works out to about 0.01 mm per hour. The evaporation tank chart indicated a very small condensation at this time.

TABLE VII

11th November, 1400-1430.

This was the occasion when an inversion of temperature was accompanied by a lapse of humidity. The wind profile was logarithmic in the layer of interest, so that N values could be derived. They are shown with the other results in Table VII. The value accepted for C(0) leads to a rate of evaporation of about 0.03 mm per hour, the tank reading being 0.03 ± 0.02 mm hr^{-1}.

TABLE VIII

24th November, 1740-1810.

In this case the humidity profile was very ill defined (see Fig. 2) and the derived f values more than usually variable. It should be noted that rejection of either the 50 cm or the 100 cm humidity reading does not increase the constancy of f, but it is suggested that the variation is due to error or inadequacy of observation, not to systematic failure of the assumptions. The wind profile was well fitted by a logarithmic curve up to 50 cm, although a simple power law was a better fit over the whole range. The N values shown with the other results, in Table VIII were computed from the logarithmic law, and they are of the same order as the Ks. There is a further uncertainty introduced by the possibility of freezing and subsequent release of latent heat, which would cause the assumed value of $|C(0) + \lambda E(0)|$ to be too great. This would result in smaller K values. Another point of interest in the proposed solution is that the ratio $\left|\lambda E(0)/C(0)\right|$ has a value much smaller than that found in other experiments of the series and considerably smaller than the maximum indicated by equation (9), whilst the evaporation tank indicated a small but definite rate of evaporation during the period of the experiment. The best which can be said of the solution proposed in Table VIII is that it rests on fewer improbabilities than would possible alternatives.

TABLE IX

26th November, 1555-1625.

The results are shown in Table IX. In this case the C(0) value used is almost certainly too high. The surface temperature was below freezing point, the surface was saturated, and ice was seen to be forming on the grass thermometer. The wind profile was not logarithmic, but we may estimate N by the usual formula, noting that Deacon's work (loc cit.) suggests that in these circumstances the values so obtained should be too high. At 25 cm N computed in this way is about 17 cm^2 sec^{-1} which suggests that the K and C values in table IX are high by a factor of about 3. On the other hand the ratio $\lambda E(0)/C(0) = 0.67$ used in the suggested solution is supported by the maximum valde at the surface, 0.78, obtained by equation (9). (Note that A is related to the ratio $\lambda E(0)/C(0)$ and not to the sum $C(0) + \lambda E(0)$. The very high values of the Richardson number are of interest.

/TABLE X

TABLE X

26th November, 1740-1750.

In this case no solution can be offered. The surface temperature was about -4°C, and a heavy deposit of ice was forming on the surface thermometer. The surface was saturated, and there were indications of rime formation on the grass and on the lower wet bulb thermometers. The indicated value of $|C(0) + \lambda E(0)|$, $1.0 \pm 0.2 \times 10^{-3}$ cals cm^{-2} sec^{-1}, was almost certainly too great. There was confirmation of this in the low value of the average gradient in the lowest 4 cm, which was approximately 0.1 °C cm^{-1}, i.e. less than the gradients between 4 and 10 cm. Assuming molecular conduction at the surface this gradient leads to values of $|C(0) + \lambda E(0)|$ of the order 1×10^{-5} cals cm^{-2} sec^{-1}, and involves changes in the fluxes in the lowest metre of the same order of magnitude as the fluxes at the ground (see Table X). It would therefore be necessary to use equation (8) rather than (6) in computing C(0) and trial showed that a solution would demand determination of the temperatures and humidities to an accuracy probably unattainable by psychrometric methods, and certainly not approached in the present experiments. The constancy of f in this case does not therefore necessarily imply the constancy of A. Table X contains the results which are believed to be unaffected by these considerations. The Richardson number is again very high.

9. VARIATION OF THE GRADIENTS WITH HEIGHT

The general wind profile law found by Deacon (loc cit.), and Robinson's analysis of some of Best's temperature profiles (M.R.P. 377), suggested a search for a power law relation between the gradients and height. With one exception it was found that a relation of this type held in the layer in which the results are considered reliable.

Table XI shows the value of the index p in

$$\frac{\partial \chi}{\partial z} = A z^p$$

for temperature, humidity and wind, on all occasions. The value of the Richardson number at 25 cm is added for convenience. With the exception of the wind profile for 24 November 1740-1810 (fig. 2), and the humidity profile for 2nd October, 1055-1125 the power laws fit the experimental values well, always at three points in the range 7, 13.5, 25, 50 cm, and often at all four. The scatter is less in the 30 minute runs than in the two ten minute runs. The exceptional case on 10th November 1735-1805 is well defined, and the anomalous behaviour of the gradients may be seen from the log z - log gradient plot in Fig. 4, Figs. 5 and 6 illustrate more normal cases, Fig. 5 showing the greatest and Fig. 6 the least scatter of the individual points so far observed. If the height variation of the fluxes is negligible the eddy diffusion coefficients vary with Z in a manner complementary to that of the gradients, and this assumption is probably valid in all the present experiments except 26th November, 1740-1750. We may therefore conclude from Tables I and XI that the eddy conductivity and diffusivity are closely related to each other, more so than is either to the eddy viscosity. (Tables II to X have of course shown the close relationship of, and have suggested equality of, K and D). Table XI suggests no systematic variation with stability of p for temperature and humidity, such as has been found by Deacon for wind speed, and it should be remembered that Best's June temperatures showed a value of $p \doteq -1.3$ in the lowest metre for both midday and midnight profiles. (Robinson, M.R.P. 377, Deacon, loc cit. fig. 22, suggests that Best's measurements indicate $|p| < 1$ in stable conditions, but his conclusions can be seen to be based on the 700 and 1700 cm measurements which are almost certainly outside the horizontally homogeneous layer and were in any case taken at some distance from the temperatures in the lowest metre).

10. SUMMARY OF RESULTS CONCERNING THE GRADIENTS AND DIFFUSION COEFFICIENTS

(i) Of eight runs, 7 (Class A) show that the ratio of the gradients of temperature and humidity does not vary with height. The other (Class B) case is doubtful.

/(ii)

(ii) In 6 of the class A runs this can be taken to mean that the ratio of eddy diffusivity to conductivity does not vary with height. In the remaining class A run no conclusions are possible.

(iii) In these 6 runs it is most probable that the diffusivity and conductivity are approximately equal. In the seventh class A run no conclusion is possible. In the class B run it is likely that the diffusivity and conductivity are approximately equal near the ground.

(iv) In seven of the eight runs the temperature and humidity gradients are proportional to a power of the height. The exception is one of the class A runs.

(v) The index of height in the power law for temperature and humidity does not appear to be related to the stability.

(vi) There is no obvious relationship between eddy diffusivity and conductivity on the one hand, and eddy viscosity on the other, but in those cases where comparison is possible (3 in number), conductivity and viscosity are approximately equal at the lowest heights.

11. THE FLUX OF HEAT NEAR THE SURFACE - THE RELATIVE ROLES OF CONVECTION AND RADIATION

Examination of tables II to IX shows that in all cases the radiative flux of heat R(Z) is greater than the convective flux C(Z). There is of course nothing surprising in this, but it also appears that the changes in R in the lowest metre are on occasions of the same order of magnitude as the changes of C, and, as the changes are usually of opposite sign both may be considerably greater than the change of total heat flux indicated by the temperatures *. It is perhaps not generally realised that the direct emission and absorption of radiation by the air near the ground plays such an important part in determining the temperature changes, e.g. Emmons and Montgomery, (1947) say "..... It must be concluded that fog can form next to a cold surface only when there is further cooling by radiation directly from the air ....." (our italics) and "There may be some heat loss by radiation direct from the air.....".

Some particular cases are of interest. On 19th July and 2nd October, in strong lapse conditions with moderate winds, the changes in radiative flux were respectively 30 and 100 times the change in total heat flux, corresponding to a change in C(Z) of 5 to 10% in the lowest metre, a confirmation of the suggestions of M.R.P.377. On 10th November 1455-1525 the conditions varied rapidly in the 30 minutes of the experiment, and the changes in radiative flux, negligible over the first 10 minutes, were practically equal to the observed changes in total flux when averaged over the whole period. (Tables IV and V). Only one case in the present series, 24th November, was comparable with the results of M.R.P.377 for June nights, since the other examples with well-marked inversions had also very light winds. The suggestion of M.R.P.377, that radiative cooling was of the order of 10 times the observed cooling, and that convection must be warming the air, was confirmed, as may be seen from Table VIII.

The observations on 26th November, 1555-1625 and 1740-1750 were particularly interesting, as there appeared to be an approach to radiative equilibrium in the layers nearest the ground. Tables IX and X show that changes in R were quite negligible up to 25 and 50 cm respectively; in fact slight radiative warming of the lowest layers was indicated. It appears that in these extreme stabilities direct radiation from the air may be the primary control of the temperature profile. In view of the suggestions of Emmons and Montgomery (loc cit.) it is interesting to note that on this occasion fog formed in a layer which was neither heating nor cooling by radiative processes.

12. THE "LONG PERIOD" FLUCTUATIONS OF TEMPERATURE

When the experiments were begun it was believed that the choice of a lag coefficient of about 1 minute for the thermometers would be sufficient to reduce the effect of random fluctuations of temperature to negligible values. This expectation was based on several reasons:-

/(a)

* It may be objected that the changes in R shown in the tables are computations. Some observations of changes in R have recently been made at Kew Observatory which confirm, within the rather wide limits of experimental error, the results of this type of radiation chart computation. It is hoped to publish these observations later.

(a) The work would be done on clear days and nights i.e. the radiative flux would be constant.

(b) The thermometers would be in a region where the mean temperature was constant in the horizontal.

(c) The thermometers would be close to the ground, so that fluctuations due to vertical movements of air would necessarily be of short period (i.e. small "mixing lengths"). The expectation was not realised. Table XII shows successive determinations of the various temperature differences on 2nd October, and the variations of temperature on other occasions can be judged from figs. 7, 8 and 9. Variations of this amplitude, with "periods" of the order of 1 minute, at these heights, cannot be explained as due to vertical movements of air if the mean temperatures are horizontally homogeneous, the observed mean profiles representative, and the radiative fluxes constant. (The way in which the temperatures follow changes in radiative flux is shown in fig. 10). The only explanation which can be offered is that the mean temperatures are not horizontally homogeneous, even in the lowest few centimetres, where the fetch of wind over the "uniform" and uniformly insolated surface is several hundred times the height above the surface *.

The consequences of such an explanation are somewhat disturbing, and we cannot discuss them at length. It suggests that a representative profile cannot be obtained by observations in one position only. (This is not necessarily true if the observation is extended over a very long period, but we must remember that the profile is often changing quickly with time, see e.g. the results for 10th November 1455-1525). It also undermines the arguments on which the definition of the diffusion coefficients is based.

We have assumed the form $K = -\frac{C}{\rho c_p\left(\frac{\partial T}{\partial z} + \Gamma\right)}$ which is usually derived from the mixing length model of turbulence (see e.g. Brunt 1939 p.225) in which the fluctuations of temperature are ascribed to vertical motion of an eddy through a distance l, and written as $-l\left(\partial T/\partial z + \Gamma\right)$ This is clearly unable to explain fluctuations with amplitudes of the order of 1°C and periods of the order of 1 minute, at heights of about 5 cm in winds of 200 cm sec^{-1}. It should also be noted that the "mixing length" derivation of the definition of K demands linearity of the temperature profile at least over lengths comparable with the mixing lengths. It may be shown to depend on the neglect of

$$\frac{l}{2!}\frac{\partial^2 T}{\partial z^2} \Big/ \left(\frac{\partial T}{\partial z} + \Gamma\right) \quad \pm \quad \text{smaller terms.}$$

Unless l is very small this is clearly unsound for many of the profiles which have been discussed here, and if l is very small even the short period fluctuations noted by other observers (e.g. Priestley and Swinbank 1947) cannot be explained as due to the vertical motion of eddies.

Montgomery (1948) has recently attempted to avoid some difficulties by defining the eddy diffusion coefficients empirically in terms of the ratio of a flux and the corresponding gradient. But if the theoretical (mixing length)

/basis

* We have of course assumed, in common with previous investigators that an aspirated thermometer of the type described gives a true indication of the temperature at the mean height of its aperture. The truth of this is by no means obvious, but can hardly be investigated experimentally (except as a major project) since alternative methods are all open to serious objections.

basis of the definition is rejected an empirical basis must be substituted, i.e. it must be shown by observation that the ratio of flux of a quantity to its gradient does not depend in any other way on the spatial distribution of the quantity, a matter of no small difficulty. Indeed the results for 10th November, 1455-1505 compared with those for 10th November, 1455-1525 suggest that in at least this instance the flux of heat near the ground was not specified solely by the local temperature gradient and local turbulent flow. Some similar speculations have recently been advanced by Priestley (1948); our own results do no more than suggest support, and further investigation is obviously needed. We hope to continue work on these lines.

G.237023/VY/5/49/40

REFERENCES

Best, A.C. Geophys. Mem. No.65 (Vol.7) 1935
Brunt, D. Physical and Dynamical Meteorology 2nd Ed. Cambridge 1939.

Deacon, E.L. Porton Technical Paper, No.39. 1948.

Emmons, G. and Montgomery, R.B. J.Met. 4. p.206 1947.

Montgomery, R.B. J.Met. 4. p.193. 1947
" " J.Met. 5. p.265. 1948

Pasquill, F. M.R.P.362
" " Not yet published
" " M.R.P.424
Priestley,C.H.B. and Swinbank, W.C. P.R.S. A189 p.543 1947
Priestley,C.H.B. Q.J.R. Met.S. 74 p.412 1948

Robinson, G.D. Q.J.R. Met.S. 73 p.127 1947
" " M.R.P. 377
" " M.R.P. 378

Sheppard, P.A. P.R.S. A188 p.208 1947.

G.237023(a)/VY/5/49/40

TABLE I. VARIATION OF f WITH HEIGHT

Date and Time	Z	7.5	13.5	25	50	100
19th July	1400-1430	$+4.63\times10^{-4}$	$+4.95\times10^{-4}$	$+4.85\times10^{-4}$	$+5.51\times10^{-4}$	$+7.2\times10^{-4}$
2nd Oct.	1055-1125	$+5.17\times10^{-4}$	$+5.15\times10^{-4}$	$+8.2\times10^{-4}$	$+11.1\times10^{-4}$	$+24\times10^{-4}$
10th Nov.	1455-1505	-7.2×10^{-4}	-8.6×10^{-4}	-8.2×10^{-4}	-7.0×10^{-4}	-10×10^{-4}
10th Nov.	1455-1525	———	INDETERMINATE		———	
10th Nov.	1735-1805	$+3.8\times10^{-4}$	$+3.2\times10^{-4}$	$+3.1\times10^{-4}$	$+3.0\times10^{-4}$	-
11th Nov.	1400-1430	-1.53×10^{-3}	-1.16×10^{-3}	-1.07×10^{-3}	-1.08×10^{-3}	-0.65×10^{-3}
24th Nov.	1740-1810	$+1.08\times10^{-4}$	$+1.29\times10^{-4}$	$+1.38\times10^{-4}$	$+1.16\times10^{-4}$	$+1.63\times10^{-4}$
26th Nov.	1555-1625	$+2.46\times10^{-4}$	$+2.35\times10^{-4}$	$+2.38\times10^{-4}$	$+2.80\times10^{-4}$	$+4.0\times10^{-4}$
26th Nov.	1740-1750	$+1.9\times10^{-4}$	$+2.1\times10^{-4}$	$+2.4\times10^{-4}$	$+2.2\times10^{-4}$	$+4.8\times10^{-4}$

TABLE II

TABLE II. RESULTS FOR JULY 19, 1400-1430

R(0) Solar $-1.53 \pm 0.05 \times 10^{-2}$ cals cm^{-2} sec^{-1}
R(0) Atmospheric $0.53 \pm 0.06 \times 10^{-2}$ " " "
G(0) $0.00 \pm 0.03 \times 10^{-2}$ " " "

Hence $C(0) + \lambda E(0) = 1.00 \pm 0.08$ cals cm^{-2} sec^{-1} $\times 10^{-2}$

Z	T (°F)	e (g/m^3)	A(Z)	C(Z)	K(Z)	F(Z)-F(0)	R(Z)-R(0)	E(Z)-E(0)	N(Z²)	Ri
0	102		-	4.5×10^{-3}	-					
5	77.77	13.09								
8	77.37	12.40	1.09	4.5×10^{-3}	190	-2×10^{-6}	(-5×10^{-5})	-2×10^{-9}	-	-
14	76.61	12.18	1.02	4.6×10^{-3}	340	-3×10^{-6}	-8×10^{-5}	-4×10^{-9}	-	-
25	75.96	12.06	1.04	4.6×10^{-3}	660	-5×10^{-6}	-13×10^{-5}	-6×10^{-9}	(240)	(-1.2×10^{-2})
50	75.32	11.74	0.92	4.7×10^{-3}	1700	-7×10^{-6}	-20×10^{-5}	-12×10^{-9}	(490)	(-2.0×10^{-2})
100	74.84	-	0.7	4.8×10^{-3}	4400	-10×10^{-6}	-30×10^{-5}	-24×10^{-9}	-	-

$E(0) = 9.5 \times 10^{-6}$

Z	u ($cm\ sec^{-1}$)
25	283
50	317
100	348
200	382

/TABLE III

TABLE III. RESULTS FOR 2 OCTOBER, 1055-1125

R(0) Solar $-1.05 \pm 0.05 \times 10^{-2}$ cals cm^{-2} sec^{-1}
R(0) Atmospheric (computed) $0.4 \pm 0.1 \times 10^{-2}$ " " "
G(0) $0.1 \pm 0.03 \times 10^{-2}$ " " "
Hence $C(0) + \lambda E(0) = 0.55 \pm 0.1 \times 10^{-2}$ cals cm^{-2} sec^{-1}

Z	T (°F)	e (g/m^3)	A(Z)	C(Z)	K(Z)	F(Z)-F(0)	R(Z)-R(0)	E(Z)-E(0)	N(Z)	Ri
0	83	-		2.5×10^{-3}						
4.5	65.07	11.66								
7.5	64.29	11.13	0.97	2.5×10^{-3}	76	-7×10^{-8}	(-1.5×10^{-5})	$+3 \times 10^{-9}$	-	-
13.5	63.31	10.96	0.97	2.5×10^{-3}	166	-11×10^{-8}	-3×10^{-5}	$+5 \times 10^{-9}$	-	-
26	62.72	10.75	0.61	2.5×10^{-3}	440	-25×10^{-8}	-5×10^{-5}	$+10 \times 10^{-9}$	-	-
51	62.12	10.33	0.45	2.4×10^{-3}	1140	-50×10^{-8}	-9×10^{-5}	$+15 \times 10^{-9}$	-	-
101	61.79	-	0.21	2.4×10^{-3}	5600	-100×10^{-8}	-13×10^{-5}	$+30 \times 10^{-9}$	-	-

$E(0) = 5 \times 10^{-6}$

TABLE IV

TABLE IV. RESULTS FOR 10 NOVEMBER, 1455-1505

R(0) Solar -2.15 ± 0.2 $\times 10^{-3}$ cals. cm^{-2} sec^{-1}
R(0) Atmospheric $+1.2 \pm 0.3$ $\times 10^{-3}$ " " "
G(0) $+0.1 \pm 0.1$ $\times 10^{-3}$ " " "
Hence $C(0) + \lambda E(0) = 0.9 \pm 0.4$ $\times 10^{-3}$ cals. cm^{-2} sec^{-1}

Z	T (°F)	e (g/m^3)	A(Z)	C(Z)	K(Z)	F(Z)-F(0)	R(Z)-R(0)	E(Z)-E(0)	N(Z)	Ri
0	48.5			-0.9×10^{-3}						
4	48.85	7.62								
7.5	49.10	7.48	1.16	-0.9×10^{-3}	240	$+3 \times 10^{-6}$	$\ll 1 \times 10^{-6}$	-3×10^{-9}	-	-
13.5	49.15	7.48	0.97	-0.9×10^{-3}	630	$+5 \times 10^{-6}$		-5×10^{-9}	-	-
26	49.20	7.46	1.02	-0.9×10^{-3}	1150	$+8 \times 10^{-6}$		-7×10^{-9}	-	-
50.5	49.30	7.39	1.19	-0.89×10^{-3}	2000	$+10 \times 10^{-6}$		-10×10^{-9}	-	-
101	49.40	-	0.83	-0.89×10^{-3}	6000	$+12 \times 10^{-6}$	$< 1 \times 10^{-6}$	-14×10^{-9}	-	-

$E(0) = 3.0 \times 10^{-6}$

/TABLE V.

TABLE V. RESULTS FOR 10 NOVEMBER 1455-1525

R(0)	Solar	$-1.35 \pm 0.15 \times 10^{-3}$ cals cm^{-2} sec^{-1}
R(0)	Atmospheric	$+1.45 \pm 0.3 \times 10^{-3}$ cals cm^{-2} sec^{-1}
G(0)		$+0.1 \pm 0.05 \times 10^{-3}$ cals cm^{-2} sec^{-1}
Hence	$C(0) + \lambda E(0) =$	$-0.2 \pm 0.4 \times 10^{-3}$ cals cm^{-2} sec^{-1}

Z	T (°F)	e (g/m^3)	A(Z)	C(Z)	K(Z)	F(Z)-F(0)	R(Z)-R(0)	E(Z)-E(0)	N(Z)	Ri
0	46.5		-	-0.2×10^{-3}						
4	47.22	7.28								
7.5	47.60	7.23	-	-0.2×10^{-3}	15	4×10^{-6}		4×10^{-9}	28	1.7×10^{-2}
13.5	47.92	7.29	-	-0.2×10^{-3}	38	6×10^{-6}	$+3 \times 10^{-6}$	5×10^{-9}	51	2.2×10^{-2}
26	48.17	7.26	-	-0.2×10^{-3}	80	9×10^{-6}	$+7 \times 10^{-6}$	9×10^{-9}	98	3.8×10^{-2}
50.5	48.45	7.24	-	-0.2×10^{-3}	155	15×10^{-6}	$+12 \times 10^{-6}$	14×10^{-9}	190	7.2×10^{-2}
101	48.65	-	-	-0.2×10^{-3}	550	25×10^{-6}	$+23 \times 10^{-6}$	20×10^{-9}	300	

$E(0) = 0$ (ie $\ll 10^{-5}$)

Z	u ($cm\ sec^{-1}$)
5	78
12	101
27.5	116
45	130

/TABLE VI

TABLE VI. RESULTS FOR 10 NOVEMBER 1735-1805

R(0) Atmospheric $+5.7 \pm 0.2 \times 10^{-4}$ cals. cm^{-2} sec^{-1}
G(0) $-2.2 \pm 0.7 \times 10^{-4}$ cals. cm^{-2} sec^{-1}
Hence $C(0) + \lambda E(0) = -3.5 \pm 0.7 \times 10^{-4}$ cals. cm^{-2} sec^{-1}

Z	T (°F)	e (g/m^3)	A(Z)	C(Z)	K(Z)	F(Z)-F(0)	R(Z)-R(0)	E(Z)-E(0)	N(Z)	Ri
0	36.5			-2.0×10^{-4}						
4	39.04	6.18								
7	39.97	6.24	0.82	-2.0×10^{-4}	7	2×10^{-6}	-	2×10^{-9}	-	0.3
13.5	40.89	6.41	0.97	-2.0×10^{-4}	20	4×10^{-6}	2×10^{-6}	4×10^{-9}	-	0.3
26	41.31	6.47	1.00	-2.0×10^{-4}	41	8×10^{-6}	4×10^{-6}	9×10^{-9}	-	0.4
51	41.84	6.53	1.03	-2.1×10^{-4}	66	16×10^{-6}	11×10^{-6}	17×10^{-9}	-	0.7

$E(0) = 2.5 \times 10^{-7}$

Z	u ($cm\ sec^{-1}$)
5	26
12	33.5
27.5	40
45	46

/TABLE VII

TABLE VII. RESULTS FOR 11 NOVEMBER, 1400-1430

R(0)	Solar	$-1.8 \pm 0.15 \times 10^{-3}$ cals. cm^{-2} sec^{-1}
R(0)	Atmospheric	$1.2 \pm 0.2 \times 10^{-3}$ cals. cm^{-2} sec^{-1}
G(0)		$0.3 \pm 0.1 \times 10^{-3}$ cals. cm^{-2} sec^{-1}
Hence	$C(0) + \lambda E(0)$	$+0.3 \pm 0.25 \times 10^{-3}$ cals. cm^{-2} sec^{-1}

Z	T (°F)	e (g/m^3)	A(Z)	C(Z)	K(Z)	F(Z)-F(0)	R(Z)-R(0)	E(Z)-E(0)	N(Z)	Ri
0	50			-1.5×10^{-4}						
4	51.34	8.48								
7	51.57	8.25	0.82	-1.5×10^{-4}	30	-1×10^{-7}	-	-	22	8×10^{-3}
13	51.65	8.24	1.08	-1.5×10^{-4}	75	-6×10^{-7}	-	-	40	11×10^{-3}
26	51.78	8.17	1.17	-1.5×10^{-4}	160	-12×10^{-7}	(5×10^{-7})	-	80	20×10^{-3}
50.5	51.82	8.07	1.15	-1.5×10^{-4}	410	-25×10^{-7}	(8×10^{-7})	-	160	30×10^{-3}
101	51.89	-	1.9	-1.6×10^{-4}	780	-55×10^{-7}	10×10^{-7}	-	310	60×10^{-3}

$E(0) = 7.5 \times 10^{-7}$

Z	u ($cm\ sec^{-1}$)	Z	u ($cm\ sec^{-1}$)
5	72	80	123
12	88	101	126
26.5	(105)	202	142
37.5	110		

/TABLE VIII

TABLE VIII. RESULTS FOR 24 NOVEMBER, 1740-1810

R(0) Atmospheric $1.6 \pm 0.1 \times 10^{-3}$ cals cm^{-2} sec^{-1}
G(0) $-0.05 \pm 0.05 \times 10^{-3}$ - - - (i.e. Very small and negative)
Hence C(0) + λ E(0) $-1.6 \pm 0.1 \times 10^{-3}$ cals cm^{-2} sec^{-1} *

Z	T(°F)	e (g/m^3)	A(Z)	C(Z)*	K(Z)*	F(Z)-F(0)	R(Z)-R(0)	E(Z)-E(0)	N(Z)	Ri
0	30			-1.2×10^{-3}						
4	34.47	5.09								
7	35.71	5.14	1.28	-1.2×10^{-3}	25	4×10^{-7}		0	20	0.1
13.5	36.80	5.22	1.08	-1.2×10^{-3}	65	6×10^{-7}	2×10^{-6}	0	40	0.15
26	37.76	5.31	1.00	-1.2×10^{-3}	140	10×10^{-7}	10×10^{-6}	0	70	0.25
51	38.61	5.37	1.20	-1.2×10^{-3}	230	15×10^{-7}	16×10^{-6}	0	140	0.3
101	39.29	5.49	0.85	-1.2×10^{-3}	770	30×10^{-7}	37×10^{-6}	0	-	0.35

E(0) = -6.7×10^{-7} *

* As the surface temperature was below freezing point these values may be in error.

Z	u ($cm\ sec^{-1}$)
5	32
12.5	48
57.5	75
100	90
200	107

/TABLE IX

TABLE IX. RESULTS FOR 26 NOVEMBER, 1555-1625

R(0) Atmospheric	$1.2 \pm 0.2 \times 10^{-3}$	cals cm^{-2} sec^{-1}
G(0)	$-0.25 \pm 0.1 \times 10^{-3}$	cals cm^{-2} sec^{-1}
Hence C(0) + λE(0)	$-1.0 \pm 0.2 \times 10^{-3}$	cals cm^{-2} sec^{-1} *

Z	T (°F)	e (g/m^3)	A(Z)	C(Z)*	K(Z)*	F(Z)-F(0)	R(Z)-R(0)	E(Z)-E(0)	N(Z)	Ri
0	30			-0.6×10^{-3}						
4	32.05	4.78								
7	33.25	4.89	1.2	-0.6×10^{-3}	15	2.5×10^{-6}	-	2.5×10^{-9}	-	0.7
13.5	34.38	5.14	1.2	-0.6×10^{-3}	25	4.5×10^{-6}	-1×10^{-6}	5.5×10^{-9}	-	2.0
26	35.55	5.37	1.2	-0.6×10^{-3}	50	8×10^{-6}	$+1 \times 10^{-6}$	11×10^{-9}	-	5.0
51	36.86	5.57	1.0	-0.6×10^{-3}	100	12×10^{-6}	4×10^{-6}	19×10^{-9}	-	10.0
101	37.89	5.83	0.7	-0.6×10^{-3}	250	15×10^{-6}	15×10^{-6}	30×15^{-9}	-	

$E(0) = 6.7 \times 10^{-7}$ *

* As the surface temperature was below freezing point these values may be in error

Z	u (cm sec^{-1})	Z	u (cm sec^{-1})
5	24	57.5	43
12.5	29	76	43+
26.5	(38)	100	46
37	38	200	64

/TABLE X

TABLE X. RESULTS FOR 26 NOVEMBER, 1740-1750

R(0) Atmospheric $1.2 \pm 0.2 \times 10^{-3}$ cal cm^{-2} sec^{-1}
G(0) $-0.25 \pm 0.05 \times 10^{-3}$ cal cm^{-2} sec^{-1}

Z	T (°F)	e (g/m^3)	F(Z)-F(0)	R(Z)-R(0)	Ri
0	24.8				
4	25.16	3.74			
7	26.52	3.94	$+1 \times 10^{-7}$	-	1.0
13.5	28.15	4.20	30×10^{-7}	-4.5×10^{-6}	1.5
26	29.61	4.42	80×10^{-7}	-3×10^{-6}	2.5
51	31.35	4.68	120×10^{-7}	0	2.5
101	32.85	4.96	120×10^{-7}	$+7.5 \times 10^{-6}$	

26 November 1740-1810

Z	u (cm sec^{-1})
5	(20)
12.5	(23)
26.5	(34)
37	32
57.5	37
100	50
200	82

/TABLE XI

TABLE XI.

VALUE OF THE INDEX p IN $\partial T/\partial z = Az^p$ ETC.

Date and Time		$\partial T/\partial z$	$\partial e/\partial z$	$\partial u/\partial z$	Ri(25)
19 July	1400-1430	-1.12	-1.12	(-1.-)	-0.01
2 Oct.	1055-1125	-1.43	(-1)	-	-
10 Nov.	1435-1505	-1	-1	(-1)	$0 < R_i < 0.01$
10 Nov.	1455-1525	-1.08	-1.08	-1	+0.04
10 Nov.	1735-1805	N/A	N/A	-0.75	+0.4
11 Nov.	1400-1430	-1.30	-1.30	-1	+0.02
24 Nov.	1740-1810	(-1.24)	(-1.24)	(-1)	+0.25
26 Nov.	1555-1625	-0.95	-0.95	-0.77	+5.0
26 Nov.	1740-1750	-0.87	-0.87	-0.77	+2.5

/TABLE XII

TABLE XII

FLUCTUATIONS OF TEMPERATURE DIFFERENCES 2 OCTOBER, 1100-1120

N.B. TEMPERATURE IN °F.

Height Range \ Reading No.	1	2	3	4	5	6	7
4-7cm	0.81	0.72	0.84	0.75	0.66	0.82	0.81
7-13cm	1.86	0.42	1.27	0.84	0.79	0.88	0.81
13-26cm	0.08	0.23	0.53	0.84	0.80	0.77	0.87
26-50cm	0.62	0.66	0.62	0.64	0.65	0.44	0.59
50-100cm	0.32	0.31	0.33	0.42	0.31	0.23	0.32
100-200cm	0.31	0.34	0.28	0.31	0.23	0.21	0.32

FIG. 1

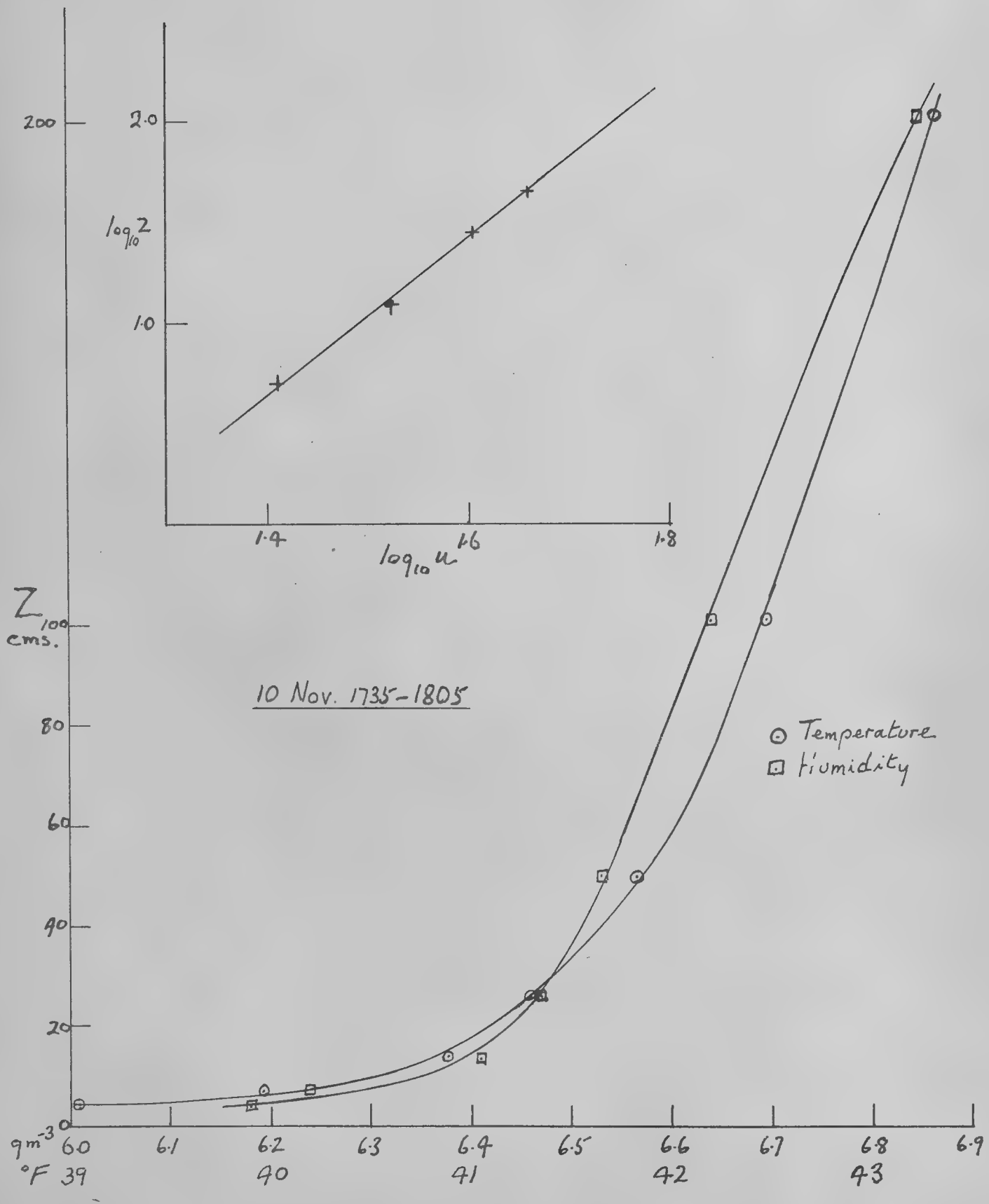
200
2·0
$\log_{10} Z$
1·0
1·4
1·6
1·8
$\log_{10} u$
Z_{100} cms.
10 Nov. 1735–1805
80
60
40
20
⊙ Temperature
⊡ Humidity
gm^{-3} 6·0 6·1 6·2 6·3 6·4 6·5 6·6 6·7 6·8 6·9
°F 39 40 41 42 43

Fig. 2

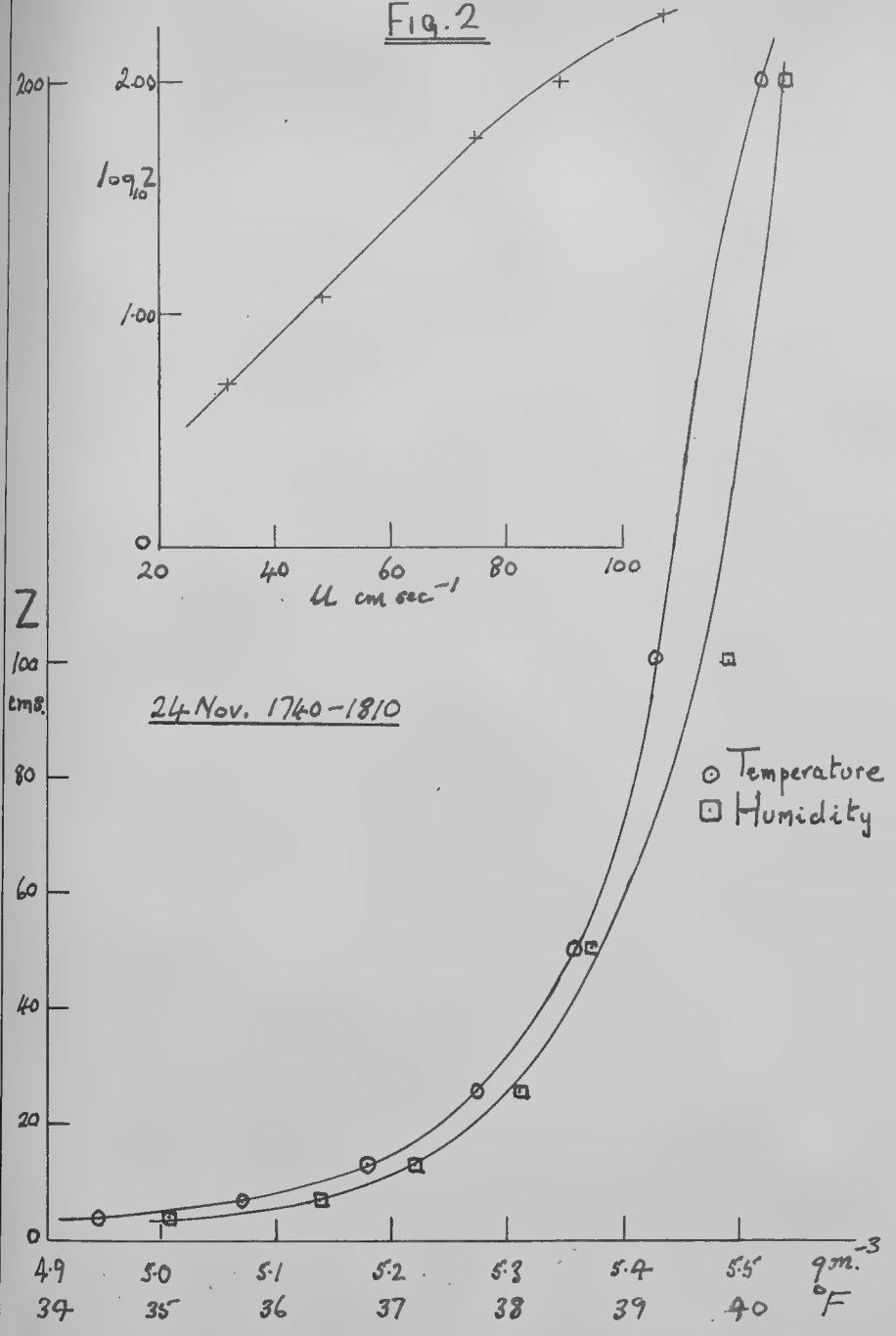

200
2.00
$\log_{10} Z$
1.00
0
20
40
60
80
100
u cm sec^{-1}
Z
100
cms.
80
60
40
20
0
24 Nov. 1740–1810
Temperature
Humidity
4.9
5.0
5.1
5.2
5.3
5.4
5.5
g.m.$^{-3}$
34
35
36
37
38
39
40
°F

Fig. 3

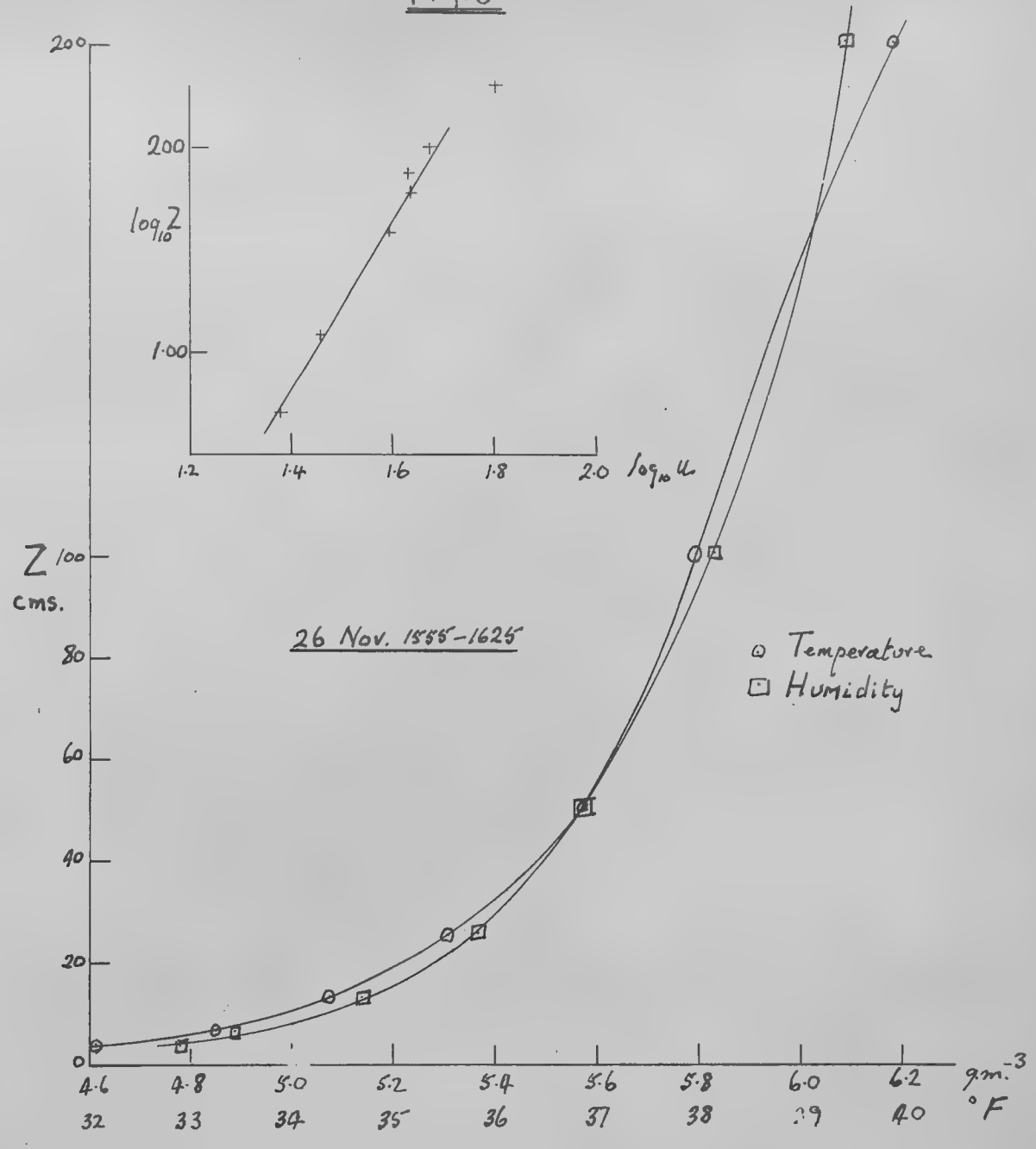

200
200
$\log_{10} Z$
1.00
1.2
1.4
1.6
1.8
2.0
$\log_{10} u$
Z
100
cms.
80
60
40
20
0
26 Nov. 1555–1625
Temperature
Humidity
4.6
4.8
5.0
5.2
5.4
5.6
5.8
6.0
6.2
g.m.$^{-3}$
32
33
34
35
36
37
38
39
40
°F

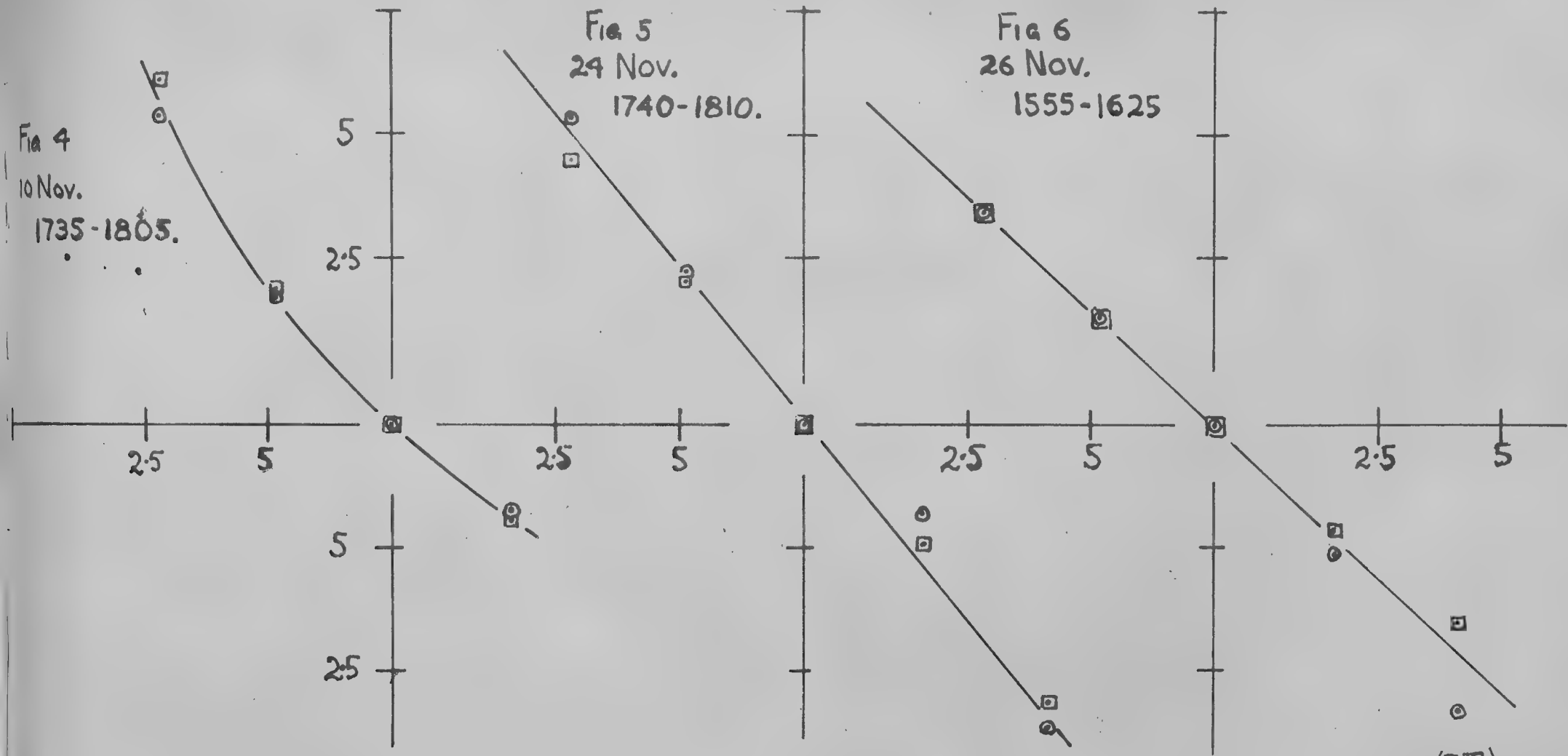

FIGS. 4-6. LOG-LOG PLOTS. ABSCISSAE - LOG $z/25$. ORDINATES - ⊙ LOG $\left(\frac{\partial T}{\partial z}\right)_z \Big/ \left(\frac{\partial T}{\partial z}\right)_{25}$

□ LOG $\left(\frac{\partial \theta}{\partial z}\right)_z \Big/ \left(\frac{\partial \theta}{\partial z}\right)_{25}$

Fig. 9

Dry Bulb Temperatures.

26 Nov.

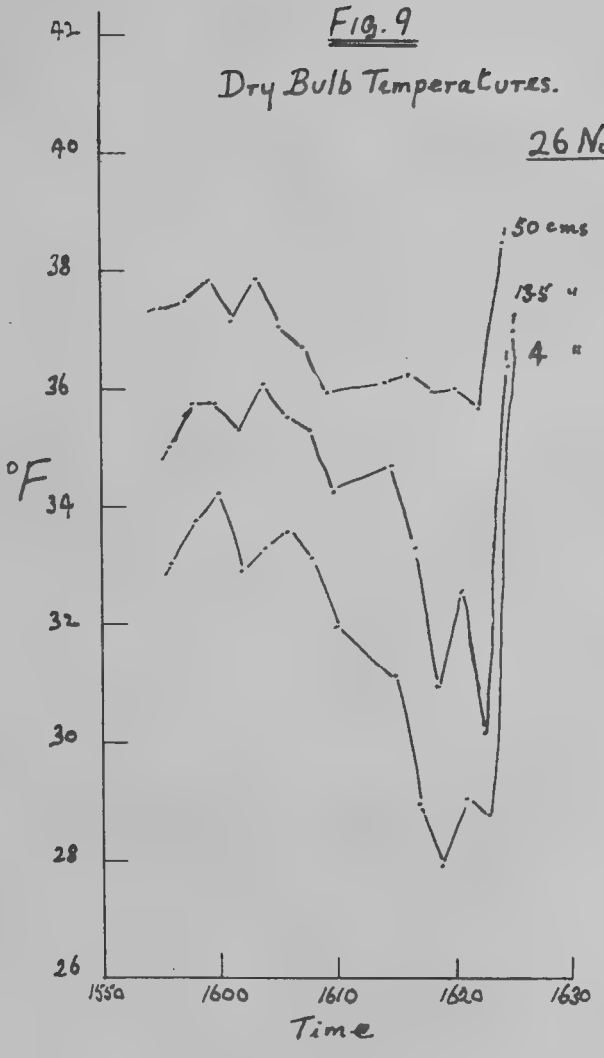

Fig. 10.

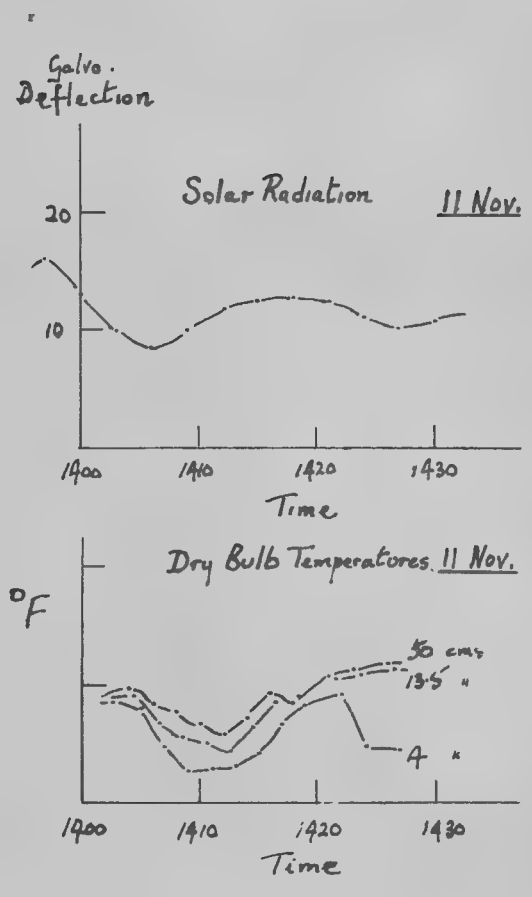

Fig. 7

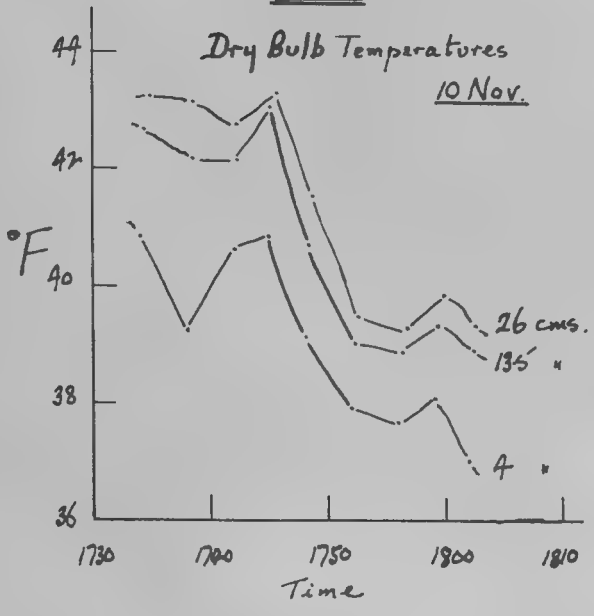

Fig. 8

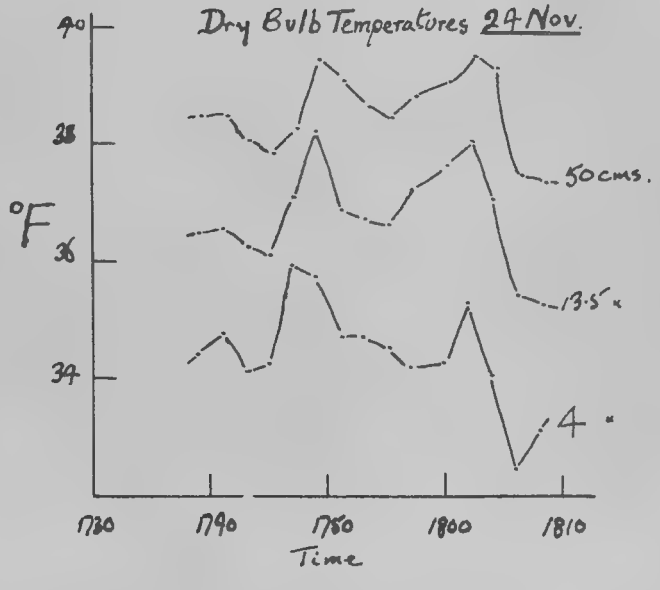

This report has not yet been published and is not to be treated CONFIDENTIAL. Its contents must not be quoted.

AIR WEATHER SERVICE
TECHNICAL REFERENCE FILES

M. R. P. 496
S. C. I/24.
30th June, 1949.

AIR MINISTRY

METEOROLOGICAL RESEARCH COMMITTEE.

The Terminal Velocity and Rate of Dispersion of 'Window' in Radar Wind Measurements.

by

A. C. Best

1. Introduction. At the fifth meeting of the Instruments Sub-Committee there was some discussion (minute 47) of the use of 'window' for the measurement of winds at great heights. It was stated that window, in the form of short threads of nylon, is now obtainable packed in cartridges similar to Verey cartridges and it was considered that such cartridges might provide a suitable source of window if they could be exploded at the required height. At the meeting reference was made to the terminal velocity of this window and to its rate of dispersion but no information on these points was available. The purpose of the present note is to discuss these two factors.

Discussion with Dr. H. G. Hopkins after the meeting indicated that the window referred to consists of nylon threads 1.5 cm. long and having a diameter of about 2 to 5 thousandths of an inch. Presumably these threads are rendered conducting by some process.

In the following paragraphs the behaviour of small cylinders, having length large compared with the diameter, at a height of 30 km. in the I. C. A. N. atmosphere is considered.

2. Terminal Velocity. If a cylinder is immersed in a fluid moving at right angles to the axis of the cylinder then we find from Lamb's Hydrodynamics (6th Edtn, p 616) that, if the Reynolds' Number is sufficiently small, the resistance per unit length of the cylinder is

$$\frac{4\pi\mu v}{1/2 - \gamma - \log_e(R/8)}$$

where μ is the coefficient of viscosity of the fluid, v the velocity, γ is Euler's constant and R is Reynolds' Number. This leads to

$$C_D = \frac{-8\pi/R}{0.0772 + 2.303\log_{10}(R/8)} \qquad \text{.....(1)}$$

where C_D is the drag coefficient.

Goldstein (Modern Developments in Fluid Dynamics - Vol 2, p. 419) reproduces a small scale curve (data from Lamb and from Bairstow) showing C_D plotted against R. Unfortunately this curve does not extend to sufficiently small values of R for the present purpose but table 1 shows that Lamb's formula is in good agreement with the experimental values quoted by Goldstein at the smallest values of R for which experimental data are available.

/Table 1.

Table 1.

Drag Coefficient C_D for a Cylinder.

R	C_D from Eqn 1	C_D from Goldstein
0.0005	5230	-
0.005	688	-
0.010	379	-
0.050	100	-
0.100	58.2	-
0.170	39.2	40
0.265	28.5	30
0.493	-	20
1.000	-	12

In the following paragraphs values from table 1 have been used, intermediate values being taken for R = 0.170 and 0.265.

By equating the forces acting on a cylinder falling through the air, and neglecting air density in comparison with cylinder density, we get

$$v^3 = \frac{\pi R \mu g \sigma}{2 C_D \rho^2} \qquad \ldots\ldots\ldots\ldots\ldots\ldots\ldots\ldots(2)$$

$$d = \frac{R \mu}{v \rho} \qquad \ldots\ldots\ldots\ldots\ldots\ldots\ldots\ldots(3)$$

where d and σ are the diameter and density of the cylinder respectively. Thus for any selected value of R, v can be computed from (2) if C_D is known, and then d can be computed from (3). Thus, by taking a number of values of R, v can be plotted against d. This has been done for various values of σ the results being given in fig 1. The values chosen for the various constants were g = 981, $\mu = 1.416\ 10^{-4}$ and $\rho = 1.819\ 10^{-5}$ c.g.s. units. The last two values correspond to a height of 30 km. in the I.C.A.N. atmosphere.

3. Rate of dispersion of smoke. Very little information is available on the degree of turbulence at 30 km. in the atmosphere and we shall consider first the rate of dispersion of smoke at this height and then examine the application to the present problem.

According to Sutton's theory of eddy diffusion (P.R.S., A.135, 1932) the rate of dispersion of an instantaneous point source is in accordance with

$$\Psi = \frac{Q}{\pi^{3/2} C^3 (ut)^{3m/2}} \exp\left[-\frac{r^2}{C^2 (ut)^m}\right] \qquad \ldots\ldots\ldots(4)$$

where

Ψ is the smoke density in gm/cc at distance r from the centre of the cloud
Q is the total smoke content of the cloud
u is the wind velocity
t is the time in seconds
C and m are constants.

From this equation Sutton deduces that if d is the visible diameter of the smoke cloud

$$\frac{d^2}{(ut)^m} = 4 m C^2 (\log_e(\text{constant}) - \log_e(ut)) \qquad \ldots\ldots\ldots(5)$$

/From

From the scatter of balloons Sutton deduced a value 1.75 for m. Using this value for m he then plotted d^2/t^m against $\log_e t$ for some observations of shell bursts at various heights and so found values for C. These values of C varied systematically with height from 0.088 at 945 metres to about 0.026 at 5350 metres. Sutton points out however that C cannot decrease indefinitely with height.

During the course of measurements of wind at 30km. by means of shell bursts during the war (M.R.P. 194 by R.J. Murgatroyd) an attempt was made to photograph the shell bursts with a kine-theodolite and to repeat Sutton's computations based upon equation 5. There were many difficulties which had not been overcome by the time the wind measurements ceased. In a departmental report Murgatroyd summarises these attempts at measuring C at 30 km. and gives the data for the occasions which were most nearly successful. In view of the present need these data have been examined to see whether they can contribute any useful information.

It must be emphasized that the values obtained are very approximate but they do seem useful in the present connection. In Murgatroyd's observations the cloud was usually elliptical so that there were two values for d. From the three best sets of data(d^2/t^m plotted against $\log_e t$) the present writer obtained the following results

21.2.45	C_x	=	?	C_y	= 0.24
24.12.44	C_x	=	0.07	C_y	= zero
9.3.45	C_x	=	0.11	C_y	= 0.07

One of the difficulties was the fact that the cloud seldom lasted longer (in the photographs) than about 100 seconds from the instant of burst and during the early part of the life of the cloud it is dispersing very rapidly under the influence of the explosion. Thus, as in Sutton's paper, the early part of the plot of d^2/t^m against $\log_e t$ was not linear and only a small part of the curve could be used to determine C. In fact on some of the curves it was difficult to be sure that the plot was linear at the larger values of t. Nevertheless these observations do suggest that at 30 km. the diffusion coefficient for smoke is of the order of 0.05 to 0.10.

In Porton Report No. 2641 D.R. Davies has applied Sutton's theory of diffusion of smoke to the diffusion of drops by writing

$$C^2(\text{smoke})/C^2(\text{drops}) = (u^2 + v^2)^{m/2} / u^m$$

where u is wind velocity and v is the terminal velocity of the drops. The justification for this procedure is not entirely clear to the writer but it seems plausible that the diffusion coefficient for smoke is applicable to aerosols having a terminal velocity small compared with the wind velocity and that as the terminal velocity increases the diffusion coefficient C decreases. Thus in the present problem we might expect C for very light threads to be of the order of 0.05 to 0.1 and to be smaller for heavier threads.

4. Application to Wind Measurement with Window. We regard a cloud of window as a target for detection by means of radar. The cloud of window is assumed to be produced by the explosion of a small container of window elements. These elements will diffuse due to the turbulent nature of the atmosphere, the cloud thus growing, and will also have a mean downward speed equal to the terminal velocity of the elements. A short while after the release of the window the number of window elements per unit volume of space (corresponding to smoke density in section 3) will vary throughout the cloud. Let us assume that equation 4 is applicable to this diffusion of window where ψ now represents the number of window elements per unit volume of space and Q is the total number of these elements contained in the cloud and, originally, in the container.

/We

We assume also that the power of the received signal from the window cloud is given by

$$P = \frac{K}{L^4} \int \psi \, dA \qquad \ldots\ldots\ldots\ldots\ldots\ldots\ldots\ldots(5)$$

where K is a constant dependent upon the radio properties of the radio equipment and of the window element, L is the slant range from the receiver to the cloud, dA is an elementary area and the integration is taken over a central cross section of the spherical cloud in a plane perpendicular to the slant range. From equation 4 the cloud is symmetrical about the centre and equation 5 becomes

$$P = \frac{K}{L^4} \int_0^\infty 2\pi r \, \psi \, dr \qquad \ldots\ldots\ldots\ldots\ldots\ldots\ldots\ldots(6)$$

Physically it is obvious that the upper limit of the integral should be a finite quantity but the integrand decreases so rapidly with increasing r that no serious error is involved in using an infinite upper limit. Substituting for ψ in equation 6 from equation 4 we get

$$P = \frac{K\,Q}{L^4\ \pi^{1/2}\ C\ s^{m/2}} \qquad \ldots\ldots\ldots\ldots\ldots\ldots\ldots\ldots(7)$$

where s has been written for ut, the distance travelled by the cloud.

It is suggested that it might be advantageous to design a special meteorological cartridge for wind measurements. In the first instance the design might take account of the following factors. Equation 7 shows that the power of the received signal is inversely proportional to C so that a small value of C is desirable. This in turn implies a high terminal velocity for the window elements. This can be achieved by choosing window elements having a large diameter or a large density (σ in section 2) or both. A large diameter however implies a smaller number of elements in a cartridge of given size. This suggests the use of copper elements. The diameter selected for the copper elements will depend upon the maximum terminal velocity which is acceptable from the meteorological angle. A radio sonde balloon ascends at about 600 cm/sec so that copper elements of about 80 microns diameter might be suitable.

The window elements being thus selected the value of K (defined by equation 5) should then be determined.

For a given ground equipment there will be a minimum acceptable value for P, say P_o. The value of Q, the number of elements in the cartridge, is then determined by

$$\frac{P_o}{K} < \frac{Q}{L^4\ \pi^{1/2}\ C\ s^{0.875}} \qquad \ldots\ldots\ldots\ldots\ldots\ldots\ldots\ldots(8)$$

The value of s depends upon the accuracy required. We might assume that reasonable accuracy can be achieved if the displacement of the cloud during the period of observation is greater than 5 km. $= 5\ 10^5$ cm. The value of L depends upon the circumstances of the observation. For a height of 30 km. L might well be 50 km. $= 5\ 10^6$ cm. The evaluation of C is subject to some uncertainty but, with window elements having a terminal velocity of 600 cm/sec it will probably be safe to assume C = 0.05. Inserting these values in equation 8 we get

/Q

$$Q > 5.42\ 10^{30}\ \frac{P_o}{K} \qquad \text{.....(9)}$$

where Q is the number of elements in the cartridge and P_o/K is the ratio of the minimum acceptable signal to K as defined by equation 5.

It will be noticed that the most important factor tending to increase Q is the value of L. A variation of 2 to 1 in the value of L outweighs any variation in C which might reasonably be expected.

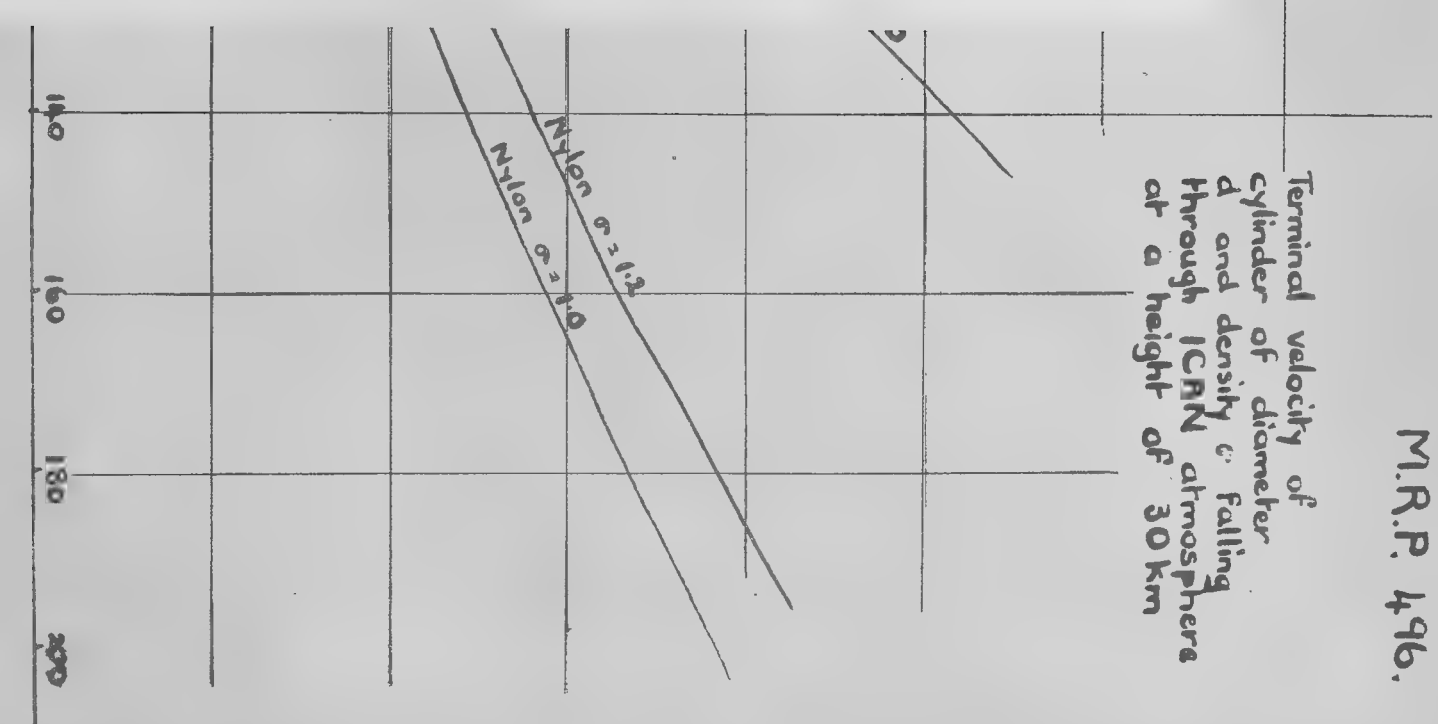

Terminal velocity of cylinder of diameter d and density σ falling through ICAN atmosphere at a height of 30 km

M.R.P. 496.

M.R.P. 496.

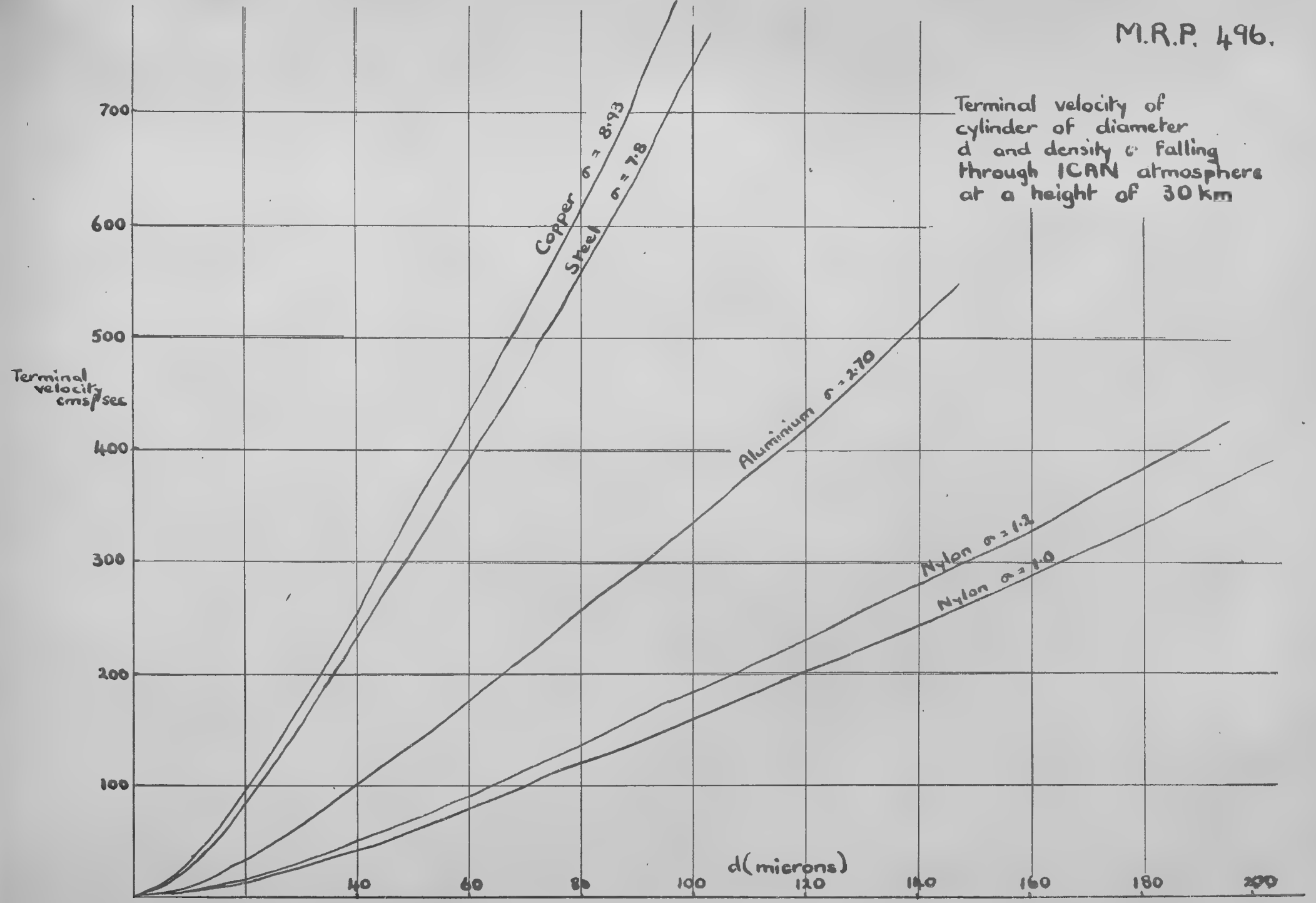
Terminal velocity of cylinder of diameter d and density σ falling through ICAN atmosphere at a height of 30 km
Terminal velocity cms/sec
700
600
500
400
300
200
100
Copper σ = 8·93
Steel σ = 7·8
Aluminium σ = 2·70
Nylon σ = 1·2
Nylon σ = 1·0
d (microns)
40
60
80
100
120
140
160
180
200

AIR WEATHER SERVICE
TECHNICAL REFERENCE FILES

M.R.P. 498.
S.C.III/38.
26th July, 1949.

AIR MINISTRY

METEOROLOGICAL RESEARCH COMMITTEE.

SOME FURTHER CONSIDERATIONS OF THE MEASUREMENT AND INDIRECT EVALUATION OF NATURAL EVAPORATION.

by F. Pasquill.

Summary.

A previous observational study (Pasquill, 1949, a) has been supplemented by further measurements of evaporation and the associated vertical profiles of wind velocity and vapour pressure in the first two metres above a clayland pasture with grass of moderate length, mainly in effectively adiabatic conditions of flow. The evaporation measurements, using a simple form of soil evaporimeter, included two series of statistically designed measurements, aimed at testing the "reliability" of the technique. The data so obtained, though not comprehensive, indicate no substantial error due to the necessary isolation of test soil from underlying layers, but there is a suggestion that the rates of evaporation ultimately adopted might be underestimates, owing to unavoidable disturbance of root and soil continuity in the vertical at the perimeters of the soil cores contained in the evaporimeters.

The observed rates of evaporation (E_o) are compared with those computed (E_c) from the following formula, which is based on the Prandtl law relating surface drag and wind profile near the surface in adiabatic conditions,

$$E_c = \frac{\rho k^2 (u_2 - u_1)(q_1 - q_2)}{\left\{ \log_e \frac{z_2 - d}{z_1 - d} \right\}^2}$$

where u_1, u_2, q_1, q_2 are the wind velocities and specific humidities at heights z_1, z_2, above the soil surface, d is a 'zero point displacement' associated with the vegetation cover, ρ is air density and k is von Karman's constant, of magnitude 0.4. For the present measurements the usual "roughness parameter", deduced from the wind profiles, was 0.51 cm., as compared with 0.25 cm. for the previous series. The two series include 19 separate determinations of rate of evaporation over periods of about one hour, and in terms of different sections of the observed profiles, provide 41 values of E_c/E_o in effectively adiabatic conditions, with wind velocities at a height of 2 m. ranging from 3 to 9 m./sec. The mean value of E_c/E_o is 0.99 and the individual deviations from 1.0 are within 10, 20 and 30% in 24, 66 and 90% of cases. It is demonstrated that deviations of this order are to be expected from local variations in the various factors involved.

Although some a priori uncertainty remains concerning the precise validity of the evaporation measurements, the consistency so demonstrated in terms of a semi-theoretical treatment which has been established in other connections (Calder, 1949) suggests that the ultimate result may be accepted with confidence. Brief consideration is then given to the validity and practicability of applying the above formula to evaporation from areas of growing crops.

1. Introduction.

An observational study during the spring of 1948 (Pasquill, 1949, a) provided data on some of the features involved in the turbulent transport of water vapour over a short grass surface and on the validity of formulae prescribing natural

/evaporation

evaporation in terms of meteorological factors. The investigation was resumed in the spring of 1949 with the aims, in particular, of justifying more firmly the method adopted for the evaporation measurements, and of carrying out these and other relevant measurements for a range of grass lengths. Due primarily to the generally dry state of ground then existing it was found practicable to apply the technique of evaporation measurement on only two occasions, during which the grass was only slightly longer than during the initial investigation; and, moreover, during which no substantial departures from adiabatic conditions were encountered.

Thus, the present investigation does not directly subscribe to the important problem of generally extending the earlier results to a surface roughness approaching the magnitude associated with crops in full growth. It does, however, add somewhat to the scanty data as yet available on direct measurement of natural evaporation and substantially reinforces the evidence for the validity of the theoretical formula for evaporation based on the Prandtl law relating wind profile and surface drag in adiabatic conditions. Furthermore, some observations of the spatial variations of wind speed and vapour pressure permit some appreciation of the reliability of individual observations. Finally, despite the lack of relevant observational data, a brief discussion is given concerning the indirect evaluation of evaporation from areas of growing crops.

2. Observational Aspects

Observations of the vertical profiles of wind velocity, air temperature and vapour pressure, and of water loss from soil evaporimeters of simple design, were carried out on the site employed previously, again avoiding wind directions in the obstructed N - E quarter. The profile observations employed anemometers and distant reading thermocouple psychrometers identical with those described previously (Pasquill, 1949, a, b) and the technique of observation differed only slightly. Differences in dry and wet bulb temperatures over the height intervals 200-100, 150-37½ and 50-25 cm. were read directly (nominally to $0.1^{\circ}F$), while absolute values of wet bulb temperature were measured at the higher level in each interval and dry bulb temperature at 200 cm. (nominally to $0.1^{\circ}F$). The nominal temperature readings were subsequently corrected on the basis of regular calibrations of the thermocouple equipment against standard mercury - in - glass thermometers, approximate corrections also being applied, as before, for the thermal lag of the temperature elements.

One reading of each temperature or temperature difference was taken every two minutes, in systematic order, for a period of 20 minutes during which the anemometers (exposed at six heights as above) were in continuous operation. Anemometers and psychrometers were then interchanged in each of the above height intervals, so as to eliminate defects in instrumental performance, and the process repeated after allowing a period of 10 minutes for adjustment of the psychrometers to their new environments. The means of the 20 individual temperature readings and of the two anemometer runs were taken as representative of the whole period of observation (approximately one hour). A thorough wind tunnel calibration of the anemometers was applied retrospectively.

The evaporation measurements were identical in principle with those described previously, but with some modifications in design, and a fairly detailed description of this aspect seems desirable. The general principle, it may be recalled, is that on a clay soil such as that which exists on the present site, and which characteristically dries out progressively from the surface downward, it may be possible to select occasions when isolation of a shallow block of soil from surrounding and underlying soil, while maintaining the original exposure at the surface, will not for some time influence the rate of loss of water from the test soil. Clearly one essential condition is that the progressive drying shall not have extended below the depth at which the soil is isolated.

The application of the technique presents two main problems. In the first place there are the mechanical features of the size, extraction, exposure and weighing of the soil. In the second place there is the designing of "control technique" on which to justify the adoption of the measured water losses as uninfluenced by the necessary isolation of the test soil. The mechanical features were similar to those of the initial investigation, soil cores of circular cross-section being extracted with "undisturbed core" samplers of conventional design, suitably exposed in Tufnol containers and weighed at intervals on an indicating balance. Further details are shown in Figure 1 (a).

/For

For the measurements over periods of one hour, which are subsequently related to the profile observations, the evaporimeters were, as before, nominally 4 inches in diameter and depth. The cutting diameter of the soil sampler was actually 3 15/16 inches, and this was adopted as the effective diameter in computing rates of evaporation from the observed water losses. Two types of control measurement were suggested and applied to some degree in the initial investigation. The first method considers the effect of a change in the depth of the soil cores, the second the effect of a difference in age of the cores, the idea being that the effects of the isolation of the cores s should show up with decreasing depth and increasing age. In the present measurements an attempt was made to apply the "depth" test in a more comprehensive fashion than hitherto, by using evaporimeters of 8 inches depth, with necessarily smaller diameter (nominally $2\frac{3}{8}$ inches, cutting diameter of sampler 2 5/16 inches) so that the total weights were still within the capacity of the indicating balance and 4 inch evaporimeters of the same cross-section for direct comparison. The final combination thus provided in addition a comparison of evaporimeters of the same depth but different cross sectional areas. Owing to the smaller evaporating areas presented by the additional evaporimeters the control measurements were made over periods of several hours or more.

In practice six evaporimeters of each type were prepared and exposed concurrently and in view of previous indications of considerable point to point variations in local rate of evaporation it was decided to set out the evaporimeters according to some suitable statistical design. The procedure adopted was to mark out a rectangle of 12 x 2 yards, 10 - 20 yards from the position of the profile apparatus in the anticipated upwind direction, with the long side lying across wind. This rectangle was divided into six plots each 2 x 2 yards, in each of which was set out one evaporimeter of each type, the plots and corresponding evaporimeters being numbered 1 - 6. In each plot the three evaporimeters were arranged as close together as possible in a random order. Soil cores were employed if inspection showed them to be completely intact, apart from shallow cracks on the outside, which appeared to be unavoidable. Thus in some cases extractions had to be repeated and a wider separation in the group had to be accepted.

Satisfactory extraction of the soil cores was generally practicable up to mid - April, during which period two series of measurements were carried out. It may be noted that on both occasions the root growth frequently extended below a depth of 4 inches, but only occasionally below 8 inches. The approximate dispositions of the evaporimeters for one of these series is indicated in Figure 1 (b). Subsequent attempts were unsuccessful, owing to the increasing dryness of the surface layers of soil and the consequent breaking up of soil cores on extraction. Indeed the experience gained during the present season demonstrated most strikingly the limited extent of the drying period during which soil cores can be extracted satisfactorily.

3. Reliability of the evaporation measurements.

The individual evaporation losses were usually of the order of 1 gm. for the hourly measurements, and frequently considerably more than this for the longer period measurements, even for the evaporimeters of small cross-section. These losses were read to 0.01 gm. on an indicating balance the scale of which was calibrated against reliable weights. A few test readings indicated that errors in individual readings were less than 0.02 gm. The accuracy of reading was thus quite adequate for an investigation of the present type.

We may now consider the implications of the control measurements as regards the ultimate reliability of the results obtained. It will be seen that some uncertainty remains. The two sets of data are summarised in Table 1 below, the water losses being expressed in the form of an equivalant depth, so as to permit direct comparison of the evaporimeters of different cross-sectional areas.

/Table 1.

Table 1. Water losses in mms. from various evaporimeters.

Date of setting out evaporimeters	Period of Measurement	Evaporimeter Depth	Evaporimeter Diam.	Plot & Evaporimeter Number. 1	2	3	4	5	6	Mean
22/3/49	1610 G.M.T. 22/3/49 to 1545 G.M.T. 24/3/49.	4"	4"	2.67	2.43	3.08	2.70	1.94	2.65	2.58
		4"	$2\frac{3}{8}$"	1.98	1.91	2.41	2.14	3.07	2.18	2.28
		8"	$2\frac{3}{8}$"	1.78	1.52	2.67	2.17	2.00	1.03	1.86
11/4/49	0915 to 1445 G.M.T. 13/4/49	4"	4"	1.16	1.41	0.90	1.27	1.36	1,15	1.21
		4"	$2\frac{3}{8}$"	0.97	0.69	1.22	0.81	0.57	0.79	0.84
		8"	$2\frac{3}{8}$"	1.06	1.03	1.20	1.03	1.18	1.09	1.10

Statistical examination of the above data leads to the following conclusions.

(a) In both sets the differences between corresponding evaporimeters of depths 4" and 8" (but of the same diameter) are insignificant. Furthermore, it is to be noted that these differences are generally of opposite signs in the two sets of data, which adds weight to the indication that the differences are chance effects of a natural point to point variation in local rate of evaporation.

(b) The differences between corresponding evaporimeters of different diameters (but of the same depth) are insignificant in the first set, but just significant in the second set. In other words there is an indication, though not a very marked one, of a genuine difference in the indications of the evaporimeters of different diameters.

The examination of the effect of depth of evaporimeter strongly suggests that over the period involved the break in soil and root continuity at a depth of 4 inches had no effect on the water loss from the surface. From this point of view, therefore, it is legitimate to accept the hourly measurements carried out with the larger diameter evaporimeters during the same period as indicative of the true water loss. Some uncertainty, however, is now introduced by the suggestion that the evaporimeters of smaller diameter indicate systematically lower than those of larger diameter. A tentative explanation of this effect is as follows. Although it may reasonably be assumed that soil and root continuity were preserved throughout the main bulk of the soil under test, it is evident that this condition would not be maintained right up to the outside of the core. As already mentioned superficial cracks seemed to be unavoidable and it is clear that cutting of some of the roots near the outside would also occur. Thus, around the edge of the soil core discontinuities in root and soil could have existed sufficiently near to the surface to reduce the local water loss. Such an 'edge effect' would presumably exert a proportionately greater effect with decrease of core diameter and so lead to differences in the direction observed. If this explanation is correct then it implies the possibility that the losses from the larger diameter evaporimeters are underestimates, but to an extent which it is not possible to estimate from the present data alone. Indeed in view of the rather slender evidence for the effect it is clear that a determination of its precise magnitude would require a much more comprehensive test than has been provided here. In the following considerations of the results, however, it will be seen that the general consistency demonstrated suggests that the effect is of a small order.

4. Profile data and Estimation of rate of evaporation.

The data on wind velocity, temperature and vapour pressure profiles are presented, with other relevant data, in Table 2. They are divided into two groups, (labelled E and F, following the grouping of the earlier data), corresponding to the two separate sets of evaporimeters. Observations 7 and 8 are omitted since owing to an accident with the evaporimeters no reliable measurements of water loss were obtained. The vapour pressure differences (Δe) for the various height intervals were evaluated from a specially prepared chart based

/on

on the formula

$$\Delta e = \beta \Delta T' + A (\Delta T' - \Delta T) \qquad \text{.....(1)}$$

where ΔT, $\Delta T'$ are the dry and wet bulb temperature differences over the interval, β is the slope of the saturation vapour pressure - temperature curve at the mean wet bulb temperature and A is the aspirated psychrometer constant. This follows immediately and with sufficient accuracy from the usual psychrometer formula when the variation of wet bulb temperature over the height interval is not more than a few degrees. For example, with wet bulb temperatures in the region of 60°F a variation of 5°F introduces an error of 0.0025 mm. Hg. The observed rates of evaporation are also given in Table 2 each figure being based on the mean water loss indicated by the six evaporimeters of 4" diameter over a period of approximately 1 hour.

Using most of the profile data we may compute rates of evaporation (E_c) from a formula the basis and derivation of which have been discussed previously (Pasquill, 1949, a). The formula is

$$E_c = \frac{\rho k^2 (u_2 - u_1)(q_1 - q_2)}{\left\{ \log_e \frac{z_2 - d}{z_1 - d} \right\}^2} \qquad \text{.....(2)}$$

where u_1, u_2, and q_1, q_2, are wind velocities and specific humidities at heights z_1, z_2. above the soil surface, k is von Karman's constant of magnitude 0.4, ρ the air density, and d a "zero point displacement" (see later). In a form suitable for direct evaluation from the present data this becomes

$$E_c = \frac{4.63 \times 10^{-5} (u_2 - u_1)(e_1 - e_2)}{T\left\{ \log_e \frac{z_2 - d}{z_1 - d} \right\}^2} \qquad \text{.....(3)}$$

where E_c is in gm/cm^2 sec., u in cm/sec., e in mm. Hg., and T is the dry bulb temperature in °A. The error involved in neglecting the variation of T over the heights involved is obviously negligible.

Basically the above formulae are valid only in "adiabatic" conditions, i.e. in conditions of zero vertical gradient of potential temperature. In the earlier investigation, however, it was demonstrated that the effective departure from adiabaticity is specified, not by the vertical gradient of potential temperature alone, but by the Richardson Number

$$R_i = \frac{g}{T} \frac{(\partial T/\partial z + \Gamma)}{(\partial u/\partial z)^2} \qquad \text{.....(4)}$$

Γ being the dry adiabatic lapse rate. Conditions are effectively adiabatic if the Richardson Number is numerically small and hence may exist even in the presence of a substantial temperature gradient provided this is associated with a large vertical gradient of wind velocity. In the present analysis the departures from effectively adiabatic conditions are conveniently examined on the basis of a pseudo - Richardson Number, S, evaluated from the formula

/ .....(5) .

$$S = \frac{(\theta_2 - \theta_1)}{(u_2 - u_1)^2} \log_e \frac{z_2 - d}{z_1 - d} \sqrt{(z_2 - d)(z_1 - d)} \qquad \text{.....(5)}$$

where θ is the dry bulb temperature in $^{\circ}F$ and d has the same meaning as before. At normal temperatures S corresponds to approximately half the Richardson Number at the geometric mean of the two heights, and follows directly from (4) by assuming a logarithmic variation with height of temperature and wind speed and neglecting Γ. The reason for evaluating (4) at the geometric mean height of the interval is that the errors due to actual departures from a logarithmic variation will be minimised.

For the evaluation of the above formulae we require, in addition to the data already specified, the value of the zero point displacement, d. This is originally introduced in the wind profile - drag relationship on which equation (2) is based, and may be said to take into account the effective raising, by the vegetation cover, of the boundary from which turbulent exchange is operative. The wind profile - drag relationship in adiabatic conditions may then be written

$$u = \frac{1}{k}\sqrt{\frac{\tau_o}{\rho}} \log_e \frac{z - d}{z_o} \qquad \text{.....(6)}$$

where τ_o is the aerodynamic drag at the surface, and z_o is the so-called roughness parameter, the magnitude of which depends on the size, shape and disposition of the roughness element. The value of d may be evaluated graphically in terms of wind velocities at three or more heights, since from (6),

$$\frac{(u_2 - u_1)}{(u_4 - u_3)} = \frac{\log(z_2 - d) - \log(z_1 - d)}{\log(z_4 - d) - \log(z_3 - d)} \qquad \text{.....(7)}$$

A similar equation in terms of vapour pressure necessarily follows from(3), since in deriving (2) and (3) it is assumed that the transport of vapour and momentum follow the same law.

During the observations of 23/3/49 the vegetation consisted of grass and young clover 1-2 cm. high as a basic cover, with frequent patches 5-10 cm. and occasional grass stalks 10-20 cm. By 12/4/49 the basic cover was 1-5 cm., frequent patches about 10 cm. and occasional stalks 15-20 cm. Preliminary evaluation of S in equation (5) indicated that Observations 3, 6 and 9-15 could be included in a suitable near-adiabatic category and could therefore be employed in evaluating 'd' from equation (7) and the corresponding equation in terms of vapour pressure. The values have been computed for the lower(50-25 and 150-37½) and higher (200-100 and 150-37½) pairs of intervals, and are reproduced in Table 3 below.

/Table 3

Table 3. Zero point displacement 'd' in wind velocity and vapour pressure profiles.

(Values from vapour pressure profiles in brackets)

Observation Number	'd' in cm.	
	Lower Intervals	Higher Intervals
3	8 (9)	7 (10)
6	11 (6)	0 (12)
9 - 15	16 (2)	0 (4)

The values for Observation 3, though slightly higher than might have been expected, are mutually consistent. In the remaining cases, however, the wide variations indicate considerable deviation from the logarithmic form of profile, particularly in the case of wind velocity. This is also immediately evident from a graphical examination of the wind profiles; for Observations 6, 9-15 and 25 cm. wind velocity seems unduly low compared with the rest of the profile. It seems probable that this is a chance effect due to the rather patchy vegetation cover, a feature which will be discussed later. For immediate purposes it appears that little reliance can be placed on the individual values of 'd' given above. The most consistent value (Observation No.3) and the visual impressions of the grass cover suggest that 'd' should be somewhat below 10 cm. Fortunately a variation of a few cm. at this range is of little practical importance in considering profiles over the height range involved here and it is therefore proposed to adopt a round value of 5 cm. The agreement then obtained with the observed wind velocity profiles is illustrated in Fig. 2. where it will be seen that the only important discrepancy occurs at the 25 cm. point in Observations 6, 9-15.

The final values of the parameter S are given in Table 2 for each of the three height intervals and on the basis of these we may finally select the cases in which it is appropriate to make comparison with equation (3). From the earlier investigation it follows that a suitable near-adiabatic category is specified by $S \leqslant 0.004$ numerically. This category, it will be seen, includes practically all the results from Observations 6 - 15 and a proportion of those from Observations 1 -5. For these cases the ratios of the computed to the observed rate of evaporation (E_c/E_o) have been evaluated and the results are summarised in Table 4 below. To these have been added the corresponding results from the earlier investigation. As an indication of the surface roughness the adopted values of d and the appropriate values of z_o (from equation (6)) are also given. For the present series z_o was evaluated from a $u_{150}/u_{37.5}$ wind ratio of 1.36, the actual values for Observations 3 and 6 - 15 being respectively 1.38 and 1.34. The lower value for Observations 6 - 15, as compared with that for Observation 3, implies a lower degree of surface roughness, despite the rather longer grass actually occurring during Observations 6 - 15. It is to be noted however that the wind velocities were considerably higher during Observations 6 - 15 than during Observation 3. A similar effect has been observed previously by Deacon (1949) in much greater detail, and has been ascribed to an effective smoothing of the surface due to deflection of the grass blades in high wind velocities.

/Table 4.

Table 4. Ratio of computed (E_c) to observed (E_o) rate of evaporation in near-adiabatic conditions

(a) $z_2 = 200$, $z_1 = 100$ cm.,
(b) $z_2 = 150$, $z_1 = 37.5$ cm.,
(c) $z_2 = 50$, $z_1 = 25$ cm.

Series	Obs. Number	u cm/sec	E_c/E_o (a)	(b)	(c)
March April 1949 (present obs.) d = 5 cm. z_o = 0.51 cm.	2	330			0.89
	3	295	0.64	0.68	0.79
	6	859	0.69	0.72	0.83
	9	579	0.81	0.78	1.03
	10	621		0.91	1.13
	11	707		0.96	1.17
	12	713	1.00	1.00	1.22
	13	702	1.06	0.96	1.25
	14	617	0.85	0.90	1.27
	15	592	0.97	0.81	1.09
March 1948. d = 0 z_o = 0.25 cm.	18	422	0.82	0.83	1.01
	21	479			1.24
	22	490		1.21	1.20
	24	522			1.11
	25	570			1.43
	26	525		1.12	1.11
	27	376	1.24	1.11	
	29	781		0.86	0.86
	30	654		0.86	

The above data present a total of 41 comparisons of observed and estimated rate of evaporation over periods of approximately one hour, based on 19 sets of measurements of rate of evaporation and covering a wind velocity range of 3 - 9 m/sec. Summarising:

Arithmetic Mean $E_c/E_o = 0.99$

Deviation of E_c/E_o from 1.0	% age of cases
< 0.1	24
< 0.2	66
< 0.3	90

/These

These deviations seem to be mainly casual in nature, the only systematic trend being in the generally higher order of the present values of E_c/E_o based on the 50 - 25 cm. interval as compared with those based on the higher intervals. This is obviously associated with the previously discussed wind profile distortion.

It will be noted that the data of Table 2 include a number of cases in which the magnitude of the parameter S falls outside the range adopted for effectively adiabatic conditions. The cases are in themselves too few to merit detailed discussion, though it has been verified that the evaporation - profile relationship exhibited is broadly consistent with that found in the earlier investigation in which greater deviations from adiabaticity were encountered. An exception occurs in the case of Observation 5 where in stable conditions (S positive) the observed evaporation and vapour pressure difference are of mutually inconsistent signs, implying a transport of vapour against a gradient. It is doubtful, however that any significance can be attached to this isolated case, particularly in view of the low orders of magnitude of the observed quantities.

5. Reliability of the evaporation - profile relationship.

In appraising the ultimate reliability of the preceding results it is important to consider the extent to which the deviations exhibited may in fact be attributed to deficiencies in the observational data, rather than to some genuine departure from the implied fundamental relationship. In testing this relationship we are employing data on evaporation, wind velocity and vapour pressure profiles appropriate to various "samples" of the atmosphere and ground. Apart from instrumental error, the various samples taken may not be mutually representative, owing to local variations of rate of evaporation and surface drag arising from the patchy nature of the ground surface.

To provide some quantitative indication of the resulting deviations observations of wind velocities at 100 and 25 cm. and of wet bulb temperature difference over this height interval were carried out simultaneously at three adjacent positions. The temperature installations were approximately 1 foot apart across wind, the anemometer installations approximately 2 m. apart, the wider separation in the latter case being necessary owing to the forms of the supporting masts employed. Table 5 below summarises the data, each value being a mean for two 10 minute observations, for the second of which the anemometers and psychrometers were interchanged over each height interval. The temperature difference readings were taken at 1 minute intervals. The grass cover was similar to that occurring during the main series of observations, though somewhat less patchy owing to subsequent grazing.

Table 5. Wind velocities and vapour pressure differences at three closely adjacent sites.

11/5/49 Cloud: 1 - 3/10 small Cu.

G.M.T.	u_{100} cm/sec.			u_{25} cm/sec.			Wet bulb Temp. differences, (100 - 25) cm., in °F.		
1147 - 1217							-1.46	-1.55	-1.48
1230 - 1250	417	421	423	279	281	267			
1310 - 1340	432	432	427	291	295	275	-1.40	-1.47	-1.38
1353 - 1413	482	468	483	329	335	311			
1505 - 1535	405	409	407	271	283	267	-0.90	-0.94	-0.88
1548 - 1608	357	360	365	239	241	231			

The wind velocities exhibit a variation which, as would be expected, is the more pronounced at the lower level. An examination of the component runs, with

/the

the anemometers in opposite orders vertically, shows the same variation fairly consistently, suggesting that these variations are for the most part genuine and not due to instrumental error. For the wet bulb temperature differences a spatial variation is also indicated, though it seemed possible that this could be a spurious effect due to the fact that a less complete sample is provided by temperature readings at minute intervals than by the continuous anemometer runs. To test this, readings were carried out at intervals of 10 seconds over 20 minute intervals intermediate with those specified in the table, and the standard deviation of the various possible means based on one minute intervals of reading evaluated in terms of the overall mean. The standard deviations were 0.01 or 0.2° F, suggesting that the variations shown in Table 5 are to some extent genuine spatial variations.

Now in the conditions of these measurements and of the majority of those considered in the main analysis the vapour pressure difference depends primarily on the first term of equation (1) and hence on the wet bulb temperature difference. It was therefore possible to infer that the above variations in wet bulb temperature difference correspond to a variation in vapour pressure of up to ± 0.02 mm. Hg. in a magnitude of about 0.5 mm. Hg., i.e. about $\pm 4\%$. The wind velocity differences over the height interval likewise show a variation of the order of ± 10 cm/sec. in about 140 cm/sec., i.e. about $\pm 7\%$ variation. Thus the rates of evaporation based on equation (3) and using values of $(u_2 - u_1)$ and $(e_1 - e_2)$ at a single position could vary by as much as $\pm 10\%$. Remembering that there is also likely to be a casual error in the observed rates of evaporation, but of a magnitude which it is not possible to specify from the present data, it is seen that deviations such as those found in the values of E_c/E_o are to be expected. It is also evident that wind velocity deviations of the above order would explain the apparent distortion at the bottom of the wind profiles in Observations 6, 9 -15, (see Fig.2).

The average value obtained for E_c/E_o (0.99) implies excellent agreement between the present observations and a semi-theoretical treatment based on well established laboratory laws for flow over a rough surface. We have to remember, however, that it has not been possible to justify the technique of evaporation measurement completely on a priori grounds, though as far as can be judged from the results discussed in section 3 it seems likely that any systematic error could only be in the form of an underestimate. On the other hand the semi-theoretical treatment, on which the computed values are based, has been shown independently to be in good agreement with the observed diffusion of artificially liberated smoke and vapour (Calder, 1949). Taken as a whole these features strongly suggest that both observed and computed values are good approximations to the actual rate of evaporation. The practical implication, therefore, is that for surfaces covered with grass up to moderate lengths, and in near-adiabatic conditions of air flow, evaporation over short periods (about one hour) may be estimated from measurements of wind velocity at three heights and vapour pressure at two heights, with a high degree of accuracy on the average. Errors in individual estimations (excepting occasions of very low rates of evaporation) may be expected to be less than those implied by the deviations shown by E_c/E_o, since some part of these is undoubtedly due to casual deviation in the values of E_o. Thus, for example, we could expect errors less than $\pm 20\%$ on more than 70% of occasions.

In conclusion it is of interest to consider briefly the validity and practicability of applying the present semi-theoretical method to the estimation of evaporation (including transpiration) from areas of crops. It is to be noted that the aerodynamic law expressed in equation (6) was generally established in the laboratory for flow over flat plates bearing roughness elements of different sizes, shapes and dispositions (Schlichting, 1936). Aerodynamically the only difference between a surface bearing grass and one bearing crops is a difference in the roughness elements and indeed it has been verified (Paescke, 1937) that, in functional form at any rate, equation (6) holds over such a wide variety of surfaces as is presented by snow, fallow land, grass, wheat and turnips. Thus there is no a priori reason why the present method of estimating natural rate of evaporation should not be applied, with equal confidence, to a cropped surface. The only obvious difficulties would appear to lie in the satisfactory specification of the vertical profiles of wind velocity and vapour pressure and it is clear that an exhaustive investigation of such features would be required. For example, measurements at conveniently accessible heights over tall crops would require careful interpretation as regards the 'zero point displacement'. Crops of large

/individual

individual size and spacing will presumably impose a pattern on the wind velocity and vapour pressure fields, so that the representative value of measurements at a single site would need to be carefully investigated. In considering areas of small extent there is the problem of ensuring that the profiles observed are truly representative of the immediate surface. Finally, in the latter connection, it is clear that for small areas, and at the upwind edges of larger areas, there will be a progressive development of the profiles as the air flows over the surface, so that some doubt then exists as to the validity of a treatment which assumes horizontally uniform conditions.

Acknowledgement.

Acknowledgement is made to Mr. F.J. Anscombe of the Statistical Laboratory, Cambridge University for advice and assistance in the statistical design and analysis of the evaporation measurements.

References.

Calder, K.L., 1949, Quart. J. Mech. Appl. Math., London.
Deacon, E.L., 1949, Quart. J.R. Met. Soc., London, 75, p.89.
Paeschke, W., 1937, Beitr. Phys. frei. Atmos., Leipzig, 24, p.163.
Pasquill, F., 1949, (a) Proc. Roy. Soc., London, in press.
(b) Quart. J.R. Met. Soc., London, in press.
Schlichting, H., 1936, Ingenieur, Archiv., 7, 1.

Table 2. Profile

Group	E				
Date	23/3/49				
Observation Number	1	2	3	4	5
G.M.T.*	1330	1430	1530	1730	18
Wind direction	ESE	ESE	ESE	ESE	ESE
Cloud	6/10 Cu.	7/10 Cu.	4/10 Cu.	1/10 Ac.	1/10
Wind velocity in cm/sec. at hts. in cm. 200	351	330	295	265	18
150	328	309	275	243	16
100	311	293	259	222	14
50	259	243	211	179	10
37½	244	227	199	165	9
25	205	193	167	139	7
Vapour pressure differences in mm. Hg. for intervals in cm. 200-100	-0.25	-0.21	-0.17	-0.09	+0
150-37½	-0.55	-0.45	-0.37	-0.15	+0
50-25	-0.31	-0.29	-0.22	-0.07	+0
Temperature differences in °F for intervals in cm. 200-100	-0.44	-0.27	-0.05	+0.64	+1
150-37½	-1.00	-0.59	-0.06	+1.20	+2
50-25	-0.55	-0.33	-0.02	+0.54	+1
Temperature °F at 200 cm.	54.3	56.1	55.7	53.0	4
Observed rate of evaporation gm/cm² sec.	0.60	0.40	0.30	0.12	0
S for intervals in cm. ✓ 200-100	-0.027	-0.019	-0.004	+0.034	+0
150-37½	-0.015	-0.009	-0.001	+0.020	+0
50-25	-0.005	-0.003	0.000	+0.008	+0

* Mid-time of observation

✓ S approximates to half t

G.239965/MBF/8/49/40.

Table 2. Profile and Evaporation Data.

Group		E					F							
Date		23/3/49					12/4/49	13/4/49						
Observation Number		1	2	3	4	5	6	9	10	11	12	13	14	15
G.M.T.*		1330	1430	1530	1730	1830	1130	1000	1100	1200	1300	1400	1530	1630
Wind direction		ESE	ESE	ESE	ESE	ESE	WSW	W	W	W	W	W	WSW	WSW
Cloud		6/10 Cu.	7/10 Cu.	4/10 Cu.	1/10 Ac.	1/10 Ac.	5/10 Sc 9/10 Ac.	9/10 Sc.	5/10 Sc.	5/10 Sc.	5/10 Sc.	2/10 Cu.	1/10 Cu.	4/10 Sc.
Wind velocity in cm/sec. at hts. in cm.	200	351	330	295	265	189	859	579	621	707	713	702	617	592
	150	328	309	275	243	167	807	543	582	665	672	658	579	553
	100	311	293	259	222	146	757	507	549	625	625	619	546	520
	50	259	243	211	179	108	640	430	461	526	535	525	462	435
	$37\frac{1}{2}$	244	227	199	165	95	601	401	434	499	497	492	435	411
	25	205	193	167	139	77	513	325	353	405	414	401	349	326
Vapour pressure differences in mm. Hg. for intervals in cm.	200-100	-0.25	-0.21	-0.17	-0.09	+0.05	-0.14	-0.18	-0.27	-0.30	-0.23	-0.26	-0.21	-0.17
	$150-37\frac{1}{2}$	-0.55	-0.45	-0.37	-0.15	+0.12	-0.31	-0.38	-0.58	-0.61	-0.50	-0.51	-0.47	-0.31
	50-25	-0.31	-0.29	-0.22	-0.07	+0.07	-0.17	-0.20	-0.29	-0.30	-0.26	-0.26	-0.25	-0.16
Temperature differences in °F for intervals in cm.	200-100	-0.44	-0.27	-0.05	+0.64	+1.58	-0.27	-0.18	-0.44	-0.44	-0.23	-0.23	-0.11	+0.12
	$150-37\frac{1}{2}$	-1.00	-0.59	-0.06	+1.20	+2.95	-0.46	-0.39	-0.92	-0.96	-0.46	-0.48	-0.21	+0.25
	50-25	-0.55	-0.33	-0.02	+0.54	+1.25	-0.23	-0.20	-0.49	-0.51	-0.25	-0.25	-0.12	+0.13
Temperature °F at 200 cm.		54.3	56.1	55.7	53.0	49.1	58.9	55.2	57.2	58.9	59.7	61.1	61.9	61.5
Observed rate of evaporation gm/cm^2 sec.		0.60	0.40	0.30	0.12	0.02	0.64	0.50	0.68	0.76	0.63	0.63	0.54	0.39
S for intervals in cm. /	200-100	-0.027	-0.019	-0.004	+0.034	+0.084	-0.003	-0.003	-0.008	-0.006	-0.003	-0.003	-0.002	+0.002
	$150-37\frac{1}{2}$	-0.015	-0.009	-0.001	+0.020	+0.058	-0.001	-0.002	-0.004	-0.004	-0.002	-0.002	-0.001	+0.001
	50-25	-0.005	-0.003	0.000	+0.008	+0.032	0.000	0.000	-0.001	-0.001	0.000	0.000	0.000	0.000

* Mid-time of observation period of approximately 1 hour.

/ S approximates to half the Richardson Number at the geometric mean height (see equation (5)).

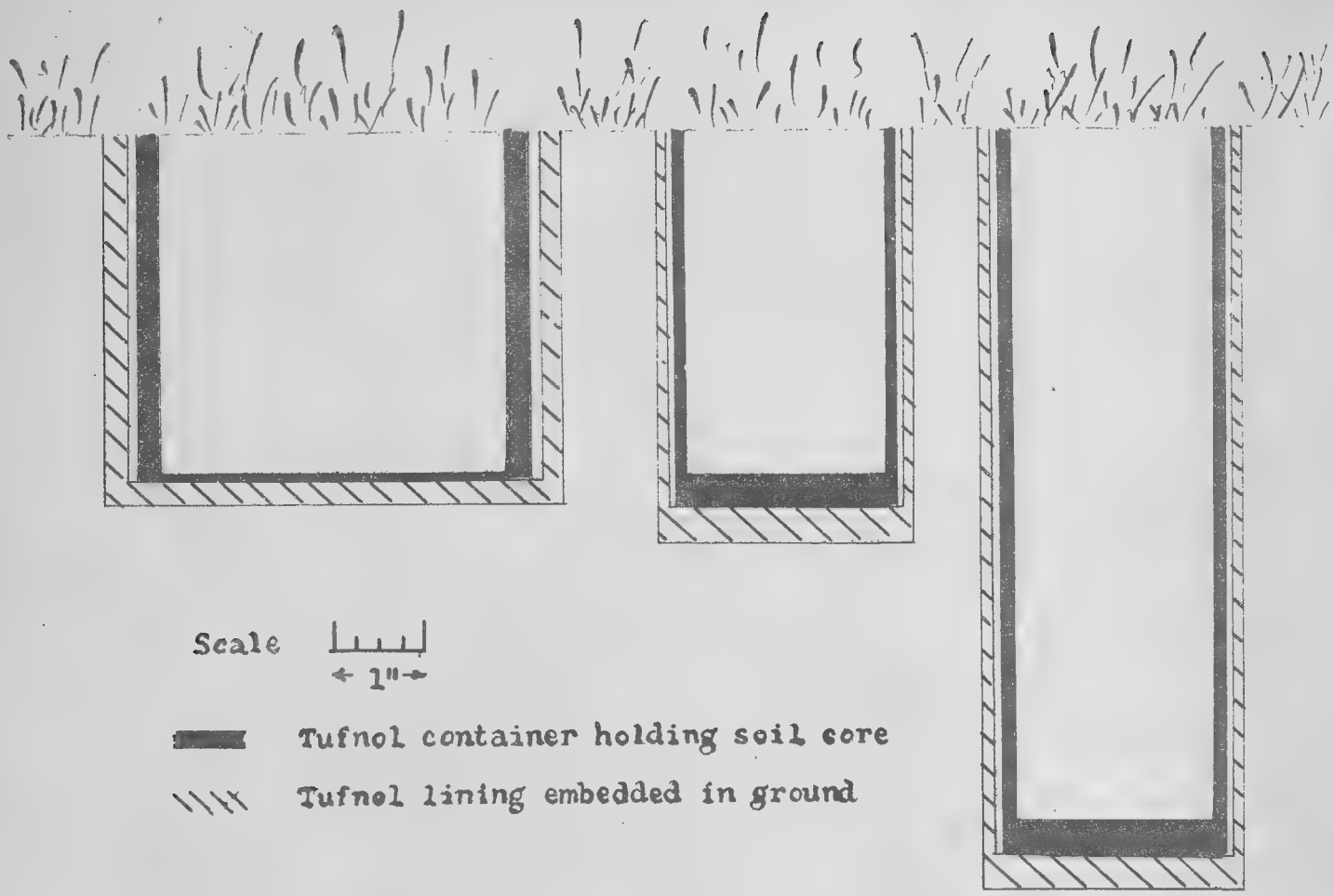

FIG.1(a)SOIL EVAPORIMETERS

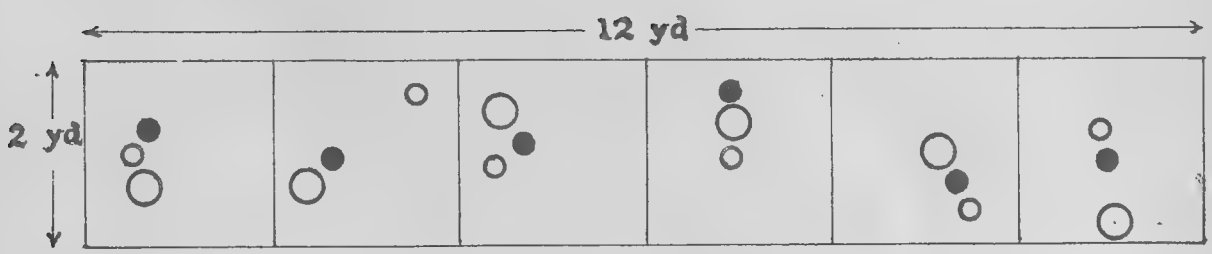

● indicates evaporimeter of 8" depth.

FIG.1(b). APPROXIMATE DISPOSITION OF EVAPORIMETERS
(22.3.49)

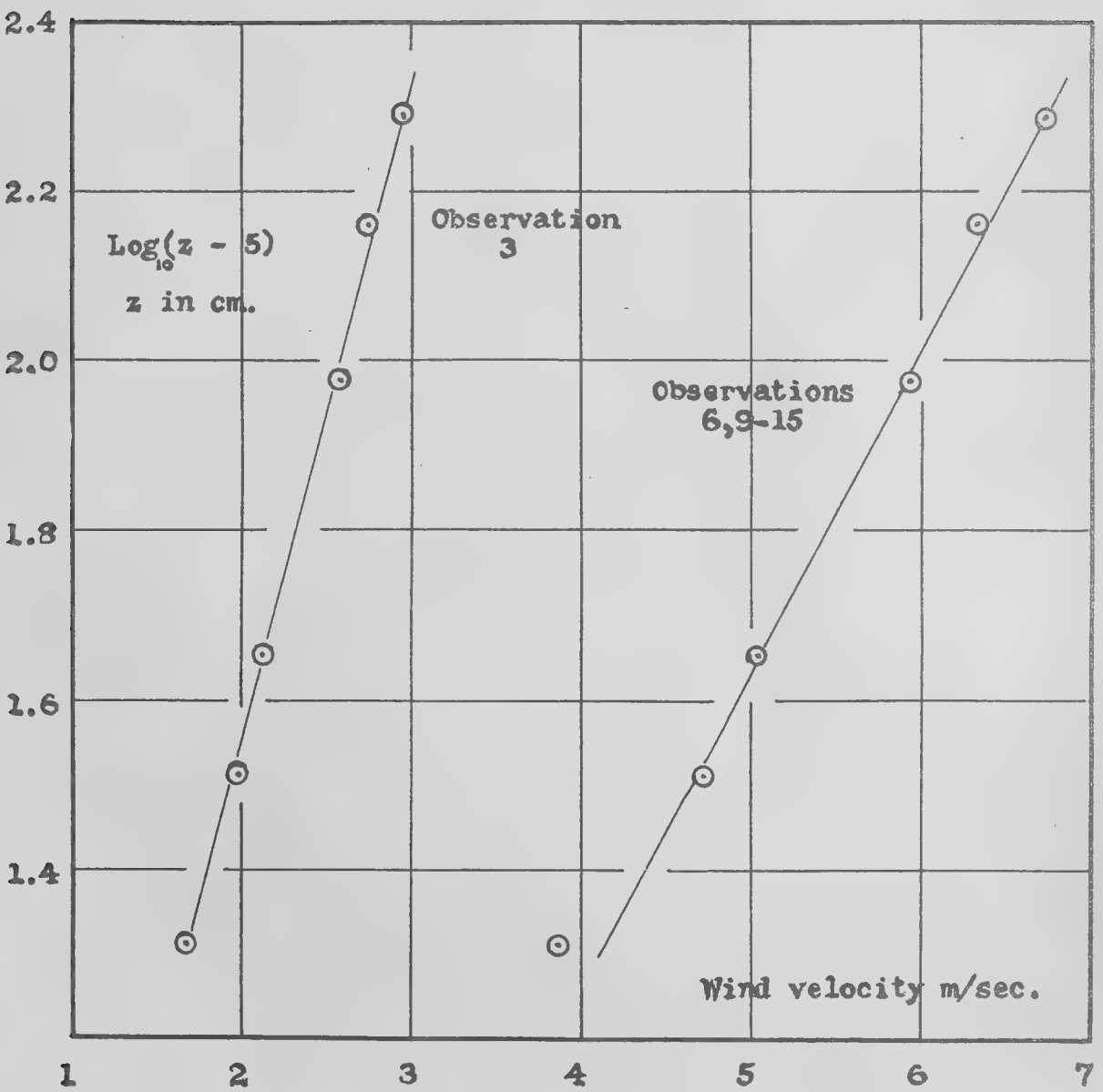

FIG.2. VERTICAL PROFILES OF WIND VELOCITY OVER GRASSLAND

Its ... must not be quoted.

M.R.P. 499
S.C.I./25
10th August, 1949.

AIR MINISTRY

METEOROLOGICAL RESEARCH COMMITTEE

AIR WEATHER SERVICE
TECHNICAL REFERENCE FILE

The Wilson Cloud Chamber as a Hygrometer

by

H.P. Palmer

(a) Introduction

The frost-point hygrometer as developed at Oxford and by the Meteorological Research Flight, is the most accurate and convenient method of measuring the water-content of the upper troposphere and lower stratosphere. Its principal disadvantage, which may become important if the instrument is used in an aircraft with a higher ceiling than the Mosquito, is that the water-content cannot be measured if the frost-point is below about -85°C. Below this temperature the water vapour is deposited on the thimble as a glassy layer which is invisible under the best conditions of illumination, though it might be detected by optical interference phenomena. It has been suggested that a Wilson cloud chamber could be used as a hygrometer, and that a cloud formed by an expansion might still be visible even at temperatures below -85°C when the vapour would be deposited on a surface as a glassy layer.

The expansion ratio required to form a cloud will depend on the water-content of the air, and the temperature of the chamber. A hygrometer could be constructed in the form of a cloud chamber in which the initial temperature of the air and the expansion required to form a cloud could be measured, provided firstly that the first trace of cloud formation can be detected and also provided that the air is not contaminated with water-vapour from the walls of the chamber. As regards detection of the first formation of cloud it may be noted that at low temperatures no trace of cloud would be expected until the air temperature fell to the dew point, but at this temperature numerous ice particles would be formed. These being in supersaturated air (i.e. air saturated with respect to water) would grow rapidly. This would greatly increase the visibility of the cloud. This paper reports experiments to examine these points, and it is concluded that below -80°C the cloud is so thin that it is invisible, and therefore such an instrument would be as useless as the frost-point hygrometer in the glassy ice region below -85°C.

(b) Apparatus

The apparatus used for these experiments was similar to that used to examine the condensation processes on ions at low temperatures, described in M.R.P. 492. The cloud chamber consisted of a closed glass tube, connected to a trap and bellows system by which expansions up to a volume ratio of 1.4 could be made. The chamber and trap could be cooled by surrounding them with cold alcohol in Dewar vessels.

A small volume at the bottom of the chamber was illuminated by light from a high pressure mercury arc which had passed through the alcohol and through a filter absorbing ultra-violet light. The method of observation was to view the illuminated volume through a glass plate waxed to the top of the chamber. The dark background was provided by a cone-and-cylinder black-body placed at the bottom of the chamber.

The air could be dried by passing it through a spiral of copper tube and a cotton wool filter both immersed in a bath of solid carbon dioxide and alcohol. Nuclei could be introduced into the dry air by passing a spark between aluminium points. At ordinary temperatures these nuclei cause condensation when the relative humidity reaches 100% relative to water, whether the condensation product be ice or water.

/(c)

(c) Procedure and Results

The drying spiral was placed in a mixture of dry ice and alcohol, at a temperature of -78°C. The trap was also cooled to this temperature. The chamber was pumped dry on a high vacuum system, and was ventilated with dry air for some hours. Immediately after ventilation was stopped, with the chamber at -70°C, no visible cloud could be formed with the largest expansions, and with final temperatures well below -78°C. After a few minutes however, even small expansions produced a faint cloud of numerous particles, and from the expansion required to form the cloud it could be calculated that the frost-point of the air was the same as the temperature of the walls of the chamber, although these had been well dried. When the chamber was cooled to -78°C no visible cloud could be formed at all. It is thought that in the earlier experiment, immediately after the chamber had been ventilated, the frost-point was -78°C. and that any cloud formed was so thin as to be invisible. In the next few minutes the air picked up water vapour from the walls of the chamber, until a frost-point of -70°C. was reached (this represents a three-fold increase of water-content) and that then the cloud was just visible.

(d) Conclusion

The important result is that with this apparatus no cloud could be seen at a temperature of -78°C. although the illumination conditions were very good. As the water-content is reduced by a further factor of three as the temperature falls to -85°C. it is most improbable that any cloud formed below this temperature could be detected. The experiments also make it clear that even carefully dried glass vessels contaminate dry air with water vapour quite quickly at these low temperatures.

LOW TEMPERATURE CLOUD CHAMBER USED AS A HYGROMETER.

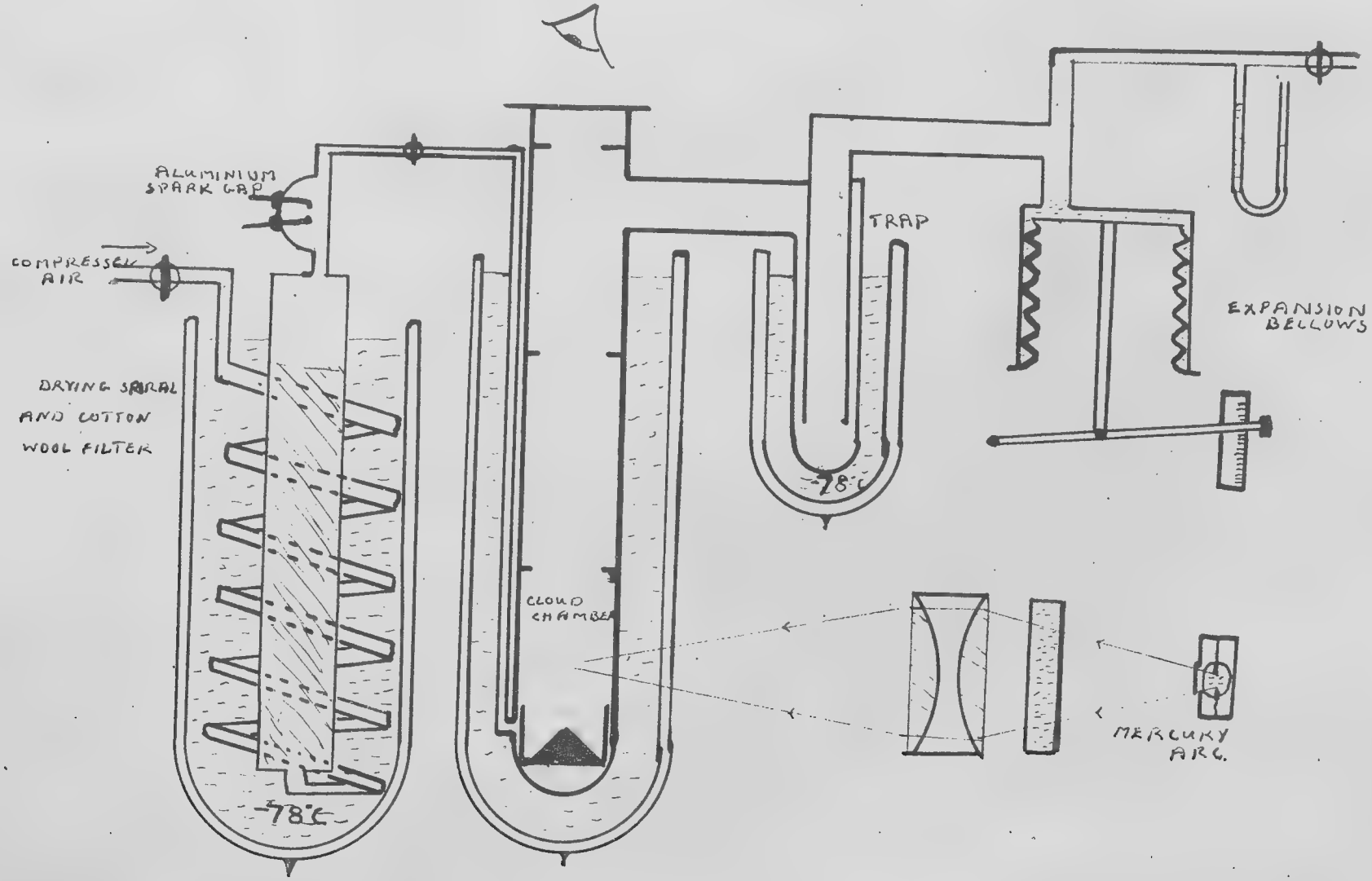

This report ... to be quoted.

M.R.P. 503.
S.C.III/39
18th August, 1949.

AIR MINISTRY

METEOROLOGICAL RESEARCH COMMITTEE.

AN APPROXIMATE MEASUREMENT OF THE AERODYNAMIC DRAG OF GRASSLAND.

by

AIR WEATHER SERVICE
TECHNICAL REFERENCE FILES

F. Pasquill

Summary

An improvised drag-plate apparatus, on the principle of that used by Sheppard (1947) on a concrete surface, but suitably modified in design, has been used for exploratory measurements of the aerodynamic drag of grassland. The grass cover was variable (1 - 15 cm. in height) and measurements were made at a number of positions (not simultaneously) in order to obtain an approximate representative value of the drag over a considerable area. Wind velocities were in the region of 5 m./sec. and, judged in terms of the Richardson Number, effectively adiabatic conditions of flow prevailed.

The drag (τ_o) and the simultaneous vertical distribution of wind velocity (u) up to a height of 2 m. were found to be expressible in terms of the law well established in the laboratory, i.e.

$$u = \frac{1}{k}\sqrt{\frac{\tau_o}{\rho}} \log_e \frac{z - d}{z_o}$$

with k (von Kármán's constant) = 0.37, d (the zero point displacement) = 8 cm. and z_o (the roughness parameter) = 0.66.

For reasons which are discussed the drag measurements are regarded as approximate and the agreement of the numerical value of k with the laboratory value of 0.4 is probably fortuitous. However the general consistency achieved in this preliminary application suggests that the technique could be profitably developed for a critical investigation of the natural drag - wind profile relationship and its dependence on atmospheric stability.

1. Introduction.

The relation between the drag of a surface and the distribution of fluid velocity in the boundary layer is fundamental in problems of turbulent motion and, for example, plays an important part in treatments of turbulent diffusion in the lower atmosphere. Experimental researches by Nikuradse (1933) and Schlichting (1936) on flow through pipes and over flat plates with artificially roughened surfaces have established the following law, written here in the form customary in meteorological application,

$$u_z = \frac{1}{k}\sqrt{\frac{\tau_o}{\rho}} \log_e \frac{z - d}{z_o} \qquad \ldots\ldots\ldots\ldots\ldots\ldots (1)$$

/In

In this expression

u_z = fluid velocity at a distance z from the pipe wall or plate, measured from the base of the roughness elements,

τ_o = shearing stress per unit area of the pipe wall or plate,

ρ = fluid density,

d = a "zero point displacement" associated with the finite size of the roughness elements,

z_o = a constant for each type of roughness, in meteorological application termed the roughness parameter,

k = a dimensionless constant = 0.4.

An equation of this form has been derived by Prandtl and von Kármán on theoretical grounds (see Brunt, 1939, p.244-247) and the constant k is usually called von Kármán's constant.

The above equation was first applied to the distribution of mean wind velocity near the earth's surface, in adiabatic conditions of flow, by Prandtl (1932), but while the functional form of the equation has since been widely observed to hold in such conditions (see Deacon, 1949), the only direct evidence for its explicit validity is that obtained by Sheppard (1947). Sheppard measured the drag exerted by the wind on a horizontal plate, floating in oil, under torsional control, and exposed in such a fashion as to effectively form part of an extensive concrete area of smoothness approximating to that of the floating plate. From simultaneous measurements of the vertical wind profile over the concrete surface Sheppard demonstrated that equation (1) held, with k = 0.46, a value which, in view of the unstable atmospheric stratification then existing, was considered to be in good agreement with that obtained in the laboratory.

The assumption of the explicit validity of the above law for adiabatic flow, i.e. flow with negligible vertical gradient of potential temperature, over grassland, with also the assumption that the eddy diffusivities for momentum and matter are identical, has been indirectly justified by recent satisfactory interpretations of data on the dispersal of smoke and vapour from artificial ground level sources (Calder, 1949) and of observations on the transport and distribution of natural water vapour (Pasquill, a, 1949). However, direct observations of the relation between surface drag and wind profile, and of the influence thereon of the thermal stratification of the atmosphere, have yet to be made over a natural vegetated surface. The present note describes some preliminary measurements, on grassland, which are possibly of interest in providing an approximate test of equation (1) and in indicating the practicability of a more searching investigation.

2. Instrumental Details and Field Technique.

The somewhat improvised apparatus used for the measurement of drag was built on the principle of Sheppard's drag-plate, with certain modifications of design to suit the application to a grassland surface. It consists of an aluminium pan floating in water in a slightly larger pan (see Fig.1). In field operation the floating pan contains a close fitting sample of the actual grassland surface and the outer pan is embedded in the ground at the original position of the sample, so that the floating element of ground is exposed approximately in its natural state. Horizontal movement of the floating pan under the action of wind drag is controlled by a flexible metal strip (actually a pen arm of the type used in a barograph) which is attached to one side of the pan and rigidly held in a small clamping block at its other end. Deflection of the pan is indicated by a long pointer attached to the opposite side of the pan. The control strip and pointer are shielded from the wind by slender cases attached to the outer fixed pan. Adjustment of the height and level of the floating pan is made by altering the quantity and positions of brass weights carried on a frame attached to

the under side of the pan and, if necessary, by altering the quantity of water in the outer pan. This adjustment is made with the control strip unclamped; the latter is subsequently carefully clamped, there then being no resultant vertical force operating on the control strip.

Calibration of the apparatus was carried out in the laboratory by placing small weights in a light paper pan attached to the centre of the floating pan by a hair passing over a light pulley. The relation between the horizontal force so applied normal to the axis of symmetry of the drag-plate assembly and the deflection of the pointer was found to be linear within satisfactory limits for a movement of the floating pan over a distance of about 3/16 inch on either side of the central position, as would be expected in view of the small displacements involved. With the shorter control strip (see Fig. 1), as used in the measurements discussed here, the corresponding overall movement of the pointer approximately 2 inches. Outside this range the linear relation was distorted by surface tension action in the then narrow gap between the two pans. All subsequent measurements were contained within the range of linear response. Calibrations carried out after dismantling and re-assembly of the apparatus showed an extreme variation of ±3% in the force/deflection ratio. This degree of reproducibility was probably as good as could be expected from the rather crude mechanical features of the apparatus and was quite acceptable for the preliminary measurements envisaged. Damping of the movement of the plate, effected by a small metal vane carried on the pointer and dipping in an oil bath, was adjusted until critical damping was achieved.

With the shorter control strip a pointer deflection of 1 inch was produced by a force corresponding to 3.0 dynes/cm^2 over the whole horizontal area of the floating pan, acting normal to the axis of symmetry of the apparatus, and full response to an applied force was obtained in approximately 15 seconds.

In field operation the drag-plate assembly was set up with its axis of symmetry across wind. The horizontal force acting at the centre of the floating plate, normal to the axis of symmetry, is then $\tau_o A \sin\theta$ where A is the area of the floating plate and θ is the angle between the wind direction and the axis of symmetry. A light vane for recording wind direction, a portable distant-reading temperature gradient assembly (described elsewhere, Pasquill, b, 1949) and masts carrying sensitive cup anemometers were set up close to and crosswind of the drag-plate.

Each series of observations was maintained over a period of 10 minutes. During this period readings of the drag-plate pointer were taken every 5 seconds by an observer lying on the ground on the crosswind side of the apparatus, so as to impose as little as possible disturbance on the air flow. As anticipated the drag-plate deflections showed considerable fluctuations, though no difficulty was experienced in taking precise readings at the above rate. Before and after each series a draught-proof cover was placed over the drag-plate and zero readings taken. The drag-plate deflections were mainly in the region of 0.5 inch, occasionally 1 inch or more, and were read to 0.01 inch. Anemometers were operated simultaneously at heights of 200, 150, 100, 50, 37½, 25 cm. and in consecutive runs were interchanged over the levels 200-100, 150-37½, 50-25 cm. The temperature profile was observed over the same height range but only the differences over the interval 150-37½ cm. and the absolute value at 2 m. are employed here. Two three-minute records of wind direction were taken, centred on 2½ and 7½ minutes from the beginning of the observation, and from these a mean wind direction was obtained for each half of the observation period. In reducing the drag-plate results the mean deflection for each half of the run was associated with the corresponding mean wind direction.

The site of the measurements was a level, well exposed clayland pasture, with at least 150 yards of similar terrain upwind of the apparatus. The grass cover, however, was variable over distances of the order of yards, and ranged in height from 1 to 15 cm. With a surface non-uniformity on such a scale it was not to be expected that a single siting of the present drag-plate (effective area approximately 250 sq. cm.) would provide a representative

/measure

measure of the drag over a substantial area. The same considerations apply to the vertical wind profile, particularly in the region close to the ground, and indeed previous observations on the same site have demonstrated a local variation of wind distribution. In order therefore to obtain a closer approach to mutually representative drag and wind profile data three adjacent areas were chosen on which the local grass length was mainly 1 - 5 cm., 5 - 10 cm. and 10 - 15 cm., and measurements were carried out with the drag-plate and wind profile apparatus set up at each of these localities in turn. Two ten-minute series of observations were made at each position, the whole process occupying approximately four hours.

3. Discussion of Observations and Results.

The observations are presented in Table 1 in the form of mean values for each ten-minute observation, except for the values of wind direction and θ, which correspond to the two three-minute records of wind direction and are adopted as means for the component five minute periods. The value given for τ_o is the average of the two values based on the mean drag-plate deflections in these five minute periods. Before describing the results ultimately derived from these data it is convenient to summarise at this stage the various limitations imposed by the improvised form of the drag-plate apparatus and the prevailing conditions of ground and weather.

The present drag measurements refer to a small area of ground which had been freed from its surroundings. In so doing an artificial gap was produced between the test area and the undisturbed ground. Although nominally this gap was very small, approximately $\frac{1}{2}$ inch, in practice it was increased somewhat by the trimming of grass around the edges, a procedure which was necessary to avoid mutual interference of trailing grass blades projecting from the fixed and free edges of the gap. Even so, the artificial irregularity so produced was not greatly dissimilar to irregularities occurring naturally. It will be noted that the cases housing the control strip and pointer projected above the soil surface by about 4 cm. Since, however, these spurious obstacles to flow were on the crosswind sides of the drag-plate and were for the most part submerged in the natural roughness elements, it seemed reasonable to accept this convenient arrangement for these preliminary measurements, rather than to complicate the manipulation and adjustment for wind direction by embedding the cases in the ground. The proximity of the observer provided another possible disturbance of flow conditions but as already mentioned this was minimised by the observer lying flat on the ground crosswind of the apparatus. The limitations imposed by the non-uniformity of surface have been stated in the previous section. Finally it should be noted that the derivation of the mean drag in the direction of the wind directly from the mean drag-plate deflection requires that the wind direction should be constant, apart from turbulent fluctuations, over the period of measurement. Most of the individual records showed an acceptably constant wind direction over the three-minute periods involved, though as will be seen from Table 1 the two values obtained in each ten-minute observation differ by as much as 24° in the extreme case. For this reason, and as already mentioned, the drag was evaluated separately for the two component five-minute periods, employing the appropriate values of θ, and averaged to give τ_o.

Turning now to the data presented in Table 1 it is seen that the vertical temperature gradient, as indicated by the temperature differences over the height range 150-37½ cm., varied from a moderate lapse at the beginning to a moderate inversion at the end of the series of observations. It has previously been demonstrated, however, by Deacon (1949), and by the present writer (a, 1949), that the effects of thermal stratification on processes of turbulent transport near the ground are controlled, not by the vertical temperature gradient alone, but by the ratio of the latter to the square of the vertical wind shear, as in the now familiar Richardson Number

$$Ri = \frac{g}{T} \frac{(\partial T/\partial z + \Gamma)}{(\partial u/\partial z)^2} ,$$

/where

where T is in °A, Γ is the dry adiabatic lapse rate, and u is in cm./sec. With high wind speeds and hence, usually, large values of $\partial u/\partial z$, the departure of the above parameter from zero (the value which occurs with zero vertical gradient of potential temperature) may be quite small even with appreciable values of $\partial T/\partial z$. The approximate values of Ri at a height of 75 cm. have been computed for the present cases, assuming a variation of temperature and wind speed with the logarithm of the height, and are reproduced in Table 1. Due to the fairly high wind speeds all values are less than 0.01 numerically, with an algebraic mean of -0.002. These values represent departures from "adiabatic" or "neutral" conditions of flow, which, in terms of the previously mentioned observations of the effect of thermal stratifications, are of a very small order. It is thus considered justifiable to bulk the present series of observations as one sample of drag - wind profile data in effectively adiabatic conditions of flow.

It will be noted that the individual wind profiles, specified in terms of u_z/u_{100} so as to facilitate comparison of the various observations, exhibit considerable variation. Furthermore, graphs of the individual results, not produced here, display some departures from smooth u, log z profiles. These features are thought to be mainly a reflection of genuine local variations in wind distribution, arising from the non-uniformity of surface. On the other hand the magnitudes of $\frac{1}{u_{100}}\sqrt{\frac{\tau_o}{\rho}}$, which might have been expected to exhibit wide variations, are surprisingly constant, though there is an indication of a slight systematic increase with increase in local grass length.

Considering now the mean results for the whole series we may note that the wind velocities show a good approach to a smooth u/log z profile (see Fig. 2, graph (a)) which is, however, slightly concave to the log z axis. This is presumably to be attributed to the existence of a "zero point displacement" (d in equation (1)). Trial plottings for a range of values of 'd' show that the best approach to a linear relationship is obtained with d = 8 cm., a value which seems reasonably in accordance with the description of the grass cover. The profile is plotted in this form in graph (b) of Fig. 2, and from this we have

$$\frac{u_z}{u_{100}} = 0.466 \left\{ \log_{10}(z - 8) + 0.182 \right\} \quad \ldots\ldots\ldots (2)$$

From equation (1)

$$\frac{u_z}{u_{100}} = \frac{2.303}{k u_{100}}\sqrt{\frac{\tau_o}{\rho}} \left\{ \log_{10}(z - d) - \log_{10} z_o \right\} \quad \ldots\ldots (3)$$

/which

which is satisfied by (2) if

$$z_o = 0.66 \text{ cm.},$$

$$\frac{2.303}{k\, u_{100}} \sqrt{\frac{\tau_o}{\rho}} = 0.466 \qquad \ldots\ldots\ldots\ldots (4)$$

From Table I

$$\frac{1}{u_{100}} \sqrt{\frac{\tau_o}{\rho}} = 0.075$$

which with (4) gives

$$k = 0.37$$

to be compared with the laboratory value of 0.4.

In view of the previously discussed limitations of the present measurements the agreement of the observed value of k with that established in the laboratory may be to some extent fortuitous. However, the satisfactory nature of this result and the general success achieved in manipulating the preliminary form of drag-plate give reason to believe that the present apparatus and technique could be profitably developed. With improvements in the design of the drag-plate, especially some increase in scale and further reduction of the various factors possibly contributing to a distortion of air flow, and with a more rigid restriction to uniformity in ground and atmospheric conditions, it seems likely that the drag - wind profile relation could be critically determined and valuable data obtained on the outstanding problem of stability influence.

References

Brunt, D., 1939, Physical and Dynamical Meteorology, Camb. Univ. Press.

Calder, K.L., 1949, Quart. Journ. Mech. & Applied Math., London, 2, Pt. 2, p153.

Deacon, E.L., 1949, Quart, J.R. Met. Soc., London, 75, No. 323, p. 89.

Nikuradse, J., 1933, Forschungsh. Ver. Deutsch, Ing. No. 361.

Pasquill, F., (a) 1949, Proc. Roy. Soc., London, (A), 198, p. 116.
(b) 1949, Quart. J.R. Met. Soc., London, in press.

Prandtl, L., 1932, Beit. Phys. frei Atmos. (Bjerknes Festschrift), 19, p.188.

Schlichting, H., 1936, Ingenieur Archiv., 7, 1.

Sheppard, P.A., 1947, Proc. Roy. Soc., London (A), 188, p. 208.

Table 1. Drag and Wind Profile Results.

(Girton Pasture, University Farm, Cambridge, 28.7.49)

Local Grass Length	G.M.T.	Wind Dirn. (°M) *	θ ∠ (degs.)	u_{100} (cm/sec)	u_z/u_{100} at heights in cm. of 200	150	50	37.5	25	Measured τ_o (dynes/cm.)	Temp. at 200 cm. (°F)	p (mb)	$\rho \times 10^3$ (gm/cc)	$\frac{1}{u_{100}}\sqrt{\frac{\tau_o}{\rho}}$	Temp. Diff. (150-37½cm) (°F)	Ri_{75}
1-5cm.	1345-55	a 270 b 282	82 70	403	1.110	1.065	0.806	0.776	0.640	0.90	72.3	1016	1.20	.068	-0.73	-.011
	1405-15	a 267 b 285	85 67	478	1.155	1.084	0.824	0.778	0.657	1.44	72.7	"	"	.073	-0.84	-.008
5-10cm.	1510-20	a 277 b 281	80 76	483	1.159	1.089	0.834	0.741	0.675	1.53	72.5	"	"	.074	-0.61	-.004
	1530-40	a 238 b 262	61 85	513	1.150	1.084	0.852	0.743	0.678	1.53	73.4	"	"	.070	-0.32	-.002
10-15cm.	1650-00	a 289 b 290	89 88	429	1.124	1.072	0.804	0.758	0.625	1.38	71.9	"	"	.079	+0.73	+.008
	1710-20	a 270 b 277	72 79	440	1.141	1.078	0.843	0.757	0.634	1.59	70.3	"	"	.083	+0.72	+.007
Means				458	1.140	1.079	0.827	0.759	0.651					.075		-.002

* a and b refer to the two separate three-minute records of wind direction.

∠ Angle between wind direction and axis of symmetry of drag-plate assembly.

G.241267(a)/DS/8/49/40.

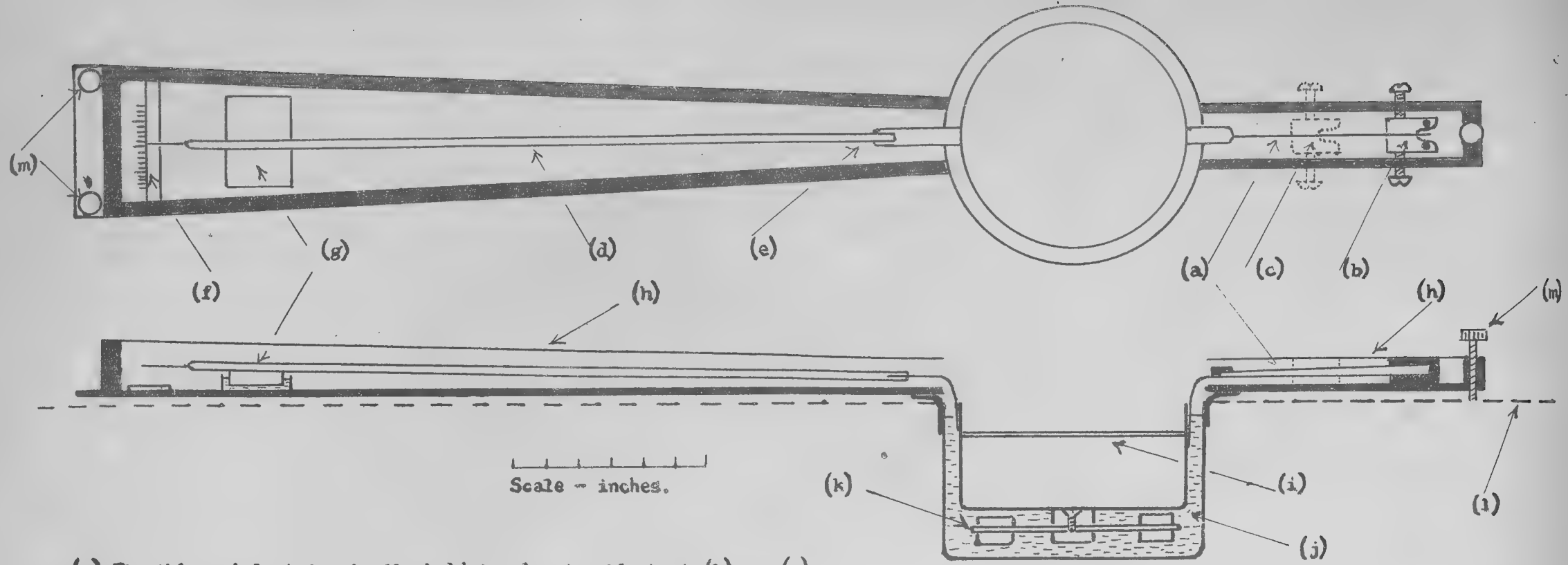

(a) Flexible metal strip rigidly held in clamping block at (b) or (c).
(d) Pointer, with horizontal & vertical adjustment at (e) (not shown).
(f) Scale and mirror.
(g) Oil bath for damping . (h) Wind shielding cases with transparent covers.
(i) False bottom to support ground sample approx. 1" thick.
(j) Water . (k) Adjustable weights for control of height and level of floating pan.
(l) Level of soil surface during field operation . (m) Levelling feet.

FIG. 1. DRAG PLATE — PLAN AND VERTICAL SECTION THROUGH AXIS OF SYMMETRY

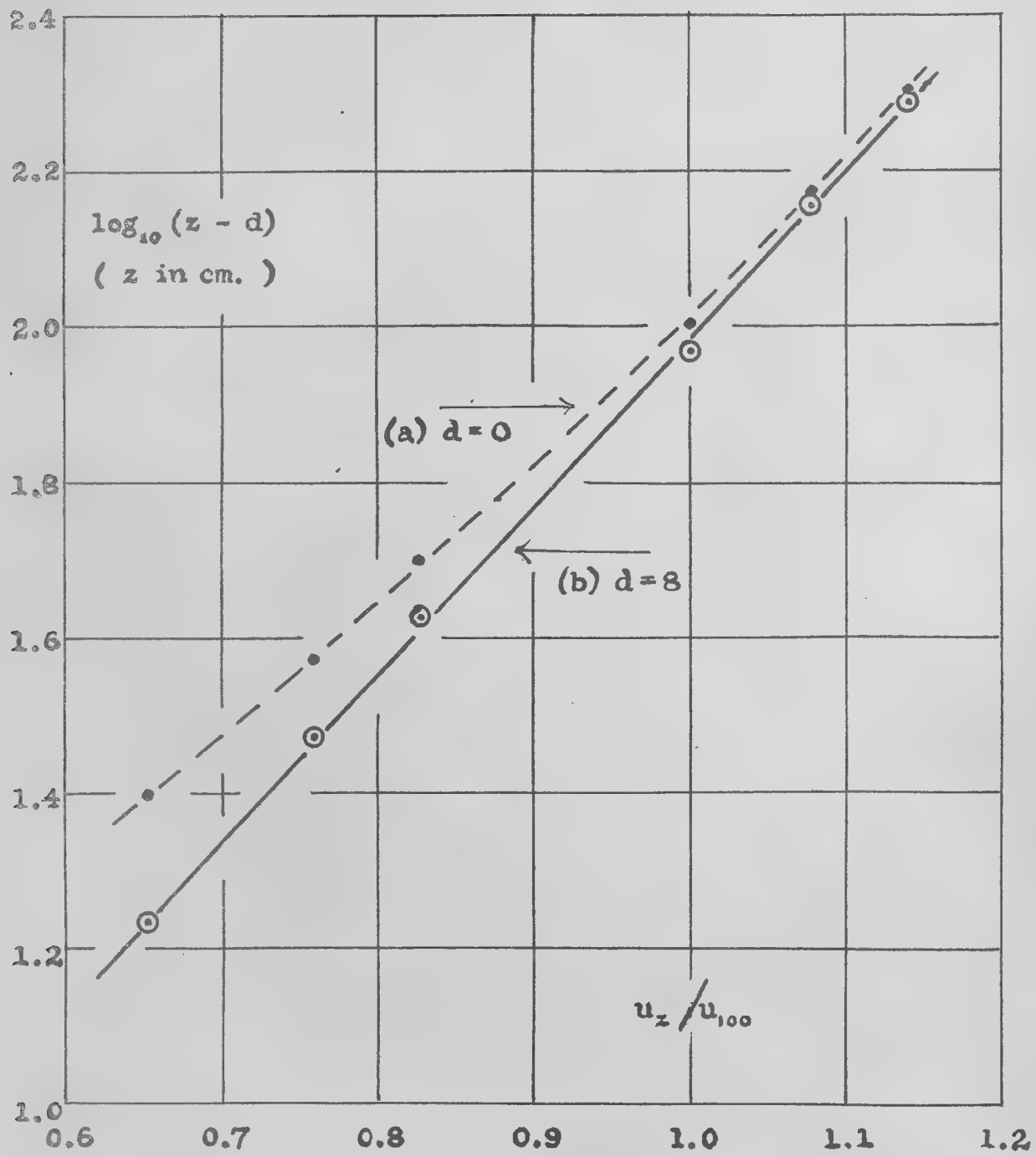

FIG. 2. VELOCITY PROFILE OVER GRASS 1 - 15 cm. HIGH IN EFFECTIVELY ADIABATIC CONDITIONS.

AIR WEATHER SERVICE
TECHNICAL REFERENCE FILE

M.R.P. 504
S.C. I/26
29th August, 1949.

AIR MINISTRY

METEOROLOGICAL RESEARCH COMMITTEE

Methods of comparison of height measurements by radio sonde and radar

by

D.N. Harrison
(Meteorological Office)

Contents.

Section 1. Radio sonde measurements of height.
Section 2. Radar measurements of height and pressure.
Section 3. Comparison of radio sonde and radar observations.
Table
Figure

Summary.

The purpose of this paper is to examine the effect of errors in radio sonde and radar observations on determinations of pressure and height, and to see what a comparison of the two sets of observations can be expected to show.

The treatment is mainly theoretical. General methods are indicated, but the results are intended to be readily applicable to particular cases. Instrumental questions are not dealt with, and where numerical values are quoted they are only round figures by way of illustration.

1. Radio sonde measurements of height.

(a) The computation of height from pressure and temperature, and of pressure from height and temperature, is based on the relation

$$dz = -\frac{kT\,dp}{p}$$

The "virtual temperature" is used, and k is treated as a constant*. Writing l for $\log p$ we have

$$z_1 = k\int_{p_1}^{p_o} T\,dl = kT_m(l_o - l_1) \quad \ldots\ldots\ldots(1)$$

where p_o is the pressure at the height $z = 0$. The mean temperature T_m is defined by this equation. If z is measured in metres and T in degrees A, and natural logs are used, $k = 29.3$. Where an integral occurs, the limits p_1 and p_o (or 0 and z_1) will be understood throughout. The symbol Δ is used to mean an error of observation.

In radio sonde observations, an error in the temperature at a given pressure

/can

* The error due to ignoring the variation of gravity with latitude and with height is negligible compared with the errors of radio sonde pressure measurements; in terms of pressure, it has a maximum value of 0.5 mb. at Z=15Km.

can arise from an error in either temperature reading $\Delta T'$ (including any error due to humidity) or pressure reading Δp ; the total error is

$$\Delta T = \Delta T' - \frac{dT}{dp}\Delta p \quad \ldots\ldots\ldots \quad (2)$$

$$= \Delta T' - \frac{akT}{p}\Delta p \quad \ldots\ldots\ldots \quad (3)$$

where a is the temperature lapse rate.

(b) The radio sonde observations may be used to compute

(i) the height z_p of a given pressure level of the atmosphere,

(ii) the height z of the balloon at a given point, e.g.at the tropopause, or at a given time.

Denoting the error in (i) by $\Delta z_{p,s}$ and the error in (ii) by Δz_s - the suffix s denoting radio sonde observations - and assuming that the error in surface pressure is zero[x], we obtain

$$\Delta z_{p,s} = k\int \Delta T\, dl = k\int\left(\Delta T' - \frac{dT}{dp}\Delta p\right) dl \quad \ldots\ldots \quad (4)$$

$$\Delta z_s = \Delta z_{p,s} + \frac{dz}{dp}\Delta p_1 = \Delta z_{p,s} - \frac{kT_1}{p_1}\Delta p_1 \quad \ldots\ldots \quad (5)$$

The relative importance of the terms on the right hand side of eqns. 4 and 5 can be estimated if Δp and $\Delta T'$ are known as functions of p, by plotting on a log p scale and taking the means by the method of equal areas. The values of $\frac{kT}{p} = -\frac{dz}{dp}$ and $\frac{akT}{p} = \frac{dT}{dp}$, taking a = .0065°C per metre, are given in the fourth and fifth columns of the table for arbitrarily chosen values of p and T, together with the corresponding heights z. From these data, taking $\Delta p = \pm$ 5mb and $\Delta T' = \pm$ 0.5°C at all levels, it can be seen that

(i) $\frac{dT}{dp}\Delta p = \frac{1}{2}$°C roughly, i.e. about equal to $\Delta T'$

(ii) ΔT_m, which is equal to the mean value of $\Delta T' - \Delta p\, dT/dp$ (eqns. 1 and 2), is of the order of 1°C, which will give rise to an error of about 1 part in 250 in z,

(iii) The height error due directly to Δp_1 (the second term in eqn. 5) is several times as large as $\Delta z_{p,s}$. This is the justification for the practice of attributing radio sonde height errors to pressure errors, but it would not hold good in the presence of systematic temperature errors of several degrees (due, for instance, to solar radiation).

It should be noted that even if $\Delta p = 0$ at pressure p_1 and $\Delta T' = 0$ throughout, there may still be an error in the computed height of this pressure level due to pressure errors lower down, through their effect on ΔT_m

/The

Footnote: [x] The ordinary errors of observation with a mercury barometer are negligible. The effect of larger errors (e.g. due to a defective instrument) depends on the way in which the control correction is applied to the radio sonde readings and on the shape of the radio sonde calibration graph.

The way in which the height errors arise is illustrated in the figure, in which the ordinates are log p and the abscissae T (curves 1) and z (curves 2). 1a represents the true temperatures, 1b the observed values, and 2a and 2b the heights computed from these. 2b is the same no matter what the combination of pressure and temperature errors that produced 1b from 1a. The true height of pressure level p_1 is z_1, the observed height z_2. $z_2 - z_1 = \Delta z_{p,s}$. If an inversion occurs at p_1, where the pressure error is Δp_1, the observed height of the inversion is z_3. $z_3 - z_2 = \Delta p_1 \, dz/dp$ and $z_3 - z_1 = \Delta z_s$. At pressure p_2 let $\Delta p = \Delta T = 0$.

Then there is still an error in the computed height of the level p_2 owing to observational errors in the lower layers.

(c) In the case of the Mk. II radio sonde, since the pressure readings are corrected for air temperature, a temperature error $\Delta T'$ will contribute to the pressure error Δp. The sign of this effect is such it tends to compensate $\Delta T'$ in both eqn. 4 and eqn. 5. The magnitude can be calculated with the aid of the pressure calibration graph and the correction ("Q") graph; it differs greatly for different instruments; it is negligible in eqn. 4, but in eqn. 5 it may make the second term larger than the first at high levels, even in the absence of other sources of pressure error (see MRP 203, section 5).

The discussion in this section has reproduced to some extent that of Section 7 of MRP.205, but it is given here for the sake of completeness

2. Radar measurements of height and pressure.

(a) The height of the balloon as measured by the range R and elevation E is

$$z = R \sin E$$

and therefore

$$\Delta z_r = \sin E \, \Delta R + R \cos E \, \Delta E \quad \ldots\ldots\ldots (6)$$

$$= \sin E \, \Delta R + z \cot E \, \Delta E \quad \ldots\ldots\ldots (7)$$

the suffix r denoting radar observations. The heights must be corrected for the earth's curvature. In comparisons with radio sonde observations this correction cannot be ignored. The correction, being proportional to $(R \cos E)^2$ will itself be subject to error, but this is negligible as a rule.

(b) The total temperature error for height z is

$$\Delta T = \Delta T' + a \, \Delta z_r \quad \ldots\ldots\ldots (8)$$

where $\Delta T'$ is the error of temperature measurement and a is the temperature lapse rate (compare eqn. 2).

Thus, assuming that the surface pressure error is zero, the error in the computed height for pressure level p_1 is theoretically

$$\Delta z_{p,r} = k \int (\Delta T' + a \, \Delta z_r) \, dl \quad \ldots\ldots\ldots (9)$$

In practice pressures are computed (see section 3c) for an arbitrary series of heights (viz. those where the lapse rate changes), and plotted on a log p scale. The heights of the required pressure levels are read off by interpolation, usually linear, between two points. The integral in eqn. 9 is thus replaced by a graphical summation.

Comparison of radio sonde and radar observations.

(a) Height of standard pressure levels.

The difference (radio sonde-radar) in the computed height for pressure p_1 is (eqns. 4 and 9)

$$\Delta z_{p,s} - \Delta z_{p,r} = -k \int \left(\frac{dT}{dp} \Delta p_s + a \Delta z_r\right) dl$$

$$= -k \int a\left(\frac{kT}{p} \Delta p_s + \Delta z_r\right) dl \quad \ldots\ldots (10)$$

provided that the summation $\int \Delta T' \, dl$ is performed in the same way in the two computations, that is, that the same temperature readings are used. This condition is fulfilled if the radar height is found for every "significant point" plotted on the "Radio sounding plotting chart" and these heights are then used for computing the pressure steps. If different levels are taken for the radio sonde and radar computations, or if some are omitted from one or the other, there will be a difference between the values of $\int \Delta T' \, dl$; but the method of selection ensures that these differences will be small compared with those due to Δp and Δz.

The relative importance of the two terms on the right hand side of eqn. 10 can be estimated if Δp_s and Δz_r are known in terms of l (or z) by plotting against l and taking the means by the equal-area method. A pressure error Δp_s = 1 mb. has the same effect as a height error Δz_r of kT/p metres. Specimen values of kT/p are shown in the fourth column of the table. In the sixth column are shown the values of Δz_r for cot E = 2 (mean wind speed twice the rate of ascent) and $\Delta E = 0.1^\circ = 1/573$ (see eqn. 7.) These are roughly equal to kT/p. Under the same conditions a range error of 15 m. would give rise to a height error of 7 m. Since systematic errors of $\pm$ 0.1° and $\pm$ 15 m. are very likely to be present unless great care is taken with the radar set, this means that a pressure error of 1 mb. may be masked by radar height errors. The magnitude of the resulting height errors $\Delta z_{p,s}$ or $\Delta z_{p,r}$ may be found by multiplying the figures of coulumns 4 and 6 by a (= .0065° C per metre). We thus obtain a mean equivalent temperature error of the order of 0.1°C, which will give rise to a height error of about 1 part in 2,500. This is therefore about the limit of accuracy with which heights of pressure levels can be determined by the G.L. III.

(b) Height of "significant point".

The difference (radio sonde-radar) in the observed height of a "significant point" is (see eqn. 5)

$$\Delta z_s - \Delta z_r = \Delta z_{p,s} - \frac{kT_1}{p_1} \Delta p_1 - \Delta z_1 \quad \ldots\ldots\ldots (11)$$

The probable value of Δz_r can be calculated from eqn. 6 or 7 if the radar errors are known. Typical values are given in the sixth column of the table. The relative importance of the first two terms of eqn. 11 is discussed in sect. 1. In observations with the Mk. II radio sonde the second term is generally much larger than the first.

/It

It might be thought that since the first term in eqn. 11 depends on $\Delta T'$ it should be possible to detect temperature errors due to solar radiation by means of height comparisons by day and night. But, as shown in sect. 1(c), there is a partially compensating pressure error of very variable magnitude, so that it would be necessary to use radio sondes having pressure units either particularly sensitive or particularly insensitive to temperature. The development of a radio sonde in which the pressure readings were independent of the air temperature might enable such a comparison to be made successfully.

Converting eqn.11 to a pressure error by the factor $\frac{dp}{dz} = -\frac{p_1}{kT_1}$ we obtain

$$\frac{dp}{dz}(\Delta z_s - \Delta z_r) = \Delta p_1 - \frac{p_1}{T_1}\int(\Delta T' - \frac{dT}{dp}\Delta p_s)\,dl + \frac{p_1}{kT_1}\Delta z_1 \qquad \ldots\ldots\ldots\ldots\ldots\ldots (12)$$

(c) Pressure of "significant point".

The pressure at height z_1 is given by

$$l = l_o - \frac{z_1}{kT_m}$$

where

$$\frac{1}{T_m} = \frac{1}{z_1}\int \frac{1}{T}\,dz$$

This definition of T_m is identical with that of eqn. 1.

In practice pressures are calculated in steps for layers having, within the experimental error, a constant value of dT/dl, and thus $T_m = (T_o + T_1)/2$. For layers a few hundred metres in depth the condition dT/dz = constant, is indistinguishable from dT/dl = constant.

If the surface pressure error is zero, the pressure error for a point at height z_1 is given by

$$\Delta l = -\frac{1}{k}\int \Delta(\frac{1}{T})\,dz - \frac{\Delta z_1}{kT_1}$$

therefore

$$\Delta p_r = \frac{p_1}{k}\int \frac{\Delta T}{T^2}\,dz - \frac{p_1}{kT_1}\Delta z_1 \qquad \ldots\ldots\ldots (13)$$

The observed pressure difference (radio sonde-radar) is therefore

+

/Substituting

$$\Delta p_s - \Delta p_r = \Delta p_1 - \frac{p_1}{k}\int \frac{\Delta T' + a\Delta z_r}{T^2}\,dz + \frac{p_1}{kT_1}\,\Delta z_1 \quad \ldots\ldots (14)$$

Substituting $dz/kt = -dl$, we see that the second (integral) term in eqn. 14 is of the same order of magnitude as the corresponding term in eqn. 12, but somewhat smaller in general since $\Delta z_r\, dT/dz$ is likely to be smaller than $\Delta p_s\, dT/dp$.

To this extent it is better to convert the radar heights to pressures and compare these with the radio sonde pressures than to convert radio sonde pressures to heights and compare with the radar heights.

Table

1	2	3	4	5	6
p mb	T °A	z m	- dz/dp m/mb	dT/dp °A/mb	2z/573 m
800	275	2,000	10	.07	7
500	250	5,500	15	.09	19
300	230	9,200	22	.15	32
200	220	11,800	32	.21	41
100	220	16,200	64	-	56

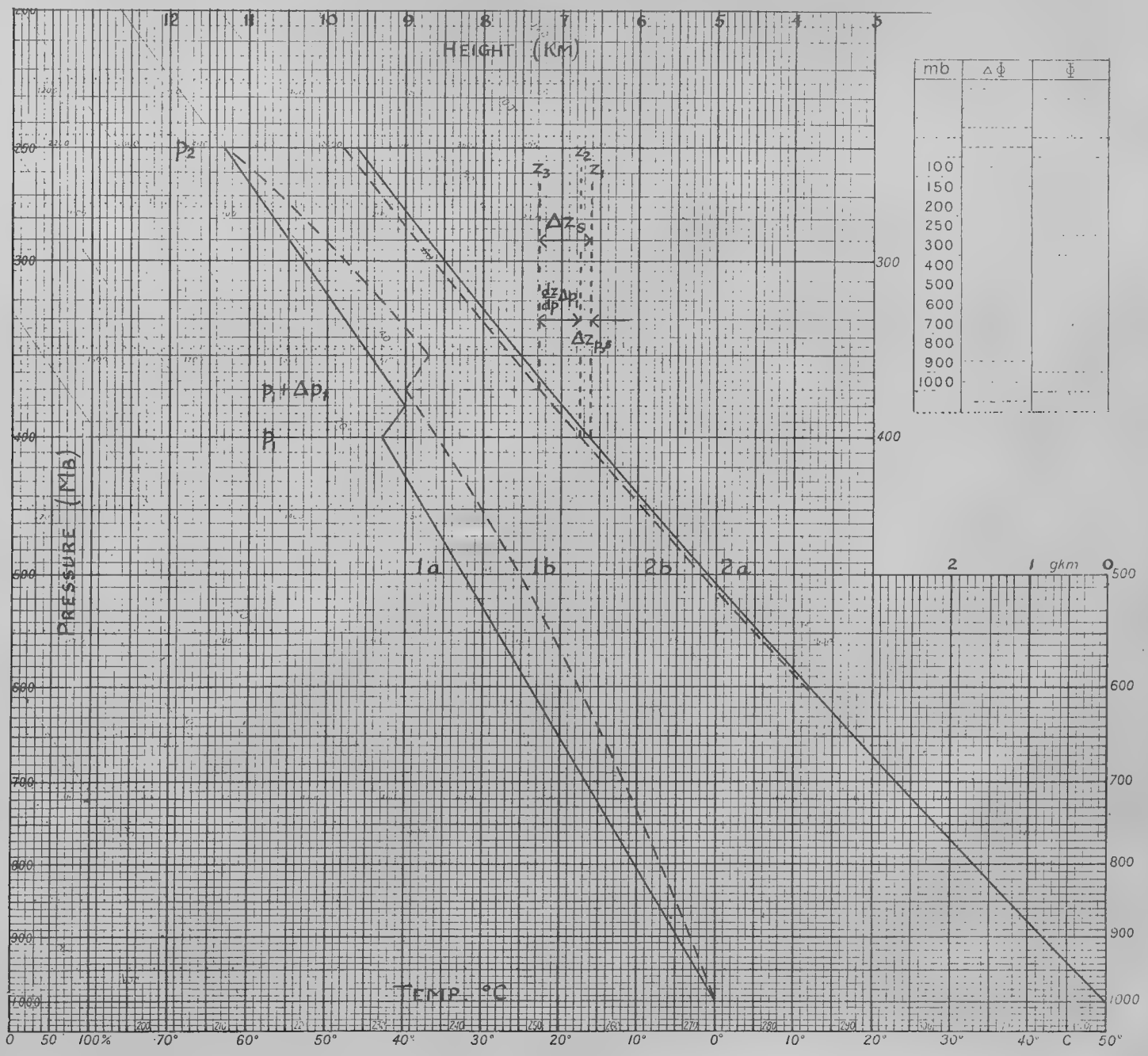
HEIGHT (Km)
PRESSURE (MB)
TEMP °C
mb
ΔΦ
Φ
100
150
200
250
300
400
500
600
700
800
900
1000
p_2
z_3
z_2
z_1
Δz_s
$\frac{dz}{dp}\Delta p_1$
Δz_{p_1}
$p_1+\Delta p_1$
p_1
1a
1b
2b
2a
gkm

AIR WEATHER SERVICE
TECHNICAL REFERENCE FILES

AIR MINISTRY

METEOROLOGICAL RESEARCH COMMITTEE

Amendment to M.R.P.510.

In Table VII, the following figures should be substituted for those given:-

Source	Less than 500'	500 to 1000'	1000 to 3000'	3000 to 6000'	Greater than 6000'	Total
R.A.E.(b)	93	3	18	17	10	141
Total (excluding B.E.A. and West Malling)	180	18	43	26	23	290

J.K. Bannon

Secretary M.R.C.

April, 1950.

G.256619/MKL/3/50/

0935 –	30,300	29,200 ; up to 0·4g other levels		II	21,000, 2·3 above	
3.11.48 1130-1230	22,000' to 24,000'	Up to ·3g	None	About 27,000' I	19·0	·17
	29,000' to 30,000'	Small			4·0	·08
4.11.48 0945-1030	Layer 26,700'	Small	None	35,900' II	125	·06
5.11.48 09-1100	29,200' to 31,200'	Small	None	28,900' I	2050	·24

AIR WEATHER SERVICE
TECHNICAL REFERENCE FILES

AIR MINISTRY
METEOROLOGICAL RESEARCH COMMITTEE

Addition to M.R.P.510

The attached tables should be inserted at the end of Table I(b).

J.H. Bannon
Secretary M.R.C.

17th April, 1950

G.256700/MKL/4/50/150

27.9.48	Layer 22,200′	Up to 0·3g	None	52,500′ II	20·0	·09
0930-1030	" 29,600′	Small			7·7	·10
29.9.48	Layer 33,000′	Small	Layers of stratus	38,800′ I	2·7	·17
0930-1020	" 36,000′	"	16,500′ to 36,000′		7·8	·02
	" 40,000′	"			—	—
30.9.48	Layer 36,000′	Small	None	39,900′ I	23·2	·03
0940-1025						
4.10.48	24,700′ to 27,700′	Up to 0·3g at 27,200′ otherwise small	None	39,100′ II	0·8 at bottom, 61·0 at top of layer	·36
8.10.48	Layer 33,000′	Small	None	44,600′ I	3·5	·25
1335-1430						
26.10.48	20,600′ to 29,500′	Small	None	37,500′ I	13·0	·11
1400-1500						
29.10.48	27,800′ to 30,300′	Up to 0·5g at 29,200′; up to 0·4g other levels	None	34,200′ II	0·7 up to 29,800′, 2·3 above	·21
0935-						
3.11.48	22,000′ to 24,000′	Up to ·3g	None	About 37,000′ I	19·0	·17
1130-1230	29,000′ to 30,000′	Small			4·0	·08
4.11.48	Layer 26,700′	Small	None	35,900′ II	12·5	·06
0945-1030						
5.11.48	29,200′ to 31,200′	Small	None	28,900′ I	20·50	·24
09-1100						

Table I (b)

Date Time	Bumpy Layers	Intensity of bumps (Accelerations)	Clouds in bumpy layer	Tropo-pause and type	R_i	Horizontal shear $(hours^{-1})$
18.3.48 1110-1220	Layer 38,100'	Small	None	About 34,000' II	160	.05
4.6.48 0915-1045	Layer 29,000'	Small	None	38,700' II	7.2	.16
	35,000' to 37,000'	Small			4.8	—
27.9.48 0930-1030	Layer 22,200'	Up to 0.3g	None	52,500' II	20.0	.09
	" 29,600'	Small			7.7	.10
29.9.48 0930-1020	Layer 33,000'	Small	Layers of stratus 16,500' to 36,000'	38,800' I	2.7	.17
	" 36,000'	"			7.8	.02
	" 40,000'	"			—	—
30.9.48 0940-1025	Layer 36,000'	Small	None	39,900' I	23.2	.03
4.10.48 1400-1500	24,700' to 27,700'	Up to 0.3g at 27,200' otherwise small	None	39,100' II	0.8 at bottom, 61.0 at top of layer	.36
8.10.48 1335-1430	Layer 33,000'	Small	None	44,600' I	3.5	.25
26.10.48 1400-1500	20,600' to 29,500'	Small	None	37,500' I	13.0	.11
29.10.48 0935-	27,800' to 30,300'	Up to 0.5g at 29,200'; up to 0.4g other levels	None	34,200' II	0.7 up to 29,800', 2.3 above	.21
3.11.48 1130-1230	22,000' to 24,000'	Up to .3g	None	About 37,000' I	19.0	.17
	29,000' to 30,000'	Small			4.0	.08
4.11.48 0945-1030	Layer 26,700'	Small	None	35,900' II	125	.06
5.11.48 09-1100	29,200' to 31,200'	Small	None	28,900' I	2050	.24

Table I (b)

Date Time	Bumpy Layers	Intensity of bumps (Accelerations)	Clouds in bumpy layer	Tropo-pause and type	Ri	Horizontal shear $(hours)^{-1}$
20.2.48 1025-1200	Layer 32,800	Small	None	About 29,000′	–	–
25.2.48 1440-1530	Layer 32,000′	Small	None	32,900′ II	12·6	–
26.2.48 1140-1225	Layer 26,000′ Layer 30,000′	Small "	Thin Ci. 30,000′	About 35,000′ I	2·0 13·0	– –
8 3.48 1025-1115	21,600′ to 37,800′	Small	1/10 Cs 21,600′ to 37,800′	About 42,000′ I	0·36 31-35,000′ otherwise 4. to 1,000	·03 up, to 30,000 – no obs. above

/9.3.48

CONFIDENTIALLY. Its contents must not be quoted.

M.R.P. 517
S.C. II/42
28th October, 1949.

AIR MINISTRY
METEOROLOGICAL RESEARCH COMMITTEE.

Advective Temperature Change in the 1000 - 700 mb and 700 - 500 mb Layers.

by J.M. Craddock (Meteorological Office)

AIR WEATHER SERVICE
TECHNICAL REFERENCE FILES

Summary

The part played by isobaric advection in affecting large scale temperature changes in the troposphere is examined. On the basis of about 700 measurements made at a particular station during a period of six months, it appears that the thermal changes due to advection alone are largely offset by the other processes at work, so that the resultant thickness tendency is a residual showing a correlation of the order of .6 with the advective component.

A subsidiary question, whether the estimate of the thermal change based on the shear hodograph of an upper wind sounding affords useful information on the resultant thickness tendency is answered in the negative.

1. Introduction.

1.1. This paper covers the first stage of an investigation into the processes leading to large scale temperature change in the troposphere. The changes considered are those which are recognisable on the synoptic chart and which therefore, the practising forecaster must estimate in making prognostic upper air charts. Hence temperatures are expressed in a way which the synoptic meteorologist has found convenient; in terms of the thickness of the layers between chosen isobaric surfaces.

The rate of change of the thickness of a particular layer above a particular point (which, expressed in units of 10 feet per 6 hours, will be called the thickness tendency) can be analysed mathematically into the sum of three components which may be called advective, dynamic (due to airflow through the isobaric surfaces) and non-adiabatic. This analysis, which is due essentially to Dr. R.C. Sutcliffe, is reproduced in Appendix A, where it is shown that under suitable conditions any one of the components may be of synoptic importance. It follows that an upper air analyst, engaged in forecasting the thermal pattern, must bear in mind all three components, but the qualitative adjustments based on experience, which are made in current synoptic practice, are lacking in precision. If the forecast thermal chart is to be used to extend the effective range of forecasting, something more than qualitative estimation is required and the present paper is intended to provide basic data for quantitative forecasting. The advective component of the thickness tendency is obviously important (it has sometimes been supposed to be the only significant component) and forms the subject of this paper.

1.2. The method of investigation is basically simple. Some radiosonde stations make simultaneous soundings of upper air temperature and wind velocity at the four main synoptic hours. The series of values of the thickness found from the temperature observations are used to estimate the thickness tendency at that place at any particular time. The advective component is found from the wind sounding and the thermal gradient, the latter being estimated both directly, from an analysed upper air chart, and indirectly, from the shear hodograph of the wind sounding itself. When a number of such measurements are made, the association between the thickness tendency and the corresponding advective component can be expressed by means of a correlation coefficient or regression equation.

1.3. The following section is concerned with the basic data, and section 3 with the statistical treatment. This latter is intended not only to ensure that the conclusions drawn are not vitiated by observational errors or other irrelevant features but also to afford a means of judging the reliability of estimates, so that the reader may judge the efficiency of the methods of approximation used and the practical value of the regression equations found. The remainder of the paper, apart from three Appendices, (one of mainly synoptic, two of statistical interest) discusses the results.

/2.

2. The Basic Data.

2.1. Direct evidence on the thickness tendency is provided by the 6-hourly soundings of upper air temperature made at Larkhill and Downham Market. The thickness of the layers are computed from the soundings at the Central Forecasting Office, and, for this investigation, the values taken were those plotted on the analysed charts. These values are subject to the basic observational errors discussed in section 3.3., and in addition appear liable in an unpredictable manner, to errors due to faulty transmission and plotting, and gross instrumental failure. Where an observation appeared to be subject to exceptional error, it was rejected, but in all fewer than 10 observations were rejected out of a total of over 4,000. To the degree of approximation used (thicknesses rounded to the nearest 10 feet) these measurements are almost free from the subjective element. A typical section of a series of thicknesses is shown in Fig.1.

2.2. The Advective Component of the Thickness Tendency.

2.2.1. It is shown, in appendix A, that the advective component of the tendency in the layer between pressures p_1 and p_2 is

$$-\frac{R}{g}\int_{p_2}^{p_1} \underline{v} \cdot \text{grad}_p T \; d\log p \qquad \ldots\ldots\ldots (3)$$

If it is assumed that $\text{grad}_p T$ is constant at all levels within the layer, this becomes

$$-\frac{R}{g}\,\text{grad}_p T \int_{p_2}^{p_1} \underline{v} \; d\log p \qquad \ldots\ldots\ldots (4)$$

The vector $-\frac{R}{g}\,\text{grad}_p T$ is proportional to the gradient of thickness of the layer in question, and for the 1000 - 700 mb and 700 - 500 mb layers can be measured from the thickness lines of an analysed upper air chart. Once this is done, the component of the vector

$\int_{p_2}^{p_1} \underline{v} \; d \log p$ in the direction of $\text{grad}_p T$ can be evaluated from an upper wind sounding, and the advective component found by multiplying the two together.

2.2.2. The thickness gradients were measured from the analysed working charts of the upper air section at the Central Forecasting Office. The station used, Downham Market, is in the part of the chart where the observational net work and analysis are most reliable but even so the measurement is difficult and subject to much uncertainty. The thickness gradient is subject to local variations which the analysed contours (at 200 ft intervals) do not express and which the comparatively sparse network of upper air soundings stations often fails to resolve. Consequently, each chart was given individual study before the gradient was estimated. Such estimates are bound to be to some extent subjective, but the resulting errors in the tendency are perhaps less considerable than might appear, because most of the uncertainty arises with the smaller gradients.

2.2.3. The component of $\int_{p_2}^{p_1} \underline{v} \; d \log p$ or $\int_{p_2}^{p_1} \frac{\underline{v}}{p}\, dp$ was estimated from the upper wind sounding for the hour in question by plotting the components of $\underline{v}$ at each 50 mb level within the layer on parallel lines, the scales along which being adjusted for the factor of p in the denominator, and by estimating the mean value by eye. In dealing with the 1000 - 700 mb layer the mean wind was taken over the layer 950 - 700 mbs., so as to avoid frictional effects. To the degree of approximation used (the nearest knot) this process is almost wholly objective. The product of the two terms, expressed as a tendency per 6 hours, was rounded to the nearest 10 feet. The value of the advective component so obtained is strictly an instantaneous value, relating only to the synoptic hour to which it refers.

/2.2.4.

2.2.4. The method is appropriate only where there is an aerological net-work good enough to enable the thickness gradient to be estimated without reference to the "thermal wind". In such a situation it does not assume any relationship between thickness gradient and the change of wind with height, and applies whatever such relationship may be. If, on the other hand, the thickness lines are drawn strictly to agree in direction and spacing with the "thermal wind", then the quantity measured by this method will be almost the same as that found more directly by the "hodograph" method now to be discussed, while if the thickness lines are a compromise taking account of both observed thicknesses and "thermal winds" the quantity measured will be of intermediate status.

2.3. The "Hodograph" Component of the Thickness Tendency.

The derivation of the "hodograph" component, which equals the advective component if the airflow is geostrophic, is given in Appendix A. (Section 3) The actual measurement is extremely simple, since all that is necessary is to plot the observed winds experienced by the radiosonde in traversing the layer in question on a polar diagram and to measure on an appropriate scale the area enclosed between the wind vectors for top and bottom of the layer and the hodograph. Each measurement was rounded to the nearest 10 ft, and, to eliminate surface effects, when the 1000 - 700 mb layer was considered the lowest wind included was that at 950 mb.

2.3.1. The relation between the observational error in the wind measurements and the error of the hodograph component is complex, but the latter error appears to be small. The estimation of the tendency from the hodograph is easily made and entirely objective, great attractions in a field where the inexactitude of data is one of the major difficulties. Like the advective component of the tendency, the measured "hodograph" component is an instataneous value relating to the synoptic hour.

3. The Statistical Treatment of the Data.

3.1. The statistical treatment of the data is intended to provide evidence from which firm conclusions can be drawn; accidental effects such as those due to observational error, or physical processes not intimately connected with synoptic temperature change are to be eliminated. Sections 3.3. and 3.4. deal with these. Further, the validity of the approximations in the basic equation resolving the thickness tendency into its components has only been established (Appendix A, Section 1.7) for mean values, taken over six hours, of the quantities involved. Thus the equation must be integrated through at least this period for a comparison based on it to be valid. What we actually compare is the mean refined thickness tendency during the 6 hours between synoptic hours, and the advective component for the same period. The thickness tendency as measured (as the change in thickness during a period) is essentially a mean value, so that the only difficulty is to find its value for the right period, but the measured advective component is an instantaneous value and we have to decide how a succession of these can be used to estimate a mean value. These are problems of estimation, to be surmounted before the comparison of tendency with advective component can begin. In Section 3.5 a standard is laid down, to enable us to choose between alternative methods of estimation, and in sections 3.5.6 to 3.5.8 it is shown that the methods actually used are satisfactory. For clarity, the formulae used are set down first and justified afterwards.

3.2. The Formulae Used.

3.2.1. Where the basic series is composed of instantaneous values (as in the advective and hodograph series) a four term moving average is made, and taken to refer to the mid-point of the period covered. If $a_1\ a_2 \ldots\ldots\ldots a_n$ are the observed values, and $a^+_{n+1/2}$ the average, then

$$a^+_{n+1/2} = \frac{a_{n-1} + a_n + a_{n+1} + a_{n+2}}{4} \quad \ldots\ldots\ldots (5)$$

3.2.2. For the observed tendency series, the value t_n at a synoptic hour is taken to be one quarter of the total change in thickness during a 24-hour period centred at that hour, and the value $t^+_{n+1/2}$ halfway through a synoptic interval is taken as the mean of the preceding and succeeding values.

$$t^{+}_{n+1/2} = \frac{t_n + t_{n+1}}{2} \qquad \text{.....} \quad (6)$$

3.2.3. These formulae require that there are no breaks in the series of basic observations. In fact a few breaks occurred, where observations were missing and were dealt with as follows:- If only a single isolated observation was missing, a value was interpolated, the mean of the preceding and succeeding observations: if a single observation was missing regularly (as when at Downham Market, during the summer of 1946 no midnight observation was made) or two or more consecutive observations were missing, the derived series t^{+}, a^{+} were stopped, and restarted, when the basic series became regular again. It is not considered that this procedure involved any significant error.

3.2.4. The series t_n defined in section 3.2.2. may be considered as a four term moving average applied to the primitive series of 6-hour tendencies obtained by subtracting from each term its immediate predecessor.

The derived series $t^{+}_{1/2}$, $t^{+}_{1+1/2}$, .., $t^{+}_{n+1/2}$ deserves special scrutiny, because it is our estimate of the function we are trying to predict. In Fig. 1. the pecked curve represents the "derived thicknesses" obtained by adding successive values of $t^{+}_{n+1/2}$ to an arbitrary initial value. This curve follows the general trends of the series of observed values, it is clear that the features of synoptic importance would not be distorted or obscured.

3.2.5. These formulae have been chosen in order to minimise the errors which would arise if crude data were used, and which are discussed in the following sections. It is shown that by their use uncertainties due to processes of estimation are made small compared with uncertainties due to sampling, discussed in Section 3.6, which are inherent in the nature of the atmosphere.

3.3. Problems of Graduation or the Elimination of Error.

3.3.1. The errors affecting meteorological series are of two kinds.

(a) non-persistent errors, such as those arising from lack of homogeneity in an air mass or the rounding of fractions in calculation, which may be expected to affect each term of the series independently, and

(b) persistent errors, such as those arising when a radiosonde is affected by direct solar radiation, or a series of observations is made in turn by observers of different personal equation, in which errors occurring in one observation may be expected to recur at regular intervals in others.

The persistent component of error is very difficult to eliminate but a major purpose of the organisers and instrument designers of the meteorological network is to make such errors as small as possible. The radiosonde stations used are well established, and such errors will be neglected. It may be noticed however that the smoothing used to eliminate diurnal effects has the incidental result of eliminating any systematic radiational error.

3.3.2. The non-persistent component of error has the effect of reducing the correlations found (see Appendix B section 2.2.). Its effects can be eliminated entirely if its variance (or mean square value) is accurately known, but should this state of perfection be unattainable (and it is in our series) the uncertainty is larger when the variance due to error forms a large proportion of the variance measured than when the proportion is small. By suitable averaging, the proportion which the mean square error bears to the variance of the quantity measured can be reduced, (Appendix B (Section 2.1)), and the best estimate possible is then used for the variance of residual error. The uncertainty in the final correlations due to the presence of error is thus reduced to less than 1%.

3.4. Problems of Refinement, or Finding the Wanted Component.

3.4.1. If average values are found for the thicknesses at each synoptic hour, a significant diurnal variation is revealed (Appendix B Section 7).

This may be due, in some part, to persistent observational error, but there is no doubt that in the main it is a real effect, attributable to the processes of temperature change already mentioned. There is, however, no reason why these processes should have the same relative importance in the diurnal change as they have in the large scale variation. On the contrary, it seems likely that non-adiabatic effects are more important, and advective effects less so, in diurnal changes than in large scale changes. The diurnal change, though real enough, is clearly best eliminated from this study of synoptic changes. The formulae quoted in section 3.2.1. and 3.2.2. do this.

3.5. Problems of Interpolation and Integration, and the Degree of Precision of Estimates.

3.5.1. The common feature of these problems is that the observed values of a function at regular intervals of time are used to estimate its values at intermediate times, or its mean value over a period of time. Any such estimate is open to uncertainty, because if the function contains a harmonic component with period equal to the time interval between observations, this component will affect means and interpolated values without being in any way detectable in the observed values. It is therefore assumed that no such component exists (or, what amounts to the same, that the mean square value of the function at any intermediate time does not differ systematically from its value at the times of observation) and this, for meteorological data, and a series interval of 6 hours, seems reasonable enough.

3.5.2. Apart from this, an indefinite number of formulae may be suggested to estimate, say, an interpolated value, and we require some means of distinguishing between these, a measure of reliability, in fact. Suppose that U is the function to be estimated, and E is an estimate obtained by a particular method, both functions being measured from their mean values.

Then $\frac{1}{N}\sum U^2 = \sigma_u^2$ is the variance of U, and $\frac{1}{N}\sum (U - E)^2$ the residual variance, or mean square deviation of observed from estimated value. The ratio $\sum (U - E)^2 / \sum U^2$ which will be called the relative residual variance, has the features we require for a measure of reliability. (The summations are understood to be over a large number, N, of observations which will be defined in any particular context). If the method of estimation is perfect, the relative residual variance will vanish, while of two imperfect estimates the one with the lower relative residual variance is the better. One obvious estimate is the mean value of U, in this case zero, which has relative residual variance unity. Hence provided this estimate is available, any other estimate for which the relative residual variance exceeds unity is worse than useless, and one whose relative residual variance is only slightly less than unity may be held not to justify the extra trouble involved in its use. Suppose, now, observed and estimated values are compared for a given body of data, an improved estimate can generally be made by multiplying the original estimate by the appropriate regression coefficient (unless exceptionally this = 1). In meteorological work however, a formula of estimation often has to be chosen before the data to which it is to be applied have been specified, so we consider the effect of multiplying the original estimate by any constant multiplier K. Let $E' = KE$ be the new estimate.

If σ_u^2, σ_e^2 are the variances of U and E and r the correlation between them, the relative residual variance of this estimate is

$$\frac{\sum (U - E')^2}{\sum U^2} = 1 - r^2 + \left(\frac{K\sigma_e}{\sigma_u} - r \right)^2 \quad \ldots\ldots\ldots \quad (7)$$

/This

This will be least if $K = r\sigma_u/\sigma_e$ that is, if E' is obtained from E by multiplying by the usual regression coefficient. If we adopt a slightly different value of K, then so long as $K\sigma_e/\sigma_u - r$ is small the loss of precision will be insignificant. If, however,

$$K\sigma_e/\sigma_u - r > r \quad \text{or} \quad K > 2r\sigma_u/\sigma_e$$

then

$$\frac{\sum (U - E')^2}{\sum U^2} > 1$$

so that the estimate E' is worse than useless, and in particular, the original estimate E will be worse than useless, however high the value of r if $r\sigma_u/\sigma_e < 1/2$. The need for adopting a value of K near the optimum $r\sigma_u/\sigma_e$ is thus demonstrated and in sections 3.5.6 to 3.5.8 it is shown that the formulae here used are satisfactory. This consideration is important, not only in discussing the details of statistical estimation, but whenever a more or less reasonable estimate is used in place of a quantity difficult or laborious to calculate. In this case the true regression coefficient not known in advance and the method of estimation cannot be considered satisfactory until it has been demonstrated, after the event that $r\sigma_u/\sigma_e$ is near the optimum value, unity. Section 4.2.5 deals with an example when this was not done.

3.5.3. When the series considered is relatively smooth, and there is a strong prior probability that the underlying variate is changing steadily (a state of affairs which occurs in actuarial data, and when an analytical function is being tabulated) the problems mentioned in section 3.5.1. may be treated by methods based on the calculus of finite differences. Our meteorological series are, however, of a different type, with the following outstanding features:-

(1) However long the series is, the terms lie within a fairly definite range.

(2) There is no prior evidence as to the nature of the underlying variate, other than what is contained in the series itself, and

(3) consecutive terms are more alike than terms chosen at random, i.e. the series all show some measure of coherence (Appendix B, Section 8).

3.5.4. These series give no ground for assuming that differences of any particular order should vanish, and the approach via the calculus of finite differences appears unpromising. It is in any case open to the objection that no numerical measure of precision is available, so that the reliability of the estimate is left as a matter of personal opinion. The methods of estimation actually used depend on the coherence of the meteorological series.

3.5.5. When a function relating to a particular time is to be estimated from the terms of a time series, we may enquire how far terms of the series relating to much different times are able to contribute to our knowledge of the required function. Suppose for example, we wish to estimate one term, u_n in terms of predecessors, by a linear relation of the form $u_n = au_{n-1} + bu_{n-2} + \ldots ju_{n-s}$. Then we may ask whether u_{n-s} is able to contribute anything to our knowledge of u_n We may solve this problem by calculating partial serial correlation coefficients r'_2, r'_3 $\ldots r'_s$ where r'_s

is defined to be the correlation between u_n and u_{n-s} when the effect of the intervening terms is eliminated. Only if r'_s is significantly different from zero is it worth while to include u_{n-s} in our expression for u_n. The theory behind this treatment may be found in "The advanced theory of statistics" by M.G. Kendall, Vol. 1, p.380, and a worked example is given in Vol. 2. p.416. The partial serial correlations, and also, the coefficients of the regression equation, when these are chosen to minimise the residual variance

$\frac{1}{N} \sum (U_n - U_m)^2$ are functions of the serial correlations of the time series.

Some of these serial correlations have been found for our meteorological series (Appendix B, Section 8) and it appears that in all cases much the most important part of our knowledge of the required function comes from the nearest terms of the time series. Accordingly, the formulae used for interpolation and integration, discussed in the following sections, make use only of the adjacent terms of the appropriate time series.

3.5.6. The interpolation formula used in section 3.2.2. for the series of observed tendencies is

$$t^+_{n+1/2} = \frac{1}{2}(t_n + t_{n+1}) \qquad \ldots\ldots\ldots\ldots\ldots (8)$$

the coefficient being adjusted to make the residual variance as low as possible. This coefficient is, in fact $\frac{r_{1/2}}{1 + r_1}$ and the relative residual variance is $1 - 2r^2_{1/2}/(1 + r_1)$. These functions depend not only on the observed correlation r_1 but also on the correlation $r_{1/2}$ between terms half a synoptic interval apart, which cannot be observed, and which must be estimated from the observed values.

The method of estimation is discussed in Appendix C, and the estimate used $r_{1/2} = \frac{1 + r_1}{2}$ gives the value $\frac{1}{2}$ for the regression coefficient, as stated in section 3.2.2. and $(1 - r_1)/2$ for the relative residual variance.

3.5.7. In this section the notation r_c will be used to denote the correlation between values of a function c apart, even if c is fractional. In dealing with the advective series, we have to estimate the mean value of the advective component during a 6-hour period, centred at a synoptic hour, and our estimate is the instantaneous value at the mid-point of the period. If the synoptic interval is our unit of time, our estimate is u_n, and the true value is $\int_{-1/2}^{1/2} u_{n+c}\, dc$. It is shown in Appendix C that the regression coefficient of the true value on the estimate is

$$2\int_0^{1/2} r_c\, dc$$

and the relative residual variance is

$$1 - 2\left\{\int_0^{1/2} r_c\, dc\right\}^2 \Big/ \left\{1 - \int_0^1 c\, r_c\, dc\right\}$$

3.5.8. It appears, therefore, that the accuracy of the formulae of interpolation and integration depends on the form of the lag correlation coefficient, r_c for small values of c. This is a question which has been studied extensively in connection with the theory of turbulence, where,

/however

however, interest attaches to the value of $\int_0^T r_c \, dc$ when T is large

rather than when it is small. It has been suggested by G.I. Taylor that r_c can be expressed by means of an even power series in c, by O.G. Sutton that it varies as c^{-n} where $0 < n < 1$ and by T.E.W. Schumann and others that it varies as e^{-c}. These alternatives are discussed in Appendix C, but it appears that none of them is very suitable to the existing data, judging from the observed values of the serial correlation coefficients. The data actually suggests that r_c is very nearly a linear function of c, and in this work it has been assumed that $r_c = 1 - c(1 - r_1)$

On this hypothesis the regression coefficient, for estimating the mean advective component from the instantaneous value, is $(3 + r_1)/4$ and the relative residual variance of the estimate is $(53 - 50r_1 - 3r_1^2)/\{16(5 - 2r_1)\}$

Values of this function for selected values of r_1 are as follows:-

r_1	.4	.7	.9
relative residual variance	.5	.3	.11

In the series actually used, the first serial correlations range from .80 to .93. It follows, not only that the relative residual variance is satisfactorily low, but also that it is legitimate to use the estimate without making the correction (multiplying by $(3 + r_1)/4$) discussed in section 3.5.2.

3.5.9. The errors arising in the process of estimation have thus been reduced to a fairly low level; further considerable reduction could be effected only by reducing the time interval between observations, and not by manipulation of existing data. In view of their comparative smallness, the effect of these errors has not been studied in detail, but in general it tends to reduce the correlations found.

3.6. Problems of Sampling.

3.6.1. A correlation coefficient provides an exact measurement of the association between the variables in the body of data from which it has been calculated. The question then arises whether another body of data would show the same correlation and if not, what magnitude of difference is to be expected. Where the data are drawn from a normal population, this question can be answered exactly, (see e.g. R.A. Fisher; Statistical Methods for Research Workers, pp. 179 - 188) but our meteorological variables do not appear to be normally distributed. There is the even more serious difficulty that the estimate of the significance of observed correlations are based on the supposition that the sample examined consists of a set of independent terms, and this condition is certainly not fulfilled when a pair of serially correlated time series are compared. The present data, in fact, lie outside the scope of existing theory, and standards of significance have therefore been omitted throughout this work. The features discussed would, however, be significant if normal sampling theory were held to apply. An alternative to predicting what the scatter of correlation coefficients ought to be on the basis of the normal distribution is to repeat the calculation on several independent bodies of data, and see what the scatter actually is. This has been done, and the tables show both the actual long term correlations, and the scatter about the long term value which short term correlations show. This is much the most important source of uncertainty to which the results are liable.

4. A Discussion of the Results.

4.1. The Advective Component.

4.1.1. When the various corrections have been made the correlations between total thickness tendency and advective component, at Downham Market during the 6 months October, 1945 to March, 1946 are as follows:-

Month	Oct.	Nov.	Dec.	Jan.	Feb.	March	Total
No. of obs.	122	120	124	124	112	124	726
1000-700 mb.	.54	.59	.56	.43	.60	.69	.64
700-500 mb.	.60	.79	.41	.53	.70	.46	.53

Using the correlations for the whole series of data, the regression of the thickness tendency on the advective component is

$$T_{71} = -0.36 + 0.54\, a_{71} \qquad \ldots\ldots\ldots\ldots (9)$$

for the 1000 - 700 mb layer and

$$T_{51} = -0.33 + 0.39\, a_{51} \qquad \ldots\ldots\ldots\ldots (10)$$

for the 700 - 500 mb layer

4.1.2. The correlations, given to two significant figures, are almost free from observational error, and bias due to methods of estimation, but the scatter due to sampling is very considerable. Correlation coefficients calculated from samples of 124 drawn from a normal population may be expected to show about as much scatter as these but the possibility also arises that the correlation may vary with the type of weather, or season of the year. It is intended that this question should be further investigated.

4.1.3. Consider now the regression equations (9) and (10). These show that the advective component has a positive bias compared with the thickness tendency, so that in the British Isles during winter advection has the overall character of a warming process, while the non-advective processes have an overall cooling effect. The regression equations give us an estimate T^+ of the total tendency based on the advective components a^+, but in view of the values of the correlations between t^+ and a^+, the estimates are not at all good ones.

4.1.4. While the advective component cannot provide a good estimate of the total tendency it may on occasion provide the only one. Should it be necessary to use it in this way, the best estimates are provided by the regression equations (9) and (10). An alternative procedure, often followed in such circumstances is to ignore the other components, and replace the total tendency by the advective component. This is equivalent to using instead of the proper regression equations, the empirical regression equation

$$T^+ = a^+ \qquad \ldots\ldots\ldots\ldots\ldots (11)$$

This estimate will have relative residual variance .89 for the 1000 - 700 mb layer, and 1.47 for the 700 - 500 mb. layer, compared with .59 and .72 for the proper equation so that the loss of precision is obvious.

/4.1.5.

4.1.5. While the advective component is not a satisfactory measure of the total tendency from the forecaster's point of view, it is nevertheless of value to show the importance of advective processes in comparison with the dynamic and non-adiabatic processes also at work. To do this the non-advective tendency, representing the sum of the dynamic and non-adiabatic components was found for the Downham Market data by subtracting the advective component from the total tendency. The corrected correlations of this with the total tendency, and with the advective component, are shown in the following tables.

Correlation between non-advective and total tendency, Downham Market, 1945, to March, 1946.

Month	Oct.	Nov.	Dec.	Jan.	Feb.	March	Total
No. of Obs.	121	120	124	124	112	124	726
1000-700 mb	.34	.35	.26	.33	.42	.36	.35
700 - 500 mb	.24	.14	.30	.08	.17	.54	.22

Correlation between advective and non-advective components Downham Market Oct. 1945 to March 1946.

Month	Oct.	Nov.	Dec.	Jan.	Feb.	March	Total
No. of Obs.	122	120	124	124	112	124	726
1000-700 mb	-.60	-.55	-.67	-.71	-.47	-.42	-.63
700-500 mb.	-.64	-.72	-.75	-.81	-.58	-.50	-.71

4.1.6. The negative correlation between advective and non-advective components is noteworthy, and supports the impression, gained from a study of synoptic charts, that the effect of isobaric advection in modifying the thermal field is largely offset by the other processes at work. It appears, moreover, that the compensation is generally more complete in the 700-500 mb. layer than it is in the 1000-700 mb. layer since in each of the six months the negative correlation is larger for the upper layer than for the lower.

4.1.7. The correlations between the tendency and non-advective component are noticeably below those between the tendency and its advective component. In fact, the lowness of the former in the 700-500 mb. layer is surprising, because there the effects of dynamic heating may be expected to be most conspicuous. The question hardly deserves further consideration at this stage, since the non-advective component is no more than the sum of various dissimilar parts, but it is hoped to investigate it further by analysing the non-advective component with the aid of additional observational data.

4.2. The "Hodograph" Component.

4.2.1. The "hodograph" component is equal to the advective component if the air-flow is geostrophic or if it does not vary with height. In other cases it forms only an approximation to the advective component, but even so, it has received wide publicity as affording a reasonable approximation to the tendency itself. The idea has been recommended for use in practical forecasting by inter alia C.G. Rossby and his collaborators (Univ. of Chicago Misc. Rep. No. 1 "A proposed method for the computation of the 10,000 foot tendency field" p.1 - 8 and Misc. Rep. No. 7 "Weather Map Construction and Forecasting in the Westerlies from Single Station Aerological Data", p.36, and Misc. Rep. No. 2 "Weather Estimates from Local Aerological Data" p. 15 - 18) and V.P. Starr ("Basic Principles of Weather Forecasting" p.217). The form of the secondary advective component of

/the

the tendency (See Appendix A Section 3.2) shows that its magnitude will be small under the conditions of gradient airflow discussed by C.H.B. Priestley in "The Dynamical Control of Atmospheric Pressure" Q.J. Vol. 73, p. 65 1947, so that under those conditions too the "hodograph" component should be a good approximation to the advective component.

4.2.2. A comparison between the "hodograph" component and the thickness tendency for the layer between 5000 and 10,000 feet has been carried out by Panofsky (Bull. Amer. Met. Soc. Vol. 25 1944 p. 271 - the effect of vertical motion on local temperature and pressure tendencies) in which he obtained a correlation of 0.50, based on 86 pairs of observations, the hodographs being obtained from pilot balloon soundings. A rough idea of the significance of this may be gathered by assuming the data to be drawn from a normal population and applying Fisher's z-transformation to find the limits between which the true value of the correlation must lie. Adopting a 5% standard of significance it appears that the true value of the correlation in the population form which Panofsky's sample was drawn should lie between .32 and .65. While, therefore, Panofsky's result does not conflict with those obtained in the following paragraph, it fails to determine the correlation with enough accuracy to be of much use. Its value is further reduced by the fact that, being based on pilot balloon observations it cannot cover synoptic developments which are accompanied by extensive cloud.

4.2.3. The present investigation covers three years observations at Downham Market and Larkhill, and in all 4000 comparisons were made. The detailed results are shown in the following Table 1, the correlations being corrected.

Table I

	Larkhill		Downham Market			
	Oct. 47 - Mar. 48	Apr. 48 - Sep. 48	Oct. 45 - Mar. 46	Apr. 46 - Sep. 46	Oct. 47 - Mar. 48	Apr. 48 - Sep. 48
1000 - 700 mb.						
Mean tendency (ft)	1.5	-.4	-1.0	-1.1	-.4	.3
Variance (sq. ft)	657	483	491	621	753	491
S.D. (ft.)	25.6	22.0	22.2	24.9	27.9	22.2
Mean hodograph cpt (ft)	36.7	12.8	21.6	18.6	37.0	14.8
Variance sq. ft.	2877	1148	2835	1278	2917	963
S.D. (ft.)	53.6	33.9	53.3	35.7	54.0	31.0
Correlation	.440	.446	.104	.391	.209	.414
Regression coefft.	.21	.29	.04	.27	.11	.29
700 - 500 mb						
Mean tendency (ft)	-.5	-.3	-1.2	-.8	-.6	.5
Variance (sq. ft.)	781	599	754	485	947	579
S.D. (ft.)	27.9	24.5	27.5	22.0	30.8	24.1
Mean hodograph cpt	8.7	-.4	.5	3.3	10.7	2.2
Variance (sq. ft.)	2906	1116	1715	1062	2164	863
S.D. (ft.)	53.9	33.4	41.4	32.6	46.5	29.4
Correlation	.46	.57	.20	.50	.49	.45
Regression coefft.	.24	.42	.13	.34	.32	.37

/This

This table shows many features of interest. The correlations between tendency and hodograph component are noticeably below those between the tendency and the advective component. Further, these correlations vary a good deal among themselves, and being based each on 500 to 700 observations, there is no doubt that these variations are significant. There is a suggestion, falling short of statistical significance, that the correlation tends to be higher in the summer half-years than in the winter half-years. Turning now to the mean values, it appears that while the mean tendency over a six months period is always very small, the hodograph component has in the 1000 - 700 mb layer a mean positive value ranging from 21.6 ft to 37.0 ft in the winter, and from 12.8 ft to 18.6 ft in the summer. In other words at both these stations, and at all seasons of the year, the wind shows an average veer with height in the layer 950 - 700 mb. It has been seen already that at Downham Market in the period October, 1945 to March, 1946 the advective component had a small positive value (about 3 ft.) in the 1000 - 700 mb layer, so that the excess of the hodograph component (21.6 ft) over this must be neutralised by the secondary advective component. It is not surprising that the hodograph component should show the very poor correlation with the tendency which in fact occurs.

The standard deviation of the thickness tendency is slightly larger in winter than in summer, that of the hodograph component is in all cases much larger still. To sum up, in winter the hodograph component has a large positive bias in the lower layer, a large variance, and a low correlation with the tendency, while in summer it has a smaller positive bias in the lower layer, a smaller variance and perhaps a slightly higher correlation with the tendency. It may therefore be stated that the "hodograph" component though smaller in magnitude in summer, is then a more reliable indicator of thermal change in the troposphere than it is in winter.

4.2.4. The regression coefficient by which the departure of the "hodograph" component frim its mean must be multiplied to give the best estimate of the thickness tendency, is also stated in Table 1. The value of this coefficient varies considerably from one period to another, and the three years data suggests that over a much longer period, the mean value would be perhaps .20 for the 1000 - 700 mb layer and .30 for the 700 - 500 mb layer.

If, however, a regression equation using the long term regression coefficients is used for forecasting, it will, when the results are considered over a six months period, suffer from imprecision not only because of the low correlation, but also because the long term regression coefficient differs from the appropriate six months value. If the relative residual variance is worked out (following Section 3.5.2.) of the estimate involving the long term regression coefficient (the best value available before the event) it will be found nearly always to exceed .9, and sometimes to exceed unity. Hence we conclude that no estimate, based only on the measured "hodograph" component provides a worthwhile amount of information as to the thickness tendency.

4.2.5. In Rossby's work already quoted, the "hodograph" component is used to obtain the correction for temperature change in an air column to enable the pressure tendency at 10,000 feet to be obtained from the surface pressure tendency. (See, e.g. Univ. Chic. Inst. Met, Misc. Rep. No. 1, equation 12, which is equivalent to a simplified form of our equation (25) in Appendix A. This is equivalent to using the inexact regression equation.

$$T^{+} = h^{+} \qquad (12)$$

instead of that embodying the long term regression coefficient. Since for each period, using the values in Table 1, $2r\,\sigma_u < \sigma_e$ it appears, following section 3.5.2. that an estimate by Rossby's equation is worse than useless in each of the six monthly periods here considered. The adjustment to the pressure tendency based on equation (12) introduces, on the average, larger errors than those involved in ignoring temperature

change altogether. This does not, of course, rule out the possibility that Rossby's treatment may be applicable in some special situations (which a synoptic meteorologist may be able to recognise) but is a powerful argument against its indiscriminate or unthinking use.

4.2.6. An examination of graphs in which total tendency and hodograph component are plotted side by side shows that the correlation between the two is not uniformly bad, but that there are periods of time, ranging from 12 hours to six days, where the correlation is noticeably lower than at other times. These periods are characterised in the 1000 - 700 mb layer by a large positive "hodograph" component and a much smaller, often negative, tendency. The question of recognising these periods, which appear to be associated with special types of synoptic situation, is to receive further attention. In the meantime, their existence shows that the indications of the "hodograph" component, or qualitatively, the wind veering or backing with height, are most suspect when they are most striking. A wind veering or backing slightly with height may throw some light on thermal change, whereas a large veering or backing throws none.

5. Conclusion.

5.1. Judging by the data here used, the advective component, taken by itself, does not afford a satisfactory estimate of the thickness tendency. On the contrary, the changes due to advection are largely offset by those due to non-advective processes, so that the resultant thermal change appears as a small residual. These conclusions apply even more strongly to the "hodograph" component, which taken by itself, provides at best very little information as to the thickness tendency. Further even that little is not a constant, but varies a good deal from one six monthly period to another.

5.2. In current synoptic practice a forecast thickness chart is based partly on an estimation of the effect of advection and the other physical processes in changing the existing thickness pattern, and partly on empirical knowledge of the behaviour of thickness patterns. The present work does not relate to such estimates of thickness change, into which many considerations enter, but it does show that satisfactory prognostic charts cannot be constructed on the basis of advection alone. The need for investigating the non-advective processes is clearly underlined.

/Appendix A.

Appendix A.

The Components of the Thickness Tendency.

1. The Basic Equation.

1.1. We have first to consider the changes in thermal energy of a unit air mass, which changes its position, pressure and temperature. The assumption is made, not implicit in the argument, that the part played by water vapour, except as a provider of latent heat, is negligible. The energy balance can then be found for the dry air, with a reduction in the complexity of the equations. It is worth noting that the energy involved under atmospheric conditions in changes of the Kinetic energy of moving air is hardly large enough to count in the balance of heat energy, (but the following analysis does not assume it negligible).

1.2. The following two paragraphs follow the well-known paper by Brunt (Q.J. Vol. 59, p. 351. 1933). The symbols, except where otherwise defined, have their usual meanings, as in Brunt's Physical and Dynamical Meteorology. Consider a unit air mass at the beginning (t) and at the end ($t + \delta t$) of a short interval of time and let the operator δ denote the change of the quantity operated on during this interval. Denote by Q the heat energy per unit air mass. Then, if the air is unsaturated the energy balance is expressed by

$$\delta Q = c_p \delta T - \frac{A}{\rho} \delta p \qquad \ldots\ldots\ldots (1)$$

Here δQ appears as the heat supplied to the air from outside during the interval, and vanishes if the process is adiabatic. If the air is saturated, then Lx, the latent heat energy of the contained water vapour, is a function of temperature and pressure, and if, now, δQ is regarded as heat supplied from outside other than latent heat of condensation we have, for any process in which the air is and remains saturated

$$\delta Q - \delta(Lx) = c_p \delta T - \frac{A}{\rho} \delta p \qquad \ldots\ldots\ldots (2)$$

and since $x = \frac{\epsilon e}{p - e}$

$$\delta Q - \epsilon \delta\left\{\frac{Le}{p - e}\right\} = c_p \delta T - \frac{A}{\rho} \delta p \qquad \ldots\ldots\ldots (3)$$

If we regard ϵ as vanishing when the air is unsaturated, this equation covers both dry and saturated processes.

/1.3

1.3. When heat is being supplied from outside, the variables p and T, which enter into $\delta\left(\frac{Le}{p-e}\right)$ are independent, so that

$$\delta\left(\frac{Le}{p-e}\right) = \frac{\partial}{\partial T}\left(\frac{Le}{p-e}\right)\delta T + \frac{\partial}{\partial p}\left(\frac{Le}{p-e}\right)\delta p \quad \ldots\ldots (4)$$

assuming now, that L does not depend on p and expanding

$$\delta\left(\frac{Le}{p-e}\right) = \left\{\frac{e}{p-e}\frac{\partial L}{\partial T} + \frac{p}{(p-e)^2}\frac{\partial e}{\partial T}\right\}\delta T - \frac{Le}{(p-e)^2}\delta p \quad \ldots\ldots (5)$$

substituting in eqn. (3) gives

$$\delta Q = \left\{c_p + \epsilon\left(\frac{e}{p-e}\frac{\partial L}{\partial T} + \frac{L\,p}{(p-e)^2}\frac{\partial e}{\partial T}\right)\right\}\delta T - \left\{\frac{A}{\rho} + \frac{\epsilon\, Le}{(p-e)^2}\right\}\delta p \quad \ldots\ldots\ldots (6)$$

subject to the initial assumptions, this equation is quite general, and can be applied, in particular, to an air element having no horizontal motion or vertical acceleration which undergoes a small upward displacement δz. If $\delta Q = 0$ the air will, if saturated, cool at the saturated adiabatic lapse rate Γ_s, and under these conditions $\delta T = -\Gamma_s \delta z$, $\delta p = -g\rho\,\delta z$, so that equation (6) gives

$$0 = \left\{c_p + \epsilon\left(\frac{e}{p-e}\frac{\partial L}{\partial T} + \frac{L\,p}{(p-e)^2}\frac{\partial e}{\partial T}\right)\right\}\Gamma_s - g\left\{A + \rho\frac{\epsilon\, Le}{(p-e)^2}\right\} \quad \ldots\ldots\ldots (7)$$

This method was in fact used by Brunt (Q.J. Vol. 59 p. 351, 1933) and Bannon (Q.J. Vol. 74 p. 161 1948) to compute the saturated adiabatic lapse rate. If the air is assumed dry, then equation (6) gives, of course, $c_p\Gamma = gA$. Writing c_p' for the coefficient of Γ_s in equation (7), and substituting for the final term in equation (6) gives

$$\frac{\delta Q}{c_p'} = \delta T - \frac{\Gamma_s}{g\rho}\delta p \quad \ldots\ldots\ldots (8)$$

1.4. This section is concerned mainly with the geometry of the moving air element. Take rectangular axes, x being directed to East, y to North and z vertically upwards, with origin in latitude ϕ (positive in the northern hemisphere) at the initial position of the air element. If w is the angular velocity of the earth, take $2\omega\sin\phi = \lambda$, $2\omega\cos\phi = \mu$. Take u, v, w the components of the air velocity relative to these axes, $\underline{v}$ the horizontal wind vector and $\underline{i}$, $\underline{j}$, $\underline{k}$, unit vectors directed along the

co-ordinate axes. Denote by grad the horizontal gradient of any quantity, and let suffix p, as in grad_p or $(\partial T/\partial t)_p$ mean that the operation in question is to be performed following an isobaric surface. Let H be the height of the isobaric surface, which initially passes through the origin

$$\text{Let } g' = g - \mu u + \frac{dw}{dt} \quad \ldots\ldots\ldots (9)$$

Then the equations of frictionless atmospheric motion are

$$\frac{d\underline{v}}{dt} + \lambda\, \underline{k} \times \underline{v} + \mu w \underline{i} = -\frac{1}{\rho} \text{grad } p \quad \ldots\ldots\ldots (10)$$

$$\text{and} \qquad 0 = -\frac{1}{\rho}\frac{\partial p}{\partial z} - g' \quad \ldots\ldots\ldots (11)$$

$$\text{Also} \qquad \text{grad } p + \text{grad } H \frac{\partial p}{\partial z} = 0 \quad \ldots\ldots\ldots (12)$$

$$\text{so that} \qquad \text{grad } p - g'\rho \text{ grad } H = 0 \quad \ldots\ldots\ldots (13)$$

and we have the relation between operators

$$\text{grad} + \text{grad } H \frac{\partial}{\partial z} = \text{grad}_p \quad \ldots\ldots\ldots (14)$$

Now define w' to be the vertical velocity of the air relative to the isobaric surface, and w'' the vertical velocity of the isobaric surface. Then

$$\delta T = \left(\frac{\partial T}{\partial t}\right)_p \delta t + \underline{v} \cdot \text{grad}_p T\, \delta t + w' \frac{\partial T}{\partial z} \delta t \quad \ldots\ldots\ldots (15)$$

$$\delta p = -g'\rho w'' \delta t \quad \ldots\ldots\ldots (16)$$

$$\text{and} \qquad w = w' + w'' + \underline{v} \cdot \text{grad } H \quad \ldots\ldots\ldots (17)$$

If, now, we substitute from eqns. (15) and (16) in equation (8), and proceed to the limit when δt is indefinitely small, and make the convention that c_p^+, Γ^+ stand for c_p, Γ when the process is dry, and for c_p', Γ_s when the process is saturated, we have

$$\frac{1}{c_p^+}\frac{dQ}{dt} = \left(\frac{\partial T}{\partial t}\right)_p + \underline{v} \cdot \text{grad}_p T + w'\left(\frac{\partial T}{\partial z} + \Gamma^+\right) + \frac{g' - g}{g} w'\Gamma^+ \quad \ldots\ldots\ldots (18)$$

1.5. We now turn to the dynamics of the air motion. Differentiating equation (10) partially with respect to p, keeping x and y constant, gives

$$\frac{\partial}{\partial p}\left(\frac{d\underline{v}}{dt}\right) + \lambda \underline{k} \times \frac{\partial \underline{v}}{\partial p} + \mu \frac{\partial w}{\partial p} \underline{i} = -\frac{\partial}{\partial p}\left(\frac{1}{\rho} \text{ grad } p\right) \quad \ldots\ldots\ldots\ldots (19)$$

Now, remembering that $p = R\rho T$ we have, omitting some algebra,

$$-\frac{\partial}{\partial p}\left(\frac{1}{\rho} \text{ grad } p\right) = \frac{1}{g'\rho} \frac{\partial}{\partial z} (RT \text{ grad log } p) \quad \ldots\ldots\ldots\ldots (20)$$

$$= \frac{R}{p} \text{ grad}_p T - \frac{1}{g'\rho} \text{ grad } g'$$

Hence

$$\frac{\partial}{\partial p}\left(\frac{d\underline{v}}{dt}\right) + \lambda \underline{k} \times \frac{\partial \underline{v}}{\partial p} + \mu \frac{\partial w}{\partial p} \underline{i} + \frac{1}{g'\rho} \text{ grad } g' = \frac{R}{p} \text{ grad}_p T \quad \ldots\ldots\ldots (21)$$

This is the full form of the 'thermal wind' equation.

1.6. Now let H_1 H_2 be the heights of the isobaric surfaces for which the pressures are p_1, p_2 $(p_1 > p_2)$. Then the thickness tendency, for this layer, is

$$\frac{\partial}{\partial t}(H_2 - H_1) = \frac{\partial}{\partial t} \int_{p_2}^{p_1} \frac{\partial H}{\partial p} \, dp \quad \ldots\ldots\ldots\ldots (22)$$

$$= \int_{p_2}^{p_1} \left(\frac{\partial}{\partial t}\right)_p \left(\frac{1}{g'\rho}\right) dp \quad \ldots\ldots\ldots\ldots (23)$$

Now

$$\left(\frac{\partial}{\partial t}\right)_p \frac{1}{g'\rho} = \left(\frac{\partial}{\partial t}\right)_p \frac{RT}{g'p}$$

$$= \frac{R}{pg'} \left(\frac{\partial T}{\partial t}\right)_p - \frac{1}{pg'^2} \left(\frac{\partial g'}{\partial t}\right)_p \quad \ldots\ldots\ldots\ldots (24)$$

Substituting from equation (30) for $(\partial T/\partial t)_p$ gives

$$\left(\frac{\partial}{\partial t}\right)_p \frac{1}{g'\rho} = \frac{R}{pg'} \left\{ \frac{1}{c_p^+} \frac{dQ}{dt} - \underline{v} \cdot \text{grad}_p T - w' \left(\frac{\partial T}{\partial z} + \Gamma^+\right) \right.$$

$$\left. + \frac{g' - g}{g} w' \Gamma^+ \right\} - \frac{1}{\rho g'^2} \left(\frac{\partial g'}{\partial t}\right)_p \quad \ldots\ldots (25)$$

/The

The work so far has been without approximation and can be continued in like manner. The following equations have, however, been simplified by the omission of terms on the right hand side which under atmospheric conditions are insignificant. Substituting from equation (25) in equation (23) gives

$$\frac{\partial}{\partial t}(H_2 - H_1) = -\frac{R}{g}\int_{p_2}^{p_1} \frac{1}{p}\,\underline{v} \cdot \mathrm{grad}_p\, T\, dp$$

$$- \frac{R}{g}\int_{p_2}^{p_1} \frac{w'}{p}\left(\frac{\partial T}{\partial z} + \Gamma^+\right) dp + \frac{R}{g}\int_{p_2}^{p_1} \frac{1}{p\, c_p^+}\frac{dQ}{dt}\, dp \qquad \ldots\ldots\ldots\ldots (26)$$

which, if the first term is expanded by substitution from equation (21) becomes

$$\frac{\partial}{\partial t}(H_2 - H_1) = \frac{\lambda}{g}\underline{k}\int_{p_2}^{p_1} \underline{v} \times \frac{\partial \underline{v}}{\partial p}\, dp - \frac{1}{g}\int_{p_2}^{p_1} \underline{v} \cdot \frac{\partial}{\partial p}\left(\frac{d\underline{v}}{dt}\right) dp$$

$$- \frac{R}{g}\int_{p_2}^{p_1} \frac{w'}{p}\left(\frac{\partial T}{\partial z} + \Gamma^+\right) dp + \frac{R}{g}\int_{p_2}^{p_1} \frac{1}{p\, c_p^+}\frac{dQ}{dt}\, dp \qquad \ldots\ldots\ldots\ldots\ldots (27)$$

These are the fundamental equations for the thickness tendency. They apply to the tropics as well as to temperate and polar regions.

1.7. Before discussing these equations, it is appropriate to consider the approximations, which they involve. If the substitution into equation (23) is carried out in full, there will appear additional terms on the right hand side of equations (25) and (26) which may easily be shown to be small, under atmospheric conditions, in comparison with the terms retained. Only one case will be considered, to show the questions which arise, namely, the substitution of g' by g wherever it occurs. By definition,

$$g' = g + \mu u + \frac{dw}{dt} \qquad \ldots\ldots\ldots\ldots\ldots (9)$$

Now, using c.g.s. units, the value of μ varies from 1.46×10^{-4} at the equator to zero at the poles, while u has typical values of say, 30 knots, or 1560 cm/sec and extreme values of 10,000 cm/sec. As for $\frac{dw}{dt}$, the value of w in large scale atmospheric processes (not of course, in convective phenomena) may be taken to lie between $\pm$ 10 cm/sec. Thus while $\frac{dw}{dt}$ may have a large value over a short period of time, its

/mean

mean value over six hours is of the order of 10^{-2}. Thus the three elements in g^1 are of order 10^3, 10^0, 10^{-2} respectively, and the second and third may without hesitation be neglected in comparison with the first. Where two approximate quantities, of which only the mean values are known to be small, enter into one integral, it is not impossible that a preferential combination of instantaneous values should produce a significant value although the product of the mean values is negligible. This possibility should not be overlooked in view of the contribution by Priestley and Swinbank to the theory of turbulence, which is founded on a similar argument (Proc. Roy. Soc. London, A. 189 p.543 1947) but in view of the absence in our present context, of any physical reason to expect it, it may be regarded rather as an escape clause, deserving attention only if after full investigation, the more obvious mechanisms fail to account for the facts.

2. The Significant Components of the Thickness Tendency.

2.1. To have a standard of comparison, we may note that the mean square value of the refined 6-hour thickness tendency at Downham Market during the 6 months October, 1945 to March, 1946 was 22.6 ft. for the 1000 - 700 mb. layer, and 28.5 feet for the 700 - 500 mb. layer. The three terms on the right hand side of equation (26) are called, respectively, the advective, dynamic and non-adiabatic components of the thickness tendency. The first forms the main subject of this note, and will not be further discussed here, but the second and third, which are to be investigated later, deserve some preliminary mention in order to provide the practical analyst with some metrical background pending the results of a full investigation.

2.2. The dynamic component $$- \frac{R}{g} \int_{p_2}^{p_1} \frac{w'}{p} \left(\frac{\partial T}{\partial z} + \Gamma^+ \right) dp$$

Taking $\partial T/\partial z + \Gamma^+ = 2°F$ per 1000 feet, and $w' = 4$ cm/sec. (a value agreeing with those found by Petterssen, Sheppard, Priestley and Johannssen (Q.J. Vol. 73 p. 57)) gives a 6-hour tendency of 108 feet per 6 hours in the 1000 - 700 mb layer, and 102 feet per six hours for the 700 - 500 mb. layer. These values are typical of active subsidence, and the resulting component of the thickness tendency is significant. With ascending air, and similar values of w', the term will remain significant so long as $\partial T/\partial z + \Gamma^+$ has the assumed value. When, however, condensation takes place, the value of $\frac{\partial T}{\partial z} + \Gamma_s$ will usually be much less than 2°F per 1,000 ft and the dynamic component may then be insignificant.

2.3. The non-adiabatic component $$\frac{R}{g} \int_{p_2}^{p_1} \frac{1}{p\, c_p^+} \frac{dQ}{dt}\, dp$$

The atmosphere gains heat from the sun, either by direct absorption, or indirectly, from the ground or sea surface, and loses it by radiation, directly from the clear air or a cloud top, or indirectly, via a radiating ground surface. Heat is transferred within the atmosphere, or from or to a surface acting as a heat source or sink, by radiative, turbulent and convective diffusion. All these processes lead to the gain or loss of heat by the individual air element, and contribute to the non-advective component of the thickness tendency. Of these processes, the only one likely to operate in saturated air is the cooling of a cloud mass by turbulent mixing when the cloud-top is losing heat by radiation. Only here, then, is c_p^+ likely to have the saturated value,

$$c_p' = c_p + \epsilon \left\{ \frac{e}{p - e} \frac{\partial L}{\partial T} + \frac{Lp}{(p - e)^2} \frac{\partial e}{\partial T} \right\}$$

/The

The value of c_p', which necessarily exceeds c_p varies with temperature and pressure, and can be calculated from the table given by Brunt (Q.J. Vol. 59 p. 355). At low temperatures the ratio $\frac{c_p'}{c_p}$ is almost unity, but it increases with rise of temperature and fall of pressure. Under temperate conditions its value is unlikely to exceed 4. This effect has not yet been examined, its contribution to the thickness tendency must be of the same order of magnitude as that due to radiative cooling at the ground surface discussed in para. 2.5.

2.4. Of the other non-adiabatic processes, which take place in unsaturated air, the most important in temperate latitudes is the warming of cold air masses over the sea. This process has been investigated by myself, and is discussed in a paper now being prepared for publication. It appears that when an arctic air current crosses the Gulf Stream in winter, a mean value of $\frac{1}{C_p}\frac{dQ}{dt}$ equal to 1°F per hour may persist throughout the 1000 - 700 mb. layer for over 24 hours. This corresponds to a component to the thickness tendency of 115 feet in 6 hours, which is evidently of major importance.

2.5. The effect of radiative cooling from the ground surface may be estimated by assuming that the earth loses one quarter of the black body radiation corresponding to the surface temperature, and that all the heat lost is taken from the air. On these assumptions, the component of the 6-hour thickness tendency due to radiative cooling at the ground is as follows:-

Surface temperature in °F	14	32	50	68
Component of 1000 - 700 mb. thickness tendency	-18 ft.	-21 ft.	-24 ft.	-27 ft.

This effect is less important than the preceding, and in much of the temperate zone, will be offset by insolation, but it is sufficient to explain the development during the polar night of cold pools of the intensity observed.

2.6. Finally, there is the question of direct insolation. It is natural to regard the diurnal variation of thickness demonstrated in Appendix B, section 7, as being due to the fluctuating balance between insolation which is an intermittent process, and radiation which is continuous. On this view the component of the 1000 - 700 mb. thickness tendency due to insolation in England during a summer afternoon must be of the order of +60 ft., and so capable of causing a significant change in thickness whenever the offsetting radiative loss is reduced, e.g. by the spreading of frontal cloud during the night. As regards tropical insolation, it may be observed that when a cold air mass is being warmed over the sea, the energy flux per sq. cm. of sea surface is of the order of half the solar constant (1.94 calories per s. cm. per minute) and that this amount of energy is about what can be made available by direct insolation. It is therefore to be expected that a contribution to the thickness tendency exceeding 100 feet in 6 hours can arise by tropical insolation.

3. Further Resolution of the Advective Component.

3.1. The "Hodograph" Component.

The transition from equation (26) to equation (27) is made by means of the "thermal wind" equation. The first term of equation (27) may be recognised as proportional to the area enclosed by the hodograph of the vector $\underline{v}$ between the vectors corresponding to the top and bottom of the layer concerned. If $\underline{v}_1$, $\underline{v}_2$ are the winds at pressures p_1, p_2, and the direction of $\partial\underline{v}/\partial p$ is the same throughout the layer, then

/If

$$\frac{\lambda}{g}\,\underline{k}\int_{p_2}^{p_1}\underline{v}\times\frac{\partial\underline{v}}{\partial p}\,dp \;=\; \frac{\lambda}{g}\,\underline{k}\,\underline{v}_1\times(\underline{v}_1-\underline{v}_2) \qquad \ldots\ldots\ldots (28)$$

If now, we take v_1 = 30 knots, $\underline{v}_1 - \underline{v}_2$ = 20 knots in a direction at right angles, and $\lambda = 1.12 \times 10^{-4}$ (corresponding to latitude 50°) then the contribution to the thickness tendency is 130 feet in 6 hours. This is of course, significant but near the equator the term will be negligible, owing to the small value of λ .

3.2. The Secondary Advective Component.

The remaining term $-\frac{1}{g}\int_{p_2}^{p_1}\underline{v}\cdot\frac{\partial}{\partial p}\left(\frac{d\underline{v}}{dt}\right)dp$ which we call the secondary advective component, is the difference between the advective component originally discussed and the "hodograph" component. This component, which depends on the acceleration of the air, will vanish if $d\underline{v}/dt = 0$ (the case of geostrophic wind) or if $\frac{\partial}{\partial p}\left(\frac{d\underline{v}}{dt}\right) = 0$. If we write $\underline{v} = \underline{v}_g + \underline{v}_a$ where $\underline{v}_g$ is the geostrophic wind, then

$$-\frac{1}{g}\int_{p_2}^{p_1}\underline{v}\cdot\frac{\partial}{\partial p}\left(\frac{d\underline{v}}{dt}\right)dp \;=\; \frac{\lambda}{g}\,\underline{k}\int_{p_2}^{p_1}\underline{v}\times\frac{\partial\underline{v}_a}{\partial p}\,dp \qquad \ldots\ldots\ldots (29)$$

Now, bearing in mind that $\underline{v}$ does not usually change direction very much in layers of the depth considered, it appears that if the secondary advective tendency is to be large, the mean value of $\partial\underline{v}_a/\partial p$ across the mean wind direction must be large. This points to large values of the secondary advective tendency as arising when the airflow across the isobars varies with height, i.e. it is associated with a wind differing from the geostrophic in direction rather than in speed.

3.3. The magnitude of the secondary advective component cannot be estimated directly but only by measuring the difference between the advective component and the "hodograph" component. A preliminary investigation shows that it is generally small, but that sometimes very large values occur, and persist for several observations (e.g. a value of 200 feet per 6 hours persisting for 30 hours). The significance of these exceptional periods, which go some way to explaining the poor correlation found between the "hodograph" component and the thickness tendency, is to be examined further.

3.4. The values of the individual terms discussed in Appendix A Section 2.2. to 2.6. are strikingly large compared with the mean square value of the thickness tendency quoted in Appendix A section 2.1. and suggest that generally when conditions favour a large value of one term its contribution is offset by those of the other terms, so that the resultant thickness tendency is only a residual. This suggestion agrees with the conclusion concerning advective processes reached in Section 4.1.6.

/Appendix B.

Appendix B.

1. Introduction.

1.1. Sections 2.1. to 5.3. which are concerned with the elimination of errors of observation, the following notation will be used. The value of a quantity actually observed or calculated from actual observation, will be denoted by a small letter, and the true value of the same quantity by the corresponding capital. The letters ϵ, α will denote the non-persistent errors of observation.

2. Measurements of Total Tendency.

2.1. The actual measurements are of thicknesses θ_1, θ_2, .. θ_n Let the observational error be ϵ_n so that

$$\theta_n = \Theta_n + \epsilon_n \qquad \ldots\ldots\ldots\ldots (1)$$

then if t_n is the tendency measured as in Section 3.2.2.

$$t_n = T_n + \frac{\epsilon_{n+2} - \epsilon_{n-2}}{4} \qquad \ldots\ldots\ldots (2)$$

and

$$t^+_{n+1/2} = T^+_{n+1/2} + \frac{\epsilon_{n+3} + \epsilon_{n+2} - \epsilon_{n-1} - \epsilon_{n-2}}{8} \qquad \ldots\ldots\ldots (3)$$

Now the series $\epsilon_1, \epsilon_2, \ldots \epsilon_n$ is entirely haphazard, and shows no serial correlation, and further, shows no correlation with the series of true values. Hence, if equation (3) is squared, and summed over a number of terms, N, large enough to make negligible any spurious correlations due to sampling,

$$\frac{1}{N}\sum(t^+_{n+1/2})^2 = \frac{1}{N}\sum(T^+_{n+1/2})^2 + \frac{1}{16N}\sum(\epsilon_n)^2 \qquad \ldots\ldots (4)$$

Or, if we write $V(t^+_{n+1/2})$ for the variance of $t^+_{n+1/2}$

$$V(t^+_{n+1/2}) = V(T^+_{n+1/2}) + \frac{1}{16}V(\epsilon_n) \qquad \ldots\ldots\ldots\ldots (5)$$

Squaring equation (2) we have

$$V(t_n) = V(T_n) + \frac{1}{8}V(\epsilon_n) \qquad \ldots\ldots\ldots\ldots (6)$$

/and

and if we write $\text{cov}\,(t_n, t_{n+1})$ for the covariance of t_n and t_{n+1}

$$\text{cov}\,(t_n, t_{n+1}) = \text{cov}\,(T_n, T_{n+1}) \quad \ldots\ldots\ldots\ldots (7)$$

and generally, for $s \neq 4$

$$\text{cov}\,(t_n, t_{n+s}) = \text{cov}\,(T_n, T_{n+s}) \quad \ldots\ldots\ldots\ldots (8)$$

but for $s = 4$

$$\text{cov}\,(t_n, t_{n+4}) = \text{cov}\,(T_n, T_{n+4}) - \frac{1}{16} V(\epsilon_n) \quad \ldots\ldots (9)$$

2.2. Denoting by r_s the serial correlation between terms s apart,

$$r_s = \frac{\text{cov}\,(t_n, t_{n+s})}{V(t_n)} \quad \ldots\ldots\ldots\ldots (10)$$

It is apparent from equations (6), (8) and (9) that the effect of the presence of observational error is to reduce all serial correlations except the fourth in the same ratio, and to reduce the fourth serial correlation even more.

3. The Evaluation of $V(\epsilon_n)$

3.1. The observational errors of the radio-sonde have been studied by Prof. P.A. Sheppard, whose results are published in an official memorandum (S.D.T.M. No. 75, Part VII). Interpolating, we estimate a probable error of ± 11.6 ft. for a computed value of the thickness from 1000 - 700 mb. and ± 20.0 ft. for a computed value of the thickness from 700 - 500 mb. The value of $V(\epsilon_n)$ (the square of the standard deviation) has accordingly been taken as 296 sq. ft. for the 1000 - 700 mb. layer and 900 sq. ft. for the 700 - 500 mb. layer. An alteration of 10% in the estimated value of $V(\epsilon_n)$ would alter the estimate of $V(T_n^+)$ by less than $\frac{1}{2}\%$.

4. Measurement of the Advective Component.

4.1. The measurement of the advective component $a = -\frac{R}{g} \text{grad}_p T \int_{p_2}^{p_1} \frac{v}{p}\, dp$ is subject to observational error α

$$a_n = A_n + \alpha_n \quad \ldots\ldots\ldots\ldots\ldots (11)$$

Thus following para. 3.

$$a^+_{n+1/2} = A^+_{n+1/2} + \frac{\alpha_{n-1} + \alpha_n + \alpha_{n+1} + \alpha_{n+2}}{4} \quad \ldots\ldots (12)$$

/Hence

Hence, squaring, summing and dividing by N

$$V(a^{+}_{n+1/2}) = V(A^{+}_{n+1/2}) + \frac{1}{4} V(a_n) \quad \ldots\ldots\ldots\ldots\ldots (13)$$

5. The Evaluation of $V(a_n)$

5.1. The measurement of the advective component has been described in section 2.2.1. to 2.2.3. The basic measurement most open to doubt is that of the magnitude and direction of the thermal gradient. What was done was to consider the analysed upper air chart, and decide, (on the basis of the analysis and observations) on the direction in degrees and spacing in miles of thickness lines differing by 100 ft. which enclosed the station in question.

5.2. The estimation which I did myself is easy in strong thermal gradients and difficult in weak, particularly as regards the direction. My impression is that I could nearly always estimate a moderate gradient to within 25% of its true value, and that my estimate of direction would be in error by less than 5 degrees in strong winds, but by 20° or more in weak. An error in the direction taken for the thermal gradient involves an error in the resolved component of wind and my impression is that this error was usually less than 4 knots.

5.3. Consider now an occasion when the thickness gradient was 250 miles per 100 ft. and the mean resolved component of wind as 8 knots, both typical values. Suppose (a) that the estimated gradient was 300 miles per 100 ft. and mean wind component 4 knots, and (b) that the estimated gradient was 200 miles per 100 feet and mean wind component 12 knots. The computed advective component is 9.2 ft. on supposition (a) and 41.5 ft on supposition (b). The true value is 22.1 ft. so that the above errors, which are larger than usually appear, would produce a positive error of 19.4 ft. or a negative error of 12.9 ft. Hence, if we adopt 16 ft. as our estimate of the standard deviation of α , about 70% of observation will lie within $\pm$ 16 ft. of the true value which if anything probably exceeds the true scatter. We therefore adopt 256 sq. ft. as our estimate of $V(\alpha)$. The value of this estimate is a matter of personal opinion, but even if it were doubled, the general nature of the results would be unaltered. My own view is that it somewhat over-estimates the true error.

6. The Hodograph Component.

6.1. The measurement of the hodograph component is almost entirely objective, and the standard deviation of the observational error is very small, of the order of 5 - 10 ft. In view of the nature of the results obtained, no correction has been made for this.

7. The Diurnal Variation.

7.1. A subsidiary investigation was made to find whether the data showed any diurnal variation, and if so, to estimate the magnitude of such variation. The period before 1st January, 1948, when upper air soundings were made at 00, 06, 12 and 18 hours G.M.T. was treated separately from the period after, when the observations were made at 03, 09, 15 and 21 hours G.M.T. If any diurnal variation exists, it will be liable to be obscured on any particular occasion by casual observational errors, or by any large scale variations, such as the passage of warm sectors, which are out of phase with the diurnal variation. We can, however, reduce the effect of casual and large scale disturbances to any desired extent simply by finding the average change in thickness between given synoptic hours from sufficiently numerous observations. On the other hand, since the mean diurnal variation may be expected to change with the season and possibly with the synoptic situation, the long term average may differ from the value to be expected during a particular period.

/7.2.

7.2. To reconcile these requirements, the measurements of thickness of the 1000 - 700 mb and 700 - 500 mb layers were sorted according to their hour of origin, and average thicknesses were found, the periods covered by the averages being in turn, 5, 15, 30 and 60 days. These were subtracted each from the general mean thickness for the same period, and a table was constructed showing the average departure during each period of the thickness measured at a particular synoptic hour from the mean thickness for that period.

7.3. When the average was over five days, the departures showed no particular regularity, but the fifteen day averages showed considerable regularity. When 30 day averages were used, the magnitude of the departures in any period showed a fairly close resemblance to those for the succeeding and preceding periods. I concluded, therefore, that the data showed a diurnal variation, not casual in origin, of which the amplitude could be estimated from its average value during a period of about a month.

7.4. This diurnal variation shows a change in amplitude and character between winter and summer. There is also a suggestion that any abnormal features occur simultaneously at Larkhill and Downham Market. A full investigation of this variation is now in progress, but the results which are here important are shown in Fig. 3 which gives, for the four seasons, the mean departures of the thicknesses from the midnight (or 0300) values.

7.5. For the season October - December, three years data are available, (the observations being at 00, 06, 12, 18 hours G.M.T.) These show an oscillation of about 10 ft. amplitude in the 1000 - 700 mb thickness, with a maximum at 1200 or 1800 hours, and a similar oscillation in the 700 - 500 mb thickness with maxima at 1200 and 2400 hours. In the other three seasons, for which two years' data are available (the observations being at 03, 09, 15 and 21 hours G.M.T.) there is in both layers a well defined maximum at 1500 hours and a minimum at 0300 hours, (except that in the period January - March in the 1000 - 700 mb layer the minimum is at 0900 hours). The amplitude is greatest in the summer, and exceeds 30 ft. in the 1000 - 700 mb layer and 20 ft. in the 700 - 500 mb layer. The two stations agree well with one another, with Larkhill showing if anything the larger amplitude.

7.6. By comparison, the standard deviation of the refined thickness tendency (Section 3.2.2.) is only about 28 ft. for the 1000 - 700 mb layer and 30 ft. for the 700 - 500 mb layer, so that the tendency due to the diurnal variation is not insignificant even in winter, and of comparable magnitude in summer, with the tendency which produces large scale thickness changes. The need for eliminating the diurnal variation is thus demonstrated.

8. The Coherence of Meteorological Series.

8.1. The serial correlations of the refined thickness tendency (t, not t^+) were calculated for the Larkhill data for the periods Oct. 1947 - March 1948 and April 1948 - Sept. 1948. After correction for residual error, the correlations are as follows:-

October 1947 - March 1948

	r_1	r_2	r_3	r_4	r_5
1000 - 700 mb	.8197	.5067	.1590	-.1209	-.1527
700 - 500 mb	.8460	.5116	.1273	-.1650	-.2495

April 1948 - September 1948

	r_1	r_2	r_3	r_4	r_5
1000 - 700 mb	.4928	.1646	-.0147	-.2139	-.3007
700 - 500 mb	.8001	.4113	.1115	-.2245	-.3061

8.2. These correlations which are required in the following sections are interesting in themselves. Since r_4 is small and negative, they show that the thickness change in any 24 hour period affords almost no information regarding the change during the 24 hour period which begins where the former ends.

8.3. Since the formulae of interpolation and integration involve only the first serial correlation, r_1 this was calculated for all the data used, the values found being as follows:-

The first serial correlation used for interpolation of the tendency series, for 6-monthly periods.

	Larkhill		Downham Market			
	Oct.47 - Mar.48	Apr.48 - Sept.48	Oct.45 - Mar.46	Apr.46 - Sep.46	Oct.47 - Mar.48	Apr.48 - Sep.48
1000 - 700 mb	.8197	.4928	.8423	.8113	.8645	.7791
700 - 500 mb	.8460	.8001	.8119	.8380	.9013	.9840

The first serial correlation of the smoothed advective component for monthly periods used for integration.

	Oct.	Nov.	Dec.	Jan.	Feb.	Mar.	Total
1000 - 700 mb	.82	.93	.89	.92	.80	.90	.869
700 - 500 mb	.81	.87	.84	.82	.85	.85	.826

9. Partial Serial Correlations.

9.1. These have been calculated from the total serial correlations by means of the formula

$$r_s' = \frac{\begin{vmatrix} 1 & r_1 & r_2 & \cdots & r_{s-2} \\ r_1 & 1 & r_1 & \cdots & \\ \cdots & \cdots & \cdots & & \\ \cdots & \cdots & \cdots & & \\ r_{s-1} & r_{s-3} & \cdots & & 1 \end{vmatrix} r_s + \begin{vmatrix} 1 & r_1 & r_2 & \cdots & r_{s-2} & r_1 \\ r_1 & 1 & r_1 & \cdots & r_{s-3} & r_2 \\ \cdots & \cdots & \cdots & \cdots & \cdots & \\ r_{s-2} & \cdots & \cdots & \cdots & & \\ r_{s-1} & r_{s-2} & \cdots & r_1 & & 0 \end{vmatrix}}{\begin{vmatrix} 1 & r_1 & r_2 & \cdots & r_{s-2} & r_{s-1} \\ r_1 & 1 & r_1 & \cdots & r_{s-3} & r_{s-2} \\ \cdots & \cdots & \cdots & \cdots & \cdots & \\ r_{s-1} & \cdots & \cdots & r_1 & & 1 \end{vmatrix}}$$

This expression is a transformation of that given on p.371 of Vol.1 of Kendall's "Advanced Theory of Statistics". The partial serial correlations are found successively starting with

$$r_2' = \frac{r_2 - r_1^2}{1 - r_1^2}$$

If these determinants are evaluated by Chio's method, (see Calculus of Observations p.71, Whittaker, Robinson) starting always with the first row and column all the terms except those involving the final rows and columns will be found to have occurred earlier in the work. Some saving of labour is effected, and the work is reasonably easy to check.

/9.2.

9.2. Using this method, and the Larkhill data set out in Appendix B, section 8.1., the partial serial correlations are as follows:-

October, 1947 - March, 1948.

	N_1	N_2	N_3	N_4
1000 - 700 mb	.8197	-.5040	-.2156	-.0958
700 - 500 mb	.8460	-.7190	.0667	-.5228

April 1948 - September 1948

	N_1	N_2	N_3	N_4
1000 - 700 mb	.4928	-.1034	-.0319	-.2867
700 - 500 mb	.8001	-.6365	-.3836	

These results are discussed in Section 3.5.5. and in Appendix C section 2.3.

/Appendix C.

Appendix C.

1. The Reliability of the Formula of Integration.

1.1. Taking the synoptic interval as the interval of time (as in para. 26 of the main paper), the function to be estimated is

$$\int_{-1/2}^{1/2} u_{n+c}\, dc$$

and our estimate is u_n. If a large number N of such estimates is made, the correlation between observed and estimated values is

$$\sum u_n \int_{-1/2}^{1/2} u_{n+c}\, dc \Big/ \left\{ \sum u_n^2 \sum \left(\int_{-1/2}^{1/2} u_{n+c}\, dc \right)^2 \right\}^{1/2} \qquad \ldots\ldots\ldots\ldots\ldots\ldots (1)$$

and the regression coefficient of the true value on the estimate is

$$\sum u_n \int_{-1/2}^{1/2} u_{n+c}\, dc \Big/ \sum u_n^2 \qquad \ldots\ldots\ldots\ldots\ldots\ldots (2)$$

Now

$$\sum u_n \int_{-1/2}^{1/2} u_{n+c}\, dc \Big/ \sum u_n^2 = \int_{-1/2}^{1/2} \frac{\sum u_n u_{n+c}}{\sum u_n^2}\, dc \qquad \ldots\ldots\ldots (3)$$

Our definition of a lag correlation coefficient has so far been restricted by analogy with the first serial correlation of a time series. We now generalise this, and say that

$$r_c = \frac{\sum u_n\, u_{n+c}}{\left[\sum u_n^2 \sum u_{n+c}^2 \right]^{1/2}}$$

where the $\sum$ denotes summation over any succession of equally spaced values of u_n. We assume that this tends to a limit independent of the sample as the number of observations is increased. It is also part of our hypothesis that

$$\sum u_{n+c}^2 \Big/ \sum u_n^2$$

tends to unity as the number of observations is increased.

Thus the regression coefficient

$$= \int_{-1/2}^{1/2} r_c\, dc = 2 \int_{0}^{1/2} r_c\, dc \qquad \ldots\ldots\ldots\ldots (4)$$

/1.2.

1.2. To find the correlation coefficient we must express

$$\frac{1}{N}\sum\left\{\int_{-1/2}^{1/2} u_{n+c}\,dc\right\}^2 \quad \text{in terms of} \quad \frac{1}{N}\sum u_n^2$$

Suppose, now, that the unit time interval is divided into m equal parts.

Then $\int_{-1/2}^{1/2} u_{n+c}\,dc$ can be approached as closely as we please by

$$\frac{1}{m}\left(u_{n-1/2+1/m} + u_{n-1/2+2/m} + \cdots + u_{n+1/2}\right)$$

Therefore

$$\left\{\int_{-1/2}^{1/2} u_{n+c}\,dc\right\}^2 = \frac{1}{m^2}\left\{\sum_{s=1}^{m} u^2_{n-1/2+s/m} + 2\sum_{s=1}^{m-1} u_{n-1/2+s/m}\,u_{n-1/2+(s+1)/m} + \text{etc}\right\}$$

Now, performing a second summation over the N estimates making up the sample

$$\sum_N\left\{\int_{-1/2}^{1/2} u_{n+c}\,dc\right\} = \frac{1}{m^2}\sum_N u_n^2\left\{m + 2(m-1)\,r_{1/m} + 2(m-2)\,r_{2/m} + \text{etc}\right\} \quad \ldots\ldots (6)$$

$$= \sum u_n^2\left\{2 - 2\int_0^1 c\,r_c\,dc\right\} \quad \ldots\ldots (7)$$

Thus the required correlation between estimate and true value is

$$R = \frac{2\int_0^{1/2} r_c\,dc}{\left\{2 - 2\int_0^1 c\,r_c\,dc\right\}^{1/2}} \quad \ldots\ldots (8)$$

2. The Form of the Lag Correlation for Small Lag.

2.1. The study of the lag correlation coefficient appears to have been started by G.I. Taylor (Diffusion by Continuous Movements. Proc. Lond. Math. Soc. 20. 196. 1921). He showed that a function which satisfied certain conditions would have a lag correlation of the form

$$r_c = 1 - \frac{\lambda c^2}{2!} + \frac{\mu c^4}{4!} - \frac{\nu c^6}{6!} + \text{etc} \quad \ldots\ldots (9)$$

/Another

Another proof embodying different conditions by L.F. Richardson was included in the same paper and a third has been developed by the present author. These proofs are purely mathematical, and will hold provided that our meteorological functions satisfy the conditions laid down.

2.2. From the aspect of the theory of turbulence, interest attaches to the value of $\int_0^T r_c \, dc$ when T is large, and equation (9) does not seem applicable to this case. Taylor assumed that $\int_0^T r_c \, dc$ tended to a finite limit as T increased, and this assumption led to difficulties. In 1932, O.G. Sutton (Proc. Roy. Soc. A. 135, p.143. 1932) suggested that r_c varies as c^{-n} where $0 \leqslant n \leqslant 1$ and it has also been suggested by T.E.W. Schumann, (Phil. Mag. 1941) and others, that r_c varies as e^{-c}. These proposals were not made with any claim to mathematical rigidity and stand or fall by the observational evidence adduced in their support. Sutton's data, obtained by observation of shell bursts, does not, and is not claimed to fit his formula when C is small, (the discrepancy being attributed to disturbances due to the explosion). Our present data does not support it (Appendix C, Section 2.4.). Schumann criticises the derivation of Taylor's equation, and concludes that it does not apply to meteorological data. His criticism, however, though valid as the proof stands, can be avoided without much difficulty. The evidence for his own form, $r_c \propto e^{-c}$ is published in the Quarterly Journal. (The problem of auto-correlation of meteorological time series, illustrated by examples from some South African Stations.) His first type of example, a series of night minimum temperatures, does not constitute a time series at all in the sense here defined, because the observations are not at fixed intervals of time. His second class of data (hourly temperatures at Germiston) is of the special kind where the variance shows a systematic fluctuation with the hour of day, and again is outside the scope of this note. His series for two-hourly pressures at Kimberley are much more amenable to the treatment developed in this section than to that which he proposes.

2.3. This question has been considered in detail, because there appears to be a tendency to regard the "simple exponential law" as one to which a series in the absence of evidence to the contrary, may be expected to conform. Actually, if the "simple exponential law" applies, the second partial serial correlation of any time series obtained from this function must vanish, as was pointed out in 1921 by G.I. Taylor (ibid). Hence the vanishing of this correlation (to within limits of sampling error) is a necessary condition for the applicability of the "simple exponential law". In the series examined in this paper, the second partial serial correlation is always negative (see Appendix B Section 9.2) and the same applies to the series of two-hourly pressures at Kimberley published by Schumann-Hofmayer (ibid) and the series of pressures at Kew published by Sir G.T. Walker (on periods and symmetry points in pressure as aids to forecasting, Q.J. Vol. 72 Oct. 1946 p. 265). These examples show that the "simple exponential law" is not to be adopted without careful consideration, and in particular, that it does not apply to the data here used.

2.4. G.I. Taylor's equation leads to the conclusion that for small values of the lag the second partial serial correlation should approach -1, and the predominance of negative values suggests that the time intervals used (2 - 24 hours) may be small enough for the theorem to have some application. Since for small c, $r_c = 1 - ac^2$ where a is constant, the graph of a plotted against c must be parabolic near the origin. The actual observations, however, shown in Fig. 4 show very little suggestion of this, any more than they conform to the exponential form. If Sutton's form were applicable, the graph of log c plotted against $\log r_c$ should be a

straight line, but Fig. 5 offers little support for this. The data rather suggests that r_c is a linear function of c and in fact the form $r_c = 1 - c(1 - r_1)$ has been assumed for the present. Since the true form must be parabolic near the origin, it is expected that the true correlation is rather higher than the assumed value. It is not, of course, claimed or suggested that this expression of r_c is of universal application, but simply that it is reasonable for use with the present body of data.

G. 248365/DS/11/49/40.

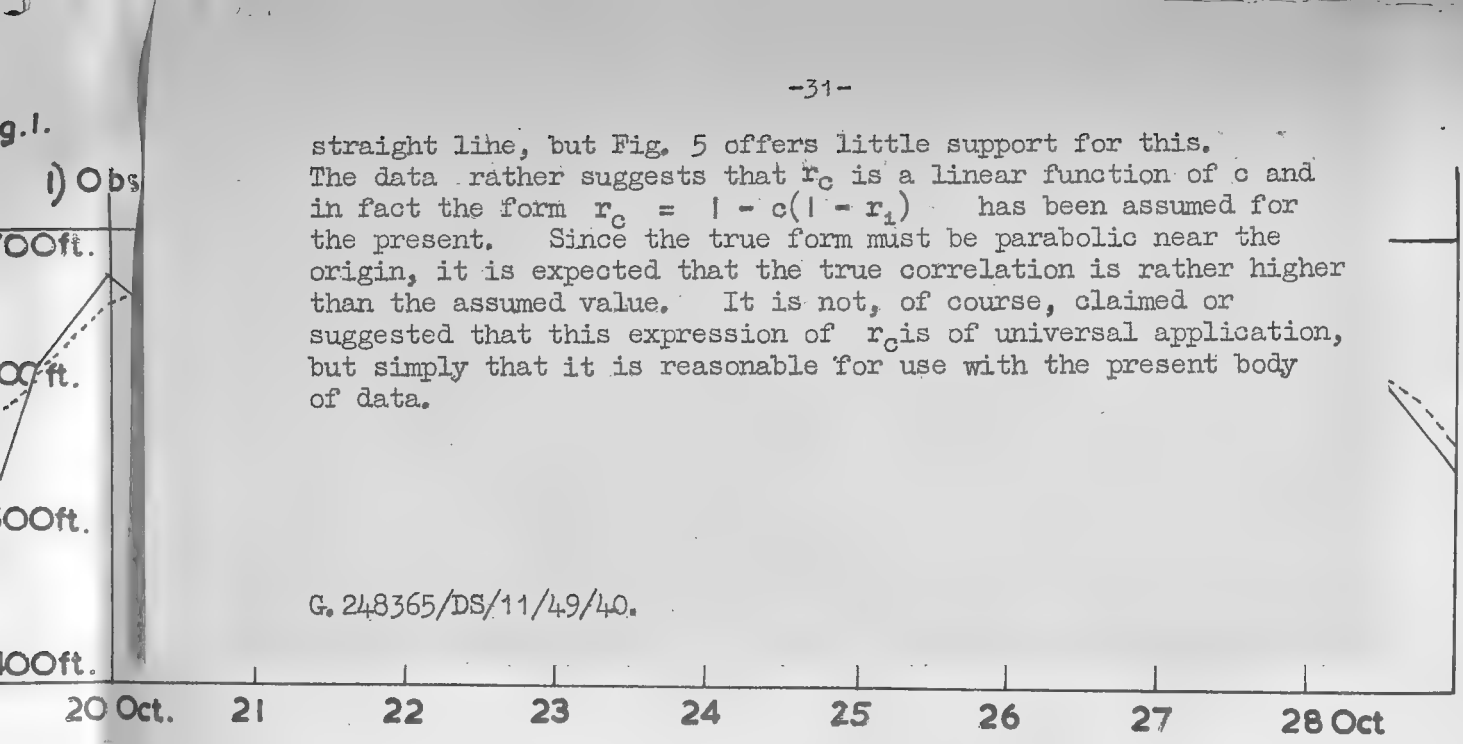

Fig. 2. Corresponding values of the thickness tendency, and advective and "hodograph" components for Downham Market for the 1000-700 mb. layer for October 20-28th 1945, exemplifying the abnormal "hodograph" component in the section BC.

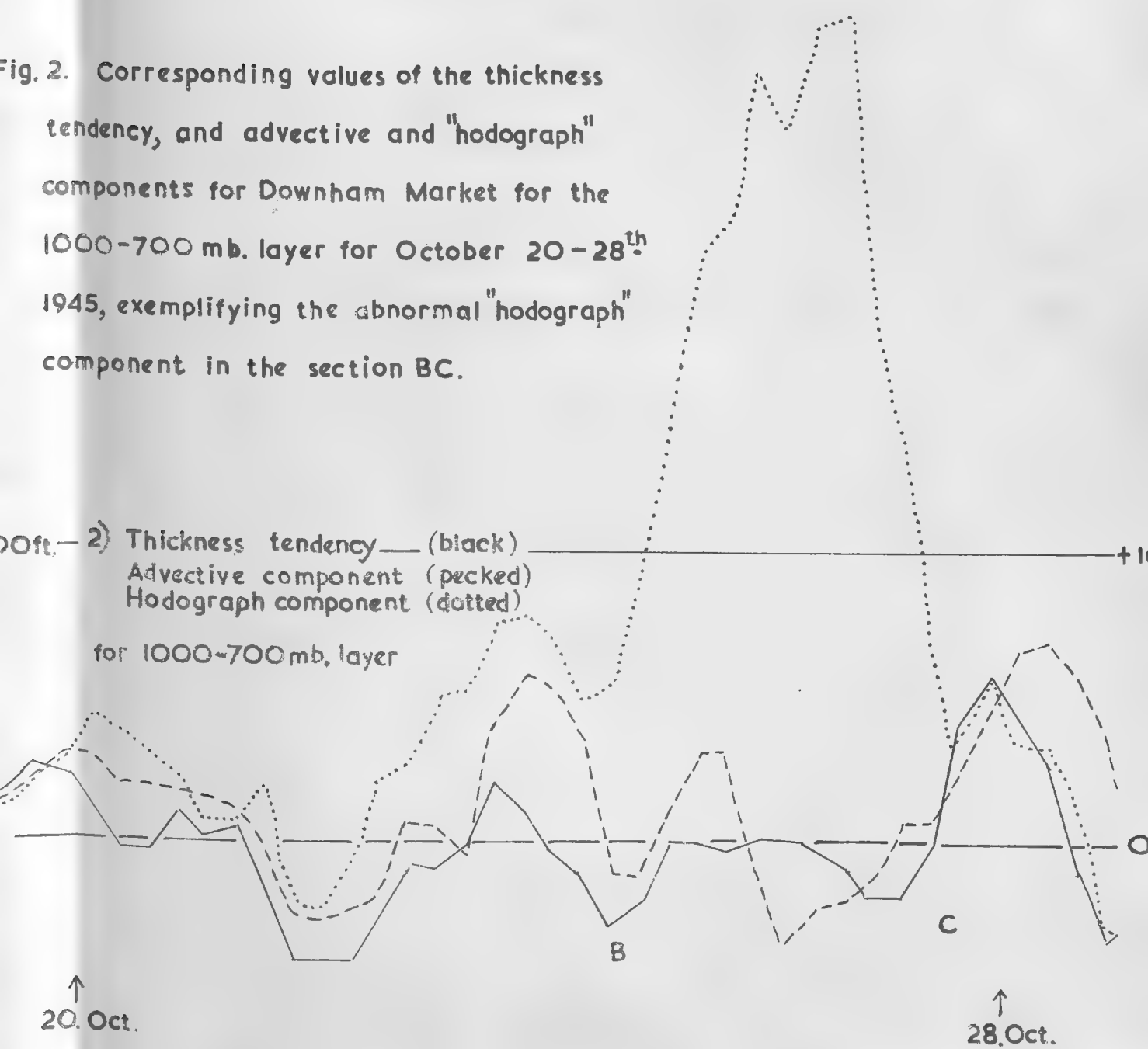

Fig.1.

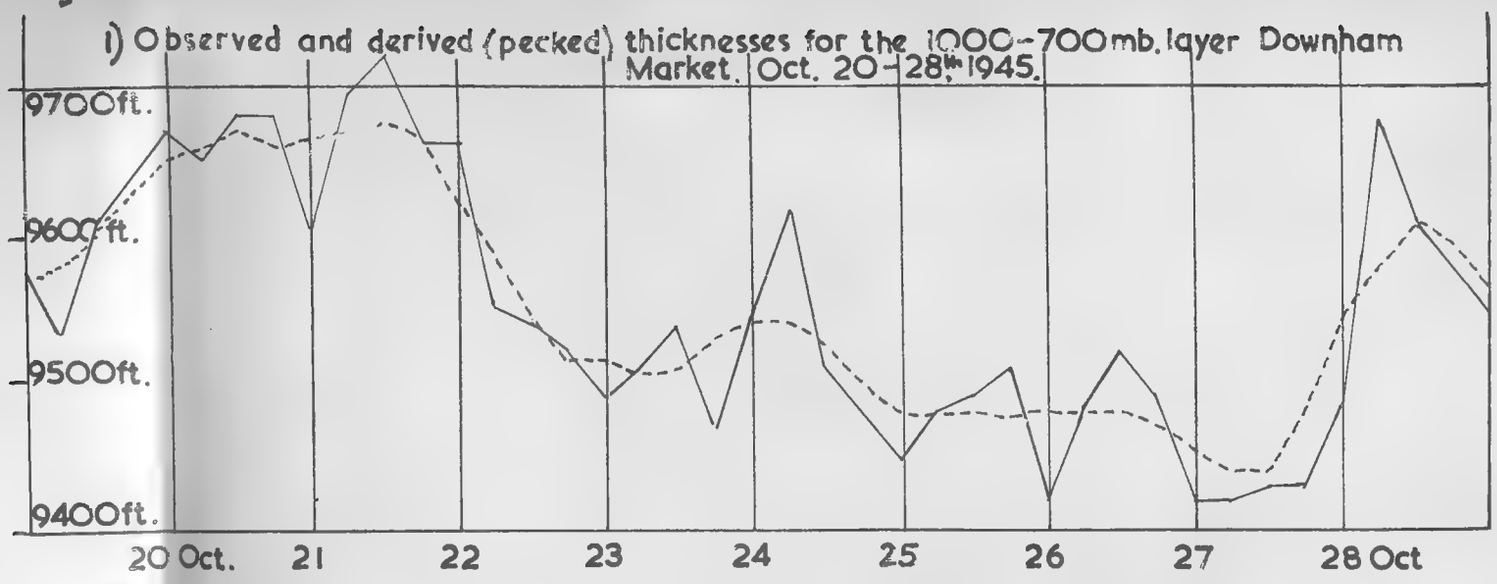

Fig. 2. Corresponding values of the thickness tendency, and advective and "hodograph" components for Downham Market for the 1000-700 mb. layer for October 20-28th 1945, exemplifying the abnormal "hodograph" component in the section BC.

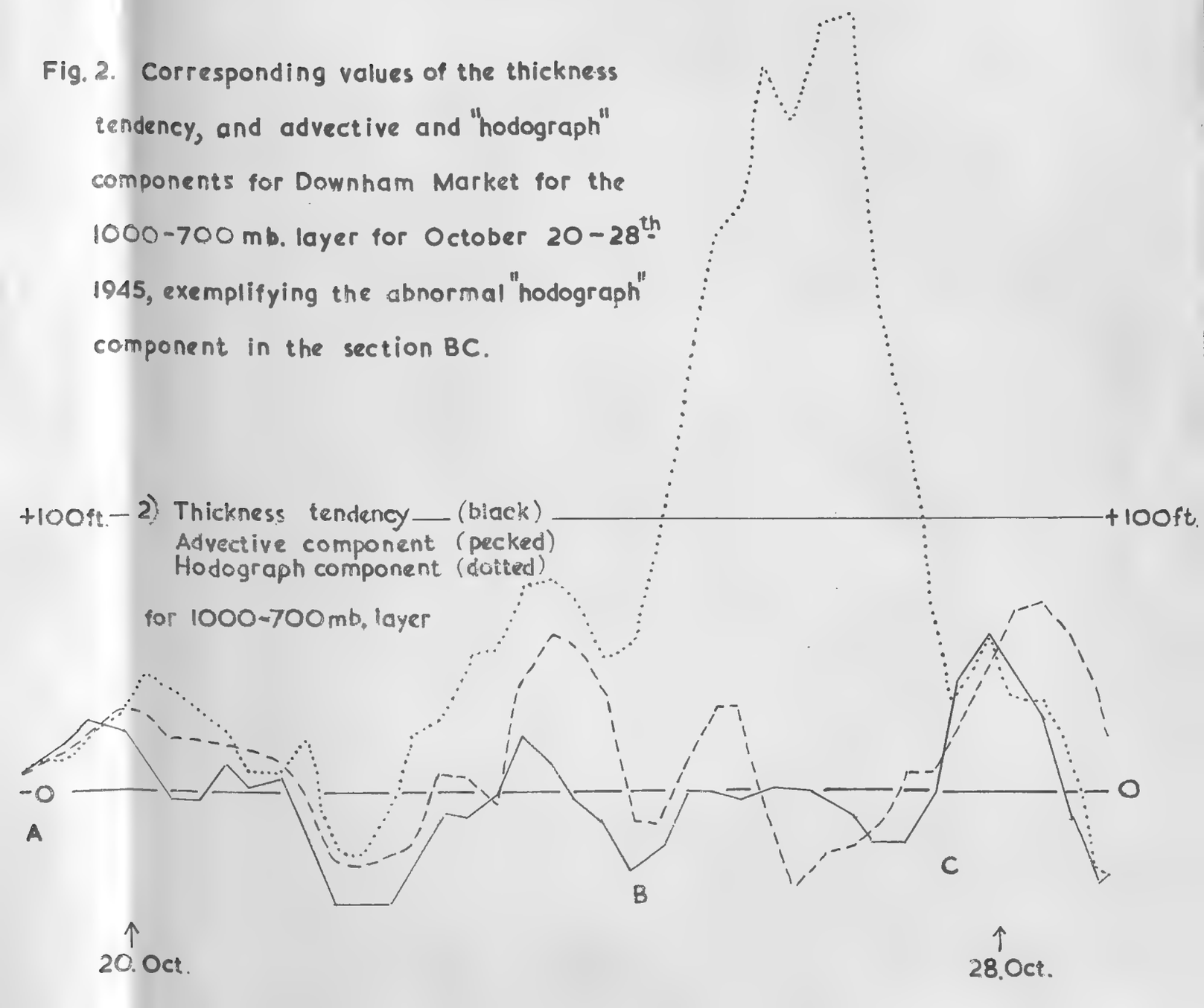

M.R.P. 517

Fig. 3. The diurnal variation of thickness - based on two or three years data

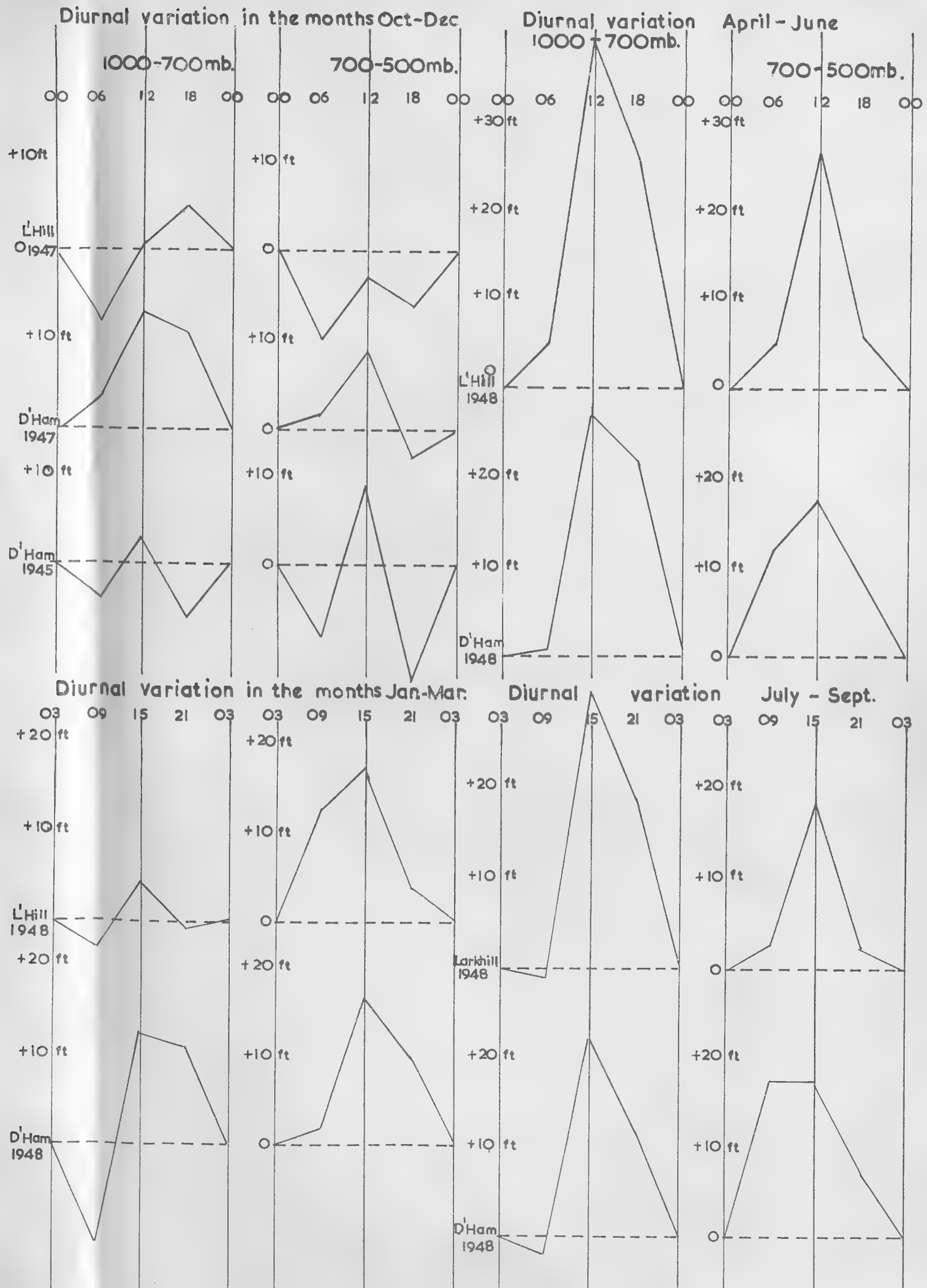

Fig.4. Serial correlations of the thickness tendency at Larkhill.

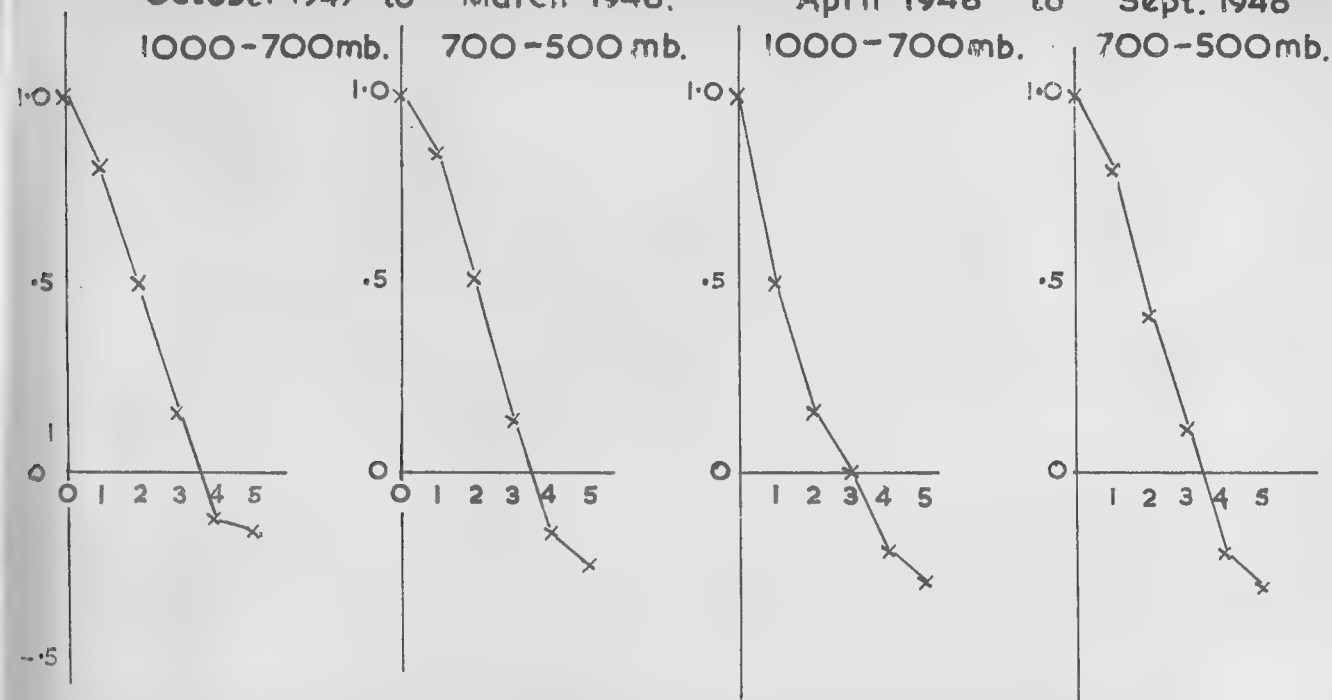

The abscissa is the number of the serial correlation whose value is the ordinate.

Fig.5. Graphs of log c plotted against $\log_{10} r_c$ for the above data to test Sutton's formula for r_c

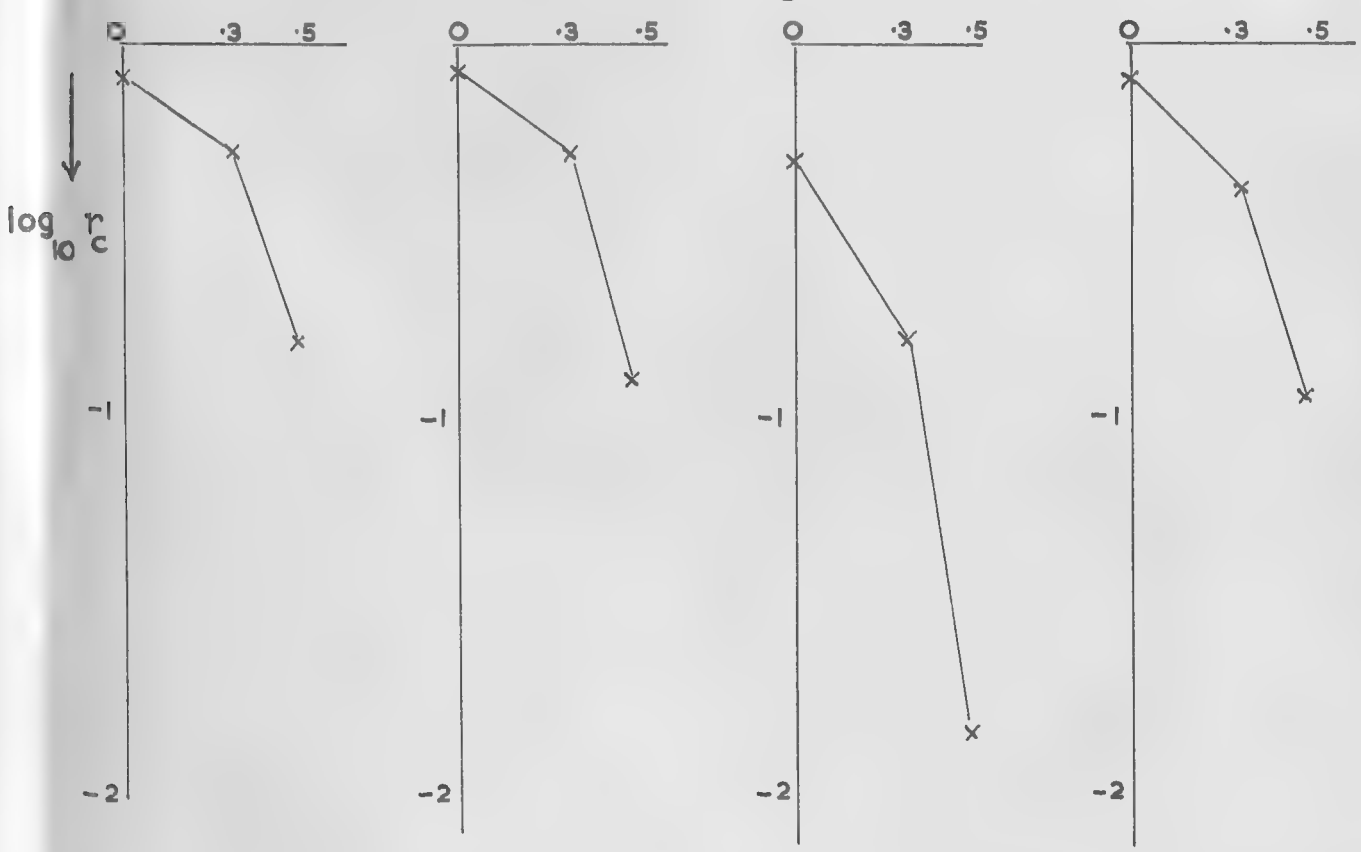

CONFIDENTIAL. Its contents must not be quoted.

M.R.P. 518
S.C. II/43
28th October, 1949.

AIR MINISTRY

METEOROLOGICAL RESEARCH COMMITTEE.

Changes of Air Temperature

Comments on M.R.P. 517

AIR WEATHER SERVICE
TECHNICAL REFERENCE FILE

by

A.H.R. Goldie (Meteorological Office)

It is possible by using already existing statistics to get some general ideas on the relative importance of the factors determining temperature change. There are two ways of considering the changes of temperature in the free air. In the first (Lagrangian) we fix our attention on the same small mass of air and follow the changes undergone by it. Let dQ represent the amount of heat communicated to it (or abstracted from it) from external sources in the interval of time dt: then:-

$$dQ = C_p\, d\theta - A\alpha\, dp \qquad \ldots\ (1)$$

(θ denotes absolute temperature, A being the heat-equivalent of work and α the specific volume)

or

$$\frac{d\theta}{dt} = \frac{1}{C_p}\frac{dQ}{dt} + \frac{A\alpha}{C_p}\frac{dp}{dt} \qquad \ldots\ (2)$$

The temperature of the air at any time is given by

$$\theta = \theta_o + \frac{1}{C_p}(Q - Q_o) + \frac{A\alpha}{C_p}(p - p_o) \qquad \ldots\ (3)$$

where θ_o, Q_o, p_o refer to some fixed time t_b. In other words the actual temperature of the mass depends on:-

(a) "origin" or advection of initial conditions,
(b) heat communicated from external sources since time t_o,
and (c) adiabatic pressure-change in the interval.

The other way (Eulerian) of considering the matter is to fix our attention upon a particular point in space and to observe what is going on there. Provided there is approximate geostrophic balance, the mathematical expression of this reduces to[1]:-

$$\frac{\partial\theta}{\partial t} = -\left(v_x\frac{\partial\theta}{\partial x} + v_y\frac{\partial\theta}{\partial y}\right) + \frac{1}{C_p}\frac{dQ}{dt} + \frac{A\alpha}{C_p}\frac{\partial p}{\partial t} + v_z\left(\frac{A\alpha}{C_p}\frac{\partial p}{\partial z} - \frac{\partial\theta}{\partial z}\right) \qquad \ldots\ (4)$$

3. The expression (3) is the more convenient when we are discussing trajectories of air. The expression (4) is the more convenient for discussing, on the basis of statistics, the changes taking place at a given place and height. It divides the temperature change at a fixed point into four parts.

/(a)

(a) Advection of air (horizontally).

(b) Gain or loss of heat from or to external sources including radiation, release of latent heat and so on.

(c) Pressure change.

(d) Ascent or subsidence.

The effect of (c) is calculable as a matter of physics. At a height of 4 km it is

$$\delta\theta = 0.12\ \delta p$$

and at 8 km it is

$$\delta\theta = 0.19\ \delta p$$

But on the other hand as a matter of experience (the statistics of W.H. Dines) it is found that on the average,

$$\delta\theta = 0.46\ \delta p \quad \text{at 4 km}$$

$$\delta\theta = 0.47\ \delta p \quad \text{at 8 km}$$

Thus as W.H. Dines(2) pointed out, the adiabatic effect in the troposphere is about one third of the total change of temperature at a given point. The conclusion of course (drawn by Hesselberg,(3) Douglas and others over 25 years ago) is that on the average the net contribution of the other elements of equation(4) is in the same direction as the pressure change. Since the term (b) is probably small for periods of the order of a few days (except where there is precipitation) it seems that the terms (a) and (d) i.e. advection and subsidence or ascent, have usually to account for well over half of the total change of temperature.

4. In the lower stratosphere however, as W.H. Dines(2) also showed, the mechanism of changes is quite different. At 12 km. for example, the adiabatic relation is

$$\delta\theta = 0.33\ \delta p$$

whilst the statistical relation is

$$\delta\theta = -0.31\ \delta p$$

Here (see M.R.P. 213) the vertical circulations associated with changing pressure run in the opposite sense to those in the troposphere and the term (d) - subsidence or ascent - gives a negative contribution with rising pressure and a positive contribution with falling pressure.

5. Thinking now of equation (3), we can say a little, from examination of trajectories of air, on how air masses of different kinds tend to change as they move.

Examination of a number of trajectories given in the "Life History of Surface Air Currents"(4) led me to the following conclusions:-

1. In polar air the pressure rises so long as it is advancing southward i.e. in general under-running tropical air.

2. In polar air the pressure falls so long as it is being over-run by tropical air which in general means that it (the polar air) is retreating northward.

3. In tropical air there is as a rule very little change of pressure along a trajectory, at least until it is about to over-run colder air.

5. In practice as a rule, it is thus polar air or at least the "cold air" which is subject to the largest and most rapid pressure changes along a trajectory. Where a big southward advance occurs it is found that the air at ground level rises in pressure and loses speed substantially and the adiabatic effect accounts for about half the rise of temperature. The remaining rise of temperature along the trajectory is presumably partly the result of the heat gained from sea or land surface and partly the effect of subsidence.

6. In tropical air on the other hand, so long as it extends right down to the surface, the changes in pressure along a trajectory are relatively insignificant and the heat loss is in the main from the surface layers. Where tropical air rises and gives precipitation the effects of the 2nd and 4th terms of equation (4) will be large and in opposite senses, though sometimes calculable.

7. In general the processes of change are at their simplest in the lowest layer of the stratosphere, so that for periods of time of the order of a few days the control of temperature in any given air mass is almost entirely dynamical. The true advection differences, after elimination of the dynamical element, are probably often virtually confined to the troposphere.

References

(1) A.H.R. Goldie Q.J. R. Met. Soc. 49 (1923) No. 205.

(2) W.H. Dines Q.J.R. Met. Soc. 51 (1925) No. 213.

(3) Hesselberg, Th. "Über den Zusammenharg zwischen Druck - und Temperatur - schwankungen in der Atmosphäre". Met. Zeit. 32, 1915, pp. 311 - 318.

(4) Lempfert and Shaw, M.O. 174, 1906.

G. 248366/DS/11/49/40.

This report has not yet been published and is to be treated CONFIDENTIALLY. Its contents must not be quoted.

21st December, 1949.

MRP 526

AIR MINISTRY

METEOROLOGICAL RESEARCH COMMITTEE

The warming of cold air masses over the sea.

by J.M. Craddock (Meteorological Office)

AIR WEATHER SERVICE
TECHNICAL REFERENCE FILES
AUG 29 1951

I. Summary

Methods are described whereby 28 measurements were made of the rates at which cold air masses were receiving heat and water vapour from the underlying sea. It is shown that the rate of heat transfer is closely associated with the difference between the sea temperature and the surface temperature representative of the air mass.

Introduction.

1. This paper describes an investigation made during the spring of 1946 to determine the rate at which cold air masses receive heat and water vapour from the sea surface. Although originally undertaken in the interests of the routine forecaster, it falls into place in the general investigation now in progress in large scale atmospheric thermal change. The method used was to find the trajectory of air which passed over one upper air sounding station and later over another, and to relate the observed changes in temperature and moisture to the surface temperature of the sea which had been traversed.

II. The difficulties

2. Since an air trajectory is based on estimates of wind velocity derived from a series of analysed charts its accuracy depends, among other things, on the original analysis, and the closeness with which the actual wind approximates to the assumed value (geostrophic or gradient) which is estimated from the isobars or contour lines. The true air track is thus subject to some uncertainty while the initial and final upper air soundings are subject to observational error. In order that the effect sought for should not be obscured by these uncertainties the cases chosen for examination all included a fairly long sea crossing - the data relate to polar outbreaks which passed over a northern station such as Reykjavik, and later over the British Isles.

3. With such distances, while the investigator can start his trajectory in the most suitable conditions (at a northern radio sonde station at a time when a sounding is being made) he has no power to arrange that it ever passes near another radiosonde station, so that most of the trajectories started proved fruitless. The methods in the next Section are considered to provide the best return for the time expended. Supposing we have two soundings such as are illustrated in Fig. 1. which gives the condition of air at Reykjavik and 24 hours later, at Liverpool, are these properly comparable? In other words, if we had enclosed a vertical column of air in a hypothetical bell glass, and taken it at the prescribed speed along the prescribed track (in this case, that of the air at 700 mb) would the changes of temperature and water vapour content have agreed with those actually observed? This question can be answered in the affirmative provided three conditions are satisfied, namely:-

(1) the horizontal thermal gradient in the air mass must be in the same direction at all heights;

(2) the vector change of wind with height, the so called "thermal wind" must be at right angles to the thermal gradient in the air mass;

/(3)

(3) and the factors making for thermal change must act with the same intensity on either side of the trajectory in the direction of the thermal wind as they do on the trajectory itself.

4. These conditions are sufficient because the first two ensure that the thermal wind is in the same direction as the isotherms at each level so that the thermal wind produces no advective temperature change, while the third ensures that air introduced by the thermal wind into the air column following the trajectory has received the same treatment as the air which it replaces. It is a matter of practical experience in upper air analysis that the first two conditions are approximately fulfilled in the type of situation here considered, as also is the third, since the thermal wind agrees approximately in direction with the isotherms of the underlying sea surface. Further, the isopleths of water vapour content also tend to follow the isotherms, so that initial and final soundings are comparable as regards humidity as well as temperature.

III. Methods of trajectory drawing.

5. Both methods used the routine upper air charts analysed at 6 hourly intervals at the Central Forecasting Office. The trajectories were drawn with wax pencil on a talc sheet which was transferred from one working chart to the next. In the first method the air at 700 mb. only was followed, a trajectory being started at a northern radiosonde station at the time of a sounding, and the air being assumed to move at the local gradient speed for the three hours preceding and the three hours succeeding the time of each chart. Working in this way, one chart was finished with before the next was looked at. Sometimes such a trajectory passed over a British upper air sounding station, but much more often it passed between the stations, or missed the British Isles altogether. When the trajectory passed between two stations, another trajectory was drawn starting at the same northern station at the hour of the next sounding, and compared with the first. Where the two trajectories lay closely alongside, and included a British upper air sounding station between them, a trajectory, relating to an intermediate hour was interpolated to pass directly over the British Station. In all about 50 trajectories were drawn this way.

6. In the second method, not only was the 700 mb trajectory drawn, but also that for air at 1000 mb proceeding with gradient speed, and an estimate was made of the projection on the earth's surface of the air column which initially was vertically over the northern station. This was not difficult as the projected segment joined isochronous points on the two trajectories and between them followed the run of the isotherms or thickness lines which appear on the analysed charts. Sometimes the segment was extended by including the 500 mb. trajectory. If the conditions laid down in para. 3. are satisfied, any point of this segment may be considered as generating a trajectory at an intermediate level, and any observation on the segment as it crosses the British Isles is properly comparable with the initial sounding. This method is clearly more fruitful than the other, since the moving segment is fairly sure, sooner or later, to pass over a second radiosonde station, and is susceptible to internal check, since simultaneous observations of different parts of a segment should, and did, confirm its uniformity along its length. Over 50 trajectories were drawn in this way, all relating to air above the layer affected by surface friction.

7. Of the final total of over 100 trajectories, each starting over one upper air sounding station and finishing over another, some started and nearly all finished at times other than synoptic hours.

Soundings for the initial and final times were then constructed by interpolating at each level between the preceding and succeeding observations (in finding moisture content, values of the humidity mixing ratio were interpolated). This was thought legitimate since the differences between the soundings were in all cases fairly small.

8. It will be seen that the drawing of trajectories in this way entails the exercise of personal judgment. All the trajectories used were drawn by the author. In order to standardise the conditions as far as possible, only

trajectories starting at Reykjavik are used in this paper: some have been rejected on internal evidence, and it is considered that the 28 which were retained show features which could be established by any experienced upper air analyst who cared to repeat the investigation. Apart from the subjective element, since all the trajectories relate to air with a fairly high surface velocity, say, exceeding 15 knots, the results apply to conditions in moving air masses, and not to semi-stagnant ones such as surround the sub-tropical anticyclones.

IV. A survey of the Data

9. In practice the trajectories were drawn first, and the soundings examined afterwards, and it then appeared that the data fell into two main classes, illustrated by Figs. 1 and 2. Transits resembling Fig.1 were accepted as satisfactory. In some of these the sea crossing had been followed by a considerable passage over land, and the air mass appeared to have been modified below the 900 mb. level. The modification, which did not occur in transits ending at coastal stations, is typical of air over a land surface subject to radiative cooling, and it was concluded that far from giving heat to the air mass the land surface was in fact abstracting heat from it. The heating in these cases was assumed to take place entirely over the sea so that the effective period of heating was in these cases less than the time between observations. The changes depicted in Fig. 2. were considered to indicate the presence of warm air overlaying the cold outbreak, implying a thermal wind changing direction with height. Any such transit in which the trajectory lay within the warm air was discarded, as violating the first condition set down in paragraph 3. (Transits Nos. 1 - 5 which are all that relate to one particular outbreak, are open to some doubt on this ground). Temperatures and humidity mixing ratios for the 28 transits, including these five, which are considered satisfactory are given in full in Appendix I.

10. Each of these air masses had received heat in the lower layers, as shown by comparing the initial and final temperatures. Further, each was, while over the sea, in a state of convective agitation, as indicated by reports of showers, gusts and hail at the coastal stations. It appears therefore, that the depth of air directly responsive to changes in the surface conditions will be indicated by the depth of convective cloud, a depth which may occasionally be observed directly, but more often has to be estimated by the use of some indicator which distinguishes an air mass subject to convective mixing from one which is not. The equivalent potential temperature, θ_e was used for this purpose, and proved very satisfactory. In all cases θ_e was fairly uniform in the lower layers and usually showed large increases with height above, so that the limit of the air mass subject to mixing was determined to the nearest 50 mb. without ambiguity. Occasionally soundings at neighbouring stations were consulted. The heights of convective cloud, where reported by aircraft, agreed with the top layer of uniform θ_e which from now on will be called the convective limit. In the transit shown in Fig. 1. the convective limit was at 800 mb. when the air was at Reykjavik, but had risen to 550 mb. by the time it reached Liverpool. This rising occurred in nearly all the transits, and in some the convective limit in the final sounding coincided with the tropopause. It appears that convection was at first shallow, but became deeper as the warming of the surface layers increased the lapse rate aloft.

11. The changes in temperature observed (e.g. in Fig. 1. an increase in 24 hours of 23°F at the 1000 mb. level, 26°F. at the 800 mb. level and by 7°F. at the 550 mb. level) are, of course, far beyond the range of observational error, and we may at this point consider how they are brought about. In this case the possibility of advective heating is excluded, so that the alternatives of dynamic heating and non-adiabatic heating remain. The distribution of temperature with height in a typical air mass subject to dynamic heating is quite unlike that actually observed, so there remains the possibility of non-adiabatic heating. The processes to be considered here are (a) lateral mixing, which can hardly be effective in a broad air mass showing little horizontal wind shear, (b) the direct absorption or emission of radiation, which has the overall character of a cooling process and in any case, cannot produce changes at the rates observed and (c) direct surface heating. If the air mass is receiving heat from the sea surface,

/than

then the rate of heat transfer may be expected to depend on the conditions in the boundary layer, and the remainder of this paper is directed to testing this possibility.

V. The relation between the rate of warming of an air mass and the conditions at the sea surface.

12. To obtain for each transit a parameter depending on the conditions in the boundary layer, an estimate was made of the mean surface air temperature during each transit (by taking the mean of the actual surface temperatures, ignoring any small inversions, of the initial and final soundings) and subtracted from the mean sea temperature along the track (estimated from the mean isotherms for the appropriate month with a small adjustment, based on synoptic experience, for the distortion of the isotherms brought about by a sustained airstream). This difference, which may be called the boundary lapse, is a rough guide to the intensity of the temperature change across the boundary layer, although of course it does not measure the gradient between particular levels.

13. For each transit there was computed the mean rate of gain of sensible heat by a column of 1 sq. cm. section extending from the surface to the final convective limit. It was assumed that the increase in mean temperature of a layer of 50 mb. depth, (e.g. between pressures 875 mb. and 925 mb.) was measured by the increase in temperature at the mean level (900 mb. in this case) and that if this increase is δT then the increase per gram of air of the heat energy in the layer is $c_p \delta T$. The values found therefore include the gain in internal heat energy, $c_v \delta T$ and also the work done against gravity in raising the overlying air. Typical and extreme values of the rate of gain of sensible heat are given in Table 1, column (a) and similar figure for the observed increase in water vapour content in Table 1, column (b). These latter are of course minimum values for any particular occasion because some water vapour taken up by the air mass is later condensed and lost as precipitation. Since, however, water vapour lost as precipitation but not that which is condensed and later re-evaporated leaves its latent heat in the air mass, the total rate of gain of water vapour cannot exceed the amount required to supply the observed increase in water vapour content together with enough water vapour later condensed and not re-evaporated to supply latent heat equal to the observed gain in sensible heat by the air mass. The exact heat gain per gram of this condensed water depends on the circumstances, and in particular whether it eventually reaches the sea or remains in the air at the time of the final sounding in the form of liquid water or of ice. In this work it is assumed that precipitation and residual cloud are in the form of water and that one gram of condensed water yields 595 calories to the air. On this basis maximum values for the rate of gain of water vapour content are given in Table 1, column (c). Table 1, column (d) gives the rate of transfer of heat energy corresponding to the maximum values for water vapour gain, or, what comes to the same thing, the sum of the rate of gain of sensible heat given in 1 (a) with the rate of gain of latent heat implied in 1 (b).

Table I

	a $cal.cm^{-2}sec^{-1}$	b $gm.cm^{-1}sec^{-1}$	c $gm.cm.^{-2}sec^{-1}$	d $cal.cm.^{-2}sec^{-1}$
Typical	$1.0x10^{-2}$	$.5x10^{-5}$	$2.0x10^{-5}$	$1.3x10^{-2}$
Extreme	$1.8x10^{-2}$	$.8x10^{-5}$	$3.7x10^{-5}$	$2.2x10^{-2}$

14. In figs. 3 and 4 the rates of gain of sensible heat and water vapour are plotted for each occasion against the boundary lapse. Each shows strong association between the variables, so that it appears that the rate at which a cold air mass gains heat and moisture is determined mainly by the magnitude of the boundary lapse. This evidence is in favour of the view reached by a process

of exclusion in para. 11, that the air mass is warmed by direct heating from the sea surface, rather than by any of the alternatives, none of which are affected directly by the boundary conditions at the sea surface. The figures in Table 1 thus give the magnitude of the flux of heat energy or water vapour which crosses the boundary layer. It is noteworthy that the difference between Cols. 1 (b) and 1 (c) (which is the maximum value for water vapour lost as precipitation) corresponds to rainfall at the moderate rate of .5mm per hour for the typical case, and 1 mm per hour in the extreme case. It appears, therefore, that the rainfall over the sea (averaged over an area of several square miles and a period of the order of 24 hours) due to instability in a cold air mass proceeding Southeast from Iceland to the British Isles is unlikely to exceed this figure.

15. The figures given in Table 1(d) for the total heat flux may be compared with the solar constant, (3.2×10^{-2} cal. cm^{-2} sec^{-1}). The heating of cold air masses over the sea appears to be comparable in intensity with the most intense heating by direct insolation, and unlike the latter, may operate on an air mass for as long as 24 hours.

16. The association shown in Fig. 3 is of interest to the practical forecaster who has to modify a thickness pattern to allow for non adiabatic heating over the sea. For his purposes, the most convenient rule is as follows:- When the boundary lapse is n°F and the convective limit is not above 700 mb. the thickness of the layer from 1000 mb. to 700 mb. will increase by n feet per hour. This rule corresponds to the relation between boundary lapse and flux of sensible heat shown in Fig. 3 by the sloping line, which is a good if not quite the best fit to the observations.

/When

X.	1.0	.7	.6	.5	.5	.6	.6	.5	.4	.3	.2

Larkhill 0600 on 4.2.44. 24 hours. M.S.T. 45°F.

T.	39	34	27	19	12	10	8	3	-4	-9	-12
X.	3.6	3.5	3.0	2.2	1.7	1.4	.7	.3	.2	.2	.2

4. Reykjavik 1200 on 3.2.1944

T.	11	5	0	-6	-5	-2	-2	-5	-11	-19	-28
X.	1.0	.7	.6	.5	.5	.6	.6	.5	.4	.3	.2

Larkhill 0800 on 4.2.1944. 20 hours. M.S.T. 45°F.

T.	39	33	27	19	12	11	6	3	-4	-8	-9
X.	3.5	3.0	2.6	2.0	1.6	1.3	.7	.4	.3	.3	.2

5. Reykjavik 1200 on 3.2.1944.

T.	11	5	0	-6	-5	-2	-2	-5	-11	-19	-28
X.	1.0	.7	.6	.5	.5	.6	.6	.5	.4	.3	.2

Ballyhalbert 0330 on 4.2.1944. 16½ hours. M.S.T. 45°F.

T.	34.5	31	25	17	13	7	5	4	0	-3	-11
X.	3.9	3.2	2.8	2.2	1.9	1.3	.9	1.1	1.1	-	-

II. Outbreak of 7th - 9th February 1944.

6. Reykjavik 1100 on 7. 2.1944.

T.	37	32	24	19	12	7	2	-3	-11	-16	-27
X.	3.2	3.0	2.3	1.9	1.5	1.2	1.0	.7	.6	.4	.3

/Leuchars

	1000	950	900	850	800	750	700	650	600	550	500
Leuchars 0700 on 8.2.1944. 20 hours. M.S.T. 45°F.											
T.	36	35	31	25	20	14	8	0	-9	-17	-23
X.	3.5	3.5	2.9	2.3	1.7	1.3	1.0	.7	.3	.3	.2
7. Reykjavik 1100 on 7.2.1944.											
T.	37	32	24	19	12	7	2	-3	-11	-16	-27
X.	3.2	3.0	2.3	1.9	1.5	1.2	1.0	.7	.6	.4	.3
Downham 1400 on 8.2.1944. 27 hours. Mean Sea Temp. 45°F.											
T.	42	36	30	24	16	9	4	-3	-4	-9	-16
X.	3.3	2.6	2.7	2.2	1.6	1.1	.5	.6	.3	.4	.4
8. Reykjavik 1800 on 7.2.1944.											
T.	36	31	24	18	12	7	3	-2	-9	-13	-23
X.	3.3	2.9	2.1	1.9	1.5	1.2	1.0	.9	.8	.6	.4
Leuchars 1330 on 8.2.1944. 19½ hours. M.S.T. 45°F.											
T.	40	35	29	23	18	12	6	0	-7	-14	-22
X.	3.7	3.2	2.7	2.1	1.8	1.4	.9	.7	.5	.4	.2
9. Reykjavik 1800 on 7.2.1944.											
T.	36	31	24	18	12	7	3	-2	-9	-13	-23
X.	3.3	2.9	2.1	1.9	1.5	1.2	1.0	.9	.8	.6	.4
Downham 1930 on 8.2. 1944. 25½ hours. M.S.T. 45°F.											
T.	39	36	31	25	17	9	6	1	-5	-10	-18
X.	3.6	3.4	3.1	2.6	1.9	1.5	.7	.9	.5	.5	.4
10. Reykjavik 0000 on 8.2.1944.											
T.	36	31	23	17	12	8	3	-1	-6	-10	-18
X.	3.3	2.7	2.0	1.8	1.6	1.3	1.1	1.1	.9	.8	.5
Leuchars 1800 on 8.2.1944. 18 hours. M.S.T. 45°F.											
T.	38	33	28	22	17	11	5	-2	-9	-18	-27
X.	3.8	3.2	2.7	2.2	1.8	1.5	1.0	.8	.5	.4	.2
11. Reykjavik 0000 on 8.2.1944.											
T.	36	31	23	17	12	8	3	-1	-6	-10	-18
X.	3.3	2.7	2.0	1.8	1.6	1.3	1.1	1.1	.9	.8	.5
Downham 0100 on 9.2.1944. 25 hours. M.S.T. 45°F.											
T.	34	35	28	20	16	10	5	2	-4	-12	-21
X.	3.4	3.4	2.7	2.1	1.8	1.3	1.0	.6	.3	.2	.2

III. Outbreak of 4th - 5th November, 1944.

12. Reykjavik 1800 on 4.11.1944.											
T.	29	25	21	11	5	3	-4	-12	-18	-20	-28
X.	2.9	2.3	2.0	.9	.8	.5	.5	.5			
Lerwick 1400 on 5.11.1944. 20 hours. M.S.T. 47°F.											
T.	39	37	34	27	21	14	6	-1	-8	-17	-28
X.	4.0	3.7	3.4	2.2	1.8	1.4	1.2	1.0	.6	.5	.2

/13.

	1000	950	900	850	800	750	700	650	600	550	500
13. Reykjavik 0600 on 5.11.1944.											
T.	32	26	20	14	7	2	-6	-12	-19	-28	-38
X.	2.8	2.7	2.4	2.0	1.4	1.1	.8	.5	.2	.1	
Stornoway 2200 on 5.11.1944 16 hours. M.S.T. 47°F.											
T.	37	33	27	21	16	10	1	-7	-16	-25	-34
X.	4.0	3.8	3.1	2.7	1.5	.9	.6	.4	.5	.4	.2
14. Reykjavik 1800 on 5.11.1944.											
T.	29	25	19	13	5	-1	-8	-12	-21	-29	-37
X.											
Lerwick 0900 on 6.11.1944. 15 hours. M.S. T. 47°F,											
T.	40	39	32	26	21	15	9	1	-6	-15	-24
X.	4.9	4.0	3.0	2.8	2.5	1.9	1.5	1.6	.9	.7	.4

IV. Outbreak of 18th - 20th January, 1945.

15. Reykjavik 0900 on 18.1.1945.											
T.	13	7	0	-6	-13	-19	-24	-29	-36	-40	-48
X.	1.1	.9	.9	.7	.2	.2	.1	.1	.1	.0	.0
Valentia 1200 on 19.1.1945. 27 hours. M.S.T. 45°F.											
T.	36	30	25	19	13	6	-2	-10	-20	-30	-34
X.	3.0	2.0	2.8	1.8	1.8	1.3	.9	.4	.3	.2	.2
16. Reykjavik 1100 on 18.1.1945											
T.	11	5	-1	-7	-14	-19	-24	-29	-36	-40	-48
X.	1.0	.8	.8	.7	.3	.2	.1	.1	.1	.0	.0
Penzance 1700 on 19.1.1945. 30 hours. M.S.T. 45°F.											
T.	35	29	22	14	8	1	-7	-15	-25	-35	-39
X.	3.8	2.8	2.3	2.0	1.4	1.0	.6	.4			
17. Reykjavik 1700 on 18.1.1945.											
T.	9	3	-3	-10	-17	-19	-24	-29	-36	-42	-49
X.	.8	.7	.6	.6	.4	.1	.1	.1	.1	.0	.0
Larkhill 2100 on 19.1.1945. 28 hours. M.S.T. 43°F.											
T.	31.5	28	22.5	15.5	9.5	2	-6	-14	-22.5	-30	-39.5
X.	3.2	3.0	2.5	1.6	1.6	1.0	.8	.3	.3	.2	
18. Reykjavik 2000 on 18.1.1945.											
T.	10	3	-3	-10	-18	-21	-25	-28	-35	-41	-49
X.	.8	.8	.7	.6	.4	.1	.1	.1	.1	.1	
Ballyhalbert 1700 on 19.1.1945. 21 hours. M.S.T. 41°F.											
T.	29	25	19	13	7	-1	-9	-16	-25	-36	-42
X.	3.3	3.0	2.4	1.8	1.4	1.0	.8	.5	.3	.2	.1

/19.

	1000	950	900	850	800	750	700	650	600	550	500
19. Reykjavik 2100 on 18.1.1945.											
T.	10	3	-3	-10	-18	-21	-25	-28	-35	-41	-49
X.	.8	.8	.7	.6	.4	.1	.1	.1	.1	.1	
Liverpool 2100 on 19.1.1945. 24 hours. M.S.T. 41°F.											
T.	32.5	28	22	15.5	8.5	0.5	-6	-14.5	-24	-34.5	-43
X.	3.3	2.9	2.1	1.7	1.4	.9	.6	.5	.3	.2	.1
20. Reykjavik 0700 on 19.1.1945.											
T.	10	3	-4	-11	-18	-21	-25	-29	-36	-42	-50
X.	.8	.8	.7	.6	.4	.1	.1	.1	.1	.0	.0
Ballyhalbert 0300 on 20.1.1945. 20 hours. M.S.T. 41°F.											
T.	30	27	21	14.5	8.5	2	-5.5	-12.5	-22	-32.5	-41-5
X.	3.3	3.0	2.5	1.9	1.5	1.0	.8	.5	.3	.2	.1
21. Reykjavik 1800 on 19.1.1945.											
T.	13	5	-2	-7	-11	-14	-19	-25	-33	-39	-46
X.	1.1	.7	.5	.6	.5	.4	.1	.1	.1	.0	.0
Valentia 1800 on 20.1.1945. 24 hours. M.S.T. 41°F.											
T.	36	31	25.5	19.5	8	6	-1	-6.5	-13.5	-23	-34.5
X.	3.4	2.4	2.3	1.5	1.1	.9	.5	.5	.4	.3	.2
22. Reykjavik 1000 on 20.1.1945.											
T.	13	7	1	-6	-10	-15	-21	-28	-35	-43	-47
X.	1.3	1.3	.9	.7	.3	.2	.0	.0			
Valentia 1000 on 21.1.1945. 24 hours. M.S.T. 44°F.											
T.	33	27	24	19	12	4	-3	-10	-16	-22	-27
X.	3.8	2.5	2.0	1.5	1.0	.9	.7	.3	.4	.2	.1

V. Outbreaks of 26th - 29th April, 1945.

23. Reykjavik 0900 on 26.4.1945. M.S.T. 49°F.											
T.	29	21	16	9	3	-1	-5	-9	-15	-18	-25
X.	2.1	1.9	1.5	1.3	1.0	.4	.2				
Ballyhalbert 0900 on 27.4.1945. 24 hours.											
T.	43	36	27	22	15	7	3	-4	-14	-17	-27
X.											
24. Reykjavik 1500 on 26.4.1945. M.S.T. 49°F.											
T.	31	22	14	7	2	-2	-6	-12	-17	-18	-25
X.	2.1	2.0	1.6	1.2	1.1	.3	.2	.2	.2	.3	.3
Penzance 1800 on 27.4.1945. 27 hours.											
T.	47	39	32	26	20	15	10	4	-3	-9	-14
X.	4.3	3.9	2.9	2.0	2.0	1.6	1.1	1.0	1.0	.6	.4
25. Reykjavik 1500 on 27.4.1945.											
T.	25	18	14	11	9	6	0	-8	-13	-12	-18
X.	2.9	2.1	1.9	1.6	1.6	1.5	1.2	.7	.4	.2	

/Larkhill

	1000	950	900	850	800	750	700	650	600	550	500
Larkhill 1400 on 28.4.1945. 23 hours. M.S.T. 49°F.											
T.	43	37	31	24	17	12	5	-2	-11	-19	-25
X.	4.1	3.9	3.3	2.5	1.9	1.5	1.1	.9	.5	.4	.3
26. Reykjavik 0300 on 28.4.1945.											
T.	21	15	10	7	4	0	-3	-6	-10	-15	-23
X.	1.4	1.5	1.1	.4	.4						
Valentia 0000 on 29.4.1945. 21 hours. M.S.T. 49°F.											
T.	42	36	29	23	17	14	14	9	3	-3	-11
X.	3.6	2.3	3.3	2.5	1.8	1.0	.4	.3	.2	.3	.2
27. Reykjavik 1500 on 28.4.1945.											
T.	29	26	20	10	5	2	1	-3	-6	-10	-16
X.	1.7	1.8	1.5	.8	.5	.4	.4	.4	.5	.6	.5
Valentia 1500 on 29.4.1945. 24 hours. M.S.T. 49°F.											
T.	41	35	29	21	16	11	9	5	-1	-7	-16
X.	3.9	3.4	2.5	2.1	1.9	1.3	.6	.8	.7	.6	.4
28. Reykjavik 0300 on 29.4.1945.											
T.	20	16	11	7	4	-1	2	-2	-7	-15	-22
X.	1.6	1.1	.6	.3	.7	1.0	1.3	.4	.9	.6	.4
Valentia 0800 on 30.4.1945. 29 hours M.S.T. 49°F.											
T.	38	33	26	19	13	9	3	0	-6	-11	-18
X.	3.7	3.2	2.6	1.7	1.5						

G.257274(a)/MBF/1/50/40.

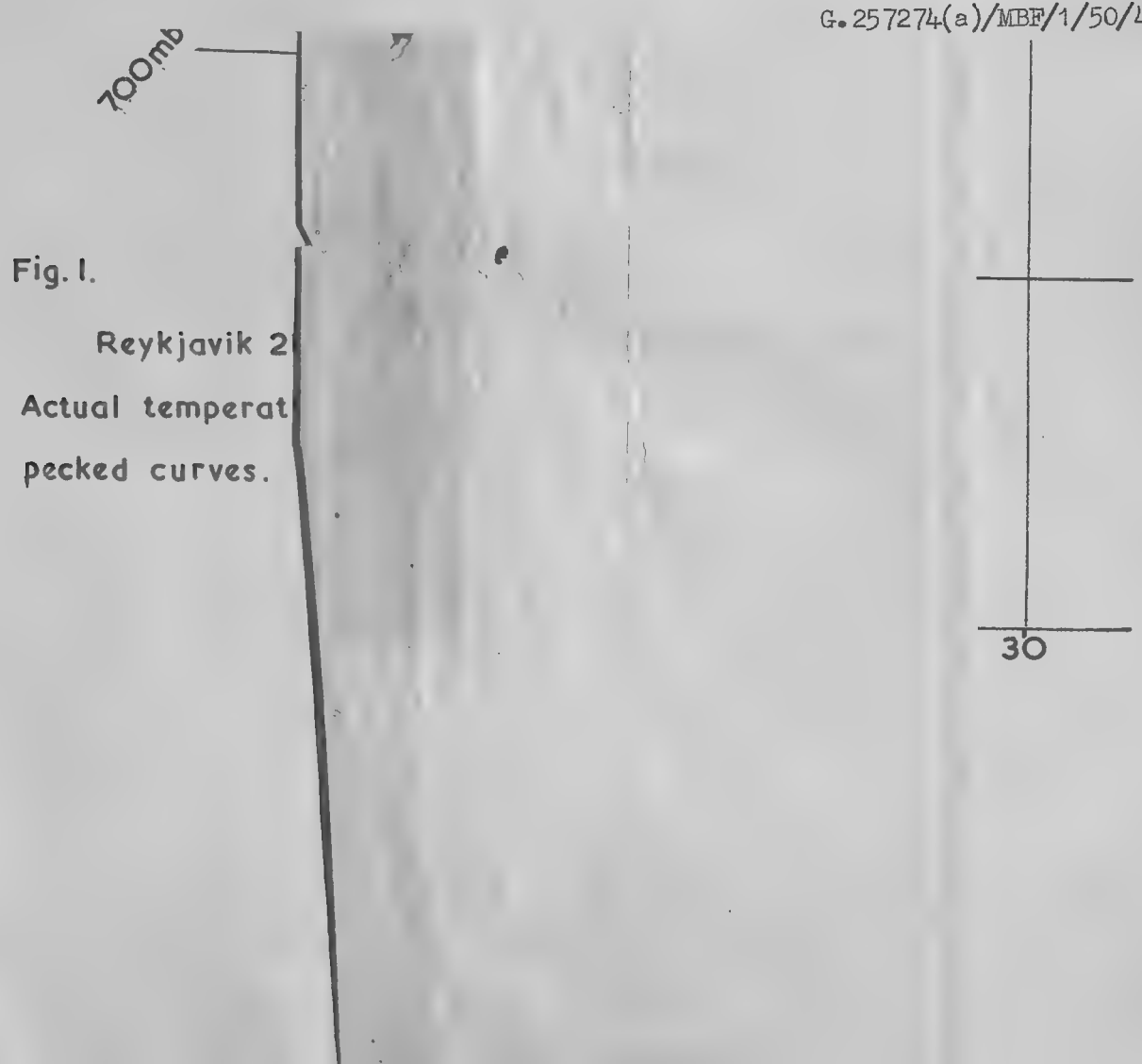

Fig. 1.

Reykjavik 2

Actual temperat

pecked curves.

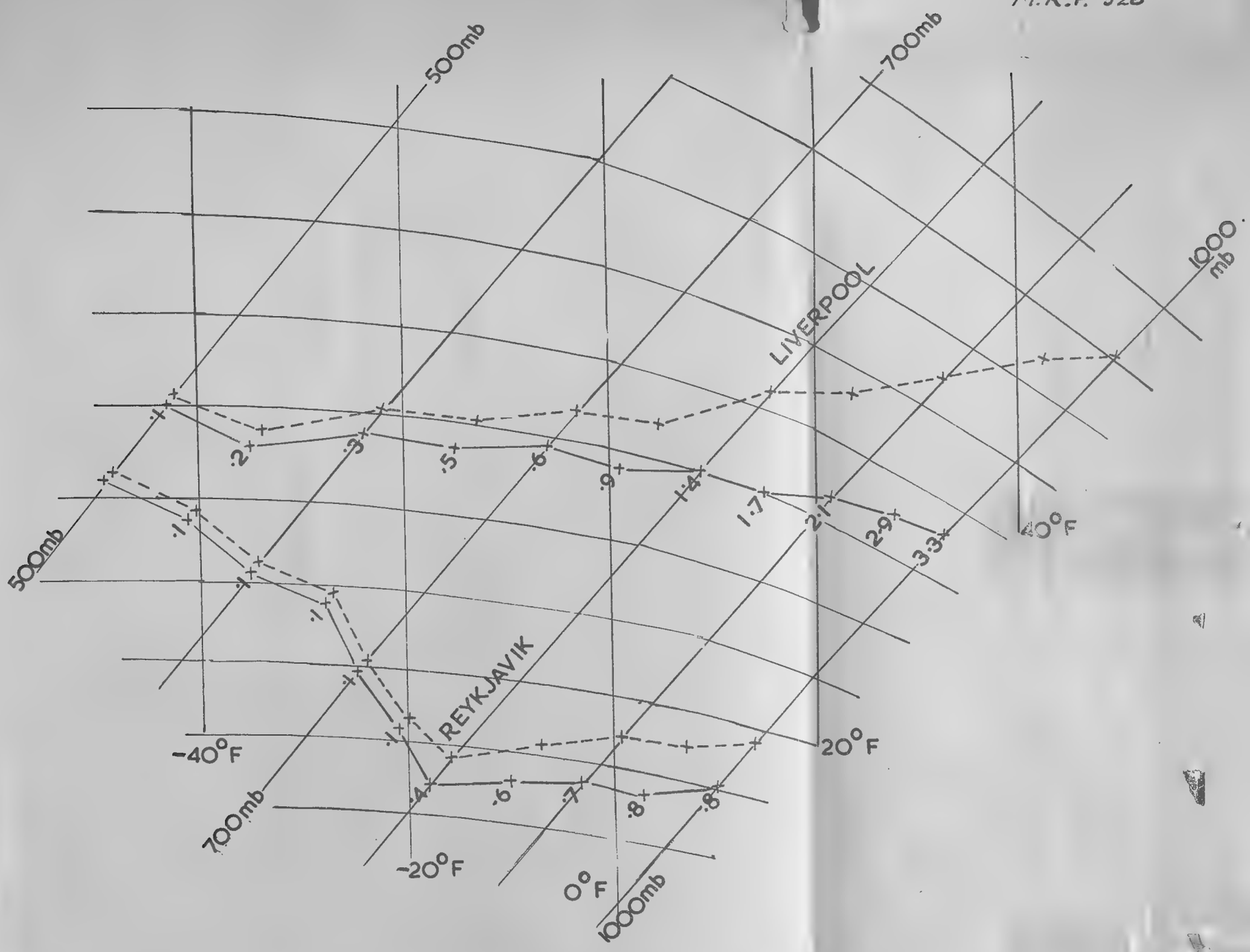

Fig. 1. Transit No.19.

Reykjavik 2100 on 18th Jan. 1945. to Liverpool 2100 on 19th Jan. 1945. Actual temperatures in full curves. Equivalent temperatures in pecked curves. Figures give humidity mixing ratio. (in gm/Kg).

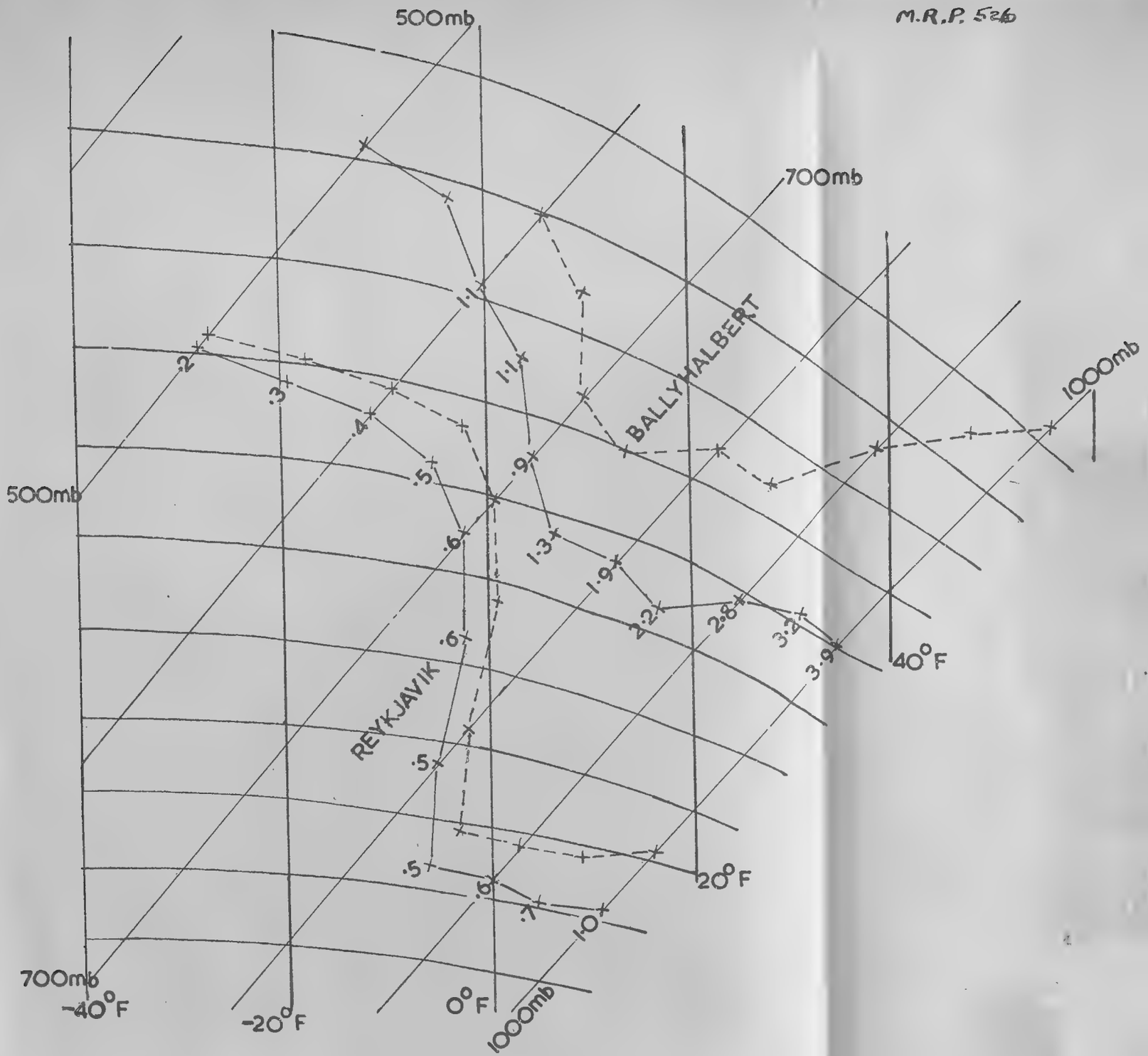

Fig. 2. Transit No.5.

Reykjavik 1200 on 3rd Feb. 1944 to Ballyhalbert 0330 on 4th Feb. 1944. Actual temperatures in full curves. Equivalent temperatures in pecked curves. Figures denote humidity mixing ratio.(in gm/Kg).

Fig. 3.

Relation between boundary lapse and rate of gain of sensible heat by air column of 1 sa.cm. cross section
Number against each point is that of the transit from which it was derived: see Appendix I.

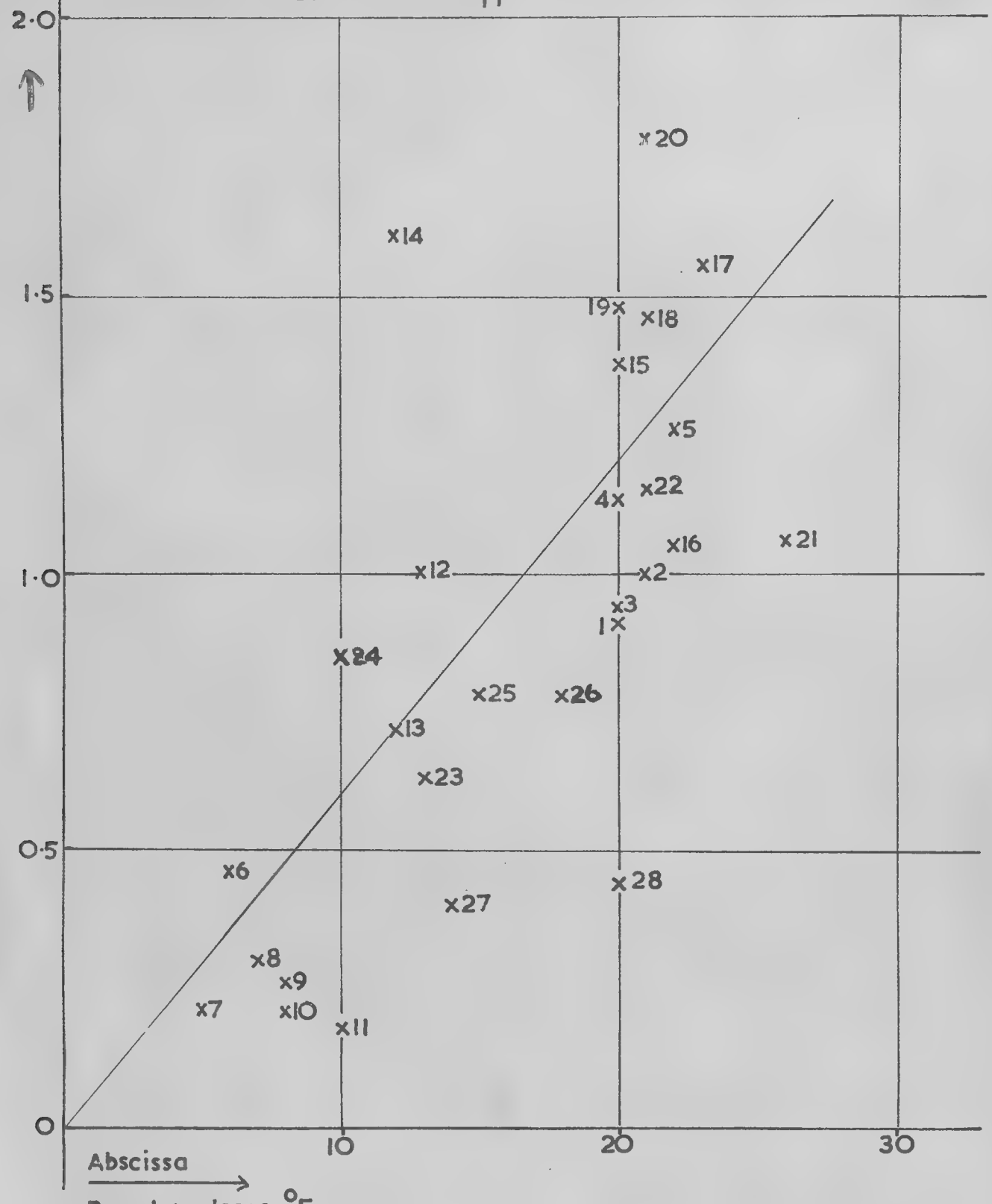

Fig. 4.

Relation between boundary lapse and rate of gain of water vapour by air column of 1 sq. cm. cross section. Number against each point is that of the transit from which it was derived.

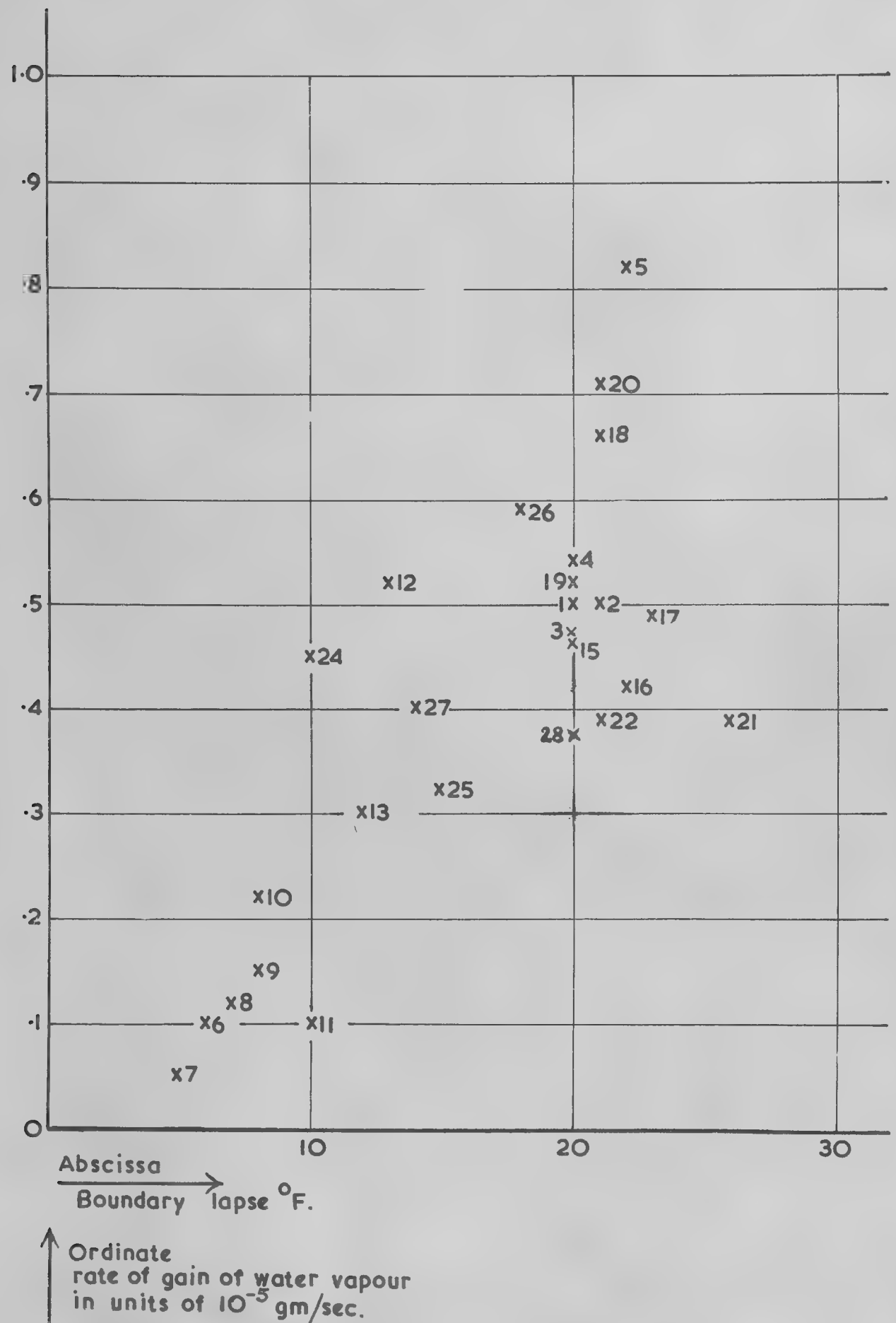

...its
...must not be quoted.

M.R.P. 527
S.C.I/32
23rd December, 1949

AIR MINISTRY

METEOROLOGICAL RESEARCH COMMITTEE

VARIATION WITH ALTITUDE OF THE SPEED CORRECTION COEFFICIENTS OF AIRCRAFT THERMOMETERS

By H.C. Shellard (Meteorological Office)

1. INTRODUCTION.

The results of some measurements by the Meteorological Research Flight of the speed correction coefficient, (denoted by α , where indicated temperature = true air temperature + α $(v/100)^2$, and v is true airspeed) of the M.O. flat plate resistance thermometer were given in M.R.P. 405.(1) Since that paper was written Mr. H.W.L. Absalom has pointed out to us that the use of a more exact formula for computing true airspeed from indicated airspeed would considerably reduce the amount of the variation of α with height which our results indicated. The values of α given in M.R.P.405 have therefore been recalculated and the new results are now presented. They still indicate a variation with height which is believed to be significant. The recalculated Mosquito results also indicate a slight but unmistakable variation of α with speed. The results of some more recent flights in Halifax aircraft are also given. In these we have concentrated on measuring the difference between the coefficients of two thermometers, one a R.A.E. pitot head resistance thermometer, and the other a M.O. flat plate thermometer. This difference in α's is also shown to decrease with height. This means that, not only does the α of the pitot head thermometer also decrease with height, but that it does so by a greater amount than that of the flat plate thermometer. Some possible explanations are considered.

2. RE-EXAMINATION OF PREVIOUS RESULTS.

In M.R.P. 405 we published the results of speed runs made at various levels in both Halifax and Mosquito aircraft to measure α for the M.O. flat plate thermometer. In the case of the Halifax the results were rather unsatisfactory mainly because most of the runs had been made before it was found that the radiation shield was inadequate when the element was mounted under the aircraft nose. On the later runs, and on all subsequent flights with the Halifax, an under-wing mounting has been used for this element. Nevertheless a decrease of α with increasing height was indicated. The Mosquito results were better because the elements could not have been appreciably affected by the sun, and also because the aircraft has greater height and speed ranges. Mean values for α at the 900, 700, 500, and 300 mb. levels were 1.79, 1.75, 1.69, and 1.58°F $(\frac{\text{knots}}{100})^{-2}$ respectively.

In computing these values the true airspeed was obtained from the approximate relation

$$v = v_i\sqrt{\frac{\rho_o}{\rho}} \qquad \text{..... (1)}$$

where v = true airspeed, v_i = indicated airspeed, ρ = air density, and ρ_o = air density at the base of the I.C.A.N. atmosphere. In other words the airspeed indicator was assumed to be calibrated in accordance with the equation

$$p = \frac{1}{2}\rho_o v_i^2 = \frac{1}{2}\rho v^2 \qquad \text{..... (2)}$$

/where

where p is the so-called impact pressure, the total pressure on the head tube minus the static pressure. In fact however the instrument is calibrated in accordance with the formula

$$p = \frac{1}{2}\rho_o v_i^2\left(1 + \frac{v_i^2}{4a_o^2}\right) = \frac{1}{2}\rho v^2\left(1 + \frac{v^2}{4a^2}\right) \quad \ldots\ldots (3)$$

where a = speed of sound and a_o = speed of sound at I.C.A.N. base. Equation (3) is actually a close approximation, for values of v less than a, to the adiabatic formula

$$p = P\left[\left\{1 + \frac{(\gamma - 1)\rho}{2\gamma P} v^2\right\}^{\gamma/\gamma-1} - 1\right] \quad \ldots\ldots (4)$$

where P = atmospheric pressure.

If we call the true airspeed obtained by using equation (1), v', and the more exact value obtained from equation (3), v, then it can be shown that

$$\left(\frac{v}{v'}\right)^2 = \frac{2P}{P_o m^2}\left[\left\{1 + m^2\frac{P_o}{P}\left(1 + \frac{m^2}{4}\right)\right\}^{1/2} - 1\right] \quad \ldots\ldots (5)$$

where P_o = atmospheric pressure at I.C.A.N. base = 1013.2 mb., and $m = \frac{v_i}{a_o}$

From equation (5) curves relating $(v/v')^2$ with v_i for different values of P can be drawn. Hence given v_i at any level the corresponding value of v can quickly be obtained.

Since v/v' clearly decreases with P, our values of α obtained from $\Delta T = \alpha(v'/100)^2$ will have been too small by an amount which is greater at lower pressures. The corrected values of α from our Mosquito flights are shown in Table I, the original values being given for comparison. The means for the 900, 700, 500, and 300 mb. levels are now 1.79, 1.78, 1.76, and 1.67 respectively. The range of the variation is thus reduced from 0.21 to 0.12, or by nearly half.

It has been suggested that the remainder of the variation might be due to position error. It can be shown however that so far as temperature measurements are concerned the effects of position error on airspeed indicator and on altimeter will generally cancel out. The total error involved is $dp(\alpha - \beta)/Jc_p\rho$, where β is the ratio of the lapse rate to the dry adiabatic lapse rate, and dp is the pressure departure from true atmospheric pressure at the static holes or vent. Since α is about 0.7 (using C.G.S. units), and β in the upper air usually lies between 0.6 and 0.8, the errors cancel and the effects of position error can thus be ignored if care is taken not to fly in isothermal layers or inversions when making runs. In any case the position errors for the Halifax and Mosquito aircraft, both types having static vents, are very small. Furthermore there seems to be no evidence for the existence of a variation of position error with height and this would be necessary to account for our result. Some flight tests carried out at the R.A.E. using different types of static vents indicated that the ground level position error curve was valid at heights up to at least 25,000 ft.(2)

/3.

3. FURTHER WORK IN HALIFAX AIRCRAFT.

The Halifax results given in Table III of M.R.P. 405 have also been recalculated using the more exact method of computing true airspeed (eqn.(5)). They are listed in Table II together with the results of a large number of additional runs made since Spring, 1948.

In the Summer of that year two new thermometer elements consisting of fine nickel resistance windings mounted inside pitot heads were obtained from the R.A.E. and one was mounted under the nose of each Halifax, connected to a suitably modified M.O. balanced bridge indicator. Several runs, on the lines described in Sect. III para. 5 of M.R.P. 405, were made between July, 1948 and February, 1949, in which temperatures indicated by one of these elements and by a M.O. flat plate element mounted under the wing were read simultaneously. In this way values of the speed correction coefficients of the pitot head thermometer (α_{ph}) and of the flat plate thermometer (α_{fp}) were obtained. Values of α_{ph} are given in column 5 of Table II (the runs of 21.7.48 and 9.2.49 gave reliable values for the difference $\alpha_{ph} - \alpha_{fp}$ only). It was expected that α_{ph} would be about 2.3 as the adiabatic heating was likely to be about 95% of the theoretical value for air brought to a complete standstill. It will be seen that this was the case, but that there was also a tendency for α_{ph} to decrease with height. It should be mentioned that the nickel wound thermometers were used for the runs of July, 1948 only, subsequently otherwise similar pitot head elements but with more robust platinum windings were used.

After the first few flights with both thermometers it coourred to us that it would be a simpler matter to measure the quantity $\alpha_{ph} - \alpha_{fp}$ than to measure the α's separately. The main cause of the uncertainty in measuring the value of α for any thermometer is the inhomogeneity of the air at any selected level in the atmosphere. The effect of a gradual temperature change along the run, i.e. a change on the synoptic scale, can be eliminated by our method of making reciprocal runs. Also the effects of rapid small scale fluctuations in temperature can be reduced by taking a number of readings in succession and averaging. It is the larger scale variations which are troublesome.(3) When only the differences between the readings of two thermometers are to be measured however these variations are of little consequence, particularly if the two elements have approximately the same lag as they had in our case. It was decided in future therefore to concentrate on obtaining values of $\alpha_{ph} - \alpha_{fp}$ only. An additional advantage was that since a fairly reliable value would be obtained in a shorter time than was needed to get absolute values of α, it was expected that values of $\alpha_{ph} - \alpha_{fp}$ at two, or perhaps three, different levels would be obtained from one flight.

Eight additional flights were made between May and July, 1949, from all of which values of $\alpha_{ph} - \alpha_{fp}$ were obtained. The flight of 29.6.49 was a joint run with a Mosquito and gave fairly reliable values of α_{ph} and α_{fp} as well as of their difference. The results of all these flights are listed chronologically in Table II. All the values in Table II were obtained by plotting indicated temperature against $(v/100)^2$ where v is true airspeed obtained from equation (5), and then finding the slope of the straight line of best fit by the method of least squares.

Table III summarises all the Halifax results and gives mean values of α_{ph}, α_{fp}, and of $\alpha_{ph} - \alpha_{fp}$, at 900, 700, and 500 mb. approximately. It is clear that all these quantities decrease with height. The really important result is the variation of $\alpha_{ph} - \alpha_{fp}$, since this quantity can be measured the most accurately. If it had been found to increase with height the increase being of the same order as the decrease already found for α_{fp}, then the indication would have been that α_{ph} was independent of height. Again if $\alpha_{ph} - \alpha_{fp}$ had been found to be approximately constant the indication would have been that α_{ph} and α_{fp} both decreased with height by the same amount. In fact it is found to decrease with height, which means not only that α_{ph} must decrease with height also but that it does so by a greater amount than α_{fp} does. The decrease in α_{ph} between 900 and 500 mb. amounts at the very least to 0.15, so that to assume a constant α for this thermometer would introduce errors of at least 1.3, 2.4, and 3.7°F in the corrections applied to indicated temperature readings at 500 mb. and at true airspeeds of 300, 400, and 500 knots respectively.

For each of our Halifax runs giving a value of $\alpha_{ph} - \alpha_{fp}$, a value of $\frac{P}{459+T}$ (which is proportional to air density) has been calculated and correlated with $\alpha_{ph} - \alpha_{fp}$ yielding a correlation coefficient of +0.59 from 20 pairs of values.

4. POSSIBLE EXPLANATIONS OF THE EFFECT.

The first possibility (considered in M.R.P. 405) is that the speed correction law may depart from the form $\alpha(v/100)^2$. If, for example, the true law were $\alpha(v/100)^n$ where $n > 2$, then the curve of indicated temperature, against $(v/100)^2$ as abcissa, would curve upwards, i.e. the apparent slope (α) would increase with increasing v. Since practically the same range of <u>indicated</u> airspeed is available at any height, so that α is measured at higher <u>true</u> airspeeds at the higher levels, the result would be an apparent increase of α with height. To explain a decrease of α with height therefore we must suppose the true law to be $\alpha(v/100)^n$ where $n < 2$. This can be tested by meaning (1) the results of the three runs in Mosquito VL621 at 300 mb., and (2) the results of the seven runs in Halifax ST796 at 500 mb. Then plotting mean indicated temperature against mean $(\frac{v}{100})^2$ we obtain for each of the above a number of points through which a mean curve can be drawn. If there is an appreciable departure from the true square law at the speeds with which we are concerned, and which could explain our result, then these curves should curve downwards. The curves are shown in Fig. 1, plotted on the same scale. Curve (1), the most suitable for this test, since it covers more than twice the speed range of curve (2), shows a slight departure from a straight line and curves upwards. Curve (2) shows no definite tendency to curve one way or the other. The curvature of (1) is in the sense that α increases with increasing airspeed. Thus we can rule out the possibility of our variation with height being due to a departure from the true square law. The indication that a departure exists in the opposite sense is very interesting however.

A more likely explanation perhaps is that α depends on the nature or pattern of the airflow over the element, i.e. on Reynolds Number (Re). Now $Re = vl\rho/\mu$ where v = true airspeed, l = a representative length, ρ = air density, and μ = coefficient of viscosity. Thus, if α increases with Re, it will increase with speed and decrease with height. Since ρ decreases more rapidly with height than μ (which depends on temperature), the ratio ρ/μ decreases with height. We have obtained definite experimental evidence for a decrease of α with height and some indication also of an increase of α with speed. For laminar flow the α for a flat plate should be constant, but if the flow becomes turbulent the available evidence indicates that α increases, at first sharply, with the onset of turbulence, then more slowly.(4) Thus if the flow is turbulent at low levels, and less turbulent, or laminar, at high levels there would be a decrease of α with height. It can be shown that if certain assumptions are made the decrease calculated theoretically would be of the right order. It is hoped to make further flights to test this possibility.

Another possible explanation which has been suggested is that the Prandtl Number might vary at low temperatures. For a flat plate the theoretical value of α for laminar flow is proportional to $Pr^{\frac{1}{2}}$, so that a decrease in Pr at low temperatures, or at low pressures, would lead to a decrease in α. It can be shown that Pr depends on $\frac{C_p}{C_v}$ of which values have been determined experimentally over a wide range of temperature and show very little variation. No values of $\frac{C_p}{C_v}$ appear to be available at low pressures. The indications are that it would decrease with decreasing pressure, but it seems unlikely that the decrease at pressures of $\frac{1}{2}$ to $\frac{1}{3}$ atmospheres would be large enough to account for an appreciable decrease in α.

/5.

LCULATED
E OF α .

5. CONCLUSIONS.

(1) The values of the speed corrections coefficients for the M.O. flat plate resistance thermometer and for the R.A.E. pitot head resistance thermometer decrease with increasing height, the decrease being greatest in the case of the pitot head element.

(2) There is some evidence for the existence of an increase in the speed correction coefficient of the M.O. flat plate thermometer with increasing airspeed.

.71
.79
.76
.78
.73
.81
.78
.77
.66
.67
.62

REFERENCES.

(1) Frith R., and Shellard H.C., M.R.P. No. 405, Air Ministry, London.
(2) Charnley, and Fleming, R.A.E. Report No. Aero. 2299.
(3) Frith R., M.R.P. No. 402, Air Ministry, London.
(4) Eckert E. and Weise W., N.A.C.A. Technical Memo. No.1000.

						α_{ph}	$\alpha_{ph} - \alpha_{fp}$
						-	-
						-	-
						-	-
						-	-
						-	-
						-	-
						-	-
						-	-
						-	-
						-	-
23.4.48	"	503	"	"	1.62	-	-
29.4.48	"	504	"	"	1.51	-	-
7.5.48	"	883	"	"	1.78	-	-
9.7.48	"	504	"	"	1.67	-	-
15.7.48	"	502	FP under wing, PH under nose		1.63	2.25	0.62
16.7.48	"	936	"	"	1.78	2.52	0.74
21.7.48	"	704	"	"	-	-	0.64
22.7.48	"	503	"	"	1.73	2.30	0.57
9.2.49	ST 817	506	"	"	-	-	0.52
10.2.49	"	697	"	"	1.71	2.32	0.61
4.5.49	ST 796	900	"	"	-	-	0.70
13.5.49	"	850	"	"	-	-	0.70
7.6.49	ST 817	506	"	"	-	-	0.63
7.6.49	"	697	"	"	-	-	0.62
23.6.49	"	892	"	"	-	-	0.70
23.6.49	"	697	"	"	-	-	0.57
24.6.49	"	506	"	"	-	-	0.68
24.6.49	"	697	"	"	-	-	0.64
29.6.49	"	506	"	"	1.61	2.11	0.50
15.7.49	"	506	"	"	-	-	0.61
15.7.49	"	697	"	"	-	-	0.59
19.7.49	"	697	"	"	-	-	0.76
19.7.49	"	506	"	"	-	-	0.62
19.7.49	"	892	"	"	-	-	0.62

/TABLE III

TABLE I. RESULTS OF SPEED RUNS IN MOSQUITO AIRCRAFT.

DATE.	AIRCRAFT.	PRESSURE LEVEL mb.	ORIGINAL VALUE OF α.	RECALCULATED VALUE OF α.
10.3.48	RG 248	300	1.60	1.71
11.3.48	"	698	1.76	1.79
11.3.48	"	500	1.67	1.76
12.3.48	"	908	1.78	1.78
22.3.48	"	500	1.68	1.73
24.3.48	"	900	1.80	1.81
24.3.48	"	500	1.73	1.78
25.3.48	"	700	1.74	1.77
14.4.48	VL 621	300	1.58	1.66
23.4.48	"	301	1.61	1.67
26.4.48	"	301	1.52	1.62

MEAN VALUES OF α (RECALCULATED).

Aircraft \ Pressure Level MB.	900	700	500	300
RG 248	1.79	1.78	1.76	1.71
VL 621	-	-	-	1.65
BOTH	1.79	1.78	1.76	1.67

TABLE II. RESULTS OF SPEED RUNS IN HALIFAX AIRCRAFT.

DATE.	AIRCRAFT.	PRESSURE LEVEL MB.	MOUNTING	α_{fp}	α_{ph}	$\alpha_{ph} - \alpha_{fp}$
17.12.47	ST 817	527	Under Nose	1.70	-	-
17.12.47	"	832	" "	2.05	-	-
24.2.48	ST 796	929	" "	1.77	-	-
24.2.48	"	929	On extension under nose	1.92	-	-
26.2.48	"	505	" "	1.84	-	-
27.2.48	"	504	Under nose	1.77	-	-
27.2.48	"	504	On extension under nose	1.80	-	-
16.3.48	"	505	" "	1.74	-	-
16.3.48	"	505	Under Wing	1.70	-	-
23.3.48	"	508	" "	1.62	-	-
23.4.48	"	503	" "	1.62	-	-
29.4.48	"	504	" "	1.51	-	-
7.5.48	"	883	" "	1.78	-	-
9.7.48	"	504	" "	1.67	-	-
15.7.48	"	502	FP under wing, PH under nose	1.63	2.25	0.62
16.7.48	"	936	" "	1.78	2.52	0.74
21.7.48	"	704	" "	-	-	0.64
22.7.48	"	503	" "	1.73	2.30	0.57
9.2.49	ST 817	506	" "	-	-	0.52
10.2.49	"	697	" "	1.71	2.32	0.61
4.5.49	ST 796	900	" "	-	-	0.70
13.5.49	"	850	" "	-	-	0.70
7.6.49	ST 817	506	" "	-	-	0.63
7.6.49	"	697	" "	-	-	0.62
23.6.49	"	892	" "	-	-	0.70
23.6.49	"	697	" "	-	-	0.57
24.6.49	"	506	" "	-	-	0.68
24.6.49	"	697	" "	-	-	0.64
29.6.49	"	506	" "	1.61	2.11	0.50
15.7.49	"	506	" "	-	-	0.61
15.7.49	"	697	" "	-	-	0.59
19.7.49	"	697	" "	-	-	0.76
19.7.49	"	506	" "	-	-	0.62
19.7.49	"	892	" "	-	-	0.62

/TABLE III

TABLE III. MEAN VALUES OF a_{fp}, a_{ph}, and $a_{ph} - a_{fp}$ from HALIFAX RUNS.

1. MEAN VALUES OF a_{fp}

MOUNTING AND AIRCRAFT.	LOW LEVEL 900 mb. approx.	MEDIUM LEVEL 700 mb. approx.	HIGH LEVEL 500 mb. approx.
Under nose ST 817	2.05 (1)	-	1.70 (1)
" " ST 796	1.77 (1)	-	1.77 (1)
On extension under nose ST 796	1.92 (1)	-	1.79 (3)
Under wing ST 796	1.78 (2)	-	1.64 (7)
" " ST 817	-	1.71 (1)	1.61 (1)
All Mountings	1.86 (5)	1.71 (1)	1.69 (13)
All under wing mountings	1.78 (2)	1.71 (1)	1.64 (8)

2. MEAN VALUES OF a_{ph}

Under nose ST 796	2.52 (1)	-	2.27 (2)
" " ST 817	-	2.32 (1)	2.11 (1)
All mountings	2.52 (1)	2.32 (1)	2.22 (3)

3. MEAN VALUES OF $a_{ph} - a_{fp}$.

ST 796 (FP under wing) (PH under nose)	0.71 (3)	0.64 (1)	0.59 (2)
ST 817 (" " ")	0.66 (2)	0.63 (6)	0.59 (6)
All mountings	0.69 (5)	0.63 (7)	0.59 (8)

N.B. Bracketed figures indicate number of measurements.

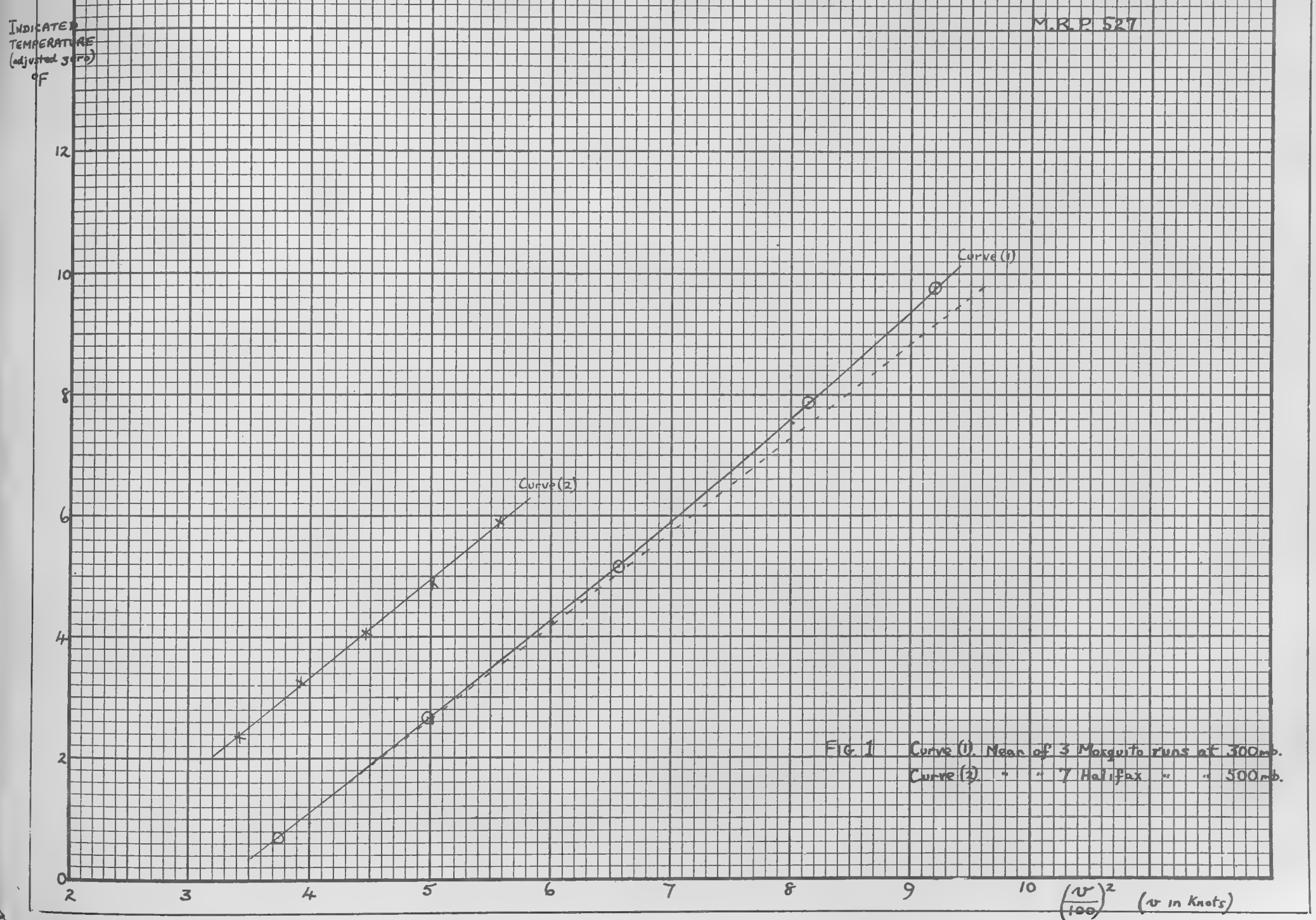

FIG 1 Curve (1). Mean of 3 Mosquito runs at 300 mb.
Curve (2). " " 7 Halifax " " 500 mb.

This report has not yet been published and is to be treated CONFIDENTIALLY. Its contents must not be quoted.

M.R.P.528
S.C.I/33
3rd January, 1950

AIR MINISTRY

METEOROLOGICAL RESEARCH COMMITTEE

AIR WEATHER SERVICE
TECHNICAL REFERENCE FILE

Frost Point Hygrometer for use on the Ground

by
D.D. Clark (Meteorological Office)

In the frost point hygrometer the temperature at which frost forms is obtained by observing the deposit on a polished metal surface. This metal surface is usually the flat top of a thimble whose temperature can be controlled and measured.

The methods employed for both control and measurement vary and depend on the purposes to which the hygrometer will be put and the conditions under which it will operate. Before plans for a frost-point hygrometer for use on the ground can be prepared information on these two points is essential.

The frost-point hygrometer enables the temperature of frost formation of an air sample to be found but, owing to the phenomenon of super-cooling of water-drops, the nature of the deposit on the thimble must be known when working in the range 0°C to approx. -12°C.

Visual observation is of course the simplest method of detecting a deposit and is effective even at the lowest frost points measurable. Prolonged observation in adverse conditions however causes fatigue and instruments required for prolonged observations are usually provided with photo-electric detection of the deposit.

The temperature of the thimble, which is also the frost-point temperature when a constant frost deposit is formed on the thimble, can be measured either by means of a platinum resistance wire wound directly on to the thimble which, in this case, is made of aluminium and anodised, or else by means of a thermo-couple inserted into a recess in the thimble underneath the polished flat surface. Temperature can be made automatically indicating or recording (the latter only if the hygrometer also is automatic) or may be obtained by manipulation of a Wheatstone bridge or a potentiometer as the case may be.

There are five practical methods of controlling the temperature of the thimble (a) by a jet of cold petrol; (b) by a jet of liquid air; (c) by conductivity cooling from a copper rod immersed in liquid air; (d) by a jet of carbon dioxide gas at liquid CO_2 pressures; (e) by a self-contained refrigerator.

The jet of cold petrol or methylated spirits issues from a pump containing the fluid which itself is immersed in a bath of solid carbon dioxide. In practice temperatures of about -60°C can be reached by this method but supplies of solid carbon dioxide must be readily available and the instrument must be replenished each time it is set up for use.

Cooling by a jet of liquid air from a pump immersed in the liquid in a Dewar flask is sufficient to reach frost points of -80°C with ease. In constant operation a quart size Dewar flask will last only a few hours. The same remarks apply to cooling by a copper rod immersed in liquid air but, in addition, electrical power is required to operate a heater coil by which means the temperature of the thimble can be raised.

/ The

The jet of carbon dioxide gas requires the supply of cylinders of carbon dioxide in liquid form. The temperature drop in the issuing gas is governed by the pressure drop so a close control on the thimble temperature can be obtained by controlling the pressure in the expansion chamber where the gas issues from the jet. The theoretical lower limit of temperature with this type of cooling is the triple point of CO_2 at -56.7°C but in practice temperatures of about -40°C are the lowest reached.

Automatic refrigeration is only required for continuous recording of frost points over a long period.

It is seem therefore, that the design of this hygrometer depends on the availability of supplies in the places where it will be used and also on the range of frost or dew points to be measured. Further, the method of temperature measurement is governed by the accuracy required.

Before work on this hygrometer can begin a clear statement therefore will be required of the exact purpose of the instrument e.g. "for field measurements in cold climates" or "for humidity control in low-pressure wind tunnels" etc., also the range of frost or dew point temperatures expected, the degree of accuracy required in the measurements, whether the hygrometer is to be used for single observations or for continuous recording and what facilities of supplies would be available where it is to be used.

It may be stated that the present pressurised version of the Dobson-Brewer frost-point hygrometer Mk.IIA which is compactly built with an airtight air supply and exhaust circuit, could be easily adapted for field use for single observations in places where solid carbon dioxide or liquid air were obtainable and that a photo-electric frost-point hygrometer using the carbon dioxide gas method of temperature control was made for the British-Norwegian-Swedish antarctic expedition 1949.

CONT... contents mus...

18th January, 1950.

AIR MINISTRY

METEOROLOGICAL RESEARCH COMMITTEE

AIR WEATHER SERVICE
TECHNICAL REFERENCE FILES

The Horizontal Dimensions of Cumulonimbus Clouds at Various Heights

by R.F. Jones (Meteorological Office)

AD 22324

1. Introduction

From time to time information is required concerning the horizontal dimensions of shower clouds, particularly in an examination of icing and turbulence hazards. Up to the present time it has only been possible to give an estimate of these dimensions without any detailed information on which to base this estimate. The fact that the radar echoes from shower clouds can be distinguished from the echoes from other weather phenomena enables information to be obtained on the horizontal extent of such echoes, and the results of a number of aircraft penetrations of these echoes enables a close estimate to be made of the horizontal extent of the clouds containing the echoes.

This paper provides the results of an analysis of a number of photographs of cumulonimbus radar echoes together with an examination of aircraft flights through cumulus and cumulonimbus clouds which gave a radar echo.

The radar equipment used was in all cases the A.M.E.S. Type 13 height-range equipment operating on a wave-length of 10 cm and more fully described elsewhere (1)

2. The radar echoes from cumulonimbus clouds

The writer has given elsewhere, (1) a description and interpretation of the various types of weather echoes, as viewed in the vertical cross-section, and has shown how it is possible to distinguish cumulonimbus weather echoes from those associated with other cloud formations. The outstanding characteristic of the cumulonimbus type of echo is the appearance of the echo in the form of a strong vertical column with sharply defined vertical edges (see photograph (1)) or, in the more extensive formations, a number of strong columns separated by well marked troughs (photograph (ii).

The P.P.I. presentation (photograph (iii)) shows the echoes associated with single column vertical cross-sections to be isolated and sharp edged with an approximately circular cross-section. Multiple column echoes on the other hand appear to be derived from masses of echo of all shapes, but sometimes forming a line of echo, which show signs of cellular structure (see photograph (iv)), each cell having associated with it a single column of echo and being approximately circular in cross-section.

It is important, however, to note that the echo received does not indicate the whole volume of the cloud but only that part of the cloud in which the drop sizes and concentrations are great enough to give a detectable signal at the radar receiver. A comparison between aircraft flights through echo and cloud is given in Section 6 below from which an approximate correction factor can be deduced to convert observed echo dimensions into probable cloud dimensions.

3. The data available and method of analysis used

Photographs of the height-range display tube on 35 mm. film are available for a large number of weather situations from March 1947 to the present day. For the purposes of this paper these photographs were examined for the period 13th May, 1947, to 4th October, 1948 and those relating to cumulonimbus echoes were extracted. A distinction was drawn between single and multiple column echoes; a total of 104 single column echoes occurring on 32 different days and 45 multiple column echoes occurring on 23 days was analysed.

/ The

The analysis consisted of examining the photographs under an enlarger and measuring the distance through the echo at height intervals of 5,000 ft., from 5,000 ft. above the station upwards. Measurements were made to the nearest $\frac{1}{4}$ mile while the vertical extent of the echo examined was noted to the nearest 500 ft. It should be noted that, by using height-range display photographs, measurements were always made along a radial line from the station; with a large number of measurements on a number of different days this is unlikely to lead to any systematic error.

In the case of the multiple column echoes, in addition to measuring the total width of the echo, the widths of the individual columns and of the clear intervals between those columns were measured.

Frequency tables were then constructed showing the distribution of the distances through the echo at each standard height for varying vertical extent of the echo. For multiple column echoes these frequency tables included not only the total distances through the echo but also the distribution of column widths and clear intervals at the standard heights.

To determine the correction factor to be applied to convert echo width into cloud width 35 cumulonimbus traverses by Spitfire aircraft from R.A.E., which co-operated with East Hill on turbulence investigations, (2), were available together with simultaneous radar echo photographs. The ratios of cloud width to echo width for these 35 flights were calculated and used to obtain mean correction factors.

4. The frequency distribution and mean values of single column echo widths.

Frequency distributions and mean values of single column echo widths, measured at height intervals of 5,000 ft. from 5,000 ft. above the station upwards, for various intervals of height of the echo top are given in Table I.

Table I indicates that for all single column echoes the most frequent column width at all heights up to 25,000 ft. lies in the range $2\frac{1}{4}$ - 3 miles, while above 25,000 ft. the number of observations available is probably too small for a representative sample to have been obtained. No single column was encountered with a width greater than 8 miles and widths greater than 7 miles were very infrequent and confined to heights of 15,000 ft. or below. At heights of 20,000 ft. and above single column widths greater than 6 miles did not occur while occurrences of widths greater than 5 miles were very infrequent.

From Table I it will also be seen that, except near the top of the echo column the mean column width was almost constant for all echoes extending to less than 35,000 ft. with a value of about $3\frac{1}{2}$ miles.

5. The frequency distributions and mean values of multiple column echo widths

(a) Total width of multiple column echoes

In Table II are shown the frequency distributions and mean values of total echo width of multiple column echoes (i.e. from the beginning of the first echo column to the end of the last echo column including the spaces between the columns clear of echo) for the standard height intervals at various intervals of height of the maximum echo top.

It will be seen that, as distinct from the single column echoes, there is no clearly defined echo width which contains a maximum frequency over any large interval of height. The greatest echo width measured was 13 miles and echo widths of over 10 miles were measured at heights up to and including 20,000 ft. Above 20,000 ft. echo widths of greater than 6 miles were rare although the number of observations is small. Except near the echo top, where the echo width probably became the width of a single remaining column, multiple column widths of less than 3 miles were rare.

/ It

It will be seen that the mean echo width is almost constant in the first 15,000 ft. of the echoes which extend higher than 20,000 ft. with a value of about $6\frac{1}{2}$ to 7 miles. At greater heights the mean echo width decreases, probably because some of the columns do not reach to the same height as others in the same echo. Smaller values of mean echo width are also encountered in those echoes which do not reach to 20,000 ft.

(b) Widths of individual columns and of the clear intervals between in multiple column echoes.

It is probable (1) that the columns of echo distinguish the parts within the cloud containing water drops of raindrop size, and those parts of the columns which extend above the freezing level probably indicate the presence of supercooled waterdrops and hence the volumes of increased icing risk. Further it has been shown (2) that the columns of echo are probably associated with the up-currents of the cumulonimbus cloud and the clear intervals between the columns with the down-currents. It is of interest therefore to determine, in echoes of the multi-column type, the widths of the individual columns and of the clear intervals between those columns.

For a large proportion of multi-column echoes (30 out of 44 examined) the echo showed no sign of breaking up into columns and clear intervals at 5,000 ft. although individual columns were visible at greater heights. At 10,000 ft. the echo appeared "solid" on 18 occasions out of 45 but at 15,000 ft. only 4 occasions out of 34 showed no sign of columns although the echo indicated column structure at greater heights. There were no occasions on which a multi-column echo appeared solid to heights as great as 20,000 ft. The distribution of echo widths on these occasions is shown in Table III.

On those occasions when individual columns were visible at the standard heights, measurements were made of the widths of the columns and clear intervals between them and a frequency table showing the distribution of these widths at the standard heights is shown in Table IV together with the mean values.

It will be seen that no columns were observed with a greater width than 7 miles and that column widths greater than 4 miles were rare. The mean column width at all heights was almost constant with a value of about $1\frac{1}{2}$ to 2 miles. No clear interval between the columns of echo exceeded 4 miles and clear intervals greater than 2 miles in width were rare. The mean clear interval was almost constant with a value of one mile.

It is of interest to note that the mean widths of individual columns in a multiple column echo are considerably less (about half the value) than the mean echo widths in a single column echo (Section 4, last paragraph); this point is returned to in Section 8(d) below.

6. The ratio between cloud width and echo width from aircraft flights.

Having, in Sections 4 and 5, obtained the frequencies of occurrence of various echo widths, it is necessary to determine the value of a correction factor to convert these echo widths into cloud widths, since it is known that the echo from a cumulonimbus cloud is not received from the whole cloud but only from that part of the cloud containing a sufficient number of large enough drops. Available for this purpose were the results of a number of flights made by a Spitfire aircraft from R.A.E. on turbulence investigations (2). On these flights the pilot switched on his recording accelerometer on entry into cloud, and off immediately on leaving cloud, while on a course directly towards or away from the radar station. At the same time photographs were taken of the radar weather echo so that the distance flown through the echo was directly comparable with the distance flown through cloud as determined by the time scale of the accelerometer record. The ratio of cloud width to echo width was determined and the results for 35 such flights are shown in Table V.

/ It

It will be seen that, although for 20 out of 35 flights the value of this ratio was less than 1.60, the ratio on a few occasions was considerably greater with a maximum value of 5.11. These abnormally large values can probably be ascribed to cloud formations which are not really part of the active cumulonimbus cloud. For example, cumulonimbus cloud sometimes extends through broken and occasionally extensive layers of stratocumulus and if an aircraft flight was made at the height of the stratocumulus layer a large part might be in the Sc cloud, (which would not give a weather echo) and not in the cumulonimbus. Similarly the cumulonimbus cloud often spreads out at high levels into an anvil cloud, which usually fails to give an echo, so that a large value of the ratio cloud width to echo width might be expected in those runs near the top of the cloud. That this is the case will be seen from Table V, for of the 8 occasions when flights were made within 2,000 ft. of the top of the echo, 6 had ratios greater than 2.0, including the four biggest ratios of all, with a mean ratio of 2.87. The mean ratio for the remaining 27 flights was 1.60.

If we take the single and multi-column echoes separately we find that for single column echoes the ratio of cloud width to echo width is 1.8, if we exclude those flights (six in number) within 2,000 ft. of the top of the echo for which the average ratio if 3.0. For multi-column echoes the ratio is 1.3, excluding those flights (two in number with a mean value of 2.6) within 2,000 ft. of the echo top.

The mean echo widths of the single and multiple column echoes examined by the aircraft, excluding those within 2,000 ft. of the top of the echo, were 3.2 and 6.0 miles respectively, which are in sufficiently close agreement with the mean echo widths obtained from a much greater sample in Tables I and II to ensure that the ratios of cloud to echo width obtained in this section are representative.

Applying the conversion factors here obtained to the mean values in Tables I and II we arrive at Tables VI and VII which show the average widths of cumulonimbus clouds of varying vertical extent in this country, Table VI for clouds giving a single radar echo column and Table VII for multiple column clouds. The larger of the two conversion factors (applicable to flights within 2,000 ft. of the echo top) is applied to the highest standard height measured in Tables I and II, although in the case of multiple column clouds this factor is based on only 2 readings and is therefore very approximate.

The close correspondence between the widths at 20,000, 25,000 and 30,000 ft. of single and multi-column clouds containing radar echoes extending to 30,000 - 34,500 ft. suggests that the values in the multi-column case relate to a single remaining column of echo, the other columns having failed to reach to 20,000 ft. The same explanation probably applies also to the 25,000 ft. reading in the multi-column cloud extending to 25,000 - 29,500 ft.

The vertical extent of the cloud is not known with any accuracy except that it must be greater than, or equal to, the vertical extent of the echo, so that the vertical extent of the echo given in Tables VI and VII represents a lower limit to the vertical extent of the cloud. Data are not available at present to relate echo top height to cloud top and it is probable that no simple relationship exists since the size and number of radar reflecting particles in the upper levels of the cloud probably depend on the stage of development the cloud has reached.

7. <u>The relation between the vertical extent of a cumulonimbus cloud and the width of the cloud at 5,000 ft.</u>

As mentioned in Section 6 (last para.) above, the vertical extent of the cloud containing an echo is not known with any accuracy but the minimum height of the cloud top will be given by the height of the radar echo top.

/ If

If we now assume that, on the average, the cloud base of a cumulonimbus cloud is 2,500 ft. we have, from the radar, the minimum vertical extent of the cloud.

The ratio of the minimum vertical extent of the cloud, obtained in this way, to radar echo width at 5,000 ft. has been determined for the 104 occasions in Table I for single cell cumulonimbus clouds and for the 44 occasions in Table II for multiple cell clouds. Frequency tables showing the distribution of these ratios are given in Table VIII.

Examination of the 5 occasions for single cell clouds when the ratio was greater than 2.3 showed that on all these occasions the range at which the echo was observed was 45 miles or greater, so that the attenuation of the radar beam due to range was considerable and the value of the ratio therefore open to question. The only other occasion of range greater than 45 miles for single cell clouds gave a ratio of 0.6 and there was one occasion for multiple cell clouds with a ratio of 0.5.

Omitting therefore these occasions, when the range of observation was 45 miles or greater, we can form mean values of the ratio for different intervals in height of the echo top (or minimum cloud top). From Section 6 we see that for single column clouds the ratio of cloud width to echo width is 1.8:1 and, for multiple column clouds, 1.3:1, so that we can obtain mean values of the ratio of minimum vertical extent of the cloud to cloud width for different intervals of height of the echo top (or minimum cloud top). These values are shown in Table IX.

The ratios so obtained indicate, as shown more clearly in Table VI, that the mean width of a single column cumulonimbus cloud is largely independent of the vertical extent of the cloud, for if the vertical extents of the cloud are 3, 4, 5 and 6 miles the ratios from Table IX give mean widths of the cloud of 6, 6.7, 6.3 and 7.5 miles respectively for single cell clouds. This point is returned to in Section 8(d) below.

8. Discussion of results

(a) The proportion of a traverse of a cumulonimbus cloud which is through the radar echo

We have seen in Section 6, that, except near the top of the echo, the ratio of cloud width to total echo width is 1.8 for single column echoes and 1.3 for multiple column echoes.

If a multiple column echo consists of n columns there must be (n - 1) clear intervals between the columns. From Table IV the mean column width in these cases is 1.82 miles and the mean clear interval 1.07 miles.

Hence the total echo width = 1.82n + 1.07(n - 1) miles

= 2.89n - 1.07 miles

The cloud width is then 1.3(2.89n - 1.07) miles

= 3.76n - 1.39 miles

The n columns have a width 1.82n miles

Therefore for multiple column echoes the ratio

$$\frac{\text{echo only}}{\text{total cloud}} = \frac{1.82n}{3.76n - 1.39}$$

which expression has values 0.59, 0.55, 0.53, 0.52 for n = 2, 3, 4, 5 respectively.

/ For

For single column echoes the ratio

$$\frac{\text{echo only}}{\text{total cloud}} = \frac{1}{1.8}$$

$$= 0.56$$

Hence it would appear that an aircraft flying through a cumulonimbus cloud giving an echo, whether composed of one or more columns, would on the average be within the part of the cloud from which the echo is received for rather more than half (0.52 to 0.59) the traverse, provided the traverse was not made near to the top of the cloud (when the proportion would be much less) and, in the case of multiple column echoes, was not made below the height at which the columns merged together to form a solid block of echo - usually below 10,000 ft. (see Table III). In this latter case, i.e. in multiple column echoes below about 10,000 ft. the aircraft might often be within the radar echo for 1/1.3 = 0.77 of the total cloud traverse, and usually if the traverse was made at 5,000 feet or below.

(b) The proportion of the area of cross-section of a cell of a cumulonimbus cloud which contains the radar echo.

If we regard a cumulonimbus cloud giving a single column echo and the echo itself as having a circular cross-section (which is probably approximately true - see photograph (iii)) and if t is the diameter of the echo and d the diameter of the cloud we have seen that

$$t/d = 0.56 \quad \text{(Section 8(a))}$$

The ratio of the area of cross-section of the echo to the area of cross-section of the whole cloud is

$$t^2/d^2 = 0.31$$

In the case of a cloud giving a multiple column echo we may regard the cloud as consisting of individual cells composed of a column of echo with a surrounding interval clear of echo. If we regard the cross-section of the individual cell and echo column as circular, and if t_1 is the diameter of the echo column and d_1 the diameter of the cell, then the ratio of cross-section of the echo to area of cross-section of the cell is t_1^2/d_1^2.

From Table IV the mean diameter of a column = t_1 = 1.82 miles and the mean clear interval between columns = $d_1 - t_1$ = 1.07 miles, assuming that on the average the echo and clear interval are concentric.

$$\text{Hence } t_1^2/d_1^2 = (0.63)^2$$

$$= 0.40$$

(It should be noted that if the vertical cross-section of a complete multi-column cloud consisted simply of cells of this type in contact with each other the ratio of cloud width to total echo width for n columns would be

$$\frac{nd_1}{nt_1 + (n-1)(d_1 - t_1)} = \frac{nd_1}{(n-1)\,d_1 + t_1}$$

which has values of 1.23, 1.14 for n = 2, 3 respectively. These values are less than the mean value of 1.3 found experimentally, although values of 1.25 or less, see Table V, occur 6 times out of 11 in traverses of multiple column echoes not within 2,000 ft. of the echo top. It is considered that the average is increased to 1.3 by the occurrence of other cloud than true cumulonimbus cloud (e.g. broken stratocumulus) at the heights of the remaining 5 traverses.).

/ The

The ratio of area of cross-section of echo to area of cross-section of cloud is therefore approximately 1:3 in all single cell cumulonimbus clouds, except near the top of the cloud, and 1:2½ for individual cells in a multiple cell cumulonimbus cloud. The ratio of area of cross-section of the echo column to the area of cross-section of the cloud or cell clear of echo will then be 1:2 for single cell clouds and 1:1½ for individual cells in a multi-cell cloud.

Now there is some evidence (2) to suggest that the columns of echo are indications of the zones of strong upward currents in the cloud and that the clear intervals between the columns correspond to down-currents. There is also some evidence that immediately on entry into the cloud and before entering the echo down currents exist.

If the cumulonimbus cloud having a single column echo or the individual cell of a multi-cell cloud is a self-contained entity, so that air flowing upwards through a part of a cross-section of the cloud or cell is balanced by air flowing downwards through the remainder of the cross-section, then the mean down current in the cross-section will bear the same relationship to the mean up-current as the area of cross-section of the echo bears to the area of cross-section of the cloud or cell free from echo, i.e. the ratio of mean down-current to mean up-current would be 1:2, in single cell clouds and 1:1½ in the individual cell of the multi-cell cloud.

American measurements (3) have indicated that in Florida thunderstorms which were almost, if not quite, entirely multi-cell storms the mean up-current is greater than the mean down-current, except at 6,000 ft. (at which height radar division into cells is rarely possible in our experience), with ratios of up-current to down-current of 1.33, 1.14, 1.41 and 1.14 at 11,000, 16,000, 21,000 and 26,000 ft. respectively, the mean ratio being 1.25. It is of interest to note that if the ratio of mean echo column diameter to mean cell diameter had been 0.66 instead of 0.63 as measured, the ratio of up-current to down-current on the above reasoning would also be 1.25. An increase of mean echo diameter from 1.82 to 2.00 miles with decrease of mean clear interval from 1.07 to 1.00 miles would be sufficient.

The fundamental assumption in the foregoing is that air carried upwards in the active cumulonimbus cloud is balanced by air flowing downwards within the cloud while the commonly accepted mechanism visualises the descent of air as taking place over a much greater area outside the cloud, citing as supporting evidence the dissipation of other clouds in the vicinity of large cumulonimbus masses. Nevertheless the large values of mean down currents within the cloud found by the Americans and the foregoing interpretation of echo columns and intervals clear of echo within the cloud suggest that a large proportion, at any rate, of the air which ascends must be replaced by down-currents within the clouds.

(c) Turbulence and icing in cumulonimbus clouds.

A corollary of the reasoning of Section 8(b) is that if the mean up-currents in a single cell and multiple cell cumulonimbus cloud are the same the mean down-currents in the single cell cloud will be less than in the multi-cell cloud. If the turbulence on traversing a cumulonimbus is principally associated with the passage from major down-currents to major up-currents or vice versa and the strength of these currents, as seems probable, then it would be expected that the turbulence would be more severe, as regards maximum gusts, in the multi-cell clouds than in the single cell clouds, while the existence of more than one, and narrower, columns in the multi-cell clouds would also be expected to give a greater frequency of large gusts than in the single cell clouds. As regards turbulence therefore the multi-cell cloud would be expected to be more dangerous to an aircraft than a single cell one. It may also be noted that since the mean up-current is likely always to be stronger than the mean down-current and the aircraft likely to be in the echo (and hence probably up-current) slightly longer than in the down-current, except near the top of the cloud, the net effect of a traverse would be expected to be reflected in a gain of height by the aircraft unless compensated by pilot's control.

/ From

From Section 8(a) it is seen that an aircraft traverse of a cumulonimbus cloud, whether single or multi-cell, above about 10,000 ft. and not near to the top of the cloud, would include rather more than half the traverse in the radar echo, and if the traverse was made above the freezing level, the aircraft would be exposed to the risk of rapid ice accretion for this period. Since the dimensions of a multi-cell cloud are normally greater than those of a single cell cloud the amount of icing to be expected in a multi-cell cloud is correspondingly greater.

While preferable to avoid flying through all cumulonimbus clouds it is clear that, if a choice has to be made, the multi-cell cloud offers the greatest hazards both from turbulence and icing. In some cases there appears to be a tendency e.g. in troughs or cold fronts, for the cells to form in a line so that the cross-section in the direction of the line may be composed of several cells while the cross-section at right angles to this line may contain only a single cell. The pilot of an aircraft equipped with radar, when faced with a multi-cell echo on his radar screen, would therefore by manoeuvring sometimes have the opportunity of making a single cell traverse of a mass of cumulonimbus by a temporary change of course.

(d) The growth of a cumulonimbus cloud

It is of interest to note (Table VI and Section 7) how little the average horizontal dimensions of a single cell cumulonimbus cloud change with increasing vertical extent of the cloud and, in a particular cloud, the little change in horizontal extent at different heights in the cloud. These results suggest that once a cumulus contains drops of raindrop size any further growth of the cloud takes place only in the vertical without any appreciable lateral spread of the cloud as long as the cloud remains a single cell. If lateral development does take place then, instead of the original cloud growing laterally, the cloud splits up into separate cells each having approximately the same diameter, but this diameter will be appreciably less (about half) the original single cell. This suggests, as first reported by Byers and Braham (4), that lateral development takes place by the initiation of new cells on the perimeter of the original cell possibly owing to the forced uplift of the air surrounding this cell by the descending air in the outer edges of the original cloud. Growth of these new cells on the perimeter of the older cloud imposes a new circulation on the old and part of the ascending current of the older cloud is "eaten away" by the growing down current of the new cell, with the result that the diameter and activity of the old cell is reduced and the cloud develops more than one cell each of less diameter than the original single cell. Some evidence of such an occurrence is provided by the examination of the multiple cell radar cross-sections in which it is seen that some of the columns are less intense and more diffuse - indicating that the process of decay has set in - than others, showing that not all the cells are in the same stage of development, the decaying cell being flanked by one or more active cells. An extreme example of such a case is shown in photograph (v) while photograph (ii) illustrates a more frequent occurrence. The growth of new cumulonimbus columns on the edge of the main thunderstorm cloud mass has also been noted on occasions by the pilots of the R.A.E. aircraft engaged in turbulence investigations.

9. Note on the P.P.I. photographs of shower type echoes

It will be noted that in the P.P.I. photographs of multi-cell cumulonimbus echoes the individual cells are not clearly defined and do not show the clear intervals between the individual columns of echo which are an integral part of the cell as defined in this paper. This is because the P.P.I. photograph shows the projection on an almost horizontal plane of a considerable interval of height of the echoing volume - the beam width

/ of

of the equipment in the vertical being about $7\frac{1}{2}$ degrees. As seen in Table III identification of individual columns in the vertical cross-section of the echo was rarely possible at 5,000 ft, the echo usually appearing solid at this height although dividing into columns at greater heights. On the P.P.I. photographs therefore the division into columns is masked by the response from about 5,000 feet so that only an indication of the possibility of clear intervals inside the echo is shown. A different P.P.I. equipment with a narrower vertical beam width and the aerial inclined to give a cross-section at 15,000 ft., say, would undoubtedly show the cellular structure much more clearly.

10. Summary

Cumulonimbus clouds can be distinguished by radar as consisting of cells which are approximately circular in cross-section and contain a column of radar echo surrounded by an interval of cloud which fails to give a radar echo.

Clouds containing a single cell are smaller than those which contain a number of cells but the isolated single cell is larger than those which exist in close proximity to each other to form a large cumulonimbus mass.

The mean diameter of a single cell cloud is of the order of 6 miles at all heights until near to the top of the cloud while a multi-cell cloud has a mean width of about 9 miles with the individual cells about 3 miles in diameter.

On a flight above the freezing level through a cumulonimbus cloud severe icing conditions are likely to be encountered on about 0.5 to 0.6 of the traverse while the turbulence both as regards magnitude and frequency of gusts is probably greater in a multi-cell cloud than in a single cell cloud.

There is some evidence to suggest that the speed of the down-currents in a single cell cloud are likely to average about half the speed of the up-currents but in a multi-cell cloud the ratio of speeds of down-currents and up-currents may average about 2 : 3 or possibly, in combination with some American results, about 4:5.

11. References

1. Jones, R.F.: The height and temperatures at the tops of radar echoes associated with various cloud systems. M.R.P. No. 458, Air Ministry, Meteorological Research Committee, London, 1949.

2. Jones, R.F.: The relation between the radar echoes from cumulus and cumulonimbus clouds and the turbulence within those clouds. M.R.P. No. 484, Air Ministry, Meteorological Research Committee, London, 1949.

3. A report on thunderstorm conditions affecting flight operations, Technical Paper No. 7, Thunderstorm Project, Chicago, Ill., Washington, April 1948.

4. Byers and Braham: Thunderstorm structure and circulation. J. Met., Milton, Mass., Vol.5, No.3, June, 1948.

TABLE I

The frequency distributions and mean values of single column echo widths at various heights for different intervals of height of the echo top

A. 5,000 FEET ABOVE STATION

Height of echo top (feet)	Echo Widths (miles)								Total	Mean echo width (miles)
	¼ - 1	1¼ - 2	2¼ - 3	3¼ - 4	4¼ - 5	5¼ - 6	6¼ - 7	7¼ - 8		
0 - 9,500	3	1							4	1.2
10,000 - 14,500	2	13	7	3					25	2.1
15,000 - 19,500	0	2	13	9	5	2			31	3.4
20,000 - 24,500	0	1	9	4	4	0	1		19	3.5
25,000 - 29,500	1	2	3	2	2	0	1		11	3.2
30,000 - 34,500	0	0	2	2	3	0	0		7	3.7
35,000 - 39,500	0	1	1	1	1	0	1	1	6	4.6
Over 39,500	0	0	1	0	0	0	0	0	1	(2.7)
Totals	6	20	36	21	15	2	3	1	104	

B. 10,000 FEET ABOVE STATION

10,000 - 14,500	9	11	4	1					25	1.4
15,000 - 19,500	0	6	9	9	6	1			31	3.1
20,000 - 24,500	0	3	8	3	3	0	1	1	19	3.6
25,000 - 29,500	0	3	3	2	1	0	2		11	3.5
30,000 - 34,500	0	0	2	3	2				7	3.6
35,000 - 39,500	0	0	1	2	1	0	1	1	6	4.8
Over 39,500	0	0	1	0	0	0	0	0	1	(3.0)
Totals	9	23	28	20	13	1	4	2	100	

/ C.

TABLE I (contd.)

Height of echo top (feet)	Echo Widths (miles)								Total	Mean echo width (miles)
	¼ - 1	1¼ - 2	2¼ - 3	3¼ - 4	4¼ - 5	5¼ - 6	6¼ - 7	7¼ - 8		
				F. 30,000 FEET ABOVE STATION						
30,000 - 34,500	6	0	0	0	1				7	1.3
35,000 - 39,500	2	0	1	1	2				6	3.0
Over 39,500	0	1							1	(1.3)
Totals	8	1	1	1	3				14	
				G. 35,000 FEET ABOVE STATION						
35,000 - 39,500	2	1	2	1					6	2.0
Over 39,500	0	1							1	(1.7)
Totals	2	2	2	1					7	

TABLE II

The frequency distributions and mean values of multiple column echo widths at various heights for different intervals of height of the echo top.

A. 5,000 FEET ABOVE STATION

Height of echo top (feet)	Echo Widths (miles)											Total	Mean echo width (miles)
	$\frac{1}{4}$ - 1	$1\frac{1}{4}$ - 2	$2\frac{1}{4}$ - 3	$3\frac{1}{4}$ - 4	$4\frac{1}{4}$ - 5	$5\frac{1}{4}$ - 6	$6\frac{1}{4}$ - 7	$7\frac{1}{4}$ - 8	$8\frac{1}{4}$ - 9	$9\frac{1}{4}$ - 10	Over 10		
0 - 9,500	0	0	0	0	0	0	0	0	0	0	0	0	-
10,000 - 14,500	0	0	2	0	2	4	2	0	0	1	0	11	5.5
15,000 - 19,500	0	0	0	3	3	1	0	0	0	0	0	7	4.3
20,000 - 24,500	0	0	0	0	0	4	2	4	1	0	0	11	6.9
25,000 - 29,500	0	0	0	0	2	4	0	0	0	2	0	8	6.6
30,000 - 34,500	0	0	0	2	0	0	0	0	0	2	1	5	8.2
35,000 - 39,500	0	0	0	0	0	0	0	0	1	0	0	1	(8.3)
Over 39,500	0	0	0	0	0	0	0	0	0	1	0	1	(10.0)
Totals	0	0	2	5	7	13	4	4	2	6	1	44	

B. 10,000 FEET ABOVE STATION

10,000 - 14,500	1	0	3	2	2	2	1	0	0	0	0	11	3.9
15,000 - 19,500	0	0	1	4	1	1	0	0	0	0	0	7	3.9
20,000 - 24,500	0	0	0	0	1	2	3	4	1	0	0	11	6.8
25,000 - 29,500	0	0	0	1	0	4	1	0	0	0	2	8	6.8
30,000 - 34,500	0	0	0	2	0	1	0	0	0	1	2	6	7.3
35,000 - 39,500	0	0	0	0	0	0	0	0	1	0	0	1	(8.3)
Over 39,500	0	0	0	0	0	0	0	0	0	1	0	1	(10.0)
Totals	1	0	4	9	4	10	5	4	2	2	4	45	

/C.

Height of echo top (feet)	Echo Widths (miles)											Total	Mean echo width (miles)
	¼ - 1	1¼ - 2	2¼ - 3	3¼ - 4	4¼ - 5	5¼ - 6	6¼ - 7	7¼ - 8	8¼ - 9	9¼ - 10	Over 10		
C. 15,000 FEET ABOVE STATION													
15,000 - 19,500	1	1	3	1	1	0	0	0	0	0	0	7	2.7
20,000 - 24,500	0	0	0	1	2	2	3	1	2	0	0	11	6.3
25,000 - 29,500	0	0	0	1	2	2	1	0	0	1	1	8	6.5
30,000 - 34,500	0	0	0	2	0	0	1	0	2	1	0	6	6.8
35,000 - 39,500	0	0	0	0	0	0	0	0	1	0	0	1	(8.3)
Over 39,500	0	0	0	0	0	0	0	0	0	0	1	1	(10.5)
Totals	1	1	3	5	5	4	5	1	5	2	2	34	
D. 20,000 FEET ABOVE STATION													
20,000 - 24,500	2	1	2	3	0	1	1	0	1	0	0	11	3.6
25,000 - 29,500	0	0	0	2	1	3	0	0	1	0	1	8	5.9
30,000 - 34,500	0	0	2	0	1	1	1	0	1	0	0	6	5.0
35,000 - 39,500	0	0	0	0	0	0	0	1	0	0	0	1	(7.5)
Over 39,500	0	0	0	0	0	0	0	0	0	1	0	1	(10.0)
Totals	2	1	4	5	2	5	2	1	3	1	1	27	
E. 25,000 FEET ABOVE STATION													
25,000 - 29,500	3	3	1	1	0	0	0	0	0	0	0	8	1.7
30,000 - 34,500	1	0	1	1	1	1	0	1	0	0	0	6	4.3
35,000 - 39,500	0	0	0	0	1	0	0	0	0	0	0	1	(5.0)
Over 39,500	0	0	0	0	1	0	0	0	0	0	0	1	(5.0)
Totals	4	3	2	2	3	1	0	1	0	0	0	16	

/F.

Height of echo top (feet)	Echo Widths (miles)											Total	Mean echo width (miles)
	¼ - 1	1¼ - 2	2¼ - 3	3¼ - 4	4¼ - 5	5¼ - 6	6¼ - 7	7¼ - 8	8¼ - 9	9¼ - 10	Over 10		
F. 30,000 FEET ABOVE STATION													
30,000 - 34,500	4	1	0	0	0	1	0	0	0	0	0	6	1.5
35,000 - 39,500	0	0	0	0	0	1	0	0	0	0	0	1	(6.0)
Over 39,500	0	0	0	0	1	0	0	0	0	0	0	1	(4.7)
Totals	4	1	0	0	1	2	0	0	0	0	0	8	
G. 35,000 FEET ABOVE STATION													
35,000 - 39,500	0	0	0	0	0	1	0	0	0	0	0	1	(6.0)
Over 39,500	0	0	0	0	1	0	0	0	0	0	0	1	(4.3)
Totals	0	0	0	0	1	1	0	0	0	0	0	2	
H. 40,000 FEET ABOVE STATION													
Over 39,500	0	1	0	0	0	0	0	0	0	0	0	1	(2.0)

TABLE III

Frequency distributions of the widths of echoes which were "solid" at the height indicated although dividing into columns at greater heights

Echo widths (miles)											Total	Total no. of multi-col. echoes observed.
$\frac{1}{4}$ - 1	$1\frac{1}{4}$ - 2	$2\frac{1}{4}$ - 3	$3\frac{1}{4}$ - 4	$4\frac{1}{4}$ - 5	$5\frac{1}{4}$ - 6	$6\frac{1}{4}$ - 7	$7\frac{1}{4}$ - 8	$8\frac{1}{4}$ - 9	$9\frac{1}{4}$ - 10	Over 10		
					A. 5,000 FEET ABOVE STATION							
0	0	1	5	6	7	2	4	0	4	1	30	44
					B. 10,000 FEET ABOVE STATION							
0	0	0	4	1	5	2	2	1	1	2	18	45
					C. 15,000 FEET ABOVE STATION							
0	0	0	1	1	0	2	0	0	0	0	4	34
					D. 20,000 FEET ABOVE STATION AND HIGHER							
						NIL					0	27

G.256083(c)/JMB/1/50/40

TABLE IV

The frequency distributions of individual column widths and of the widths of the clear intervals between them in multiple column echoes at various heights

COLUMN WIDTHS (Miles)								WIDTHS OF CLEAR INTERVALS (Miles)					MEAN VALUES (Miles)	
$\frac{1}{4}$ - 1	$1\frac{1}{4}$ - 2	$2\frac{1}{4}$ - 3	$3\frac{1}{4}$ - 4	$4\frac{1}{4}$ - 5	$5\frac{1}{4}$ - 6	$6\frac{1}{4}$ - 7	Over 7	$\frac{1}{4}$ - 1	$1\frac{1}{4}$ - 2	$2\frac{1}{4}$ - 3	$3\frac{1}{4}$ - 4	Over 4	Column	Clear
						A. 5,000 FT. ABOVE STATION								
8	10	11	3	2	0	0	0	16	3	1	0	0	2.13	0.95
						B. 10,000 FT. ABOVE STATION								
23	21	9	7	1	1	0	0	20	14	0	1	0	1.75	1.05
						C. 15,000 FT. ABOVE STATION								
20	26	11	7	3	2	1	0	28	9	3	0	0	2.00	0.96
						D. 20,000 FT. ABOVE STATION								
21	25	7	3	3	0	0	0	19	8	5	0	0	1.72	1.22
						E. 25,000 FT. ABOVE STATION								
14	8	1	2	1	0	0	0	7	1	1	1	0	1.38	1.27
						F. 30,000 FT. ABOVE STATION								
6	2	0	0	1	1	0	0	1	1	0	0	0	1.70	1.37
						TOTALS FOR ALL HEIGHTS							MEAN VALUES (miles) for all heights	
92	92	39	22	11	4	1	0	91	36	10	2	0	1.82	1.07

G.256083(d)/JMB/1/50/40

TABLE V

Aircraft flights through echo and cloud

(1) No.	(2) Date	(3) Type of echo (single or multi-column)	(4) Height of echo top (feet)	(5) Height of aircraft traverse (feet)	(6) Distance through cloud (yds)	(7) Distance through echo (yds)	(8) Ratio of Col. (7) to Col. (6)	(9) Remarks
1	25/5/48	Single	9,500	9,00	9,280	3,030	3.06	Through top of echo.
2	1/6/48	Multiple	22,000	16,000	10,510	8,480	1.24	
3	1/6/48	Multiple	21,000	10,500	6,900	4,840	1.43	
4	2/6/48	Multiple	17,000	10,000	6,120	4,900	1.25	Echo rather diffuse this height.
5	2/6/48	Multiple	11,000	7,500	12,420	11,700	1.06	
6	3/6/48	Single	21,000	15,000	4,220	2,200	1.92	Isolated col. out of much larger echo.
7	3/6/48	Single	14,500	10,000	10,200	3,520	2.90	
8	3/6/48	Single	15,000	7,000	8,330	4,400	1.89	
9	3/6/48	Single	14,000	5,000	10,640	3,700	2.88	
10	3/6/48	Multiple	14,000	12,000	7,480	3,460	2.16	Near echo top.
11	3/6/48	Multiple	19,000	7,000	14,800	11,000	1.35	
12	9/6/48	Single	15,500	15,000	4,320	2,315	1.87	Near echo top.
13	9/6/48	Single	14,000	8,000	7,040	3,000	2.35	
14	10/6/48	Multiple	22,000	10,000	18,450	12,500	1.48	
15	10/6/48	Multiple	25,000	14,000	22,700	19,500	1.16	
16	17/6/48	Single	14,000	12,000	8,139	1,590	5.11	Near echo top.
17	17/6/48	Single	15,000	8,000	15,922	7,440	2.14	
18	17/6/48	Multiple	10,000	5,000	13,476	8,550	1.58	
19	28/6/48	Single	19,000	11,000	8,740	8,740	1.00	Diffuse echo
20	28/6/48	Single	20,000	10,000	14,640	11,500	1.27	
21	28/6/48	Multiple	26,000	24,000	14,860	5,030	2.95	Near echo top.
22	13/7/48	Single	11,500	10,000	8,090	3,460	2.34	Near echo top.
23	13/7/48	Single	13,000	9,000	7,460	3,100	2.40	
24	13/7/48	Single	16,000	15,800	2,590	2,000	1.29	Near echo top.
25	13/7/48	Single	14,000	13,000	7,740	1,850	4.17	Near echo top.

G.256083(e)/JMB/1/50/40

(1) No.	(2) Date	(3) Type of echo (single or multi-column)	(4) Height of echo top (feet)	(5) Height of aircraft traverse (feet)	(6) Distance through cloud (yds)	(7) Distance through echo (yds.)	(8) Ratio of Col. (7) to Col. (6)	(9) Remarks
26	13/7/48	Single	16,000	8,000	7,450	5,280	1.41	
27	13/7/48	Multiple	13,500	10,000	10,040	7,550	1.33	
28	30/7/48	Single	38,500	18,000	9,200	5,870	1.56	
29	30/7/48	Single	39,000	36,000	16,140	10,860	1.49	
30	13/8/48	Single	15,000	11,000	7,600	3,500	2.17	
31	13/8/48	Single	10,000	5,000	5,780	4,850	1.19	
32	3/9/48	Single	15,000	6,000	8,000	7,000	1.14	
33	3/9/48	Single	13,000	6,000	6,360	5,280	1.20	
34	4/10/48	Multiple	12,000	8,000	19,280	16,400	1.17	
35	4/10/48	Multiple	10,500	5,000	12,520	10,720	1.17	

TABLE VI

Mean widths (miles) of single echo column cumulonimbus clouds at various heights for varying vertical extent of the radar echo.

Height of echo top (feet)	HEIGHT (feet)						
	5,000	10,000	15,000	20,000	25,000	30,000	35,000
0 - 9,500	3.6	-	-	-	-	-	-
10,000 - 14,500	3.8	4.2	-	-	-	-	-
15,000 - 19,500	6.1	5.6	4.5	-	-	-	-
20,000 - 24,500	6.3	6.5	6.1	5.1	-	-	-
25,000 - 29,500	5.8	6.3	5.9	4.7	4.8	-	-
30,000 - 34,500	6.7	6.5	5.9	6.1	5.6	3.9	-
35,000 - 39,500	8.3	8.6	6.8	6.8	6.1	5.4	6.0

TABLE VII

Mean widths (miles) of multiple echo column cumulonimbus clouds at various heights for varying vertical extent of the radar echo.

Height of echo top (feet)	HEIGHT (feet)						
	5,000	10,000	15,000	20,000	25,000	30,000	
10,000 - 14,500	7.1	10.1	-	-	-	-	
15,000 - 19,500	5.6	5.1	7.0	-	-	-	
20,000 - 24,500	9.0	8.8	8.2	9.4	-	-	
25,000 - 29,500	8.6	8.8	8.5	7.7	4.4	-	
30,000 - 34,500	10.7	9.5	8.8	6.5	5.6	3.9	

TABLE VIII

Frequency distributions of the ratio of minimum vertical extent of cloud to radar echo width at 5,000 ft., for single and multiple cell cumulonimbus clouds

A. Single cell cumulonimbus clouds

Ratio:-	0.4	0.5	0.6	0.7	0.8	0.9	1.0	1.1	1.2	1.3	1.4	1.5	1.6	1.7	1.8	1.9	2.0	2.1	2.2	2.3	Over 2.3
No. of Occasions:-	1	2	9	10	10	14	10	5	7	11	6	2	3	2	2	1	2	1	0	1	5

Total Number of Occasions:- 104

B. Multiple cell cumulonimbus clouds

Ratio:-	0.2	0.3	0.4	0.5	0.6	0.7	0.8	0.9	1.0	1.1	1.2	1.3	1.4
No. of Occasions:-	1	7	5	7	7	8	4	2	1	0	0	1	1

Total Number of Occasions:- 44

G.256083(g)/JMB/1/50/40

TABLE IX

Mean values of the ratios of minimum vertical extent of the cloud to cloud width for different intervals of height of the minimum cloud top.

Echo Top (Minimum cloud top) (feet)	Ratio of minimum vertical extent of cloud to cloud width at 5,000 ft. Single column clouds.	Multi-column clouds.
0 - 9,500	0.6	-
10,000 - 14,500	0.5	0.3
15,000 - 19,500	0.5	0.5
20,000 - 24,500	0.6	0.4
25,000 - 29,500	0.8	0.6
30,000 - 34,500	0.8	0.6
35,000 - 39,500	0.8	(0.6)

G.256083(h)/JDG/1/50/40

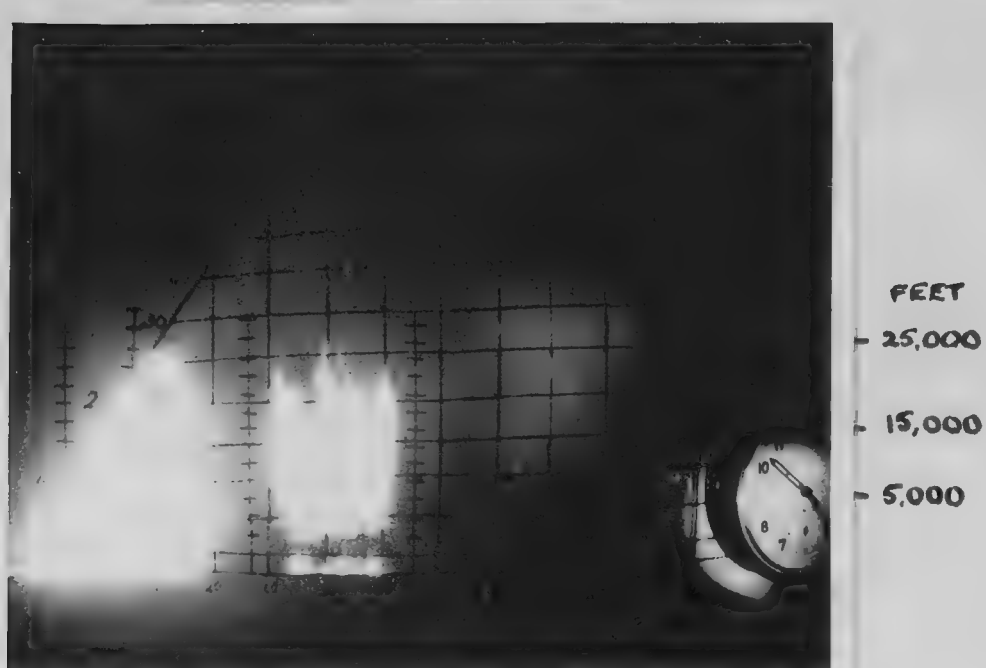

Photograph (ii)

Multiple column cumulonimbus echo.

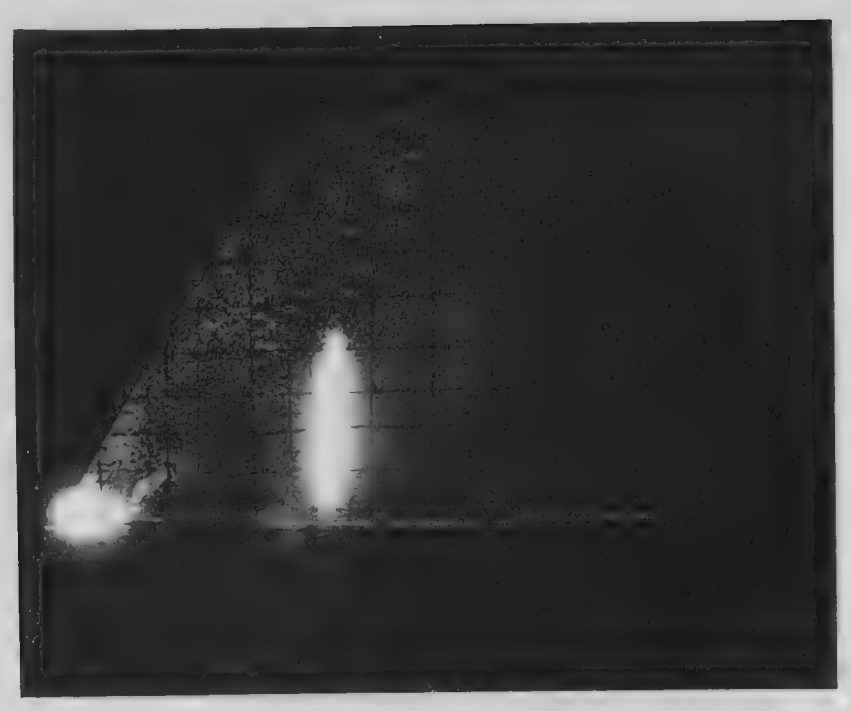

Photograph (i)

Single column cumulonimbus echo.

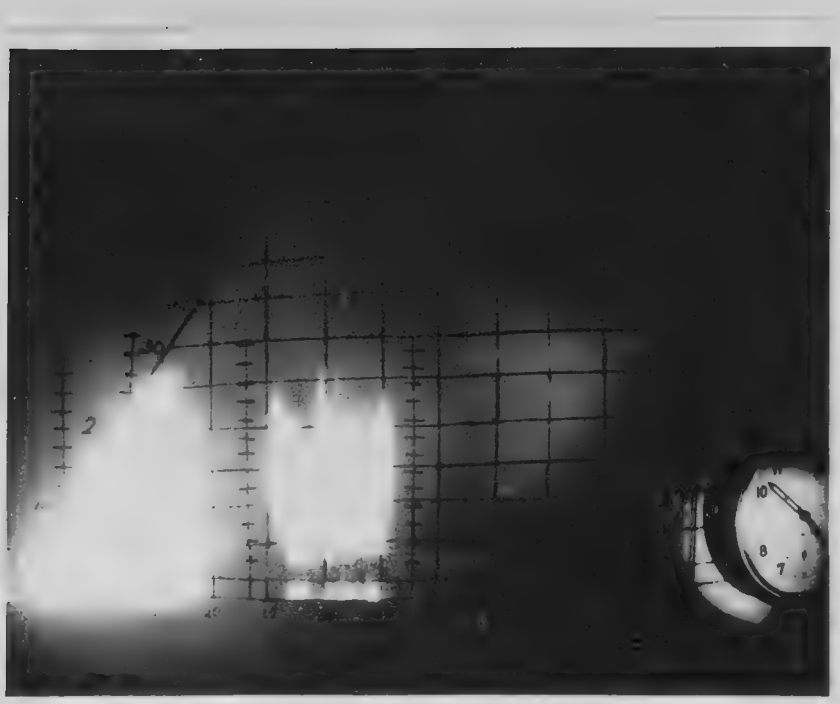

Photograph (ii)

Multiple column cumulonimbus echo.

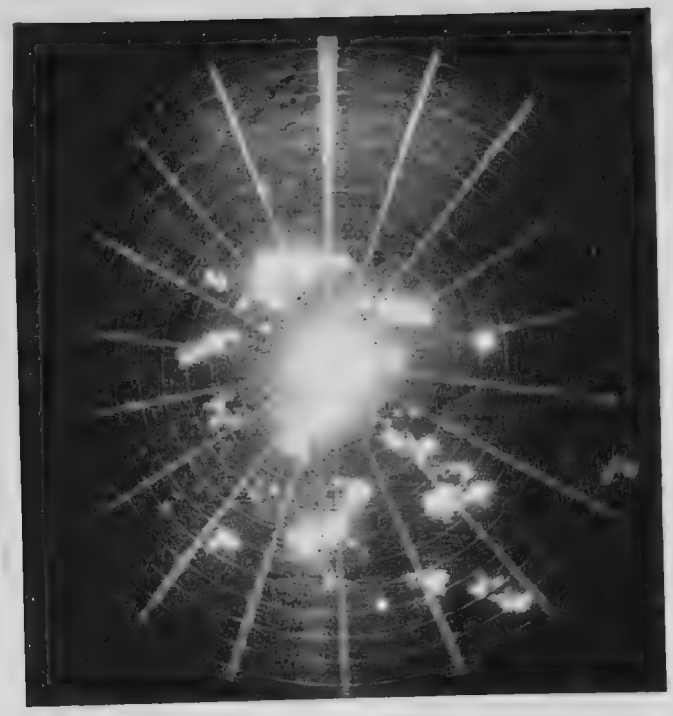

Photograph (iii)

P.P.I. photograph of cumulonimbus echoes showing single and multiple cell echoes (Range markers at 5 mile intervals.)

↑

Photograph (iv)

Multiple cell cumulonimbus echo (arrowed). Indications of 8 cells in contact with each other. Large mass of echo is from storm overhead.

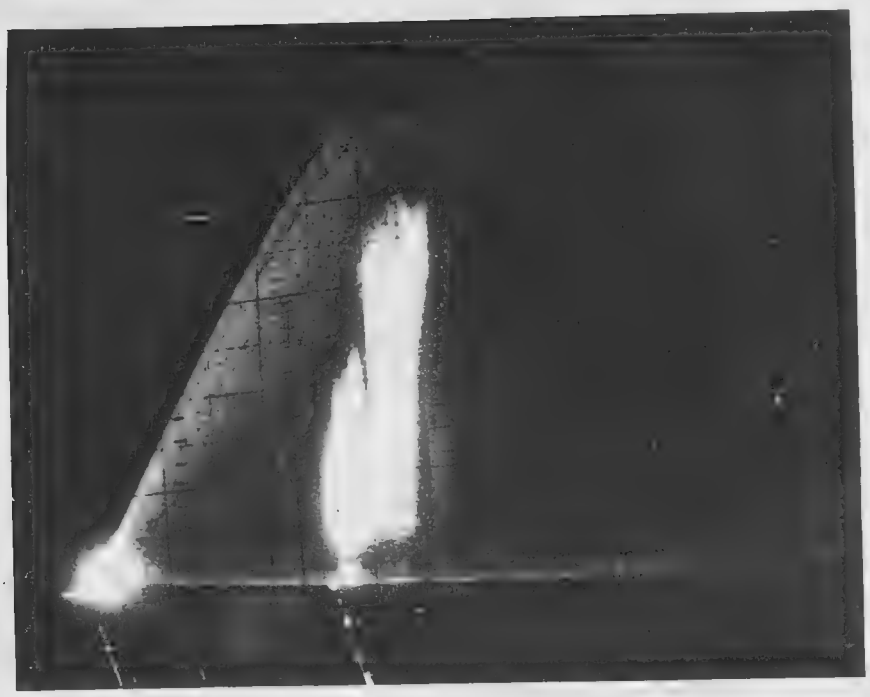

Photograph (v)

Double cell cumulonimbus echo showing growth of new vigorous cell at edge of older cell. The top of the older cell is at 39,000 ft. while the new cell at this time has only reached 24,000 ft.

This report has not been published and is to be treated CONFIDENTIALLY. Its contents must not be quoted.

M.R.P. 538
S.C.III/50
23 rd January, 1950.

AT 488 401
AIR WEATHER SERVICE
TECHNICAL REFERENCE FILES

AIR MINISTRY

METEOROLOGICAL RESEARCH COMMITTEE.

The Size of Cloud Droplets.

by A. C. Best. (Meteorological Office).

Summary.

The rate of growth of cloud droplets round a salt nucleus is examined and it is shown that, with nuclei of the size quoted in published measurements, the drop radius achieved in the period before the droplet is carried out of the cloud layer by turbulent diffusion is in reasonable accord with published measurements of the mean drop radius. It is also shown that the maximum drop radius reached when the droplet leaves the cloud due to fall under gravity is of the same order as the largest cloud drop measurements. The effect of temperature is considered.

Finally it is shown that the high rate of condensation which occurs in convective clouds is likely to lead to a small decrease in the average size of cloud particles.

1. Introduction.

Most of the measurements of the size of cloud particles show that these particles have diameters within the range 5 to 40 microns. The present note is an attempt to explain why this should be so. Cloud particles form by condensation of water vapour onto a nucleus and condensation is essentially a time process. Several authors have computed the time required for the formation - by condensation - of drops of various sizes but as far as the present writer is aware none of these computations has taken account of the properties of the nucleus.

2. Vapour Pressure over a drop of Salt Solution.

Wright (1936) has given the equation for vapour pressure over a drop of salt solution in the following form

$$\frac{p'}{p} = \exp\left(\frac{P}{d}\right) - \frac{8Q}{\rho_1 d^3} \qquad \text{.....(1)}$$

where

p' = vapour pressure over the drop.
p = saturation vapour pressure over a plane water surface at the same temperature.
d = drop diameter.
ρ_1 = drop density
P = $4TM/\rho_1 R\theta$
Q = $750 m_1 G/\pi\beta$
T = surface tension (= 74)
M = molecular weight of water (= 18)
R - gas constant per gram molecule (= $8.314\ 10^7$)
θ = temperature (absolute)
m_1 = mass of solute in drop
β = molecular weight of solute (= 58 for NaCl)
G = the proportionality factor in the relation between the fractional lowering of vapour pressure and the number of gram molecules of solute per 1000 grams of water and has a value 0.04 for NaCl.

It has been pointed out by Simpson (1941) that the second term on the right hand side of equation 1 contains a small error which is significant only at high salt concentrations. The approximate form of the equation given above is convenient for our present purpose and, since we shall be primarily concerned with dilute solutions, will be retained here. For the same reasons we shall also assume $\rho_1 = 1$.

As Wright mentions, we easily see from equation 1 that there is a value of d which makes p' a maximum. This critical value of d is given by

$$P \exp\left(\frac{P}{d}\right) = \frac{24\,Q}{d^2} \qquad \ldots\ldots\ldots\ldots\ldots\ldots\ldots (2)$$

Now evaluating P and Q we find

$$P = 6.408\ 10^{-5}/\theta \qquad Q = 0.165\ m_1$$

Thus P is of the order 10^{-7} whereas d is at least 10^{-5} and P/d is small. We may accordingly expand the exponential in equation 2 and retain only the first term in P/d. This leads to a quadratic equation in d the solution of which is

$$2d = -P + \sqrt{(P^2 + 144\,Q/P)} \qquad \ldots\ldots\ldots\ldots\ldots (3)$$

The work of Kohler (1936), Wright (1940) and of Houghton and Radford (1938) indicates that the mass of the salt nucleus lies between 10^{-14} and 10^{-12} gm. We shall accordingly consider the six cases given by θ = 273°A and 293°A and $m_1 = 10^{-14}$, 10^{-13} and 10^{-12} gm. For each case we obtain numerical values for P and Q, substitute in equation 3 and solve for d. Having obtained the critical diameters we can then substitute in equation 1 and so get p'/p. The results for the six cases are given in table 1.

Table 1.
Droplet size for maximum vapour pressure.

θ °A	m_1 gm	d cm	p'/p
273	10^{-14}	$5.0\ 10^{-4}$	1.000363
273	10^{-13}	15.9	1.000115
273	10^{-12}	50.3	1.000037
293	10^{-14}	5.2	1.000327
293	10^{-13}	16.5	1.000103
293	10^{-12}	52.1	1.000033

We may note here that unless the relative humidity exceeds 100p'/p the cloud drop diameter will not exceed the value given in table 1. Moreover, since values of m_1 as small as 10^{-14} gm have been deduced as the mean size of the nucleus, and since no measurements of cloud particle diameters have shown the mean drop diameter as small as 5 microns, it follows that the relative humidity must, on occasions, exceed 100.036 per cent. On the other hand it seems plausible that the amount of supersaturation is unlikely to be of a greater order of magnitude than 0.036 per cent both because this would lead to nuclei much smaller than 10^{-14} becoming effective and because - as the humidity rises - the excess vapour is absorbed by the larger nuclei. In the following paragraphs we shall need an estimate of the relative humidity in a cloud. The argument above suggests that 100.05 is a value which is unlikely to be exceeded.

3. Rate of growth of cloud droplets.

Condensation on, or evaporation from, a cloud droplet leads to the drop having a temperature greater or less, respectively, than the ambient temperature. If the droplet is so small that the relative motion between the air and the droplet can be neglected it can be shown that (see for example Fuchs(1934) and Topley and Whytlaw-Gray (1927)) the temperature difference between the droplet and the air, and the rate of growth of the

droplet, are described by the following equations

$$\Delta\theta = \frac{\lambda D}{R\theta k}(hp_a - p') \quad \ldots\ldots\ldots\ldots\ldots\ldots(4)$$

$$a\frac{da}{dt} = \frac{MD}{R\theta}(hp_a - p') \quad \ldots\ldots\ldots\ldots\ldots\ldots(5)$$

where
- $\Delta\theta$ = excess of droplet temperature over ambient temperature (°A)
- λ = latent heat of evaporation (cal./gm molecule)
- D = coefficient of diffusion
- k = specific conductivity of air
- $100\ h$ = relative humidity per cent
- p_a = saturation vapour pressure at air temperature
- p' = vapour pressure over drop (of salt solution)
- a = drop radius

and other symbols have meanings as before. Inserting numerical values appropriate to temperatures 273°A and 293°A and, for D, to a pressure of 900 mb we get the following results

θ	$\frac{\lambda D}{R\theta k}$	$\frac{MD}{R\theta}$
273°A	$2.041\ 10^{-3}$	$1.955\ 10^{-10}$
293°A	$2.009\ 10^{-3}$	$2.078\ 10^{-10}$

For a given set of conditions equation 4 may be regarded as defining the temperature difference between droplet and air. Having obtained a solution to (4) the quantity $(hp_a - p')$ can be computed, inserted in (5) and this latter equation integrated to show the rate of growth of the drop.

Unfortunately equation (4) cannot be solved explicitly and the following procedure was adopted. From equation (1) we can write

$$p' = Cp_d \quad \ldots\ldots\ldots\ldots\ldots\ldots(6)$$

where p_d is the saturation vapour pressure over a plane water surface at the temperature of the drop and

$$C = \exp\left\{\frac{P}{2a}\right\} - \frac{Q}{a^3} \quad \ldots\ldots\ldots\ldots(7)$$

(after putting $\rho_1 = 1$). We thus obtain

$$\Delta\theta = \frac{\lambda D}{R\theta k}(hp_a - Cp_d) \quad \ldots\ldots\ldots\ldots\ldots(8)$$

where $\lambda D/R\theta k$ is independent of drop size but C is a function of a as well as of θ and m_1. For given values of θ, m_1 and a we can compute C. Inserting the numerical value of C in (8) we can then compute the right hand side of (8) for selected values of $\Delta\theta$ (θ being known) provided h is known. From the pairs of values so obtained ($\Delta\theta$ and the right hand side of equation 8) the value of $\Delta\theta$ which satisfies equation 8 can then be obtained graphically. This procedure was followed for various values of a from $0.75\ 10^{-4}$ to $50\ 10^{-4}$ cm for each of the six cases listed in table I and assuming h to have the value 100.05. The computations were repeated for one case with h = 100.5. Having obtained $\lambda D(hp_a - Cp_d)/R\theta k$ (= $\Delta\theta$) the quantity $MD(hp_a - Cp_d)/R\theta$ was then computed for each drop size in each case. Now from equation 5 we see that

$$t_2 - t_1 = \int_{a_1}^{a_2} \frac{R\theta}{MD}\frac{a}{(hp_a - Cp_d)}\,da \quad \ldots\ldots\ldots\ldots(9)$$

where $t_2 - t_1$ is the time required to grow from radius a_1 to radius a_2.

The integration was performed graphically. The results are given in table 2.

Table 2.
Time of growth of droplet.

Case	1	2	3	4	5	6	5a
θ	273	273	273	293	293	293	293
m_1	10^{-14}	10^{-13}	10^{-12}	10^{-14}	10^{-13}	10^{-12}	10^{-13}
h	100.05	100.05	100.05	100.05	100.05	100.05	100.5
	Time (seconds) to grow from radius a = 0.75 10^{-4} cm						
a (cm)							
1 10^{-4}	2.4	0.15	0.013	1.1	0.80	0.0059	0.06
2 ..	130	7.0	0.61	52	3.4	0.31	1.4
5 ..	1000	320	62	410	150	27	18
10 ..	2700	1800	870	1200	870	440	80
15 ..	5200	4200	2900	2500	2100	1500	210
20 ..	8500	7400	5900	4100	3600	3000	350
25 ..	12500	11500	9700	6000	5600	4900	540
30 ..	17500	16000	14500	8400	7900	7300	760
35 ..	23000	22000	20000	11000	11000	10000	1000
50 ..	44500	43500	41500	22000	22000	21000	1600

Now a cloud is always in a more or less turbulent state and during this mixing process elements of the cloud are transferred from the middle of the cloud to the boundary and vice versa. One result of this is that although the cloud as a whole may preserve its identity over long periods it is likely that the individual droplets are continually changing as a result of turbulence transferring droplets to the cloud boundaries and then into the unsaturated air outside the cloud and, at the same time bringing in nuclei from outside the cloud. Thus the life of an individual cloud particle is limited by the turbulent processes. We can form an idea of the order of magnitude of the life of one droplet as follows. Sutton (1932) has shown that the standard deviation of airborne smoke particles from the mean path is given by

$$\sigma^2 = \tfrac{1}{2} c^2 (ut)^m \qquad \ldots\ldots\ldots\ldots\ldots\ldots\ldots\ldots (10)$$

where c has a value about 0.08 and m is 1.75 (c.g.s. units) As a first approximation we may apply this formula to cloud droplets. Inserting numerical values in equation 10 and putting σ = 300 metres (= about half the thickness of a layer cloud) and u = 10 m/sec. we find t = 3500 seconds or approximately 1 hour. Referring to table 2 we see that this time corresponds to growth to radii of 11.5, 13.5 and 16 microns for cases 1, 2 and 3; 18.5, 19.5 and 21.5 microns for cases 4, 5 and 6.

It is not to be expected that equation 10 will do more than indicate the order of magnitude of the particle life since, amongst other things, it implies isotropic turbulence. This is probably valid while the particles are not too far apart but may not be true when the separation is comparable with the thickness of the cloud.

We may note from table 2 that an increase of 20°C in the cloud temperature is slightly more effective in increasing particle size than a tenfold increase in the mass of the nucleus.

The final column of table 2 has been included to show the effect of the degree of supersaturation though, as indicated in paragraph 2, it seems probable that the supersaturation does not normally reach such a high value as 100.5 per cent.

4. Distance of fall during growth.

The distance of fall of a particle while it is growing is given by

$$z = \int_{t_1}^{t_2} v \, dt \quad \ldots\ldots\ldots\ldots\ldots\ldots\ldots\ldots (11)$$

where v is the appropriate terminal velocity at any instant and $t_2 - t_1$ is the time of fall. The terminal velocity is obtained from Stokes' law

$$v = \frac{2g(\rho_1 - \rho)}{9\mu} a^2 \quad \ldots\ldots\ldots\ldots\ldots\ldots\ldots\ldots (12)$$

(where μ is the coefficient of viscosity) for radii up to about 25 10^{-4} cm (Best. 1949). For slightly larger radii the error involved is not large and we shall use the formula for cloud droplets of all sizes. Neglecting ρ in comparison with ρ_1 and substituting numerical values for the other quantities the coefficient of a^2 on the right hand side is 1.271 10^6 for θ = 273°A and 1.201 10^6 for θ = 293°A. Using these values and the value of a as a function of t from table 2 we can integrate equation 11 graphically. Table 3 shows the distance fallen while the droplet radius grows from 0.75 microns to a microns.

Table 3.
Fall distance while growing from
a radius of 0.75 10^{-4} cm.

a (cm)	Case Number 1	2	3	4	5	6	5a
				centimetres			
1 10^{-4}	0.023	0.0015	0.00013	0.011	0.00075	0.00005	0.00056
2 ..	4.5	0.24	0.021	1.7	0.11	0.010	0.044
5 ..	160	60	12	62	27	5.0	3.0
				metres			
10 ..	15	13	6.9	6.6	5.6	3.3	0.50
15 ..	67	61	49	31	29	23	3.0
20 ..	200	190	170	90	88	80	8.5
25 ..	460	450	420	210	210	200	20
30 ..	930	910	870	430	420	420	40
35 ..	1700	1700	1600	790	780	780	74
50 ..	5100	5100	5100	2400	2400	2400	160

This table is of interest because it provides an upper limit, which depends upon the cloud thickness, to the size of the droplets. Thus if the cloud thickness is 600 metres we see that the maximum droplet radius is about 26.5 microns in case 1 and 32.5 microns in case 4, values which are in reasonable accord with observations. Reference to table 2 however shows that the time required for this fall would be about 3.8 hours in case 1 and 2.7 hours in case 4. The higher temperature not only leads to a larger maximum drop radius: the periods required to grow to the maximum size are comparable with the mean life of a cloud particle and in view of this the reduction of the period from 3.8 hours to 2.7 hours may make a significant difference to the probability that some droplets will reach the maximum size.

Another point brought out by table 3 is the fact that the maximum droplet size is but little affected by the size of the nucleus. This contrasts with the effect of nucleus mass on mean drop size already noted.

5. Drop temperature during condensation.

In the computations described in section 3 it was necessary to compute $\Delta\theta$ - the excess of drop temperature over ambient temperature - on the basis of equation 4. As a matter of interest, and also because we shall need to refer to these values below, the values obtained for $\Delta\theta$ are tabulated in table 4.

Table 4.
Values of $\Delta\theta$ - excess of drop temperature over ambient temperature (°C)

a cm.	Case Number. 1	2	3	4	5	6	5a
0.75 10^{-4}	0.018	0.25	3.11	0.035	0.467	6.54	0.522
1.0 ..	0.006	0.103	1.16	0.013	0.186	2.23	0.245
1.5 ..	0.0013	0.030	0.323	0.0031	0.056	0.60	0.112
2.0 ..	0.0008	0.013	0.135	0.0020	0.024	0.25	0.077
5.0 ..	0.0018	0.0026	0.010	0.0036	0.0051	0.019	0.058
10.0 ..	0.0025	0.0026	0.0036	0.0046	0.0051	0.0066	0.058
15.0 ..	0.0027	0.0028	0.0030	0.0051	0.0051	0.0056	0.058
25.0 ..	0.0029	0.0029	0.0030	0.0056	0.0056	0.0056	0.059
35.0 ..	0.0030	0.0030	0.0030	0.0056	0.0056	0.0056	0.059
50.0 ..	0.0031	0.0031	0.0031	0.0056	0.0056	0.0061	0.059

It is apparent from table 4 that except at the smaller sizes, say below a = 5 10^{-4}, the excess of drop temperature over ambient temperature is almost independent of the radius. From the present point of view $\Delta\theta$ is to be interpreted in terms of its effect on the water vapour pressure difference between the drop surface and the surrounding air and we see from equation 4 that at a given ambient temperature this vapour pressure difference $(hp_a - p')$ is proportional to $\Delta\theta$. The table also demonstrates the physically obvious fact that the mass of the nucleus has very little effect at the larger drop sizes. In fact, except at the smaller sizes, the value of $(hp_a - p')$ will be independent of drop size and will approximate closely to the value appropriate to a drop of pure water.

6. Convective cloud.

So far we have considered only the early stages in the life of a cloud. In layer type cloud with a limited liquid water content and continual change in the individual elements constituting the cloud it is probable that the factors outlined above govern the drop size in the cloud throughout the life of the latter. We shall now consider the effect of substantial condensation within a short time - as happens in convective cloud - on the drop size distribution. When condensation first starts in a newly forming convective cloud the factors outlined above are applicable but the drop size distribution later on may be modified by the rapid condensation which occurs as the cloud grows.

The condensation process will still be described by equations 4 and 5 and in view of the inferences drawn from table 4 in section 5 we shall now neglect the influence of drop curvature and salt nucleus. This amounts to replacing p' in equations 4 and 5 by p_o - the saturation vapour pressure at the drop temperature. With this approximation equation 5 becomes

$$a \frac{da}{dt} = F \quad \ldots\ldots\ldots\ldots\ldots\ldots\ldots\ldots (13)$$

where F is dependent upon temperature but is independent of drop size, i.e. of a. Integrating equation 13 we get

$$A^2 - a^2 = 2\int F\, dt = K \text{ say} \quad \ldots\ldots\ldots (14)$$

where a is the initial drop radius, A the final drop radius and K depends upon temperature, period of condensation etc but is independent of a.

Let us suppose the drop size distribution at the base of the cloud is given by

$$1 - f = \exp\left[-\left(\frac{2a}{b}\right)^n\right] \quad \ldots\ldots\ldots\ldots\ldots\ldots(15)$$

where

f = the fraction of liquid water in the cloud comprised by drops with diameter less than 2a,

and b and n are constants.

This type of formula is very elastic and, by suitable choice of b and n, can be made to give a reasonable fit to many measured drop size distributions.

If w is the liquid water concentration near the cloud base we see that

Total volume of drops (per unit volume of air) with radius between a and a + da $= wn\left(\frac{2}{b}\right)^n a^{n-1} \exp\left[-\left(\frac{2a}{b}\right)^n\right]da$

Number of drops with radius between a and a + da $= \frac{3wn}{4\pi}\left(\frac{2}{b}\right)^n a^{n-4} \exp\left[-\left(\frac{2a}{b}\right)^n\right]da$

After further condensation due to ascent the drops with initial radius a grow to a radius A defined by equation 14 and we have

Final volume of drops which had initial radius between a and a + da $= wn\left(\frac{2}{b}\right)^n a^{n-4}(a^2+K)^{3/2} \exp\left[-\left(\frac{2a}{b}\right)^n\right]da$

Final volume of water comprised by drops with final radius less than A $= wn\left(\frac{2}{b}\right)^n \int_o^a \phi(a)\, da \quad \ldots\ldots(16)$

Final concentration of water $= W$ (say)

$$= wn\left(\frac{2}{b}\right)^n \int_o^{\infty} \phi(a)\, da \quad \ldots\ldots(17)$$

where

$$\phi(a) = a^{n-4}(a^2+K)^{3/2} \exp\left[-\left(\frac{2a}{b}\right)^n\right] \ldots\ldots(18)$$

$$A = \sqrt{(a^2 + K)} \quad \ldots\ldots\ldots\ldots\ldots\ldots(19)$$

We can choose an arbitrary value of K. Putting this in 18 evaluation of the integral in 17 then gives the proportional increase in the liquid water concentration and evaluation of 16 gives the cumulative volume as a function of drop size. The final drop size distribution can be obtained by differentiating the final cumulative volume curve. Alternatively it is easily verified that the volume of drops with radius between A and A + dA is given by the expression

$$wn\left(\frac{2}{b}\right)^n \phi(a)\, \frac{A}{a}\, dA$$

Following the procedure outlined above the drop size distribution has been determined for five values of K on the assumption thatthe initial distribution is given by equation 15 with n = 2 and b = 5 10^{-4} cm. It is not suggested that these two values of the parameters are necessarily the best values to make equation 15 fit a drop size distribution in cloud. They are convenient values for computation and give a reasonable initial size distribution. The integral in equation 17 was evaluated graphically,

the lower limit being taken as $0.5\ 10^{-4}$ cm instead of zero. This particular value of the lower limit was chosen because it is about the size of a salt nucleus in air of normal humidity.

Equation 17 determines only the proportional increase in liquid water concentration and accordingly, when plotting the final drop size distribution in the figure it has also been assumed that w = 1. The increase in liquid water concentration for each value of K is shown in table 5.

Table 5.

Liquid water concentration for selected values of K assuming $w = 1,\ b = 5\ 10^{-4},\ n = 2$

K	0.1	0.5	1	2	3
W	1.029	1.314	1.801	2.868	4.155

The size distribution of drops for each value of K is shown in the figure, the curve for K = 0 corresponding to the initial size distribution given by equation 15. The following features may be noted about these curves

(a) All curves have a sharp cut off at the end near the origin owing to the assumption that initially the smallest drops have a radius $0.5\ 10^{-4}$ cm. On the scale adopted for the figure it has not been possible to plot the curves for K = 2 and 3 at the smaller sizes.

(b) Apart from the artificial maximum at the smallest radius - introduced by the artificial assumption regarding the smallest drop in the initial cloud - only the curves for K = 0 and 0.1 show a true maximum.

(c) The assumption that F (equation 13) is independent of drop size affects the shape of the curves for small radii. If allowance is made for the increased value of $(hp_a - p')$ at the smaller radii (see section 5) the ordinates at the smaller radii in the figure would be increased. On the other hand new nuclei are undoubtedly entrained at all levels in a real convective cloud. The combined effect of these two factors would be to give the curves a true maximum at some radius smaller than the radius corresponding to the maximum ordinate in the curve for K = 0

We may conclude from the figure that condensation in a convective cloud will probably affect the shape of the size distribution curve. The drop radius corresponding to maximum volume of water may become slightly smaller as condensation continues but is not likely to increase. These conclusions are based on the analysis for the special case of n = 2 and $b = 5\ 10^{-5}$ but it is improbable that other values for these parameters would affect the character of the conclusions.

References.

Best. A. C. 1949 M.R.P.469

Fuchs. N. 1934 Phys. J. Sov. Union, 6

Houghton. H.G. and Radford W.H. 1938 M.I.T. Papers in Phys. Ocean. and Met. VI

Kohler. H. 1936 Trans. Far. Soc. 32

Simpson. Sir G.C. 1941 Q. J. Roy. Met Soc. 67

Sutton. O.G. 1932 Proc. Roy. Soc. A 135

Topley. B. and Whytlaw-Gray. R.W. 1927 Phil. Mag. IV (Seventh Series)

Wright. H.L. 1936 Proc. Phys. Soc. 48

.. .. 1940 Q. J. Roy. Met. Soc. 66

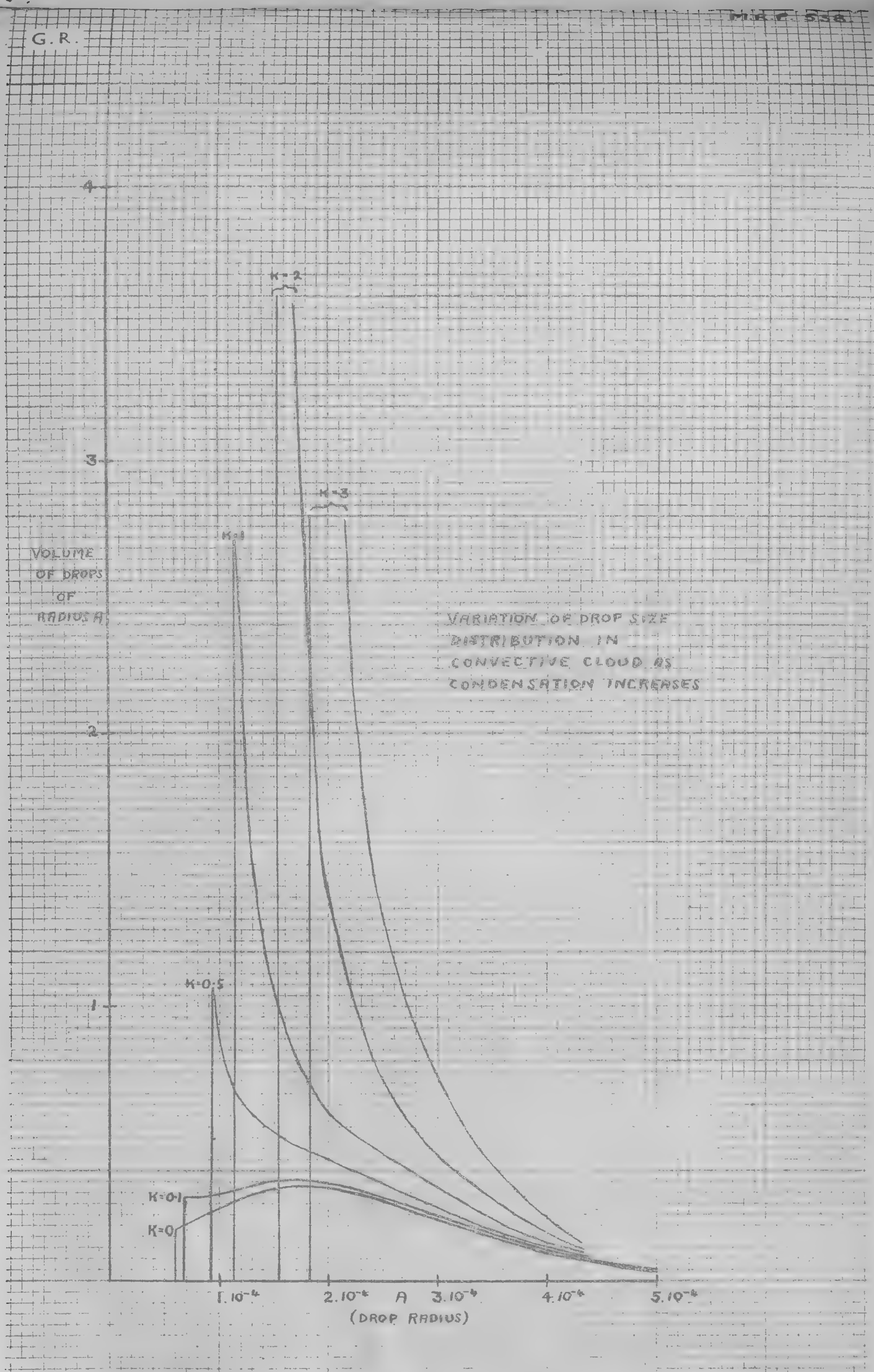
G.R.
M.R.C. 538
4
3
2
1
K=2
K=3
K=1
K=0.5
K=0.1
K=0
VOLUME OF DROPS OF RADIUS A
VARIATION OF DROP SIZE DISTRIBUTION IN CONVECTIVE CLOUD AS CONDENSATION INCREASES
1.10⁻⁴
2.10⁻⁴
A
3.10⁻⁴
4.10⁻⁴
5.10⁻⁴
(DROP RADIUS)

AIR MINISTRY

METEOROLOGICAL RESEARCH COMMITTEE

Addendum to M.R.P.539

At the meeting of the Meteorological Research Committee on 16th November, 1950, it was agreed to add the following problem (priority P.1) to the Research Programme (M.R.P. 539):-

Item No. II. 14. Investigation of conditions associated with the occurrence of ice on the Icelandic fishing grounds.

2. The problem is assigned to Commander Frankcom and A.D.M.O.(F.R.) jointly.

28th November, 1950.

AIR WEATHER SERV
TECHNICAL REFERENCE FILES

G.278401/JMB/11/50/100

II.8.(a) The three dimensional structure of fronts in relation to temperature, humidity and wind with special reference to clouds and rainfall.

II.12.(b)(i) The development and use of regression equations for forecasting upper winds.

II.13.(c) Temperature at standard pressure levels; frequencies and standard deviations.

III.2.(d)(i) Exploration of physical structure of rain producing clouds.

III.2.(e) Investigation of meteorological factor affecting ice accretion on aircraft.

III.3.(a) Investigation of the velocity and dimensions of gusts associated with cumulonimbus clouds.

III.3.(b) Investigation of clear air turbulence.

III.8.(b) Investigation of the relation between air-to-ground and horizontal visibilities.

/Investigation

G.256451/DC/3/50/25

To Members of the Meteorological Research Committee and Sub-Committees.

Will you please note the following amendment to M.R.P.539 (Programme of Investigations, 1950/51):-

The priority category for Item No.I, 7(b)(iv), should be PI not P3, as shown.

A.C. Best

Secretary.
Meteorological Research Committee.

18 May, 1950.

G.269066/MKL/5/50/120

AIR WEATHER SERVICE
TECHNICAL REFERENCE FILES

III. Physical Investigations. r of frontal

Each section is divided into groups of problems.

3. The system of priority markings used in previous Programmes has been retained, viz:-

SERVICE
ENCE FILES

PX Exceptionally important and urgent investigations.

P1 Important and urgent investigations. atures Hemisphere).

P2 Important investigations, but not particularly urgent.

P3 Less important investigations.

/4. jet streams

256451/DC/3/50/25

AIR WEATHER SERVICE
TECHNICAL REFERENCE FILES

importance of n the synoptic

II.8.(a) The three dimensional structure of fronts in relation to temperature, humidity and wind with special reference to clouds and rainfall.

II.12.(b)(i) The development and use of regression equations for forecasting upper winds.

II.13.(c) Temperature at standard pressure levels; frequencies and standard deviations.

III.2.(d)(i) Exploration of physical structure of rain producing clouds.

III.2.(e) Investigation of meteorological factor affecting ice accretion on aircraft.

III.3.(a) Investigation of the velocity and dimensions of gusts associated with cumulonimbus clouds.

III.3.(b) Investigation of clear air turbulence.

III.8.(b) Investigation of the relation between air-to-ground and horizontal visibilities.

/Investigation

G.256451/DC/3/50/25

published and is to be treated CONFIDENTIALLY. Its contents must not be quoted.

RESTRICTED

M.R.P.539
March, 1950.

Air Ministry

Meteorological Research Committee

Programme of Investigations 1950/51
(Revised March, 1950)

1. The accompanying Research Programme broadly follows the lines of the previous programme (M.R.P.471), though a few new problems have also been added.

2. Problems are classified according to the practical purposes which each investigation is designed to serve. There are three main headings, viz:-

I. Development of Meteorological Instruments.

II. Investigations in Synoptic and Dynamical Meteorology.

III. Physical Investigations.

Each section is divided into groups of problems.

3. The system of priority markings used in previous Programmes has been retained, viz:-

PX Exceptionally important and urgent investigations.

P1 Important and urgent investigations.

P2 Important investigations, but not particularly urgent.

P3 Less important investigations.

/4.

256451/DC/3/50/25

AIR WEATHER SERVICE
TECHNICAL REFERENCE FILES

II.8.(a) The three dimensional structure of fronts in relation to temperature, humidity and wind with special reference to clouds and rainfall.

II.12.(b)(i) The development and use of regression equations for forecasting upper winds.

II.13.(c) Temperature at standard pressure levels; frequencies and standard deviations.

III.2.(d)(i) Exploration of physical structure of rain producing clouds.

III.2.(e) Investigation of meteorological factor affecting ice accretion on aircraft.

III.3.(a) Investigation of the velocity and dimensions of gusts associated with cumulonimbus clouds.

III.3.(b) Investigation of clear air turbulence.

III.8.(b) Investigation of the relation between air-to-ground and horizontal visibilities.

/Investigation

4. The list contains certain problems, such as the investigation of the radiative equilibrium of the atmosphere, which although not under examination by the Meteorological Research Committee, are of definite interest to it.

5. The numbers of problems of each priority are shown in the following table.

No. of Problems

Nature of Problem	Section	Priority					
		PX	P1	P2	P3	Not assigned	Total
Instruments	I	7	30	19	14	0	70
Synoptic and Dynamical	II	11	11	20	7	0	49
Physical	III	7	14	21	6	5	53
		25	55	60	27	5	172

6. A list of P.X. problems is shown overleaf.

London

April, 1950

G.256451/DC/3/50/25

Problems with Priority PX.

Investigations

Item No.	
I.1.(a)(i)	Temperature and humidity. Speed corrections for thermometer elements.
I.1.(a)(ii)	Thermometer suitable for high speed aircraft.
I.1.(d)(i)	Hoar frost point hygrometer, extension to photo electric, to automatic cooling and heating and to automatic recording.
I.5.(c)	Design of instrument to assess air to ground or ground to air visibility from scattered light of searchlight beam, for use by day and night.
I.7.(a)(iii)	Development of meteorological elements for radar sonde.
I.7.(b)(ii)	Development of radar sonde theodolite.
I.8.(b)	Application of radar methods for detecting and investigating cloud, precipitation and turbulence.
II.3.(d)	The forecasting of incidence, duration and intensity of frontal rain over the British Isles.
II.6.(a)	Large scale circulation types: classification.
II.6.(b)	Studies of change of type.
II.6.(c)	Zonal, meridional and other indices.
II.6.(d)	Development, movement and decay of major synoptic features (according to season and location in the Northern Hemisphere).
II.7.(f)	Early stages of anticyclogenesis.
II.7.(h)	General studies of upper winds and contour patterns: jet streams in particular.
II.7.(i)	General studies of temperature changes and relative importance of advection, dynamical and non-adiabatic processes, in the synoptic problem.
II.8.(a)	The three dimensional structure of fronts in relation to temperature, humidity and wind with special reference to clouds and rainfall.
II.12.(b)(i)	The development and use of regression equations for forecasting upper winds.
II.13.(c)	Temperature at standard pressure levels; frequencies and standard deviations.
III.2.(d)(i)	Exploration of physical structure of rain producing clouds.
III.2.(e)	Investigation of meteorological factor affecting ice accretion on aircraft.
III.3.(a)	Investigation of the velocity and dimensions of gusts associated with cumulonimbus clouds.
III.3.(b)	Investigation of clear air turbulence.
III.8.(b)	Investigation of the relation between air-to-ground and horizontal visibilities.

AIR WEATHER SERVICE
TECHNICAL REFERENCE FILES

/Investigation

III.9.(d) Investigation of the temperature and water content of the troposphere and lower stratosphere under various conditions.

III.9.(h) The formation of simple and miltiple tropopauses, types of tropopause, exchange of mass between the stratosphere and the troposphere.

Meteorological Research Programme

M.R.P.539 Part I.

Note: In the "Latest papers" column an asterisk indicates an M.R.P. which has been approved for distribution.

Item No.	Investigation	Priority	Branch or Individual	Latest Papers, Remarks, etc.
	I. Development of Meteorological Instruments and Observing Technique.			
I.1	Temperature and Humidity, measurement and recording			
	(a) (i) Speed corrections for thermometer elements.	PX	M.R.F., M.O.17	M.R.P. 169* 355* 405* 527*
	(ii) Thermometer suitable for high speed aircraft.	PX	M.O.17	
	(iii) Development of low lag thermometers for aircraft.	P1	M.R.F., M.O.17	
	(b) Design of hygrometer for routine use.			
	(i) Electrical absorption type.	P3	M.O.16	M.R.P. 222*/240*
	(ii) Other types, improvements to hygrometer elements	P3	M.O.16	M.R.P. 185*, 187*, 256, 267, 499*.
	(iii) Aspiration of hygrometers.	P2	M.O.16	
	(iv) Development of recording dew point hygrometer.	P1	M.O.16	
	(c) Design of hygrometer for routine use on aircraft.			
	(i) Electrical resistance (dry and wet bulb) automatic type.	P2	M.O.17	
	(ii) Open scale instrument.	P3	M.O.17	For exploring detailed structure of lower layers of atmosphere.
	(d) Design of hygrometers for use as standards.			
	(i) Hoar frost point type, extension to photo electric, to automatic cooling and heating and to automatic recording.	PX	Prof.Dobson M.O.17	M.R.P. 254
	(ii) Infra-red absorption type.	P1	Gassiot Committee	
	(iii) Frost point hygrometer for ground use.	P1		M.R.P. 528*

Item No.	Investigation	Priority	Branch or Individual	Latest Papers, Remarks etc.
	(e) Development of autographic recording apparatus for use with aircraft meteorological instruments.	P3	M.O.17, M.R.F.	
I.2	Pressure, measurement and recording			
	(a) Development of a precision surface aneroid for use in place of mercury barometer, especially for mobile purposes.	P1	M.O.16	
	(b) Improvements to Kew pattern barometer.	P3	A.D.M.O.(I.D.) M.O.16	
	(c) Use of hypsometers as a means of measuring surface pressure.	P2	M.O.16	
	(d) Barographs, improvement in design.	P1	M.O.16	
I.3	Wind, measurement and recording			
	(a) Development of Distant Reading Anemograph.			
	(i) Design of wind velocity recorder.	P1	M.O.16	
	(ii) Design of wind direction recorder.	P1	M.O.16	
	(iii) Development of a true wind resolver.	P2	M.O.16	Development contract being arranged by Admiralty.
	(b) Recording Pens, Ink and Paper. Investigation of means of improving quality or records.	P3	M.O.16	
	(c) Development of maximum gust recorder.	P2	M.O.16	

Item No.	Investigation	Priority	Branch or Individual	Latest Papers, Remarks etc.
I.4	Rain, measurement and recording			
	(a) Improvement of existing rainfall recorders.	P3	M.O.16	
	(b) Development of suitable recording gauges and observing technique for measuring intensity and frequency of heavy rainfall.	P2	M.O.16	
	(c) Measurement of rainfall on ships.	P1	M.O.16	
	(d) Development of Monthly Rainfall Recorder.	P2	M.O.16	
I.5	Visibility, measurement and recording			
	(a) Design of photo-electric visibility meter and adaptation for use in daylight and as visibility warning device and recorder.	P1	M.O.16	J.Sci.Inst.Vol.26. Nov. 1949. p.357.
	(b) Design of visibility meter on scattered light principle or other method suited for use on ships and aircraft.	P1	A.D.M.O.(I.D.) M.O.16	See also III.8(a), II.2(d).
	(c) Design of instrument to assess air to ground or ground to air visibility from scattered light of searchlight beam, for use by day and night.	PX	M.O.16,M.O.17	R.C.(G)40, G.E.C. Rep. 8303, M.R.P.403. See also III.8(b).
I.6	Cloud height, measurement and recording			
	Determination of cloud height by day.			
	(a) (i) Optical radar method.	P1	T.R.E.,M.O.17	
	(ii) Use of rockets, tracer bullets, etc.	P3	C.E.A.D.(M.of S.)	
	(iii) Application of modulated searchlight.	P1	M.O.16	

Item No.	Investigation	Priority	Branch or Individual	Latest Papers, Remarks etc.
	(b) Method of estimating cloud amount at night.	P2	M.O.16	
I.7	Radio-sonde and Radio Wind Instruments and Equipment			
	(a) Temperature, humidity and pressure.			
	(i) Improvement in accuracy of readings of pressure, temperature and humidity in Mk.2 radio-sonde.	P1	M.O.17	M.R.P. 202* - 206*, 294, 366, 422*, 504*, 525.
	(ii) Development of a transmitter for giving detailed structure of the lower layers of the atmosphere (over land and sea).	P1	M.O.17	
	(iii) Development of meteorological elements for radar sonde.	PX	M.O.17	M.R.P. 441, T.R.E. Report No. 15.
	(iv) Development of calibration procedure.	P2	M.O.17	
	(v) Development of cloud indicator for attachment to radio-sonde.	P3	A.D.M.O.(I.D.) M.O.17	
	(vi) Comparison of British and Foreign radio-sondes.	P1	M.O.17	
	(b) Wind.			
	(i) Application of radar methods including detection of gustiness and vertical velocity.	P1	M.O.17	Work also in progress by Admiralty with rockets. Use of window and ionized clouds. M.R.P. 364*, 427, 496*, 505, 513. T.R.E. Report No. 49.
	(ii) Development of radar-sonde theodolite.	PX	T.R.E., M.O.17	
	(iii) Investigation of errors in wind measurements up to 60,000 feet.	P2	M.O.12, M.O.17	M.R.P. 340, 387*, 406*.
	(iv) Improvement of radar wind targets.	P3	M.O.17	M.R.P. 398*.
	(v) Improvement of equipment for use on ships.	P3	M.O.17	M.R.P. 477*, 508.

/(e)

Item No.	Investigation	Priority	Branch or Individual	Latest Papers, Remarks, etc.
	(c) Miscellaneous Items.			
	(i) Improvement of balloons to increase height attained.	P1	M.O.16, M.O.17	M.R.P. 341*.
	(ii) Development of batteries.	P1	M.O.17	
	(iii) Development of attachment to measure vertical currents.	P2	M.O.17	
	(iv) Development of hydrogen generators.	P3	M.O.16 A.D.(Eng)C.G.	Development work in hand by Admiralty.
	(v) Development of radio-sonde for potential gradient measurement.	P2	M.O.17	
	(vi) Improvement of accessories for radio-sonde stations.	P2	M.O.17	
I.8	Thunderstorms, rainstorms etc., Location of.			
	(a) Improvement of R.D.F. technique for locating thunderstorms.	P1	N.P.L., M.O.17 M.O.12	Work by N.P.L.
	(b) Application of radar methods for detecting and investigating cloud, precipitation and turbulence.	PX	East Hill M.O.17	
I.9	Instruments for use at Sea			
	(a) Investigation of errors due to limitations of exposure.	P2	M.O.1., M.O.16	M.R.P. 481*
	(b) Development of instrument for measuring sea swell.	P1	A.R.L., M.O.16	M.R.P. 289, 291, 292, 295.
	(c) Development of instruments for use in submarines.	P1	M.O.16, D.N.M.S.	
I.10	Adaption of instruments and equipment for tropical and arctic use.			
	(a) Adaption of standard instruments for polar conditions with special regard to protection of moving parts and to providing adequate exposure.	P2	M.O.16 M.O.17	

Item No.	Investigation	Priority	Branch or Individual	Latest Papers, Remarks etc.
	(b) Survey of means of preventing deterioration of instruments under tropical or polar conditions.	P2	M.O.16 M.O.17	
I.11	Instruments for other special purposes			
	(a) Vertical Currents. Development of instrument to measure vertical component of wind near the ground.	P1	M.O.16	In connection with Severn Bridge Scheme.
	(b) Radiation.			
	(i) Development of absolute radiometer.	P1	Kew	
	(ii) Development of illumination recorder.	P1	M.O.16, Kew	
	(iii) Development of bimetallic actinograph.	P1	M.O.16, Kew	
	(c) Automatic Radio Reporting Stations. Application of radio-sonde technique to fixed or floating reporting stations.	P3	M.O.17	B.C.S.O. reports 204 and 290.
	(d) Cloud micro-physics			
	(i) Development of instruments for measuring water content in clouds and in rain.	P1	M.O.17 M.R.F.	Related to III 2(b).
	(ii) Development of instruments for measuring size distribution of water particles in clouds and in rain.	P1	M.O.17 M.R.F.	Related to III 2(b) and d(ii).
	(e) High atmosphere exploration.			
	(i) Development of high altitude searchlight.	P2	R.R.D.E. A.D.M.O.(I.D.)	Work in hand at R.R.D.E. M.R.P. 421, 485. See III 11(c) (i).
	(ii) Application of high altitude rockets.	P3	A.D.M.O.(R) W.R.D.(M.of S) M.O.17	

/(f)

Item No.	Investigation	Priority	Branch or Individual	Latest Papers, Remarks etc.
I.11	(f) Fog Instrumentation for F.I.D.O.	P2	M.O.17	
	(g) Microclimatology Instrumentation for item III 6.	P1	M.O.16 M.O.19 Cambridge	
	(h) Wind The development of means of obtaining winds up to 2,000 feet above ground in conditions of low cloud.	P2	A.D.M.O.(I.D.)	
	(i) Nuclei Development of a pressurized Aitken nucleus counter for use in aircraft at high levels.	P1	A.D.M.O.(I.D.)	

Note:- In the "Latest Papers" column an asterisk indicates an M.R.P. which has been approved for distribution.

Item No.	Investigation	Priority	Branch or Individual	Latest Papers, Remarks etc.
	II. Investigation in Synoptic and Dynamical Meteorology.			
II.1	Examination of Forecasting Technique Generally.			
	Development of a system for checking the accuracy of forecasts and to determine in particular the frequency and magnitude of the errors of the component parts.	P2	A.D.M.O. (F.R) M.O.2.	M.R.P's 170, 260, 399, 414, 514, 536
II.2	The Forecasting of Fog.			
	(a) Radiation fog, its formation, persistence and dispersal	P1	A.D.M.O. (F.R)	M.R.P's 159, 434
	(b) Study of advection fog and the influence of the thermal properties of the ground and sea.	P2	A.D.M.O. (F.R)	M.R.P's 167, 435
	(c) Geographical distribution of smoke pollution.	P3	A.D.M.O. (I) A.D.M.O. (F.R)	Atmos. Poll. Re. Ctte. Leicester Report S.D.T.M. 26. At. Poll. Com. Report No. 9 June, 1946 National Smoke Abatement Socy. (Brooks) Conf. Edinburgh, 1947. Q.J. R.Met. Soc. 73, 1947, pp 426-36 (Sutton) Q.J. R.Met. Soc. 74, 1948. pp. 133-143. (Dobson).
	(d) To investigate the variation of visibility at small heights.	P2	-	See also I.5(c)

/II.3

Item No.	Investigation	Priority	Branch or Individual	Latest Papers, Remarks etc.
II.3	The Forecasting of Cloud and Precipitation			
	(a) Convectional cloud and precipitation	P2	A.D.M.O.(F.R.)	M.R.P. 161
	(b) A synoptic statistical investigation of medium and high cloud.	P2		
	(c) Investigation of factors which govern the formation and dispersal of low stratus cloud over the British Isles.	P2	M.O.21	
	(d) Incidence, duration and intensity of frontal rain over the British Isles.	PX	A.D.M.O. (F.R.)	M.R.P. 353*
	(e) Conditions favourable for snow	P2	M.O.21	
	(f) Investigation of cirrus cloud with a view to forecasting more exactly its depth and upper level.	P1		
II.4	Investigation of Local and Topographical Characteristics			
	(a) Behaviour of fronts on encountering obstacles such as high mountains.	P3	M.O.21	
	(b) Föhn effect of the Welsh mountains on the west Midlands	P3	A.D.M.O.(F.R.)	
	(c) Study of land and sea breezes in relation to topography	P3	A.D.M.O.(F.R.) A.D.M.O.(I)	
II.5	Investigations relating primarily to long range forecasting.	P1	A.D.M.O.(F.R.)	To be broken down into detailed problems later. M.R.P. 433

/ II.6

Item No.	Investigation	Priority	Branch or Individual	Latest Papers, Remarks etc.
II.6	Investigations relating primarily to medium range forecasting			M.R.P. 514
	(a) Large scale circulation types: classification	PX		M.R.P. 433
	(b) Studies of changes of type	PX	A.D.M.O.(F.R) M.O.22	
	(c) Zonal, meridional and other indices	PX		M.R.P. 428*, 475
	(d) Development, movement and decay of major synoptic features (according to season and location in the Northern Hemisphere)	PX		
II.7	Investigations of circulation problems relating primarily to short range forecasting			
	(a) Wave-like depressions on cold fronts	P2		M.R.P's 411, 446
	(b) Wave-like depressions on warm fronts (break away depressions)	P2		M.R.P's 411, 446, 476
	(c) Depressions developing along the line of occlusion	P2		M.R.P's 476, 494
	(d) Polar air depressions	P1		
	(e) Cold pool depressions	P1		
	(f) Early stages of anticyclogenesis	PX	A.D.M.O.(F.R) M.O.21	
	(g) Inter-relation of vorticity, divergence and vertical motion generally.	P2		
	(h) General studies of upper winds and contour patterns: jet streams in particular	PX		M.R.P. 426
	(i) General studies of temperature changes and relative importance of advection, dynamical and non-adiabatic processes, in the synoptic problem.	PX		M.R.P.'s 517*, 526*

Item No.	Investigation	Priority	Branch or Individual	Latest Papers, Remarks etc.
II.8	Frontology			
	(a) The three dimensional structure of fronts in relation to temperature, humidity and wind with special reference to clouds and rainfall.	PX	M.O.21	
	(b) Frontogenesis and frontolysis; investigation of cases where relevant upper air information is available.	P2	M.O.21	
II.9	Conditions at Great Heights.			
	Synoptic and statistical investigation of wind temperature and weather conditions between 20,000 and 60,000 feet.	P1	A.D.M.O.(F.R) A.D.M.O.(I) M.O.18	M.R.P. 511
II.10	Problems of Tropical Meteorology *			
	(a) Relation between wind and pressure distribution.	P2	A.D.M.O.(I) Mr. Crossley Dr. Forsdyke	* The following papers are related to many of the individual problems listed in this item. M.R.P's 279, 298*, 311, 318* 326, 329* and 454. Q.J. Roy. Met. Soc. Vol.74, pp 379 - 382. (Crossley).
	(b) Upper air and convection.			
	(i) Investigation of the effect of high ground on the upper level pressure distribution and on wind flow.	P3		
	(ii) Investigation of the effects of convective turbulence on the upper air temperature distribution.	P2		
	(iii) Investigation of whether radiation from cloud tops affects the lapse rate sufficiently to affect stability and cause night precipitation.	P2		Could perhaps be referred to a tropical service.
	(c) Lower atmosphere.			
	(i) Investigation of turbulent and radiative cooling of the lower layers of the atmosphere in the tropics at night.	P3		
	(ii) Investigation of the forecasting of early morning fog and low stratus cloud in tropical regions.	P3		

Item No.	Investigation	Priority	Branch or Individual	Latest Papers, Remarks etc.
	(d) Frontal zones and discontinuities.			
	(i) Calculation of convergence and divergence in connection with the formation, activity and disappearance of convergence zones.	P2		) Could perhaps be) referred to a tropical) service.
	(ii) Study of pressure surges.	P2		))
II.11	Space and Time Variations of Sea Temperature.			
	Analysis of variations in space and time of sea surface temperature in relation to synoptic situation.	P1	M.O.22, M.O.1	
II.12	Application of Computing Machinery to Forecasting Problems.			
	(a) General	P1	A.D.M.O.(F.R) A.D.M.O.(I)	Work in progress at Imperial College. M.R.P.412
	(b) The development and use of regression equations for forecasting:-			
	(i) Upper winds	PX	A.D.M.O.(I)	M.R.P's 408, 456, 457
	(ii) Other items	P2	A.D.M.O.(I)	M.R.P. 457
II.13	Statistical Study of Upper Air Pressure, Temperature, Humidity and Wind Observations.			
	(a) Seasonal variation of mean isobaric surfaces and tropopause.	P2	))A.D.M.O.(I))A.D.M.O.(C)	M.R.P. 316
	(b) Seasonal variation of upper winds at various levels.	P1	)	M.R.P. 299, S.D.T.M. 118
	(c) Variation of wind up to 60,000 feet with time.	P1	))	M.R.P. 408
	(d) Accuracy of gradient wind and geostropic wind approximations.	P2	A.D.M.O.(F.R)	M.R.P. 383*, 392*, 443
	(e) Temperature at standard pressure levels; frequencies and standard deviations.	PX	A.D.M.O.(C)	M.R.P. 511
	(f) Temperature in the upper air in relation to the temperature at the tropopause.	P1	A.D.M.O.(C)	

Meteorological Research Programme
M.R.P.539 Part III

Note: In the "Latest Papers" column an asterisk indicates an M.R.P. which has been approved for distribution.

Item No.	Investigation	Priority	Branch or Individual	Latest Papers, Remarks etc.
	III. Physical Investigations			
III. 1	Vertical gradients of temperature, humidity and wind in the lower troposphere.			
	(a) Analysis of continuous records of temperature and humidity up to heights of 350 feet.	P1	M.O.15	Station in operation at Rye.
	(b) Detailed temperature, humidity and wind profiles over land	P2	M.O.15 Cardington	Observations being made from captive balloon. M.R.P.270*, 349, 370, 382.
	(c) Measurement of temperature and humidity gradients over the sea.	P3		
III. 2	Micro-physics of water in the atmosphere.			
	(a) Atmospheric nuclei. Determination of number and nature of condensation and sublimation nuclei at various heights in the atmosphere and investigation of condensation and sublimation of water vapour at very low temperatures.	P1	Prof. Dobson M.R.F.	M.R.P. 212, 218*, 361, 368, 371, 393, 394, 492, 493, 515
	(b) Clouds. (i) Investigation of liquid water content in clouds.	P1	M.R.F.	M.R.P. 268, 339. See also I.11(d)
	(ii) Investigation of drop size distribution in clouds.	P2	M.R.F.	M.R.P. 309*, 472*, 483*, 519, 538*
	(c) Fog Investigation of liquid water content and size distribution of water particles in fogs.	P2	M.O.15	M.R.P.208

Item No.	Investigation	Priority	Branch or Individual	Latest Papers, Remarks etc.
	(d) Rain			
	(i) Exploration of physical structure of rain-producing clouds.	PX	M.R.F. East Hill	M.R.P. 458*
	(ii) Investigation of drop size distribution in rain.	P2	M.O.15	M.R.P. 352*, 452* See also I.11(d)(ii) 453*, 469*, 519
	(iii) Artificial production of rain and dispersal of cloud	P1	M.R.F.	
	(e) Ice accretion on aircraft			
	Investigation of meteorological factors affecting ice accretion on aircraft.	PX	M.R.F., M.O.15	M.R.P. 168*, 176*, 268, 359, 430, 482*. See also I.11(d)
	(f) Contrails			
	Investigation of meteorological factors affecting contrails.	P2	Dr. Goldie, M.R.F., M.O.15	M.O. 479, 489.
	(g) Atmospheric electricity.			
	Electrical charges on, and field changes during, precipitation both near the surface and up to, and in, cloud.	P3	Kew	Geophys. Mem. No.84 (Sir G.C. Simpson)
III.3	Atmospheric turbulence.			
	(a) Investigation of the velocity and dimensions of gusts associated with cumulonimbus clouds.	PX	Dr. Goldie, East Hill	M.R.P. 155*, 192, See also I.7 b(i), 484*, 535*
	(b) Investigation of clear air turbulence.	PX	Dr. Goldie, M.O.15	M.R.P.338*, 436*, 437*, 510*, 512, A.R.C. No.11202 (I.G.P.20), A.R.C. No.10565 Civ.22, A.R.C. No.11185 (I.G.P.19). A.R.C. No.12877
	(c) Investigation of temperature and humidity inhomogeneities in the atmosphere.	P1	M.R.F.	M.R.P. 402*.
	(d) Investigation of small scale turbulence in the lower atmosphere.	P1	Cambridge, Kew	M.R.P. 265, 278, 314, 365, 377* 378, 424*, 429, 491*, 503*.

Item No.	Investigation	Priority	Branch or Individual	Latest Papers, Remarks etc.
	(e) Diffusion of pollution from chimneys.	P2	A.D.M.O.(I)	Q.J.R. Met. Soc. Vol.73, p.426, and Vol.74, p.133.
III.4	Radiation			
	(a) Study of Solar Radiation - total diffuse and according to spectral region.	P2	Kew	M.R.P.372*. Work to be extended to Eskdalemuir, Lerwick, Mildenhall, Aberporth and possibly to Leeds. See also I.11.b.
	(b) Measurement of flux of long wave (greater than 3 μ) atmospheric radiation (from atmosphere and ground)	P1	Kew	
	(c) Analysis of records of daylight illumination.	P2	Kew	Proc. Roy, Soc. 191A. 1947 pp.467 - 484 by Atkins and Ellison. D.S.I.R. A.P. Paper No.40 by J.M. Stagg. See also I.11 b(ii). A recorder is now installed at Victory House as well as at Kew.
	(d) Absorption coefficients of atmospheric gases.	-		Gassiot Committee.
III.5	Meteorological factors affecting radio transmission.			
	Investigation of the factors which govern the propagation of short-wave radio transmissions.	P1	M.O.15	In collaboration with the T.W.P.C.
III.6	Meteorological factors affecting agriculture.			
	(a) Statistical investigations in microclimatology.	P2	M.O.19	
	(b) Experimental study of microclimatology.	P1	Cambridge M.O.19	See also III.3(d) and III.7(b)

/(c)

Item No.	Investigation	Priority	Branch or Individual	Latest Papers, Remarks etc.
	(c) Measurement of water deposited in dew and hoar frost.	P2	M.O.19 Cambridge	
	(d) Detailed study of factors leading to liability to frost of particular localities.	P1	M.O.19	Work also being done at Fuel Research Station.
III.7	Assessment of water resources and the condition of the ground.			
	(a) Investigation of the monthly and annual variation of evaporation and the factors affecting the rate of evaporation.	P2	M.O.19	M.R.P. 337.
	(b) Interchange of water vapour between ground and air.	P1	Kew, Cambridge	M.R.P. 362*, 363*, 424*, 498*. See also III.3(d) and III.6(b)
	(c) Investigation of factors affecting ground conditions for traffic.	P3	A.D.M.O.(I)	In collaboration with Rothamsted. M.R.P. 197.
III.8	Study of visibility from the air.			
	(a) Investigation of visibility from aircraft to aircraft and its variation with height.	P2	-	Awaiting development of instrument. See I.5(b).
	(b) Investigation of the relation between air-to-ground and horizontal visibilities.	PX	M.O.16 initially	See I.5 (c)
	(c) Visibility of ground from aircraft at great heights.	P2	A.D.M.O.(I)	
III.9	Stratospheric phenomena.			
	(a) Investigation of the ozone content of the lower stratosphere under various conditions.	-	)Prof. Dobson)Sir Charles) Normand	M.R.P. 37, 37A, 60. Gassiot Committee
	(b) Measurement of ozone in different parts of the world.	-	)	Gassiot Committee.
	(c) Investigation of relation between ozone content and tropopause height.	-	)	Gassiot Committee.

Item No.	Investigation	Priority	Branch or Individual	Latest Papers, Remarks, etc.
	(d) Investigation of the temperature and water content of the troposphere and lower stratosphere under various conditions.	PX	M.R.F.	M.R.P. 189, 272*, 375, 397, 486* Gassiot Committee
	(e) Measurement of water vapour CO_2 and helium in the stratosphere.	P3	M.O.17, Prof. Simon	Gassiot Committee
	(f) Investigation of the conditions of radiative equilibrium in the stratosphere.	-	-	M.R.P. 84, 85, 308. Gassiot Committee.
	(g) Large scale air movements in the stratosphere, including seasonal variations.	P1	Dr. Goldie	
	(h) The formation of simple and multiple tropopauses, types of tropopause, exchange of mass between the stratosphere and the troposphere.	PX	M.O.21 M.R.F.	M.R.P.524.
III.10	The ionosphere and magnetic conditions.			
	Investigation of possible relationships between the radio reflecting conditions of the ionosphere and the prevailing terrestrial magnetic conditions.	P2	A.D.M.O.(R)	Work in progress Radio Research Station, N.P.L.
III.11	Observations at great altitudes.			
	(a) Temperature and wind from propagation of sound of explosions.	P2	-	M.R.P. 195, 284*, 346*, 413, 439, 470.
	(b) Observations made with the aid of large rockets.	P2	-	
	(c) (i) Exploration of the high atmosphere by searchlights.	P1	A.D.M.O.(I.D.) R.R.D.E.	M.R.P. 300, 315, 485. See I.11(e)(i)
	(ii) Exploration of the high atmosphere by balloons.	P1	M.O.17 M.O.12	See also I.7(c)(i)

Item No.	Investigation	Priority	Branch or Individual	Latest Papers, Remarks, etc.
III.12	Climatology			
	(a) Climatological features of specified areas.	P3	A.D.M.O.(I)	
	(b) Physical causes of climatic features.	P3	A.D.M.O.(I)	
	(c) Collation of data relating to the temperature likely to be reached by objects exposed to sunshine in various parts of the world.	P2	A.D.M.O.(C)	S.D.T.M.24 Q.J.R. Met. Soc. Vol.72, pp.87-97.
	(d) Investigation of the best data to supply to engineers in connection with heating and air conditioning.	P2	A.D.M.O.(C)	The Institution of Electric Engineers have raised the question of the worst conditions for which space heating equipment should be designed.
III.13	Marine Meteorology			
	(a) Seasonal variation of sea surface temperature.	P2	M.O.1	
	(b) Diurnal variation of meteorological elements over the ocean.	P2	M.O.1	
	(c) Variation of wind with height in the first few thousand feet over the sea and the relation between surface and geostrophic wind velocity.	P2	M.O.1	

This report has not yet been published and is to be treated CONFIDENTIALLY. Its contents must not be quoted.

M.R.P.542

S.C.I./37

24th February, 1950.

AIR MINISTRY

METEOROLOGICAL RESEARCH COMMITTEE

An Ultra-Rapid Aircraft Thermometer

by D.R.Grant. (Meteorological Office)

AIR WEATHER SERVICE TECHNICAL REFERENCE FILE

Summary

A description is given of an aircraft thermometer with a lag coefficient of less than 10m secs and sensitivity of 1/20°F per mm. deflection. It can be used both to measure temperature and to record temperature fluctuations and is sufficiently robust for use in research aircraft flying at speeds of up to at least 220 knots in clear air.

Because of the conversion of the kinetic energy of air motion into heat, on impact, the thermometer temperature fluctuations may be caused by changes in either airspeed or air temperature.

The thermometer element is a length of fine platinum wire and is connected in an A.C. bridge circuit, the out of balance voltage from which is amplified and rectified. The output is displayed on a cathode ray tube with a second tube in parallel for photographing the fluctuations.

The method used to measure the lag is also described.

The thermometer element

As amplification of the output from the thermometer is required to operate robust high speed recording instruments (e.g. recording galvanometer or cathode ray tube with camera) it was decided to use a resistance thermometer on an A.C. bridge. A.C. amplification is then used. This is preferable to D.C. amplification which would be necessary with thermo-couple elements. Moreover, it was considered that a resistance thermometer would be easier to construct than a fine wire thermo-couple. A thermistor was considered but there appear to be none produced in this country with a lag as small as obtained with fine gauge platinum wire.

Two inch lengths of platinum wire of 25μ diameter were found to stand up to airspeeds of 220 knots in clear air and in water clouds above 32°F, but not in supercooled water clouds or precipitation. Arrangements have been made, therefore, to withdraw the element into the aircraft before clouds and precipitation are entered. No attempt has been made to measure temperatures in cloud and precipitation.

The design of the element has to be such that the supports of the wire do not affect the lag. An element consisting of platinum wire wound round four thin insulated rods was tried, but although only 1/10th of the length of the wire was in contact with the insulator, the temperature of this part of the wire was influenced by the temperature of the rods, and the overall lag impaired. 9°F of 10°F temperature change were followed almost immediately but the remaining 1°F decayed with a time constant of the order of one minute in still air.

In order to avoid using the parts of the wire in contact with the supports, short lengths of wire are connected by thick copper strips, which, having negligible resistance, do not contribute to the variations of resistance with temperature. Ten 2in. lengths of 50 S.W.G. platinum wire are connected in series

/in

in this way, giving an element of resistance of approx. 115 ohms at room temperature.

A photograph of the element is shown in Plate 1.

Measurement of lag.

The lag of the element was measured using the arrangement shown in fig.(1). Fig.(1a) is a multivibrator circuit which is used to operate the switch S (fig.1b) at a frequency of 8 c/s. S changes over every 1/16th of a second and as the time of change-over is short, the relays R_2 (operating S_2 in fig.1c) and R_3 (operating S_3) are energised in turn for periods of just less than 1/16th second. The position of the relay contacts when the relays are not energised are shown dotted in fig.1c.

When R_2 is energised the thermometer T_1, (fig.1c) is connected in one arm of an A.C.bridge, and when R_3 is energised the thermometer is heated electrically. A double beam cathode ray oscilloscope (C.R.O.) is used to indicate the out of balance voltage across the bridge and it is short circuited when T_1 is heating to avoid a large voltage being applied to it when the thermometer arm of the bridge is on open circuit. A 2000 c/s oscillator to supply power to the A.C.bridge is shown in Fig.1c.

The C.R.O. is used with a slow running time base on the X plates and the out of balance voltage (amplified to give a suitable deflection) on the Y plates. When the bridge is balanced the C.R.O. trace is a straight horizontal line, but with the bridge out of balance the alternating voltage appears on the C.R.O. as a vertical deflection.

The method of operation is as follows:- With X closed (fig.1) and relay R not operating (i.e. the multivibrator switched off) R_2 is energised and fig.1c is an A.C.bridge. The bridge is balanced and the multivibrator is then switched on. When R_3 is energised the thermometer heats up and when R_2 is energised the thermometer cools down, the envelope of the 2000 c/s waveform on the C.R.O. giving the cooling curve. It is possible to obtain a stationary picture by synchronising the C.R.O. and multivibrator and a photograph can then be taken. The speed of the time base is measured by applying 50 c/s mains voltage to the second beam of the C.R.O. and this appears on the photograph alongside the cooling curve. The type of photograph obtained is shown in Plate II. The slight assymmetry is caused by a slow voltage drift on the plates of the C.R.O. but the amplitude of the 2000 c/s oscillation can be shown to decay exponentially by plotting the logarithm of the deflection (corrected to allow for the diameter of the spot) against time. The lag can be obtained either from the slope of this graph or simply by reading from the photograph the time taken for the deflection to decay to $\frac{1}{e}$ of its orginal value.

The result obtained with airspeeds of 20 knots was 12 milliseconds. As the lag decreases very approximately as the square root of the airspeed, the lag of the element must be about 4 milliseconds at 220 knots.

Oscillator, Bridge, Amplifier and Display Circuits

The circuit diagram of these is given in fig.2 and is described in detail in Appendix I. For convenience, a block schematic diagram (fig.3) will be discussed here and will suffice to give a general description of the operation.

Power supplies are obtained from a vibrator unit and H.T. batteries. The output of an oscillator giving a 2000 c/s 2 volts sine waveform is applied to the bridge in one arm of which is the thermometer. Heating of the thermometer was found to be negligible with this voltage on the bridge.

The output from the bridge is a 2000 c/s waveform modulated in amplitude because of the resistance fluctuations of the thermometer. When the bridge is balanced the amplitude of the output voltage is zero and the output increases as the bridge becomes more and more removed from the balanced position. An

/example

example of the waveform applied to the amplifier is shown in fig.4a.

The amplifier has a maximum gain of about 20,000 but this can be adjusted in steps of about 3:1 by a gain control switch.

The output from the amplifier is applied to a detector after which the waveform is as shown in fig.4b. This is filtered to remove the 2000 c/s and other unwanted frequencies introduced by the rectification and the waveform left is that caused by the temperature fluctuations only (fig.4c). This is applied to a cathode ray tube to deflect the spot vertically.

It is possible to arrange that the time constant of the whole instrument is smaller than that of the thermometer. It could in fact be made very much smaller if the "carrier" frequency of 2000 c/s were increased.

The circuit described above has a number of limitations when applied to measuring temperature fluctuations. Firstly, if the bridge is originally balanced, the fluctuations may go from one side of the balanced position to the other and there is no way of discerning whether the individual oscillations are in the "warm" direction or the "cold". It is, therefore, necessary to have the bridge in an "off balance" position initially and never allow the spot to move into the balanced position. Thus there is a limit to the drift of temperature in one direction as the bridge would reach the balance point. There is also a limit in the other direction because the "off balance" voltage would eventually become so large that the amplifier would become overloaded. The range of temperature between these two limits can, however, be adjusted by the gain control and the sensitivity is such that on maximum gain a peak to peak fluctuation of 1°F can be accommodated. If the expected amplitude of the fluctuation is greater than this, a lower sensitivity must be used or alternatively the spot must be moved away from the two extremes by changing the original setting of the bridge.

A photograph of the instrument is shown in Plate III.

The Recording Apparatus

The cathode ray tube on the main instrument has in parallel with it another tube past which a film is moved at a speed of approximately 1 cm/sec. As the spot is about $\frac{1}{2}$ mm in diameter this limits the period of temperature fluctuations which can be resolved to about 1/20th second. It may be possible to improve this slightly but the speed of the emulsion puts a limit to the rate at which the film can be moved. A much brighter cathode ray tube would increase this limit.

A time scale can be applied to the film either by flashing a light on the edge of the film or by applying a pulse periodically to the plates of the cathode ray tube to deflect the spot. The latter method is being developed for incorporation in the existing equipment.

Speed Correction

By flying at various speeds and taking readings of the balance position at different speeds, the slope of the graph of indicated temperature against (true airspeed)^2 gives the speed correction. This was found to be approximately 1.6 i.e. the true air temperature in °F = $T_i - 1.6\, V_a/100^2$ where V is the true airspeed in knots and T_i indicated temperature in °F.

Hence for a change in airspeed of 10 knots (from say 150-160 knots) the temperature of the thermometer changes by $\frac{1.6}{100^2}(160^2-150^2) \simeq \frac{1}{2}$°F.

Thus a 1 cm deflection of the spot may indicate either a 10 knot airspeed change or a $\frac{1}{2}$°F temperature change.

/Stretching

Stretching of wire under wind forces

Any change in resistance due to stress of wind forces is measured with the speed correction. There is no permanent change of resistance caused by wind forces.

Flight Tests

A number of flights have been made to test the operation of the equipment and an example of the type of trace obtained is shown in Plate IV. These are fluctuations as the aircraft was flying at a steady indicated airspeed of 130 knots, at a height of 10,000 ft. There is no time scale on this film but 1 cm ≡ 1 second (approx) and $\frac{1}{2}$ degree (F).

Uses of Equipment

It is proposed to carry out the following work using this instrument:-

(1) By taking a synchronised record on a recording accelerometer find whether there is any correlation between clear air bumpiness and indicated temperature fluctuations.

(2) Carry out an ascent simultaneously with a radio-sonde balloon measuring temperatures on a rapid thermometer and see if there is any correlation between indicated temperature fluctuations and Richardson's number. (In this experiment a thermometer with a comparatively long lag is used in one arm of the bridge.) This follows the slow change of temperature with height and frequent adjustments of the setting of the bridge are obviated.

(3) Examine the fluctuations for periodic variations and see if there is a correlation between a certain periodicity and bumpiness.

(4) Investigate the rate of change of lapse rate at an inversion.

Appendix I.

Detailed description of oscillator, bridge, amplifier and display circuits

V_1 is a phase shift oscillator the output from which is fed by an impedance matching transformer (25:1 step down) to the bridge.

The value of the resistances in the bridge circuit are the same as in the standard M.O. bridge. This allows for a balance to be obtained over a range of temperature from -110°F to +100°F. It was found necessary to balance out stray capacities in the bridge and leads in order that the output from the bridge caused by unbalanced capacities was always small.

V_2 and V_3 are R C coupled amplifiers with negative current feedback and decoupling. V_3 is followed by a gain control and V_4 is a third amplifer.

V_5 is a cathode follower detector. The value is biassed to cut off by adjusting the grid potential, the cathode potential being fixed by a bleeder chain across the H.T. Because of the curvature of the valve characteristic near cut-off, when the voltage applied to the grid is small the peak output voltage in the positive half cycle is not proportional to the peak input voltage and the sensitivity is reduced. This reduction is applied over a very small range of input voltage as the valve used is a sharp cut-off type. It makes the instrument comparatively insensitive near its balance point which is another reason for operation at a point removed from the balanced position. It has the advantage, however, of eliminating small rapid temperature flunctuations when actual temperatures are being measured.

The output from the detector is filtered to remove the undesired frequencies, leaving only the modulation frequencies caused by the temperature fluctuations. V_6 is a phase splitter of the "long tailed pair" type the outputs from which are fed to opposite plates of the cathode ray tube V_9. The voltage on one grid of V_6 is fixed and the other has an adjustment which moves the spot on the C R T across the tube. The cathode ray tube is a V C R 522 which is a $1\frac{1}{4}$" tube with a sensitivity of 100 volts/cm when an anode voltage of 1000 volts is used.

V_7 and V_8 are two voltage stabilisers in series which were found to be necessary to stabilise the 350 volts supply from the vibrator unit. The H.T. for the first two stages of amplification was taken from batteries to avoid instability and amplification of any ripple which would be present in a rectified H.T. supply.

Across the other plates of the tube it is intended to apply timing pulses. In the camera box the spot oscillates behind a slit and the timing pulses will deflect the spot perpendicular to the slit causing a temporary black out in the photograph.

Operation

With the input to V_4 earthed, the potential of the grid of V_5 is increased until the spot on the tube begins to move, i.e. until the cut-off point of V_5 is reached. The potential of the grid of the first part of V_6 is then adjusted so that the spot is on the edge of the tube. This is then the position the spot will take up when the output from the bridge is zero.

The gain is then increased in steps, the bridge being balanced more accurately at each step until full sensitivity is attained. The bridge potentiometer is then moved until the spot is near the centre of the tube and the temperature fluctuations can then be observed.

Note on circuit diagrams

The value of the resistances are shown in ohms unless followed by K or M in which case they are in kilohms or megohms respectively. Condensers are shown in μ F unless followed by **p** in which case they are in $\mu\mu$F.

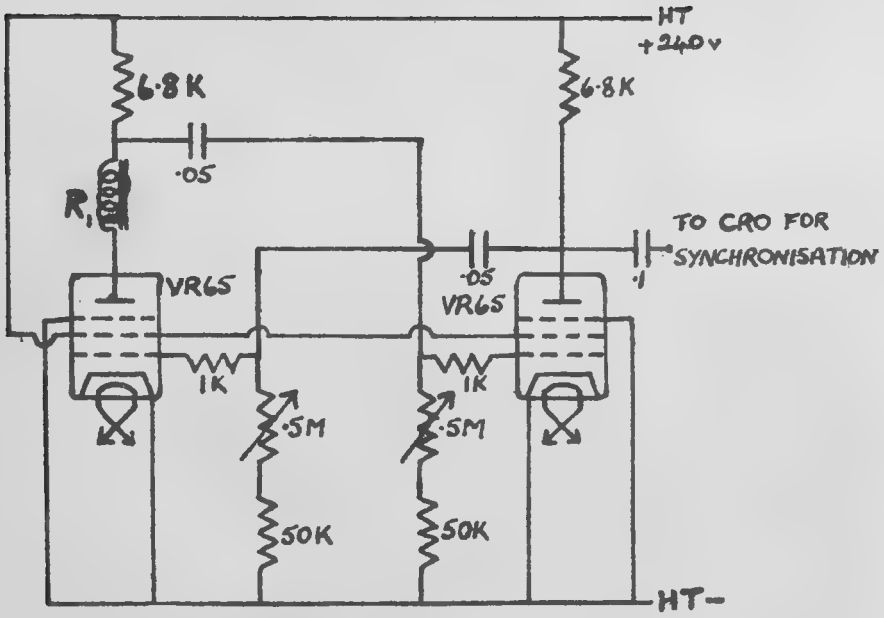

FIG 1(a)

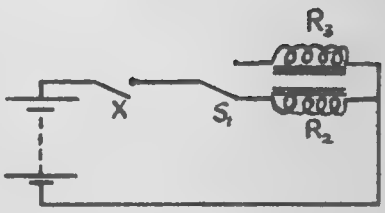

FIG 1(b)

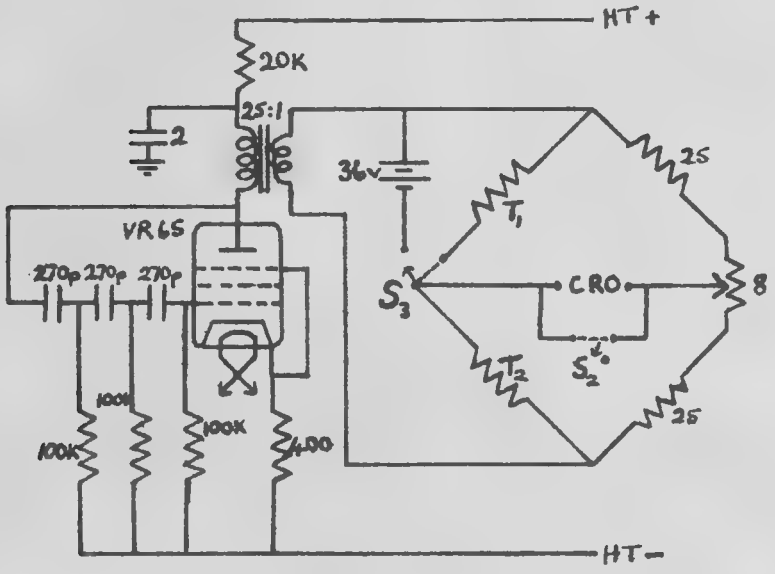

FIG 1(c)

FIG 1

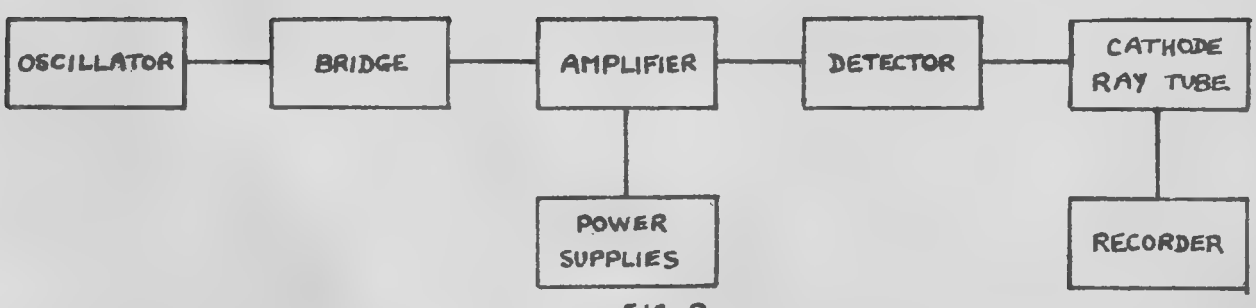

FIG 3

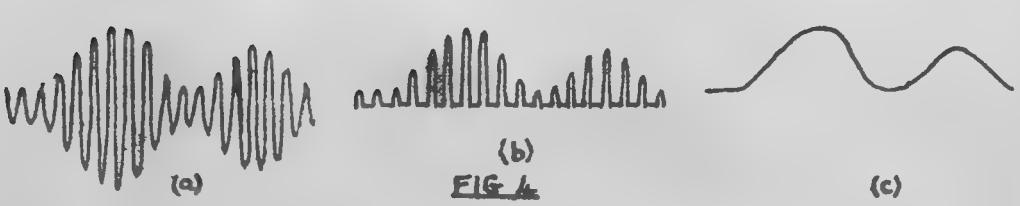

FIG 4

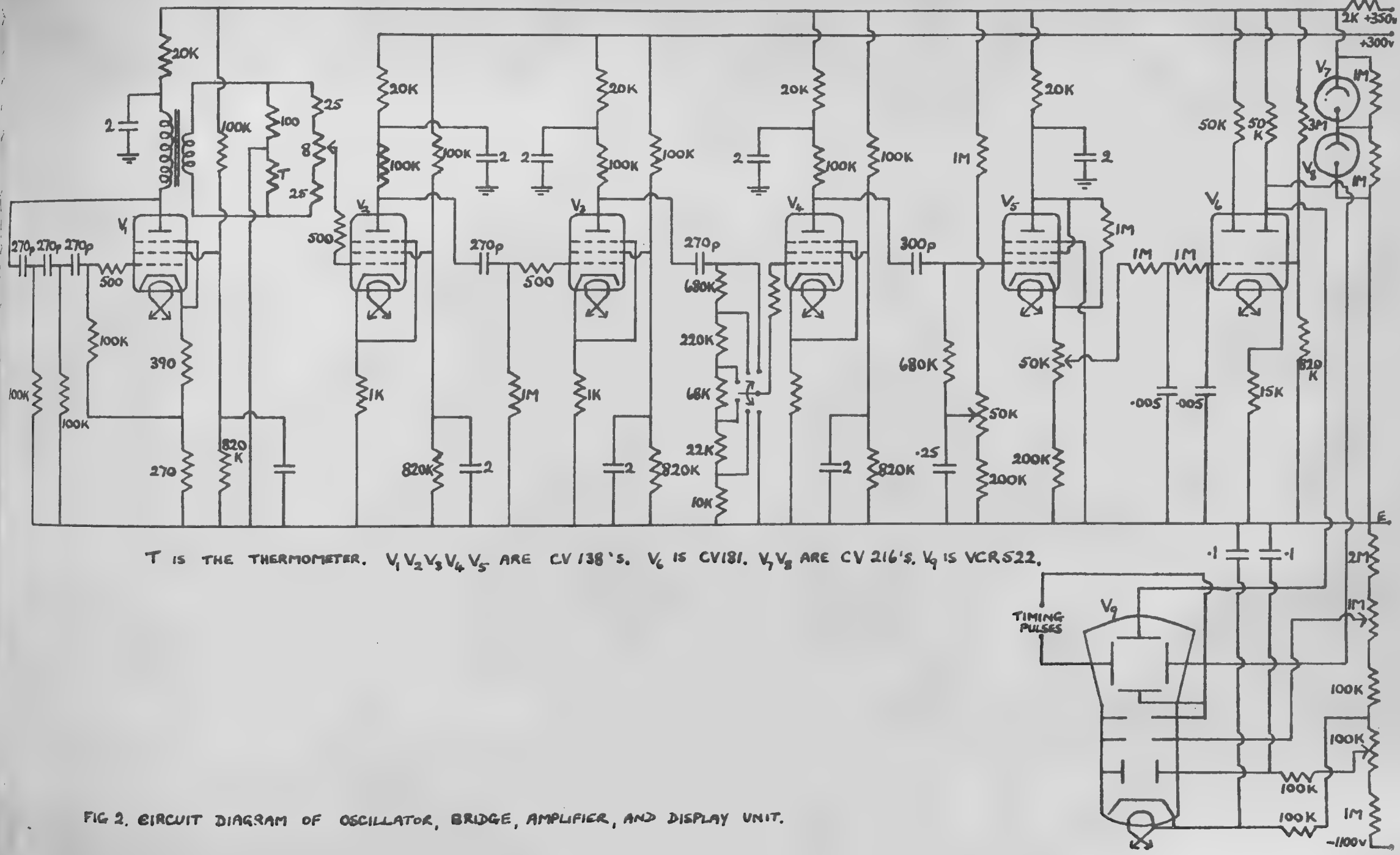

T IS THE THERMOMETER. $V_1 V_2 V_3 V_4 V_5$ ARE CV 138's. V_6 IS CV181. $V_7 V_8$ ARE CV 216's. V_9 IS VCR522.

FIG 2. CIRCUIT DIAGRAM OF OSCILLATOR, BRIDGE, AMPLIFIER, AND DISPLAY UNIT.

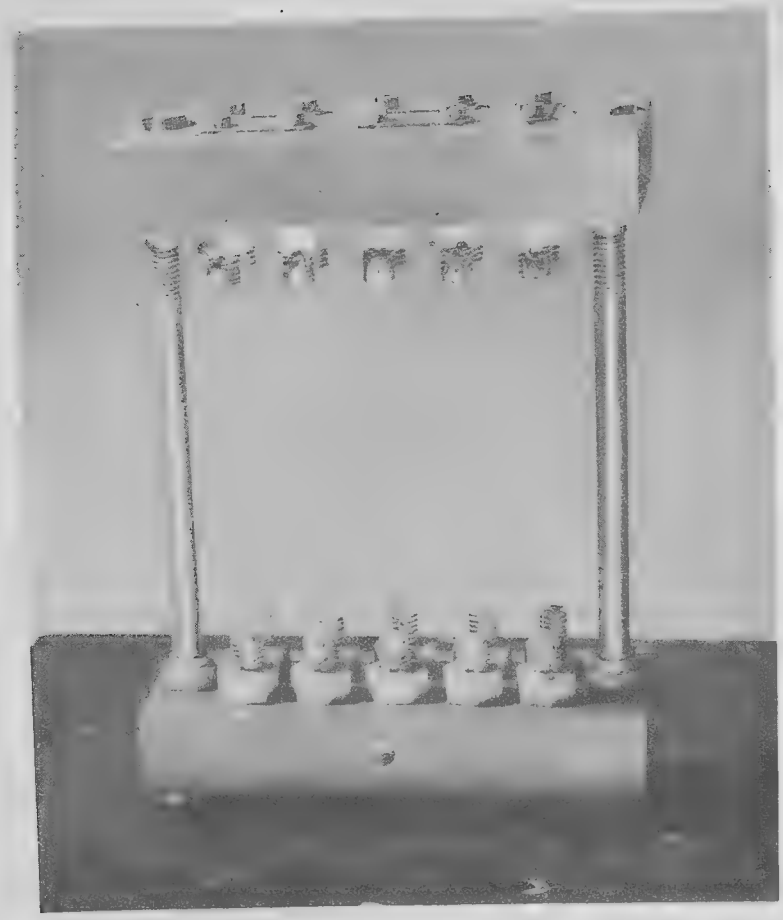

PLATE I

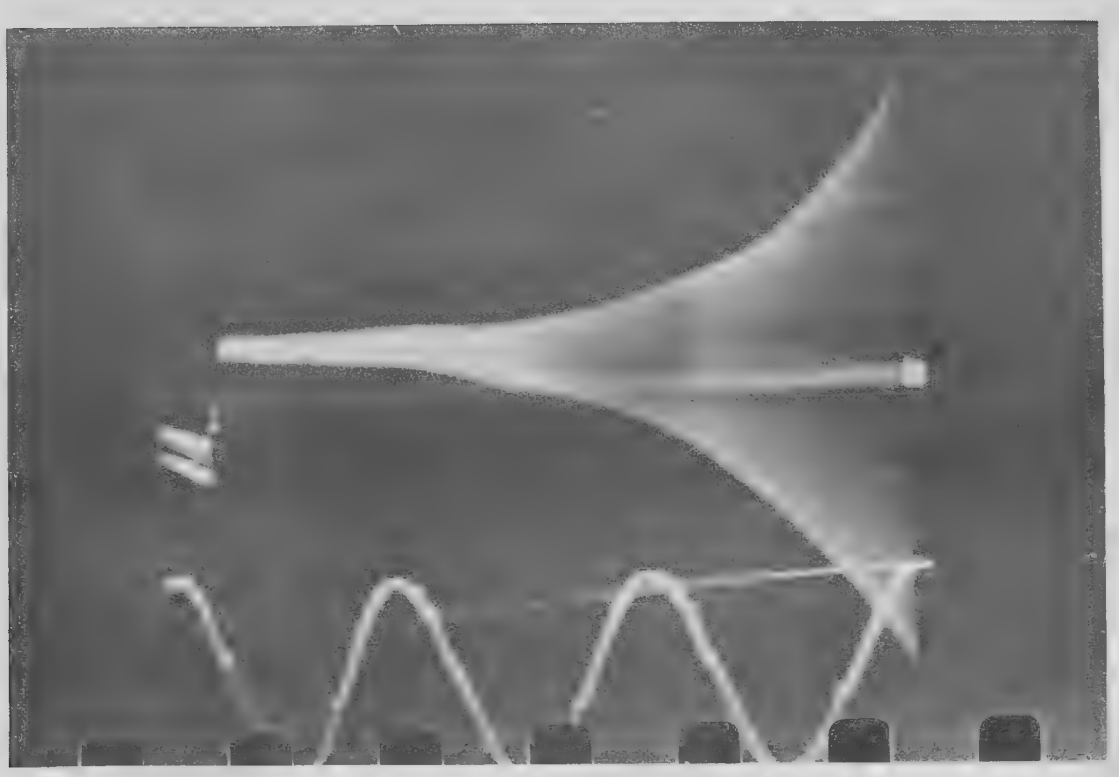

PLATE II

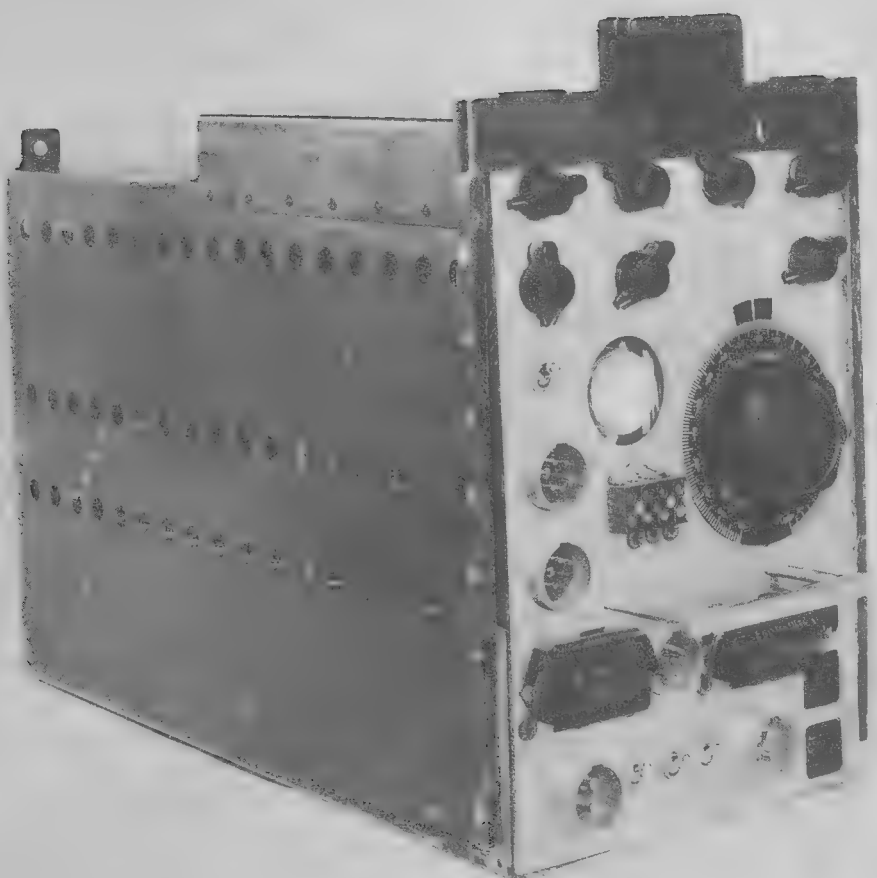

PLATE III

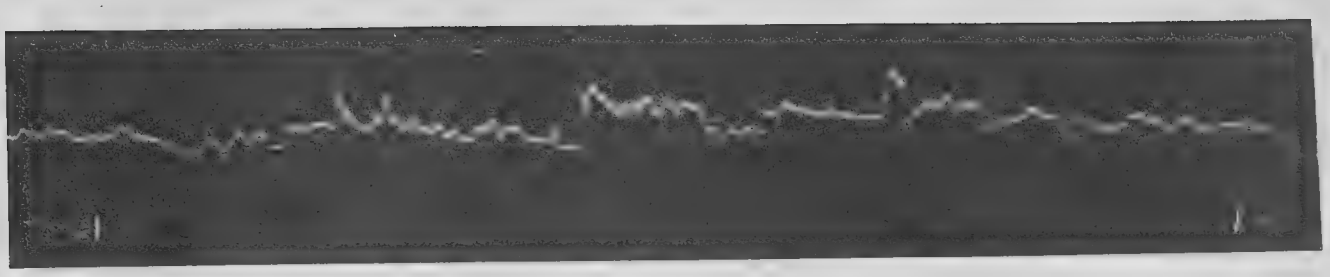

PLATE IV

This report has not yet been published and is to be treated CONFIDENTIALLY. Its contents must not be quoted.

M.R.P. 546
S.C.III/54
5th April, 1950

AIR MINISTRY
METEOROLOGICAL RESEARCH COMMITTEE

TEMPERATURE AND HUMIDITY GRADIENTS IN THE FIRST HUNDRED METRES AT RYE

by
A.C. Best, E. Knighting, R.H. Pedlow and
K. Stormonth (Meteorological Office)

Introduction

The thermal structure in the first hundred metres of the atmosphere has been investigated in experiments carried out at Leafield (1) and Porton (2) and referred to later in the text. Although desirable on many meteorological grounds, corresponding information on the distribution of humidity was not available. The need for such information was emphasized in connection with the propagation of radio and radar signals for the propagation path depends upon the refractive index of the medium through which it is passing. The refractive index of the atmosphere depends upon the temperature and humidity structure. Observations were therefore instituted at Rye with the object of investigating the thermal and hydral structure in the first hundred metres of the atmosphere. The results are given below. The humidity data presented are the first of their kind to be published; the temperature data supplement those referring to Leafield and Porton.

PART I

MAY 1 1951

Instrumental

1. The Site

The meteorological station at Rye is situated in latitude 50°58'10"N. and longitude 0°48'50" E., at an altitude of 3.8m. (12 feet) above sea level. It is towards the western end of Romney Marsh, 5 Km. NNE from the nearest point of the coast of the English Channel. From ENE to WSW through S, the ground is practically flat to the coast; to the N and NE it is 15 to 20 Km. before rising ground is encountered in the Downs and the Weald; and to the W and NW it is 4 to 6 Km. before the land rises fairly sharply to about 60m. (200 feet).

The marsh is predominantly grassland with a little arable, dissected by dykes with only rare low embankments. There are few trees, no woodlands, and only scattered farmsteads. A broken line of buildings from 3 to 8m. high, however, stretches to the SW from within 40m. of the enclosure and instrument tower to a distance of about 320m., and to the ENE of the instrument tower are two similar towers in line at intervals of 62m. Four wooden towers 76m. (200 feet) high stand 220m, to the SW, and two 37m. (120 feet) towers stand 180m. to the SE. The site is surrounded by a 3m. - high iron fence which is about 55m. distant to the SE where it most nearly approaches the enclosure.

Plate 1 shows two views of the terrain.

AIR WEATHER SERVICE
TECHNICAL REFERENCE FILE

2. The Instruments

(a) General

Normal climatological instruments were maintained as well as the temperature and humidity apparatus. Continuous records were made of the following meteorological quantities:-

1. Aspirated dry-bulb temperature at a height of 1.1m. (3ft. 6in.)
2. Differences in air-temperature over the height intervals between 15.2, (50 feet) and the levels 1.1m (3ft. 6in.), 47.2m (155 feet) and 106.7m. (350 feet).

/3

3. Relative humidity at the height of each thermometer.
4. Wind velocity and direction at a height of 12.7m. (42 feet) - effective height 10m.
5. Sunshine
6. Starshine

(b) The Tower

Instruments were mounted at 15.2m., 47.2m and 106.7m. on the W side of the most westerly of three steel towers which lie in an ENE-WSW line. The tower is of an open lattice construction, 23m. square at the base, with cantilevered wooden-floored platforms at heights of 15, 61 and 107m, projecting 7, 11 and 7m. respectively from the side of the tower. Wooden-floored gangways run round the tower within its circumference at approximately every 15m., one of these being used in mounting a screen at 47.2m. (155 feet).

(c) The Aspirated Screens

The temperature and humidity elements were housed in aspirated screens (see plate 2), each of which consisted of a box of sheet-iron 25 x 25 x 40 cm., the front plate being detachable for access to the sensitive elements. The screen and front-plate were so constructed that when fully assembled the four sides of the screen were of double sheeting separated by 2.5 cm. In the base was fitted an inflow duct of 15 x 9 cm. cross-section and 15 cm. long; and to the top was fitted an open cylinder 23 cm. high and 18 cm. diameter in which was suspended an electric motor driving a four-bladed fan with about 2mm. clearance from the cylinder walls. The speed of the motor was 2700 r.p.m. giving a rate of aspiration over the elements of about 3.5 m/sec. A canopy over the cylinder protected the whole from rain. All surfaces were painted white.

One screen was mounted at 1.1m. on a metal stand in the enclosure, about 3m. from the foot of the tower. The other three were mounted to slide on angle - iron rails projecting 1.5m. from the tower (see plate 2). Normally the screens occupied positions at the ends of the rails, though at times vibration set up by individual motors made it necessary to bring in the appropriate screen to a distance of about 1m. for quieter running. The screens could be retracted on to the platforms for maintenance. Those at 15.2m. and 106.7m. projected from the western edge of the western cantilever platforms; that at 47.2m. from the western edge of the gangway at that height. Heights are measured to the levels of the inflow ducts at the bottom of the screens.

(d) Temperature Measurements

(i) Elements and Housings. The temperature of the air was measured by nickel resistance thermometers mounted in the screens, two at 1.1m. and one each at 15.2m, 47.2m, and 106.7m. These elements had a resistance which was 100 ohms at 32°F and which varied by approximately 0.25 ohm for each degree F. change in temperature.

(ii) Electrical Circuits and Recorders. The elements were connected by 'Pyrotenax" cable (in which the copper core is held in compressed magnesium oxide insulation, the whole being sheathed in copper tubing) to 'recording pyrometers' made by Messrs. Negretti and Zambra Ltd. These are essentially out-of-balance Wheatstone bridges with a device by which the galvanometer needle is pressed against an inked ribbon and chart for 5-10 seconds every 30 seconds. A system of mercury switches, cam-operated by an electric clock, brought the various elements in turn into circuit, their records being differentiated by the use of different colours of inked ribbon. The travel of the chart was 12.77mm/hr.

/One

One of these recorders was used with one of the 1.1m. thermometers as the unknown resistance to give a single trace of actual temperature at that height.

In the other recorder, the 15.2m. element was used as one 'standard' resistance, and the second 1.1m. element and those at 47.2m. and 106.7m. were compared with it in turn, so that the three traces on the chart indicated the temperature differences over the intervals 15.2 - 1.1m, 47.2 - 15.2m, and 106.7 - 15.2m. A shunt could be placed across the galvanometer to double the range of the instrument (from ±10°F. to ±20°F.) on occasions when large inversions were expected. All the leads were compensated to allow for variation of their resistance with temperature. The recorder-room was kept, as far as possible, at a temperature of 60 - 62°F. to prevent convectional disturbances inside the recorder casings.

(e) Humidity Measurements

(i) Elements and Housings. Humidity was measured by Gregory Hygrometers made by Negretti and Zambra Ltd. In these, the sensitive element was a strip of fabric impregnated with lithium chloride and stretched on platinum-coated electrodes carried on a styrene frame. The electrical resistance of the treated fabric varies in an inverse manner with relative humidity.

In detail, two styrene annuli of 5cm. diameter were separated by 20 platinum-coated rods 35mm. long and 6mm. apart, the whole forming a cylindrical cage. The treated fabric, 3 cm. wide, lay over the electrodes and was kept taut by two small helical springs. Alternate electrodes were connected together, so that the resistance measured was that of 19 strips of fabric in parallel, each 6mm. long and 30mm. wide. The resistance at the standard temperature of 59°F varied with relative humidity as follows:

Rel. Hum. %	Resist. ohms.	Rel. Hum. %	Resist. ohms.
30	158490	80	241
45	8091	90	135
50	3908	95	103
60	1099	100	80
70	457		

The element was protected from dust etc. by a metal box 9 x 9 x 8 cm., with four fine copper-gauze windows 7 x 2.5 cm., two on the underside of the box, and one on each of two vertical sides. Two elements (one for high and the other for low humidities) were housed in each screen.

(ii) Electrical Circuits and Recorders. Pyrotenax leads from the elements led to two recorders with circuits as shown in Fig. A. A stabilising and reducing unit transformed the mains supply to 2 volts A.C. (to prevent electrolysis) which was passed through the element. The resultant current was measured, after being rectified, by a galvanometer with a recording mechanism similar to that of the temperature recorders. The charts, which travelled at 12.77mm/sec., had a non-linear scale of relative humidity. On the original instrument the spacing was:-

30-40%	40-50%	50-60%	60-70%	70-80%	80-90%	90-100%
2.5mm	14mm	29.5mm	29mm	21mm	16mm	12.5mm

/Because

Because of the crowding of the scale at the lower end, a second recorder and corresponding set of elements were introduced with a different mains unit and galvanometer setting, whereby low humidities were recorded on a chart with the spacing:-

10-20%	20-30%	30-40%	40-50%
14mm	32.5mm	60mm	16.5mm

Because of the large changes in resistance of the elements, no compensating leads are required in the hygrometer circuit.

3. Calibrations and Accuracy

(a) Temperatures

Calibrations were carried out as often as opportunity allowed in suitable weather - i.e., under conditions of overcast sky with fresh to strong breeze and no fog or precipitation. On the average, such occasions occurred ten or twelve times a year. Assmann psychrometers were placed beside the screens taken in pairs, and readings taken every minute for 20 minutes. The means of the dry-bulb readings were compared with the means recorded (as actual temperatures or as temperature differences) over the same period. In general, the corrections to the recorder readings indicated by these tests were less than ±0.3°F., and variation with temperature or with the passage of time was very slight.

The scale of the actual temperature chart (0°F - 10°F = 1.5cm.; 90°F - 100°F = 1.2cm.) only allowed of readings correct to ±0.2°F, and individual readings at times of rapid change may have been 0.3°F in error.

The temperature-difference record, with a uniform scale of 2°F = 1.25 cm., permitted a margin of error as low as ±0.05°F.

(b) Humidity

Humidity calibrations were carried out in the same way and at the same time as temperature calibrations, though the relative humidity indicated by the recorders had to be corrected for temperature before it could be compared with the psychrometer readings.

The temperature-coefficient of the elements is a function of the relative humidity, and corrections are applied according to a chart supplied by the makers of the instrument. These corrections are of the order of 3% relative humidity per 10°F departure from the standard temperature of 59°F. No calibration has been carried out below 32°F however, and though the correction curves are sensibly straight lines from above 60°F to 32°F., some error may have been introduced in assuming that the curves continue in the same fashion below that range.

Relative humidities can be read to 0.1%, but no attempt was made to read to finer limits than 0.5%. With the possible exception of occasions of very low temperature, corrections for temperature and instrument error can be guaranteed to well within this margin. The correction resulting from calibration is of the order of ± 2% for new elements, but increases slowly with time. Elements have generally been used for some six months or so, by which time the error is of the order of + 6%, but is then liable to sudden and large increase. Similar sudden increases may occur whenever the elements are exposed to wet fog, which greatly increases their subsequent resistance due to the loss of lithium chloride dissolved in the water which collects on the elements and then drains away.

/In

In general, then, relative humidities correct to ± 0.5% have been obtainable. These, together with the temperatures deduced from the recorded temperature at 1.1m. and the temperature-differences between 1.1m. and the other heights, have been used to obtain absolute humidities in mgm/cu.m. The possible errors of ± 0.2°F and ± 0.5% relative humidity produce errors in absolute humidity which vary from about ± 30 mgm/cu.m. at, say, 15°F., to about ± 200 mgm/cu.m. at 85°F.

(c) Lag

At the speed of aspiration (approximately 3.5 m/sec airflow over the elements) the lag coefficient of the thermometers was about 5 minutes and that of the humidity elements about 3 minutes. As calibration was always performed at times of almost steady temperature and humidity, this slight asynchronism was ignored.

4. Period of the Observations

(a) The observations were, as nearly as could be achieved, continuous over the period July 1945 to June 1948 inclusive. It was necessary, however, to cease all recording during January 1948. The separate monthly records represent the following numbers of complete days of observations:-

Jan.	Feb.	Mar.	Apr.	May	June	Jly.	Aug.	Sep.	Oct.	Nov.	Dec.
55	62	77	83	85	74	70	77	77	71	81	67

(b) With only three years observations it is desirable to assess the extent to which the average weather during the observations agrees with the average weather over a longer period. For this purpose the mean monthly sunshine total for the period of observations is compared below with the mean monthly values for the neighbouring town of Hastings during the period 1906 - 1935.

Sunshine during period of Observations as a percentage of normal (Hastings)

Jan.	Feb.	Mar.	Apr.	May	June	Jly.	Aug.	Sep.	Oct.	Nov.	Dec.
118	71	99	125	99	99	113	104	78	110	84	99

(c) Figures used in the compilation of tables and curves for "clear and overcast summer and winter days" relate to the following occasions:-

Winter Clear: 1947; Jan. 16 and 18th.
1948; Feb. 25th.

Winter Overcast: 1945; Dec. 22nd.
1946; Jan. 24 and 29th; Feb. 7, 12, 13, 14, 15 and 26th; Dec. 23rd.
1947; Feb. 11 - 17th (inclusive) and 20th.; Dec. 6, 12 and 13th.

Summer Clear: 1945; July 8 and 13th.; Aug. 3, 4 and 5th.
1946; July 2, 7 and 10th.
1947; June 25th.; July 15th; Aug. 9, 13 - 16th (inclusive) and 24, 25, 27 and 28th.

Summer Overcast: 1945; July 10th.; Aug. 1 and 20th.
1946; Aug. 20th.

/PART II

PART II

The Temperature Records

1. Preliminary Remarks

A broad survey of the temperature records obtained during the three years of observation at Rye show that the main properties of the temperature field are little different from those described by Sir Nelson Johnson and G.S.P. Heywood in "An Investigation of the Lapse Rate of Temperature in the Lowest Hundred Metres of the Atmosphere" (1), which treats the results of similar experiments carried out at Leafield. (This publication will be referred to as GM.77). We have, therefore, presented the results in a somewhat brief fashion, indicating from time to time particular points of similarity with the results to be found in that publication.

The method of analysis of the records and the method of presentation of the results follow closely those methods initiated in GM.77, which are akin to those used by Sir Nelson Johnson in "A Study of the Vertical Gradient of Temperature in the Atmosphere near the Ground".(2) (This publication will be referred to as GM.46).

GM.46 deals with experiments carried out at Porton. Direct comparison of the results obtained at Leafield and at Porton can thus be made with the results obtained at Rye. All temperatures are given in degrees Fahrenheit and Greenwich Mean Time is used throughout. Hourly values were extracted from the traces, the value allotted to each hour being the mean over a period of twenty minutes centred on the hour in question. The temperature differences are taken as positive when temperature increases with height, and negative when it decreases upwards. The former of these conditions is generally known as an inversion whilst the latter will be referred to as a lapse.

It is convenient to denote the intervals between 1.1m. and successive heights by letters as in the following scheme, which also includes the dry adiabatic lapse rate over each interval.

Interval	X	1.1m	to	15.2m	-0.25°F
"	Y	1.1m	to	47.2m	-0.83°F
"	Z	1.1m	to	106.7m	-1.90°F

2. Mean Hourly Values and Diurnal Variation of Lapse Rate

The mean hourly values of the temperature differences over each height interval for each month are given in Table I. If the values in Table I are plotted in the form of temperature height profiles as in Fig.8 of GM.77 it can be seen that the general appearance of the two sets of curves is remarkably similar; for this reason we have not included such a figure, but conclude that the main physical features are as discussed by Johnson and Heywood. Detailed features are different, as might be expected bearing in mind the differences in the sites chosen for the experiments. For example the mean lapse rate between 1.1m and 15.2m at 1200 in January is practically zero compared with adiabatic rate found at Leafield between 1.2m and 12.4m; in June the mean lapse rates at 1200 over the intervals 1.1m to 15.2m and 1.1m to 106.7m are respectively 7.2 and 3.5 times the adiabatic lapse rate compared with lapse rates 8.0 and 2.2 times the adiabatic lapse rate found at Leafield over similar intervals.

The values given in Table I have been plotted in Fig.1 showing the diurnal variation of the lapse rate for the three intervals X, Y and Z. It is interesting to compare these curves with similar curves in GM.46 and GM.77. In the first place the curves are similar in shape, as might be

/expected

expected since they are graphical representations of the effects on temperature of the same genus of physical causes. Although the lowest intervals are not the same in each series of experiments we may compare the curves relating to the interval 1.2m to 17.1m in GM.46, interval A (1.2m to 12.4m) in GM.77 and interval X of figure 1. With the exception of January the time of change over from mean inversion to lapse is nearly the same in each series of experiments for any month. At Rye the figure shows that in January there is never a mean lapse from 1.1m to 15.2m, but in the mid-day period there is an almost isothermal layer.

The feature noted at Leafield and Porton that the change over from inversion to lapse occurs almost simultaneously at all levels is not quite so marked in some months at Rye and the difference in time of the change from lapse to inversion in the evening shows differences of the same order as given in GM.77.

It will be noted that the July lapses in the top layer, between the levels 47.2m and 106.7m are small compared with the June and August lapses in the same layer, and at 1300 there is a small inversion. This may be a sea breeze effect and requires further investigation.

3. Mean Monthly and Yearly Values of the Lapse Rate

The hourly values of the temperature differences given in Table I have been meaned by months and the results are given in Table II.

It will be seen that in every month the average temperature structure between 1.1m and 15.2m is an inversion and that the mean inversion is stronger than that found at Leafield over the interval 1.2m to 12.4m, even allowing for the height difference between corresponding levels. In the summer months the mean gradient at Leafield and Porton was a lapse in contradistinction to the inversion found at Rye.

The mean inversion generally decreases with height with exceptions in May, June and August, but the higher levels do not show a small lapse at all times of the year; there is a lapse in summer months and an inversion in winter months, the annual mean being almost isothermal. The winter month inversion is probably due to the presence of the sea which is warmer than the land. The warm air from the sea will, for certain wind directions, ascend over the cold air over the land at a small angle of say 1/200 and will affect the temperatures inland above a height of 100 ft. or 30m; there will be no marked frontal effect owing to mixing.

4. Lapse Rates on Clear and Overcast Days

In this section it is proposed to examine the effect which the state of the sky produces upon the lapse rate in a similar manner to the investigations in GM.46 and GM.77. A departure from the selection of data made in those publications is made in order that a larger number of cases may be included in each category. The criterion for a clear day remains as continuous or almost continuous traces on the sunshine recorder and night sky camera over the 24 hour period from midnight to midnight. For an overcast day a complete absence of trace on both recorders has been required. In addition the conditions for the six hours (instead of twelve, as for Porton and Leafield) preceding the 24-hour period in question were required to conform to the appropriate criterion. The definition of summer days was extended to include the months July and August as well as June, while that of winter days was extended to include January and February as well as December. The criteria for a strict set of conditions and the extension of the meaning of summer and winter days still yields only very few cases of overcast days in summer and clear days in winter. The observations used in the compilation of tables and curves for clear and overcast days relate to the occasions which are tabulated in Part I, Section 4.

/Table III

Table III gives the mean hourly values of the temperature differences over the three height intervals for clear and overcast days in summer and winter and Figure 2 shows the graphical representation.

Table IV gives the wind velocity for each of the groups of observations as measured on the Dines Pressure Tube Anemograph at a height 12.7m.

On clear days in summer the maximum lapse over interval X is - 2.1°F, occurring at 1200, while that over interval Z is - 4.2°F occurring at 1100 and 1200. From the mean curves for summer months the corresponding maximum lapses are - 1.6°F at 1200 in August and - 3.5°F at 1200 in August. The inversion maxima over X and Z for clear nights in summer are +2.6°F at 0200 and +8.1°F at 0400, while the mean curves for the three months give +1.9°F at 0100 in June and +3.6°F at 0100 and 0200 in June. The mean curves for the summer months and those for clear skies are similar with increased amplitudes in the latter set. The inversion is seen to build up more rapidly in the evening with clear skies. The figures quoted for lapses and inversions are similar to those in GM.77 except that the night inversions in the upper layers at Rye are greater than those at Leafield. This may be a reflection of the difference in site. It would be expected that there would be a greater tendency to drainage of cold air from the Leafield site, which would lower the ceiling of the night inversion and diminish the intensity of the inversion at the greater heights.

On clear days in the winter there is no lapse in interval X in the mid-day period; there is a minimum inversion of +0.2°F. The maximum lapse in interval Z is - 1.5°F at 1200 and 1300. The comparison figures for all states of the sky are -0.3°F and -1.8°F at 1300 in February. On clear winter days the maximum inversions are respectively +1.3°F at 2300 and 4.1°F at 0300 the comparable maxima for all states of the sky being +1.7°F and +2.4°F at 0400 in January. The number of clear days in winter is only three and we have not drawn any conclusions from such meagre data. Nevertheless an interesting point arose with regard to the three clear days examined. There was snow cover on only one of these days, 25th February, 1948 and on this day only was there a lapse of temperature in interval X in the mid-day period. The air stream was from the East and over Europe was very cold near the surface combined with a strong surface inversion which inhibited turbulent transfer. On passing over the much warmer surface in England (and over the sea) a lapse of temperature was set up. On both the other occasions the air passing over Rye, from the South West, was warmer at the surface although there was a strong surface inversion, and this led to a persistence of the inversion.

Turning to overcast days, in summer the maximum lapses in the two layers we are considering, are -1.2°F and -2.9°F at 1100, the comparable lapse rates for all states of the sky being -1.6°F and -3.5°F as given above. The maximum inversions are +0.1°F and +1.1°F. These figures show the small variations of temperature on overcast days compared with those on mean days and, of course, with those on clear days. In winter the maximum lapses are -0.0°F and -1.4°F about mid-day; there is a maximum inversion of 0.4°F in interval X and a minimum lapse of -0.3°F in interval Z. On overcast days in winter the temperature variations are small, as is easily seen in fig. 2. It will be noted that above 15.2m there is always a mean lapse of temperature on overcast days in winter.

These conclusions from the Rye data serve to bear out those made by Johnson and Heywood from the Leafield data.

5. Maximum values of the Lapse Rate

From the hourly values of the temperature differences over the three height intervals the largest hourly values of both lapses and inversions occurring during each month have been extracted. These values are given in

/Tables

Tables V and VI together with the hour and date of occurrence, the state of the sky and the wind velocity at 12.7m.

(a) Maximum Lapses

During the three years in which observations were recorded the greatest lapse between 1.1m and 15.2m was - 5.2°F, between 15.2m and 47.2m was -5.0°F and between 47.2m and 106.7m was -4.5°F. They occurred in May, June and May respectively and represent 20 times, 8.7 and 4.2 times the dry adiabatic lapse rate. The maximum December lapses over the same three intervals were -2.5°F, -1.6°F and -2.2°F or 10, 2.8 and 2.1 times the adiabatic lapse rate.

The maximum lapses occur in the lowest layer about noon; of the 40 recorded maxima set out in Table V (on five occasions the maximum for a given month occurred twice) 26 were between 1100 and 1300. In the interval 15.2m to 47.2m although the maximum lapse is still most frequent about mid-day there is a wider dispersion in time of occurrence and in the interval 47.2m to 106.7m the dispersion is more marked, the maximum lapse occurring as late as 2400 in December.

As regards the state of the sky, in the lowest layer the maximum lapse occurs mainly with clear skies or broken cloud, although one example of the maximum lapse occurring in a thunderstorm is noted in June 1947. In the upper layers however the maximum lapse occurs more frequently with cloudy conditions than it does in the lowest layer.

The mean values of the wind speeds (at 12.7m) on occasions of maximum lapse are 3.5, 5 and 4m.sec^{-1} respectively for the layers X, Y, Z. On some occasions of maximum lapse in the two upper layers the wind speed was 10 - 14 m.sec^{-1} (at 12.7m.).

(b) Maximum Inversions

During the three years of observation the maximum inversions in the layers 1.1m to 15.2m, 15.2m to 47.2m and 47.2m to 106.7m were 13.6°F, 14.8°F and 14.5°F respectively, the months of occurrence being January, 1947, September, 1946 and February, 1947.

Inversion extremes occur at all times of the night in the lowest layer; out of 38 readings 17 occurred after midnight. In the middle layer out of 44 readings only 8 occurred at or before midnight and 19 occurred at or before 0300; in the top layer out of 39 readings only 9 occurred at or before midnight while 17 occurred at or after 0500. These figures are indicative of the upward growth of the nocturnal inversion.

The sky is almost always clear or only partially clouded at the time of the maximum inversion in the layer 1.1m to 15.2m; the same is true of the middle layer except that fog is occasionally reported and the frequency of fog at the time of maximum inversion in the upper layer increases. This agrees with the general physical picture that we envisage in the building up of the nocturnal inversion, the inversion in upper layers often reaching its maximum when the lower layers are already sufficiently cooled for fog to form.

The wind velocity at the time of maximum inversion is invariably small, the mean wind measured in the lowest layer at the times of occurrence in the three layers starting at the lowest, being 0.6m/sec, 0.8m/sec, and 1.4m/sec.

/(c)

(c) An Exceptional Inversion

It is noticed that in Table VI all the maximum inversions for February 1947 fall on the same day. We have therefore considered 24th February, 1947 in rather more detail. The general synoptic situation shows a high pressure system centred over France. Rye being in the North west of the anticyclone. A light wind not exceeding 2.5m.sec^{-1} from the north east was recorded during the day. There was a blue sky with slight haze, the visibility being about 7,000m. The snow depth was rather less than four inches. These conditions are ideal for the formation of a large inversion near the ground, for it is well known that the fall of temperature at the surface consequent upon the nocturnal radiation is enhanced by the presence of snow cover, clear skies and slight wind. The temperatures recorded in the first twelve hours of the day are given in Table VII.

It is seen from the table that the temperatures at three of the heights reach their minimum value at about the same time, 0700. At this time the inversion from 1.1m to 47.2m was a maximum, but the maximum inversion from 1.1m to 106.7m occurred later than 0900, while the maximum inversion from 1.1m to 15.2m occurred earlier at 0200. The early time of occurrence of the maximum inversion layer X can be explained in terms of heat transport. The nocturnal radiation draws its heat supply from both the earth and the atmosphere above. In the early stages before heat diffuses downwards sufficiently rapidly the surface temperature falls quickly and sets up a strong inversion from the surface upwards. As the temperature further falls the contribution from the air makes itself felt more and the inversion near the surface decreases while that in the layer Y is increased. Even after sunrise when the surface temperatures are rising heat is being diffused downwards more rapidly from above thus increasing the inversion in the upper layer Z. This is plain from the table for the increase of temperature at 1.1m from 0700 to 0900 is 6.3°F while that at 106.7m is 11.2°F.

6. Frequency of Occurrence of Lapse Rates of Various Magnitudes

The hourly values of the temperature differences between the levels 1.1m to 15.2m, 15.2m to 47.2m and 47.2m to 106.7m during the three years have been analysed to show the frequency of occurrence of temperature differences of given magnitude. Table VIII shows the monthly frequencies of temperature differences between the stated limits expressed as percentages of the total number of hourly readings.

In the interval 1.1m to 15.2m it will be seen that the maximum frequencies, all lie in one of the two ranges (-0.1 to -1.0) and (0.0 to 0.9), their general distribution follows that in the interval 1.2m to 12.4m of GM.77. The layer between 47.2m and 106.7m is similarly in agreement with the Leafield results for the layer 57.4m to 87.7m, while the intermediate layer 15.2m to 47.2m generally leans to the distribution in the upper layer at Leafield.

The average frequencies for the year are given in Table VIII and plotted in the form of an ogive in Figure 3*. The co-ordinates in the ogive are lapse rate in °F/m and percentage frequency with which the lapse rate is exceeded. Any ogive thus takes all ordinate values between 0 and 100; we have drawn the central part on a large scale and all the curves become zero to the left and 100 to the right. The three curves are thus represented on one diagram and can be compared directly. The frequency of large lapses near the ground is much greater than at the other levels, as is the frequency of large inversions. It is also true that the frequency of large lapses and inversions is greater in the middle layer than it is in the top layer.

* See Appendix I.

/8.

7. Mean Diurnal Variation at Each Height

(a) Three Year Means

Table IX gives the mean hourly values of the aspirated dry bulb element at 1.1m; the mean hourly values in this case were obtained in the same way as for the differential temperature charts. Curves showing the actual temperatures for the four heights 1.1m, 15.2m, 47.2m and 106.7m are shown in Figure 4, the values being obtained by using Table I and Table IX.

The curves are similar to those of GM.77, and the features noted in that publication are substantiated by the present results from Rye. An interesting feature not noted before is the small maximum about midnight, noticeable in the January curve. This feature has a corresponding minimum in the inversion of temperature as can be seen in fugure 1. It is perhaps difficult to assert whether this is a real effect in the physical sense or an oddity of the curves for the three years in question. We make no attempt to deal with small irregularities in the observations which are shown up on the curves.

The times of occurrence of maximum temperature at each height have been determined by the accurate plotting of the temperature observation on an open scale. The results for June and December are shown in the upper part of Table XI together with the lag in the time of maximum over each interval of height. The figures in rounded brackets are the time lags in minutes. The flatness of the December curves in the region of the maximum introduces uncertainties; in June certain of the points do not lie on a smooth curve and so permit alternative curve constructions and consequent uncertainty in the time of occurrence of a maximum. In June the time of occurrence of maximum temperature at 1.1m is 1414, at 106.7m is 1528 so that the lag is 74 minutes which is comparable with the lag of 85 minutes found at Leafield over the interval 1.2m to 87.7m. In December the lag is 42 minutes, the maximum near the ground occurring 50 minutes before that in June, which is comparable with the relevant figures of GM.77. In general the time estimations are too unreliable to draw firm conclusions for the intermediate levels.

(b) Means for Clear and Overcast Days

The temperatures at the four heights have been plotted in Figure 5 for clear and overcast days in summer and in winter in the same way as the mean temperature curves considered in (a), the basic data being provided by Table III and Table X which gives the mean hourly values of the aspirated dry bulb temperature at 1.1m.

On clear days the morning minima occur at about the same time at sunrise, the minimum at the level 1.1m occurring earlier by between one-half and one hour. On overcast days in summer the morning minimum at 1.2m occurs before sunrise and the minima at higher levels occur later according to height, that at 106.7m occurring about two hours after sunrise. In winter on overcast days the temperature variation at all levels is small and the maxima and minima are so flat that precision of timing is not possible. It will be seen that the maximum temperatures at 1.1m and at 15.2m, are the same.

The curves and tables show that on the average clear summer day the temperature at the end of the 24 hour period exceeds that at the beginning by 1.6°F. On clear days in December there is a gain in temperature over the 24 hour period of 0.6°F compared with the loss quoted in GM.77.

The times of occurrence of maximum temperature have been determined and are shown in the lower part of Table XI. On clear summer days the maximum occurs at 1.1m at 1410 which is practically the same time as for mean June days, while at 106.7m the maximum occurs at 1512, the lag being 62 minutes which is rather less than on a mean June day, in contradistinction to the

/result

result found in GM.77. On clear winter days the maximum temperature at 1.1m occurs at 1336 and the lag at 106.7m is 87 minutes compared with 42 minutes on the mean December day. On clear summer days the greatest portion of the lag occurs between 1.1m and 15.2m but on clear days in winter the greatest lag is between 15.2m and 47.2m.

(c) Diurnal Range of Temperature

The mean diurnal range of temperature for each height in each month, and also the mean diurnal range for clear and overcast days in summer and winter are given in Table XII. The range is greatest in summer and least in the winter. On clear summer days the range is greatly increased at all levels being about twice that of the mean range. On overcast winter days the mean diurnal range is small at all levels.

8. The Effect of Snow Cover

In order to consider the effect of snow cover on the gradient of temperature we have extracted and meaned the data for days when there was a complete cover throughout the 24 hours and predominantly the snow was not melting. There were 15 such days viz. 16 - 17 December, 1946, 25 - 28 and 30 - 31 January, 1947 and 22 - 25 February, 1947 and 20 - 21 February, 1948; out of the 360 hourly readings there are only seven at which the temperature recorded at 1.1m exceeded 32°F and there were no occasions upon which the snow remained unfrozen throughout the 24 hours. The results are given in Table XIII and have been plotted in Figure 6 which show in Figure 6(a) the diurnal variation of temperature lapses over the three intervals X, Y, Z, and in 6(b) the diurnal variation of temperature at 1.1m and 106.7m.

In the interval X the inversion is strengthened by the presence of snow covering the earth, the maximum inversion being 2.3°F compared with the February maximum of 1.7°F. The maximum inversion in the interval Z is little changed however, being 2.7°F compared with the January maximum of 2.4°F. The times of occurrence of these maximum lapses is a little earlier than those for all states of the ground. There is a mean lapse in interval X at only one hour, 1400, when there is snow cover. In this respect the results follow those of the mean January results, in which there is no lapse recorded. The maximum lapse in the Z interval is -1.7°F at 1400 which is rather less than the maximum lapse of -1.8°F at 1300 in February.

Turning to the actual temperatures at 1.1m the maximum temperature occurs at 1400, the same time as for all states of the ground; the minimum temperature occurs at 0200 which is earlier than for all states of the ground, when the minimum occurs about dawn. We can explain this on considering the heat flow to the surface, which is compounded of heat flow in the air and in the ground itself. The temperature at the surface must be such that the heat lost, mainly by radiation, balances the heat reaching the surface. The rate of loss of heat from the surface by radiation is substantially constant, being proportional to the fourth power of the absolute temperature, whereas the rate of supply increases as the surface temperature falls and sets up a larger temperature gradient near the surface. Often the temperature gradients in the earth and air are too small to prevent the temperature continuing to fall until insolation is effective. With snow cover there is a rather more rapid fall of temperature at the surface combined with an originally lower temperature at sunset; the net result is that the temperature gradient in the ground is enhanced and the equilibrium reached more quickly after which the temperature falls no further. This explanation is idealised but accounts for the main physical effects occurring at the surface. The minimum temperatures at levels near the surface correspondingly occur earlier.

/PART III

PART III

The Humidity Records

All humidities are expressed in milligrams water vapour per cubic metre; as in the case of the temperature records Greenwich Mean Time is used throughout. Hourly values were computed from hourly values of temperature and relative humidity for the three years, the value allotted to each hour being the mean value of the humidity over a period of 20 minutes centred on the hour in question. The humidity differences constructed from these reading are taken as positive when humidity increases with height and negative when it decreases upward. The former of these conditions is termed an inversion, the latter a lapse, agreeing with the terminology used in presenting the temperature records.

2. Mean Hourly Values and Diurnal Variation of Humidity Lapse Rate

The mean hourly values of humidity differences over the three height intervals, X from 1.1m to 15.2m, Y from 1.1m to 47.2m, Z from 1.1m to 106.7m, for each month are given in Table XIV. These values have been plotted in two ways.

In Figure 7 they are plotted to shew the mean variation of humidity with height for each hour. Taking the curves as a whole the most obvious feature is the rapid decrease of gradient with height; the largest variations occur in the lower layers which are nearest to the boundary surface between earth and atmosphere. In the upper layers there is usually a fairly constant mean gradient, generally a lapse.

During the middle of the day there is a humidity lapse near the surface in all months. In the summer months this lapse is much greater than in the winter months; at midday over the interval X the mean lapse for December and January is -120 mgm/cu.m., whereas the mean for June and July is -680 mgm/cu.m or rather more than five times the winter lapse. In the layer from 15.2m to 47.2m. the similar means are -105 mgm/cu.m and -390 mgm/cu.m. so that the summer lapse is about four times as great as the winter lapse. As we have already seen the temperature curves similarly shew a greater lapse near the surface in summer than in winter. At the lower winter temperatures the humidity lapse rate is less for saturated air than in summer, when temperatures are higher, for the same temperature difference, e.g. if the temperature at the 1.1m. level is 42°F and that at 15.2m. is 40°F then the humidity gradient is only about half that if the temperatures are 62°F and 60°F. There exists a potentially greater lapse in summer than in winter, even when the temperature lapses are the same. In summer at midday the turbulent convection processes carry away the moisture more readily than they do in winter which again tends to greater humidity lapses in summer than in winter.

Figure 7 also shews the general humidity structure throughout the day. In January there is an inversion of humidity near the surface at the beginning of the day. This inversion of humidity is broken down after sunrise to give way to a lapse which in its turn is broken down and an inversion is reformed during the afternoon and persists until midnight. These features are repeated in all months with the period in which there is a lapse of humidity gradually lengthening as the summer is approached. In June the humidity inversion in the night period is not at all well marked. In the autumn months the reverse series of events takes place, the lapse period gradually shortening.

The October, November and December curves are worth noting. In part of the period when there is a lapse near the surface they shew a different structure in the middle layer from that of other months; there is an inversion of humidity or greatly reduced lapse of humidity above the lapse near the surface. There is no parallel feature in the temperature records.

/The

The distribution of humidity in the vertical depends largely upon two factors, diffusion by turbulent processes and advection. When measurements are made at a single site it is difficult to deal with advection, since we have no comparable measurements in the direction from which the air is coming. We may concentrate upon diffusion in attempting to explain points arising from the experimental results, at least in the lowest layers, since for the most part the immediately surrounding country is not dissimilar from that at the site and we may expect a horizontal uniformity in the structure of the atmosphere.

A notable exception may arise when there is an onshore wind; advection may well need accounting for then if the turbulence is insufficient for the effects from the new boundary conditions to spread through the layer up to the top of the tower by the time the air reaches the observation site. The turbulent structure in the atmosphere depends upon many factors, including the thermal structure of the atmosphere.

We must also bear in mind the limitation of the saturation vapour density at a given temperature. This is particularly important near the ground which is often the source of moisture during the day when evaporation takes place. For example, in March at 1200 the mean temperature at 1.1m is 47.5°F, in October 56.9°F. The ratio of the saturated vapour densities at these temperatures is about 1:1.4. We may expect the mean vapour density in March to be less than in October; it is, in fact, and in the ratio 1:1.4 which means that the relative humidities are about the same for both months.

To return to the profiles for October, November and December, we first point out that investigation shewed that in cases of onshore winds the mean humidity profile shewed a general lapse and the vapour densities were greater than in the cases of offshore winds. Details are given in Table XIV A. of the humidity records at 1500 for October. In cases of offshore winds the mean humidity profile evidences the small inversion in the middle layers. A possible explanation may be found in the relatively greater supply of moisture which may be expected from the surface in the last three months of the year, compared with that in the first three months. The moisture supply is dependent upon the temperature of the air near the surface. With higher temperatures there is greater evaporation and a correspondingly greater supply of moisture from the surface, and the mean temperatures are greater in December than January, November than February and October than March. The feature we are investigating is most marked in October and we compare October and March, when the difference of mean temperature is the greatest. We may expect more moisture to be transferred upwards near the ground owing to the greater supply. If however the rate of diffusion is much the same in both months in the upper levels there will be a greater tendency to accumulate moisture in the middle levels in October than in March, which will result in a much less steep lapse in the middle layers and a steeper lapse in the top layers in October, as is found.

Figure 8 displays the data of Table XIV in a different manner shewing the diurnal variation of lapse rate from 1.1m. upwards for each month. In January in the interval X an inversion of humidity predominates. At midnight there is an inversion of about 150 mgm/cu.m which rises to a maximum at 0400 and then falls fairly steadily until at about two hours after sunrise the inversion changes over to a lapse. The maximum lapse occurs some hours after sunrise and there is a secondary maximum, usually much smaller; later in the afternoon after which the lapse decreases steadily until at about sunset the lapse changes over to an inversion which generally increases steadily in magnitude until after sunset, and thereafter remains fairly constant. The sequence of changes described for the interval X is repeated in all other months although the time of change over from inversion to lapse and vice versa bears no well defined relation to the time of sunrise and sunset. As the year proceeds lapses increase in magnitude and the daytime period of lapse increases until in June the inversion is ill defined and short lived, a lapse

/predominating.

predominating. The double maxima become marked and in August there are three distinct maxima. The time of the first maximum lapse comes earlier until in May, June and July it is approximately at 0700. In the autumn the reverse series of events takes place, the duration of the lapse period decreasing.

The general features of the night inversion and day lapse are explained by the cooling and extraction of moisture by the deposition of dew during the night, followed by the heating and evaporation during the day and the setting up of a turbulent regime. We will treat the question of double maxima later.

Over the interval Z in January the mean lapse persists over a much longer period than does that in interval X. The curves in Figure 7 shew that this is not generally true. In March, April, October, November and December the lapse occurs over much the same period for the two intervals, while in the remaining months the period of inversion is very short, being non-existent in June.

Apart from the first two months of the year the change over from inversion to lapse after sunrise occurs almost simultaneously in all three intervals, so that the atmosphere is approximately isohydral. The same is not true of the change over from lapse to inversion, so that in the evening there is no time when the atmosphere is isohydral.

Another feature of the curves of figure 8 is the correlation between the shapes for any given month. The time co-ordinates of the maxima and minima are nearly the same for the three curves, so that the maximum lapse, for example, occurs at nearly the same time for each of the intervals X, Y and Z. We may trace this to the same agency acting at all levels. This feature, of course, was noticed in the case of temperature, and in GM.77 use was made of the fact in order to elicit information about the turbulent structure in the lowest levels.

We may remark in passing on the occurrence at night in some months of double night maxima of inversions. The differences are not great and probably may be traced to the variation in cloud cover. When the sky clears there is a tendency for the inversions to increase owing to the cooling near the ground; when the sky becomes overcast there is a reverse tendency. The net average effect may well be to produce local small maxima.

3. Mean Monthly and Yearly Values of the Lapse Rate

The hourly values of the humidity differences given in Table XIV have been meaned by months and the results are given in Table XV.

It will be seen that except in January, March, October and December the average humidity structure in the lowest layer is a lapse; of the exceptional months October and December shew small inversions and the last three months of the year can be said to have zero humidity gradient. January and March have, on the other hand, appreciable inversions. Over the height interval 15.2m. to 47.2m. there is a lapse excepting for the last three months of the year and in March and April when the layer is isohydral. The tendency to form an inversion in the last three months of the year in the middle layer during the day has already been noted and is reflected in the appreciable figures for the whole month. The lapses over this height interval and also over interval X are greatest in the summer months.

Over the height interval from 47.2m. to 106.7m. there is a general lapse with the exception of may and June. These lapses are greatest in late summer and early autumn and least in late spring and early summer.

The mean annual lapse rate is entered at the foot of Table XV. For the three years under consideration the average humidity structure was a lapse at all heights.

/4.

4. Lapse Rates on Clear and Overcast Days

In this section it is proposed to examine the effect which the state of the sky produces upon the lapse rate of humidity. The criteria for clear and overcast days has already been given in Part II§4 and the following observations of humidity correspond to the same days for which the temperature observations were given in Table III and the wind observations in Table IV. The mean hourly observations of humidity difference are given in Table XVI and plotted in Figure 9.

On clear days in summer the maximum inversion of humidity over the interval X is 770 mgm./cu.m. while the maximum inversion from the mean monthly curves is 410 mgm./cu.m; both these maxima occur at 0400. The maximum lapse on clear days in this interval is -920 mgm./cu.m., that from the mean curves -860 mgm./cu.m., both occurring at 0800. Hence the rate of change of lapse rate on clear days is -1690 mgm./cu.m/4 hrs.; for all states of the sky it is -890 mgm./cu.m/4 hrs. in July. (The maximum inversion and maximum lapse (for all states of the sky) do not occur in the same month). In the evening the change from lapse to inversion occurs on clear days after 2000 and the magnitude of the change from 1900 to 2200 is 630 mgm./cu.m/3 hrs., while the maximum change for all states of the sky occurs in July at about the same time, the change being 470 mgm./cu.m/3 hrs. In the interval X the curves for clear days and for all states of the sky are much the same in general shape with the clear day amplitudes and slopes magnified. In the interval Z the period of inversion on clear days is from about 0100 to 0500, longer than in any of the three summer months for all states of the sky. The magnitude of the inversion +800 mgm./cu.m. is eight times that of the maximum inversion occurring at 0400 in July. The maximum lapse, -1770 mgm./cu.m. exceeds that for all states of the sky, -1310 mgm./cu.m. occurring in August. The change from inversion to lapse is -2570 mgm./cu.m/3 hrs. In interval Z the amplitudes and slopes of the curves are again increased on clear days compared with those for all states of the sky.

It is interesting to consider the layers 15.2m to 47.2m., and 47.2m. to 106.7m. In the former there is a maximum inversion of 220 mgm./cu.m., compared with 90 mgm./cu.m., for all states of the sky, while the comparative maximum lapse figures are respectively -730 and -520mgm./cu.m. In the latter there is always a lapse on clear days, ranging from -100 to -480 mgm./cu.m. whereas for all states of the sky there is a maximum inversion of 70 mgm./cu.m. at 2300 in June and a maximum lapse of -360 mgm./cu.m. at 1900 in August.

Turning to clear days in winter there is a predominant inversion in interval X with only a slight lapse at 1100. This is a reflection in humidity of the slight temperature inversion noted in Part II § 4. The maximum inversion is 500 mgm./cu.m. which is about 2/3 that for clear summer days and about double that for all states of the sky at 0400 in January. In interval Z the maximum lapse is almost -600 mgm./cu.m. compared with a maximum for all states of the sky of -410 mgm./cu.m. at 1200 in January and a maximum inversion of 200 mgm./cu.m. compared with a maximum for all states of the sky of 270 mgm./cu.m. in December. As there are only three examples of clear days in winter it would be unsafe to draw any conclusions to be regarded as firm.

On overcast days in summer it is noticeable that there is a persistant lapse of humidity in interval X, with a maximum of -330 mgm./cu.m., corresponding to the normal thermal structure in overcast conditions, the maximum inversion corresponding to the inversions of temperature, and the minimum inversions with the midday temperature lapses. The damping of the amplitude of humidity gradient corresponds, of course, to the small temperature changes in this interval and below, and a diminishing of the variations in evaporation at the surface. There is sometimes little turbulence on such days which indicates a tendency for gradients to persist. In the intervals Y and Z

/there

there is also a persistent lapse of humidity, the maxima and minima being -160 mgm./cu.m. and -770 mgm./cu.m., -410 and -1130 mgm./cu.m. respectively; the range in which the humidity lies is thus less than for all states of the sky and hance than on clear days. Turning to the interval 15.2m to 47.2m. there is a persistent lapse of humidity from -40 to -590 mgm./cu.m. which is to be compared with a maximum inversion of 220 mgm./cu.m. on clear days and 90 mgm./cu.m. on all occasions and a maximum lapse of -730 mgm./cu.m. on clear days and -520 mgm./cu.m. on all occasions. The maximum inversion of 590 mgm./cu.m. on overcast days is exceptional and on a whole the overcast day curve in this interval has a smaller amplitude than that for either clear days or that for all states of the sky. It will be remembered that there are only four cases of overcast summer days, too few to form reliable opinions.

On overcast days in winter there is an almost universal lapse of humidity; the smallness of the lapse gradients is remarkable, just as in the corresponding temperature curves.

5. Maximum Values of the Lapse Rate of Humidity

From the hourly analysis of the humidity differences over the three height intervals the largest hourly values of both lapses and inversions occurring during each month have been extracted. These values are given in Tables XVII and XVIII together with the date and time, the state of the sky and the wind velocity at 12.7m.

(a) Maximum lapses

During the three years the greatest hourly lapses in the three intervals 1.1m. to 15.2m., 15.2m. to 47.2m. and 47.2m. to 106.7m. were respectively -5750 mgm./cu.m. in May 1947, -4200 mgm./cu.m. in November 1947 and -4480 mgm./cu.m. in October 1947. It is interesting to note the months in which these lapses occur for the corresponding maximum temperature lapses occurred in May or June. There is also a marked variation in lapses from year to year. In the lowest layer there are four maximum lapses exceeding -3000 mgm./cu.m., three occurring in May, June and August 1947 and one in June 1948. In the middle layer there are again four lapses exceeding -3000 mgm./cu.m. in May, August, October and November 1947. In the top layer there are ten lapses exceeding -3000 mgm./cu.m. three occurring in 1946, five in 1947 and two in 1948. The figure -3000 mgm./cu.m. taken here as critical has no physical significance as a criterion; also, there is a half year of 1945 and of 1948 in the observations, so that certain months are missing that might have contributed to the number of cases exceeding a lapse of -3000 mgm./cu.m. Nevertheless it seems that the three 12 monthly cycles, starting in July 1945, shew well marked differences in maximum lapses.

Reverting to a consideration of the lowest layer it is seen that, although clear or only partially cloudy skies are predominant, an overcast sky often does occur at the time of maximum lapse, in contradistinction to the conditions prevailing at the time of maximum lapses of temperature. The average wind velocity at the time of maximum lapse rate is a little over 3m/sec. while winds up to 9m/sec. are found.

In the middle layer the maximum lapse rate can occur with either overcast clear or partially clouded skies as in the lowest layer. Two points of special interest are worthy of note. Firstly in July 1946 the maximum lapse rate occurred in a thunderstorm with heavy rain and no wind. Secondly in October and November the maximum lapse rate occurred in the presence of fog. The average wind on occasions of maximum lapse is lighter than in the lowest layer, being a little over 2m./sec. and the wind range reaches only to 6.7m./sec. as compared with 8.9m/sec. in the layer beneath.

/In

In the top layer it is noted that the maximum lapse occurs much more frequently on clear or partially cloudy days and correspondingly less frequently on overcast days. There is also a greater number of occasions on which there is a calm at the time of maximum lapse, and the mean wind speed is only 1.5m./sec. The occasions of strong wind speeds are associated with comparatively small maximum lapses; we note in particular that of February 1946.

The times of occurrence of maximum lapse rate are of interest. We recall that an examination of the times of occurrence of the maximum lapse rate of temperature (Part II Sect.5) shewed that they were grouped about noon with the dispersion increasing with height. In the lowest layer the times of occurrence of maximum lapse rate of humidity are grouped about 0900, 16 of the 35 cases falling between 0800 and 1000 but there is a wider dispersion about the mean than in the case of temperature. In the second layer the times are grouped about 1100 with 13 of the 35 cases falling between 1000 and 1200 and with quite a wide dispersion; in the top layer there is little grouping at all and the maximum lapse rate occurs at almost any time of the day. Thus the expected time of occurrence of the maximum lapse rate of humidity is less definite than that of temperature.

Comparing the times of occurrence of the maximum lapse rate with the time of occurrence of the minimum in the curves of Figure 8 we see that there is fair agreement in many cases, as we might expect. In May and August 1947 the maximum lapse occurs at about the time of the second minimum in the curves of Figure 8, while in July the minimum is very flat and covers the period from 1000 to 1500. There are some wide divergences, which could not be explained except by detailed consideration of the situation at the time, notably in October 1945 and December 1946.

(b) Maximum Inversions

During the three years the maximum hourly inversions in the three layers were respectively 3130 mgm./cu.m. in October 1947, 3610 mgm./cu.m. in September 1946 and 3300 mgm./cu.m. in May 1947. It should be noted that these values are of the same order as the maximum lapse values, being about 2/3 of them. In the lowest layer there are four monthly maxima exceeding 2500 mgm./cu.m., three of them occurring in July, September and October 1947 and one in October 1945. In the middle layer there are five occasions upon which the arbitrary figure is surpassed, three in May, June and October 1947, one in September 1946 and one in October 1945. In the top layer there are three occasions, in May and October 1947, and in April 1948. We may conclude that 1947 shewed greater inversions than 1946, just as we concluded that it shewed greater lapses.

Consider now the state of the sky and the wind velocity at times of maximum inversion. It is immediately seen from the table that in the first layer there is very frequently a clear or only partially clouded sky with maximum inversion, and that when the sky is clouded the maximum inversion is generally small. It is interesting to note that fog is reported several times. The mean wind velocity accompanying maximum inversions is only about 1m./sec. and many calms are reported. The upper two layers shew mainly the same characteristics with wind velocities less than 2 m./sec., and we may expect maximum inversions to occur with light winds and clear or only partially clouded skies, although once, in January 1947, rain and cloud were reported.

The times of occurrence of maximum inversions are also of interest. In the lowest layer the times are grouped about 0100, 15 of the cases falling in the period 2400 to 0200; in the middle layer the times are grouped about 0500, 19 of the cases falling in the period 0300 to 0700.

/There

There is a wider scatter in the top layer, the most favoured times being 0100 and 0200. The maxima of the curves in Figure 8 cover quite an appreciable period, not being well defined like the minima, and it is difficult to compare the times of maxima for the months with the curve maxima. Nevertheless some of the maxima in Table XVIII occur when the monthly mean curves shew a maximum lapse; such indivdual cases would need special scrutiny with regard to the prevailing conditions.

6. Frequency of Occurrence of Lapse Rates of Various Magnitudes

The hourly values of humidity difference over the height intervals 1.1m. to 15.2m., 15.2m. to 47.2m. and 47.2m. to 106.7m. during the three years have been analysed to shew the frequency of occurrence of humidity differences of various magnitudes. Table XIX shews the monthly frequencies of humidity differences between the stated limits, expressed as a percentage of the total number of hourly readings.

Considering the lowest layer, in November, December and January the maximum frequency lies between -10 and -100 mgm./cu.m. which is, of course, a lapse. In February and March the maximum frequency lies between 0 and 90 mgm./cu.m. In the remainder of the months, except for May, the maximum frequency lies in the lapse region; in May we notice that the frequencies in the contiguous regions 0 to 90, -10 to -100 and -110 to -200 mgm./cu.m. are all much the same. so that a very slight change enables one to fit May into the general scheme having maximum frequency lying in the lapse region, except for February and March. In the case of February it is noticeable that the maximum is not sharp on the lapse side, but in March it is sharper on the lapse side than it is on the inversion side.

In the layer from 15.2m. to 47.2m. the maximum frequency for all months, except February, April and November, lies in the lapse region. In the layer 47.2m. to 106.7m. the maximum frequency for all months except, May and November, lies in the lapse region. It is worthy of note that when the maximum frequency lies in the inversion region it is always in the interval 0 to 90 mgm./cu.m.

The average frequencies for the year are also listed in Table XIX and are plotted in Figure 10.

The curves shew that great lapses and great inversions, expressed in mgm./cu.m/m., are much more frequent in the lowest layer, and least frequent in the upper layer, while the frequency of lapses and inversions near the isohydral state is greatest in the top layer and least in the lowest layer.

7. Mean Diurnal Variation of Humidity

The mean hourly values of the humidity at 1.1m. are given in Table XX, the hourly mean being found by the same method of averaging as used for all other charts. By using Table XIV we can construct the mean hourly values at the other three levels. The data are plotted in Figure 11.

A point worthy of notice is that the humidity is greater in summer than in winter, largely owing to the fact that the saturated vapour pressure at winter temperatures is less than at summer temperatures. At 60°F the saturated vapour pressure is about twice that at 40°F. There is also potentially a greater supply of moisture by evaporation at the highor summer temperatures. A second point to be noticed is the general similarity in the shape of the four curves for any given month; in particular the maxima and minima occur at much the same time within the accuracy of timing and gradient maxima are therefore not due to changes at any one level while the other levels remain roughly constant in humidity.

/A

A feature of all the curves, with few exceptions, is a distinct minimum in the dawn period when the temperature curves also shew a minimum and the saturated vapour pressure is a minimum. After dawn the humidity rises sharply to a maximum about midday in winter, but advancing in time as the summer is approached so that the maximum occurs as early as 0700 - 0800 in June. The humidity then falls but rises again to a second maximum in the midday period; this second maximum is not noticeable in winter, when it is masked by the first maximum, but is quite marked in summer, when more than one local maximum can be found. The explanation of the double maxima lies in the role that turbulence plays in redistributing the moisture content of the air. After dawn there is evaporation at the surface owing to the temperature rise caused by insolation and the humidity rises at all levels, the diffusing agency being slight turbulence. As the morning proceeds turbulence increases and carried away moisture from the lower atmosphere rather more quickly than it is supplied by evaporation, so that the net effect is a decrease in humidity. At midday the evaporation is a maximum at the surface, counter balancing the loss of water vapour carried upward by turbulence and shortly after midday there is a second maximum. In the afternoon both evaporation and turbulence decrease, but the turbulence acts through a deeper layer than that in which the readings were taken and the humidity decreases. Secondary maxima later are probably due to water vapour being diffused downwards, from a humidity inversion above, as the temperature falls and condensation takes place at the ground level.

The humidities at the four heights have been obtained for clear and overcast days in summer and in winter, and are given in Table XXI and plotted in Figure 12.

On clear days in summer we notice that at 1.1m. the maximum humidity is about 12600 mgm./cu.m., occurring at 0800, the corresponding maximum for all states of the sky being 11690 mgm./cu.m. in August. On overcast days the maximum is about 11000 mgm./cu.m. at 1700. The outstanding feature on clear days in summer is that there is no second maximum in the early afternoon which shews that on clear days the increased turbulence is more effectively transporting moisture upwards. There is a secondary maximum at 1.1m. at 1900.

A second feature worthy of note is that the vapour density increases on a clear summer day, being greater at the end of the day than at the beginning. The corresponding increase in temperature has already been noted in Part II § 7, and we may explain the humidity increase by remarking that the temperature increase allows some of the evaporated moisture to remain uncondensed at the end of the day. On overcast days in summer the reverse is true of temperature and humidity. Examination of the curves for clear winter and overcast summer days shews some erratic features which, in a statistic of such few cases, are dependent upon the smallness of the sample and probably have no physical significance.

On overcast winter days there is a small range of humidity with a flat minimum about dawn and a flat maximum a little after midday. The corresponding temperature curves shewed similar small variations.

The diurnal ranges of humidity at the four levels have been extracted and are given in Table XXII. We may remark that at all levels the diurnal range generally increases in the first eight months of the year and decreases again in the last four months. On clear days in summer the diurnal range is considerably enhanced, and on overcast days is rather greater except at 1.1m., compared with the range for all states of the sky. On clear winter days the diurnal range is greater at the lowest level, being half as great again as the range for all occasions. The diurnal range for overcast winter days is small.

/The

The times of occurrence of maximum humidity at various heights have been found and are tabulated in Table XXIII. There is little difference between the figures for mean June and for clear summer days, or between those for mean December and overcast winter days.

8. The Effect of Snow Cover

The data for humidity on those occasions when snow cover was present, as in Part II § 8, have been extracted and the hourly means are given in Table XXIV. The vapour density is small, as we might expect in view of the low temperatures. The inversions and lapses are small and there is a general lapse of humidity above 15.2m. The lapse in interval X extends from 1300 to 1600, and occurs later than on the mean winter days.

PART IV

The Structure of Radiation Fogs

The temperature structure in radiation fogs has been considered by Johnson and Heywood (2), and we are concerned here with expanding that account taking into consideration the humidity structure.

It will be appreciated that the experiments carried out at Rye were not primarily concerned with the structure of early morning fogs. No visual observations, such as observations of cloud visibility or depth of fog, were made at Rye between about 1800 and 0800 the next morning and the sole guide during this period is the record of the night sky camera. Since the incidence of radiation fog is often local it has been thought best not to use the observations of weather from nearby meteorological stations, for it cannot be

/ concluded

concluded that the weather conditions on nights of strong nocturnal cooling at a given station are representative of an area about it.

We have considered cases that satisfy two criteria. Firstly that the fog was caused by nocturnal cooling, eliminating those cases when the fog was probably due to advection or to advection and radiation combined. Secondly that fog was actually reported at Rye next morning when the first visual observations were made. In the summer many radiation fogs have cleared before 0800; the two criteria therefore bring under review more fogs in the autumn to spring period than in the summer period. On this count no statistics of the occurrence of radiation fogs are offered.

In considering the full records from the instruments during the period from before the formation of fog to after the dispersal, we have placed reliance upon the night - sky camera records to determine the time of onset of fog. The obscuration of Polaris has been taken to indicate the presence of fog, except in certain cases where obscuration has been transient and the relevant records of temperature and humidity have indicated that fog was not probable; in these cases it is probable that small amounts of cloud have temporarily obscured Polaris.

(a) The General Conclusions

As might be expected, individual fogs vary very considerably in detail. Having examined the cases we have drawn general conclusions as to the structure of radiation fogs. The temperature structure in a radiation fog has been described in GM.77 in some detail; the conclusions reached here agree in the main with those found in that publication. The conclusions drawn from the Rye data are:-

(1) Inside the fog the relative humidity is almost constant.

(2) Well below the fog top there is little gradient of temperature.

(3) Well below the fog top there is little gradient of vapour density.

(4) Across the top of the fog there is an inversion of temperature which is often large.

(5) Above the fog there may be quite dry air and a lapse of vapour density which may be quite large.

of these conclusions (3) follows from (1) and (2).

(b) The Sequence of Events

Before proceeding to illustrate the general conclusions by examples we remark first upon the sequence of events that normally takes place in the formation of fog. When the outgoing radiation at the earth's surface exceeds the incoming radiation the temperature commences to fall, and the temperature of the air above falls; at 1.1m. the temperature falls steadily. At the same time the vapour density at 1.1m. falls steadily. but in such a way that the relative humidity increases steadily. At some relative humidity, dependent upon the structure and constitution of the air, fog commences to form near the surface and to build upwards. During this period of temperature fall the temperature inversion builds up and at the same time the humidity inversion builds up. As the fog deepens the rate of fall of temperature at 1.1m. is retarded, as is the rate of fall of vapour density. This retardation of the rate of fall of temperature and vapour density occurs at successive levels as the fog

/depth

depth increases. After dawn the temperature and vapour density rise rapidly; while the temperature and humidity inversions, which have been breaking down in the lower parts of the fog commence to break down across the fog top and some time later the fog disperses. Figure 13 shews the trend of events for temperature and vapour density at the four levels; the data refer to 30 - 31st October, 1945. The times at which the various phenomena take place and the gradients formed vary from fog to fog and Figure 13 should not be taken as more than a general indication of the sequence of events.

(c) The Relative Humidity inside the Fog

The first general conclusion is that the relative humidity inside the fog is almost constant. We first note that at Rye it is not necessary for the relative humidity to be 100% for fog to form. Fogs are noted with relative humidities of as low as about 89%: it should be added that in cases of fog with low relative humidities it was often found that there was a northerly wind drift and undoubtedly part of the poor visibility was due to pollution from the industrial areas to the north.

In almost all the cases of fog that were examined it was found that after the fog commenced to form the relative humidity at 1.1m. shewed little variation usually with a slight increase. Moreover as the fog top became higher the relative humidities at successive levels also assumed this fairly constant value. An illustrative example is the fog of 30 - 31st October, 1945 and the relevant data are given below in Table XXVI.

Table XXVI. Data referring to the radiation fog of 30 - 31st October, 1945 at Rye

Hour	Relative Humidity %				Temp.	Temp. Differences			Humy.	Humidity Differences		
					°F	15.2m-	47.2m-	106.7-	mgm/m³	15.2-	47.2-	106.7-
GMT	1.1m	15.2m	47.2m	106.7m	1.1m	1.1m	15.2m	47.2m	1.1m	1.1m	15.2m	47.2m.
2000	82.0	83.0	81.0	75.0	41.7	+5.4	+2.5	+1.7	5740	+1400	+550	-120
2100	84.5	85.5	83.5	81.5	39.0	+6.8	+2.8	+1.5	5330	+1680	+590	+220
2200	83.0	85.5	84.5	79.5	38.6	+4.8	+4.1	+2.7	5230	+1180	+1030	+270
2300	92.0	91.5	89.5	84.5	38.0	+6.8	+2.4	+3.0	5610	+1620	+560	+410
2400	94.5	93.0	90.5	82.5	35.9	+4.4	+6.2	+3.0	5390	+710	+1390	+170
0100	94.5	94.0	90.5	86.5	34.6	+2.2	+8.8	+3.2	5100	+450	+1850	+560
0200	95.0	93.0	90.5	88.5	34.2	+0.1	+10.8	+2.6	5040	-110	+2310	+640
0300	95.0	94.5	92.0	87.5	34.0	+0.8	+10.6	+2.6	5010	0	+2340	+350
0400	94.5	93.5	90.5	86.0	33.0	+0.2	+12.6	+3.0	4770	0	+2660	+480
0500	91.5	93.5	89.5	86.5	33.5	0.0	+13.5	+2.8	4670	+150	+2880	+600
0600	91.5	93.5	85.0	85.5	32.9	-0.3	+15.7	+2.5	4620	+60	+2970	+810
0700	92.5	93.5	91.5	90.5	33.4	0.0	+10.7	+4.9	4720	+100	+2230	+1370
0800	93.5	93.5	92.5	92.0	35.9	-0.2	+7.8	+5.4	5330	-90	+1700	+1620
0900	94.0	94.5	93.5	93.5	39.0	+0.5	+6.5	+1.8	5920	+210	+1630	+560
1000	94.5	94.5	93.5	94.0	43.7	-0.6	+3.5	+0.6	7180	-190	+960	+300
1100	94.5	94.0	93.5	93.5	48.0	-0.5	+0.4	-0.1	8510	-240	+50	0
1200	95.0	95.0	95.0	94.5	50.2	-0.4	-0.4	-0.4	9220	-100	-190	-140
1300	94.0	96.0	92.0	92.0	54.0	-0.1	-0.6	-0.5	10430	+230	-720	-190
1400	82.0	86.5	81.5	82.5	55.9	-0.7	-0.3	-0.2	9760	+270	-660	+40
1500	67.0	65.5	70.5	69.5	55.1	+0.6	-0.4	-0.6	7700	+30	+450	-260

30.10.45 1500h. Weather b. Cloud tr. Cu.Ci. Vis. $6\frac{1}{4}$-$12\frac{1}{2}$ mi.

31.10.45 0900h. " f Sky obscured. " 200-500 yd.
09-1500h. " f,cm_o,b.
1500h. " b Cloud 1/10Cu.Sc. " $6\frac{1}{4}$-$12\frac{1}{2}$ mi.

Wind at 10 m. light variable throughout.

/We

We choose this example having used it for the figures illustrating the general sequence of events. The underlined values are those in which the elements were probably in fog although it may not have been as thick at the higher as at the lower elements. It is clear from the readings of relative humidity that the fog built upwards from the surface and that there is little variation in the relative humidity either vertically or in time once any element is engulfed.

(d) The Temperature inside and above the Fog.

Reverting to Table XXVI it is seen that while the fog was below the level 15.2m. there was a strong temperature inversion between the levels 1.1m. and 15.2m. As the fog deepened this inversion was broken down and after 0100 the gradient of temperature in this layer is quite small. As the fog deepened the temperature inversion in the layer 15.2m to 47.2m. increased rapidly but decreased again as the fog top approached 47.2m. As the decrease in this layer took place the inversion in the top layer increased, but at this stage the process is checked by insolation. The features noted here are repeated in many of the examples that have been examined, and the physical explanation is not far to seek. There is nocturnal radiation from the earth's surface; this sets up an inversion near the surface. In fog the radiation is absorbed and re-emitted both upward and downward with the effect that the radiative surface is virtually moved to some surface in the fog while the layer below is almost isothermal. There is, of course, cooling at all levels but the level near the fog top which is acting as the virtual radiative surface must cool most rapidly and hence the strong inversion measured is from the element somewhere below the fog top to that above the fog top. In this case before the strong inversion is completely transmitted to the layer between 47.2m and 106.7m. insolation after dawn halts the process. We see that the general conclusions (2) and (4) are capable of physical explanation.

(e) Humidity Structure in the Fog

Reverting again to Table XXVI we see that there is a strohg humidity inversion which breaks down near the surface as the fog deepens. At the same time the humidity inversion builds up in the next layer and finally in the top layer. In this case there is downward diffusion of water vapour and the vapour density at 106.7m. gradually increases through the night. The humidity inversion is through the fog top and the gradient of vapour density in the fog itself is small. On the other hand cases in which the air above the fog is dry and there is a lapse of humidity are quite common. An example is afforded by the fog of 6 - 7th October, 1947. A short representative extract from the data covering the middle period of the fog is given in Table XXVII.

Table XXVII. The Radiation Fog of 6 - 7th October, 1947

Hour	Values at stated heights R.H.				Humidity difference mgm./cu.m.		
	1.1m.	15.2m.	47.2m.	106.7m.	15.2-1.1m.	47.2-15.2m.	106.7-47.2m
2300	91.5	92.0	50	44.5	+1400	-3150	-210
2400	91.5	92.0	71	48.0	+1320	-870	-1850
0100	92.0	92.5	84	48.5	+1750	-10	-2850
0200	92.0	92.0	67	45.0	+1850	-1490	-1540
0300	92.5	91.5	63.5	47.5	+1400	-1370	-940

In this case the shallow fog did not extend much above 15.2m. There was therefore a temperature inversion between 1.1m. and 15.2m. and so with constant relative humidity an inversion of vapour density.

/This

This may well be concentrated in the upper portion of the fog. Above the fog there is a strong lapse of vapour density.

References.

(1) Johnson N.K. and Heywood G.S.P.

An Investigation of the Lapse Rate of Temperature in the Lowest Hundred Metres of the Atmosphere. 1938. Geophysical Memoir No.77. Meteorological Office, London.

(2) Johnson N.K.

A study of the Vertical Gradient of Temperature in the Atmosphere near the Ground. 1929. Geophysical Memoir No. 46. Meteorological Office, London.

(3) Cowling T.G. and White A. The Eddy Diffusivity and the Temperature of the Lower Layers of the Atmosphere. 1941 Quart. J.R. Met. Soc. 67 p.276.

/Appendix I

The Ogive

In a work that is closely modelled on GM.77 because it deals with very similar experimental results it may seem that some explanation is necessary for our departure in representing the frequency distributions graphically. We have preferrred to use the ogive rather than the more usual forms of representation because it has certain advantages.

Consider the method of setting up frequency curves from given data. We select an interval x_r, x_{r+1} of length δx_r and count the number of cases, n_r in which the experimental results fall in this interval; e.g. if x measures lapse rate we count the number of cases in which the lapse rate falls between two specified values. Thus n_r is a function of δx_r . In order that frequencies over intervals shall be directly comparable it is necessary that we choose the interval δx_r the same, say δx , over the whole stretch of x. The frequency curve is then constructed by taking n_r/N as ordinate at the centre of the interval x_r, x_{r+1} of length δx where $N = \sum n_r$ is the total number of observations.

The area under the frequency curve is

$$\sum \frac{n_r}{N} \delta x = \delta x \sum \frac{n_r}{N} = \delta x$$

Thus the frequency curve and the area under it are both dependent upon the dissection of the x-axis.

It is often not convenient to choose δx the same for <u>two</u> sets of data, but if we do not do so the frequency curves are not directly comparable. We seek therefore a form of curve which is independent of the dissection; such a curve, called the ogive, has as ordinate at x_r, $\sum n_r/N$ taken over the stretch to the left of x_r . This ordinate is obviously independent of the dissection and depends only on x_r . Denoting the ordinate by y, in the integral form we have

$$y = \frac{1}{N} \int_{-\infty}^{x_r} n.dx$$

and the integral is the limit of sums independent of the method of dissection. The derivative at x_r is

$$y' = n(x_r) / N$$

which is the frequency of distribution. Hence the relative frequencies of distribution at x_r and x_s are proportional to the slopes of the ogive at these points; moreover two different distributions, have relative frequencies at x_r and x_s in proportion to the slopes at x_r, x_s of the ogives representing the distributions, providing the ogives are drawn to the same scale. It is this independence of the dissection - analysis which allows distributions to be directly compared that led us to use ogives in preference to frequency distributions.

/The

The ogive takes all values from 0 to 1 and is monotonic; most often it is continuous. Where the experimental results can lead only to certain specified values the ogive is a step function. For example, if the temperature gradient can only take one value, say the dry adiabatic lapse rate, then the ogive is zero to the left of the value representing the dry adiabatic lapse rate and +1 to the right.

TABLE I – MEAN HOURLY VALUES OF THE TEMPERATURE DIFFERENCE IN °F. OVER THREE HEIGHT INTERVALS FOR EACH MONTH

Month & Range		Time G.M.T.																						
		0100	0200	0300	0400	0500	0600	0700	0800	0900	1000	1100	1200	1300	1400	1500	1600	1700	1800	1900	2000	2100	2200	2300	2400
Jan.	A	1.38	1.55	1.60	1.69	1.57	1.41	1.39	1.33	1.00	0.41	0.16	0.02	0.00	0.09	0.42	0.93	1.36	1.45	1.40	1.33	1.46	1.52	1.32	1.39
	B	0.48	0.54	0.49	0.38	0.32	0.24	0.29	0.27	0.09	-0.08	-0.44	-0.49	-0.49	-0.42	-0.30	-0.15	0.05	0.14	0.13	0.18	0.23	0.35	0.45	0.28
	C	0.26	0.28	0.30	0.33	0.22	0.18	0.19	0.19	0.21	0.03	-0.10	-0.32	-0.40	-0.41	-0.37	-0.20	-0.03	0.05	0.14	0.16	0.22	0.19	0.23	0.22
Feb.	A	0.95	1.00	0.92	0.82	0.82	0.74	0.69	0.46	0.03	-0.16	-0.17	-0.14	-0.30	-0.15	0.00	0.23	0.53	0.78	0.90	1.00	1.04	0.98	1.15	1.18
	B	0.17	0.16	0.18	0.24	0.23	0.19	0.18	0.09	-0.18	-0.49	-0.74	-0.91	-0.86	-0.81	-0.69	-0.52	-0.34	-0.09	0.06	0.15	0.18	0.24	0.16	0.19
	C	-0.04	0.02	0.04	0.14	0.10	0.02	0.05	-0.06	0.02	-0.25	-0.48	-0.57	-0.60	-0.57	-0.50	-0.50	-0.41	-0.24	-0.13	-0.17	-0.11	-0.03	-0.09	0.02
Mar.	A	1.93	1.94	1.88	1.77	1.58	1.54	1.14	0.25	-0.36	-0.65	-0.99	-1.12	-1.08	-1.00	-0.72	-0.37	0.00	0.53	1.17	1.51	1.74	1.68	1.72	1.70
	B	0.84	0.88	0.96	1.02	1.08	1.00	0.74	0.13	-0.60	-0.74	-0.77	-0.77	-0.77	-0.71	-0.63	-0.57	-0.04	0.13	0.50	0.67	0.80	0.86	0.79	0.82
	C	0.88	1.01	0.88	0.79	0.69	0.73	0.53	0.08	-0.33	-0.73	-0.90	-0.95	-0.87	-0.79	-0.64	-0.46	-0.02	0.12	0.35	0.54	0.61	0.70	0.77	0.77
Apr.	A	2.06	2.14	2.17	1.88	1.76	0.94	-0.11	-0.55	-0.88	-1.20	-1.31	-1.40	-1.34	-1.19	-1.01	-0.63	-0.35	0.05	0.65	1.33	1.63	1.86	2.12	2.10
	B	1.49	1.54	1.59	1.77	1.70	1.28	0.35	-0.79	-1.09	-1.07	-0.97	-0.91	-0.91	-0.87	-0.82	-0.75	-0.61	-0.22	0.21	0.51	0.61	0.80	0.92	1.18
	C	0.40	0.47	0.49	0.54	0.46	0.60	0.33	-0.23	-0.60	-0.72	-0.95	-0.97	-0.91	-0.92	-0.88	-0.81	-0.63	-0.38	-0.26	-0.12	0.06	0.26	0.25	0.28
May	A	1.87	1.57	1.65	1.75	1.25	0.05	-0.73	-1.04	-1.15	-1.43	-1.57	-1.57	-1.58	-1.41	-1.18	-1.06	-0.76	-0.40	0.09	0.83	1.26	1.52	1.62	1.64
	B	0.88	1.11	1.01	0.97	0.96	0.18	-0.74	-1.01	-1.20	-1.19	-1.11	-1.08	-1.23	-1.13	-0.94	-0.88	-0.75	-0.48	-0.13	0.27	0.48	0.67	0.76	0.82
	C	0.86	0.79	0.73	0.68	0.69	0.25	-0.30	-0.61	-0.63	-0.73	-0.82	-0.92	-0.76	-0.77	-0.92	-0.95	-0.80	-0.45	0.07	0.29	0.50	0.68	0.89	0.96
June	A	1.88	1.84	1.77	1.56	0.67	-0.21	-0.68	-0.79	-1.10	-1.41	-1.39	-1.43	-1.49	-1.33	-0.98	-0.77	-0.45	-0.11	0.36	0.90	1.43	1.69	1.69	1.74
	B	0.86	0.94	0.95	0.91	0.80	-0.19	-0.69	-0.90	-1.06	-1.19	-1.15	-1.10	-1.38	-1.32	-1.07	-0.86	-0.52	-0.59	0.20	0.37	0.78	0.74	0.76	0.79
	C	0.81	0.77	0.71	0.69	0.51	0.16	-0.35	-0.68	-0.81	-0.68	-0.89	-0.93	-0.59	-0.56	-0.72	-0.75	-0.56	-0.44	-0.05	0.23	0.66	0.71	0.65	0.79
Jly.	A	1.28	1.33	1.41	1.41	0.51	-0.17	-0.60	-0.88	-1.07	-1.37	-1.49	-1.51	-1.52	-1.40	-1.15	-0.87	-0.40	-1.10	0.30	0.81	1.19	1.44	1.45	1.57
	B	0.51	0.71	0.74	0.69	0.56	-0.36	-0.83	-0.96	-1.14	-1.17	-1.18	-1.21	-1.38	-1.33	-1.13	-1.05	-0.78	-0.64	-0.21	0.25	0.35	0.51	0.56	0.52
	C	1.02	1.01	0.98	1.07	0.97	0.67	-0.11	-0.05	-0.07	-0.12	-0.11	-0.14	+0.09	-0.03	-0.13	0.02	0.13	0.19	0.26	0.52	0.93	1.07	1.05	1.09
Aug.	A	1.42	1.42	1.36	1.32	1.15	0.07	-0.72	-0.93	-1.20	-1.43	-1.56	-1.59	-1.47	-1.39	-1.21	-0.84	-0.43	-0.03	0.46	1.18	1.57	1.66	1.53	1.47
	B	1.08	1.12	1.21	1.26	1.23	0.74	-0.39	-0.89	-1.16	-1.15	-1.21	-1.24	-1.22	-1.19	-1.03	-0.88	-0.77	-0.49	0.01	0.46	0.68	0.84	1.01	1.14
	C	0.90	0.96	0.88	0.95	0.95	0.75	0.17	-0.24	-0.35	-0.53	-0.63	-0.64	-0.64	-0.63	-0.54	-0.49	-0.39	-0.27	-0.07	0.16	0.43	0.61	0.68	0.87

Month & Range		Time G.M.T.																						
		0100	0200	0300	0400	0500	0600	0700	0800	0900	1000	1100	1200	1300	1400	1500	1600	1700	1800	1900	2000	2100	2200	2300	2400
Sept.	A	1.56	1.74	1.51	1.59	1.43	1.12	0.13	-0.21	-0.72	-0.93	-1.06	-1.13	-1.05	-1.05	-0.78	-0.45	-0.06	0.54	1.15	1.73	1.81	1.74	1.79	1.73
	B	0.96	1.01	1.22	1.19	1.32	1.21	0.55	-0.29	-0.88	-0.91	-0.98	-1.02	-1.03	-1.02	-0.89	-0.81	-0.59	-0.19	0.28	0.69	0.88	0.82	0.92	0.86
	C	0.58	0.65	0.63	0.62	0.61	0.72	0.59	~~-0.70~~ 0.22	-0.18	-0.43	-0.51	-0.51	-0.52	-0.50	-0.47	-0.42	-0.32	-0.13	0.07	0.37	0.37	0.51	0.55	0.70
Oct.	A	1.97	1.81	1.60	1.76	1.69	1.80	0.97	-0.03	-0.41	-0.69	-0.77	-0.86	-0.87	-0.83	-0.47	-0.14	0.45	1.27	1.72	2.06	2.22	2.13	1.91	1.77
	B	1.89	1.95	2.13	2.28	2.31	2.27	1.99	1.17	0.21	-0.31	-0.58	-0.68	-0.68	-0.59	-0.43	-0.23	0.19	0.64	1.08	1.40	1.64	1.89	1.77	1.82
	C	0.93	0.86	0.74	0.86	0.89	0.98	0.92	0.81	0.38	-0.18	-0.45	-0.58	-0.59	-0.57	-0.45	-0.25	-0.63	0.11	0.33	0.48	0.58	0.72	0.71	0.87
Nov.	A	1.09	0.95	0.88	0.72	0.74	0.80	0.80	0.47	-0.05	-0.33	-0.38	-0.39	-0.32	-0.17	0.05	0.57	0.97	1.13	1.27	1.30	1.24	1.21	1.09	1.12
	B	1.52	1.48	1.54	1.45	1.23	1.34	1.44	1.04	0.65	0.05	-0.25	-0.30	-0.36	-0.31	-0.07	0.27	0.55	0.73	0.86	0.87	1.06	1.19	1.27	1.36
	C	0.46	0.56	0.57	0.58	0.55	0.49	0.41	0.63	0.22	-0.05	-0.14	-0.30	-0.27	-0.29	-0.22	-0.15	-0.03	0.06	0.12	0.27	0.28	0.35	0.39	0.48
Dec.	A	0.97	0.88	0.81	0.64	0.73	0.76	0.65	0.69	0.57	0.21	-0.11	-0.20	-0.17	-0.05	0.26	0.77	1.05	1.17	1.15	1.11	1.10	1.16	1.31	1.12
	B	0.07	0.90	0.86	0.81	0.80	0.78	0.71	0.77	0.77	0.34	-0.02	-0.25	-0.27	-0.23	-0.15	0.08	0.32	0.42	0.51	0.56	0.56	0.65	0.77	0.81
	C	0.55	0.54	0.49	0.39	0.35	0.34	0.30	0.29	0.33	0.22	0.02	-0.16	-0.25	-0.30	-0.21	-0.10	-0.02	0.08	0.16	0.19	0.27	0.24	0.27	0.38

A = temperature difference 15.2 m. - 1.1 m.
B = temperature difference 47.2 m. - 15.2 m.
C = temperature difference 106.7 m. - 47.2 m.

TABLE II - MEAN VALUES OF THE TEMPERATURE DIFFERENCE IN °F. OVER THREE HEIGHT INTERVALS FOR EACH MONTH

M.R.P. 546

Month	Height Interval		
	1.1 m. to 15.2 m.	15.2 m. to 47.2 m.	47.2 m. to 106.7 m.
January	+1.09	+0.11	+0.07
February	+0.55	-0.13	-0.18
March	+0.66	+0.24	+0.16
April	+0.45	+0.21	-0.18
May	+0.05	-0.16	-0.05
June	+0.14	-0.17	-0.06
July	+0.01	-0.33	-0.43
August	+0.08	-0.05	+0.12
September	+0.50	+0.14	+0.09
October	+0.84	+0.96	+0.31
November	+0.62	+0.78	+0.21
December	+0.69	+0.96	+0.18
Annual Mean	+0.47	+0.21	+0.02

M.R.P. 546

TABLE III - MEAN HOURLY VALUES OF THE TEMPERATURE DIFFERENCE IN °F. OVER THREE HEIGHT INTERVALS FOR CLEAR AND OVERCAST DAYS IN SUMMER AND WINTER

Height interval (metres)	Time G.M.T.																							
	0000	0100	0200	0300	0400	0500	0600	0700	0800	0900	1000	1100	1200	1300	1400	1500	1600	1700	1800	1900	2000	2100	2200	2300	2400
	SUMMER																								
	Clear days and nights (19 occasions)																								
15.2- 1.1	+3.5	+3.1	+2.8	+3.1	+3.1	+2.4	+0.5	-0.8	-1.0	-1.3	-1.8	-2.0	-2.1	-1.9	-1.9	-1.7	-1.2	-0.3	+0.2	+1.0	+2.1	+3.0	+3.1	+2.9	+2.7
47.2-15.2	+1.7	+2.1	+2.3	+2.4	+2.7	+2.6	+1.6	-0.3	-1.3	-1.6	-1.6	-1.7	-1.6	-1.8	-1.8	-1.4	-1.3	-1.2	-0.5	+0.3	+0.8	+1.0	+1.2	+1.4	+1.5
106.7-47.2	+1.8	+2.4	+2.6	+2.3	+2.3	+2.1	+1.3	+0.5	-0.1	-0.2	-0.4	-0.5	-0.5	-0.4	-0.2	-0.3	-0.3	-0.1	+0.1	+0.2	+0.5	+1.1	+1.8	+1.8	+2.2
	Overcast days and nights (4 occasions)																								
15.2- 1.1	-0.4	-0.3	+0.1	0.0	-0.2	-0.3	-0.7	-0.8	-0.8	-1.0	-1.1	-1.2	-1.0	-1.1	-1.1	-1.0	-0.9	-0.8	-0.6	-0.3	0.0	+0.4	+0.8	+0.7	+0.5
47.2-15.2	+0.1	+0.4	+0.2	+0.4	+0.1	-0.1	-0.3	-0.7	-0.9	-0.9	-1.0	-1.1	-1.0	-0.9	-1.2	-1.0	-1.0	-0.9	-0.8	-0.8	-0.4	-0.1	+0.3	-0.2	-0.1
106.7-47.2	+0.1	-0.2	-0.1	-0.1	+0.1	-0.2	-0.4	-0.4	-0.5	-0.5	-0.6	-0.6	-0.5	-0.6	-0.5	-0.4	-0.4	-0.4	-0.5	-0.3	-0.1	-0.1	0.0	+0.1	-0.3
	WINTER																								
	Clear days and nights (3 occasions)																								
15.2- 1.1	+2.2	+1.8	+2.5	+2.7	+2.2	+2.1	+2.5	+2.9	+1.8	+1.4	+0.4	+0.2	+0.3	+0.3	+0.4	+0.4	+1.3	+2.2	+2.0	+2.1	+2.4	+2.7	+2.1	+1.8	+1.4
47.2-15.2	+0.4	+0.5	+0.5	+0.3	+0.3	+0.3	+0.1	+0.1	+0.2	+0.1	-0.4	-0.9	-1.0	-0.9	-0.9	-0.9	-0.2	+0.3	+0.6	+0.4	+0.3	+0.2	+0.3	+0.3	+0.3
106.7-47.2	+0.6	+0.8	+0.9	+1.1	+1.3	+0.8	+1.1	+1.1	+1.0	+0.6	-0.3	-0.6	-0.8	-0.9	-0.6	-0.4	-0.2	+0.3	+0.5	+1.0	+1.0	+0.9	+1.1	+1.3	+1.1
	Overcast days and nights (2) occasions)																								
15.2- 1.1	+0.2	+0.4	+0.4	+0.3	+0.4	+0.4	+0.4	+0.4	+0.4	+0.3	+0.1	+0.1	0.0	0.0	0.0	+0.1	+0.2	+0.4	+0.4	+0.4	+0.3	+0.3	+0.3	+0.3	+0.4
47.2-15.2	-0.3	-0.5	-0.5	-0.5	-0.5	-0.5	-0.5	-0.4	-0.4	-0.7	-0.8	-0.9	-0.9	-0.9	-0.9	-0.8	-0.6	-0.6	-0:6	-0.6	-0.7	-0.7	-0.7	-0.7	-0.6
106.7-47.2	-0.2	-0.2	-0.2	-0.2	-0.3	-0.3	-0.3	-0.4	-0.4	-0.4	-0.5	-0.5	-0.5	-0.5	-0.5	-0.5	-0.4	-0.4	-0.4	-0.4	-0.4	-0.4	-0.4	-0.4	-0.4

M.R.P. 546

Table IV - MEAN HOURLY VALUES OF WIND VELOCITY IN METRES PER SECOND CORRESPONDING TO THE OCCASIONS SHOWN IN TABLE III

	Time G.M.T.																							
	0100	0200	0300	0400	0500	0600	0700	0800	0900	1000	1100	1200	1300	1400	1500	1600	1700	1800	1900	2000	2100	2200	2300	2400
SUMMER																								
Clear	1.3	1.2	1.2	1.2	1.2	0.8	1.6	2.2	2.6	3.1	3.6	4.0	4.1	4.1	4.5	4.4	3.8	3.4	2.4	1.6	1.4	1.5	1.4	1.4
Overcast	1.1	1.0	1.0	1.6	1.6	2.1	2.2	3.1	3.4	2.9	3.6	3.1	3.1	2.9	3.3	3.6	4.1	3.7	2.5	1.9	1.1	1.6	1.7	2.5
WINTER																								
Clear	4.2	4.3	3.7	3.6	2.2	3.6	3.0	3.3	3.3	4.8	5.8	6.3	6.4	5.7	5.8	5.1	4.2	3.7	3.1	3.9	4.6	5.2	4.6	4.8
Overcast	3.7	3.9	3.8	3.9	4.1	4.1	4.1	4.3	4.3	4.4	4.5	4.3	4.4	4.1	4.2	4.1	4.3	3.9	4.4	4.8	5.1	5.2	4.9	4.8

TABLE V - MAXIMUM HOURLY VALUES OF TEMPERATURE LAPSE IN EACH MONTH.

(a) Over the height interval 1·1m. to 15·2m.

M.R.P. 546

Month	1945 Day	Max. Lapse °F.	G.M.T.	Sky	Wind m/s	1946 Day	Max. Lapse °F.	G.M.T.	Sky	Wind m/s	1947 Day	Max. Lapse °F.	G.M.T.	Sky	Wind m/s	1948 Day	Max. Lapse °F.	G.M.T.	Sky	Wind m/s
Jan.	.....					3	-2.1	1300	b	3.6	1	-0.6	1300	bc	1.0	.....				
Feb.	.....					24	-1.8	1000 1100	b	6.2 6.7	18	-1.7	1300	c	7.1	15	-1.6	1300	c	2.2
Mar.	.....					25	-4.6	1300	bc	3.6	25	-2.6	1000	b	3.6	29	-3.8	1300	c	4.5
Apr.	.....					19	-4.6	0900	b	0.9	10 29	-2.2	1200	b	2.2 8.5	23	-4.8	1000	bc	4.5
May	.....					7	-2.5	1400	bc	8.9	24	-3.1	1100	bc	4.0	30	-5.2	1200	bc	4.0
June	.....					12	-2.6	1000	c	3.6	28	-3.2	1200	ctlnm	3.6	11	-4.4	1800	bc	1.3
July	3	-3.8	1100	bc	3.6	3 10	-3.1	1200 1100	bc b	1.3 3.1	26	-3.5	1400	b	4.5	.....				
Aug.	3	-3.4	1200 1400	b	2.2 3.1	27	-2.1	1100	b	4.5	8	-2.9	1100	b	1.3	.....				
Sept.	17	-4.4	1400	bc	5.3	30	-1.8	1300	b	1.3	17	-2.6	1100	bc	1.8	.....				
Oct.	8	-2.6	1100	bc	4.9	11	-1.5	1300	b	6.7	17 21	-1.8	1100 0900 1000	c b b	3.5 4.2 0.4	.....				
Nov.	3	-3.0	1200	bc	2.7	5	-2.0	1200	bf	0.0	6	-1.4	1000	of	0.9	.....				
Dec.	20	-2.5	1300	b	4.0	18	-1.1	1200	b	7.6	1	-1.5	1000	bm	0.0	.....				

Table V (contd.) – Maximum hourly values of temperature lapse in each month

(b) Over the height interval 15.2 m. to 47.2 m.

Month	1945					1946					1947					1948				
	Day	Max. Lapse °F	G.M.T.	Sky	Wind m/s	Day	Max. Lapse °F	G.M.T.	Sky	Wind m/s	Day	Max. Lapse °F	G.M.T.	Sky	Wind m/s	Day	Max. Lapse °F	G.M.T.	Sky	Wind m/s
Jan.						14 15	- 1.0	1400 1500	bc b	8.0 4.0	24	- 1.9	1200	cps	4.5					
Feb.						21	- 1.9	1200	bc	12.0	18	- 3.0	1400	c	6.7	18	- 1.5	1200	b	9.3
Mar.						30	- 2.0	1100	b	3.1	25	- 2.9	0900	b	3.6	13	- 2.0	1600	bc	clm.
Apr.						15	- 3.4	0900	b	0.4	13	- 2.2	0900	b	3.6	12	- 4.3	1000	b	-
May						12	- 2.0	1300	bc	4.5	1 30	- 1.9	1200 1300	c b	5.8 1.3	7	- 4.0	1000	b	1.3
June						*	- 2.0				12 26	- 2.5	1400	b c	6.2 1.8	11	- 5.0	1300	b	0.4
July	8	- 3.0	0800	b	0.9	30	- 1.9	1100	c	8.5	26	- 3.4	1400	b	4.5					
Aug.	2	- 3.0	1300 1400	b	4.0 3.1	4 9	- 1.4	1500 1100	b c	2.2 1.3	29 30	- 2.6	1000 1100	bc c	3.1 4.5					
Sept.	2	- 2.3	1300	bc	8.0	1	- 1.0	1400	bc	6.7	3	- 2.8	1300	bc	1.3					
Oct.	7	- 1.9	1300	bc	1.3	17 18 21	- 0.9	12,1400 1100 1200	bc,c c c	8.5,8.9 6.2 4.9	26	- 1.6	1100 1200	bc	6.7 5.8					
Nov.	18	- 1.5	1200	bc	4.0	30	- 0.9	1600	c	8.0	8	- 0.8	1400	c	6.2					
Dec.	9 18 18	- 0.8	1500 1100 1200	bc	clm. 12.9 13.7	28	- 1.6	1600	c	0.4	8	- 1.4	1100	bc	5.3					

* June 1946: On six occasions the lapse of temperature reached -2.0°F. Times, states of sky etc., and wind-speeds for the various days are: 14th; 1400, c, 6.2: 18th; 1400, bc, 10.2: 27th; 1100, c, 6.2: 27th; 1200, c, 7.6: 28th; 1400, bc, 6.7: 30th; 1000, c, 4.5.

Table V (contd.) - Maximum hourly values of temperature lapse in each month.

(c) Over the height interval 47.2 m. to 106.7 m.

M.R.P.546

Month	1945					1946					1947					1948				
	Day	Max Lapse °F.	G.M.T.	Sky	Wind m/s	Day	Max. Lapse °F.	G.M.T.	Sky	Wind m/s	Day	Max. Lapse °F.	G.M.T.	Sky	Wind m/s	Day	Max. Lapse °F.	G.M.T.	Sky	Wind m/s
Jan.						27	-1.9	1500	b	clm	12	-1.9	1500	b	5.3					
Feb.						9	-1.5	1100	b	10.2	24	-2.9	1700	bc	clm	26	-1.5	1000	b	10.2
Mar.						29	-2.2	1300	b	4.9	9	-3.6	1400	bc	4.0	28	-3.5	1300	b	0.9
Apr.						8	-1.8	1400	bc	6.7	22	-2.0	0900	c	5.3	12	-2.4	1700	bc	-)
May						19	-3.1	1500	bc	3.1	15	-1.7	1500	bc	6.2	7	-4.5	0700	b	0.9
June						1	-1.9	1700 1800	bc	6.2 6.7	7	-1.4	1500	bc	8.5	11	-4.4	1800	bc	1.3
July	20	-1.5	1400	c	11.1	1 4	-1.7	0900 10, 1100	c bc	1.3 clm, 0.9	19	-0.9	0700	cf	clm					
Aug.	28	-2.9	1600	bc	4.0	19 27	-0.8	1100 1200	c bc	6.7 5.3	27	-0.8	1300	b	5.8					
Sept.	30	-1.6	2100 2200	c	clm.	30	-0.9	1500	b	2.7	23	-1.2	1600	bc	1.3					
Oct.	30	-2.1	1400	b	2.7	21	-1.0	1700	bc	0.0	16	-1.4	1700	c	1.8					
Nov.	3	-1.0	1300 1400 1500	bc	5.3 3.6 3.1	5	-1.6	1200	b	0.0	8	-1.2	1600	c	3.1					
Dec.	20	-2.2	1300	bc	4.0	18	-1.3	1600	c	5.8	1	-1.0	2300 2400	c	3.6 2.7					

Table VI - Maximum hourly values of temperature inversions in each month

(a) Over the height interval 1.1 m. to 15.2 m.

M.R.P. 546

Month	1945					1946					1947					1948				
	Day	Max. Invsn °F	G.M.T.	Sky	Wind m/s	Day	Max. Invsn °F	G.M.T.	Sky	Wind m/s	Day	Max. Invsn °F	G.M.T.	Sky	Wind m/s	Day	Max. Invsn °F	G.M.T.	Sky	Wind m/s
Jan.	.....	.....	.....	.....	.....	8	9.3	0100	b	1.8	30	13.6	0200	bc	clm	.....	.....	.....	.....	.....
Feb.	.....	.....	.....	.....	.....	24	4.4	2400	b	0.4	24	12.7	0200	b	0.9	29	9.2	2300 2400	b	1.3 1.8
Mar.	.....	.....	.....	.....	.....	27	6.8	0200	bm	1.8	3	6.4	0600	b	clm	12	10.0	2000	b	clm
Apr.	.....	.....	.....	.....	.....	15	9.2	0500	b	1.3	26	7.9	2300	b	clm	18	8.5	0300	bf	clm
May	.....	.....	.....	.....	.....	15 16 19	6.4	2100 2300 2300	bc bc b	clm	30	7.5	0400	b	clm	22	8.6	0100	b	1.8
June	.....	.....	.....	.....	.....	7	7.3	0100	b	clm	25	9.0	0100	b	clm	20	6.2	2200	bc	3.1
July	16	6.5	2400	b	0.4	7	6.6	2200	b	clm	3	6.8	2200	b	clm	.....	.....	.....	.....	.....
Aug.	5	7.4	0100	b	clm	16	6.9	0200	bc	clm	8	8.6	2100	b	clm	.....	.....	.....	.....	.....
Sept.	29	7.1	2000	b	0.9	16	8.7	0200	b	clm	10	10.6	2400	b	clm	.....	.....	.....	.....	.....
Oct.	9	10.6	2100	bc	clm	6	5.8	2400	c	1.8	22	11.8	0500	bc	1.8	.....	.....	.....	.....	.....
Nov.	15	8.1	1900	bc	3.1	4	9.2	2000	bm	clm	1	9.9	0700	c	clm	.....	.....	.....	.....	.....
Dec.	7	7.8	2200	bcm	clm	21	8.2	2400	b	clm	8	6.2	0100	cf	clm	.....	.....	.....	.....	.....

G.269698/JDG/8/50/60

Table VI (contd.) - Maximum hourly values of temperature inversions in each month.

(b) Over the height interval 15.2 m. to 47.2 m.

M.R.P. 546

Month	1945					1946					1947					1948				
	Day	Max. Invsn °F	G.M.T.	Sky	Wind m/s	Day	Max. Invsn °F	G.M.T.	Sky	Wind m/s	Day	Max. Invsn °F	G.M.T.	Sky	Wind m/s	Day	Max. Invsn °F	G.M.T.	Sky	Wind m/s
Jan.	.....					7	5.9	2300	bcm	clm	3	8.0	0200 0300	bm	clm	.....				
Feb.	.....					28	3.2	0700	bcf	2.7	24	8.7	0600	b	2.2	29	7.4	0800	bm	clm
Mar.	.....					26	8.2	0600	bm	clm	9	4.7	1400	bc	4.0	6 12	10.6	2100 0700	bff b	clm
Apr.	.....					10	8.6	0400	bm	2.2	14	8.6	0300	b	clm	13	7.7	0200	b	---
May	.....					1 22	4.2	0500 0400	b bc	3.1 1.3	31	9.6	0500	b	clm	7	5.6	0700	b	0.9
June	.....					7	5.0	0500	b	clm	2	10.1	2000	bc	1.8	14 24	2.8	01,0400 0500	b,bc bc	0.9,0.4 0.9
July	14	2.8	0200	b	3.1	10 12	4.8	0400 0500	b bc	clm	27	6.4	0300	bcf	clm	.....				
Aug	3	6.8	0500	b	0.9	16	8.8	0500	bc	clm	9	7.8	0600	b	clm	.....				
Sept.	30	6.8	0100 0200	bm	1.3 0.9	16	14.8	0600	bc	clm	4	10.2	0500	bm	clm	.....				
Oct.	9	11.1	0500	bcm	clm	7	5.9	2400	b	clm	22	11.4	0200	b	1.8	.....				
Nov.	25 29	8.0	2400 0100	cf bm	clm	4	13.4	2300 2400	bf	clm	7	13.5	0600	bc	0.4	.....				
Dec.	20	10.1	0900	b	clm	22	12.4	0400	bc	clm	1	7.8	0900	bm	0.9	.....				

Table VI (contd.) - Maximum hourly values of temperature inversions in each month

(c) Over the height interval 47.2 m. to 106.7 m.

M.R.P. 546

Month	1945					1946					1947					1948				
	Day	Max. Invsn °F	G.M.T.	Sky	Wind m/s	Day	Max. Invsn °F	G.M.T.	Sky	Wind m/s	Day	Max. Invsn °F	G.M.T.	Sky	Wind m/s	Day	Max. Invsn °F	G.M.T.	Sky	Wind m/s
Jan.	.....	.....	.....	.....	.....	27	4.5	1100	bcf	1.8	8 19	4.1	0200 1100	bcf bc	1.3 2.7	.....	.....	.....	.....	.....
Feb.	.....	.....	.....	.....	.....	28	5.0	0400	bf	1.8	24	14.5	0900	b	1.8	28	5.4	2200	bcm	clm
Mar.	.....	.....	.....	.....	.....	30	8.4	0400	bff	1.8	29	3.8	0600	cpr	5.3	9	12.3	2400	b	1.3
Apr.	.....	.....	.....	.....	.....	13	7.2	0700	bm	clm	13	8.9	2200	b	clm	18	6.6	0600	bff	clm
May	.....	.....	.....	.....	.....	30	4.6	0200	bc	clm	29	11.8	2000	b	1.3	2	4.0	1300	c	4.5
June	.....	.....	.....	.....	.....	7	4.2	0200	bc	clm	3	13.6	2300	b	clm	23	4.0	0200 0500	bc	clm 0.9
July	13	10.5	2200	b	4.9	2	6.9	0100	bc	clm	28	8.1	0600	bc	3.6	.....	.....	.....	.....	.....
Aug.	4	5.3	0100	b	clm	22	5.1	0500	c	clm	16	5.1	0500	b	1.8	.....	.....	.....	.....	.....
Sept.	12 30	3.5	2200 0300	cm bm	8.0 1.3	26	4.8	2200	c	clm	15	9.4	2400	b	0.4	.....	.....	.....	.....	.....
Oct.	14	6.3	0600	bm	1.3	7	3.1	0600	bc	clm	21	8.0	0900	b	4.5	.....	.....	.....	.....	.....
Nov.	11 29	4.8	0100 0400	bc bcm	4.0 clm	5	10.2	0800	bm	clm	6	11.4	0800	oF	0.4	.....	.....	.....	.....	.....
Dec.	7	6.5	1000	c	0.9	22	5.8	0100	b	clm	1	9.3	0300	oF	clm	.....	.....	.....	.....	.....

TABLE VII - EXCEPTIONAL INVERSION OF TEMPERATURE OF 24.2.1947

	G.M.T. (2400h. 23/2) 00	01	02	03	04	05	06	07	08	09	10	11	12
Temp. (°F) at 1.1m.	9.0	8.8	4.8	5.4	6.1	3.9	3.9	2.1	5.3	8.4	14.3	21.2	25.4
" " " 15.2m.	17.5	17.5	17.5	16.1	11.8	11.2	10.5	10.6	11.7	12.3	17.8	26.2	33.4
" " " 47.2m.	19.4	18.8	19.9	18.3	18.4	18.7	19.2	19.1	20.0	19.4	23.2	29.7	32.9
" " " 106.7m.	24.2	23.8	23.8	23.8	23.7	23.9	23.6	22.7	25.9	33.9	33.6	34.8	34.1
Lapse of Temp. 15.2-1.1m	7.9	8.7	12.7	10.7	5.7	7.3	6.6	8.5	6.4	3.9	3.5	5.0	8.0
" " " 47.2-15.2m	1.9	1.3	2.4	2.2	6.6	7.5	8.7	8.5	8.3	7.1	5.4	3.5	-0.5
" " " 106.7-47.2m	4.8	5.0	3.9	5.5	5.3	5.2	4.4	3.6	5.9	14.5(+)	10.4	5.1	1.2
Lapse of Temp. 47.2-1.1m	9.8	10.0	15.1	12.9	12.3	14.8	15.3	17.0	14.7	11.0	8.9	8.5	7.5
" " " 106.7-1.1m	14.0	15.0	19.0	18.4	17.6	20.0	19.7	20.6	20.6	25.5(+)	19.3	13.6	8.7

Grass min. temp. 1°F. Weather bm. Vis 4 - 6 miles at 0900h. State of ground 8 - rather less than 4 in. snow. 8 in. earth temp., 33.2 at 0900h.

(+) At 0900 the 106.7 - 15.2 differential temperature trace exceeded even the double range of the chart. The figures entered in the record are, if anything conservative estimates; the true figures may be 0.1 or 0.2°F in excess of these.

TABLE VIII PERCENTAGE FREQUENCY OF OCCURRENCE OF TEMPERATURE DIFFERENCES (°F.) OF VARIOUS VALUES

(a) Over the height interval 1.1m. to 15.4m.

M.R.P. 546

Month	-4.1 to -5.0	-3.1 to -4.0	-2.1 to -3.0	-1.1 to -2.0	-0.1 to -1.0	0.9 to 0.0	1.9 to 1.0	2.9 to 2.0	3.9 to 3.0	4.9 to 4.0	5.9 to 5.0	6.9 to 6.0	7.9 to 7.0	8.9 to 8.0	9.9 to 9.0	10.9 to 10.0	11.9 to 11.0	12.9 to 12.0	13.9 to 13.0
Jan.	..	..	0.1	0.2	12.4	53.4	16.9	5.5	3.6	2.9	1.7	1.5	0.5	0.7	0.4	..	..	0.2	0.1
Feb.	..	..	..	1.4	34.2	46.6	8.0	3.3	2.2	1.3	1.0	0.7	0.5	0.5	0.1	0.1	0.1	0.1	..
Mar.	0.1	0.4	2.3	9.1	25.3	34.2	10.1	6.0	4.4	2.6	2.4	1.1	0.5	0.2	0.4	0.1	..	..	..
Apr.	0.6	0.7	2.9	14.4	29.6	22.4	10.2	6.0	4.6	3.5	3.0	1.4	0.5	0.1	0.1	..	..	..	..
May	0.4	1.5	7.0	17.0	27.5	25.2	8.7	4.3	3.4	2.4	1.1	1.2	0.1	0.1	..	..	..	..	..
Jun.	0.3	2.0	4.4	14.3	27.0	29.5	9.9	4.8	2.5	1.9	1.0	0.8	0.5	0.3	0.1	..	..	..	..
July	..	1.5	6.3	15.0	29.6	28.5	8.2	5.2	2.9	1.7	0.7	0.4	..	..	..	..	..	..	..
Aug.	..	0.4	4.7	23.9	28.7	19.8	9.0	5.6	3.8	2.2	1.5	0.8	0.1	0.2	..	..	..	..	..
Sept.	0.1	0.2	2.2	11.6	29.1	30.7	10.2	5.8	3.6	2.8	1.2	1.3	0.5	0.5	0.3	0.1	..	..	..
Oct.	..	..	0.6	7.6	35.3	27.4	7.6	6.4	3.9	3.9	3.1	2.1	0.8	0.8	0.3	0.2	0.1	..	..
Nov.	..	..	0.1	1.2	36.6	38.6	9.6	5.9	2.8	2.6	1.3	0.7	0.4	0.1	0.1	..	..	..	..
Dec.	..	..	0.1	0.5	17.5	57.7	11.8	5.0	3.2	1.9	1.3	0.6	0.4	0.1	..	..	..	..	..
Year	0.1	0.6	2.7	10.1	28.1	33.6	10.0	5.3	3.4	2.5	1.6	1.0	0.4	0.2	0.1	..	..	..	..

Table VIII - Page 2

(b) Over the height interval 15.2m. to 47.2m.

M.R.P.546

Month	-3.0 to -3.4	-2.5 to -2.9	-2.0 to -2.4	-1.5 to -1.9	-1.0 to -1.4	-0.5 to -0.9	0.0 to -0.4	0.5 to 0.1	1.0 to 0.6	1.5 to 1.1	2.0 to 1.6	2.5 to 2.1	3.0 to 2.6	3.5 to 3.1	4.0 to 3.6	4.5 to 4.1	5.0 to 4.6	5.5 to 5.1	6.0 to 5.6	6.5 to 6.1	7.0 to 6.6	7.5 to 7.1	8.0 to 7.6	8.5 to 8.1	9.0 to 8.6	9.5 to 9.1	10.0 to 9.6	10.5 to 10.1
Jan.	..	..	..	0.6	7.9	19.1	33.2	17.7	7.7	5.3	2.3	2.2	1.1	1.1	0.5	0.1	0.5	0.2	0.2	0.2	..	0.2	0.2	..	..	..	..	..
Feb.	0.1	0.1	0.4	5.2	20.5	11.6	29.7	15.7	6.0	4.3	1.9	0.9	0.7	0.5	0.4	0.3	0.5	0.3	0.1	0.1	0.1	0.2	..	0.1	0.1	..	..	..
Mar. 1	..	0.1	0.3	2.5	16.0	24.6	21.2	10.8	6.8	3.6	2.9	1.8	2.0	0.9	1.6	1.3	0.6	0.5	0.3	0.3	0.2	0.2	0.5	0.2	0.2	0.2	0.2	0.2
Apr. 2	0.1	0.5	2.0	4.4	10.0	23.3	22.4	9.7	7.2	4.8	3.6	2.2	2.1	1.7	1.3	1.2	1.1	1.0	0.1	0.4	0.3	0.3	0.2	0.1	0.1	..	..	..
May 3	0.5	1.0	2.7	6.1	15.3	25.6	18.8	10.0	5.2	3.1	2.8	1.9	2.2	1.3	1.0	0.7	0.6	0.3	0.2	..	0.1	0.1	..	..	..	..	..	..
June 4	0.3	1.1	2.7	7.4	15.9	25.4	17.4	11.4	5.5	4.2	2.1	1.6	1.0	0.6	0.5	0.5	0.5	0.5	0.3	0.2	0.2	0.2	0.2	..	0.1	0.2	0.1	0.1
July	0.1	0.2	2.6	9.9	17.7	25.6	17.7	8.8	6.7	4.3	2.6	1.4	0.4	0.5	0.7	0.2	0.1	0.1	0.2	0.1	..	..	..	..	..	..	..	..
Aug.	0.1	0.4	2.9	9.4	13.8	17.6	18.2	10.8	7.8	5.4	4.4	3.4	2.5	1.6	0.8	0.2	0.2	0.1	0.1	0.2	0.2	..	0.1	..	0.1	..	..	..
Sept. 5	..	0.1	1.1	4.3	16.9	17.3	22.6	12.7	7.7	5.0	3.3	1.8	1.6	1.7	0.9	0.6	0.3	0.2	0.4	0.1	0.2	0.3	0.1	0.2	0.2	0.2	..	0.1
Oct. 6	..	..	..	0.6	6.0	13.3	22.3	17.4	9.9	6.5	4.6	3.3	3.8	1.8	1.5	1.3	0.9	1.2	1.4	0.5	0.3	0.8	0.5	0.1	0.3	0.2	0.2	0.2
Nov. 7	..	..	..	0.1	0.4	7.7	32.9	21.7	13.6	8.1	4.3	2.3	2.3	1.1	1.3	0.4	0.3	0.4	0.3	0.3	0.2	0.2	0.4	0.3	0.1	0.1	0.3	0.3
Dec. 8	..	..	..	0.1	1.6	9.3	36.4	21.8	11.8	7.9	2.9	1.7	1.6	1.1	1.0	0.7	0.4	0.2	0.2	0.3	0.3	0.1	0.1	..	0.2	..	0.2	0.2
Year	0.1	0.3	1.3	4.3	11.9	18.6	24.0	13.8	8.0	5.2	3.2	2.1	1.8	1.2	1.0	0.6	0.5	0.4	0.3	0.2	0.2	0.2	0.2	0.1	0.1	0.1	0.1	0.1

Notes:- (1) A Further 0.2% of March observations fall between +10.6 and +11.0
(2) " " 0.2% " April " " " -3.5 and -4.4
(3) " " 0.2% " May " " " -3.5 and -3.9
(4) " " 0.3% " June " " " -3.5 and -5.4
(5) " " 0.3% " Sept. " " " +10.6 and +15.0
(6) " " 0.6% " Oct. " " " +10.6 and +16.0
(7) " " 1.0% " Nov. " " " +10.6 and +13.5
(8) " " 0.3% " Dec. " " " +10.6 and +12.5

(c) Over the height interval 47.2m. to 106.7m.

M.R.P.546

Month	-3.0 to -3.4	-2.5 to -2.9	-2.0 to -2.4	-1.5 to -1.9	-1.0 to -1.4	-0.5 to -0.9	0.0 to -0.4	0.5 to 0.1	1.0 to 0.6	1.5 to 1.1	2.0 to 1.6	2.5 to 2.1	3.0 to 2.6	3.5 to 3.1	4.0 to 3.6	4.5 to 4.1	5.0 to 4.6	5.5 to 5.1	6.0 to 5.6	6.5 to 6.1	7.0 to 6.6	7.5 to 7.1	8.0 to 7.6	8.5 to 8.1	9.0 to 8.6	9.5 to 9.1	10.0 to 9.6	10.5 to 10.1
Jan.	..	..	..	0.6	2.4	17.1	48.8	13.6	5.9	3.8	2.9	2.3	1.1	0.8	0.4	0.2	..	..	..	..	..	..	..	..	..	..	..	..
Feb.[1]	..	0.1	..	0.1	5.5	35.4	44.8	5.5	2.7	1.3	0.7	0.7	0.5	0.5	0.7	0.6	0.2	0.3	0.1	..	..	..	..	..	..	..	..	0.1
Mar.[2]	0.1	0.3	1.2	3.7	12.1	26.0	22.0	10.1	6.9	4.5	3.7	1.8	1.8	1.0	0.9	0.9	0.8	0.3	0.3	0.1	0.4	0.2	0.2	0.2	0.1	0.2	0.1	0.4
Apr.	..	..	0.3	4.4	22.5	31.4	14.5	8.7	5.0	2.9	2.7	2.0	2.0	0.9	0.7	0.4	0.7	0.3	0.2	0.2	0.2	0.2	..	..	0.1	..	..	..
May[3]	..	0.7	1.1	2.9	18.6	28.2	21.2	6.7	5.1	3.3	2.9	1.9	1.7	1.6	1.0	0.8	0.3	0.1	0.3	..	0.2	0.2	0.1	0.1	0.2	0.2	..	...
June[4]	0.1	0.1	0.4	2.9	17.1	28.6	23.4	9.6	5.3	2.5	2.1	2.3	1.5	0.8	1.0	0.3	0.1	0.2	0.3	0.3	0.1	0.1	0.1	0.2	0.1	0.2	0.1	..
July	..	..	..	0.1	1.7	11.7	42.4	17.3	8.0	4.8	3.9	2.8	2.3	1.1	1.1	1.0	0.7	0.4	0.3	0.1	0.2	0.1	..	0.1	..	0.1	..	0.1
Aug.	..	0.9	3.1	2.7	5.1	14.7	38.4	21.1	7.7	4.9	3.6	2.8	2.3	1.2	0.9	0.4	0.1	0.2	..	..	..	..	..	..	..	..	..	..
Sept.	..	..	..	0.2	4.1	23.8	37.6	15.0	6.5	3.7	2.2	2.3	1.9	1.1	0.4	0.5	0.2	0.1	0.1	0.1	0.1	0.1	0.1	0.1	..	0.1	..	..
Oct.	..	..	0.2	1.6	3.3	12.8	42.9	16.7	8.4	3.9	2.9	2.1	2.5	0.8	0.7	0.5	0.7	0.6	0.6	0.2	0.2	0.4	0.1	..	..	..	..	..
Nov.[5]	..	..	..	0.1	0.3	12.4	53.2	16.2	6.7	3.7	2.4	1.8	1.1	0.8	0.2	0.1	0.3	0.1	..	0.2	0.2	0.2	0.1	0.1	..	0.1	0.1	0.1
Dec.	..	..	0.1	0.1	1.1	19.9	49.3	17.9	8.3	2.8	1.7	1.0	1.2	0.6	0.3	0.6	0.2	0.3	0.1	0.1	..	0.2	0.1	0.1	0.1	0.1	..	..
Year	..	0.2	0.6	1.7	8.3	21.7	34.8	13.2	6.1	3.5	2.6	2.0	1.7	1.0	0.7	0.5	0.4	0.2	0.2	0.1	0.1	0.1	0.1	0.1	..	0.1	..	..

Notes:- (1) A further 0.1% of February observations fall between +10.6 and +14.5
(2) " " 0.4% " March " " " +10.6 " +12.5, and 0.1% between -3.5 and -3.9.
(3) " " 0.1% " May " " " -3.5 " -3.9
(4) " " 0.4% " June " " " +10.6 " +14.0, and 0.3% between -3.5 and -4.4.
(5) " " 0.1% " November " " " +10.6 " +11.5.

TABLE IX – MEAN HOURLY VALUES OF AIR TEMPERATURE AT A HEIGHT OF 1.1M. FOR EACH MONTH

M.R.P. 546

Month	Hour G.M.T. 0000	0100	0200	0300	0400	0500	0600	0700	0800	0900	1000	1100	1200	1300	1400	1500	1600	1700	1800	1900	2000	2100	2200	2300	2400
January		33.2	33.0	32.9	32.7	32.8	32.8	32.5	32.2	32.9	34.3	35.9	36.7	37.5	37.7	37.1	35.7	34.2	33.9	33.9	34.0	33.8	33.8	34.0	34.0
February		32.6	32.4	32.4	32.3	32.3	32.3	32.2	32.7	34.1	35.6	36.9	37.6	38.6	38.6	38.1	37.3	36.0	34.8	34.2	33.9	33.5	33.1	32.7	32.2
March		36.9	36.6	36.5	36.4	36.3	36.2	36.8	39.2	42.3	44.2	46.4	47.5	48.2	48.4	48.1	47.2	45.5	42.7	40.5	39.4	38.7	38.4	38.0	37.8
April		40.1	39.7	39.3	38.9	38.9	40.1	43.3	46.8	49.5	51.2	52.8	53.3	53.5	53.6	53.4	52.7	51.4	48.9	45.9	44.0	43.1	42.3	41.8	40.6
May		45.4	45.1	44.8	44.4	44.9	47.8	50.9	53.6	55.2	56.7	58.0	58.8	59.5	59.6	59.1	58.7	57.5	55.5	52.8	50.0	48.5	47.4	46.6	46.2
June		50.4	49.9	49.6	49.6	51.0	53.9	56.5	58.9	60.3	61.2	61.8	62.7	62.9	63.2	63.0	62.4	61.4	59.9	57.7	55.2	53.4	52.3	51.7	51.0
July		55.2	54.5	54.3	54.0	54.8	57.1	59.9	62.1	64.2	65.4	66.6	67.4	67.9	68.3	68.0	67.6	66.1	64.8	62.4	59.5	57.9	57.0	56.4	55.7
August		54.5	54.1	53.5	53.3	53.5	55.3	58.4	61.3	63.7	65.5	66.9	67.9	68.3	68.5	68.1	67.3	66.3	64.1	60.9	58.3	56.9	56.1	55.5	54.9
September		53.3	52.7	52.4	52.0	52.0	52.3	54.5	57.2	59.5	61.0	62.3	63.3	63.8	64.1	63.4	62.6	61.1	58.6	56.3	54.9	54.4	54.2	53.7	53.3
October		46.6	46.5	46.2	45.8	45.5	45.3	46.1	48.6	51.4	54.0	55.8	56.9	57.5	57.5	56.4	55.2	52.9	50.7	49.3	48.4	47.7	47.3	47.3	46.9
November		40.9	40.9	40.9	41.0	41.0	40.8	40.7	41.3	43.1	45.1	46.5	47.3	47.9	47.6	46.6	45.1	43.6	43.1	42.6	42.3	41.8	41.5	41.3	40.9
December		37.4	37.3	37.4	37.7	37.7	37.2	37.2	37.0	37.4	38.8	40.5	41.6	42.1	42.0	41.3	39.9	39.1	38.7	38.3	38.0	37.8	37.5	37.2	37.2

TABLE X – MEAN HOURLY VALUES OF AIR TEMPERATURE (°F) AT A HEIGHT OF 1.1M. FOR CLEAR AND OVERCAST DAYS IN SUMMER AND WINTER

	Hour G.M.T. 0000	0100	0200	0300	0400	0500	0600	0700	0800	0900	1000	1100	1200	1300	1400	1500	1600	1700	1800	1900	2000	2100	2200	2300	2400
SUMMER																									
Clear	54.2	53.4	52.9	52.3	51.8	52.6	56.5	62.1	66.8	69.9	72.7	74.4	75.3	75.6	75.9	75.7	75.0	72.8	69.9	65.3	61.0	58.2	57.2	56.2	55.8
Overcast	56.7	56.3	55.4	54.6	54.7	54.8	55.3	55.8	56.7	58.1	59.4	59.8	59.6	60.1	60.6	59.7	60.8	59.9	59.3	58.0	56.5	56.6	55.4	55.4	54.9
WINTER																									
Clear	35.5	35.5	34.3	34.0	34.1	34.1	33.8	33.0	34.2	36.3	39.5	41.3	43.2	43.9	43.6	43.2	40.6	37.7	37.1	36.7	36.5	36.1	36.3	35.8	36.1
Overcast	35.5	35.5	35.4	35.3	35.2	35.1	35.0	34.9	34.9	35.3	36.0	36.5	36.8	36.9	36.7	36.4	36.1	35.7	35.6	35.6	35.7	35.7	35.8	35.7	35.6

TABLE XI - TIMES OF OCCURRENCE OF MAXIMUM TEMPERATURE AT VARIOUS HEIGHTS

Month	G.M.T. of maximum temperature at stated heights.			
	1.1 m.	15.2 m.	47.2 m.	106.7 m.
Mean June	1414 (30)	1444 (34)?	1518? (10)?	1528?
Mean December	1324 (6,	1330 (6)	1336 (30)?	1406?
Clear Summer	1410 (35)	1445 (25)?	1500 (12)	1512
Clear Winter	1336? (-3)?	1333? (12)?	1445? (12)?	1457?
Overcast Winter	1252? (8)?	1300? (3)?	1303? (0)?	1309?

Uncertainties are introduced by (a) flatness of December and Wintercurves;
(b) certain points in June and Summer curves not lying on smooth curve and so permitting alternative constructions.

TABLE XII - Diurnal Range of Temperature at Various Heights

Month	Mean diurnal range in °F. at stated heights			
	1.1m.	15.2m.	47.2m.	106.7m.
January	5.5	4.3	3.6	3.0
February	6.4	5.6	4.6	3.9
March	12.2	9.7	8.2	7.1
April	14.7	11.7	9.2	7.9
May	15.2	10.8	8.8	7.4
June	13.6	10.8	8.8	7.4
July	14.3	11.6	9.9	8.8
August	15.2	12.5	10.1	8.5
September	12.1	9.6	7.4	6.2
October	12.2	9.6	7.0	5.5
November	7.2	6.1	4.4	3.6
December	5.1	4.2	3.2	2.6
SUMMER				
Clear	24.1	19.3	15.0	12.6
Overcast	6.2	5.4	4.6	4.6
WINTER				
Clear	10.9	8.3	7.3	5.4
Overcast	2.0	1.6	1.1	1.0

TABLE XIII - MEAN HOURLY TEMPERATURES AT 1.1M. AND MEAN HOURLY LAPSE RATES ON OCCASIONS OF SNOW COVER

Time G.M.T.	00	01	02	03	04	05	06	07	08	09	10	11	12	13	14	15	16	17	18	19	20	21	22	23	24
ean Temp. 1.1m	22.0	21.7	21.5	21.7	22.0	21.9	22.0	21.8	22.1	23.0	24.1	25.7	26.4	27.3	27.5	27.0	26.1	24.7	24.0	23.3	23.0	23.2	23.2	23.0	22.7
apse of 15.2m-1.1m	2.0	2.2	2.3	1.8	1.3	1.7	1.7	1.5	1.3	0.7	0.7	0.7	0.6	0.2	-0.3	0.9	1.3	1.7	1.6	2.0	1.8	1.6	1.2	1.5	1.8
emp. 47.2m-15.2m	0.0	0.2	0.2	0.3	0.3	0.2	0.3	0.3	0.4	0.1	0.0	-0.5	-0.9	-0.9	-0.9	-0.8	-0.6	-0.5	-0.5	-0.3	0.0	-0.1	0.0	0.0	0.0
106.7m-47.2m.	0.2	0.2	0.2	0.3	0.3	0.3	0.1	0.0	0.1	0.7	0.3	-0.2	-0.4	-0.4	-0.5	-0.3	-0.4	-0.6	-0.3	-0.1	-0.2	-0.1	0.0	0.0	0.3

TABLE XIV - MEAN HOURLY VALUES OF THE HUMIDITY DIFFERENCE IN MCM/CU. METRE OVER THREE HEIGHT INTERVALS FOR EACH MONTH

Month & Range		Time G.M.T.																					
		0100	0200	0300	0400	0500	0600	0700	0800	0900	1000	1100	1200	1300	1400	1500	1600	1700	1800	1900	2000	2100	2200	2300	2400
Jan.	A	150	180	190	220	170	140	100	100	70	-80	-70	-100	-60	-80	-20	30	120	110	100	80	130	130	130	150
	B	-80	-70	-80	-110	-100	-100	-70	-100	-160	-160	-130	-190	-210	-160	-170	-140	-150	-160	-180	-150	-150	-110	-100	-100
	C	-30	-40	-40	-50	-40	-50	-50	-50	-50	-50	-60	-120	-100	-130	-120	-120	-100	-100	-80	-70	-50	-40	-40	-70
Feb.	A	20	40	30	30	20	10	10	-20	-80	-100	-80	-70	-70	-60	-50	-60	-60	-40	-30	-10	20	20	10	40
	B	-50	-50	-50	-40	-30	-30	-40	-50	-100	-120	-80	-90	-70	-30	-20	-20	-20	-30	-10	-50	-50	-30	-30	-70
	C	-40	0	0	20	20	0	-10	-10	-30	-60	-50	-50	-40	-50	-50	-60	-30	-20	-30	-30	-20	-20	-20	-10
Mar.	A	260	270	260	250	240	240	170	0	-110	-90	-80	-70	-60	-60	-20	10	70	130	160	220	280	260	260	250
	B	40	60	90	80	50	70	30	-60	-180	-190	-100	-10	30	30	20	20	0	0	10	0	-10	10	30	50
	C	10	0	-10	0	30	40	40	-40	-100	-120	-50	-20	-30	-50	-70	-60	-80	-50	-20	-20	-10	-20	-10	0
Apr.	A	160	190	220	200	180	30	-260	-380	-310	-310	-280	-290	-290	-270	-230	-190	-120	-100	0	50	80	140	180	190
	B	90	60	80	120	130	70	-70	-180	-100	-20	-20	-40	-60	-50	-30	-10	-50	0	-10	40	30	30	30	40
	C	-10	30	40	30	20	70	20	-50	0	-40	-60	+10	-20	-30	-20	-30	-50	-50	-70	-30	-30	-40	-30	-10
May	A	140	100	150	110	0	-300	-550	-610	-530	-530	-540	-530	-590	-620	-490	-490	-390	-290	-220	-50	-10	80	80	110
	B	-200	-140	-140	-90	-90	-300	-480	-250	-220	-220	-170	-190	-180	-100	-160	-190	-210	-200	-290	-280	-290	-220	-220	-210
	C	20	-10	60	40	30	-40	-80	-70	-50	50	-20	30	90	30	40	70	70	90	70	70	110	60	50	20
June	A	10	-20	20	0	-270	-600	-810	-860	-810	-780	-730	-770	-760	-780	-710	-710	-670	-610	-490	-340	-180	-90	-60	-40
	B	-200	-120	-140	-120	-170	-410	-360	-260	-240	-240	-280	-260	-240	-200	-210	-190	-210	-220	-250	-200	-200	-220	-180	-130
	C	0	-40	-50	-60	+20	-10	-130	-30	40	70	-20	-30	+20	-50	10	40	30	-40	20	20	60	10	70	20
July	A	240	360	350	410	230	-50	-340	-460	-460	-560	-590	-590	-590	-570	-570	-540	-450	-380	-330	-90	80	140	200	290
	B	-410	-330	-340	-280	-320	-560	-570	-380	-400	-430	-470	-510	-520	-470	-440	-480	-470	-460	-420	-450	-460	-440	-410	-420
	C	-170	-120	-10	-30	-70	-140	-250	-90	-20	-40	-80	-70	-70	-120	-130	-60	-110	-110	-220	-170	-200	-170	-200	-150

/ Aug.

Month & Range		Time G.M.T.																					
		0100	0200	0300	0400	0500	0600	0700	0800	0900	1000	1100	1200	1300	1400	1500	1600	1700	1800	1900	2000	2100	2200	2300	2400
Aug.	A	100	120	120	130	90	-250	-570	-730	-580	-530	-520	-530	-430	-460	-420	-400	-430	-540	-420	-240	-60	0	0	60
	B	-60	-30	50	70	90	-70	-340	-320	-300	-340	-390	-380	-380	-330	-340	-330	-320	-370	-360	-350	-270	-230	-180	-100
	C	-210	-150	-110	-120	-100	-130	-350	-260	-200	-200	-220	-250	-220	-190	-200	-240	-260	-280	-360	-280	-310	-360	-320	-180
Sept.	A	130	210	170	230	180	90	-150	-220	-450	-450	-490	-480	-450	-410	-410	-380	-340	-270	-130	50	90	100	160	170
	B	-80	-30	20	20	70	40	-150	-330	-340	-320	-270	-260	-250	-260	-190	-180	-230	-210	-140	-120	-180	-200	-110	-130
	C	-180	-130	-110	-90	-80	-100	-160	-250	-300	-250	-220	-260	-270	-290	-280	-270	-290	-270	-310	-320	-310	-300	-310	-280
Oct.	A	300	260	200	260	270	320	70	-210	-370	-380	-390	-340	-350	-280	-280	-220	-120	20	150	250	290	270	240	220
	B	210	210	270	320	310	310	220	20	-90	-120	-130	-160	-80	-30	10	0	-60	-60	60	90	100	150	100	180
	C	-260	-230	-250	-200	-120	-70	-70	-90	-240	-360	-370	-430	-400	-430	-310	-330	-350	-260	-260	-280	-220	-190	-180	-210
Nov.	A	70	40	20	0	30	60	40	-10	-160	-260	-250	-180	-150	-120	-70	-10	0	40	70	80	70	80	70	80
	B	200	190	220	220	180	180	210	120	30	-60	-60	0	70	90	80	160	110	100	80	90	120	160	170	170
	C	-30	0	-10	-30	-20	-40	-50	-10	-90	-110	-80	-100	-60	-50	-60	-60	-20	-50	-40	-40	-20	-50	-60	-40
Dec.	A	60	50	40	30	40	40	50	50	30	-50	-110	-140	-160	-130	-80	30	50	70	70	60	60	90	110	80
	B	140	170	170	130	140	140	120	140	120	70	0	-20	-10	40	50	50	120	90	90	110	120	130	150	150
	C	50	50	40	20	0	10	0	10	0	-20	-80	-110	-80	-80	-50	-20	-20	0	0	0	0	10	10	20

A = humidity difference 15.2m. - 1.1m.
B = humidity difference 47.2m. - 15.2m.
C = humidity difference 106.7m. - 47.2m.

TABLE XIVA. - MEAN HOURLY VALUES OF THE HUMIDITY AT 1.1 m AND OF HUMIDITY DIFFERENCES AT 1500 IN OCTOBER. FOR OFFSHORE AND ONSHORE WINDS.

	Humidity at 1.1m mgm./cu.m.	Humidity Difference mgm./cu.m.		
		15.2m - 1.1m.	47.2m - 15.2m.	106.7m - 47.2m.
Off shore winds 25 cases	8390	-270	+40	-380
On shore winds 5 cases	9680	-320	-250	-570

Off shore winds defined as those between 050° and 240°

On shore winds " " " " 135° and 210°

All other Directions, and winds less than 4 m.p.h. regarded as indeterminate except for the first hour of less than 4 m.p.h. following at least three hours in one of significant categories.

TABLE XV - MEAN VALUES OF THE HUMIDITY DIFFERENCE IN MGM./CU. METRE OVER THREE HEIGHT INTERVALS FOR EACH MONTH.

M.R.P. 546

Month	Height Interval		
	1.4m. to 15.2 m.	15.2 m. to 47.2 m.	47.2 m. to 106.7 m.
January	+80	-130	-70
February	-20	-50	-30
March	+120	0	-30
April	-60	0	-10
May	-250	-210	+30
June	-460	-220	0
July	-180	-430	-120
August	-270	-230	-230
September	-130	-160	-230
October	+10	+80	-250
November	-20	+120	-50
December	+20	+100	-10
Annual Mean	-90	-90	-80

TABLE XVI - MEAN HOURLY VALUES OF THE HUMIDITY DIFFERENCE IN MGM./CU METRE OVER THREE HEIGHT INTERVALS FOR CLEAR AND OVERCAST DAYS IN SUMMER AND WINTER

M.R.P. 546

HEIGHT Interval (Metres)	Time G.M.T.																						
	0000	0100	0200	0300	0400	0500	0600	0700	0800	0900	1000	1100	1200	1300	1400	1500	1600	1700	1800	1900	2000	2100	2200	2300	2400
SUMMER																									
Clear days and nights (19 occasions)																									
15.2- 1.1	+580	+490	+580	+750	+770	+590	-120	-730	-920	-650	-560	-480	-570	-400	-360	-390	-440	-340	-450	-340	-80	+190	+290	+380	+430
47.2-15.2	-320	-160	-190	+20	+220	+190	-90	-670	-540	-470	-530	-700	-600	-600	-570	-470	-580	-600	-670	-700	-730	-630	-710	-370	-370
106.7-47.2	-340	-360	-260	-120	-190	-310	-260	-370	-140	-120	-190	-200	-230	-130	-140	-100	-160	-210	-350	-480	-390	-410	-350	-330	-240
Overcast days and nights (4 occasions)																									
15.2- 1.1	-300	-270	-130	-170	-210	-220	-270	-290	-240	-160	-280	-190	-290	-250	-180	-220	-320	-330	-250	-170	-150	-10	-10	-10	-160
47.2-15.2	-440	-390	-480	-290	-260	-370	-40	-290	-310	-350	-350	-290	-270	-230	-590	-310	-230	-220	-220	-320	-270	-370	-150	-340	-250
106.7-47.2	-470	-470	-450	-260	-130	-400	-140	-140	-30	0	-10	-90	-30	+20	+50	-80	-90	-130	-150	-90	-30	-200	-250	-320	-190
WINTER																									
Clear days and nights (3 occasions)																									
15.2- 1.1	+370	+340	+450	+500	+400	+380	+440	+470	+310	+250	+20	-80	+60	+50	+110	+110	+90	+260	+290	+380	+410	+400	+280	+290	+180
47.2-15.2	-150	-50	-90	-80	-110	-220	-240	-180	-140	-50	-380	-340	-370	-310	-260	-280	-160	-190	-180	-170	-180	-170	-110	-80	-20
106.7-47.2	-190	-230	-270	-220	-140	-190	-120	-130	-180	-50	-100	-230	-270	-330	-300	-270	-360	-350	-130	-130	-160	-130	-170	-120	-140
Overcast days and nights (21 occasions)																									
15.2- 1.1	-70	-50	-70	-80	-30	-20	-60	-70	-70	-110	-130	-130	-120	-110	-110	-90	-60	-70	-80	-90	-100	-80	-70	-70	-50
47.2-15.2	+80	-110	-70	-80	-70	-80	-50	-20	-30	-70	-100	-120	-100	-100	-70	-90	-70	-30	-30	-30	-20	-40	-50	-40	-40
106.7-47.2	-10	0	+10	-10	-30	-20	-10	-40	-40	-30	-60	-60	-70	-50	-60	-50	-40	-20	-40	-40	-40	-30	-40	-60	-50

NOTE: Mean hourly values of wind velocity ocrresponding to these occasions will be found in Table IV.

G.269040/JMB/5/50/40

TABLE XVII - MAXIMUM HOURLY VALUES OF HUMIDITY LAPSE IN EACH MONTH

(a) Over the height interval 1.1 m. to 15.2 m.

M.R.P. 546

Month	1945					1946					1947					1948				
	Day	Max. Lapse mgms/m^3	G.M.T.	Sky	Wind m/s	Day	Max. Lapse mgms/m^3	G.M.T.	Sky	Wind m/s	Day	Max. Lapse mgms/m^3	G.M.T.	Sky	Wind m/s	Day	Max. Lapse mgms/m^3	G.M.T.	Sky	Wind m/s
Jan.	.....					22	-470	1200	cm	1.8	1	-780	1300	bc	clm	.....				
Feb.	.....					6	-4010	1600	c	7.6	25	-340	1400	bc	0.9	29	-1380	1000	b	clm
Mar.	.....					20	-1080	0900	bc	8.9	7 28	-650	1800 1200	bc c	6.2 4.0	10	-2420	1000	b	5.8
Apr.	.....					13	-1930	1000	bm	1.3	27	-1990	0800	bc	clm	13	-1550	0900	b	---
May	.....					16	-2000	0800	c	clm	30	-5750	1400	b	3.6	26	-1520	0600	bc	5.8
June	.....					17	-2740	0800	c	4.9	3	-3390	1200	b	0.4	26	-3810	0800	c	0.9
July	6	-1410	1200	bc	6.2	3	-2060	1600	bc	2.7	4	-2890	1500	c	2.7	.....				
Aug.	6	-1820	0900	bc	4.0	16	-2250	0900	c	4.0	19	-4810	1800	c	3.1	.....				
Sept.	3	-1740	1300	c	3.6	16	-2700	0900	bc	2.7	3	-2940	0900	b	0.9	.....				
Oct.	25	-1870	0900	c	7.1	8	-1940	1000	bc	2.7	9	-1820	0900	b	clm	.....				
Nov.	3	-1570	1100	c	clm	6	-2100	1100	b	4.5	7	-2390	1000	c	5.8	.....				
Dec.	20	-1520	1300	bc	4.5	2	-1010	0100	c	7.6	10	- 880	1400	b	1.8	.....				

Table XVII (Contd.) - Maximum hourly values of humidity lapse in each month.

(b) Over the height interval 15.2 m. to 47.2 m.

M.R.P. 546

Month	1945					1946					1947					1948				
	Day	Max. Lapse $mgms/m^3$	G.M.T.	Sky	Wind m/s	Day	Max. Lapse $mgms/m^3$	G.M.T.	Sky	Wind m/s	Day	Max. Lapse $mgms/m^3$	G.M.T.	Sky	Wind m/s	Day	Max. Lapse $mgms/m^3$	G.M.T.	Sky	Wind m/s
Jan.						31	-530	1400	c	6.7	3	-980	0500	b	4.5					
Feb.						25	-690	1000	c	clm	24	-830	1200	b	clm	29	-1520	2000	b	1.3
Mar.						30	-940	1100	b	3.1	28	-890	2000	c	1.8	13	-2640	1100	b	clm
Apr.						20	-1510	1700	b	3.6	26	-1290	2300	b	clm	27	-2020	0900	c	clm
May						19	-2420	2200	b	2.2	28	-2060	0700	b	3.1	25	-1380	0700	c	4.9
June						28	-2050	1100	c	3.6	3	-3530	0600	b	clm	8	-1960	1000	c	3.1
July	14	-2510	0800	c	1.8	13	-2450	1600	cTR	clm	29	-2250	1300	bc	5.8					
Aug.	3	-2800	2200	b	clm	13	-1430	2300	bc	2.2	18	-3700	1200	bc	3.6					
Sept.	8	-1350	0700	c	5.8	26	-1260	1700	c	clm	19	-2060	1000	c	1.3					
Oct.	9	-2030	1100	b	6.2	3	-1130	1200	c	2.7	6	-3500	1800	bcf	clm					
Nov.	15	-820	0800	c	2.2	6	-990	1000	b	4.5	6	-4200	1200	bf	clm					
Dec.	20	-770	1300	bc	4.5	20	-810	1200	b	4.0	1	-400	1400	c	2.2					

TABLE XVII (contd.) - Maximum hourly values of humidity lapse in each month.

(c) Over the height interval 47.2m to 106.7m.

M.R.P. 546

Month	1945 Day	Max. Lapse $mgms/m^3$	G.M.T.	Sky	Wind m/s	1946 Day	Max. Lapse $mgms/m^3$	G.M.T.	Sky	Wind m/s	1947 Day	Max. Lapse $mgms/m^3$	G.M.T.	Sky	Wind m/s	1948 Day	Max. Lapse $mgms/m^3$	G.M.T.	Sky	Wind m/s
Jan.	.....					27	-980	1400	b	clm	15	-1320	1800	b	8.5	.....				
Feb.	.....					3	-390	2300	c	11.1	27	-360	1400	c	2.7	29	-1050	1000	b	clm.
Mar.	.....					26	-1520	1000	b	clm	25	-1260	2400	b	6.7	6	-3000	1500	b	0.4
Apr.	.....					13	-1330	0900	b	clm	16	-1050	2100 2400	bm bm	clm 0.9	18	-3190	1000	b	clm
May.	.....					23	-1590	0800	b	0.9	28	-3150	0200	b	0.9	7	-1380	0800	b	1.8
June	.....					7	-1400	0700	bc	clm	24	-3040	0200	b	clm	8	-2600	2100	c	0.9
July	13	-2070	0500	bc	0.4	10	-2460	0100	b	0.4	24	-2500	2200	c	clm	.....				
Aug.	3	-1500	0500	b	0.9	4	-3450	1900	bc	clm	8	-3400	2200	b	clm	.....				
Sept.	10	-1070	0200	c	clm	30	-3300	1900	bc	clm	15	-4070	2400	b	0.4	.....				
Oct.	14	-1660	1200	bc	3.6	3	-1550	1300	c	1.3	6	-4480	1900	bf	clm	.....				
Nov.	3	-1020	1200	bc	3.1	5	-3390	1200	b	clm	6	-1000	0700	c	1.8	.....				
Dec.	17	-1010	0700	c	8.9	26	-570	1200	bc	4.5	1	-1610	1100	bcm	0.9	.....				

TABLE XVIII - MAXIMUM HOURLY VALUES OF HUMIDITY INVERSIONS IN EACH MONTH.

(a) Over the height interval 1.1 m. to 15.2 m.

M.R.P. 546

	1945					1946					1947					1948				
Month	Day	Max. Inv. $m.gms/m^3$	G.M.T.	Sky	Wind m/s	Day	Max. Inv. $m.gms/m^3$	G.M.T.	Sky	Wind m/s	Day	Max. Inv. $m.gms/m^3$	G.M.T.	Sky	Wind m/s	Day	Max. Inv. $m.gms/m^3$	G.M.T.	Sky	Wind m/s
Jan.	.....					8	1650	0100	c	1.8	3	2220	0400	b	0.9	.....				
Feb.	.....					1	750	1300	bc	7.6	24	1310	1200	b	clm	27	1000	2300	b	clm
Mar.	.....					29	1190	1800	b	3.1	17	1000	1300	bc	3.6	13	950	0700	b	1.3
Apr.	.....					15	1550	0500	bcm	1.3	20	1450	0200	b	0.9	18	1910	0300	b	clm
May.	.....					20	1460	0100	b	1.3	24	1710	0100	bf	clm	7	600	0400	b	1.3
																12		1300	c	0.9
June.	.....					7	1860	0100	b	clm	23	2160	0200	bc	clm	26	1210	0400	bc	clm
July	11	1150	2400	b	clm	2	1080	0400	b	0.4	27	2540	0100	bcf	clm	.....				
Aug.	4	1570	0200	b	clm	4	2030	0100	b	clm	9	2420	0400	b	clm	.....				
Sept.	16	2470	1400	bc	9.3	16	2020	0200	b	clm	10	2630	2400	b	clm	.....				
Oct.	9	3000	2100	b	clm	21	1120	2000	bc	1.8	22	3130	0600	b	1.8	.....				
Nov.	4	1970	2400	bf	clm	4	2220	0700	b	clm	1	1850	0700	c	clm	.....				
Dec.	7	1240	1600	cm	clm	21	880	2400	b	clm	8	1160	0100	cf	clm	.....				

TABLE XVIII (contd.) - Maximum hourly values of humidity inversions in each month.

(b) Over the height interval 15.2 m. to 47.2 m.

M.R.P. 546

Month	1945					1946					1947					1948				
	Day	Max. Inv. mgms/m^3	G.M.T.	Sky	Wind m/s	Day	Max. Inv. mgms/m^3	G.M.T.	Sky	Wind m/s	Day	Max. Inv. mgms/m^3	G.M.T.	Sky	Wind m/s	Day	Max. Inv. mgms/m^3	G.M.T.	Sky	Wind. m/s
Jan.	.....					7	1210	2300	bcm	clm	10	630	1000	cpr	clm	.....				
Feb.	.....					5	520	2300	b	3.6	24	610	0800	b	2.2	13	1010	0500	bm	clm
Mar.	.....					26	1190	0600	bm	1.8	10 17	240	0700 1700	cf c	4.5 4.9	7	2050	0200	bff	clm
Apr.	.....					13	1440	0500	bm	clm	16	600	0300	bffs	1.3	18	1620	0400	b	clm
May	.....					20	760	1400	c	4.9	30	2560	1300	b	1.3	11	1790	1400	bc	1.3
June	.....					7	1060	0500	bc	clm	27	2690	2000	b	0.4	11	1210	1400	b	2.7
July	4	240	0500	bc	clm	2	1420	0400	b	0.4	14	2480	1100	bc	clm	.....				
Aug.	12	2010	0500	bc	1.3	16	2120	0500	bc	clm	17	1820	1300	bc	3.6	.....				
Sept.	17	1300	2000	c	1.8	16	3610	0600	bc	clm	5	2430	0500	bm	clm	.....				
Oct.	31	2970	0600	bff	clm	12	1020	0500	bc	3.6	13	2950	0300	bff	clm	.....				
Nov.	5	1660	0300	bf	clm	4	3230	2300	bf	clm	6	1500	0700	OF	1.8	.....				
Dec.	20	20	0900	b	clm	22	1400	0500	bc	clm	1	1150	0900	bm	0.9	.....				

TABLE XVIII (contd.) - Maximum hourly values of humidity inversions in each month.

(c) Over the height interval 47.2 m. to 106.7 m.

M.R.P. 546

Month	1945					1946					1947					1948				
	Day	Max. Inv. mgms/m^3	G.M.T.	Sky	Wind m/s	Day	Max. Inv. mgms/m^3	G.M.T.	Sky	Wind m/s	Day	Max. Inv. mgms/m^3	G.M.T.	Sky	Wind m/s	Day	Max. Inv. mgms/m^3	G.M.T.	Sky	Wind m/s
Jan.	.....					21	1070	2100	bm	0.9	8	720	0200	bcf	1.3	.....				
Feb.	.....					9	590	2300	bc	3.1	24	1190	0900	b	1.8	14	690	0400	bm	1.3
Mar.	.....					30	1620	0400	bff	1.8	22	470	0700	c	6.2	16	1920	1200	c	3.6
Apr.	.....					17	1130	1200	c	6.7	16	1550	0200	bffc	0.9	19	2510	0200	bc	2.2
May	.....					19	990	1600	bc	2.7	31	3300	2100	c	2.2	10	2410	1300	bc	2.2
June	.....					7	1500	0200	bc	clm	3	2230	2100	bc	2.2	5	1720	0900	c	4.5
July	15	1170	1300	bc	8.9	2	1980	0100	bc	clm	27	1710	2400	bc	2.2	.....				
Aug.	4	1880	0500	b	clm	16	1380	0600	c	clm	4	1400	0100	b	clm	.....				
Sept.	8	1110	0100	b	1.8	7	910	0300	c	0.4	4	1160	0400	bm	clm	.....				
Oct.	12	1740	1900	bff	clm	7	590	0600	bc	clm	7	2920	0800	bcm	clm	.....				
Nov.	5	990	0800	bc	2.7	5	2050	0800	bm	clm	6	670	1300	b	clm	.....				
Dec.	14	1230	1900	c	clm	11	1050	0100	b	clm	12	860	0200	c	1.8	.....				

TABLE XIX - PERCENTAGE FREQUENCY OF OCCURRENCE OF HUMIDITY DIFFERENCES, IN MGM./CU. METRE, OF VARIOUS VALUES.

(a) Over the height interval 1.1 m. to 15.2 m.

M.R.P. 546

Month	2410 to 2500	2310 to 2400	2210 to 2300	2110 to 2200	2010 to 2100	1910 to 2000	1810 to 1900	1710 to 1800	1610 to 1700	1510 to 1600	1410 to 1500	1310 to 1400	1210 to 1300	1110 to 1200	1010 to 1100	-910 to 1000	-810 to -900	-710 to -800	-610 to -700	-510 to -600	-410 to -500	-310 to -400	-210 to -300	-110 to -200	-10 to -100	0 to 90	100 to 190	200 to 290	300 to 390	400 to 490	500 to 590	600 to 690	700 to 790	800 to 890	900 to 990	1000 to 1090	1100 to 1190	1200 to 1290	1300 to 1390	1400 to 1490	1500 to 1590	1600 to 1690	1700 to 1790	1800 to 1890	1900 to 1990	2000 to 2090	2100 to 2190	2200 to 2290	2300 to 2390	2400 to 2490	2500 to 2590	2600 to 2690	2700 to 2790	2800 to 2890	2900 to 2990
Jan.	..	..	..	..	..	..	..	..	..	..	..	..	..	..	..	..	..	0.2	..	0.1	0.4	1.2	4.5	13.2	29.1	17.9	11.3	7.7	5.6	4.8	3.6	2.8	2.4	1.1	1.0	0.5	0.2	0.2	0.3	0.2	0.2	0.1	..	..	..	..	..	0.1	..	..	..	..	..	..
Feb.	..	..	..	..	..	..	..	..	..	..	..	..	0.1	..	..	0.1	..	..	0.1	..	0.5	1.1	4.8	7.5	12.4	27.0	20.0	8.3	2.6	2.3	1.4	0.7	0.5	0.3	0.3	0.1	0.1	..	..	0.1	..	..	..	..	..	..	..	..	..	..	..	..	..	..	..	..
Mar.	0.1	..	..	..	..	..	..	..	..	..	..	..	..	0.1	0.1	0.1	..	0.3	0.2	0.6	0.8	1.4	2.4	3.8	7.9	15.0	21.2	13.0	7.1	4.8	5.1	3.2	2.0	1.7	0.9	0.4	0.4	0.6	0.2	0.1	0.1	0.1	0.2	0.1	..	0.1	..	..	..	..	..	..	..	..	..
Apr.	..	..	..	..	..	0.1	..	0.1	0.1	0.1	0.1	0.2	0.1	0.2	0.4	0.5	1.0	1.0	1.9	2.8	5.0	7.6	10.6	14.1	13.3	12.5	9.3	5.9	3.6	3.1	2.8	1.3	0.8	0.5	0.3	0.4	0.3	0.3	0.1	0.2	0.1	..	..	..	0.1	..	..	..	..	..	..	..	..	..	..
May [1]	..	0.2	0.2	0.1	..	0.1	0.4	0.3	0.2	0.7	0.7	0.9	1.0	1.2	1.7	2.2	2.5	3.3	5.0	4.1	5.8	7.4	9.1	9.8	9.9	10.0	7.4	4.9	2.9	1.9	1.5	0.9	0.8	0.6	0.6	0.2	0.2	0.3	0.2	0.2	..	..	..	..	..	..	..	..	..	..	..	..	..	..	..
June [2]	0.1	0.3	0.3	0.5	0.6	0.3	0.6	0.3	0.6	0.6	1.0	1.2	2.0	2.3	3.5	4.2	4.6	5.7	5.8	8.4	8.4	8.4	8.3	7.1	5.7	5.0	2.8	1.6	1.1	1.2	0.8	0.7	0.7	0.3	0.2	0.3	0.4	0.7	0.2	0.2	0.2	0.1	0.2	0.2	0.1	0.1	0.1	..	..	..	..	..	..	..
July [3]	..	..	..	..	0.2	0.1	..	0.1	0.2	0.2	0.7	0.7	1.1	0.8	1.8	3.0	3.6	4.5	6.1	5.5	6.2	7.5	8.2	8.2	8.9	6.9	6.0	4.2	2.3	1.7	1.6	1.5	0.7	1.0	0.7	0.9	0.7	1.1	0.7	0.5	0.2	0.5	0.2	0.2	0.1	0.3	0.1	0.1	0.1	0.1	0.1	..	..	..	..
Aug. [4]	0.1	..	0.1	0.3	0.1	0.1	0.3	0.1	0.3	0.2	0.4	0.8	0.6	1.3	1.8	2.8	3.8	5.1	6.7	6.7	9.0	10.1	9.0	9.6	6.4	4.4	3.9	3.1	2.2	1.7	1.5	1.6	1.1	1.1	0.7	0.4	0.6	0.4	0.5	0.3	0.2	0.2	..	0.2	0.2	0.1	0.1	0.1	..	0.1	..	..	..	..
Sept. [5]	..	..	0.1	0.1	0.1	..	0.1	0.1	0.2	0.1	0.2	0.3	0.7	1.2	1.6	2.3	3.4	2.9	5.0	6.3	7.6	9.3	8.6	6.7	6.0	6.4	6.9	5.8	4.1	2.3	2.1	1.7	1.4	1.1	0.9	0.8	0.8	0.5	0.3	0.3	0.4	0.3	0.3	0.2	0.3	0.2	..	0.1	0.1	0.1	0.1	0.1	..	..	..
Oct. [6]	..	..	..	..	..	0.1	0.1	0.1	..	0.2	0.1	0.1	0.3	0.6	0.9	1.2	2.0	2.2	3.2	4.9	5.7	10.1	8.3	8.9	8.0	8.7	6.3	4.3	3.7	3.0	2.8	2.5	2.0	1.2	1.5	0.9	1.1	0.3	0.8	0.9	0.7	0.8	0.3	0.4	0.2	0.1	0.2	0.1	0.1	0.2	0.1	..	..	..	0.1
Nov.	..	0.1	..	..	0.1	..	0.1	0.1	0.1	0.1	0.1	..	0.1	0.1	0.1	0.1	0.2	0.9	0.7	1.5	1.6	4.3	7.7	17.1	25.2	19.0	7.6	2.8	2.1	2.2	2.0	0.5	0.9	0.8	0.6	0.4	0.3	0.1	0.1	0.1	0.2	..	0.2	0.1	0.1	..	..	0.1	..	..	..	..	..	..
Dec.	..	..	..	..	..	..	..	..	..	0.1	..	..	..	0.1	0.1	..	0.1	0.1	0.2	0.7	1.6	3.5	10.1	13.9	21.2	17.7	12.4	6.7	5.0	1.9	1.5	1.4	0.9	0.3	0.3	0.1	0.1	0.1	..	..	..	..	..	..	..	..	..	..	..	..	..	..	..	..	..	..
Year	..	0.1	0.1	0.1	0.1	0.1	0.1	0.1	0.1	0.2	0.3	0.4	0.5	0.7	1.0	1.4	1.9	2.3	3.0	3.6	4.6	6.5	8.1	10.7	14.1	13.0	8.0	4.9	3.3	2.4	1.9	1.3	1.1	0.8	0.6	0.5	0.4	0.4	0.3	0.2	0.2	0.2	0.1	0.1	0.1	0.1	..	..	..	..	..	..	..	..	..

NOTES: - (1) A further 0.2% of May observations fall between -2510 and -3100.
(2) " " 1.3% " June " " " -2510 " -3900
(3) " " 0.1% " July " " " -2510 " -2900
(4) " " 0.3% " Aug. " " " -2510 " -4300
(5) " " 0.4% " Sept. " " " -2510 " -3000
(6) " " 0.2% " Oct. " " " +3000 " +3190

TABLE XIX contd. - Percentage frequency of occurrence of humidity differences (in mgm./cu.m.) of various values.

(b) Over the height interval 15.2 m. to 47.2 m.

Table XIX (b)

M.R.P. 546

Month	-2410 to -2500	-2310 to -2400	-2210 to -2300	-2110 to -2200	-2010 to -2100	-1910 to -2000	-1810 to -1900	-1710 to -1800	-1610 to -1700	-1510 to -1600	-1410 to -1500	-1310 to -1400	-1210 to -1300	-1110 to -1200	-1010 to -1100	-910 to -1000	-810 to -900	-710 to -800	-610 to -700	-510 to -600	-410 to -500	-310 to -400	-210 to -300	-110 to -200	-10 to -100
Jan.	..	..	..	..	..	..	..	..	..	..	..	..	..	..	..	0.2	0.2	0.3	0.6	1.7	5.0	11.3	16.0	18.6	21.8
Feb.	..	..	..	..	..	..	..	..	..	0.1	0.1	..	..	..	0.1	0.2	0.1	0.3	0.5	0.4	1.0	2.8	7.5	24.2	16.7
Mar.	..	..	0.1	..	..	..	..	..	..	..	..	0.2	0.1	0.1	0.1	0.2	0.5	0.5	1.1	2.3	3.1	5.3	9.4	13.7	15.0
Apr.	..	..	..	..	0.1	..	..	..	..	0.1	..	0.1	0.1	0.1	0.3	0.4	0.6	0.7	0.7	1.6	2.1	3.6	6.8	12.2	17.0
May	..	..	..	..	0.1	..	..	0.1	..	..	0.4	0.2	0.5	0.3	0.8	1.0	1.3	1.6	3.4	5.1	7.8	10.4	14.2	15.2	13.1
June	0.1	0.1	..	..	0.3	0.2	0.2	0.1	0.2	0.1	0.2	0.3	0.6	0.5	1.0	1.1	1.6	2.1	3.4	4.9	8.4	10.5	15.1	13.6	10.7
July	0.2	0.1	0.1	0.2	0.4	0.1	0.4	0.5	0.7	0.5	0.8	1.3	1.7	1.4	2.5	2.9	3.3	3.7	6.2	6.7	9.0	13.2	14.1	12.6	7.2
Aug.	0.1	..	..	..	..	0.1	0.3	..	0.2	0.1	0.2	0.4	0.5	0.7	1.1	1.5	2.2	2.9	4.1	6.5	7.3	11.3	13.7	13.7	10.2
Sept.	..	..	..	..	0.1	0.1	0.1	0.1	..	0.1	0.1	0.2	0.3	0.8	1.0	1.3	0.7	2.7	3.9	6.4	8.7	8.8	12.0	11.4	8.7
Oct.	..	..	..	..	0.2	..	0.1	..	0.1	..	0.2	0.2	0.2	0.1	0.3	0.3	0.9	0.4	1.1	2.8	4.2	7.4	12.5	12.4	10.0
Nov.	..	..	..	..	..	..	..	..	..	..	..	..	..	..	..	0.1	0.2	0.2	0.2	0.3	0.5	1.9	4.8	11.3	17.7
Dec.	..	..	..	..	..	..	..	..	..	..	..	..	..	..	..	..	0.1	0.1	0.1	0.1	0.4	0.9	2.3	10.4	34.7
Year	..	..	..	..	0.1	..	0.1	0.1	0.1	0.1	0.2	0.2	0.3	0.3	0.6	0.8	1.0	1.3	2.2	3.3	4.9	7.2	10.6	14.0	14.2

Month	0 to 100	100 to 200	200 to 300	300 to 400	400 to 500	500 to 600	600 to 700	700 to 800	800 to 900	900 to 1000	1000 to 1100	1100 to 1200	1200 to 1300	1300 to 1400	1400 to 1500	1500 to 1600	1600 to 1700	1700 to 1800	1800 to 1900	1900 to 1990	2000 to 2090	2100 to 2190	2200 to 2290	2300 to 2390	2400 to 2490	2500 to 2590	2600 to 2690	2700 to 2790	2800 to 2890	2900 to 2990
Jan.	4.3	1.9	1.1	0.4	0.2	0.2	0.1	..	0.1	..	..	0.1	..	..	..	..	..	..	..	..	..	..	..	..	..	..	..	..	..
Feb.	13.1	3.4	1.2	0.4	0.3	0.1	..	0.1	0.1	0.1	..	..	..	..	..	..	..	..	..	..	..	..	..	..	..	..	..	..	..	..
Mar.	12.9	9.3	4.9	2.5	2.2	1.3	0.8	0.4	0.2	0.3	0.2	0.1	0.1	0.2	..	0.2	0.1	0.2	0.1	0.1	..	..	..	..	..	..	..	..	..
Apr.	16.3	7.9	3.4	2.3	1.3	0.9	0.5	0.3	0.3	0.2	0.2	0.2	..	0.1	..	0.1	..	..	..	..	..	..	..	..	..	..	..	..	..	..
May	6.8	2.9	2.1	0.8	0.8	0.5	0.4	0.2	0.1	..	0.1	..	..	..	..	..	0.1	0.1	..	..	..	..	..	..	..	..	..	..	..	..
June	6.6	3.3	1.6	1.9	0.8	0.3	0.4	0.3	0.3	0.2	0.1	0.1	0.1	..	0.1	..	..	0.1	0.1	..	..	..	..	..	0.1	..	0.1	..	..	..
July	1.8	1.8	0.8	0.8	0.2	0.2	0.3	0.1	0.2	..	0.1	0.1	0.1	0.1	..	0.1	..	..	..	..	..	..	..	..	0.1	..	..	..	..	..
Aug.	4.7	2.7	1.8	1.0	0.8	0.5	0.5	0.5	0.4	0.2	0.3	0.3	0.1	0.1	0.1	0.1	0.2	0.2	..	0.1	0.1	..	..	..	..	..	..	..	..	..
Sept.	6.3	5.5	2.7	2.3	1.7	0.8	0.4	0.5	0.2	0.3	0.1	0.1	0.1	0.2	0.1	0.2	0.1	0.1	0.1	0.2	0.2	..	0.1	0.1	..	..	..	..	0.1	..
Oct.	5.5	5.7	4.8	7.0	3.5	3.1	2.5	1.2	1.2	0.7	0.4	0.2	0.4	0.4	0.4	0.2	0.3	0.2	0.1	0.2	0.1	0.4	0.4	0.1	0.2	0.2	..	0.1	0.1	..
Nov.	14.0	8.8	6.0	5.4	2.5	1.5	0.8	0.3	0.4	0.5	0.1	0.4	0.3	0.3	0.2	0.2	0.1	..	0.1	0.1	0.1	0.1	..	0.2	..	..	..	0.1	..	..
Dec.	13.4	8.2	6.0	4.8	2.9	1.1	0.7	0.7	0.6	0.1	0.2	0.2	0.1	0.1	..	0.1	..	0.1	..	0.1	..	..	..	..	..	..	..	..	..	..
Year	8.9	5.3	3.1	2.5	1.5	0.9	0.6	0.4	0.3	0.2	0.1	0.1	0.1	0.1	0.1	0.1	0.1	0.1	..	..	..	..	..	..	..	..	..	..	..	..

NOTES: - (1) A further 0.1% of March observations fall between -2510 and -2700
(2) " " 0.1% " June " " " -2510 " -3600
(3) " " 0.1% " July " " " -2510 " -2600
(4) " " 0.4% " August " " " -2510 " -3700
(5) " " 0.1% " September " " " +3000 " +3690
(6) " " 0.2% " October " " " -2510 " -3500
(7) " " 0.2% " November " " " -2510 " -4200 and 0.2% between +3000 and +3290

TABLE XIX contd. - Percentage frequency of occurrence of humidity differences (in $gm./cu.m.$) of various values.

(c) Over the height interval 47.2 m. to 106.7 m.

TABLE XIX (c)

M.R.P. 546

Month	-2910 to -3000	-2810 to -2900	-2710 to -2800	-2610 to -2700	-2510 to -2600	-2410 to -2500	-2310 to -2400	-2210 to -2300	-2110 to -2200	-2010 to -2100	-1910 to -2000	-1810 to -1900	-1710 to -1800	-1610 to -1700	-1510 to -1600	-1410 to -1500	-1310 to -1400	-1210 to -1300	-1110 to -1200	-1010 to -1100	-910 to -1000	-810 to -900	-710 to -800	-610 to -700	-510 to -600	-410 to -500	-310 to -400	-210 to -300	-110 to -200	-10 to -100	0 to 90	100 to 190	200 to 290	300 to 390	400 to 490	500 to 590	600 to 690	700 to 790	800 to 890	900 to 990	1000 to 1090	1100 to 1190	1200 to 1290	1300 to 1390	1400 to 1490	1500 to 1590	1600 to 1690	1700 to 1790	1800 to 1890	1900 to 1990	2000 to 2090	2100 to 2190	2200 to 2290	2300 to 2390	2400 to 2490
Jan.	..	..	..	..	..	..	..	..	..	..	..	..	..	..	..	..	0.1	..	..	..	0.4	0.3	0.3	0.7	1.0	1.7	3.2	6.0	9.2	31.5	22.7	6.7	2.3	0.9	0.2	0.3	0.3	0.3	0.1	0.1	..	0.2	..	..	..	..	..	..	..	..	..	..	..	..
Feb.	..	..	..	..	..	..	..	..	..	..	..	..	..	..	..	..	..	..	..	0.1	0.2	0.2	0.1	0.2	..	0.4	0.8	3.8	12.8	42.0	23.5	11.0	2.8	1.4	0.3	0.2	0.2	..	..	..	..	0.1	..	..	..	..	..	..	..	..	..	..	..	..	..
Mar.	0.1	..	..	..	..	0.1	..	..	..	..	..	..	..	0.1	0.3	..	0.1	0.2	0.2	0.2	0.2	0.1	0.8	1.0	1.6	2.3	3.4	7.3	10.1	25.5	15.3	19.6	5.4	3.8	2.5	1.5	0.6	0.4	0.6	0.3	0.3	0.1	0.1	0.2	0.1	..	0.1	0.1	..	0.1	..	..	..	..	..
Apr.	..	..	..	0.1	..	..	..	..	..	..	..	..	..	..	0.1	..	0.1	0.1	0.3	0.3	0.1	0.3	0.7	1.1	1.5	1.0	3.5	8.9	18.2	16.8	15.4	9.9	6.8	4.8	2.8	1.7	1.0	0.5	0.4	0.2	0.3	0.2	0.2	..	0.1	0.1	0.1	0.1	..	..	..	..	..	..
May	..	..	..	..	0.1	..	..	..	..	..	..	..	0.1	..	0.1	0.1	0.1	0.1	0.2	0.4	0.5	1.0	1.1	1.7	2.2	2.9	4.4	7.1	8.9	14.7	15.1	12.5	9.5	5.4	3.7	1.3	1.3	0.9	0.8	0.6	0.4	0.3	0.4	0.1	0.3	0.4	0.2	0.1	0.1	0.1	..	0.1	..	..	0.1
June	0.1	..	0.1	..	0.1	..	..	..	..	...	0.1	..	0.2	0.1	0.1	0.2	0.2	0.2	0.3	0.5	0.6	0.6	1.1	1.6	1.8	2.5	5.8	8.0	11.0	10.1	15.2	13.9	7.8	5.7	2.9	1.5	1.1	1.0	1.0	0.4	0.2	0.5	0.2	0.1	0.1	0.3	0.1	0.1	..	0.1	0.1	..	0.1	..	..
July	..	..	..	..	...	0.2	0.2	0.1	..	0.2	0.1	0.3	0.1	0.1	0.3	0.4	0.4	0.6	0.6	1.0	1.0	1.2	1.5	1.9	3.2	3.3	4.9	7.7	12.7	16.3	14.0	10.8	6.2	3.8	2.5	1.2	0.8	0.7	0.1	0.1	0.2	0.2	0.1	0.3	0.2	..	..	0.1	..	0.1	..	..	..	..	..
Aug.	..	..	..	0.1	..	0.2	..	0.1	0.1	0.1	0.1	..	0.2	0.2	0.4	0.2	0.3	0.5	1.1	0.8	1.4	1.6	2.6	3.5	4.7	6.0	9.9	12.7	14.4	12.6	9.6	5.6	3.6	2.5	1.4	0.8	0.6	0.7	0.5	0.1	0.2	0.1	..	0.2	0.1	0.1	..	..	0.1	..	..	..	..	..
Sept.	..	0.1	0.2	0.2	..	..	0.1	0.1	0.1	0.2	0.1	0.2	0.2	0.2	0.5	0.3	0.4	0.1	0.6	0.9	1.1	1.4	2.1	2.7	3.9	7.3	12.7	14.9	13.1	10.9	8.8	5.6	3.2	2.8	1.3	1.9	0.7	0.6	0.3	0.3	..	0.2	..	..	..	..	..	..	..	..	..	..	..	..
Oct.	..	0.1	..	..	0.1	0.1	..	..	0.1	0.1	0.2	0.1	0.1	0.3	0.2	0.1	0.3	0.3	0.5	0.3	0.9	1.4	2.2	2.7	6.1	10.9	14.4	17.4	13.6	9.7	6.9	3.8	1.8	1.2	0.7	0.9	0.4	0.1	0.2	0.2	0.1	0.2	0.2	0.2	0.2	..	0.1	0.1	..	..	..	0.1	..	..	..
Nov.	..	..	..	..	..	..	..	..	..	..	..	0.1	0.1	..	..	..	0.1	..	0.1	0.2	0.4	0.2	0.3	0.2	1.0	1.2	3.0	6.1	15.9	27.8	28.6	8.7	3.2	0.9	0.4	0.5	0.4	0.2	0.3	0.1	0.1	..	..	..	0.1	..	..	..	..	0.1	..	..	..	..	..
Dec.	..	..	..	..	..	..	..	..	..	..	..	..	..	0.1	..	0.1	0.1	..	0.1	0.1	..	0.1	0.1	0.1	0.3	0.4	1.4	2.5	12.4	37.0	29.6	8.3	3.2	1.6	0.8	0.9	0.1	0.3	0.1	0.1	0.1	..	0.1	..	..	..	..	..	..	..	..	..	..	..
Year	..	..	..	..	..	0.1	..	..	..	..	..	0.1	0.1	0.1	0.2	0.1	0.2	0.2	0.4	0.4	0.6	0.7	1.1	1.5	2.3	3.4	5.9	8.7	13.9	24.2	16.8	8.9	4.8	3.0	1.7	1.1	0.6	0.5	0.4	0.2	0.2	0.2	0.1	0.1	0.1	0.1	..	..	..	..	..	..	..	..

NOTES:- (1) A further 0.1% of April observations fall between -3010 and -3200 and 0.1% between +2500 and +2590.
(2) " " 0.1% " May " " " +2500 and +3090
(3) " " 0.1% " June " " " -3010 and -3100
(4) " " 0.4% " August " " " -3010 and -3500
(5) " " 0.3% " September " " " -3010 and -4100
(6) " " 0.4% " October " " " -3010 and -4500 and 0.2% between +2500 and +2990.
(7) " " 0.2% " November " " " -3010 and -3400.

TABLE XX - MEAN HOURLY VALUES OF HUMIDITY IN MGM. /CU.METRE AT A HEIGHT OF 1.1 M. FOR EACH MONTH

M.R.P.546

Month	Hour G.M.T.																						
	0100	0200	0300	0400	0500	0600	0700	0800	0900	1000	1100	1200	1300	1400	1500	1600	1700	1800	1900	2000	2100	2200	2300	2400
Jan.	4650	4620	4580	4520	4550	4560	4460	4400	4510	4710	4890	4920	5010	5000	4920	4780	4640	4690	4750	4780	4750	4750	4810	4830
Feb.	4430	4430	4440	4460	4450	4450	4420	4470	4670	4860	4880	4920	4930	4850	4780	4720	4600	4530	4490	4490	4450	4400	4360	4320
Mar.	5110	5070	5070	5070	5080	5060	5180	5640	6150	6250	6110	5860	5720	5730	5680	5530	5460	5280	5210	5220	5190	5220	5200	5220
Apr.	5490	5430	5400	5350	5400	5640	6240	6660	6550	6330	6220	6160	6000	5890	5830	5790	5690	5580	5580	5560	5640	5660	5590	5530
May	6720	6700	6680	6600	6770	7460	7950	7990	7700	7550	7550	7630	7630	7540	7390	7270	7070	6920	6890	6730	6800	6790	6810	6810
June	8320	8230	8220	8260	8680	9440	9910	9920	9950	9430	9340	9440	9460	9370	9220	9140	9130	9080	8990	8790	8650	8620	8540	8430
July	9800	9590	9540	9470	9710	10290	11000	11100	11000	11120	11330	11340	11360	11410	11250	11130	11020	10830	10710	10450	10300	10130	10040	9980
Aug.	10090	9980	9860	9790	9680	10460	11380	11690	11240	10750	10640	10550	10320	10340	10220	10240	10400	10570	10560	10350	10330	10310	10240	10130
Sept.	9510	9370	9340	9270	9320	9450	9970	10480	10850	10580	10360	10380	10310	10310	10130	9940	9890	9790	9630	9500	9520	9580	9470	9450
Oct.	7530	7500	7450	7350	7310	7260	7500	8130	8620	8700	8480	8440	8330	8250	8200	8130	7970	7790	7690	7600	7550	7540	7620	7550
Nov.	6130	6170	6170	6220	6210	6200	6200	6330	6710	7020	7000	6870	6820	6700	6600	6400	6240	6310	6260	6240	6130	6150	6180	6150
Dec.	5550	5550	5570	5630	5570	5530	5500	5470	5520	5740	6010	6120	6130	6010	5890	5700	5600	5600	5570	5550	5490	5490	5470	5510

TABLE XXI - MEAN HOURLY VALUES OF HUMIDITY IN MGM. /CU. METRE AT A HEIGHT OF 1.1 M. FOR CLEAR AND OVERCAST DAYS IN SUMMER AND WINTER

	Hour G.M.T.																						
	0000	0100	0200	0300	0400	0500	0600	0700	0800	0900	1000	1100	1200	1300	1400	1500	1600	1700	1800	1900	2000	2100	2200	2300	2400
SUMMER																									
Clear	9670	9550	9480	9370	9280	9520	10680	12420	12590	11780	11180	11060	10470	10250	10090	9950	10200	10270	10430	10440	10470	10080	10210	10170	10270
O'Cast	10650	10700	10370	10190	10260	10140	10170	10190	10180	10040	9850	9710	9970	10030	10180	10400	10990	11000	10750	10800	10280	10630	10140	10190	9650
WINTER																									
Clear	4780	4930	4770	4740	4790	4760	4660	4540	4710	4980	5480	5540	5450	5450	5430	5310	5180	4970	5050	5000	4850	4760	4840	4840	4950
O'cast	5290	5320	5350	5330	5280	5190	5170	5140	5150	5250	5410	5470	5490	5510	5450	5440	5400	5340	5350	5350	5390	5400	5450	5420	5390

TABLE XXII - DIURNAL RANGE OF HUMIDITY AT FOUR HEIGHTS

Month	Mean diurnal range in mgm./cu.m. at stated heights			
	1.1 m.	15.2 m.	47.2 m.	106.7 m.
January	610	480	480	540
February	610	500	500	470
March	1190	860	60	520
April	1200	800	660	710
May	1390	770	750	690
June	1700	890	710	720
July	1940	960	820	790
August	2900	1160	1180	1120
September	1580	900	750	650
October	1440	750	450	480
November	890	500	420	380
December	660	620	660	690
SUMMER				
Clear	3310	2130	2040	2070
Overcast	1350	1180	1230	1300
WINTER				
Clear	1000	760	770	440
Overcast	370	330	280	270

TABLE XXIII - TIMES OF OCCURRENCE OF MAXIMUM HUMIDITY AT VARIOUS HEIGHTS.

M.R.L. 546

Month	G.M.T. of maximum humidity at stated heights.			
	1.1 m.	15.2 m.	47.2m.	106.7 m.
Mean June	0730 (0)	0730 (5)	0735 (25)?	0800?
Mean December	1233 (15)	1248 (21)	1309 (6)	1315
Clear Summer	0736 (-3)	0733 (6)	0739 (6)	0745
Overcast Winter	1242 (23)	1305 (7)	1312 (6)?	1318?

M.R.P.

TABLE XXIV. Mean hourly values of Humidity at 1.1m and Mean hourly values of lapse rate of Humidity on occasions of Snow Cover.

M.R.P. 546

Time		01	02	03	04	05	06	07	08	09	10	11	12	13	14	15	16	17	18	19	20	21	22	23	24
Mean Humidity at 1.1m mgm./cu.m.		2830	2800	2790	2790	2760	2730	2660	2650	2740	2830	2990	2990	3060	3050	2980	2920	2850	2830	2760	2790	2830	2810	2830	2850
Lapse of Humidity	15.2m -1.1m	130	150	120	90	70	50	70	70	50	20	20	70	-60	-70	-50	-10	10	0	40	20	20	20	70	100
	47.2m - 15.2m	-70	-70	-90	-110	-110	-80	-60	-30	-60	-60	-120	-180	-140	-110	-110	-80	-110	-100	-90	-120	-100	-80	-100	-90
	106.7m - 47.2m	-60	-60	-70	-40	-50	-50	-90	-50	10	-30	-90	-100	-80	-70	-70	-90	-110	-100	-100	-90	-110	-60	-60	-60

M.R.P. 546.

View from instrument tower looking W.

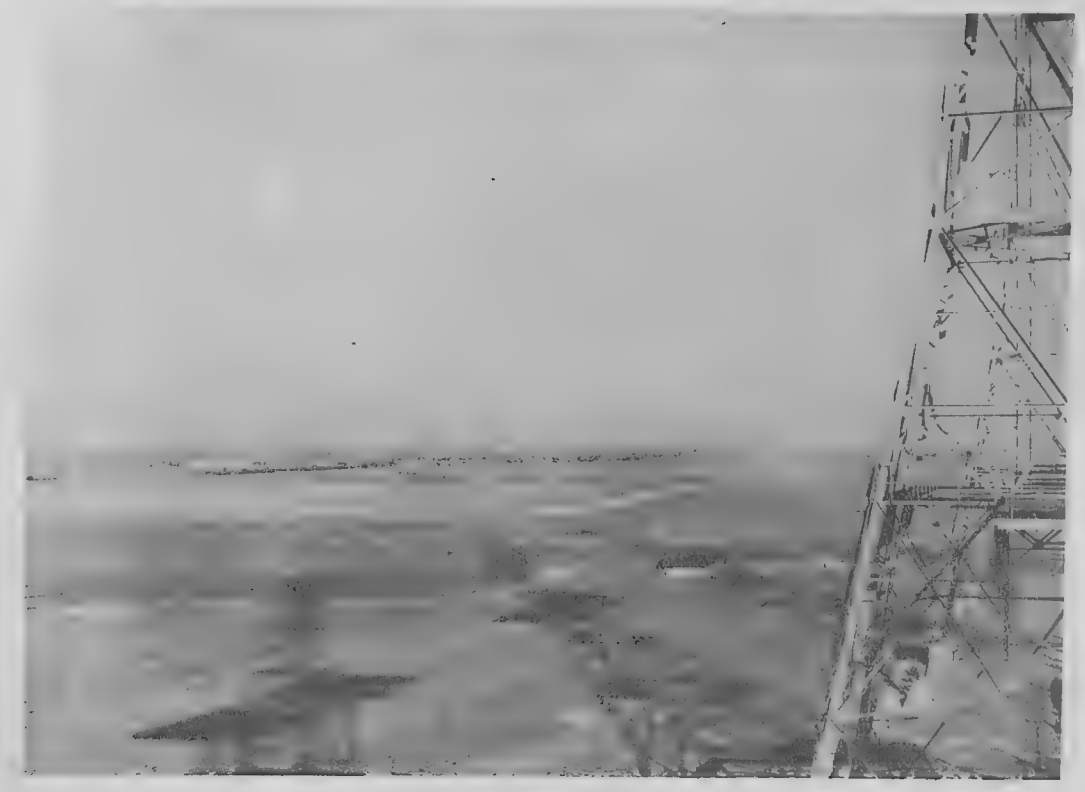

View from instrument tower looking N.E.

Plate I.

M.R.P. 546.

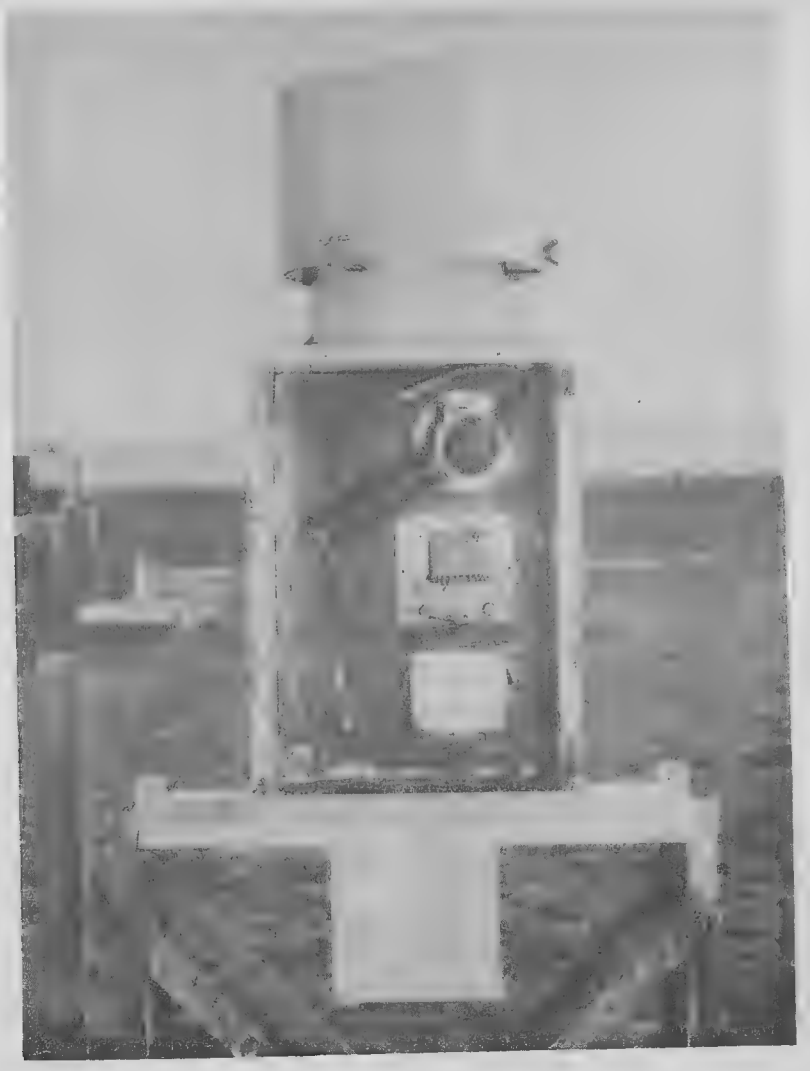

Arrangement of thermometer and humidity element in aspirated screen. (Dust cover of upper element removed)

Device for retraction of screen (50 ft. level)

Plate 2.

M.R.P. 546.

Diagram A.– Circuit Diagram for Gregory Humidiometer.

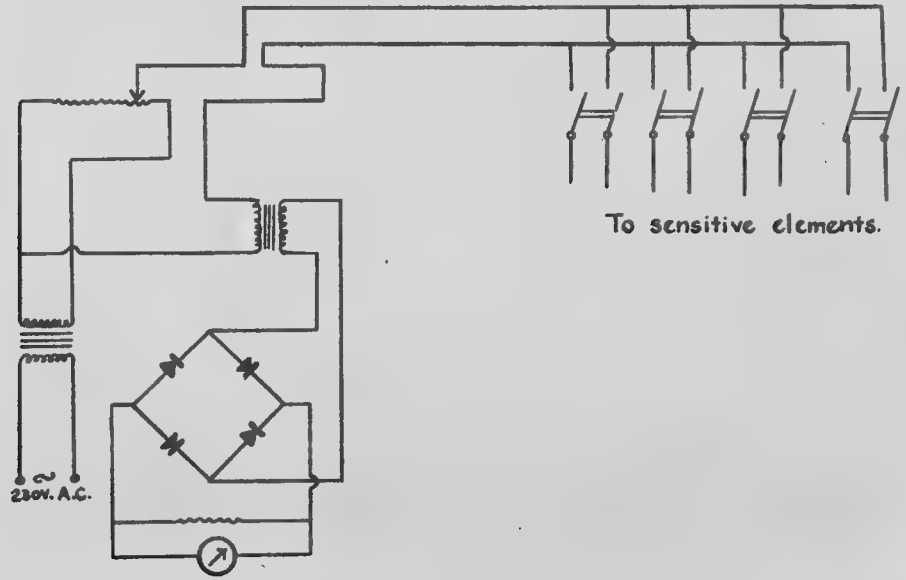

FIG. 1. DIURNAL VARIATION OF LAPSE OF TEMPERATURE FOR EACH MONTH.

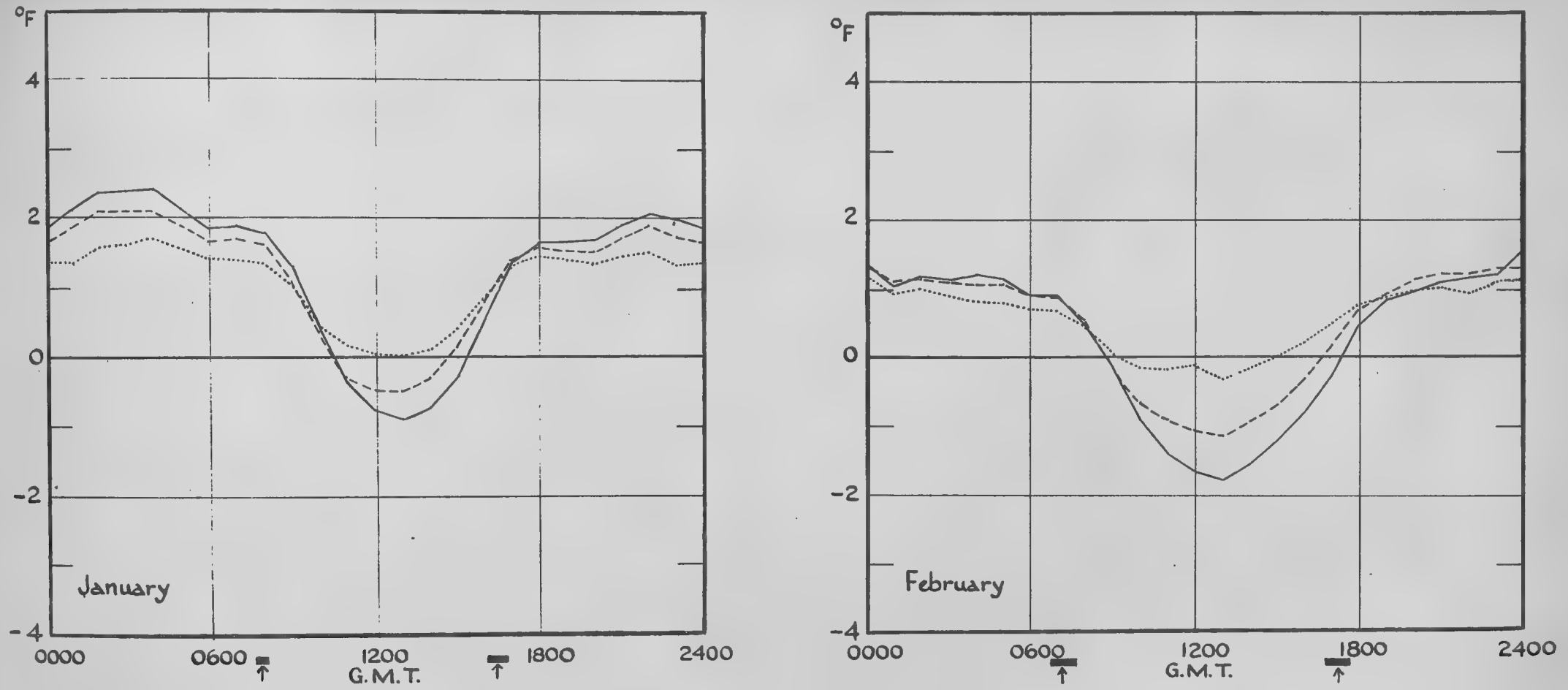

The curves show the temperature differences over the following intervals

..... 15·2 – 1·1 m. ------ 47·2 – 1·1 m. —— 106·7 – 1·1 m.

The arrows indicate times of sunrise and sunset, the limits for each month being shown by the length of the bar immediately above the arrow.

M.R.P. 5146.

FIG. 1 cont.

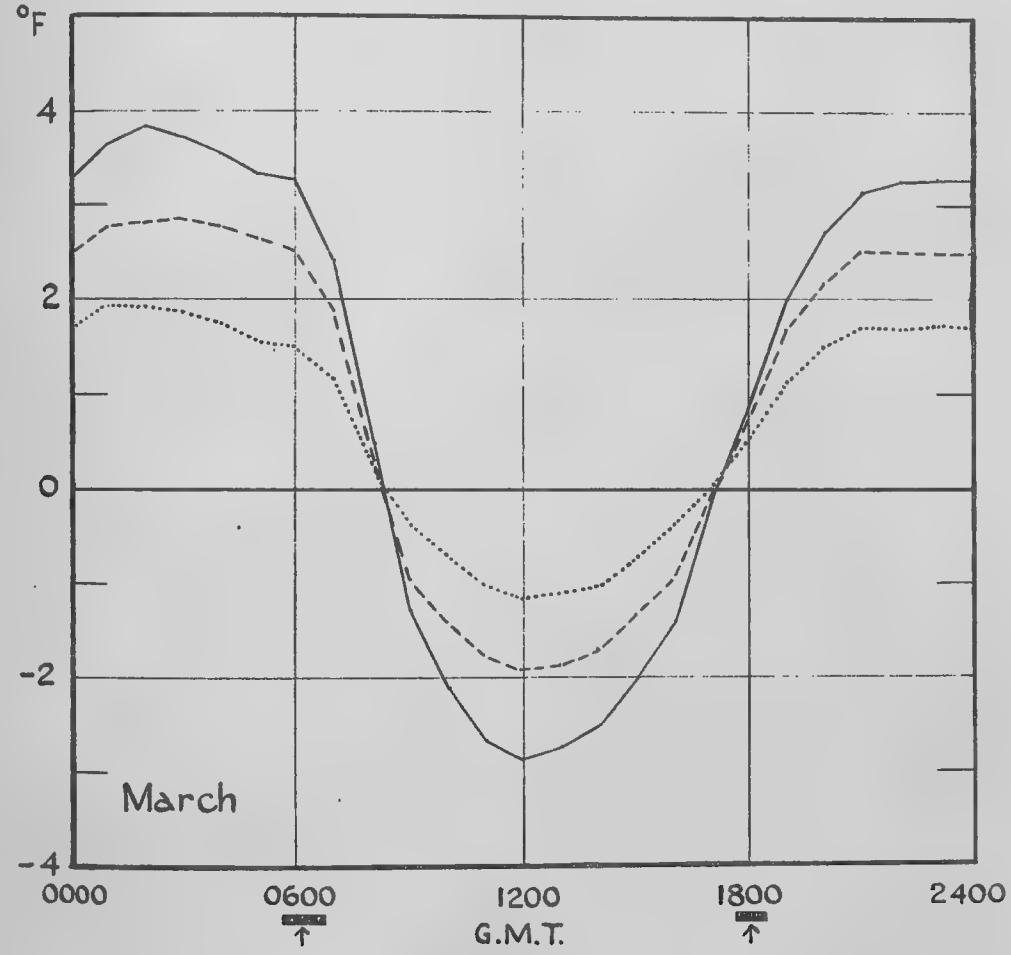

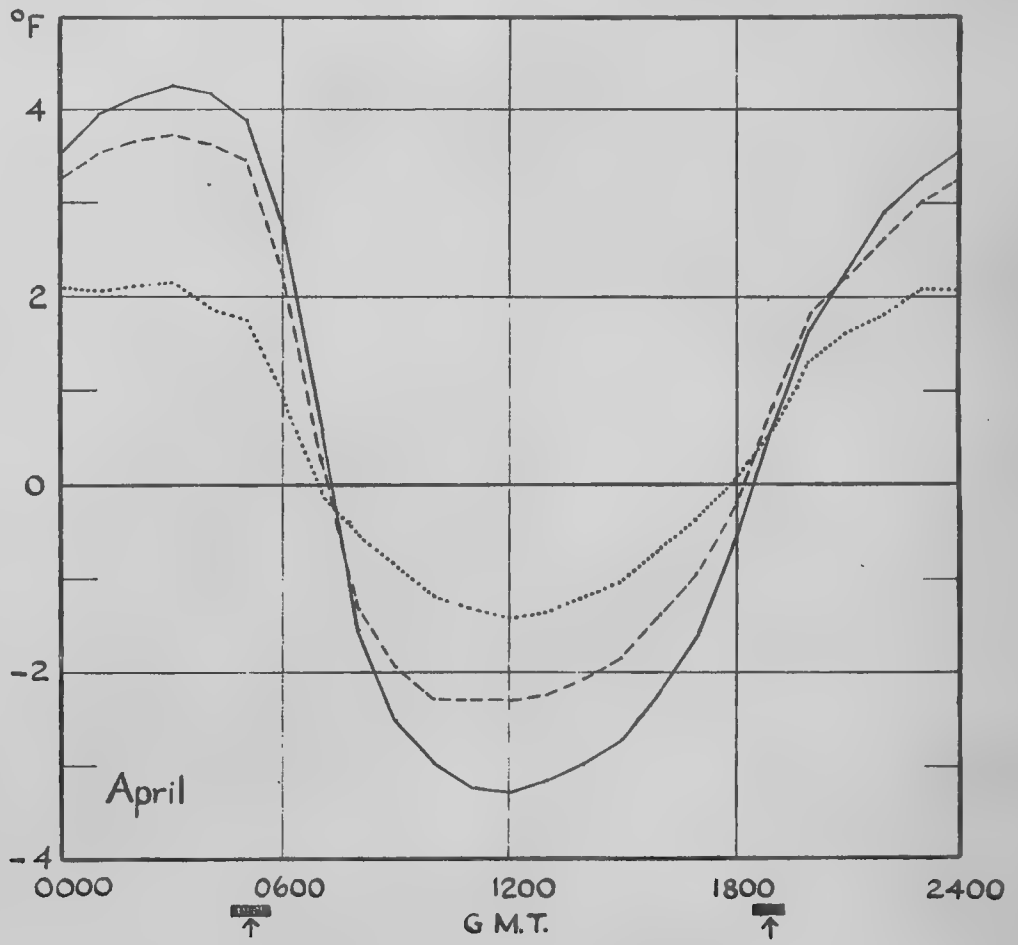

FIG. 1. cont.

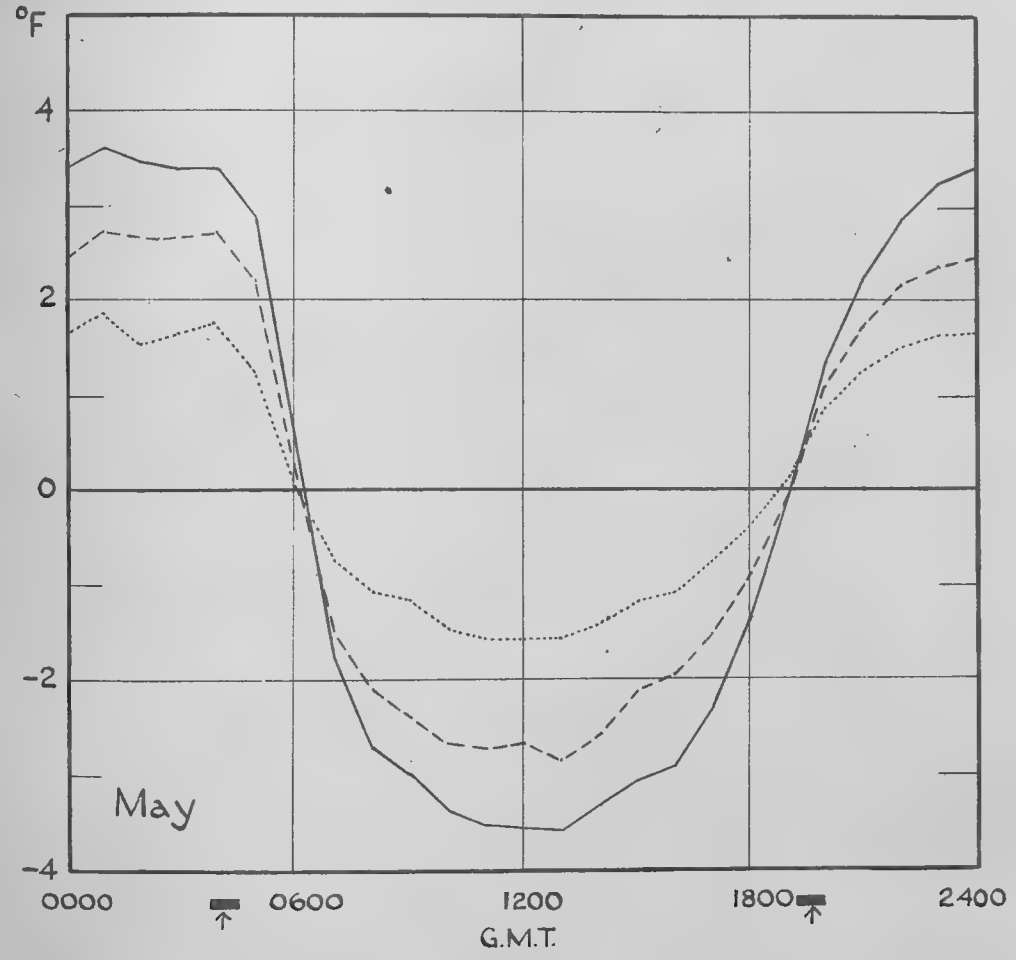
°F
4
2
0
-2
-4
May
0000
0600
1200
1800
2400
G.M.T.

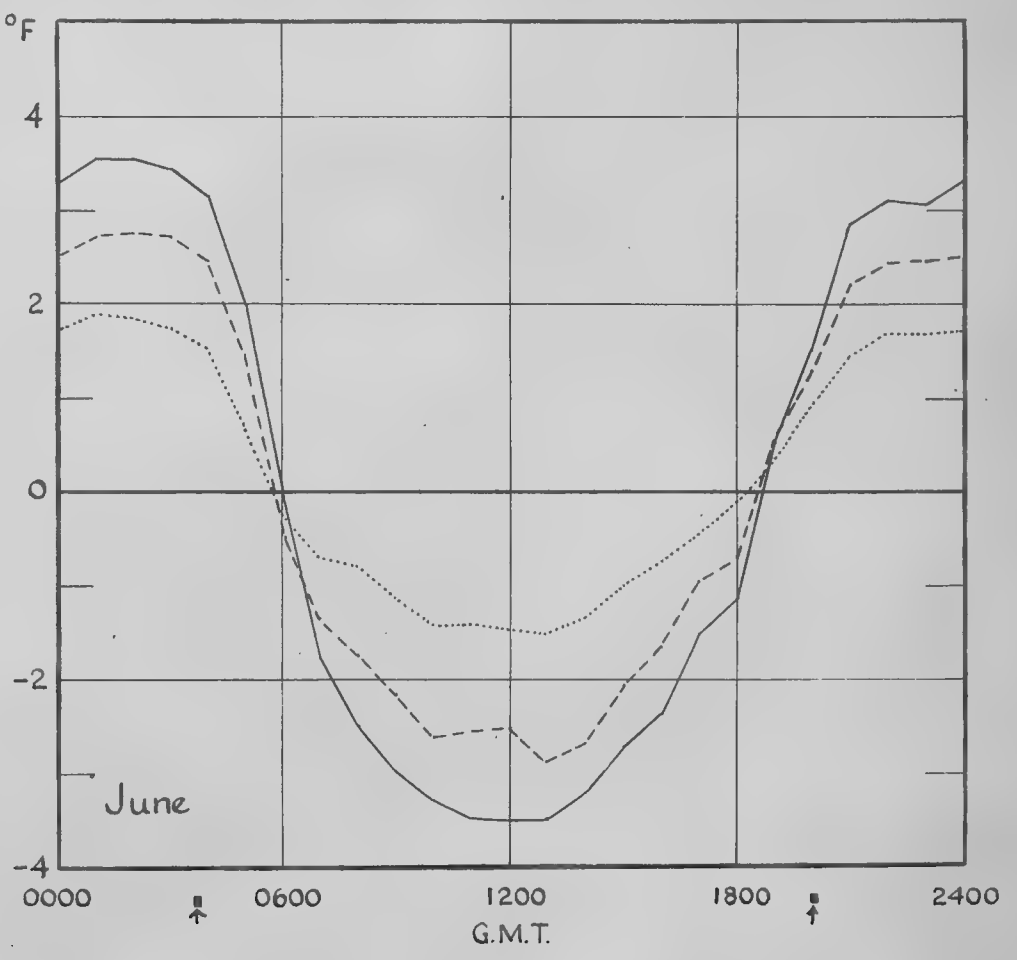
°F
4
2
0
-2
-4
June
0000
0600
1200
1800
2400
G.M.T.

M.R.P. 5446.

FIG. 1 cont.

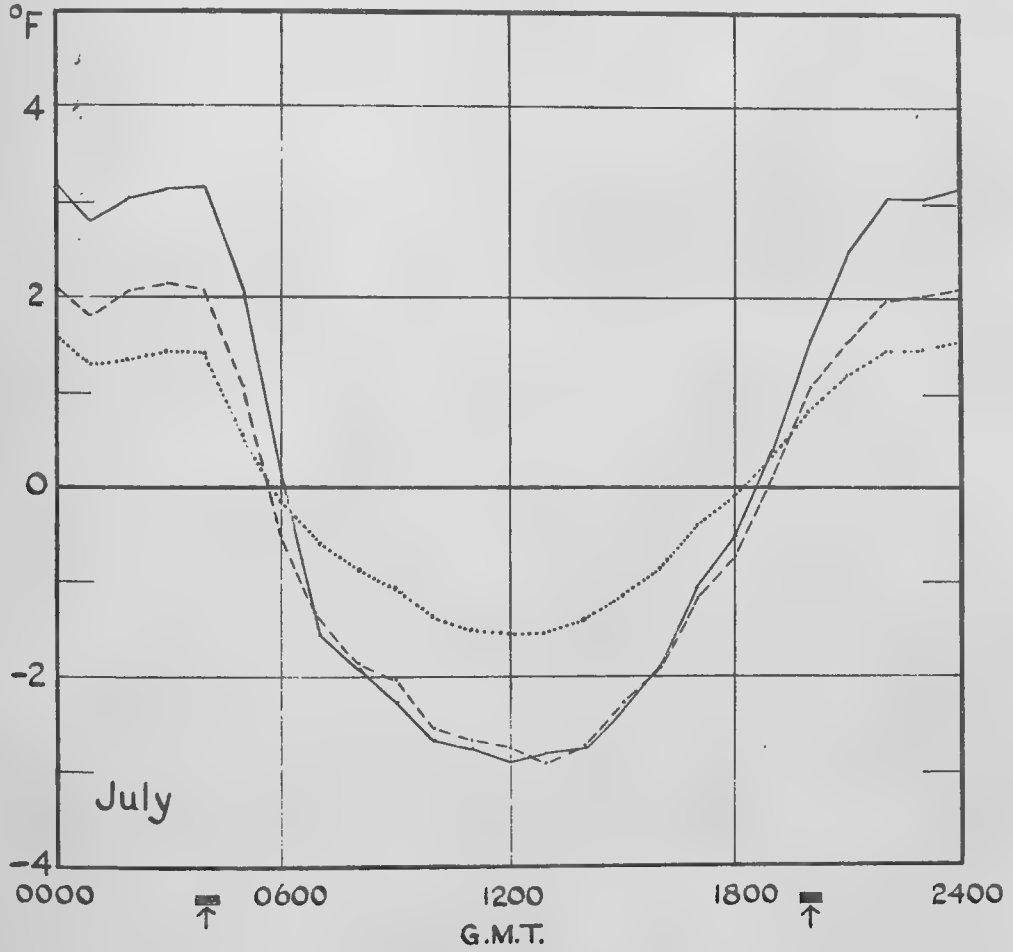

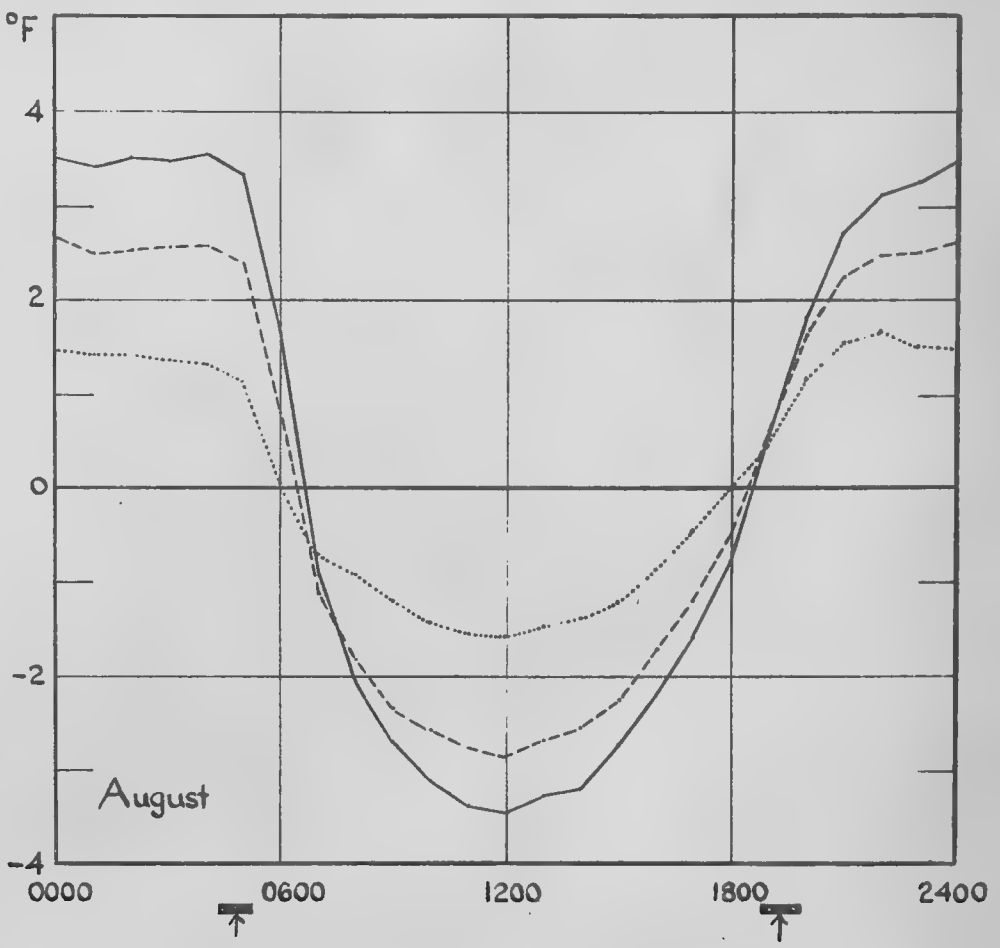

M.R.P. 5146.

FIG. 1 cont.

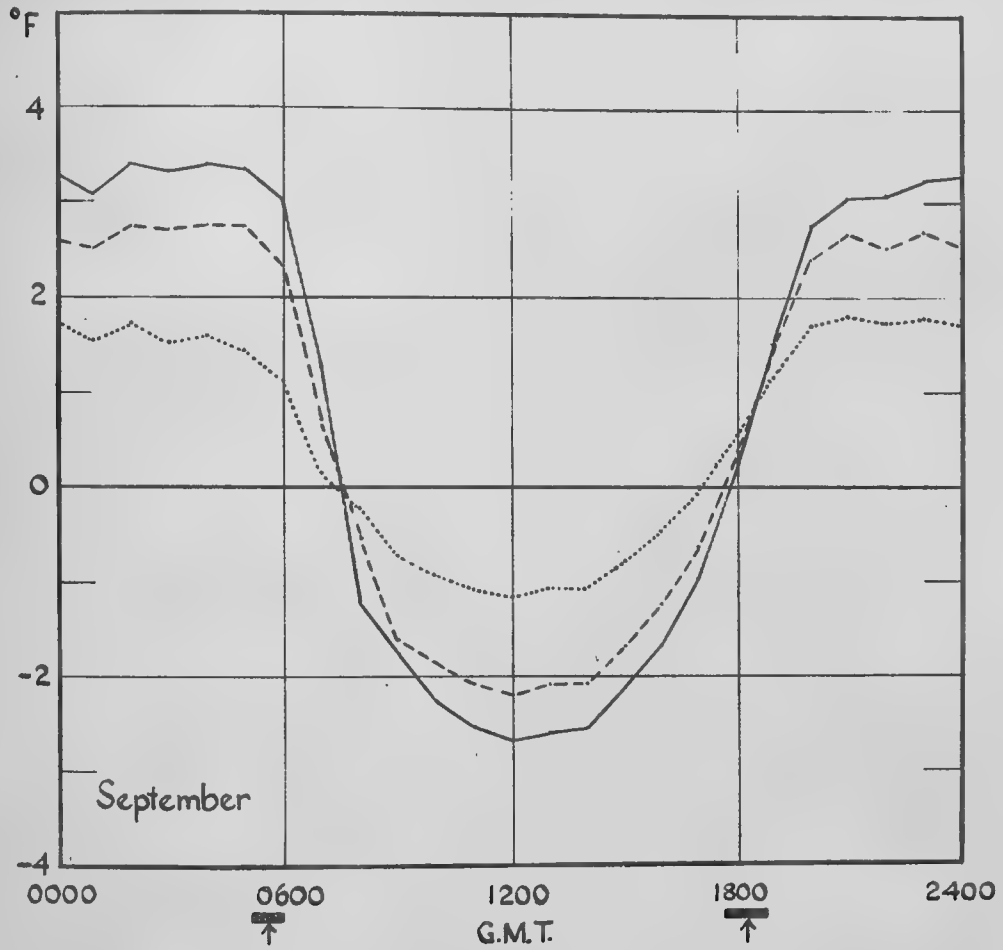

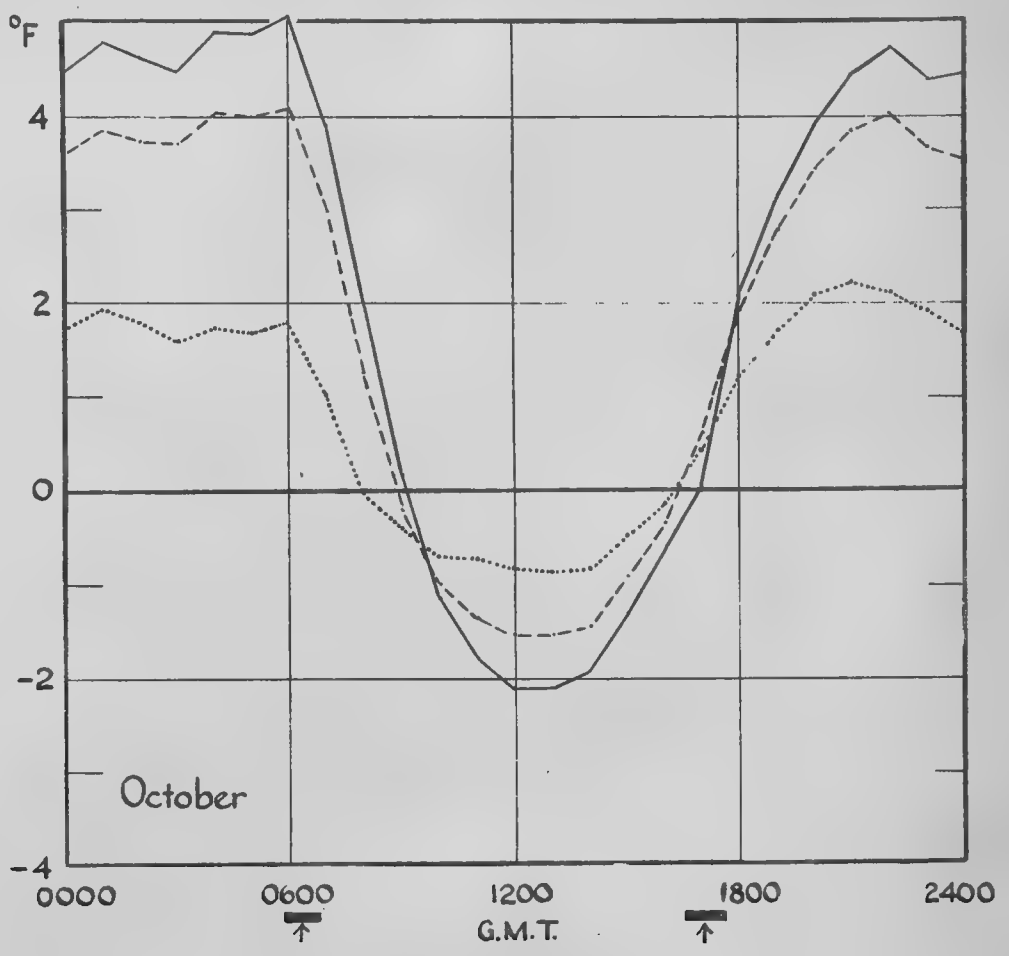

R.R.P. 546.

FIG. 1 cont.

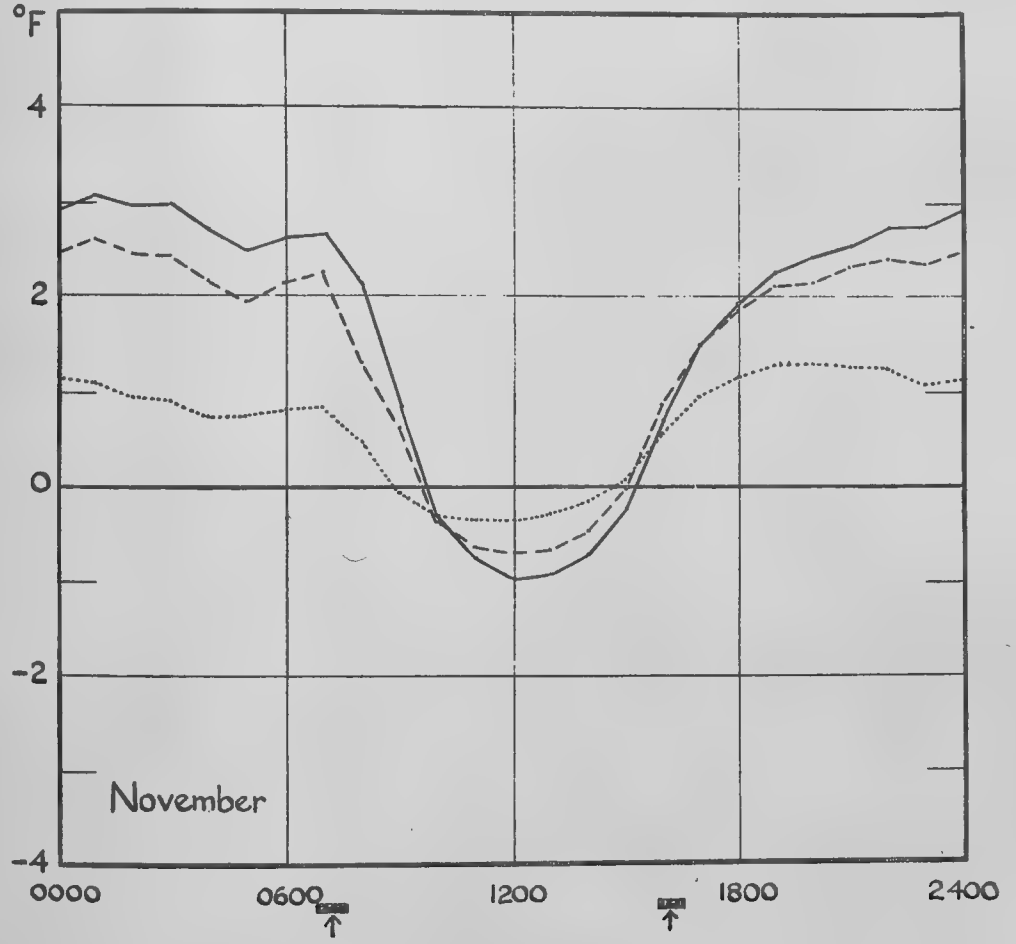

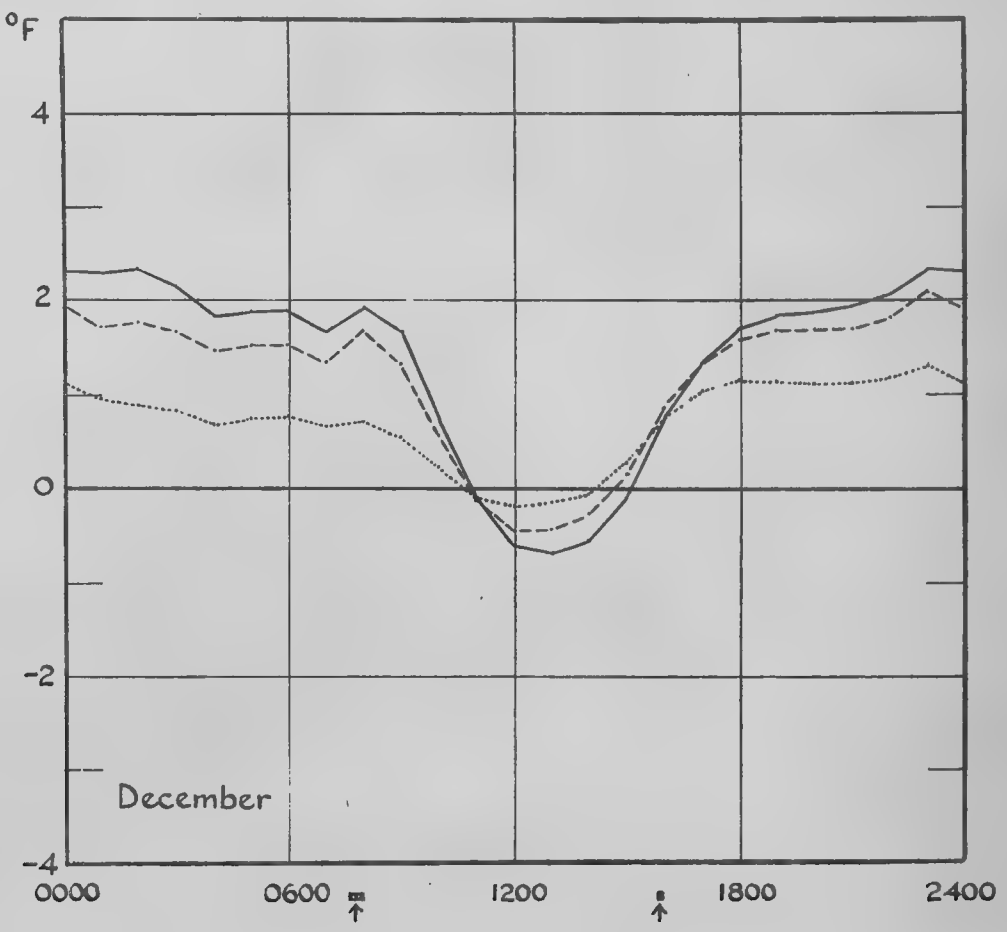

FIG. 2. DIURNAL VARIATION OF LAPSE OF TEMPERATURE FOR CLEAR AND OVERCAST DAYS IN SUMMER AND WINTER.

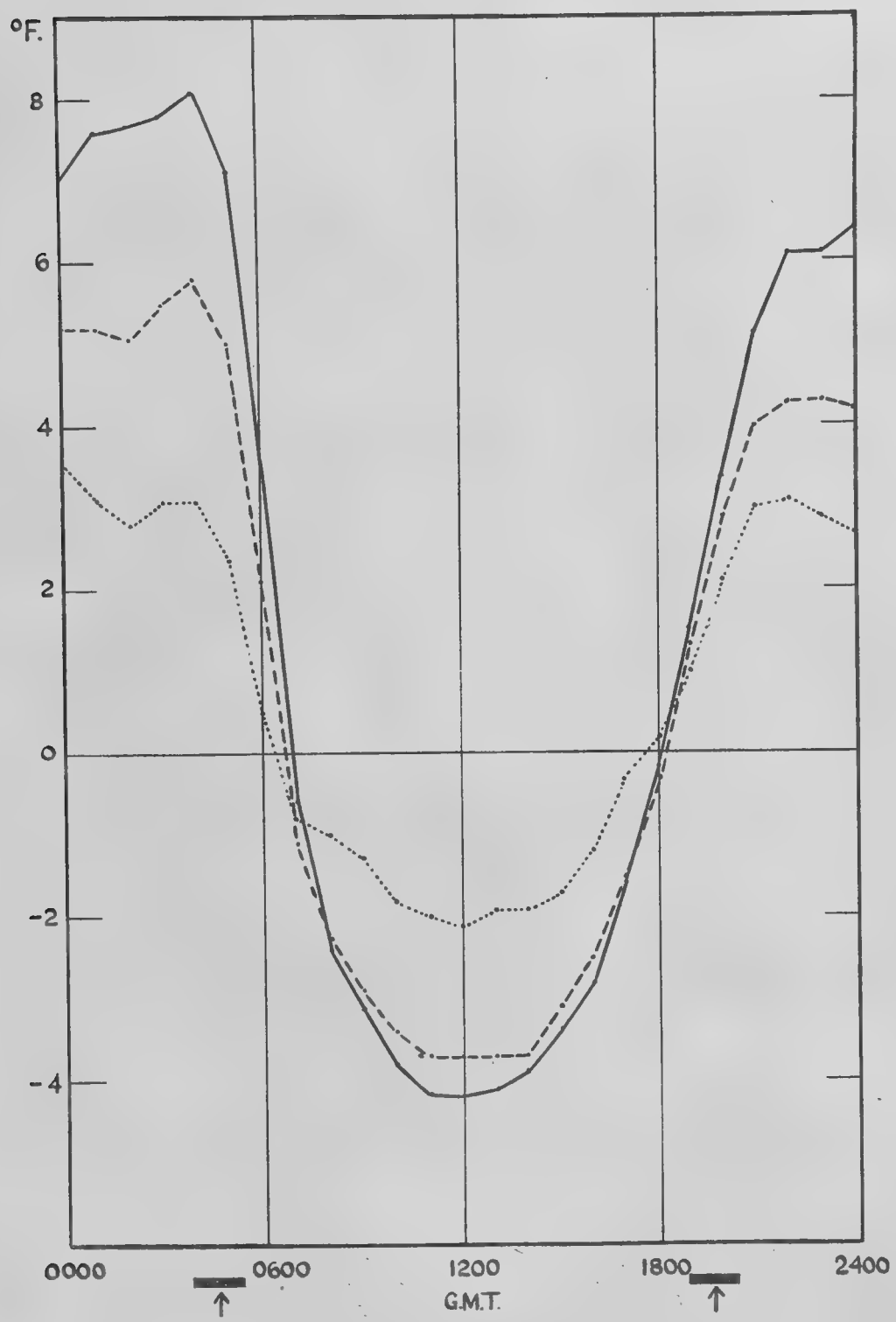

CLEAR DAYS IN SUMMER

The curves refer to the height intervals thus:-

..... 15·2 – 1·1 m. ----- 47·2 – 1 1 m. ——— 106·7 – 1·1 m.

FIG. 2 cont.

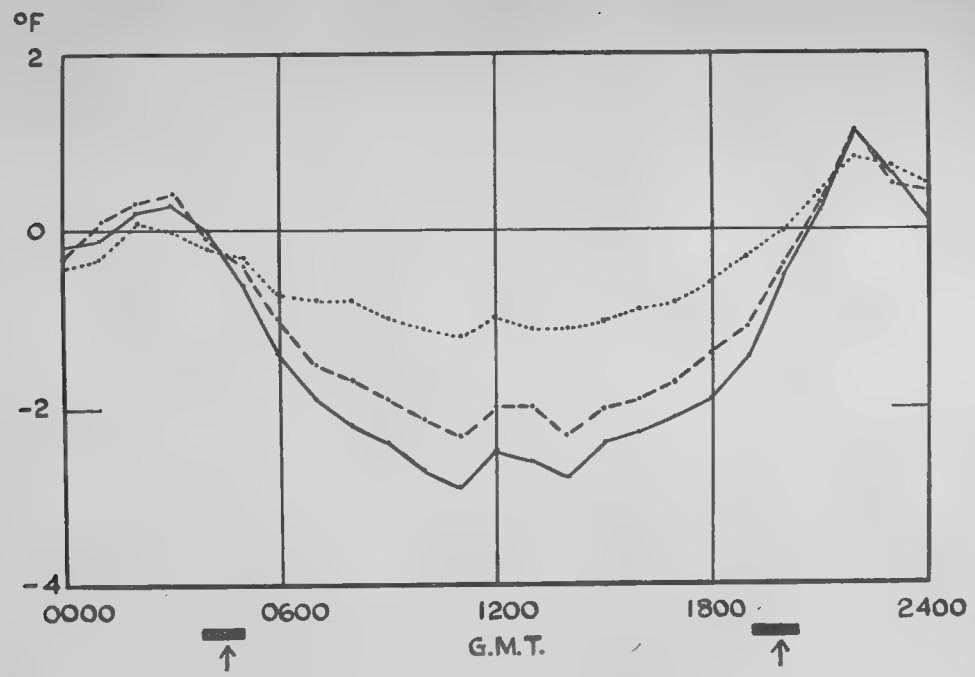

OVERCAST DAYS IN SUMMER

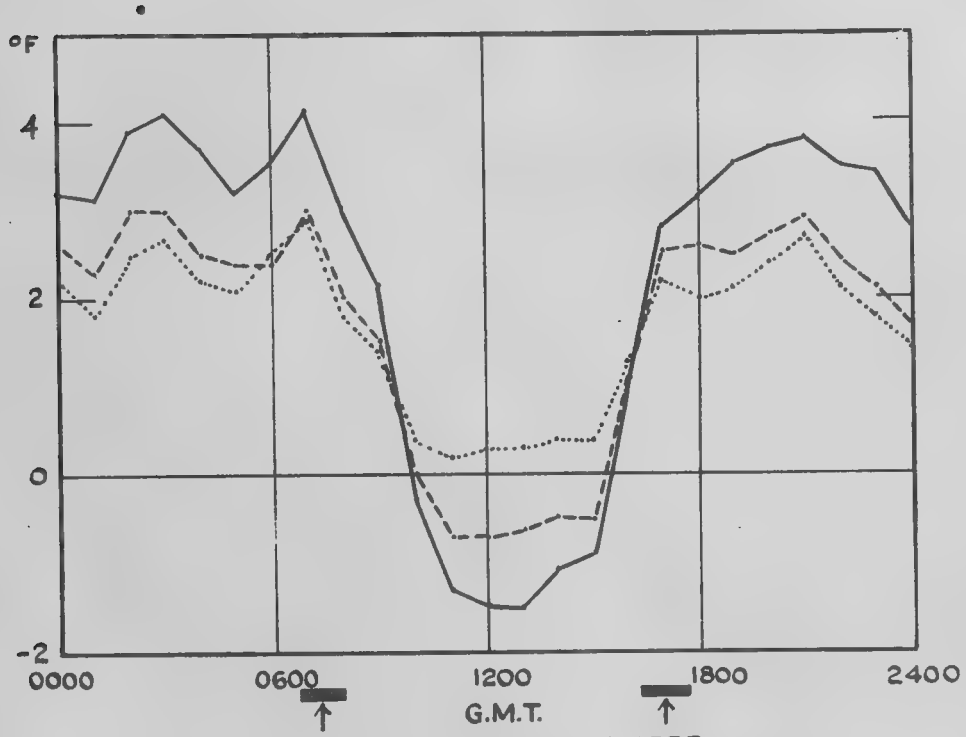

CLEAR DAYS IN WINTER

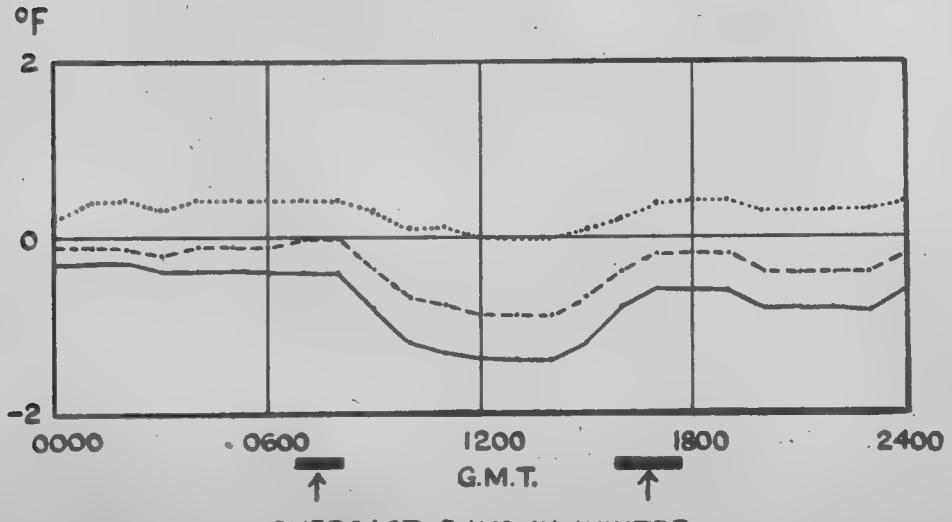

OVERCAST DAYS IN WINTER

FIG. 3. OGIVE OF PERCENTAGE FREQUENCIES OF LAPSE RATES OF TEMPERATURE.

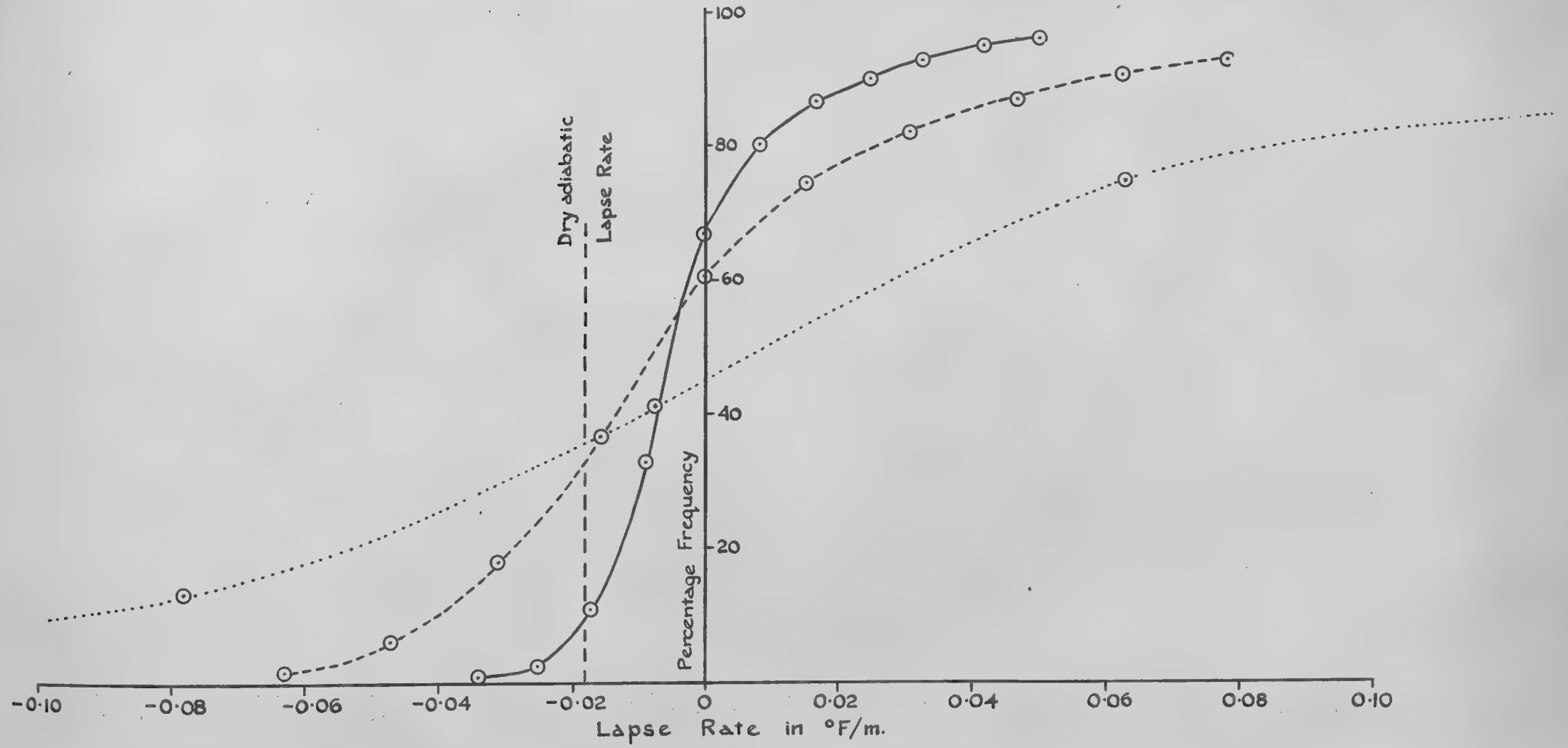

The curves are represented thus:- ..... 15·2 – 1·1 m. ----- 47·2 – 15·2 m. ——— 106·7 – 47·2 m.

FIG. 4. DIURNAL VARIATION OF TEMPERATURE AT FOUR HEIGHTS.

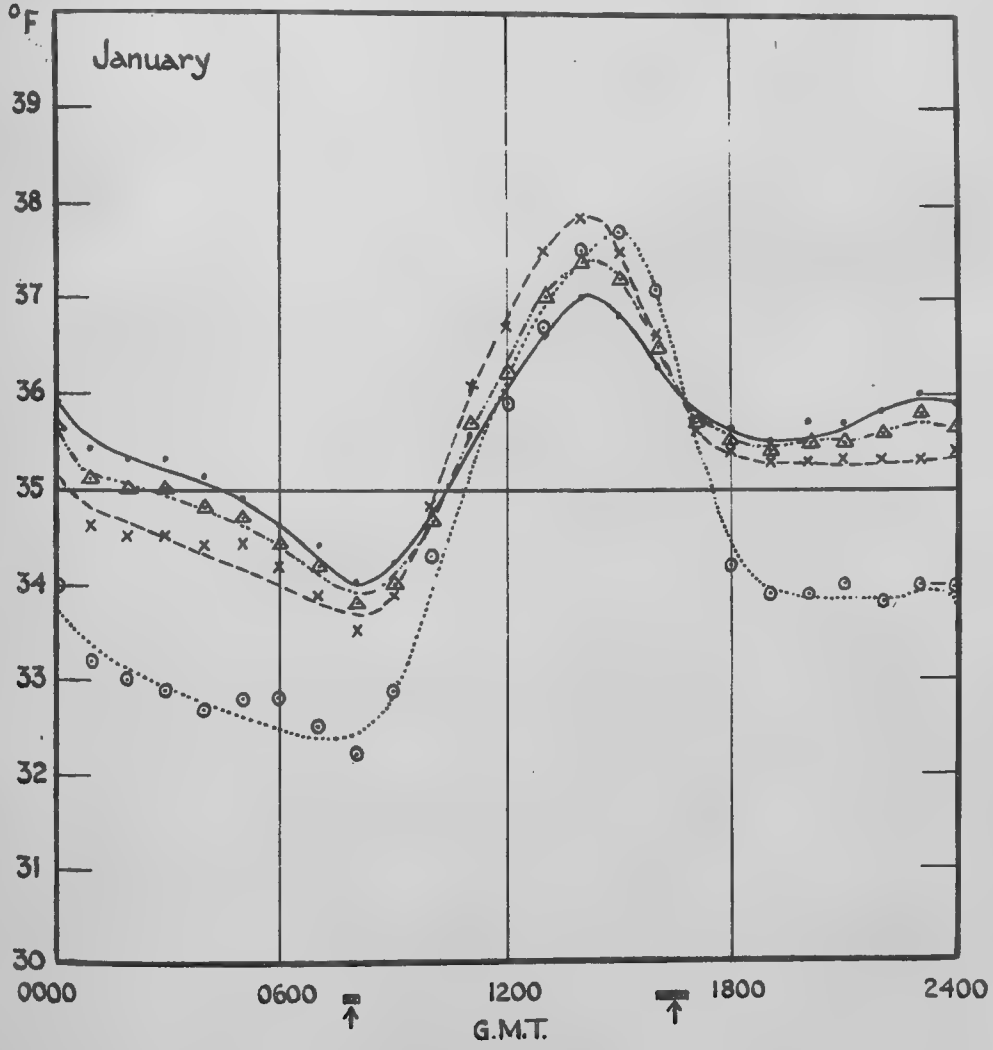

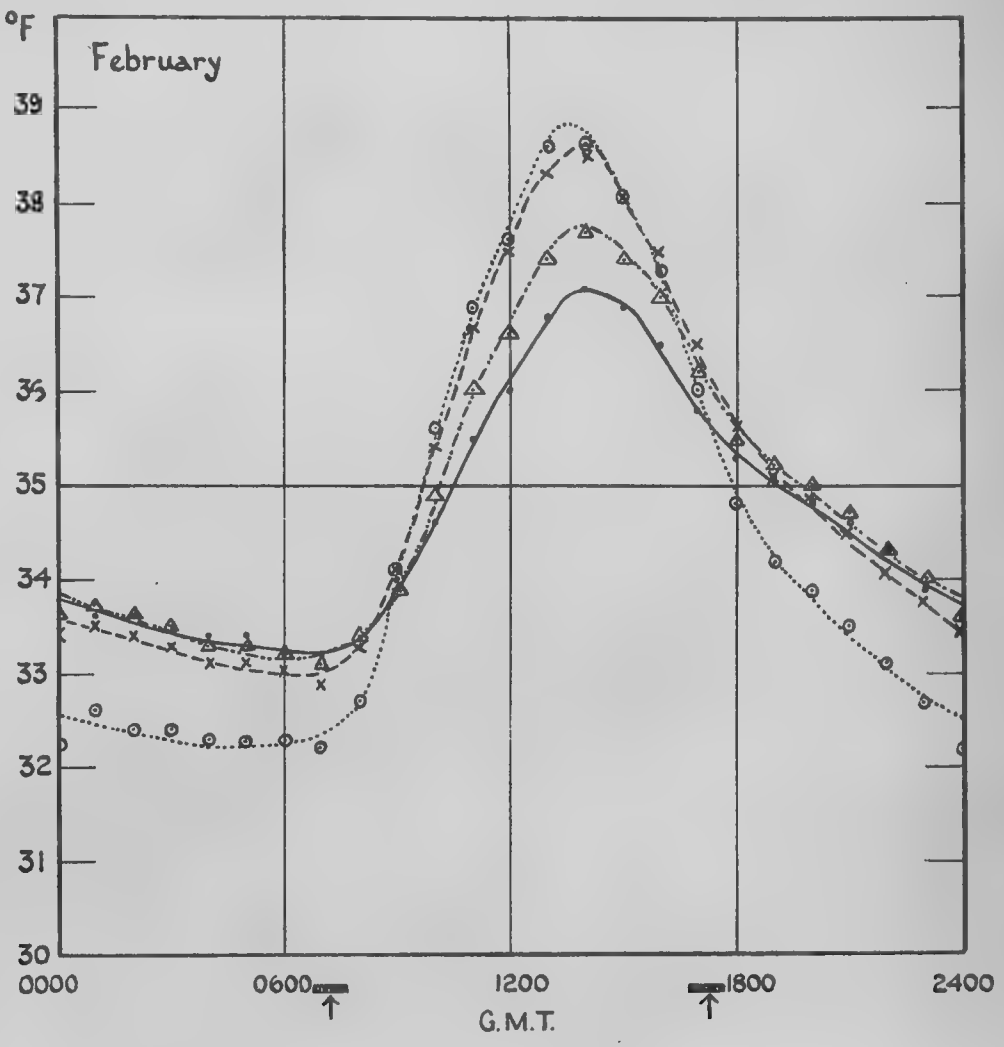

Temperature at height of { 1·1 m. ⊙·····⊙ 15·2 m. ×------× 47·2 m. △------△ 106·7 m. •——•

FIG. 4 cont.

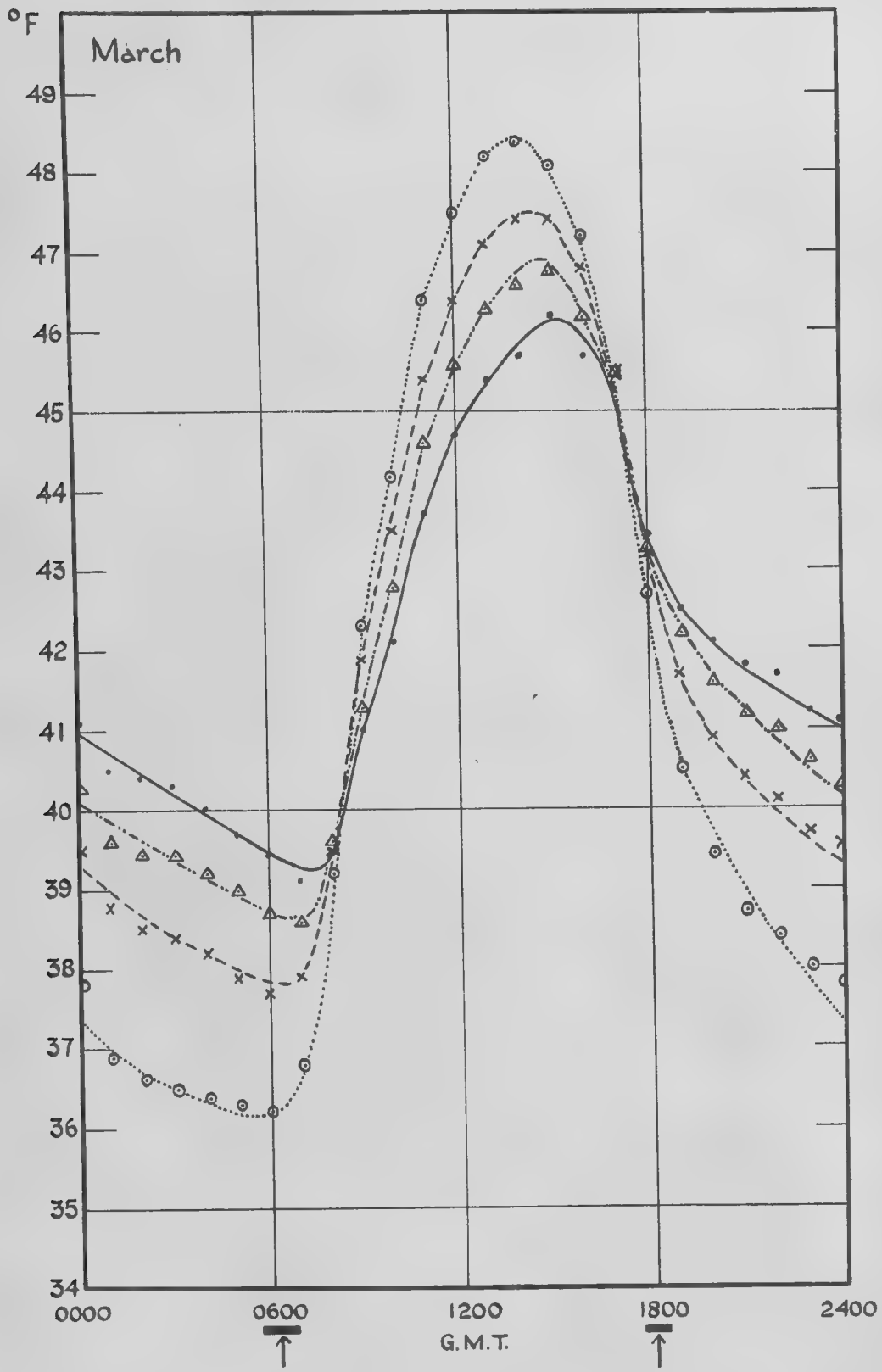
°F
March
49
48
47
46
45
44
43
42
41
40
39
38
37
36
35
34
0000
0600
1200
1800
2400
G.M.T.

FIG. 4 cont.

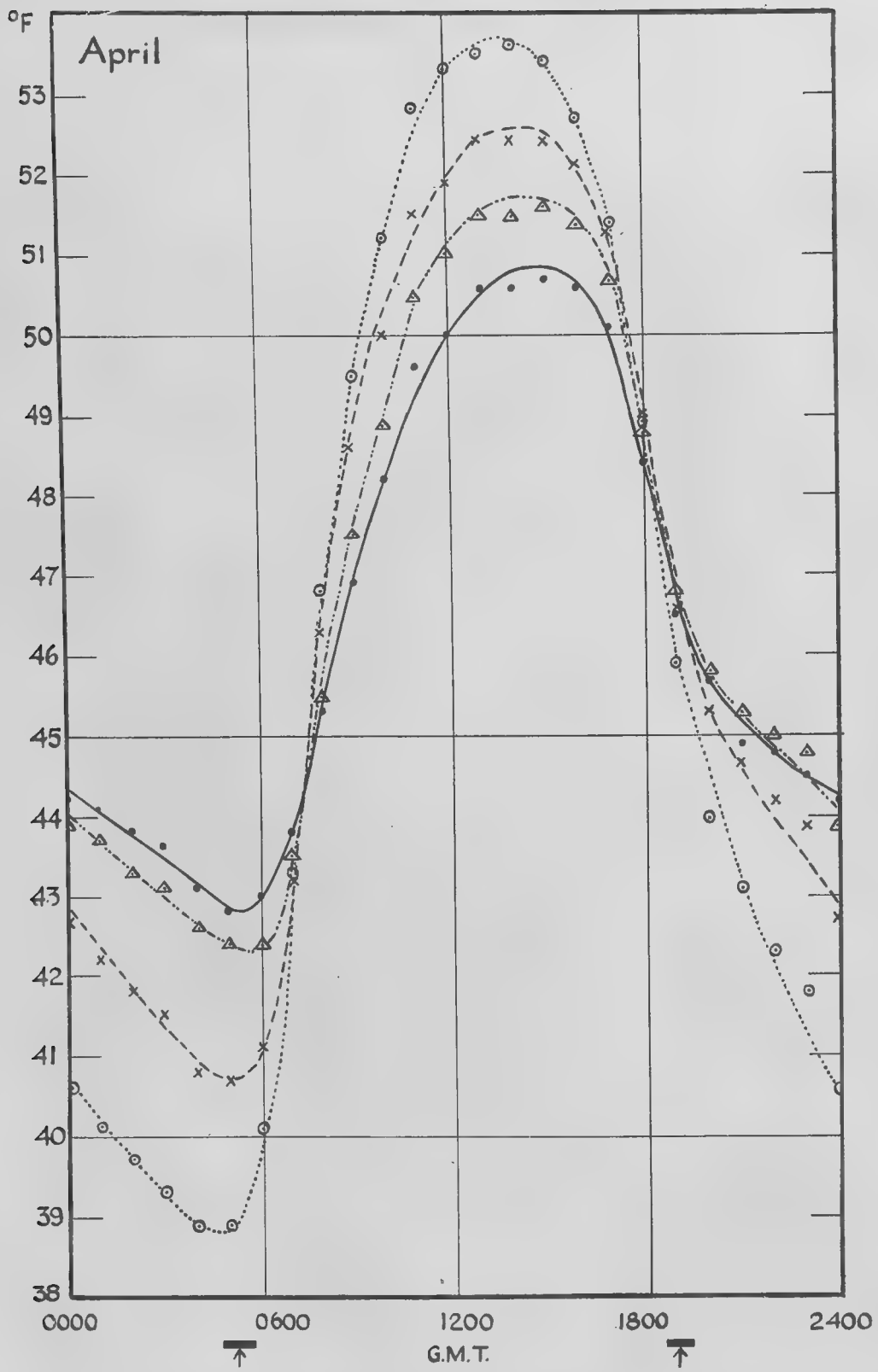
°F
April
53
52
51
50
49
48
47
46
45
44
43
42
41
40
39
38
0000
0600
1200
1800
2400
G.M.T.

FIG. 4 cont.

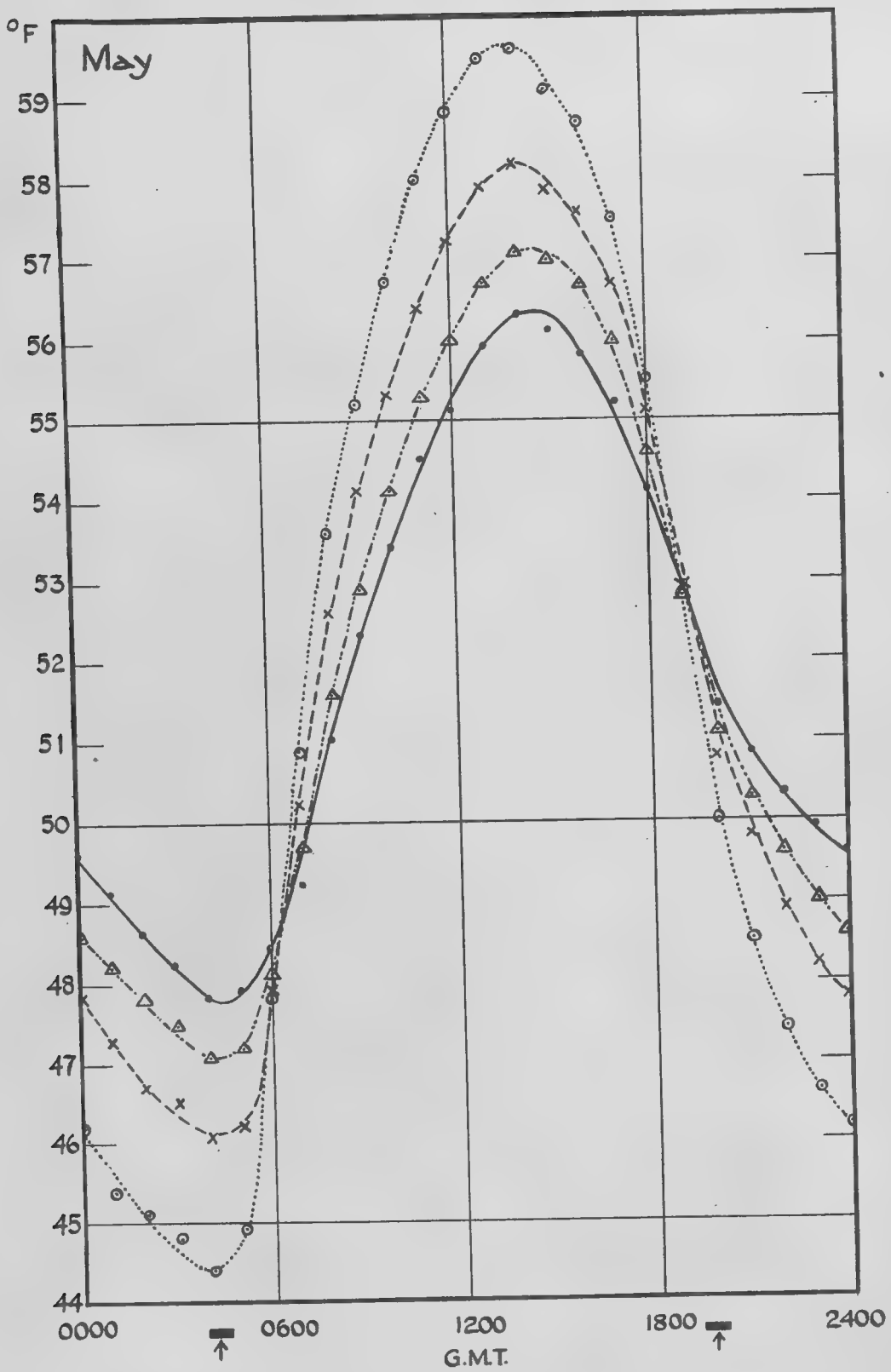
°F
May
59
58
57
56
55
54
53
52
51
50
49
48
47
46
45
44
0000
0600
1200
1800
2400
G.M.T.

FIG. 4 cont.

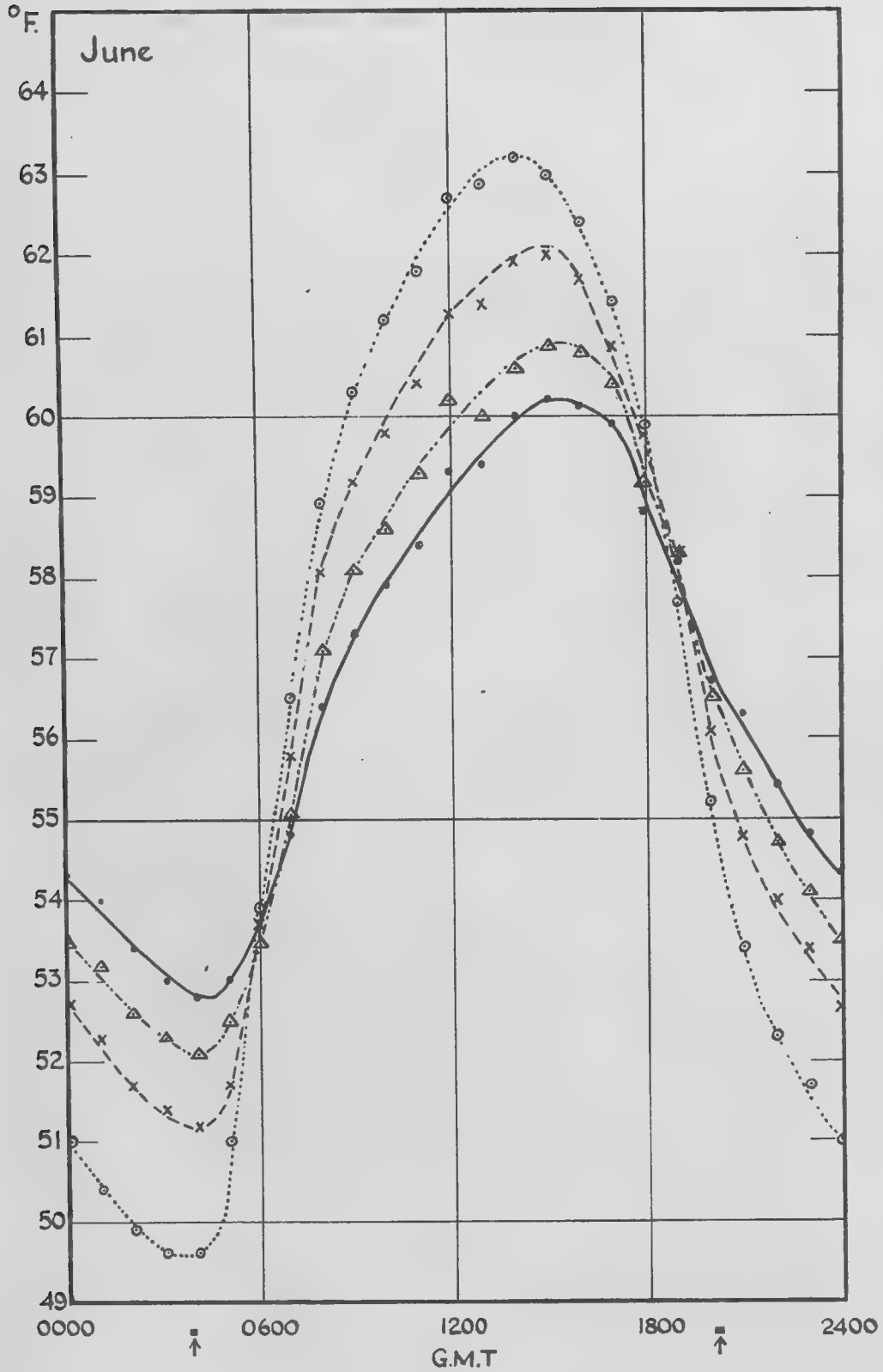
°F.
June
64
63
62
61
60
59
58
57
56
55
54
53
52
51
50
49
0000
0600
1200
1800
2400
G.M.T

FIG. 4 cont.

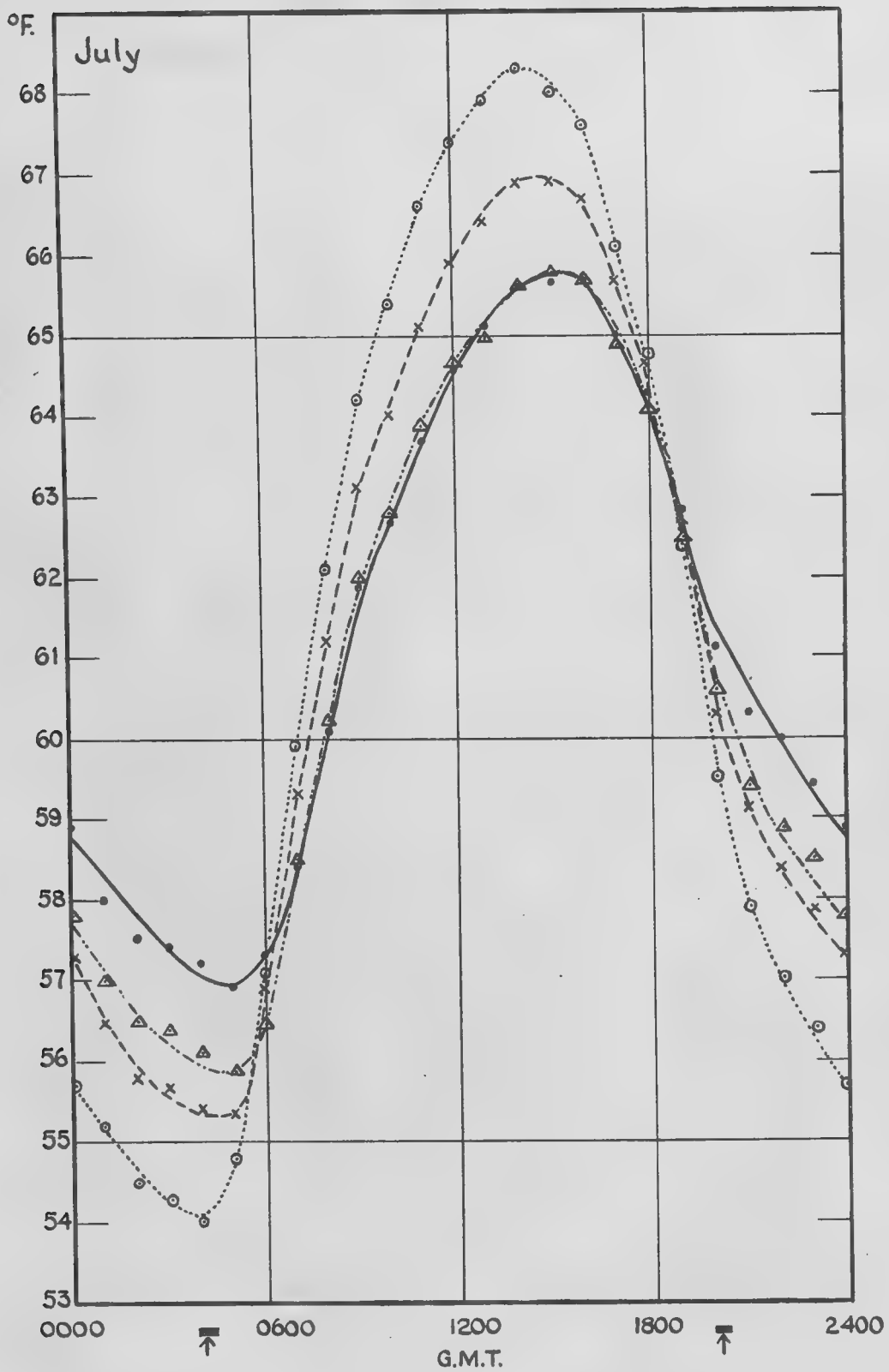
°F.
July
68
67
66
65
64
63
62
61
60
59
58
57
56
55
54
53
0000
0600
1200
1800
2400
G.M.T.

FIG. 4 cont.

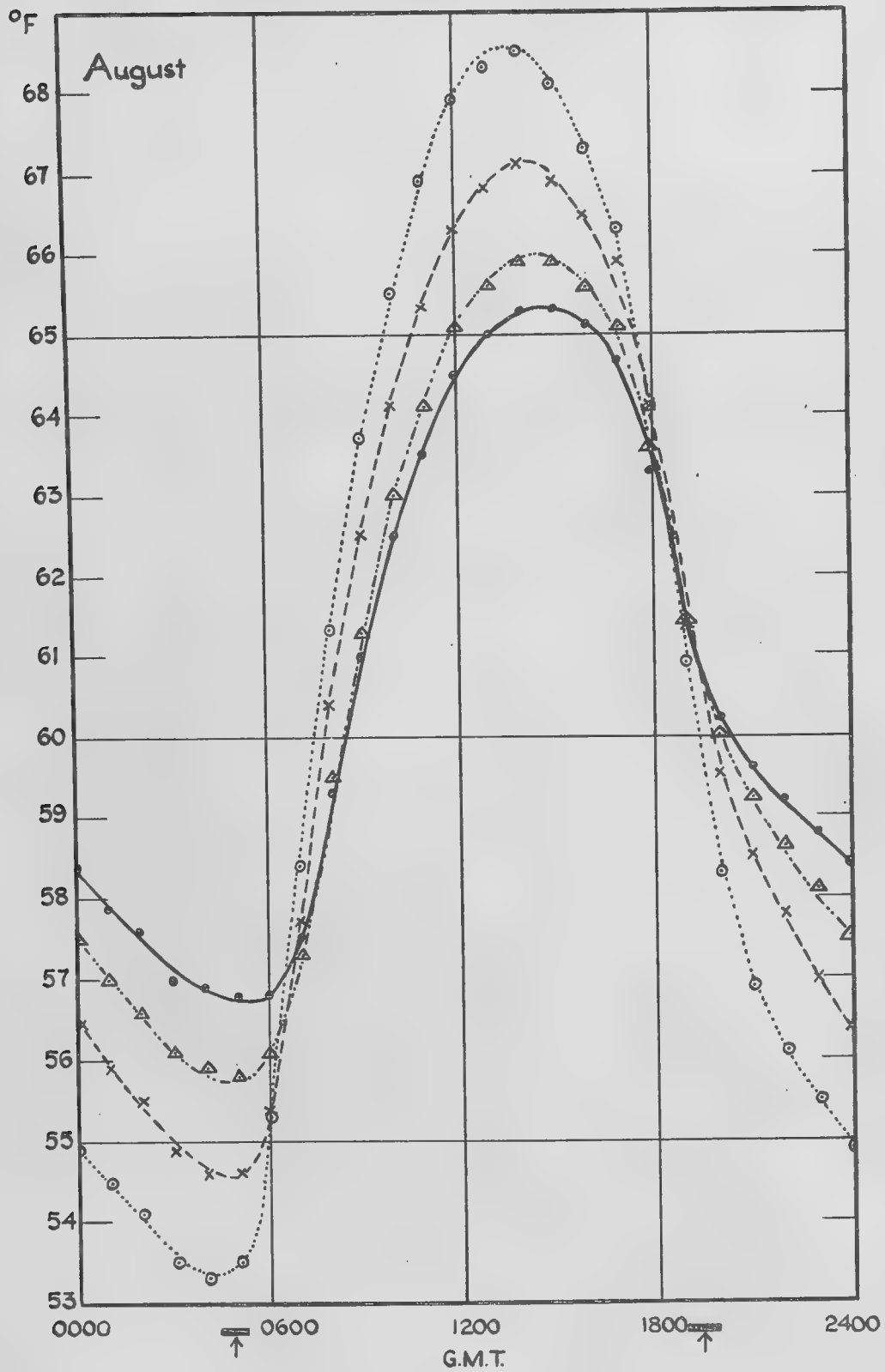
°F
August
68
67
66
65
64
63
62
61
60
59
58
57
56
55
54
53
0000
0600
1200
1800
2400
G.M.T.

FIG. 4 cont.

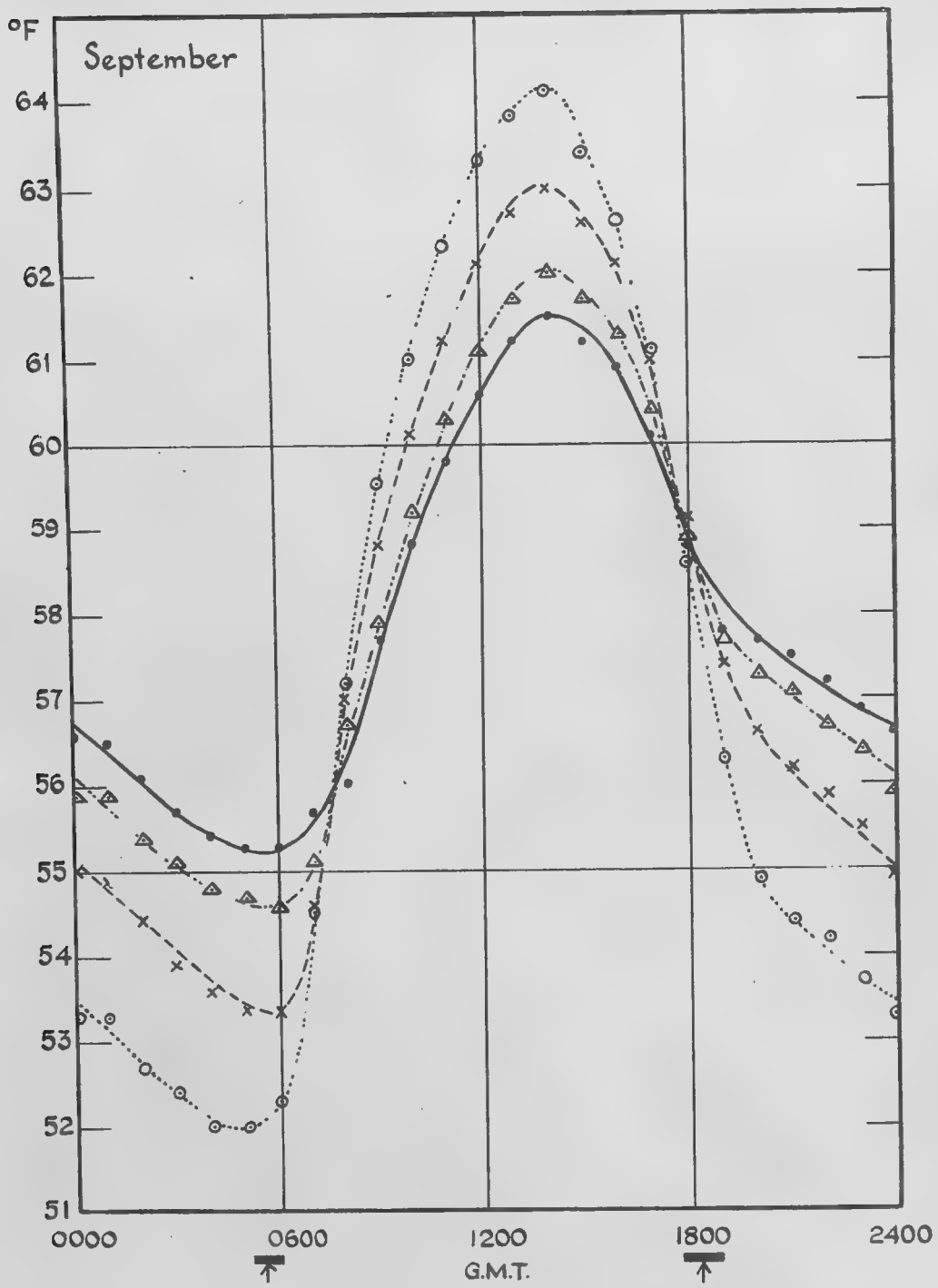
°F
September
64
63
62
61
60
59
58
57
56
55
54
53
52
51
0000
0600
1200
1800
2400
G.M.T.

FIG. 4 cont.

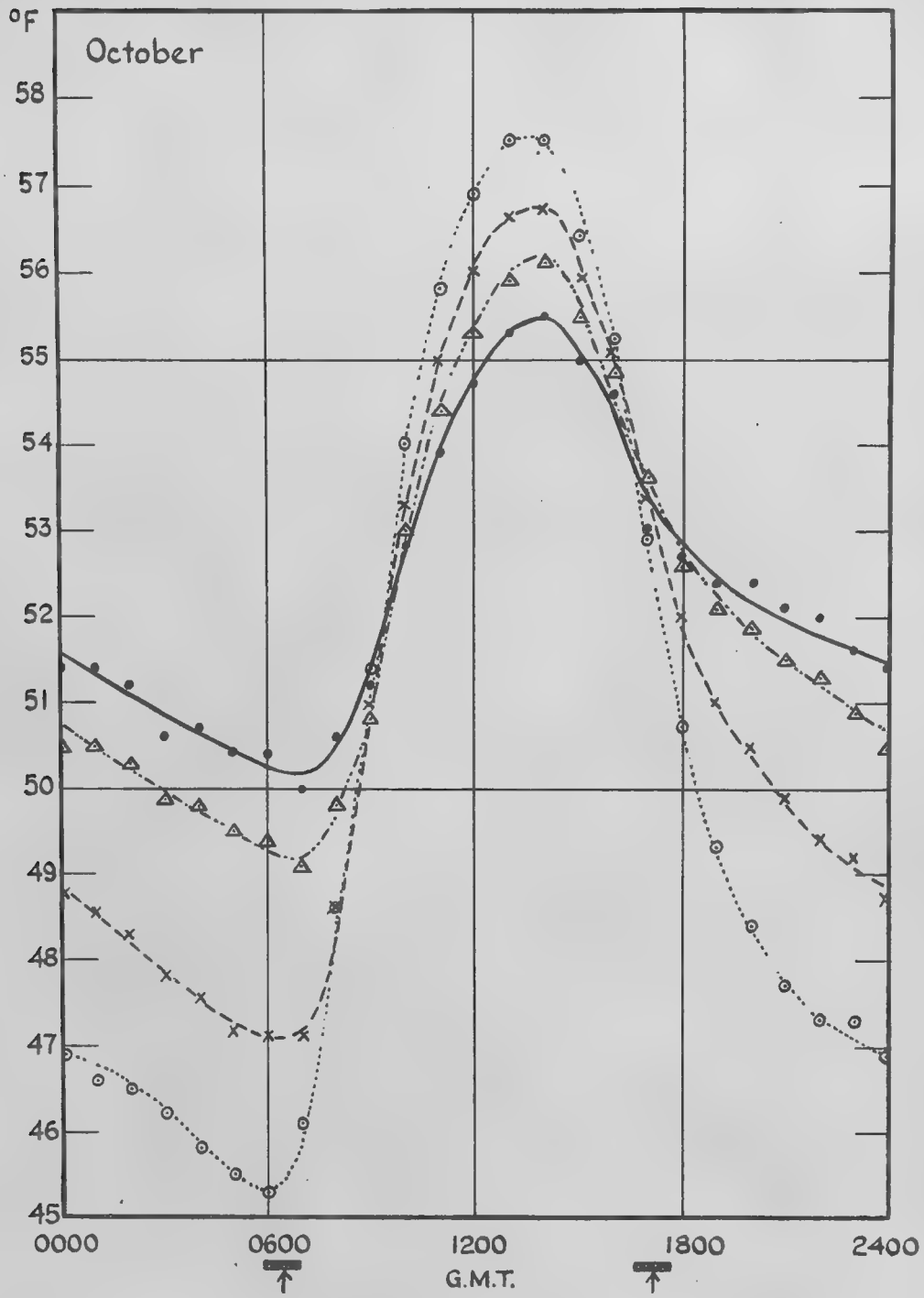
°F
October
58
57
56
55
54
53
52
51
50
49
48
47
46
45
0000
0600
1200
1800
2400
G.M.T.

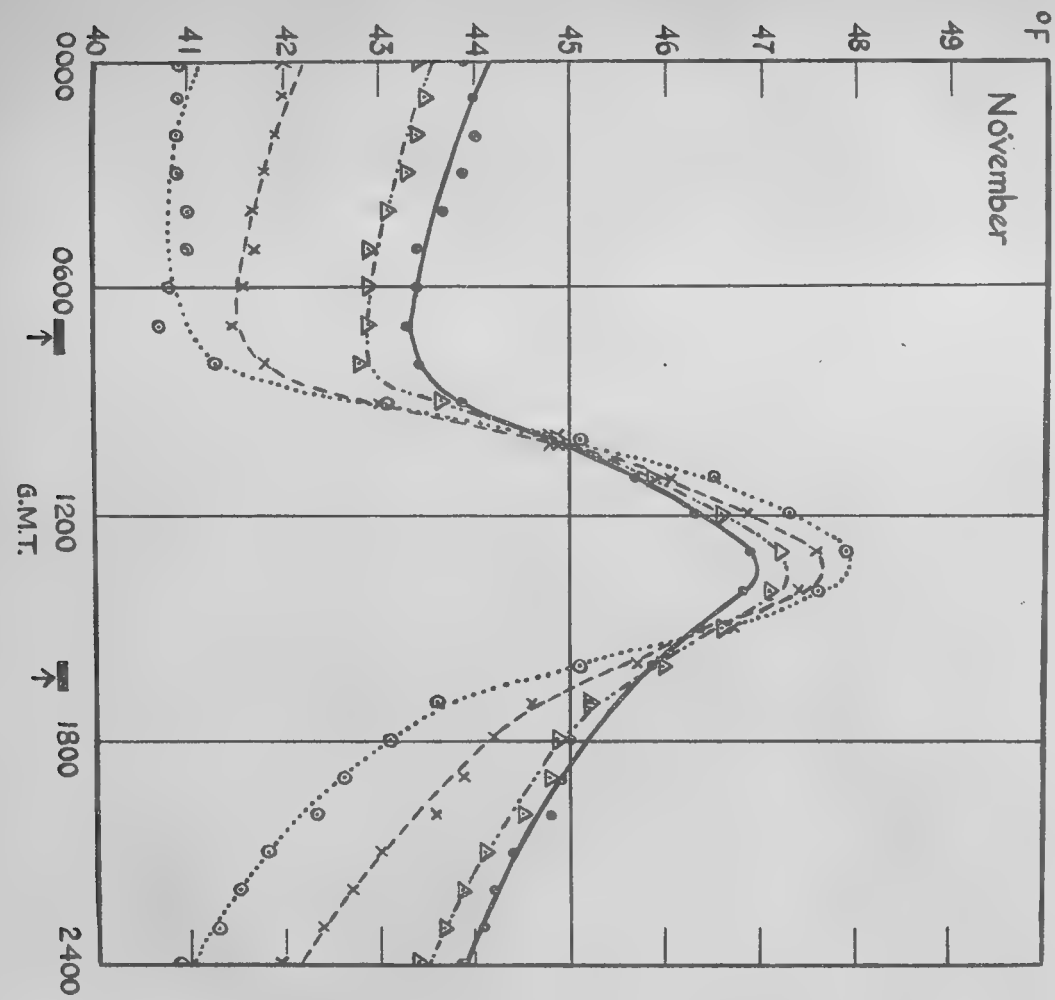
November
°F
49
48
47
46
45
44
43
42
41
40
0000
0600
1200
1800
2400
G.M.T.

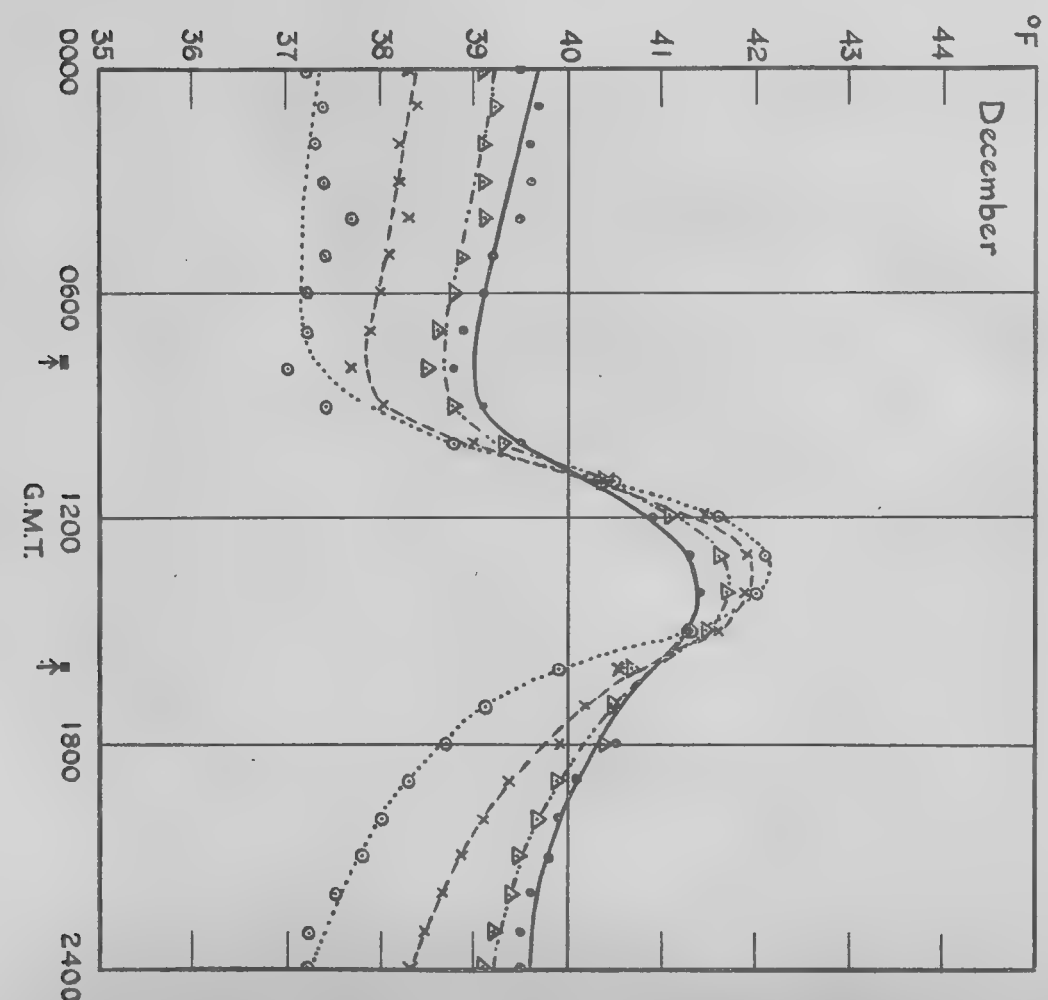
December
°F
44
43
42
41
40
39
38
37
36
35
0000
0600
1200
1800
2400
G.M.T.

FIG. 4 cont

FIG. 5. DIURNAL VARIATION OF TEMPERATURE AT FOUR HEIGHTS FOR CLEAR AND OVERCAST DAYS IN SUMMER AND WINTER.

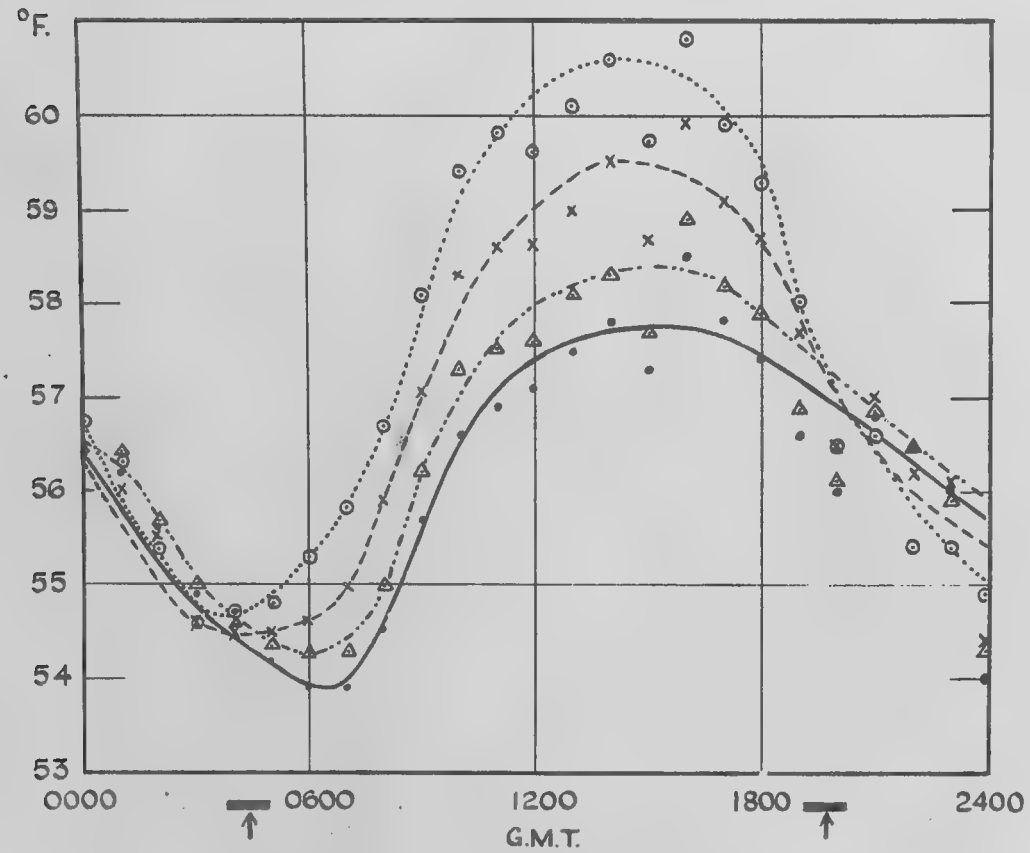

(a) OVERCAST DAYS IN SUMMER

Temperature at height of

⊙·····⊙ = 1·1 m. x- - - - -x = 15·2 m.

△-·-·-△ = 47·2 m. •——— • = 106·7 m.

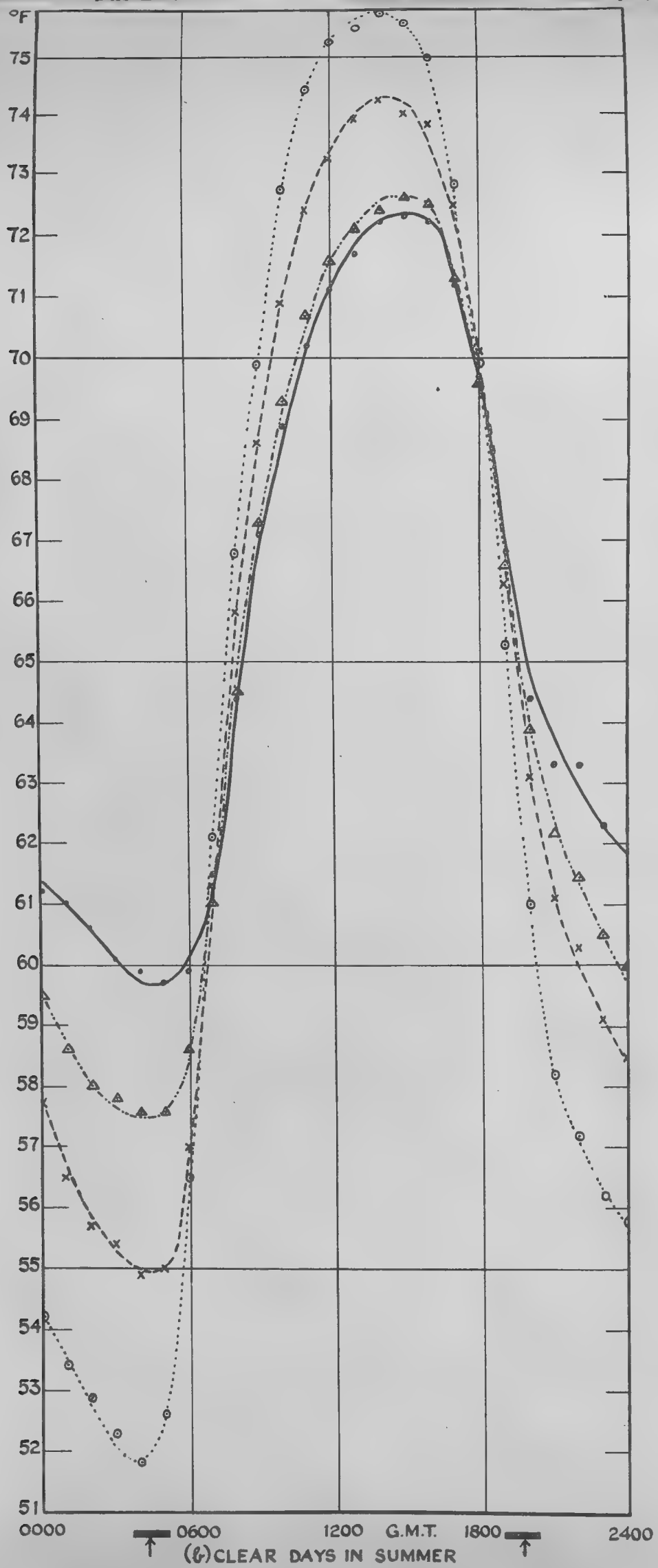

(b) CLEAR DAYS IN SUMMER

FIG. 5 cont.

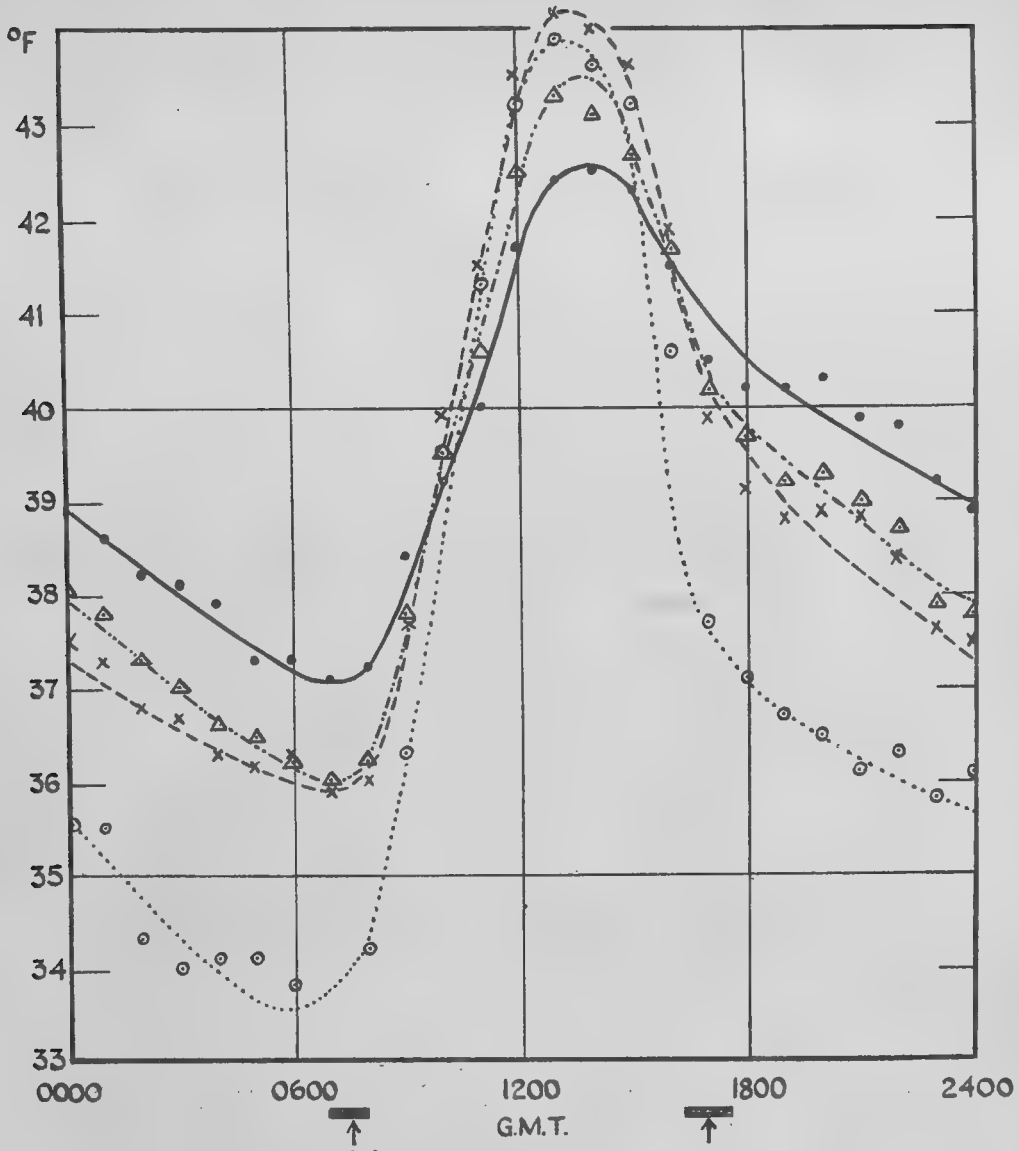

(c) CLEAR DAYS IN WINTER

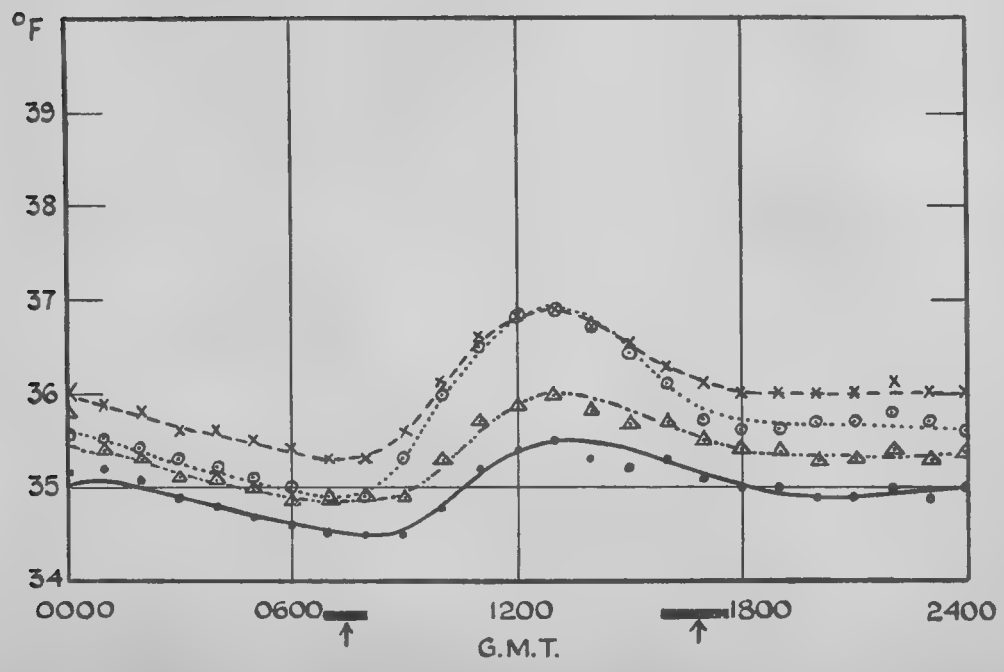

(d) OVERCAST DAYS IN WINTER

FIG. 6. DIURNAL VARIATION OF LAPSE OF TEMPERATURE ON OCCASIONS OF SNOW COVER.

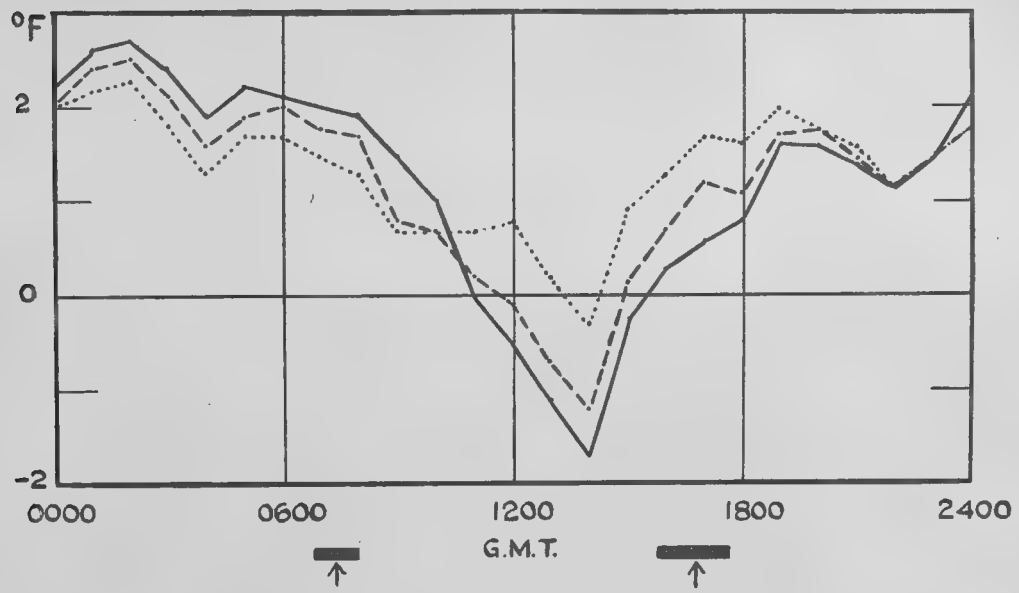

The intervals are represented ····· 15·2 – 1·1 m. ---- 47·2 – 1·1 m. —— 106·7 – 1·1 m.

FIG. 6B. DIURNAL VARIATION OF TEMPERATURE ON OCCASIONS OF SNOW COVER.

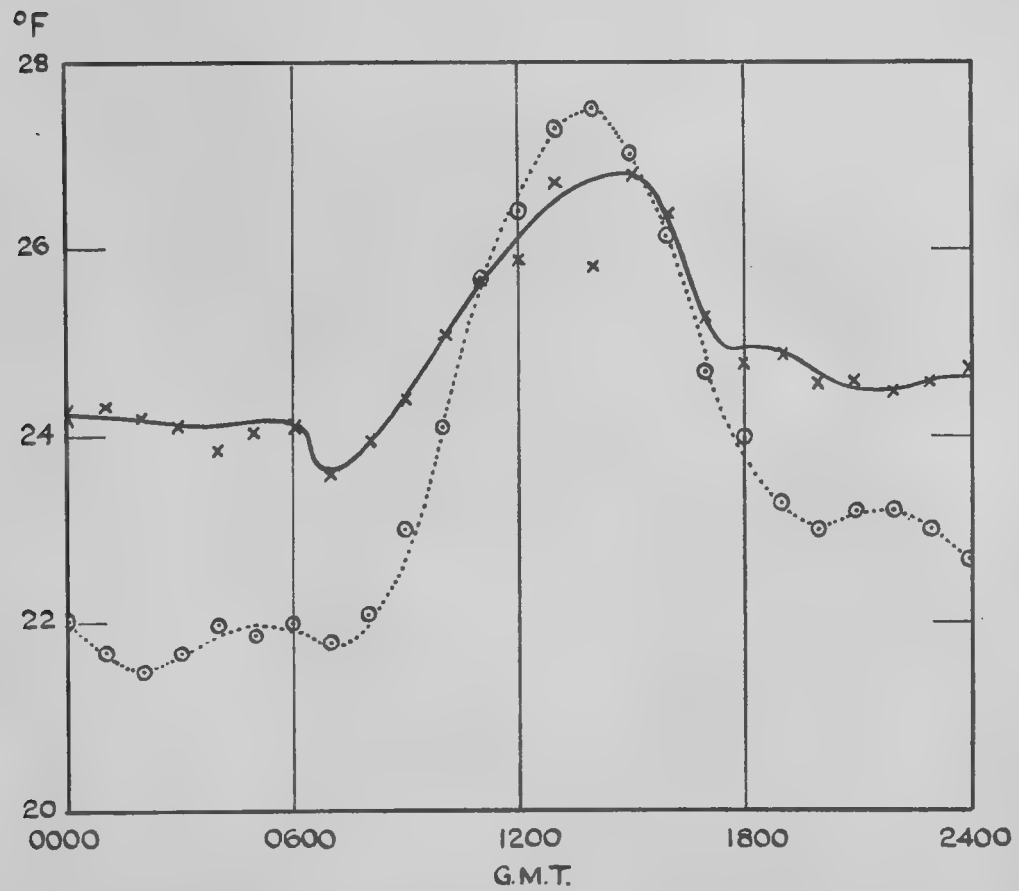

The heights are represented ⊙·····⊙ 1·1 m. ×——× 106·7 m.

MEAN VARIATION OF HUMIDITY WITH HEIGHT FOR EACH HOUR – FIG. 7.

M.R.P 546

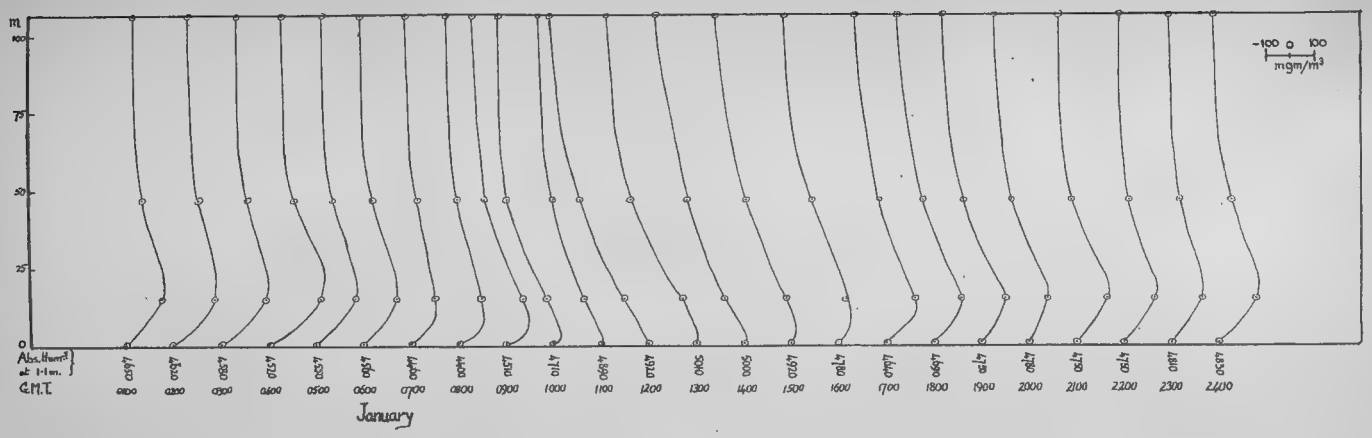

January

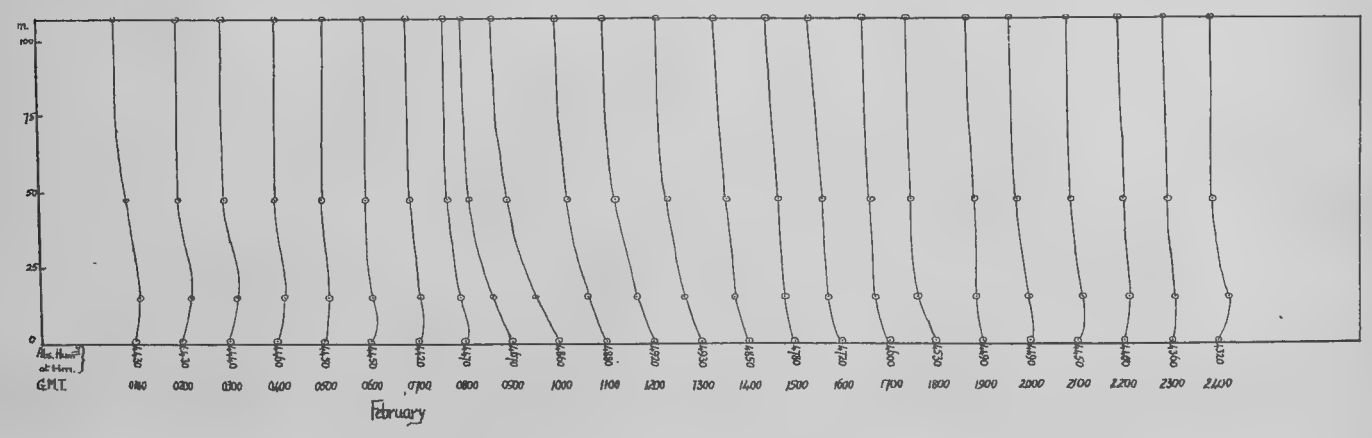

February

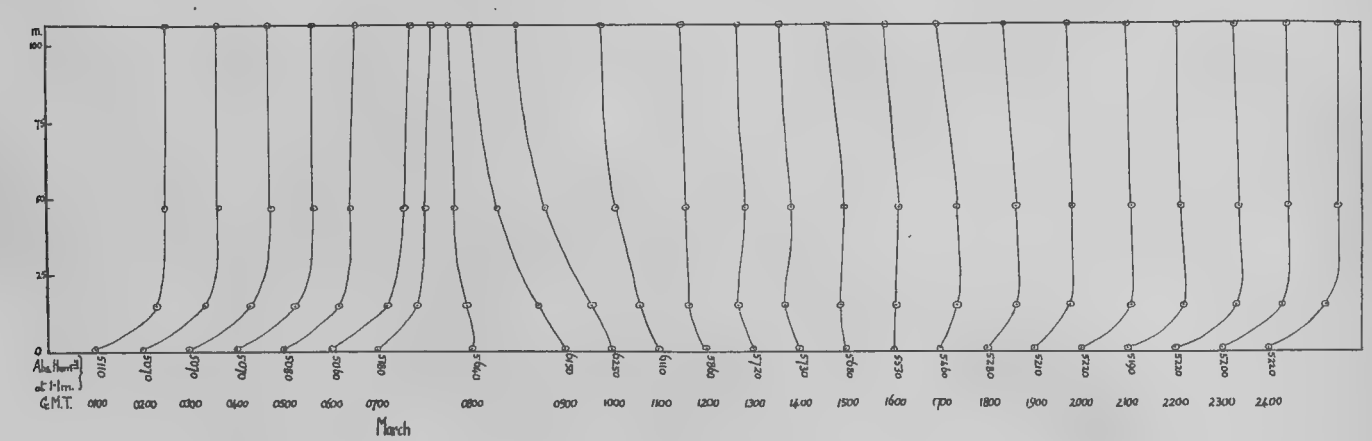

March

FIG, 7 cont.

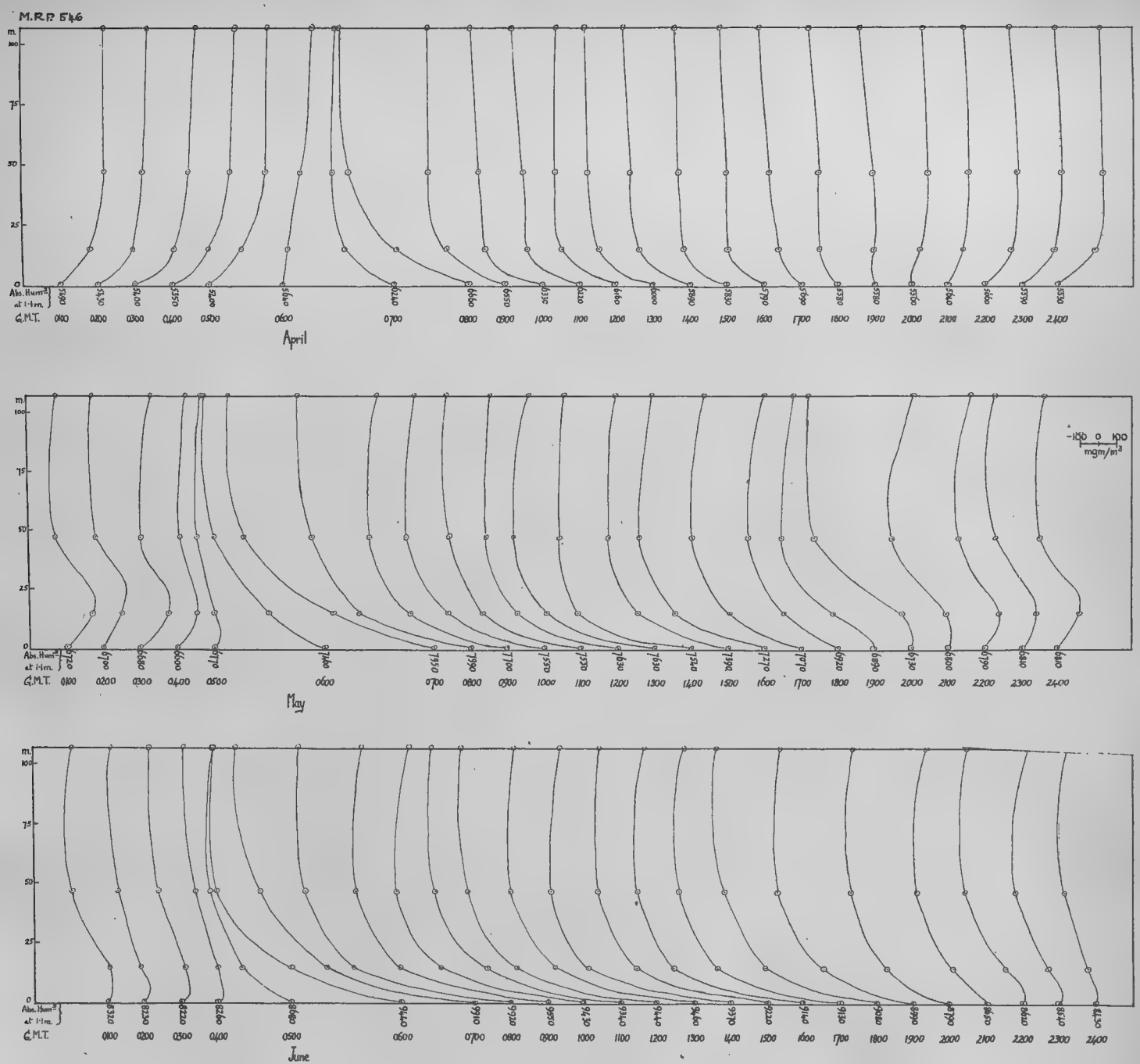
M.R.P 546
m.
100
75
50
25
0
Abs. Hum² at 1·1m.
G.M.T.
April
-100 0 100
mgm/m³
May
June

FIG. 7 cont.

M.F.P 546

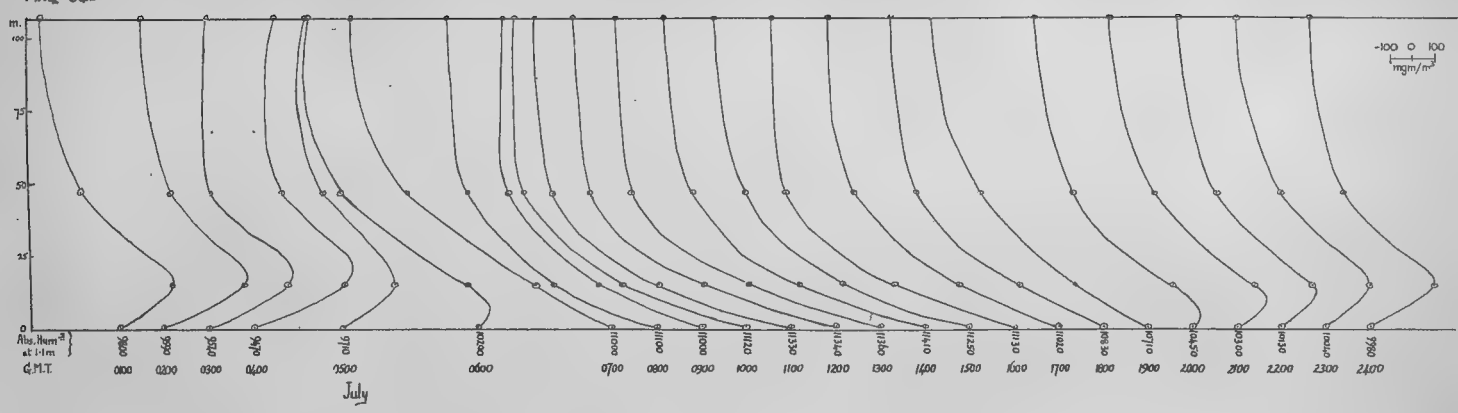

July

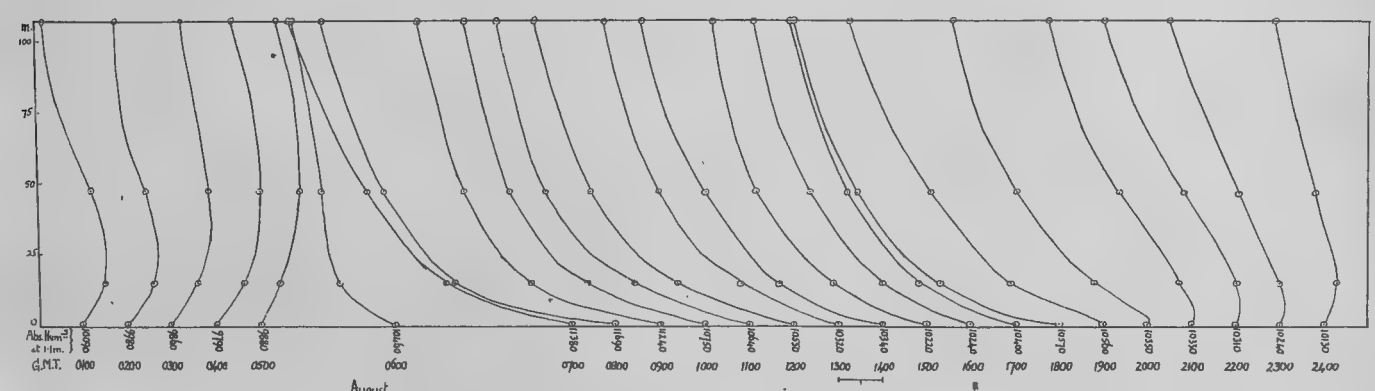

August

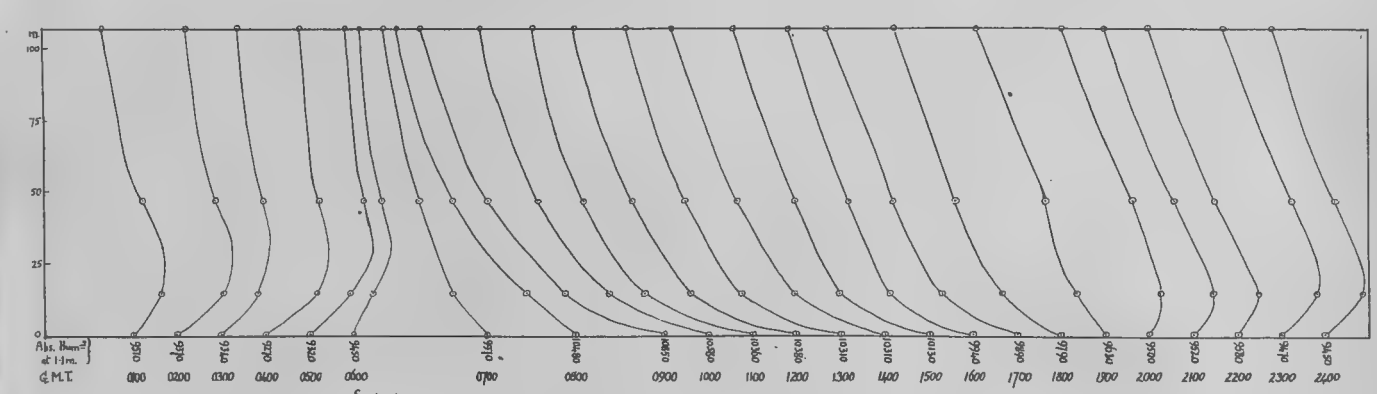

September

FIG. 7 cont.

M.R.P. 546

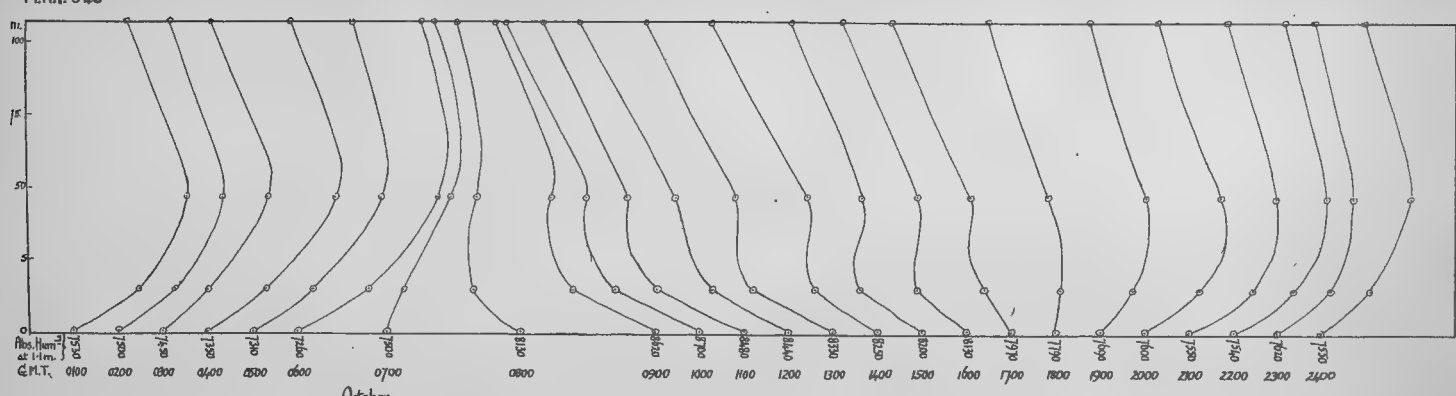

October

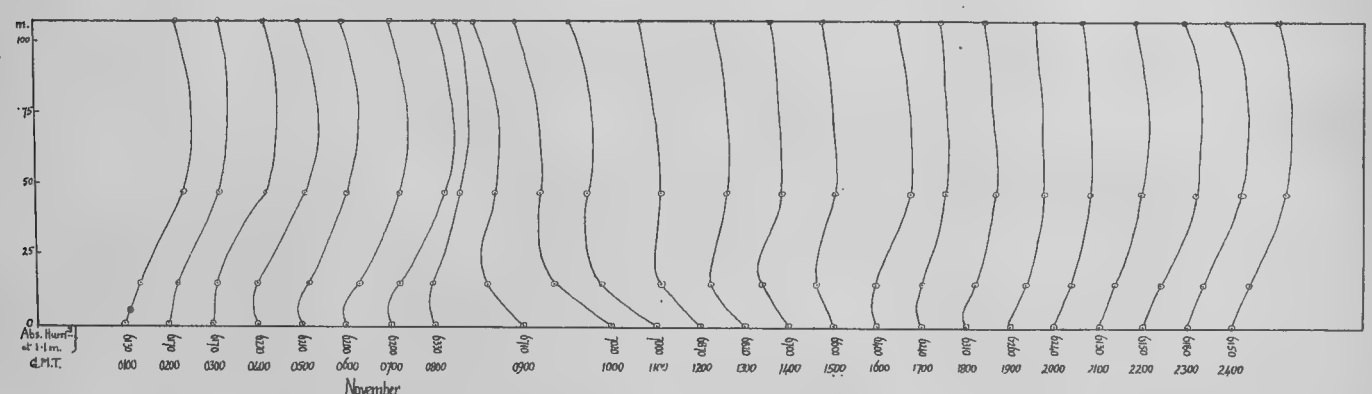

November

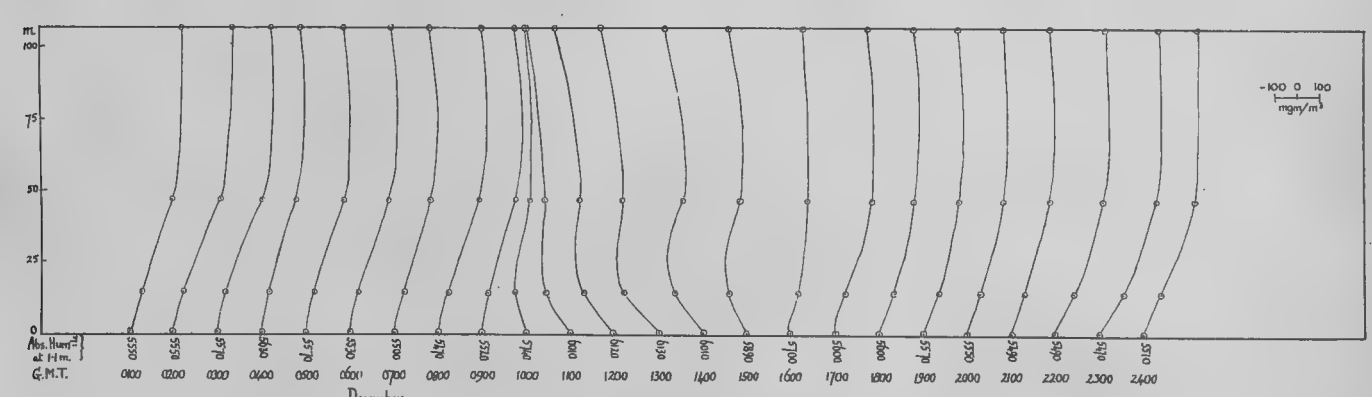

December

M.R.P. 5146.

FIG. 8. DIURNAL VARIATION OF LAPSE OF HUMIDITY FOR EACH MONTH

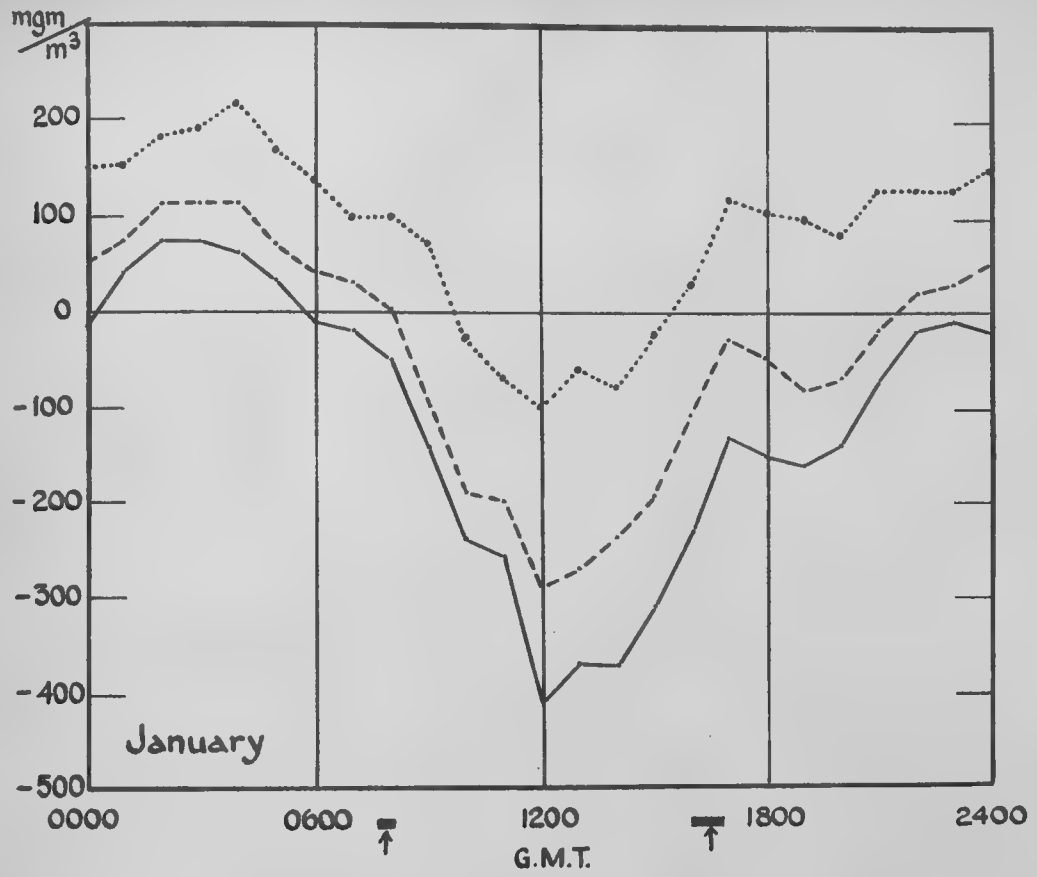

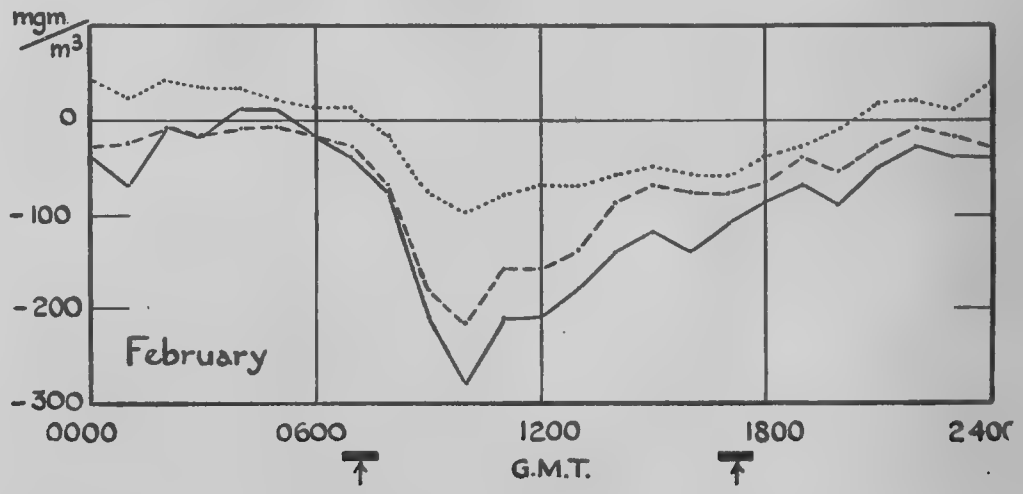

The curves show the humidity differences over the following height intervals: ····· 15·2 – 1·1m. – – – – – 47·2 – 1·1m. ——— 106·7 – 1·1m.

FIG. 8 cont.

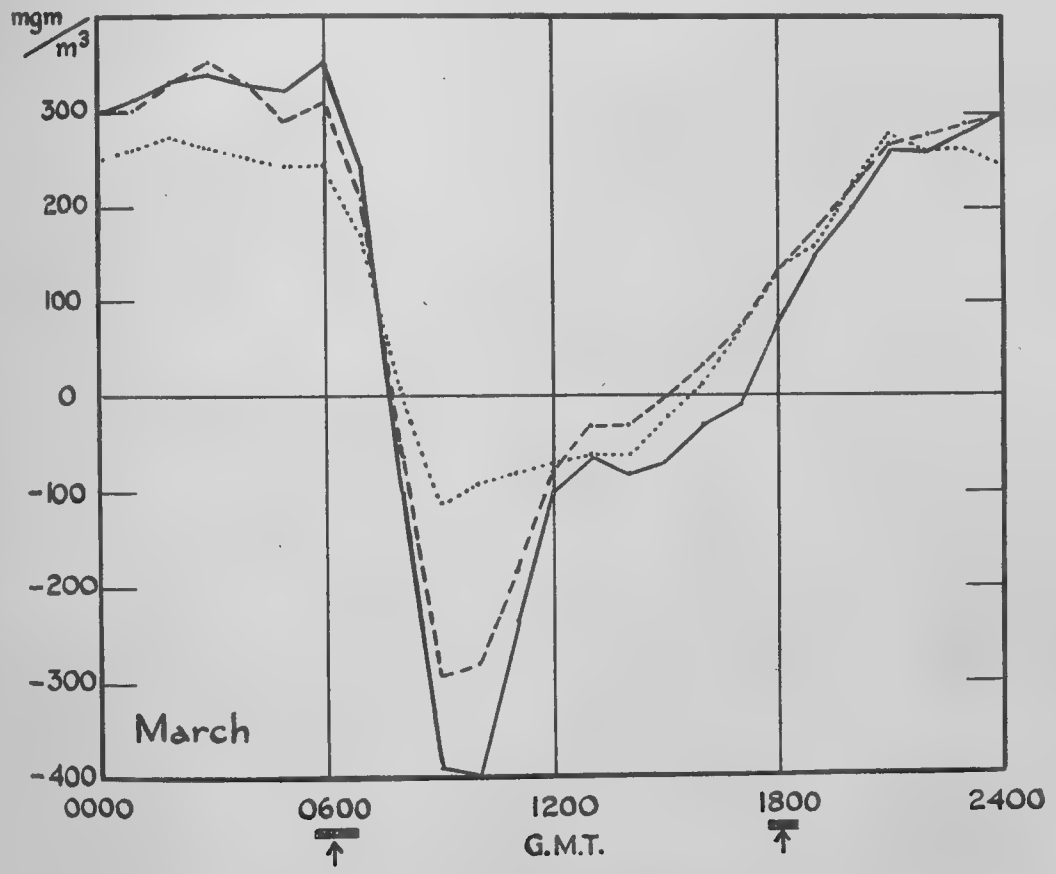
mgm
m³
300
200
100
0
-100
-200
-300
-400
March
0000
0600
1200
1800
2400
G.M.T.

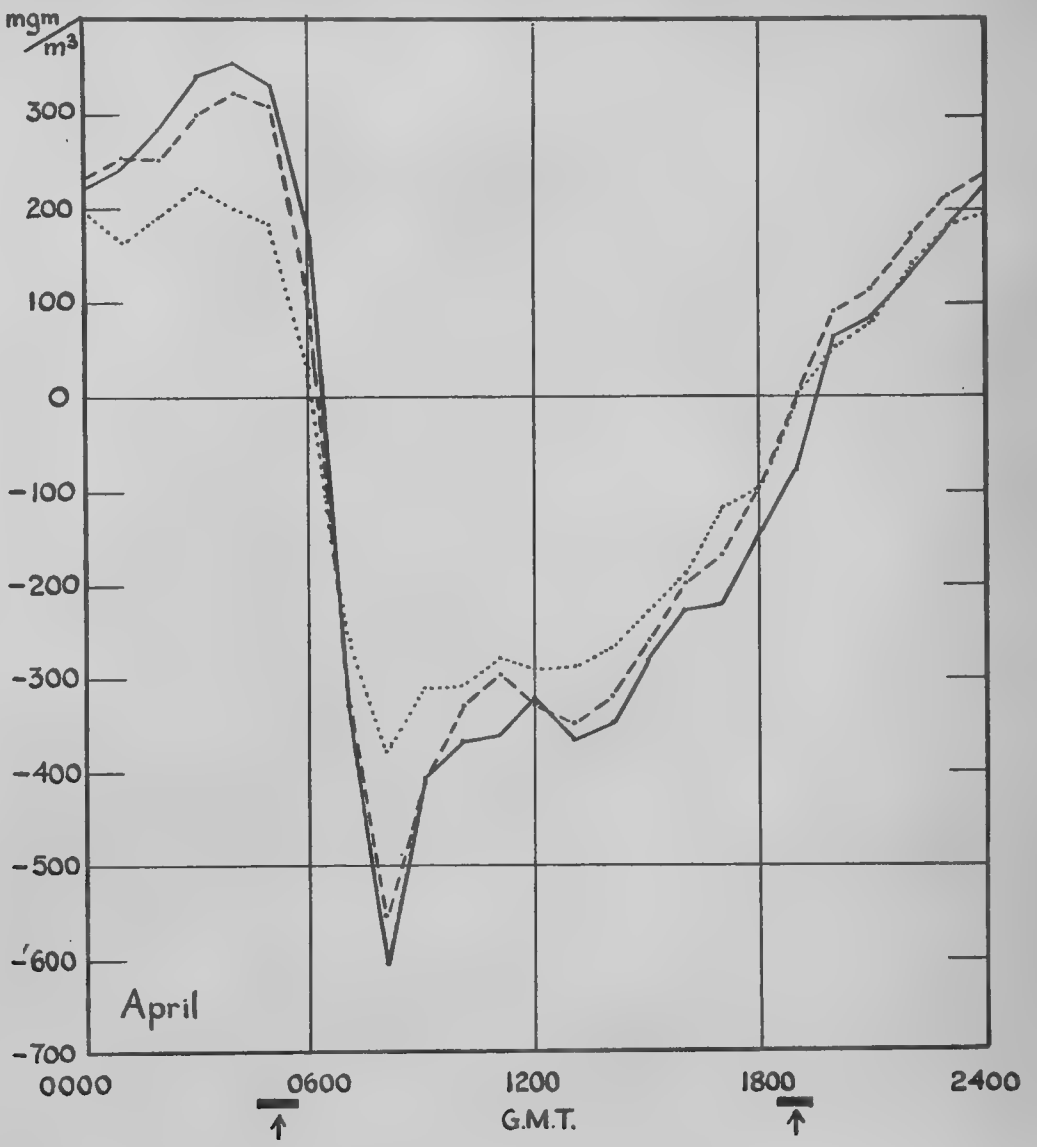
mgm
m³
300
200
100
0
-100
-200
-300
-400
-500
-600
-700
April
0000
0600
1200
1800
2400
G.M.T.

FIG. 8 cont.

N.R.P. 346.

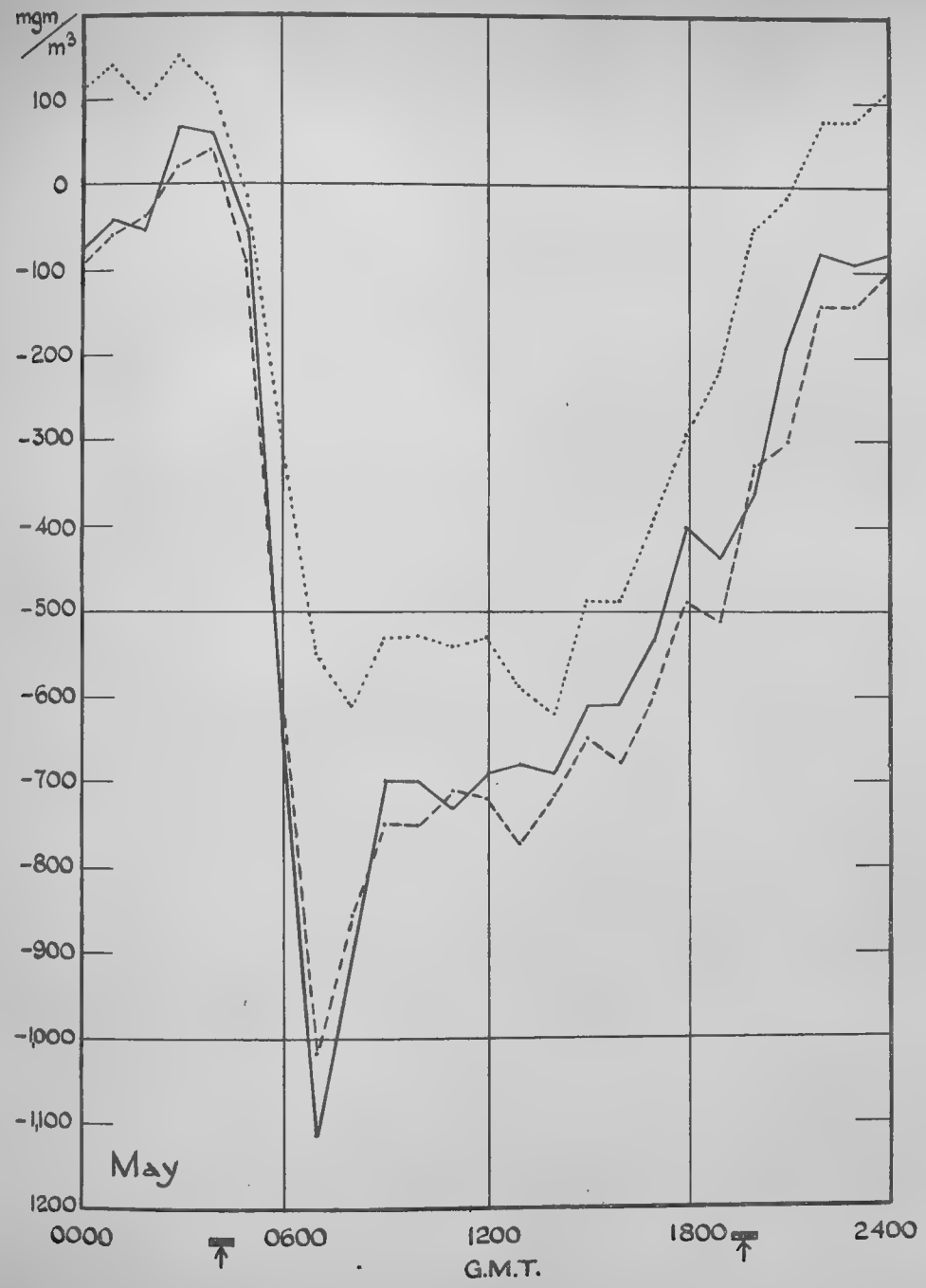

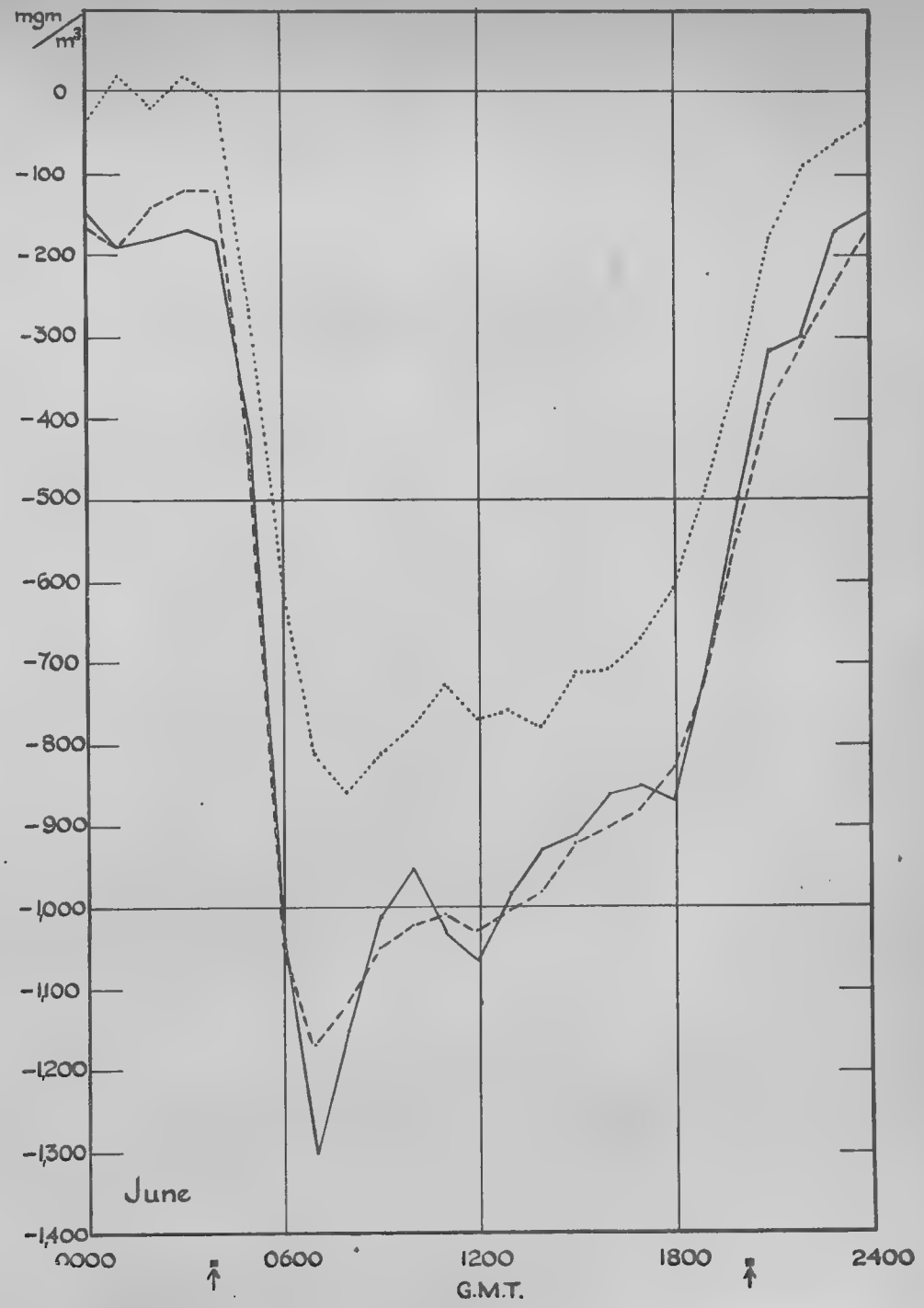

FIG. 8 cont.

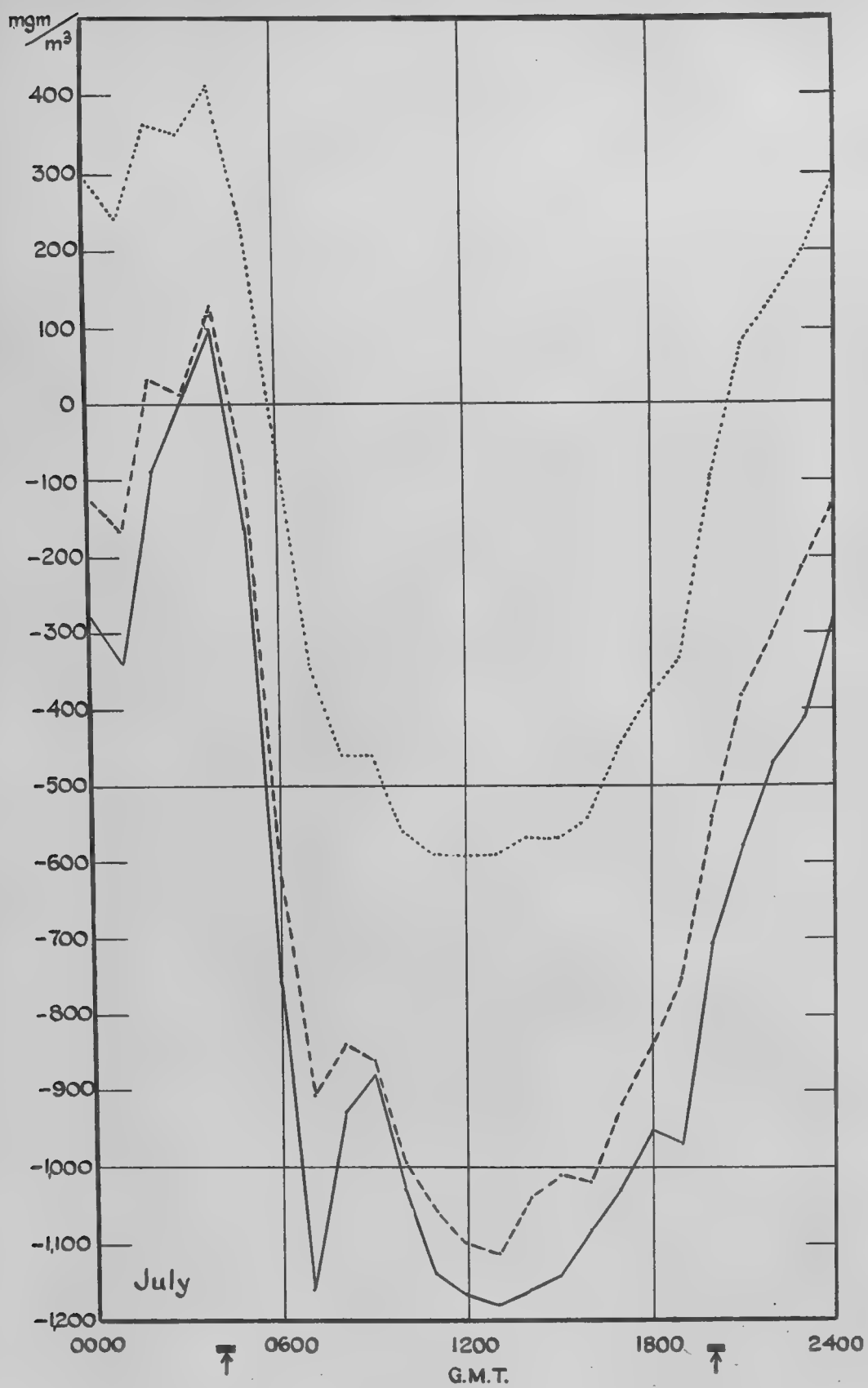
mgm/m³
400
300
200
100
0
-100
-200
-300
-400
-500
-600
-700
-800
-900
-1,000
-1,100
-1,200
July
0000
0600
1200
1800
2400
G.M.T.

FIG. 8 cont.

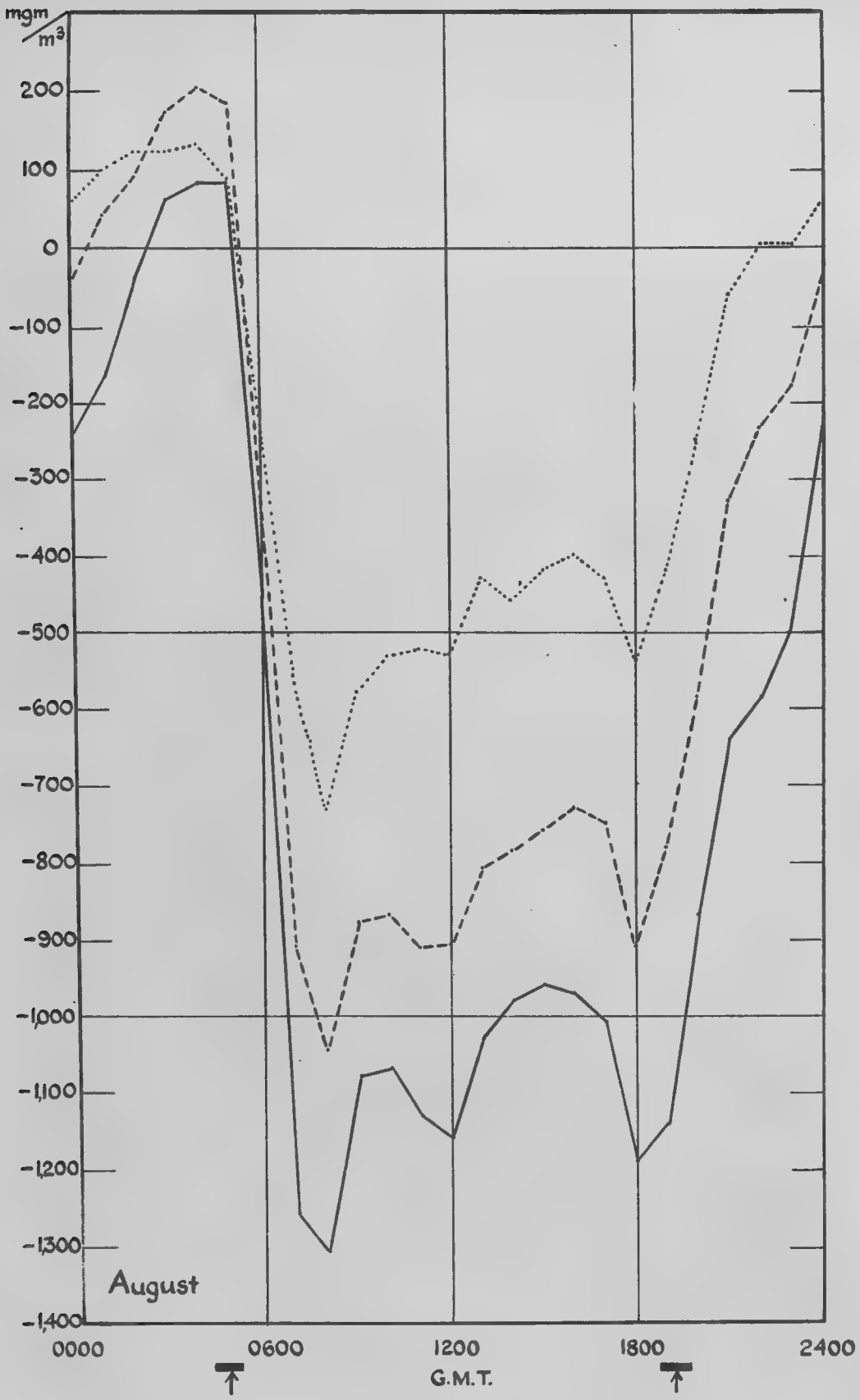
mgm
m³
200
100
0
-100
-200
-300
-400
-500
-600
-700
-800
-900
-1,000
-1,100
-1,200
-1,300
-1,400
August
0000
0600
1200
1800
2400
G.M.T.

FIG. 8 cont.

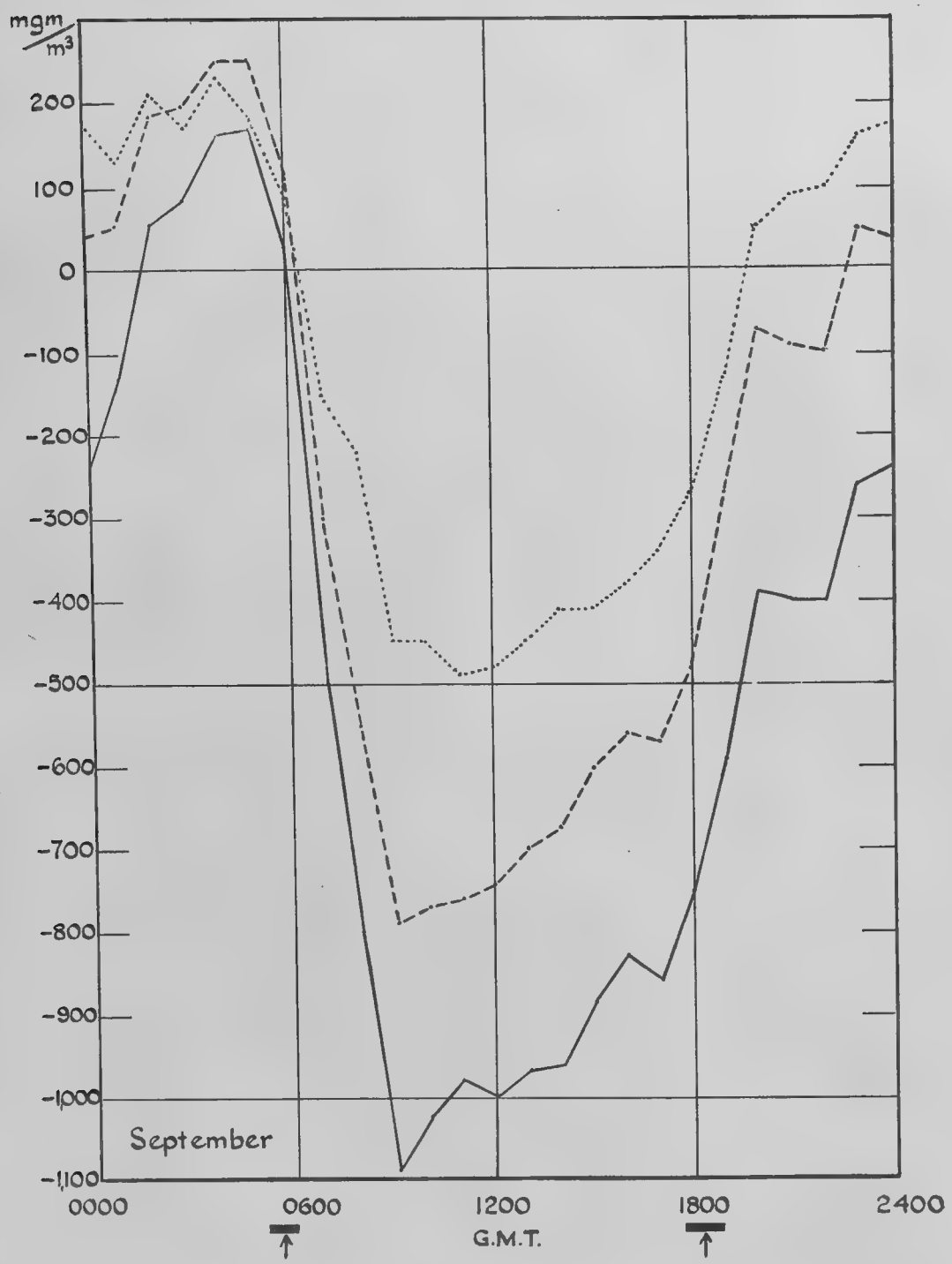
mgm/m³
200
100
0
-100
-200
-300
-400
-500
-600
-700
-800
-900
-1,000
-1,100
September
0000
0600
1200
1800
2400
G.M.T.

FIG. 8 cont.

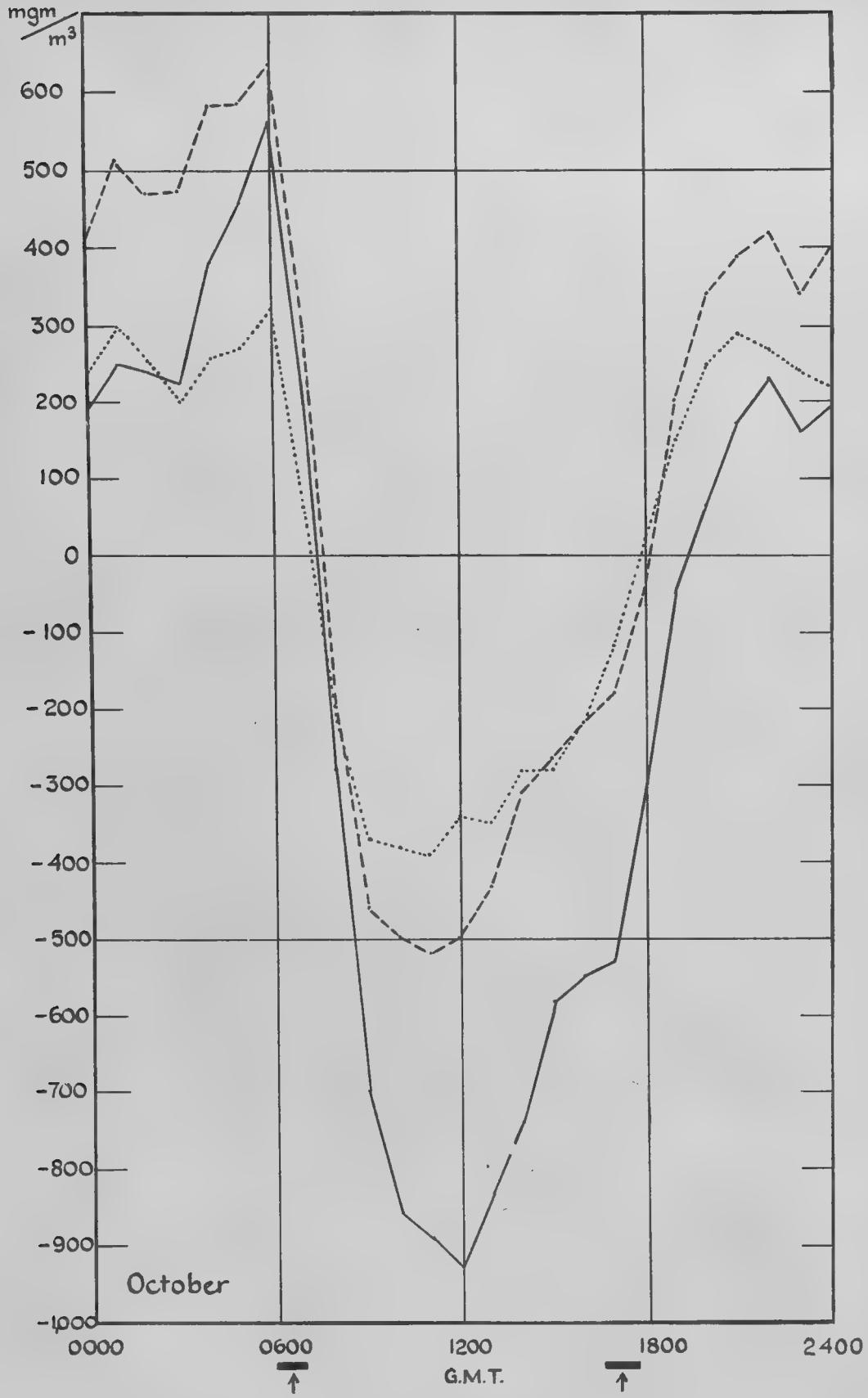
mgm/m³
600
500
400
300
200
100
0
-100
-200
-300
-400
-500
-600
-700
-800
-900
-1000
October
0000
0600
1200
1800
2400
G.M.T.

FIG. 8 cont.

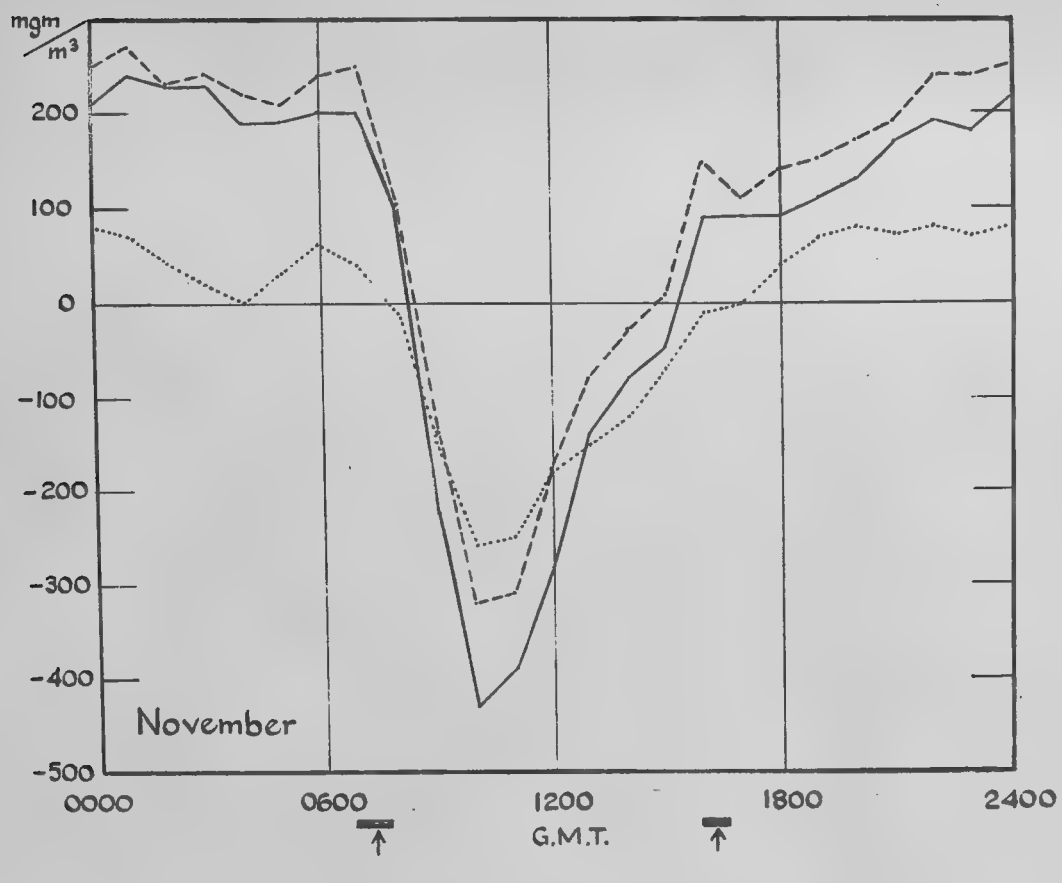
mgm
m³
200
100
0
-100
-200
-300
-400
-500
November
0000
0600
1200
1800
2400
G.M.T.

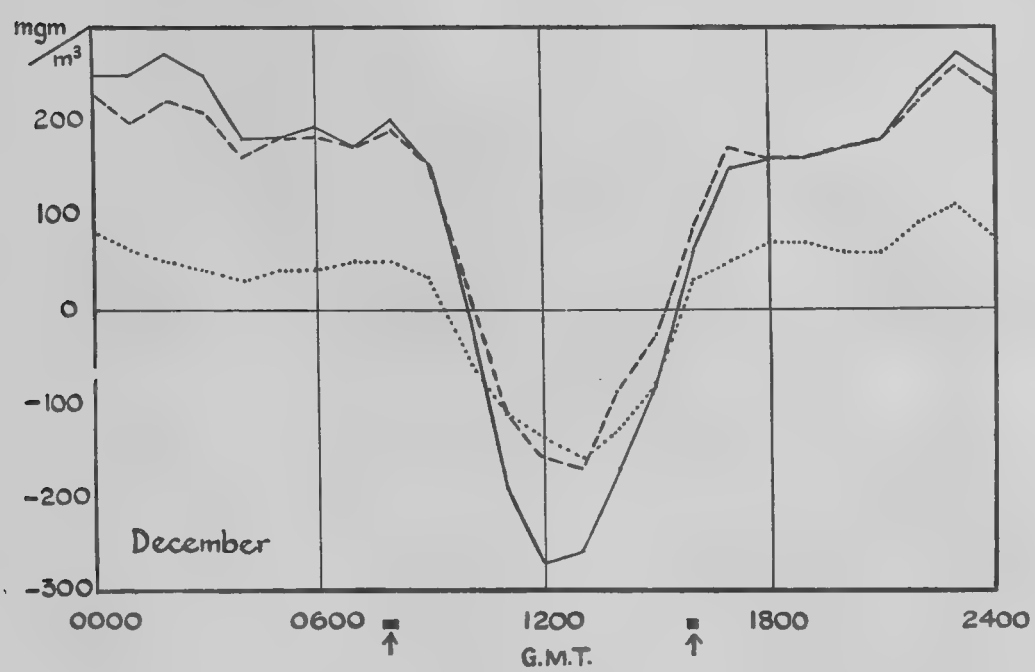
mgm
m³
200
100
0
-100
-200
-300
December
0000
0600
1200
1800
2400
G.M.T.

FIG. 9 DIURNAL VARIATION OF LAPSE OF HUMIDITY OVER 3 HEIGHT INTERVALS — CLEAR AND OVERCAST DAYS IN SUMMER AND WINTER.

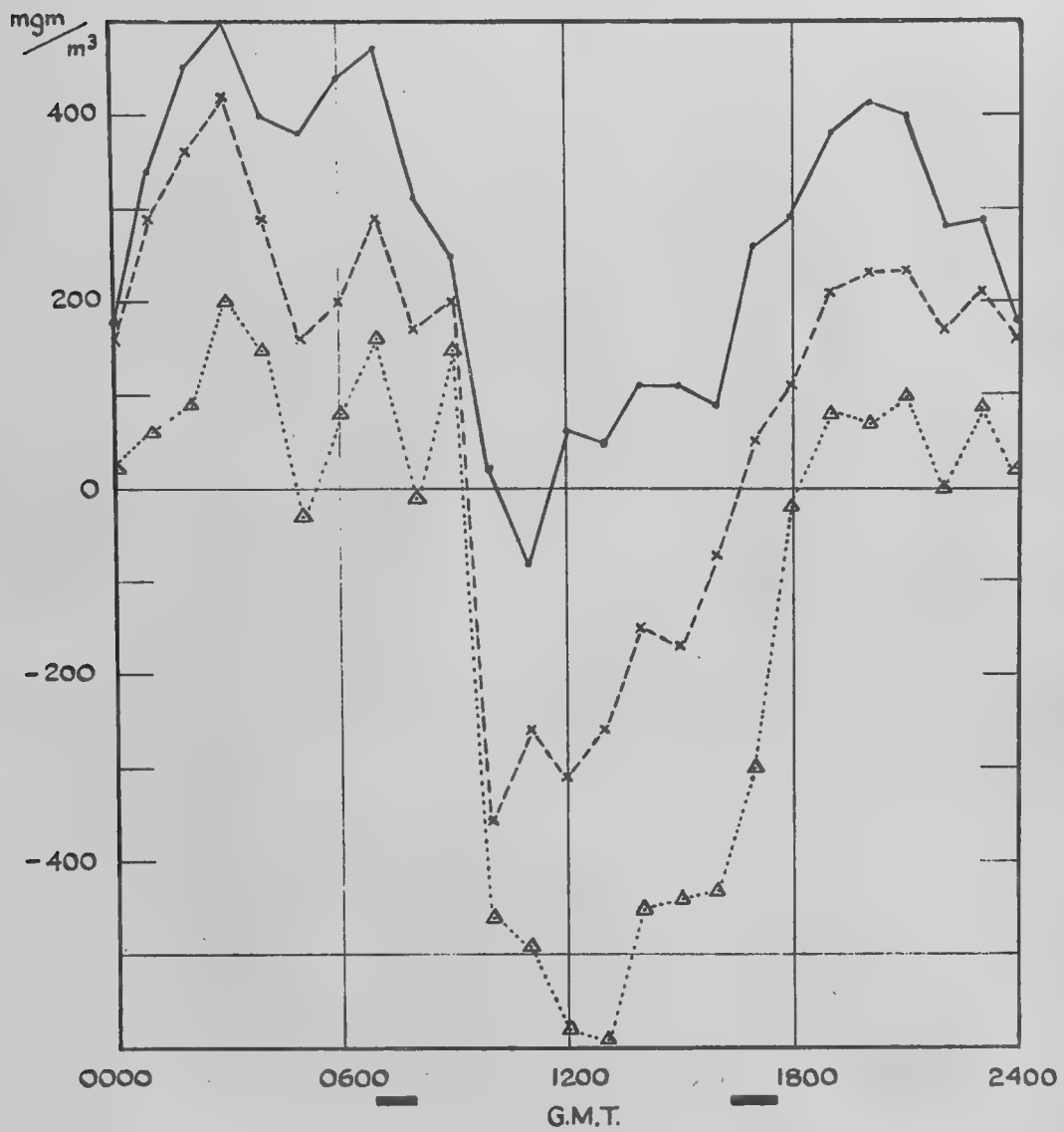

CLEAR DAYS IN WINTER

The lapse rates are represented by

——• 15·2 – 1·1 m. ×- - - - × 47·2 – 1·1 m. Δ·····Δ 106·7 – 1·1 m.

FIG. 5 Cont.

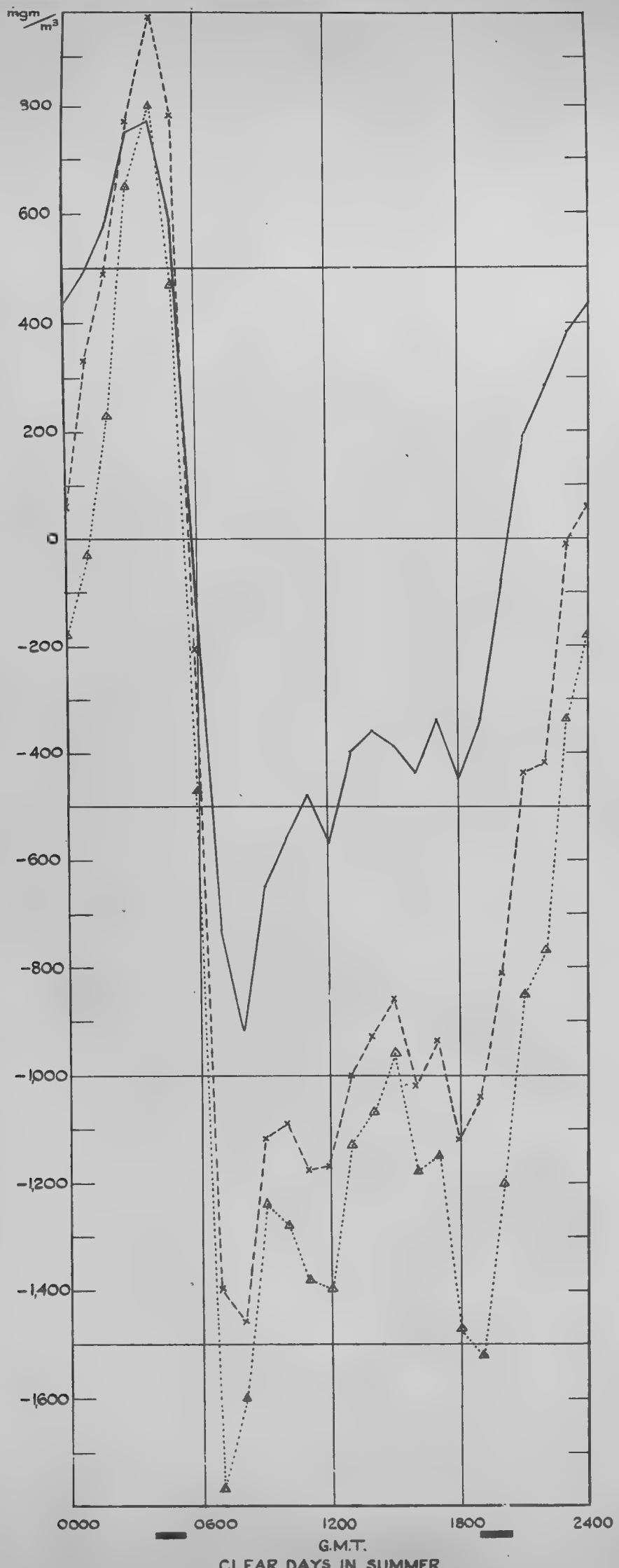

CLEAR DAYS IN SUMMER

FIG. 9 cont.

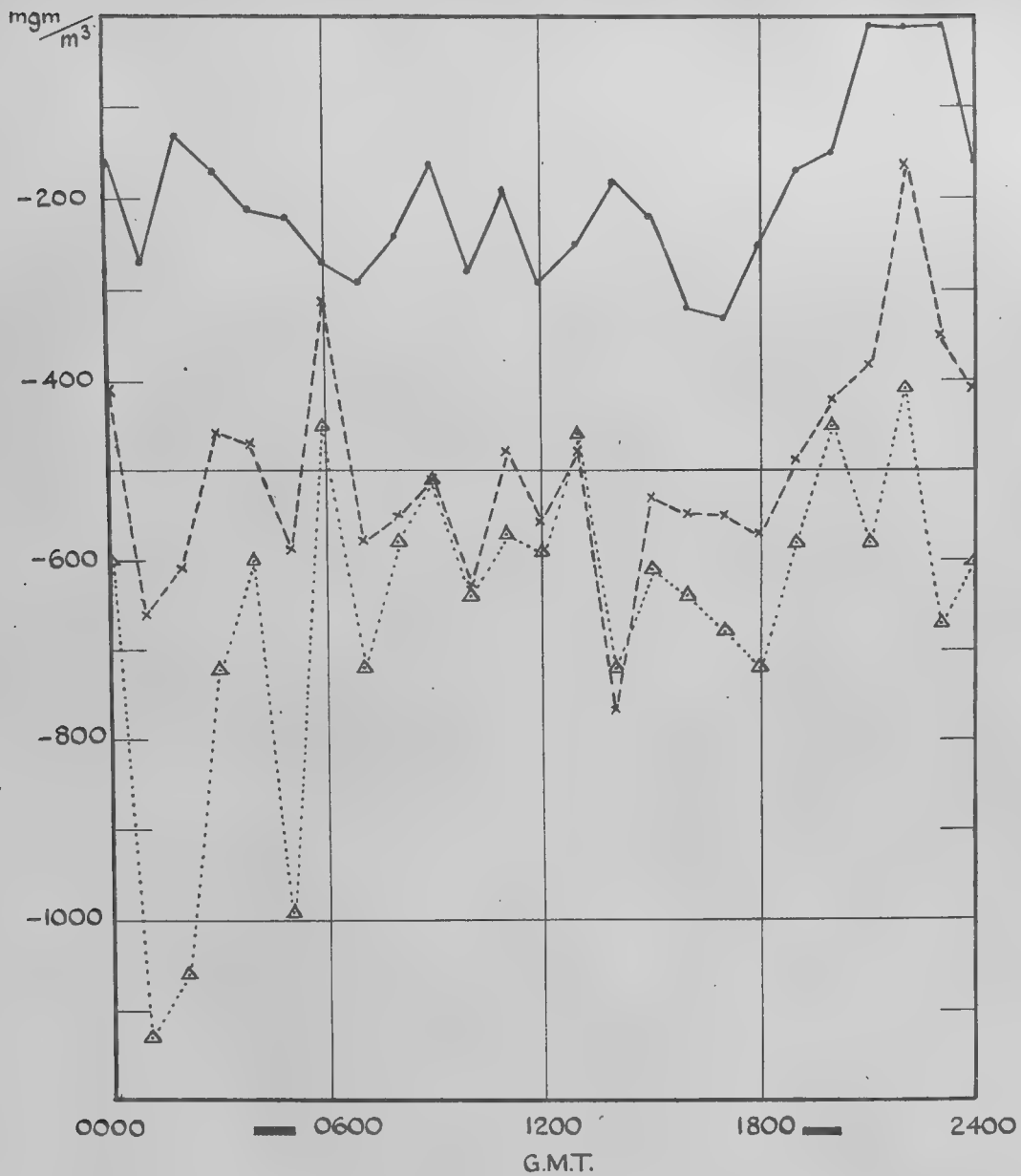

OVERCAST DAYS IN SUMMER

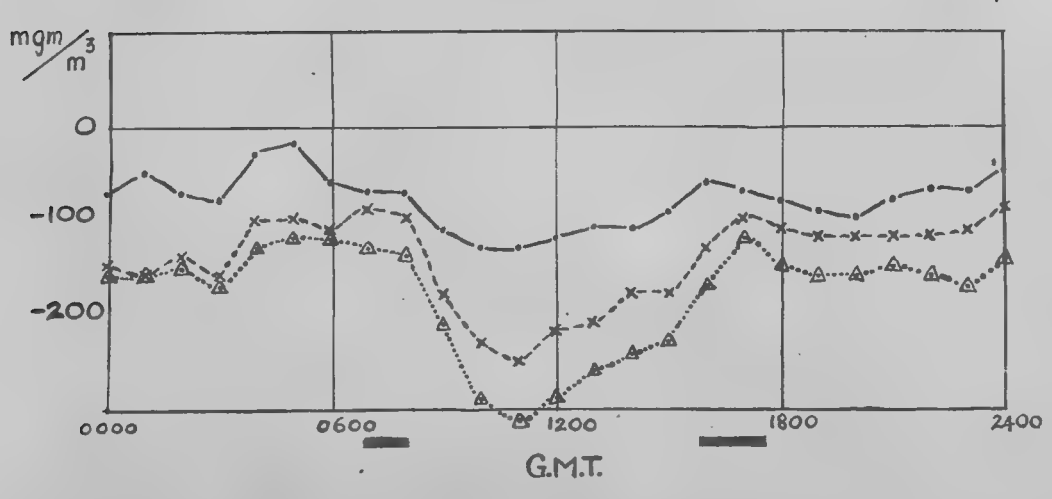

OVERCAST DAYS IN WINTER

FIG. 10. OGIVE OF PERCENTAGE FREQUENCY OF LAPSE RATES OF HUMIDITY

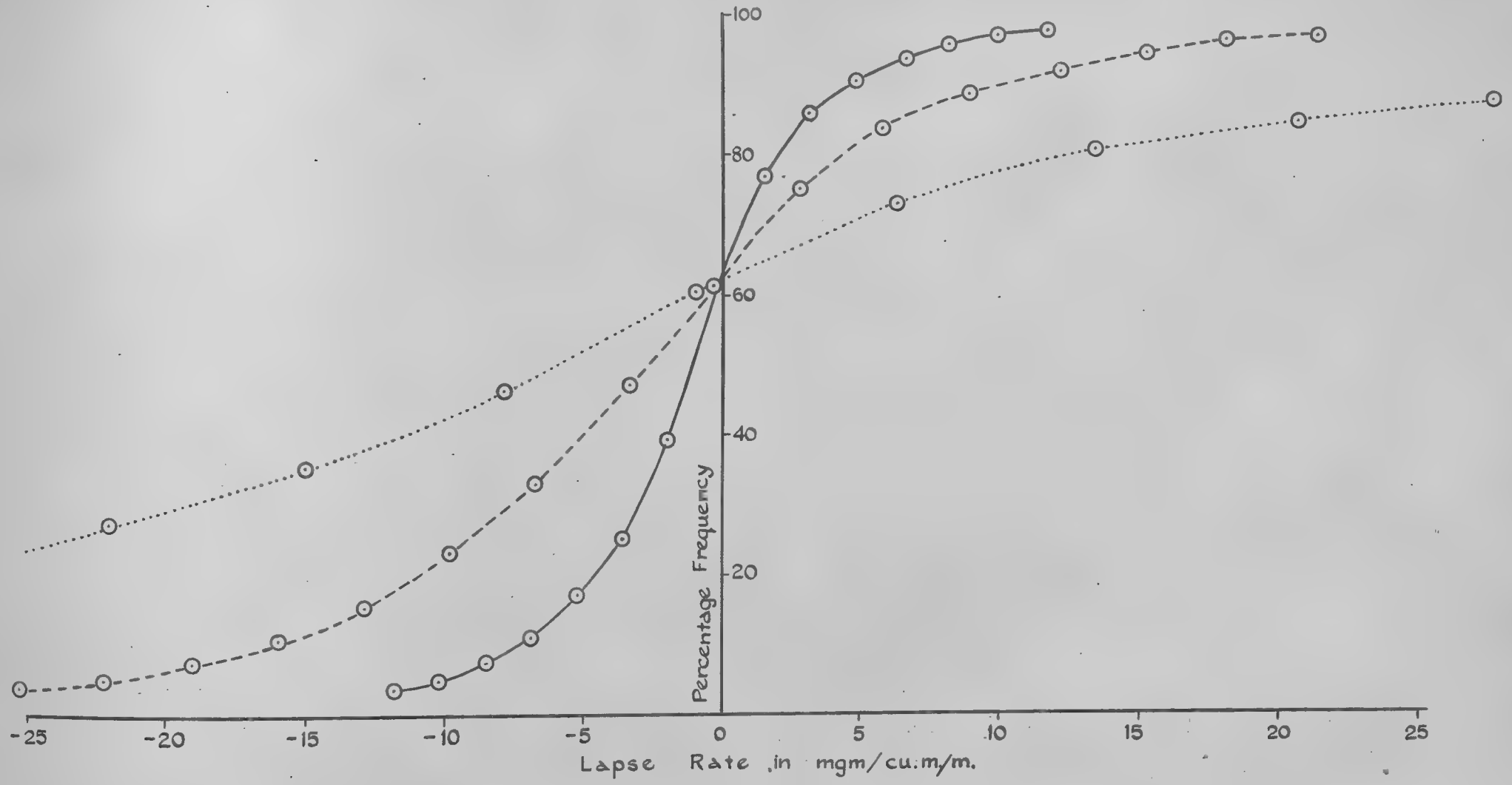

The lapse rates are represented ····· 15·2 – 1·1 m. ----- 47·2 – 15·2 m. ——— 106·7 – 47·2 m.

FIG. 11. DIURNAL VARIATION OF HUMIDITY AT FOUR HEIGHTS.

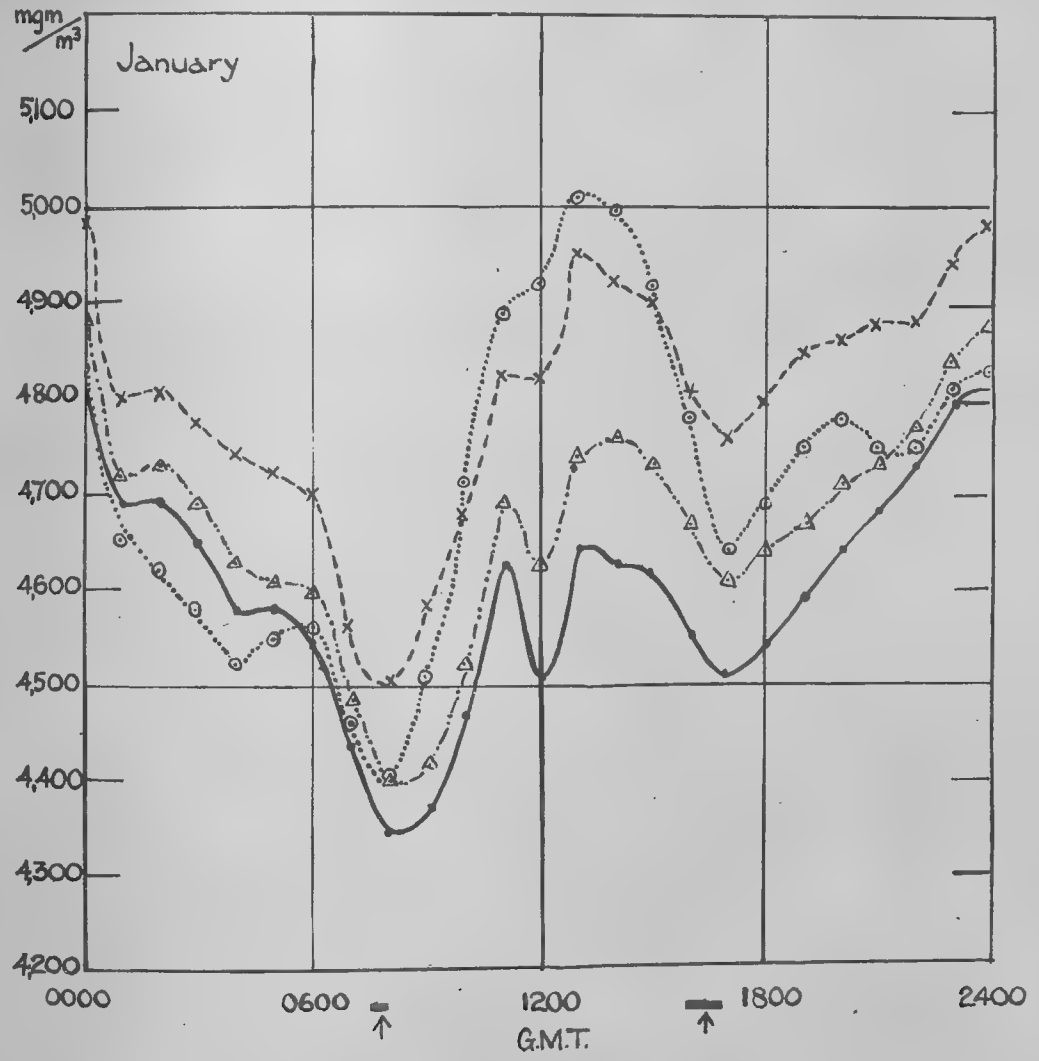

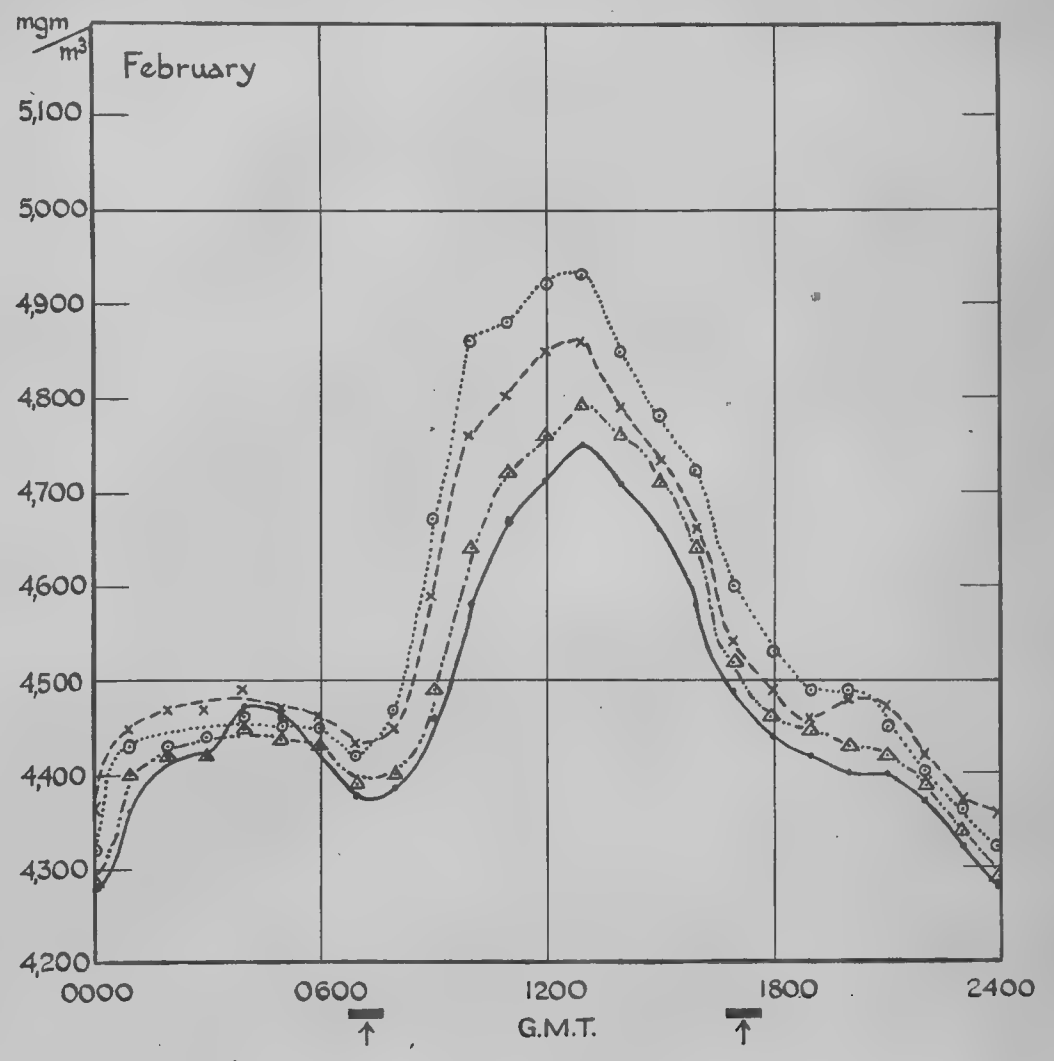

Humidity of height of ⊙·····⊙ = 1·1 m. △·-·-·-△ = 47·2 m.
×-----× = 15·2 m. ●——● = 106·7 m.

FIG. 11 cont.

M.R.P. 546.

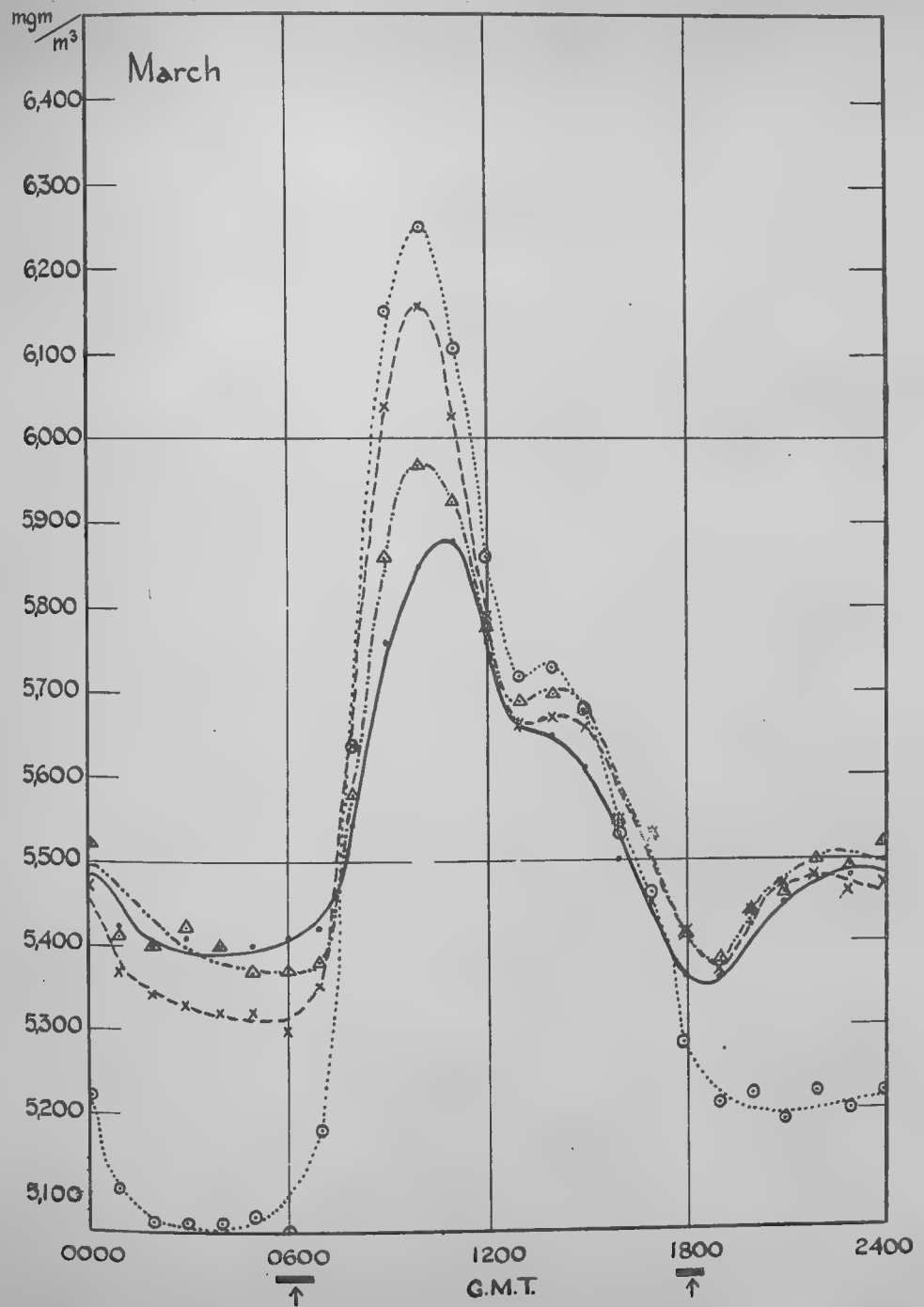

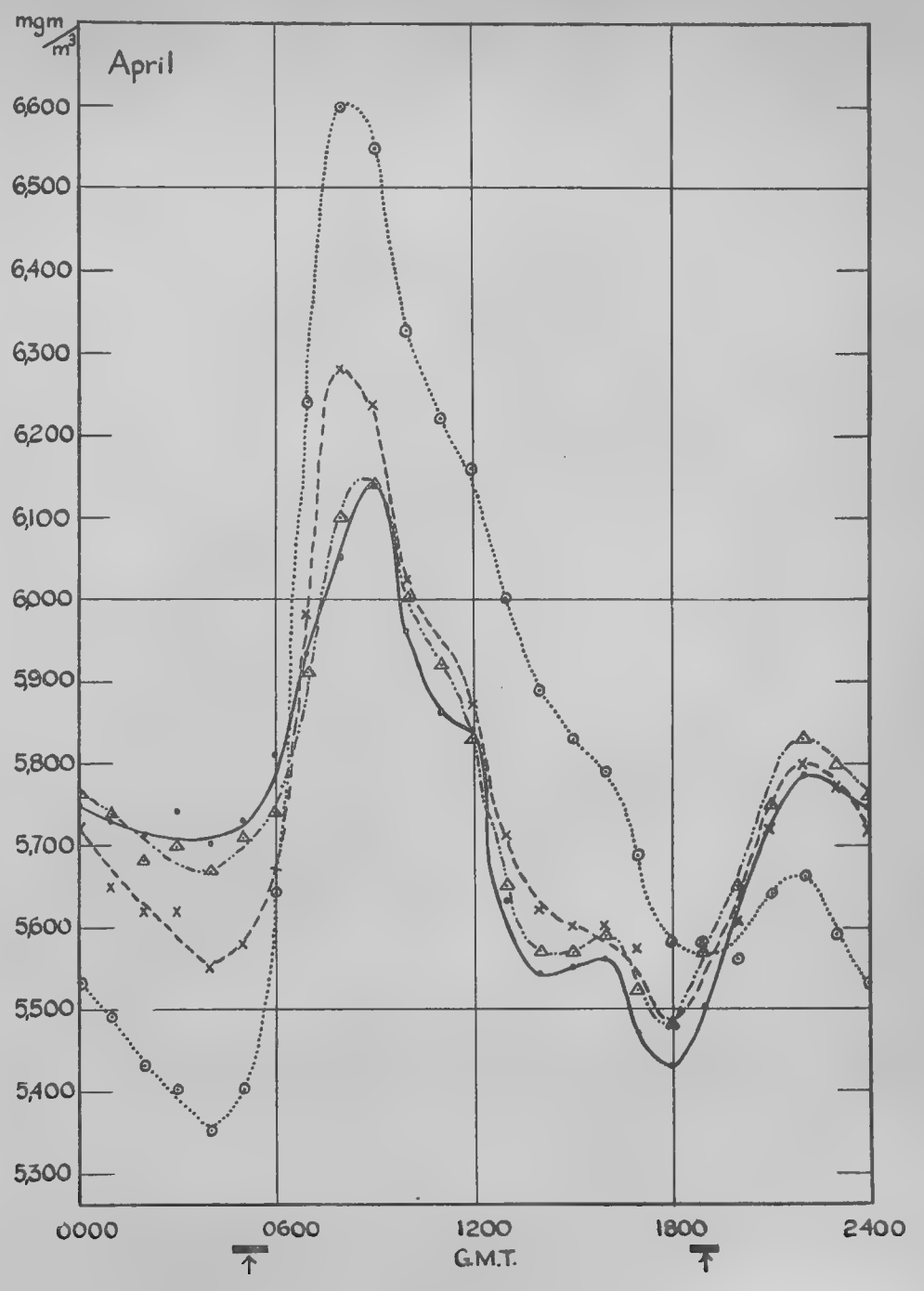

FIG. 11 cont.

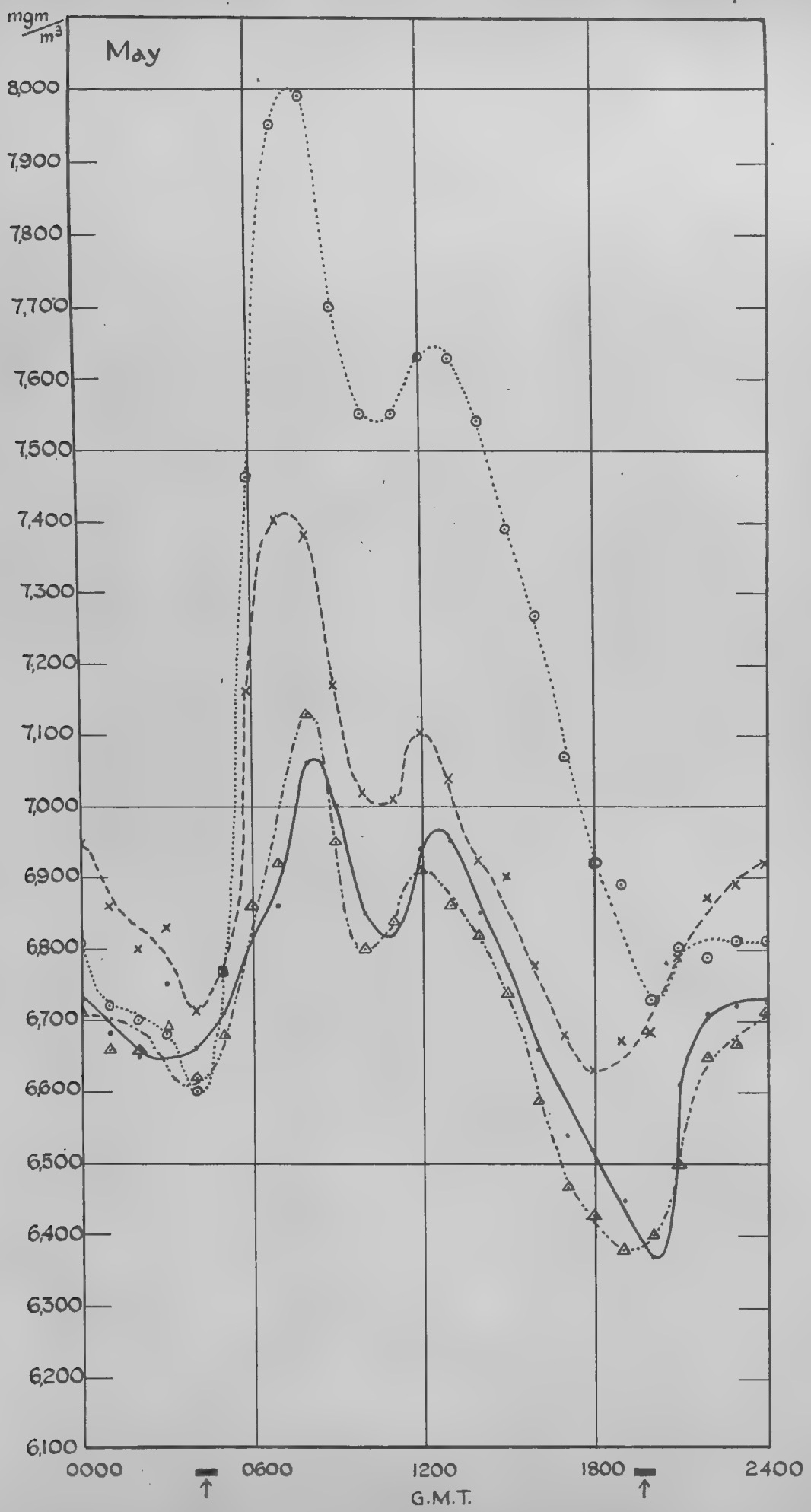
mgm/m³
May
8,000
7,900
7,800
7,700
7,600
7,500
7,400
7,300
7,200
7,100
7,000
6,900
6,800
6,700
6,600
6,500
6,400
6,300
6,200
6,100
0000
0600
1200
1800
2400
G.M.T.

FIG. 11 cont.

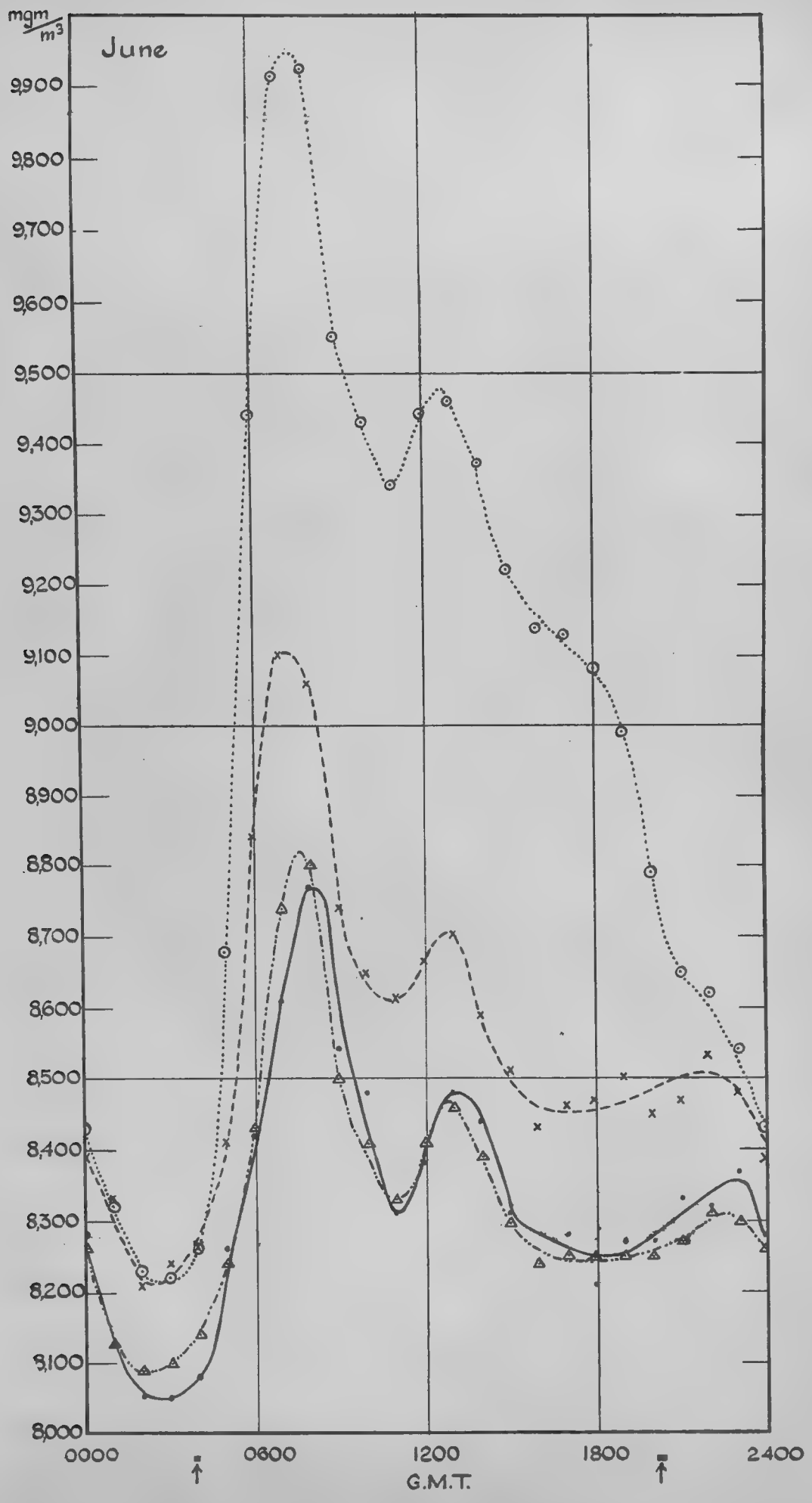
mgm/m³
June
9,900
9,800
9,700
9,600
9,500
9,400
9,300
9,200
9,100
9,000
8,900
8,800
8,700
8,600
8,500
8,400
8,300
8,200
8,100
8,000
0000
0600
1200
1800
2400
G.M.T.

FIG. 11 cont.

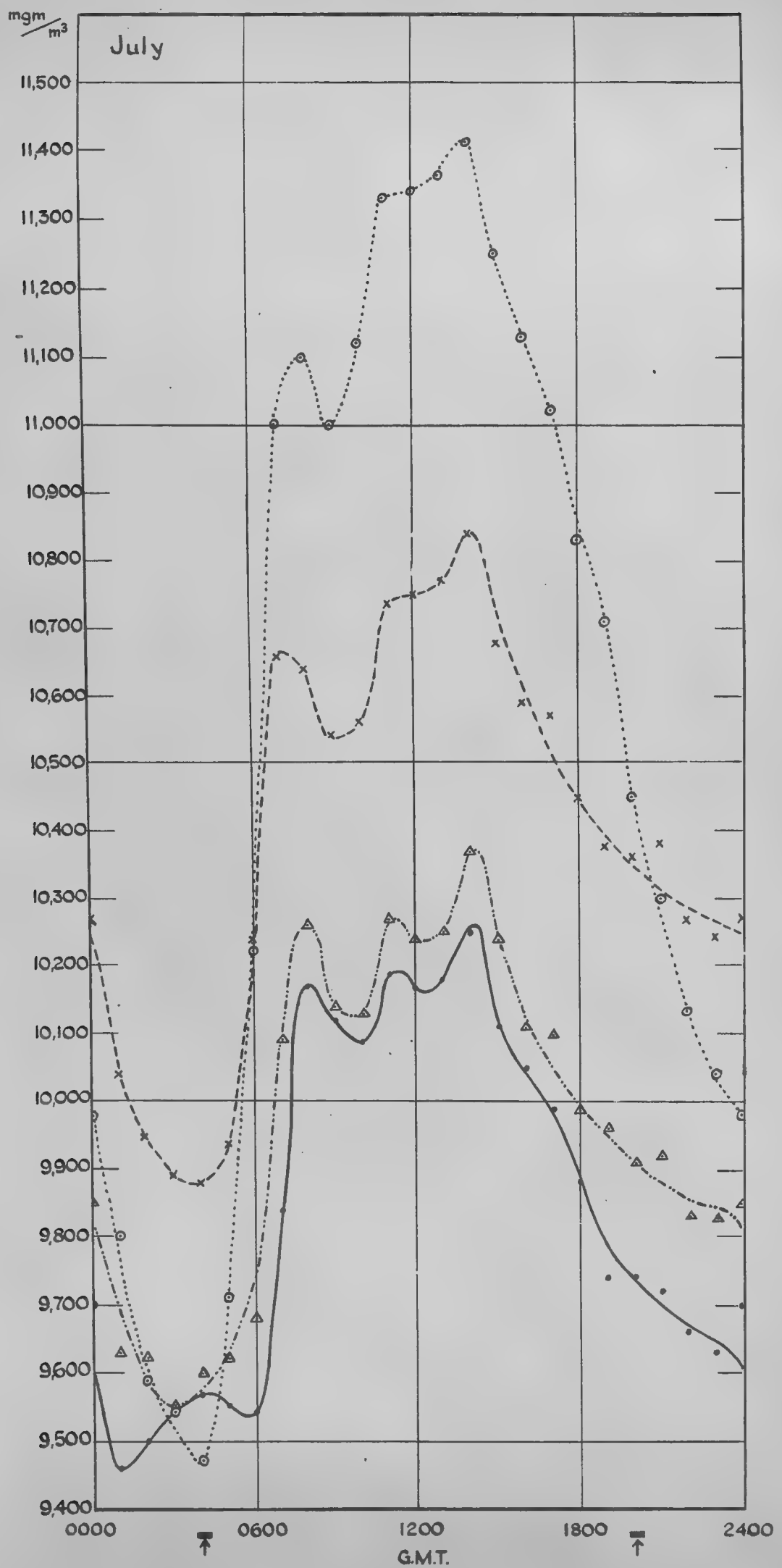
mgm/m³
July
11,500
11,400
11,300
11,200
11,100
11,000
10,900
10,800
10,700
10,600
10,500
10,400
10,300
10,200
10,100
10,000
9,900
9,800
9,700
9,600
9,500
9,400
0000
0600
1200
1800
2400
G.M.T.

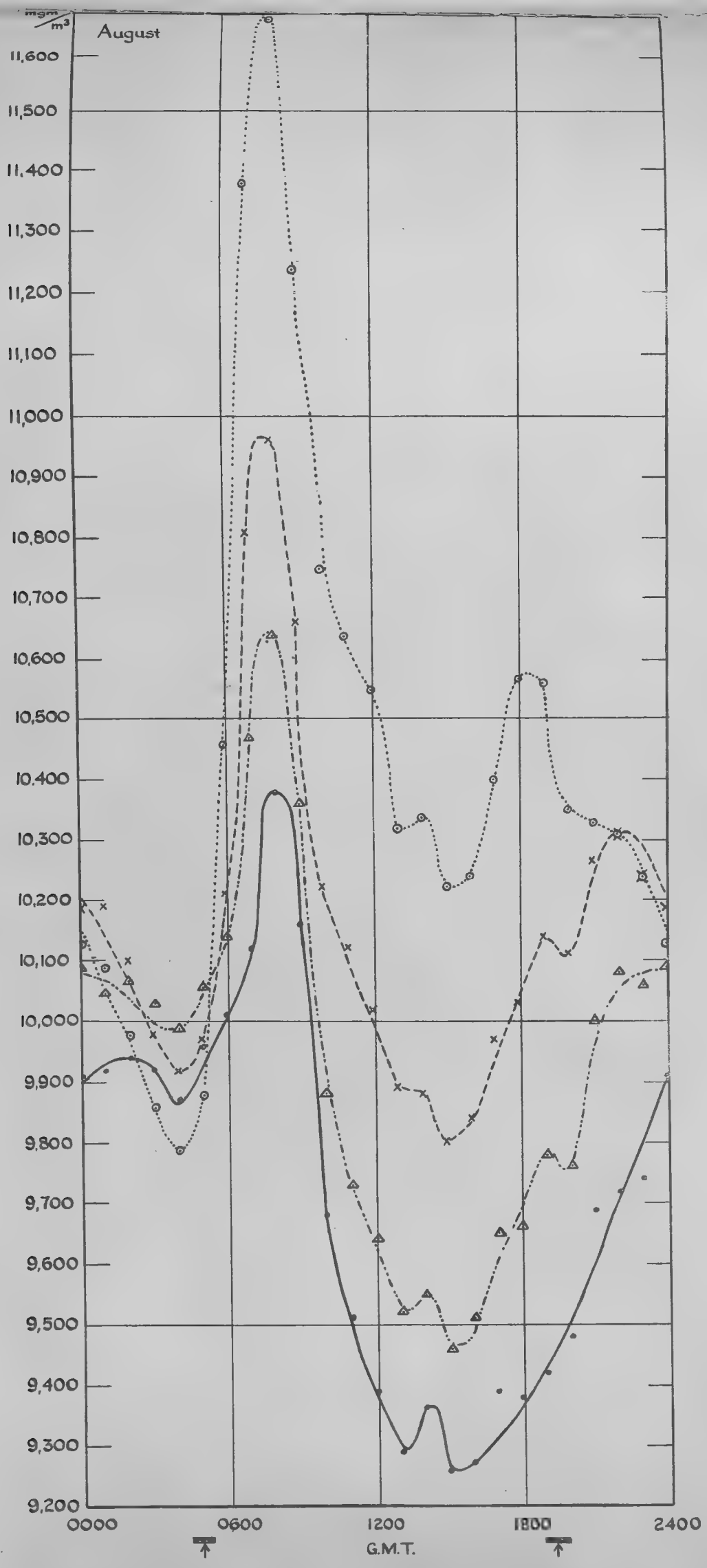
mgm/m³
August
11,600
11,500
11,400
11,300
11,200
11,100
11,000
10,900
10,800
10,700
10,600
10,500
10,400
10,300
10,200
10,100
10,000
9,900
9,800
9,700
9,600
9,500
9,400
9,300
9,200
0000
0600
1200
1800
2400
G.M.T.

FIG. 11 cont.

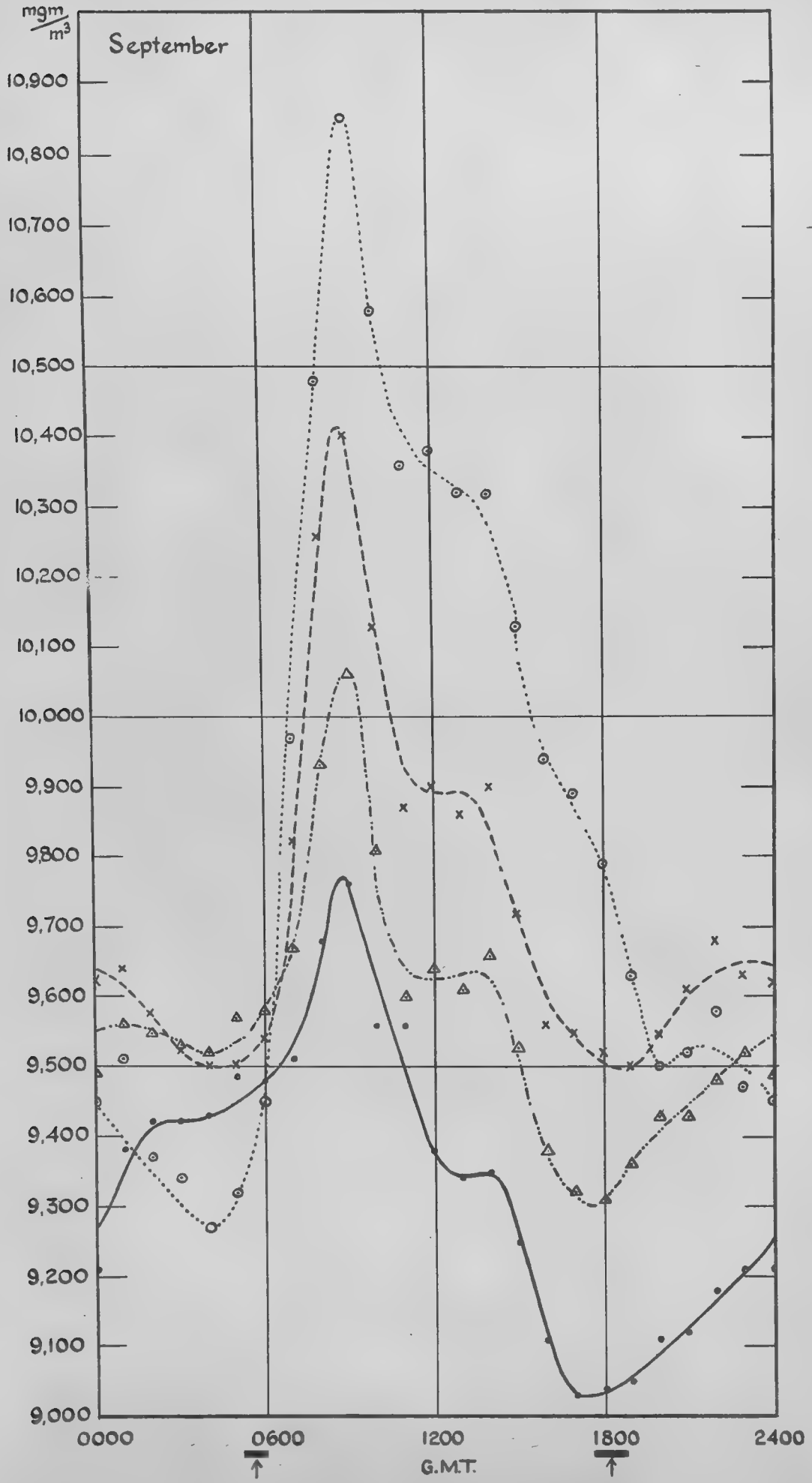
mgm/m³
September
10,900
10,800
10,700
10,600
10,500
10,400
10,300
10,200
10,100
10,000
9,900
9,800
9,700
9,600
9,500
9,400
9,300
9,200
9,100
9,000
0000
0600
1200
1800
2400
G.M.T.

FIG. 11 cont.

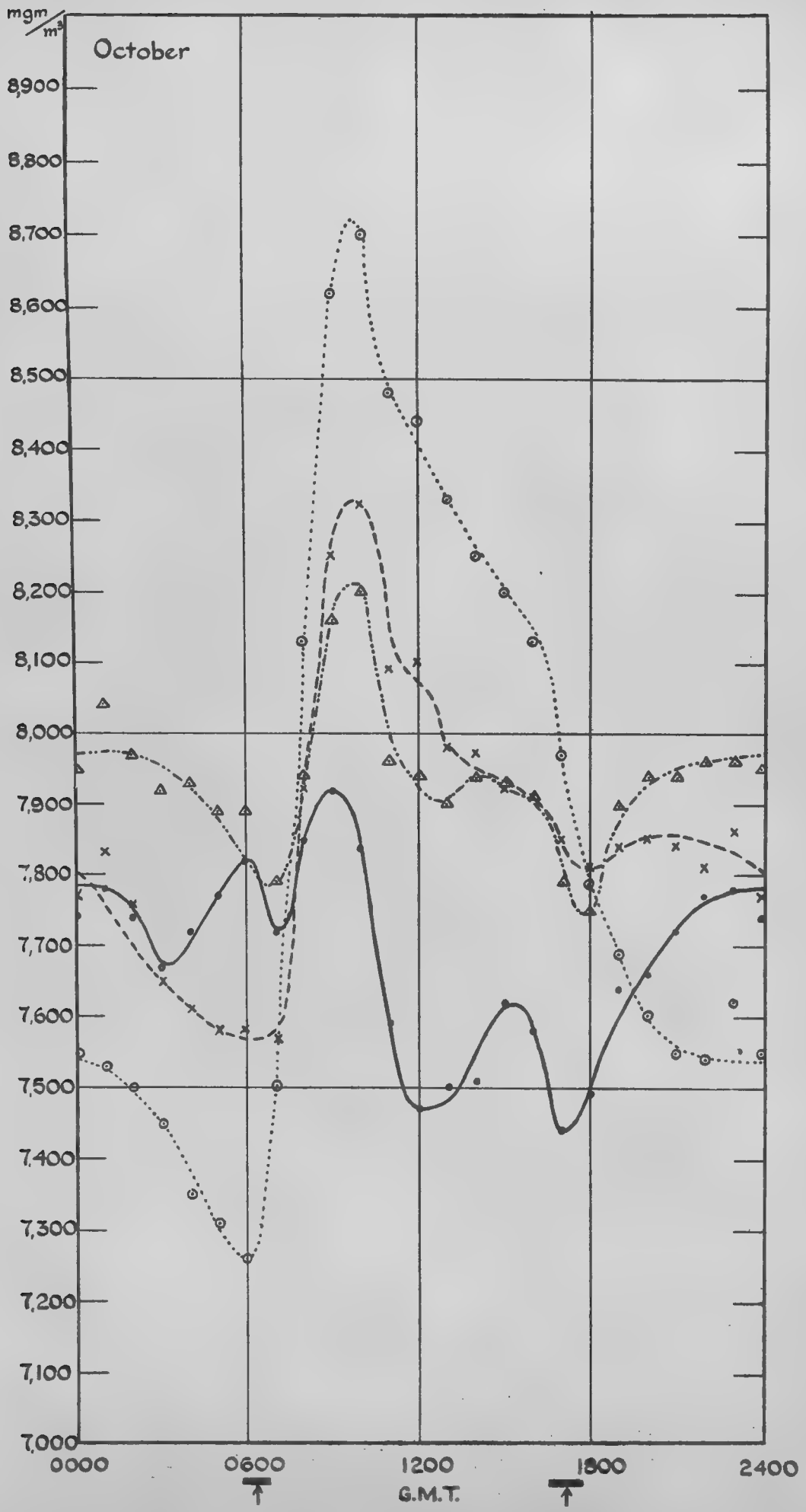
mgm/m³
October
8,900
8,800
8,700
8,600
8,500
8,400
8,300
8,200
8,100
8,000
7,900
7,800
7,700
7,600
7,500
7,400
7,300
7,200
7,100
7,000
0000
0600
1200
1800
2400
G.M.T.

M.R.P. 546.

FIG. 11 cont.

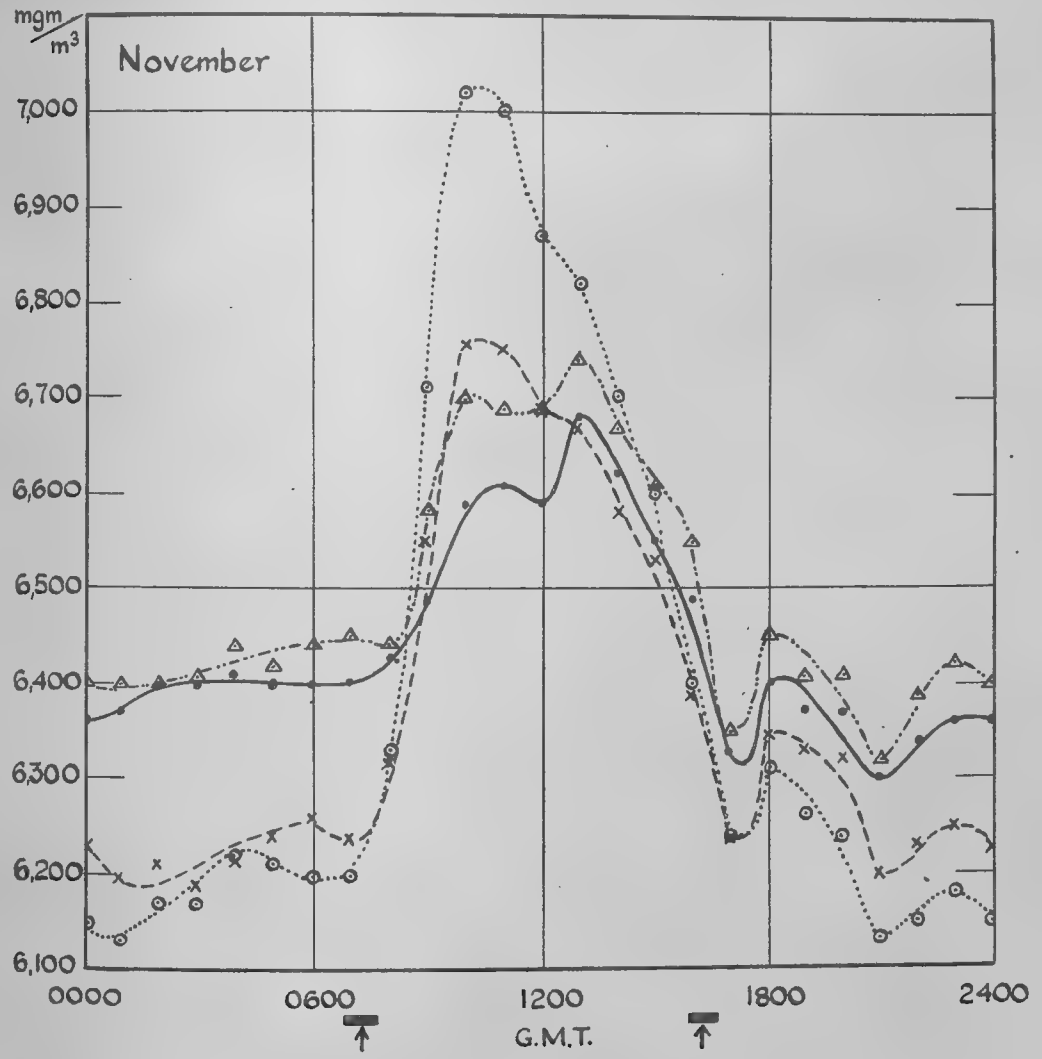

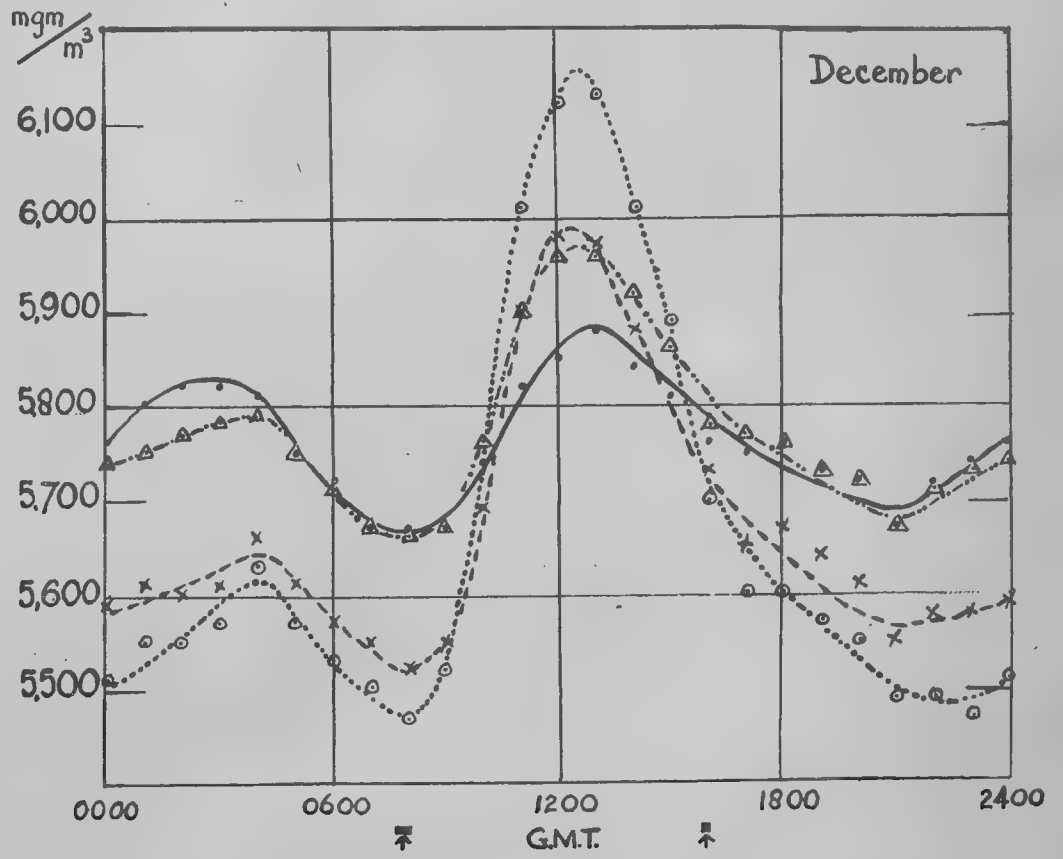

FIG. 12. DIURNAL VARIATION OF HUMIDITY AT FOUR HEIGHTS FOR CLEAR AND OVERCAST DAYS IN SUMMER AND WINTER.

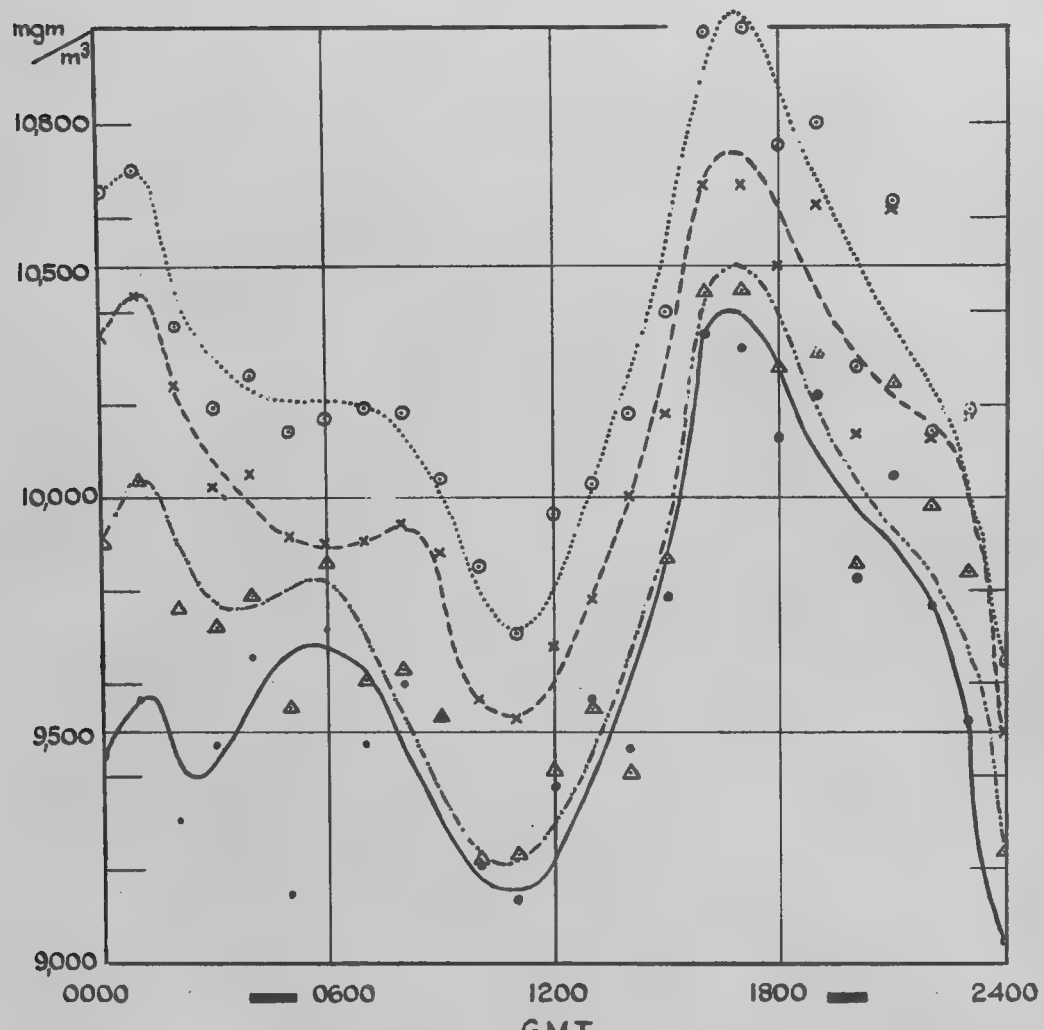

(a) OVERCAST DAYS IN SUMMER

Humidity at height of ⊙·····⊙ = 1·1 m. △------△ = 47·2 m.
x----x = 15·2 m. •———• = 106·7 m.

FIG. 12 cont.

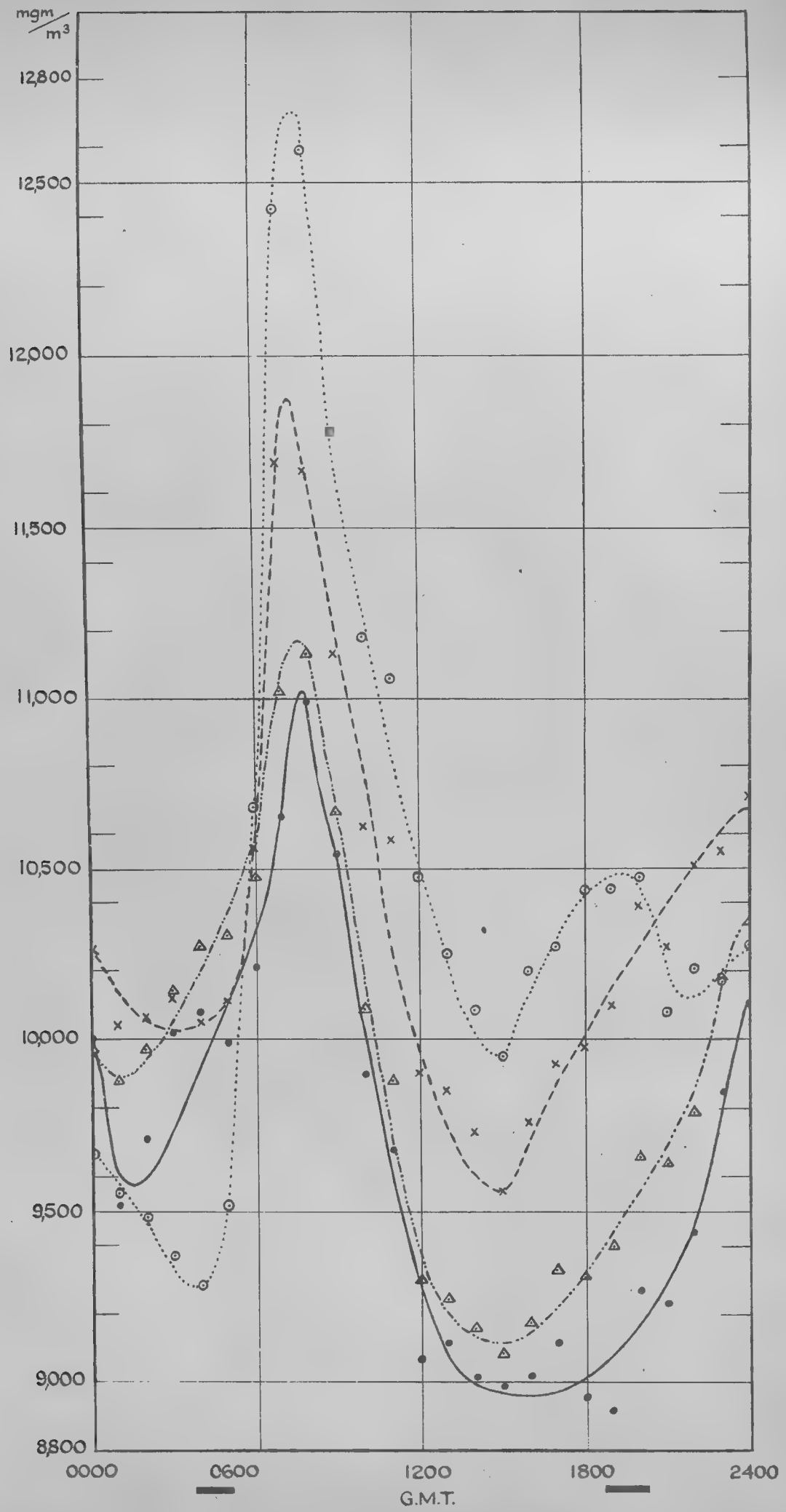

(b) CLEAR DAYS IN SUMMER

FIG. 12 cont.

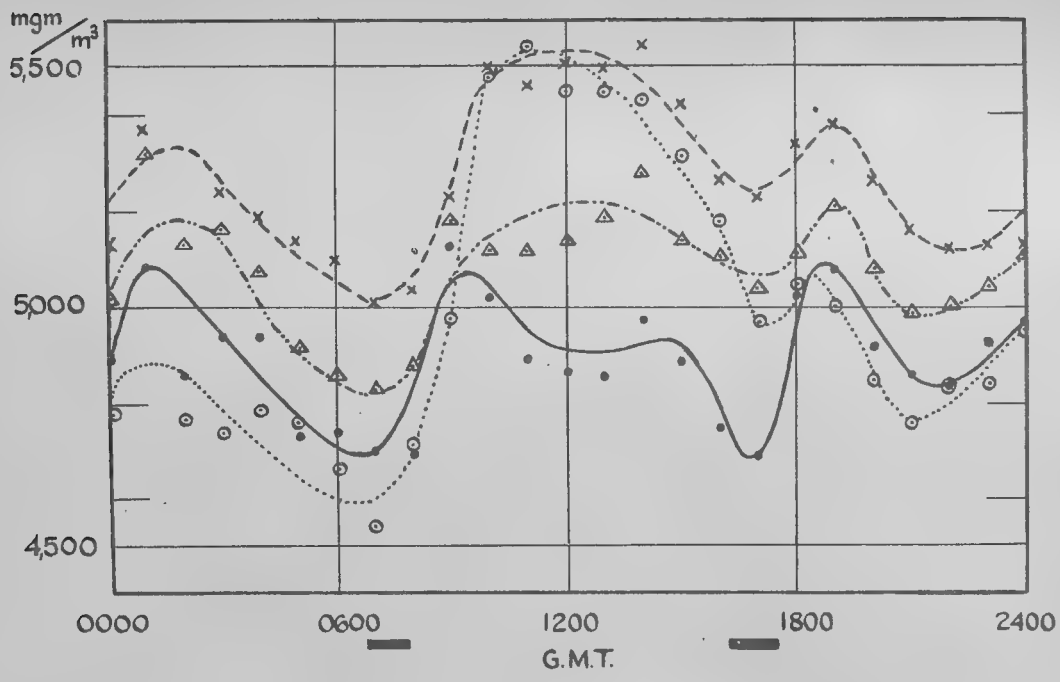

(c) CLEAR DAYS IN WINTER

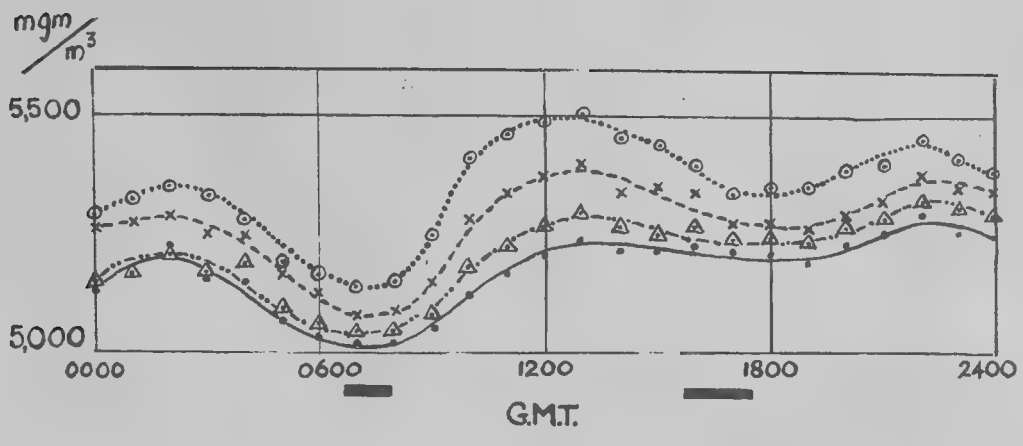

(d) OVERCAST DAYS IN WINTER

FIG. 13. VARIATION OF TEMPERATURE AND HUMIDITY DURING 30 - 31st. OCTOBER 1945.

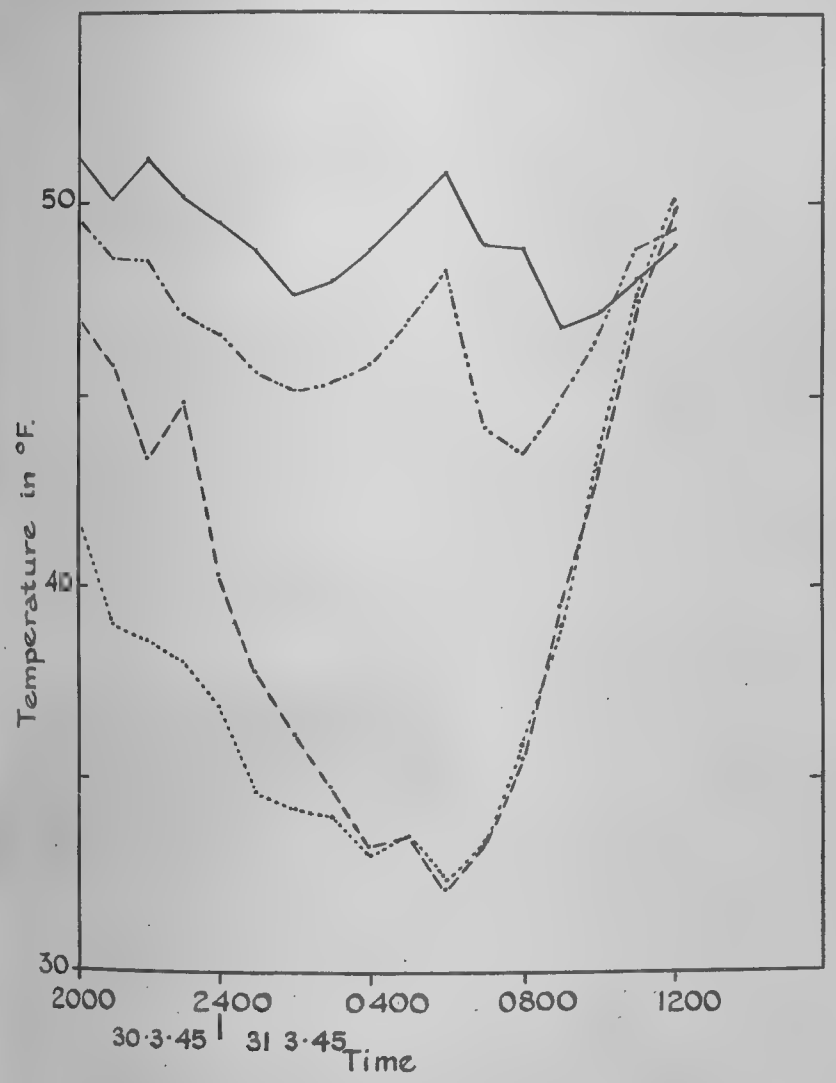

(a) Temperature Variation

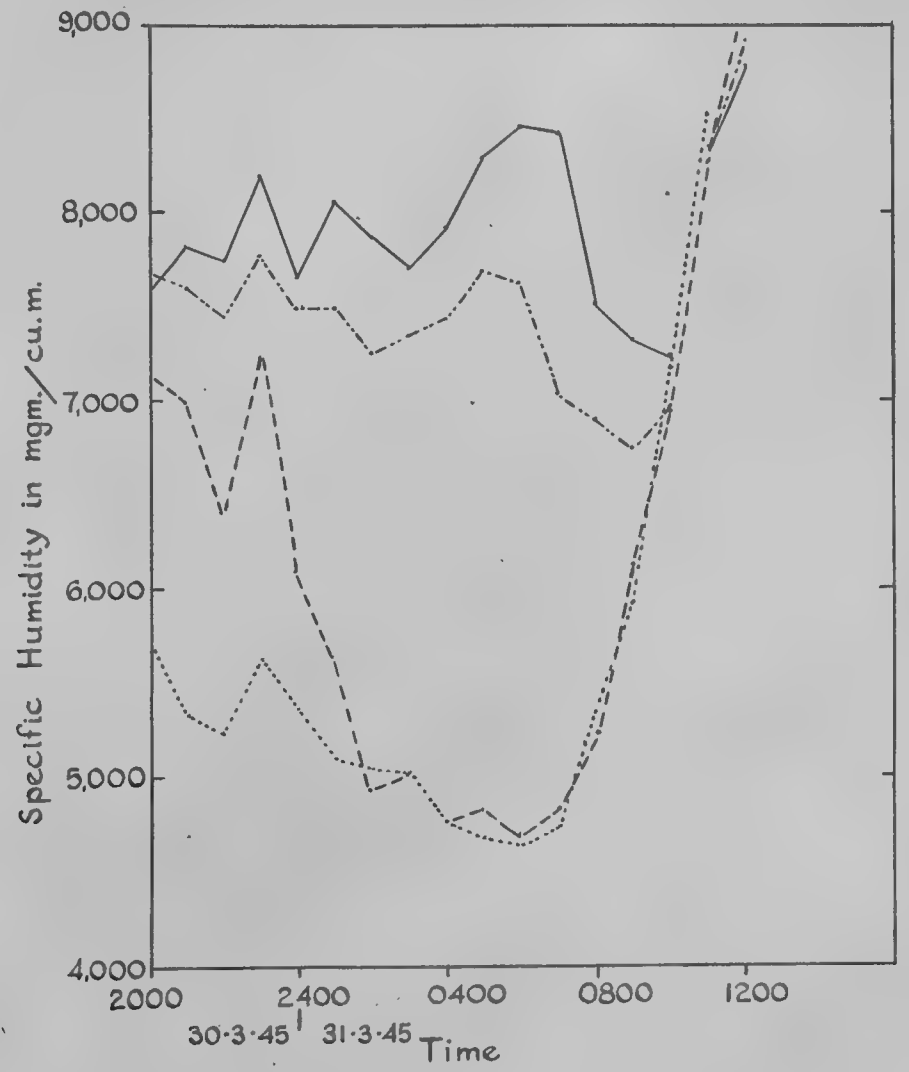

(b) Humidity

Variations shown thus:- 1·1 m. ..... 15·2 m. ------ 47·2 m. -·-·-·- 106·7 m. ———

CONFIDENTIAL. Its contents must not be quoted.

M.R.P. 547
S.C.III/52
31st March, 1950.

AIR MINISTRY

METEOROLOGICAL RESEARCH COMMITTEE

A study of the transfer of heat and water vapour above a surface of short grass.

by
N.E. Rider and G.D. Robinson
(Meteorological Office).

AIR MINISTRY METEOROLOGICAL OFFICE REFERENCE FILE

SUMMARY

The profiles of temperature, humidity and wind have been determined by conventional methods in the lowest 2 metres of the atmosphere above a close-cut grass surface. Simultaneous observations were made of the heat absorbed in the soil and of the short wave and long wave radiative flux of heat. The results of 29 sets of observations are presented and the accuracy and generality of the results discussed.

It is shown that the observed profiles of temperature and humidity have the same form, and that the vertical flux of latent and sensible heat changes only slowly with height; in consequence it is most probable that the ratio of the coefficients of eddy diffusion of heat and water vapour have a ratio constant with height. A modification of Bowen's method, which assumes equality of these coefficients, is then used to determine separately the convective flux of heat and of water vapour. These are computed also from the wind profile, assuming equality of the eddy viscosity with the appropriate coefficient. The results of the two method agree in most cases, the exceptions are discussed, as is the divergence of the present results and those of Pasquill.

By means of a radiation chart the importance of direct absorption of radiation in the layer of air investigated is shown, and the relative roles of radiation and convection in the control of temperature and relative humidity of the lowest layers of air in various weather conditions discussed. It is suggested that the usual approach to the problems of formation of radiation fog and air temperature on radiation nights may give misleading results.

I. INTRODUCTION.

The meteorology of the lowest few metres of the atmosphere over various terrains has been much studied, chiefly under the stimulus of its importance in the problems of chemical warfare. We may cite particularly the observations of Best (1935) and of Deacon (1948, 1949). Such investigations have aimed mainly at prediction of the diffusion or evaporation of exotic materials, and have therefore not included many of the factors necessary to an understanding of the transfer of heat and water vapour, a notable exception being the recent work of Pasquill (1949c). This problem has immediate practical importance in the forecasting of frost and fog, and the estimation of natural evaporation for agriculture, but it has potentially a more fundamental application in theoretical meteorology, for the earth's surface is the largest energy source of the atmospheric engine, and a better knowledge of conditions there must lead in the end to a better knowledge of the mechanism of the major circulations. The question to be investigated is "what happens to the energy of sunlight?"; the observations to be described attempt to answer this question for a few specific occasions at one place.

II. APPARATUS AND METHODS OF OBSERVATION.

(i) General

Heat is transferred to or from the surface of the earth in four principal ways. These are radiation, convective exchange of heat with the air, transfer by processes involving the latent heat of freezing and

 / evaporation

evaporation, and conduction to or from the deeper layers of the soil. The radiative flux has two main components; the "short wave" component of solar origin, and the "long waves" of atmospheric and terrestrial temperature radiation. There is no satisfactory instrument for the accurate direct measurement of total radiative flux, and the two components are conveniently measured separately, division being achieved by the limit of transmission of small thicknesses of crown glass at a wave length of 2.5 to 3 μ where the energy of both components is small. The exchange of sensible heat with the soil may be obtained from earth temperatures at various depths, and the sum of the convective and latent heat exchanges by difference. It is customary to separate the two last named terms, in the absence of direct measurements of either, by use of the profiles of temperature and humidity near the ground.

(ii) Site.

The observations were made at Kew Observatory, on a surface of level grass which was kept mown to an average length of 1 to 2 cm. This was surrounded by a solid fence about 1.5 m. high, which was about 50 m. away from the site at its nearest point. In certain directions there were huts, buildings, and very large trees at distances of 50 to 100 m.; in almost all the experiments the wind blew from directions clear of these obstacles. It is usually accepted that reproducible profiles representative of a given surface can be obtained up to a height of about 1/100 of the distance of unobstructed flow over the surface; we therefore expected our results to be of general interest at heights up to about 50 cm. The surroundings of the Observatory, to distances of about 1 Km., are level and predominantly of short grass, but are much more broken up by trees, etc., than has been usual at sites previously used for similar work.

(iii) Duration of observations.

The time over which mean values should be taken has long been recognised as a source of difficulty in work of this type. We wished to exclude the effects of diurnal variations from our means, and chose 30 min. as probably the maximum time allowable. It proved possible to take sufficient readings in this time to give smooth mean profiles, but it did not seem advisable to reduce the number of observations much further. Such reduction might be advantageous, but could only be effected by the use of more observers or an elaborate system of recording instruments. The times of observation given in this paper are the mid-points of the 30 minutes run, unless otherwise stated.

(iv) Air Temperature.

This was measured by the dry bulbs of an installation of aspirated thermocouples similar to that described by Pasquill (1949a), the "bulbs" being at heights of about 4, 8, 12, 25, 50, 100 and 200 cm., above the surface. The linear dimensions of bulbs and housings were about half those used by Pasquill, and with the ventilation rate employed, about 3 m. sec^{-1}, the lag coefficient was about 65 sec. The standard junction was attached to a copper block similar to the thermometer bulb, and immersed in a Dewar flask which contained paraffin and a heavy copper coil to facilitate heat exchange. It was placed in contact with the bulb of the reference thermometer which had an open scale calibrated to 0.2°F and read to 0.01°F, readings being taken at frequent intervals in the course of each observation.*

The main purpose of the temperature readings was the determination of mean vertical temperature gradients, secondary considerations being the variation with time and the absolute values of the temperatures. The choice of equipment therefore requires some justification since it is obviously not ideal for its purpose; and we can only plead that any more

/ direct

* This thermometer is the cause of the regrettable mixture of Fahrenheit and Centigrade scales which follows, and for which we apologise. We were unable to obtain a suitable Centigrade thermometer at short notice.

direct method of determining the gradient (e.g. by freely exposed thermocouples or thermistors at equal small height intervals) would have required a major research to establish its validity. It is by no means obvious that the air disturbance caused by ventilation of the thermometers used would be without effect on the measured values, but Best (1935) and Pasquill (1949b, 1949c) had obtained very consistent results with similar apparatus, and in the event we confirmed their experience. It must however be borne in mind that there is no direct external evidence that the method gives "true" temperature values, particularly at the lowest heights, in all circumstances.

In all except the first two experiments the circuits were arranged to switch each "bulb" in turn against the reference bulb, readings being made on a low resistance galvanometer of fairly short period. (8ω about 1 sec, sensitivity 8 mm. μ a^{-1}, giving, with a total circuit resistance of about 26ω ., a sensitivity of about 6.6 mm. $^{o}F.^{-1}$). Each differential circuit was calibrated a total of four times during the course of the observations, and the galvanometer sensitivity was checked from time to time. No significant variation in the sensitivity of the circuits was found, nor were deviations from linearity significant over the small range of temperature involved in any one observation. In the 30 min. of each experiment about 15 separate readings of the dry bulb temperature, nominally to 0.01°F, were obtained at each height, the number being rather less in the early runs. Fluctuations of temperature were found to be greater than had been expected, but the profiles given by the means of this relatively small number of individual readings were remarkably smooth.

(v) Humidity.

The wet bulbs of the aspirated psychrometer were of the same size as the dry. Their lag coefficients were not determined, but no doubt Pasquill's (1949a) observations of the relative lags of similar dry and wet bulbs held for our smaller instruments. Circuits were arranged to give directly the wet bulb depression at the various heights. Calibrations of the thermometers and circuits were carried out as for the dry bulbs; the sensitivity for most of the experiments was 7.5mm. $^{o}F^{-1}$, so that a nominal accuracy of about 0.01°F was possible. The procedure was to take a dry bulb reading at each height, then the wet bulb depression at each height, then another set of dry bulb readings. The wet bulb depression at each height was then associated with the mean of the two dry bulb readings to determine the humidity. Fifteen values for the humidity at each height were obtained in the 30 min. run and the means taken. In criticising this procedure it must be remembered that the three readings necessary for one determination were completed inside 2 minutes, and that the lag coefficients were of the order of 1 minute, and differed for wet and dry bulbs. In fluctuating temperature and humidity conditions, simultaneous readings of wet and dry bulb will not give a "true" humidity value, and results obtained by our method should be little different from those given by simultaneous readings. Graphical interpolation was necessary to determine the humidity from temperatures and wet bulb depressions expressed to 0.01°F. Marvin's (1912) tables were used as a basis, being the only tables available to us for aspirated Fahrenheit thermometers.

The general accuracy of the humidity readings will be discussed later, but we should remark here that a few of the readings were grossly in error. This is believed to have been due mainly to the muslin touching the housing during the course of a run. Pasquill's large instruments apparently did not suffer from this trouble to the same extent; the smaller size we used was dictated by the small separation of the lower thermometers, but is not to be recommended if avoidable.

(vi) The flux of heat in the ground.

The instrument used for earth temperature measurement was similar to that employed by Pasquill (1949c) in which a number of copper strips were set on an ebonite rod which was pushed into the ground. The strips were

/ insulated

insulated electrically by a thin varnish layer and had differential thermocouple circuits attached, the wiring being accommodated in a channel in the ebonite and protected by wax. Long lengths of fine gauge (47 S.W.G.) copper wire were used, to minimise direct heat conduction between the copper strips. In the first model six strips were used, at depths of 1, 2, 4, 8, 16 and 32 cm. below the surface, a later design had additional strips at 3 and 6 cm. The 32 cm. strip was referred to a standard junction contained in the same Dewar flask as the air temperature standard. Three sets of readings were taken during each observation, before, during, and after the air temperature measurements. The sensitivity was 4.5 mm.$^{o}F^{-1}$.

The method normally adopted to obtain the rate of heat absorption in the ground was to determine the temperature changes at various depths over a period of about 40 mins., and use values of the density and specific heat of the soil appropriate to each depth. Unfortunately in a number of cases it was not possible to do this owing to a fault in the apparatus. In these circumstances, however, a reliable measurement of the temperature gradient in the soil was available, and the required rate of heat transfer was computed using the thermal conductivity of the soil deduced from the more complete observations. Several independent determinations of this conductivity were in good agreement, and it is not thought that the results of the second method were much more uncertain than those of the first. It will be seen later that uncertainties in the heat transfer to and from the ground were in any case normally small, compared with those of measurements of the radiative flux, and had only a secondary effect on the overall accuracy of the work.

The nature of the soil at Kew may be judged from the following figures:- The density after drying for several hours at 105°C was about 0.3 g.cm^{-3} for the top two centimetres, then about 1.1 g.cm^{-3} down to at least 30 cm. Drying at this temperature after a prolonged rainless spell expelled about 10% by weight of water; when saturated (but not muddy) after rain about 45% by weight was expelled. The specific heat of the oven dried material was 0.30 ± 0.02 cal. $^{o}C^{-1}g^{-1}$, with no significant variation with depth. A number of determinations (from the earth temperatures) of the thermal conductivity of the top layers of soil in the naturally dry condition gave results between 2×10^{-4} and 5×10^{-4} cal. cm.$^{-1}$sec.$^{-1}$°C^{-1}; with a mean of 3.2×10^{-4}.

(vii) The radiative flux of heat.

The flux of "short wave" radiation was measured by a Moll solarimeter mounted horizontally near the site, its output being recorded continuously. From time to time during each observation the instrument was inverted to give a measurement of the flux reflected from the grass. This instrument was supplemented by two similar thermopiles mounted on the Observatory roof. The solarimeters were standardised from time to time by shading the thermopiles from direct solar radiation by a small disc and simultaneously determining the solar intensity by means of a standard Ångström pyrheliometer (No.24). It was not possible to perform a standardisation during the course of each experiment, and our experience with the solarimeters suggests that the results may be in error by as much as 10%, this being the largest source of error in an observation. This view of the accuracy obtainable from these instruments, less optimistic than that of Pasquill (1949c) appears to be confirmed by Nicolet (1948).

The long wave radiation, of atmospheric or terrestrial origin, was measured by means of a Linke-Fuessner radiometer directed alternately on sky and ground at an angle of $52\frac{1}{2}^{o}$ to the vertical, the surface temperature being checked directly by a grass thermometer (Robinson 1947, 1950 - these papers also contain details of the standardisation of the radiometer). In most of the experiments cloud amounts were negligible, but one run (16th June 1949 1620 G.M.T.) was made with 10/10 fairly uniform cloud, and during two others (15th June 1949 2130 G.M.T. and 17th June 1949 2133 G.M.T.) up to 6/10 of thin medium cloud was present. In these circumstances an attempt was made to

/ examine

examine a representative sample of the sky when using the radiometer. In daylight it was possible to take 3 or 4 radiometer determinations each on ground and sky during the course of an experiment, at night 6 to 8 determinations were made on each. The grass thermometer was read at frequent intervals. In uniform sky conditions, and particularly at night in the absence of short wave radiation, the determination of the long wave flux was by meteorological standards, quite precise. The probable errors of this measurement, even in the worst cases of partly clouded skies, were less than those of the short wave radiative flux.

(viii) The change of temperature and humidity with time.

To compute the changes with height in the fluxes of heat and water vapour it was necessary to know the time rate of change of temperature and humidity. For each experiment the individual readings at each height were plotted against time, and a smoothed curve drawn through them. The mean rates of change over the experimental periods were computed from the end points of the smoothed curves rather than from the first and last readings, in order to minimise the effects of the fluctuations.

(ix) Wind.

Wind measurements were made with sensitive cup anemometers similar to that described by Sheppard (1940). The number available varied, and in one case no wind profile was obtained, but for most of the observations 8 anemometers were exposed at heights (mid-point of cups) of about 5, 12, 25, 37, 50, 75, 100 and 200 cm. For each of the two lowest heights it was necessary to sink the dial of the anemometer below the surface, and to work the control by means of a spring and cord. This entailed some disturbance of the surface, but this was well within the area swept by the cups. Because of lack of observers the anemometers were left to record for the 30 minutes of each run, providing a mean wind for the whole period. It was found that the calibrations initially supplied were mutually inconsistent, and we are indebted to Mr. G.W. Hartley of the Meteorological Office, Harrow, who made wind tunnel calibrations on two occasions, and to Mr. B.A. Eagle who made intercomparisons in the field. Owing to limited wind tunnel facilities it was not at first possible to secure an absolute standardisation of the anemometers, and the calibrations used were referred to one of the instruments as a sub-standard. An absolute calibration carried out by Mr. Hartley in December, 1949, i.e. after completion of the observations, showed that the wind speeds which had been used were too great by an almost constant factor of approximately 10 cm. $sec.^{-1}$ except in extremely light winds. Retrospective corrections were not attempted, as the calibrations and intercomparisons showed that there were slight changes from time to time in the relative sensitivities of the instruments, and, since gradients rather than absolute speeds were the chief interest, it was considered advisable to rely on relative calibrations made during the course of the observations.

Anemometers of the type used measure the run of the wind, not its component in a given direction, and will respond to the transverse velocities of eddies with dimensions larger than the circle swept by the cups. It is however customary to identify their indications with the "magnitude of the vector mean wind" of theoretical treatments. The point is mentioned because the present experiments contain a number of occasions when large variations of wind direction were observed on the site. Another point of interest is connected with the stopping of the cups in very light winds of about 15 cm. $sec.^{-1}$ or less. This was seen to occur during one of the runs, and probably did so during at least two others. No correction to these results was possible, but they were not rejected. It can be seen that the effect would probably lead to an underestimation of wind speed greater for lighter winds, i.e. for lower heights, and hence to an over-estimation of wind gradient of magnitude decreasing with increasing height.

/ III.

III. METHOD OF ANALYSIS OF THE RESULTS

(i) Notation

The following symbols, units, and conventions will be used.

z Height above surface (cm).

T Temperature (°C unless otherwise stated)

e Water vapour concentration (g. per g. of air)

u Wind speed (cm. sec.$^{-1}$)

$F(z)$ Total vertical flux of heat at height z (cal. cm^{-2} sec.$^{-1}$)

$C(z)$ Non-radiative " " " " " " " " "

$R(z)$ Radiative " " " " " " " " "

$G(o)$ Flux of heat in ground at the surface " " " "

$E(z)$ Vertical flux of water vapour at height z (g. cm^{-2} sec^{-1})

$M(z)$ Vertical flux of momentum " " " (g. cm^{-1} sec^{-2})

$\tau(o)$ Shearing stress at the surface (g. cm^{-1} sec^{-2})

$K(z)$ Eddy conductivity defined by $-C(z)/\rho c_p\left(\frac{\partial T}{\partial z}+\Gamma\right)_z$ (cm^2 sec^{-1})

$D(z)$ Eddy diffusivity of water vapour defined by $-E(z) \,/\, \rho\left(\frac{\partial e}{\partial z}\right)_z$ (cm^2 sec^{-1})

$N(z)$ Eddy viscosity defined by $-M(z) \,/\, \rho\left(\frac{\partial u}{\partial z}\right)_z$ (cm^2 sec^{-1})

k, d, ν Molecular thermal diffusivity, diffusivity of water vapour, and kinematic viscosity respectively (cm^2 sec^{-1})

$A(z) = D(z)/K(z)$

$f(z) = \frac{\partial e}{\partial z} \,/\, \left(\frac{\partial T}{\partial z}+\Gamma\right)$

Γ The dry adiabatic lapse rate $= 1\times10^{-4}$ °C cm^{-1}

Ri Richardson's number $g\left(\frac{\partial T}{\partial z}+\Gamma\right) \,/\, T°\text{Abs}\left(\frac{\partial u}{\partial z}\right)^2$

Fluxes directed away from the surface are considered positive.
In practically every instance to be discussed the temperature gradient is numerically much greater than Γ and $\partial T/\partial z$ is used to replace $\partial T/\partial z + \Gamma$ with negligible error.

In the numerical work, necessarily very approximate, ρ and c_p the density and specific heat at constant pressure of air, are taken as 1.2×10^{-3}g. cm^{-3} and 0.25 cal. °C^{-1} g.$^{-1}$ respectively. For the latent heat of condensation of water, λ the value 600 cals. g.$^{-1}$ is used.

/ (ii)

(ii) The radiative and non-radiative flux of heat.

Heat is transferred in the atmosphere by radiation, convection, and conduction, the last being negligible except in immediate proximity to the surface. Convection may be free, i.e. due purely to buoyancy forces initially set up in air heated by radiation and conduction, or forced, the air being driven in turbulent motion by the pressure gradients. The two types have been distinguished in some meteorological literature as "convective turbulence" and "frictional turbulence", this distinction will not be made here.

Direct absorption of short wave radiation by the air near the ground will be regarded as negligible, changes with height in radiative flux being considered as due entirely to changes of the long wave component. These changes are measurable in principle, or may be calculated, e.g. by means of a radiation chart, if temperatures and humidities are known. Trials using the Elsasser chart (Elsasser 1942) or the Kew chart described by Robinson (1950) showed that the temperature and humidity results up to 2 metres were sufficient to allow fair accuracy in computing the flux changes near the ground. These changes were found to be often of order 10 to 100 times the total heat flux change computed from the increase or decrease of temperatures, i.e., the magnitude of the terms on the right of the equation.

$$-\int_0^z \rho c_p \frac{\partial T}{\partial t}\, dz \quad = \quad F(z) - F(o) \quad = \quad \left[R(z) - R(o)\right] + \left[C(z) - C(o)\right] \qquad \ldots\ldots\ldots\ldots\ldots\ldots (1)$$

was often considerably greater than that of their algebraic sum.

The Kew radiation chart was used to compute the radiative flux changes for all the cases investigated, the effect of CO_2 being neglected. The question of the validity of such computations has been discussed by Robinson (1950), who also reports a few confirmatory measurements. General experience with the charts suggests that $\pm 25\%$ is a reasonable estimate of the likely error of this type of computation.

(iii) The relation of convective flux and gradient - Advection.

We have defined eddy conductivity and eddy diffusivity in terms of the ratio of the appropriate flux to its corresponding vertical gradient, but since this ratio is known to be variable over a very wide range of values, according to position and meteorological conditions, it is obvious that the definition is not based on direct experimental evidence. Historically it originated by analogy with molecular conduction and diffusion, and its wide acceptance depends on its deduction by the aid of mixing-length theories (e.g. Brunt 1939 p.225). In this derivation in addition to the artificial mixing length hypothesis, three assumptions are made

(a) That there is no correlation between the subsequent vertical motion of a parcel of air instantaneously at rest in the vertical and its excess of the property considered over the mean value at the level at which it is at rest.

(b) That the appropriate vertical gradient is linear over the range of vertical motion of individual parcels of air.

(c) That the corresponding horizontal gradients are negligible.

Of these, (a), at least in the case of transfer of heat, may be inconsistent with the existence of free convection, (b) is questionable on several counts (compare, e.g., with the definition of v. Karman's constant in terms of the ratio of the first and second derivatives), and whilst (c) is not a fundamental objection in theory, we shall find ~~that it raises a number of practical~~

/ difficulties.

difficulties. If the horizontal gradients are not negligible a certain proportion of the convective flux will be associated with them, and in investigations in which observations are made in one position only it is not possible to separate this advective term.

Advection may be on a large scale -detectable on a synoptic chart - or on a small scale, due to local inhomogeneity of terrain. The advection term is most easily dealt with in the case of momentum transfer, where large scale advection implies a rapid change of pressure gradient, and where small scale advection has been to some extent studied in the search for wind profiles representative of different surfaces. It is now generally accepted that the wind profile over a uniform surface is effectively independent of surroundings up to a height of about 1/100 of the fetch of wind over the surface. This was suggested by wind tunnel experience, and has been confirmed by the internal consistency of a long series of wind profile observations culminating in those of Deacon (1948, 1949). It is clear that elimination of advection of momentum does not necessarily imply no advection of heat or of water vapour. For large scale advection this is disclosed by a study of synoptic charts, indeed advection of heat is recognised as a major climatic factor, whilst for small scale advection a surface of uniform roughness may be obviously inhomogeneous in thermal properties or dampness. The difficulty is inherent in all methods of estimation of convective exchange of heat and water which, like the present, employ the concept of eddy coefficients, and it must be kept in mind when the results are considered.

(iv) Determination of the fluxes by the heat balance method. - Bowen's ratio.

Conservation of energy in the vanishingly thin surface layer gives

$$C(0) + \lambda E(0) + R(0) + G(0) = 0 \qquad \ldots\ldots\ldots (2)$$

Thus the convective loss of sensible and latent heat, $C(0) + \lambda E(0)$ is determined by the observations, but to separate the terms a new relation is required. The usual method of establishing such a relation follows that of Bowen (1926) who determined $C(0)/\lambda E(0)$ often called Bowen's ratio, from measurements of temperature and humidity at two heights. The conception of eddy diffusion is not explicit in Bowen's original paper, but subsequent modifications of his method have been made (see e.g. Sumner 1947) in which it is found necessary to assume equality of K and D. The following treatment is a simple variant of the method. We have,

$$\lambda E(z) / C(z) \equiv (\lambda/c_p) A(z) f(z) \qquad \ldots\ldots (3)$$

$$E(z) - E(0) = -\int_0^z \rho \frac{\partial e}{\partial t} dz \qquad \ldots\ldots (4)$$

$$C(z) - C(0) = -\left[R(z) - R(0)\right] - \int_0^z \rho c_p \frac{\partial T}{\partial t} dz \qquad \ldots\ldots (5)$$

It will be shown from the observations (section IV, iii) that the term on the right of (4) is always small, of the order 1% of E(o) up to 1 metre, whilst that on the right of (5) though larger and more variable, is probably less than 10% of C(o) up to 1 metre. Within these limits of error (3) becomes

$$\lambda E(0) / C(0) \simeq (\lambda/c_p) A(z) f(z) \qquad \ldots\ldots (6)$$

/ The

The observations also show (Section IV, ii)

$$f(z) = \text{constant}$$

for each observation, within similar limits of error, which, together with (6) implies

$$A(z) = \text{constant}$$

i.e. the ratio of eddy diffusivity and eddy conductivity does not vary with height. The ratio A cannot be determined by this method, for although an equation involving A and quantities theoretically measurable in certain conditions can be set up, these quantities include terms containing

$\frac{\partial^2 T}{\partial z^2}$ and $\frac{\partial^2 e}{\partial z^2}$ and it is not possible to obtain the profiles with anything approaching the precision required for a reliable determination of the second derivative.

We are therefore compelled to fall back on the assumption made by most users of Bowen's method namely K=D, i.e. A=1. Since we have shown A constant with height it is indeed difficult to explain any value other than unity, which has the support of the mixing length theory. Emmons and Montgomery (1947) have pointed out the difficulties that arise when considering transition between turbulent and molecular diffusion owing to the non-equality of the molecular diffusion coefficients k and d, and a case might be made out for the assumption A=d/k, i.e. about 1.2 at surface layer temperatures and pressures.* The accuracy of the present measurements is however not sufficiently great to make the distinction between A=1 and A=1.2 of much significance, and the former value will be adopted. We therefore write

$$\lambda E(0) / C(0) \simeq (\lambda/c_p) f \qquad \ldots\ldots\ (7)$$

which, with (2), allows computation of the fluxes and eddy coefficients.

(v) Determination of the fluxes by the aerodynamic method.

The variation of mean wind speed near a rough boundary surface has been thoroughly investigated, and a profile law of the form

$$u = \frac{1}{k}\left\{\tau(o)/\rho\right\}^{1/2} \log \frac{z + z_o}{z_o} \qquad \ldots\ldots\ (8)$$

established empirically, z_o being a constant, with dimensions of length, associated with the nature of the surface, and k (v. Karman's constant) having the value 0.40 in a wide variety of circumstances. Sheppard (1947) working over an artificial surface, confirmed that this law is valid for atmospheric flow if the lapse rate is near the adiabatic value, and Pasquill (1949d) has extended the confirmation with minor modifications, to natural grass surfaces. We shall regard it as an empirically established law.

/ If

* Pasquill (1942, p.88) in studying the evaporation of a number of liquids has advanced empirical evidence that the eddy coefficients are functions of the corresponding molecular coefficients. It is also noteworthy that although Bowen in his original paper nowhere speaks of eddy diffusion, his work is most readily interpreted on these lines, and his numerical values imply the assumption A=d/k.

If we identify $\tau(o)$ with $-M(z)$ in the steady state (which is equivalent to assuming local conservation of momentum in the turbulent flow, but which has not been experimentally established), (8) leads to

$$N(z) = k^2 z^2 \frac{\partial u}{\partial z} \quad \ldots\ldots\ldots (9)$$

This is strictly valid only if (8) holds. Deacon (1949) has shown that this is not the case except in neutral stability. A convenient index of stability is provided by Richardson's number, which is zero for neutral stability, negative in unstable and positive in stable conditions. Deacon's experiments (and the present results at smaller heights) show that Ri usually becomes small as the surface is approached, and it seems clear, as pointed out by Deacon, that, at least over short grass, (8) provides a close approximation to the profile near the boundary in practically all stabilities, and that (9) holds generally for small values of z.

We have thus an empirically established method for determination of the eddy viscosity from the wind profile alone, without the need for simultaneous determination of a momentum flux or shear. If now we equate eddy viscosity to eddy conductivity or diffusivity, we may estimate the convective loss of sensible or latent heat from simultaneous measurements of the profiles of wind and of temperature or humidity, providing the measurements are made sufficiently close to the ground. It has been customary to regard the eddy viscosity, diffusivity, and conductivity as equal, but the only justification has been in the rather vague ideas of the mixing length theory. If however the use of this (the aerodynamic) method of estimating evaporation and convection is found to give the same results as direct measurement, or as the "energy balance" method using Bowen's ratio, the equality of the coefficients may be regarded as established in the conditions of the experiment. We shall see that the present results indicate approximate equality of the fluxes determined by the two methods, indicating approximate equality, at least in many circumstances, of the eddy coefficients.

IV. ANALYSIS OF THE RESULTS - COMPUTATION OF THE CONVECTIVE FLUX BY THE HEAT BALANCE METHOD.

(i) Are the profiles representative of the surface?

As remarked in section II (ii)., it was expected that representative profiles would be obtained up to about 50 cm. It is obvious that there could be no direct confirmation of this, since we were not prepared to make any assumptions concerning the form even of a representative profile. However it was found that discontinuities of the wind profile were rather common between the 25 cm. and 37 cm. anemometers, though sometimes they were noted only at greater heights. Examples of this are shown in Fig.1, in which the wind profiles of 12th September, 1949, 2200 hrs. and 28th September, 1949, 1905 hrs. are plotted on a logarithmic height scale. The effect may also be seen on the profiles in Fig.2, for example 21st June, 1949, 1111 hrs. (75 cm.), 21st June, 1949, 1400 hrs. (30 cm.), and 1st July, 1949, 1413 hrs. (30 cm.). The effect was much less marked on the temperature profiles, but was probably present to a slight degree in some cases, e.g. 16th June, 1949, 1620 hrs., and was very large on 3rd May, 1949, 1407 hrs. between 50 and 100 cm. It seems reasonable to suggest that these discontinuities mark the top of the region of horizontal homogeneity of wind velocity.

(ii) Determination of the gradients and the ratio f.

The choice of method of deducing the gradients from the observations is probably the most important step in the analysis of the results. It was soon apparent that although smooth curves could usually be drawn through the observed temperatures it was very difficult to construct a humidity profile at all satisfying as a unique representation. Pasquill (1949c) avoided this difficulty by assuming a definite functional form for the

/ profiles

profiles, the same for both temperature and humidity. This included three "constants" one of which was allowed to differ in different height ranges. We were reluctant to base conclusions regarding the ratio of the gradients of temperature and humidity at different heights on a method which assumed the same functional form for the profiles, and which at the same time obscured the considerable observational scatter of the humidity points. It was therefore decided to draw (without mechanical aid) smooth curves through the temperature and humidity points, and to obtain the gradients by tangent drawing at the points of observation. In this process a number of humidity points were rejected, in circumstances which made it almost certain that a large systematic error was present. (The criterion of rejection was that the observed humidity should be higher than that suggested by the other points by an amount at least four times that of the deviation of any other point from the curve. Practically all the rejected points were from either the 100 cm or the 4 cm. wet bulb, and were over a consecutive series of observations. They are thought to have been due to the wet bulb fouling the housing, temporary obstruction of ventilation, or faulty insulation of the two thermocouple leads in the 'stem' of the thermometer). Even after rejection of these points many of the humidity profiles looked by no means convincing, but it is doubtful whether more careful work with existing methods will ever produce really definite humidity profiles, since in most of our observations the deviation of the observed point from the curve drawn was less than 1% of the concentration, and few of the deviations were more than 2%. In contrast to this scatter of the humidity observations, the smoothness of the temperature profiles was most surprising. Although based on 15 (or less) readings of a fluctuating quantity, the deviations from a smooth curve were only of the order of 1% of the fluctuations, and of the order 0.01% of the absolute temperature.

The gradients obtained by tangent drawing were used to compute values of f at each height for each observation, and the results are shown in Table I for all observations taken between 19th July, 1948 and 1st July, 1949. No physical significance is attached to the means, but they should eliminate to some extent errors due to uncertainties in the drawing of individual profiles and tangents. Remembering that the profiles were probably often not representative above 30 cm., and that there was much uncertainty in deriving gradients by tangent drawing at 7.5 and 100 cm., it seems reasonable to conclude from Table I that f is constant with height.

A more convincing demonstration was obtained by superposition of the temperature and humidity profiles. The scales were adjusted so that the profiles drawn by hand coincided at 10 cm. and 100 cm., and temperature and humidity points were plotted on one curve using the appropriate scales. These superposed curves are shown in Fig.2, and the f values derived from the ratios of the scales are listed in Table I Col.8. The curves of Fig.2 are the most direct evidence available in the present results that the temperature and humidity profiles have the same form; the most doubtful occasion is 2nd October, 1948, 1110 hrs. but even here the deviations of the humidity observations are within the estimated range of experimental error.

In fig.2 the wind profiles have been fitted to the temperature profiles in the same way, by superposition at 10 cm., and adjustment of the scales. The indications are that the wind and temperature profiles frequently have the same, or nearly the same, form, but that significant deviations may occur on some occasions.

(iii) The heat balance.

Table II contains details of the measurement of R(o) and G(o), together with values of the changes in F, R, C, and E between the surface and 100 cm. F(100)-F(o) was computed from eqn. (1), E(100)-E(o) from (4), R(100)-R(o) by means of the radiation chart, and C(100)-C(o) from (5). Tables II and III show that $C(100)-C(o)+\lambda\{E(100)-E(o)\}$ was not more than about 5% of $C(o)+\lambda E(o)$ on any occasion on which the latter was known with certainty.*

/ The

* There was a possibility of overestimation of $C(o)+\lambda E(o)$ in the observations of 24th November, 1949 and 26th November, 1949, as the surface temperature was below freezing point, although freezing was not observed in the water on undisturbed grass. Such freezing would constitute an undetected source of heat.

The change in C was normally much greater than that in λE, a consequence of the radiative heat transfer. If we assume a value of $\lambda E(o)/C(o)$ not greater than about 3 (i.e. Bowen's ratio of magnitude not less than 1/3) we find E constant with height within 2% to 3%, and C constant with height within 20% in all cases. For Bowen's ratio 1, C is constant within 10%. Within this range of uncertainty we may therefore, by (6), regard A as constant, and, as explained in section III, (iv) it is difficult to choose for it any value other than 1. The restriction on Bowen's ratio is of course only necessary when there is considerable variation in R(z) i.e. when surface temperature and air temperature differ widely. These are the circumstances in which C(o) would be expected to be large, a justification of the assumption. To recapitulate: we have arrived at the conclusion K = AD from observations of the profiles, the changes with height of C(z) and $\lambda E(z)$, and the values of $C(o) + \lambda E(o)$, combined with the assumption that the magnitude of Bowen's ratio is usually not very much less than 1. We have then made the further not unreasonable assumption A=1.

This allows computation of C(o) and E(o) by combining (2) and (7), and the results are shown in Table III, the values of f deduced from superposition of the curves (Table I, col.8) having been used.

(iv) Comparison with Pasquill's results.

The assumption K=D, usually made in this type of work, and partially established by our results, has been questioned in recent work of Pasquill (1949c). It is therefore necessary to compare critically his and our methods. Pasquill was able to give definite values to K and D by measuring E(o), together with other quantities in (2), simultaneously with profile measurements. He finds (his Fig.5, p.136) good agreement between K and D in stable stratifications, but K>D in unstable conditions. As mentioned in section IV, (ii), Pasquill obtained his gradients by an objective method, and f values which may be deduced from these gradients show in some cases a variation with height. We found, however, that if his profiles were superposed they showed, as did ours, constancy of f within the range of observational error, some examples being shown in Fig.3. By (6) then, Pasquill's measurements are consistent with K=AD at all heights for all his observations. This is inconsistent with his Fig 5, which suggest a relation between K and D depending on Ri, which itself changes with height. In view of this inconsistency we do not consider Pasquill's results as invalidating our assumption of A=1, even though his argument is supported by a direct measurement of E.

In further justification we may point out a fact not explicitly stated by Pasquill, that his "unstable" cases were all occasions with substantial short wave radiation, and could in fact be reconciled with the assumption K=D if his estimates of the incident flux of short wave radiation were high by about 15%. In our view he has overestimated the accuracy obtainable from a Moll-Gorczynski solarimeter, and our experience suggests that these instruments, if not frequently standardised, may give rise to quite large systematic errors.

V. COMPUTATION OF THE CONVECTIVE FLUX BY OTHER METHODS.

(i) The aerodynamic method.

The main practical difficulty in the application of (9) to the computation of the flux of heat or water vapour by equating the eddy viscosity to eddy conductivity or diffusivity is to obtain accurate values of the gradients. We have

$$C(z) = -\rho c_p K \left(\frac{\partial T}{\partial z} + \Gamma \right)$$

$$= -\rho c_p k^2 z^2 \frac{\partial u}{\partial z} \left(\frac{\partial T}{\partial z} + \Gamma \right) \qquad \ldots\ldots \quad (10)$$

/ and

and

$$E(z) = -\rho D \frac{\partial e}{\partial z} = -\rho k^2 z^2 \frac{\partial u}{\partial z} \frac{\partial e}{\partial z} \qquad \ldots\ldots (11)$$

expressions which contain the product of two gradients. Since these expressions are to be applied at the lowest possible values of z, where tangent drawing is most imprecise it is necessary to find an alternative method for determination of the gradients.

It was decided to limit discussion to occasions when the observations allowed confident drawing of smooth curves through the temperature and wind observations below 30 cm., the plotted points lying strictly on the curves. Values were then read from these curves at 2cm. height intervals, and Rutledge's (1932) method of numerical differentiation applied at heights of 10, 15, 20 and 25 cm.* This procedure ruled out any direct use of the humidity profiles, only one of which (21st June, 1949, 1111 hrs.) was sufficiently free from scatter, and f $\partial T/\partial z$ was substituted for $\partial e/\partial z$ in computing the water vapour flux, the f values in Table I Col.8 being used. The results are shown in Table IV, and Figs. 4 and 5 show C(z) and E(z) computed in this way for z=10 cm. plotted against the corresponding results of the heat balance method from Table III, the limits of error shown in the latter being estimated from the uncertainties of the measured quantity $C(o) + \lambda E(o)$. Table IV contains some examples of calculation of the flux at heights above 10 cm. When these were plotted against height it was found that in most cases extrapolation to z=0 improved the agreement with the flux as determined from the heat balance, but that there were two notable exceptions, 21st June, 1949, 1400 hrs. and 1st July, 1949, 1428 hrs. The computed flux was also plotted against the Richardson number for the same height, and again it was found that extrapolation to Ri=0 improved the agreement with the fluxes determined from the heat balance, except on the same two occasions. The observations did not however conform to any universal relation of the type proposed by Holzman (see Pasquill, 1949c, p.130); the constant σ in

$$N = K = D = k^2 z^2 \frac{\partial u}{\partial z} (1 - \sigma Ri)$$

having a different value for each occasion. Figs.6 and 7 illustrate the extrapolations for 21st June, 1949 1111 hrs. and 21st June, 1949, 1428 hrs., the former the most convincing example of extrapolation to the heat balance value of E(o), the latter one of the obviously exceptional cases.

We conclude from this that the heat balance method of flux computation, with the assumption K=D often leads to the same result as the aerodynamic method with the assumption K=D=N, so long as the latter method is used for z small, or when extrapolation to z=0 or Ri=0 can be made. There are, however, exceptional cases, and our observations are insufficient to explain these, or even to allow an estimate of their frequency of occurrence. They may be connected with the presence of a large advective term, but there is no evidence on this point. The occasions on which the two methods agree include both stable and unstable conditions, and constitute further indirect evidence against Pasquill's conclusion that K is greater than D in unstable conditions.

(ii) Computation of the heat flux as a problem in forced convection.

Neither the heat balance nor the aerodynamic method of estimation of the fluxes, in the form described, is simple or convenient for routine use.

/ Bearing

* The method assumes that the data may be fitted by a quartic or lower order curve in the immediate vicinity of the point considered. To this minor extent it is contrary to the rule we adopted at other times to make no assumptions concerning the functional form of the profiles. The method was found more convenient than more general difference formulae.

Bearing in mind the object of estimating heat flux and evaporation in a wide variety of conditions and localities, it is clear that a method is required based on fewer and much simpler observations. The most obvious approach is to regard the matter as a problem of forced convection. The theory of this form of heat transfer, based on dimensional methods, is very limited in scope, and its applications have been mainly concerned with convection from relatively small bodies immersed in stream of fluid (see e.g. Roberts 1940 p.250). It does however suggest that the flux of heat due to forced convection is directly proportional to the "temperature difference between the body and the air" and is an unspecified junction of the "velocity of the air stream". For a variety of cylindrical objects it has been found empirically that the form $(a + bu^{1/2})$ fits the observations closely.

Fig.8 is a plot of $C(o)/\{T(o)-T(100)\}$ against $\{u(100)\}^{1/2}$, the wind speeds used having been obtained from the absolute calibration of the anemometers mentioned in section II, (ix), and it will be seen that.

$$C(o) / \{T(o) - T(100)\} = a \{u(100)\}^{1/2} - b \quad \ldots\ldots\ldots (12)$$

fits most of the points within the range of error of the observations, with $a = 0.17$, $b = 0.5$ for $C(o)$ positive and $a = 0.26$ $b = 1.0$ for $C(o)$ negative. (The very large range of uncertainty of some of the points is associated with very small values of $C(o)$ and $T(o) - T(100)$). There is no obvious reason why the relations should differ for different directions of the flux, but this seems well established by the observations. If surface temperatures and temperatures and wind speeds at 1 metre are known, the convective heat loss from mown grass appears to be given by (12) with reasonable accuracy, particularly if the integrated value over a period is required. A similar approach might yield useful results for the heat flux over other crops. Its direct application to evaporation computation is not possible since $E(o)$ cannot be determined.

(iii) The evaporation from an open tank.

An evaporation tank of standard M.O. pattern (1942 Meteorological Observer's Handbook, H.M.S.O. London, p.106), surrounded by a grass surface similar to that over which the profile observations were made, and fitted with a recording system designed by Mr. L.H.G. Dines, was in use continuously during the period of the observations. It has long been realised that the readings of this and other types of evaporimeter may not bear much relation to the actual evaporation from a bare or cropped soil surface, since both the energy absorption at the surfaces and the air flow conditions over them differ. Nevertheless the total evaporation in a year from such tanks agrees reasonably well with the evaporation computed from rainfall and run-off statistics.

The recording device enabled the rate of evaporation from the tank to be obtained for the period of each heat balance measurement, and this rate is given in Table III col.7. In Figs. 9 and 10 the ratio of $E(o)$ to the tank reading is plotted against time of day, for daylight observations only, the former figure referring to cases when the grass was described as green and healthy, the latter to occasions when the grass was brown and dry. With healthy grass it is seen that in the forenoon, when ground and air temperature are rising, the tank has a lower rate of evaporation than the surrounding surface, but that the rates become equal at about the time of maximum temperature at 1400 hrs., and that the relation is reversed during the time of falling temperatures. The total evaporation during daylight hours is approximately the same from tank and grass. When the grass is brown and dry $E(o)$ is less than the tank reading throughout the day, the ratio of $E(o)$ to tank evaporation rate falling continuously. The integrated evaporation from the tank during daylight is probably about 50% higher than that from the grass. At night in summer Table III shows that the tank readings are quite unrelated to $E(o)$, as the tank continues to show large rates of evaporation, whilst $E(o)$ becomes very small or even negative. The few winter (November) readings indicate that the tank

/ evaporation

evaporation and E(o) are about the same by day and night.

The variation of the ratio of E(o) to tank evaporation readings, and the tank readings for summer nights may be explained qualitatively by the greater thermal lag of the water surface and the effect on the water level of the relative thermal expansion of tank and water. We may conclude that the Kew tank gives a reasonable approximation to the natural evaporation from the surrounding short grass surface, so long as the vegetation is healthy, and if integrated values for daylight hours only are considered. It seems likely that further investigation of the readings of such tanks will confirm the existence of empirical factors whereby the tank evaporation may be converted into natural evaporation from grassland with an accuracy sufficient for climatological purposes.

VI. THE VARIATION OF TEMPERATURE AND HUMIDITY WITH TIME.

(i) The fluctuations of temperature

In previous sections we have been mainly concerned with the magnitude of the various components of the heat flux. We now consider their variation with height, which controls the change with time of temperature and humidity. Fig.11 shows a number of examples of the variation of individual temperature readings during the course of an observation, and it is apparent that there are fluctuations of temperature of magnitude quite comparable with the temperature change in 30 minutes. The existence of a convective flux of heat implies temperature fluctuations, indeed the flux through any level may be written as

$$C(z) = c_p \overline{\rho t' w'}$$

where t' is the instantaneous departure from mean temperature at a point in the level, and w' the simultaneous vertical component of wind at the point. Very near the ground, however, in a horizontally homogeneous layer, it can readily be seen from a study of the temperature profiles that if t' is of order 1°C or more, the fluctuations, which can only be caused by vertical motion, must be of very short period. It was therefore expected that the relatively large lag of the thermometers used in the present experiments would reduce the observed fluctuations to very small values. Temperature variations of the observed amplitude, with "periods" of order 1 minute or more, at these heights, cannot be caused by vertical movements of air if the mean temperatures are horizontally homogeneous and the radiative fluxes constant in time. The only explanation which can be offered is that the mean temperatures are not horizontally homogeneous, even in the lowest few centimetres, where the fetch of wind over "uniform" and uniformly insolated surface is several hundred times the height above the surface. It has been suggested in section III, (iii) that this inhomogeneity might lead to a local advective flux, but the existence of the long period fluctuations does not necessarily imply such a flux, since the temperature excess is not necessarily correlated with the wind fluctuations. The matter could be settled only by simultaneous observations of temperature and horizontal and vertical wind components. For the present we can only note the existence of the fluctuations, and the fact that they may possibly be inconsistent with the fundamental assumption of the heat balance analysis, that the flux is proportional to the corresponding vertical gradient and to no other function of position.

(ii) The relative roles of convection and radiation in heat transfer.

It has been customary, in considering temperature changes near the ground, to neglect the effects of direct radiation from the air, but Table II cols. 9 and 10 shows that it is of great importance in most cases, for, as mentioned in section III, (ii), the temperature changes observed are of order 1/10 to 1/100 of those which would be expected from radiative exchange alone, so long as the wind is not very light nor the temperature difference

/ between

between the surface and say 100 cm. very small. This implies that during the daytime, when the lowest layer of air is being warmed by radiative exchange with the hot surface, convection is cooling this layer, whereas at night, when radiative exchange is cooling the air, the effect of convection is to warm the lowest layer. For a given humidity, so long as the wind is not very light, the change in radiative flux in the first metre is roughly proportional to T(o)-T(100). Fig. 12 is a record of the variation of this temperature difference for 21st June, 1949, obtained by means of a fine thermocouple in the bulb of a glycol-filled grass thermometer, and it will be seen that this implies a considerable variation in radiative flux in the lowest metre throughout the 24 hrs. It therefore appears that in the majority of cases investigated direct radiation from the lowest layers of air is one of the controlling factors in the diurnal variation of temperature, a fact which is perhaps not generally appreciated. Table V gives a more detailed analysis of the change in radiative and convective flux in the first metre for mid-afternoon and early night in clear June weather with moderate winds.

With very light winds different conditions obtain, as may be seen from Table VI, which gives details of the change of heat flux with height for a number of occasions when the mean wind at 1 metre was less than 50 cm. sec^{-1}. It is seen that, although the temperature gradients were considerable, the radiative flux changed comparatively little with height, and that in the lowest levels there was an approach to radiative equilibrium. This condition is probably typical of very calm nights. Study of thermograph records for such nights shows that the "long period" fluctuations of temperature become very marked, and Fig. 11 shows a good example of this for 26th November, 1948, 1610 hrs. It will also be noted that values of C(o) remained comparatively high on the occasions listed in Table VI, in spite of the fact that the existence of radiative equilibrium strongly suggests an absence of convection. It seems likely that the convective flux in these cases was almost wholly advective, and that the process which we have described as local or small scale advection was dominant in the heat exchange.

(iii) Humidity changes - the formation of ground fog.

It can be seen from Table II col.12 and Table III col.5 that the change with height of the water vapour flux is normally very small compared with E(o). Its meteorological importance becomes apparent when it is realised that a value of -1×10^{-8} $g.cm^{-2}$ sec^{-1} for E(100)-E(o) implies an increase of water content of 0.36 $g.m.^{-3}$ $hr.^{-1}$ and that 0.1 $g.m.^{-3}$ of condensed water can form a thick fog. Any investigation of fog formation is concerned with the change in water vapour flux with height. Emmons and Montgomery (1947) in a preliminary note have considered fog formation near the surface, regarding it as a problem in eddy diffusion, equating eddy conductivity and diffusivity, and considering the effects of molecular conduction and diffusion in a saturated layer very close to the surface. They conclude that loss of water vapour to the surface would be greater than loss of heat, and that fog should not form by diffusion alone. They suggest that fog formation in these conditions involves some loss of heat by direct radiation from the air. We have seen, in section VI (ii), that on the nights most suitable to fog formation the air close to the ground was neither gaining nor losing heat by radiative exchange. In two of these cases, 26th November, 1949, 1745 hrs. and 10th September, 1949, 2128 hrs., fog did in fact form during the course of the observation. In the former case a thick fog with an extremely well-marked horizontal top began to form close to the ground at 1750 hours, and by 1805 hrs. its top was above 2 metres. The profile of Fig. 2 applies to the 10 minute period immediately before fog formation was first observed. On 10th September, 1949, the fog was much thinner and patchy, and did not persist. It was first observed at 2125 hrs. about the middle of the period to which the profile of Fig. 2 refers, and drifted slowly in patches during the remainder of the observation. There seems little doubt that in these two cases fog formed in air which was not losing heat by direct radiation, and in which we have suggested that the main process of heat and water vapour exchange was by horizontal rather than vertical mixing. These

/ considerations

considerations suggest that it may be misleading to regard "radiation fog" formation as a problem of turbulent exchange in a horizontally homogeneous body of air with the fluxes assumed proportional to the corresponding vertical gradients.

The time variations of temperature on these two occasions of fog formation have some points of interest, and are shown in Fig. 11. A common feature is the rise of temperature at the time when fog formation was first noted. This seems too great to be caused by the release of latent heat (condensation of 0.5 g.m.$^{-3}$ could cause a temperature rise of about 1°C at the most), and may merely indicate that fog forms on the advection of a supply of warmer saturated air, in accordance with the speculations which we have advanced. The observations are insufficient for critical discussion, but are reported now since further similar material cannot be expected to accumulate rapidly.

VII. THE VARIATION OF THE GRADIENTS WITH HEIGHT.

Deacon (1948, 1949) found that to a high degree of precision the **wind** gradient over a short grass surface between heights of 0.5m. and 8 m. could be represented by a power law of the type

$$\frac{\partial u}{\partial z} = a\, u^{-\beta}$$

He further demonstrated a general relation between β and the stability which implied

$$\beta > 1 \quad \text{for} \quad Ri < 0$$

$$\beta < 1 \quad \text{for} \quad Ri > 0$$

and was consistent with (8) for Ri=o. Sheppard (1947) and Pasquill (1949c), working in the height range from 25cm. to 2m., confirmed that u varied with z more rapidly than log z for Ri<o, and less rapidly than log z for Ri > o. The present measurements which were made closer to the surface, were examined to see if the same relation was obeyed. Only those occasions for which the gradients had been obtained by numerical differentiation were used, and in Figs. 13 and 14 plots are shown of log z against log $\partial T/\partial z$ and log $\partial u/\partial z$ for a number of these cases. It will be seen that the law established by Deacon at greater heights does not hold for the present observations at small heights, for although the power law for $\partial u/\partial z$ is indicated sufficiently clearly, the relations (13) are not obeyed, in fact we have $\beta \geq 1$ for each instance of the Ri $>$ o, whilst for Ri $<$ 0 there are a number of examples with $\beta \leq 1$. The two cases discussed in Section VI, which gave anomalous results for the fluxes by the aerodynamic method, have Ri $<$ 0 and $\beta \leq 1$, but on 23rd June, 1949, 1636 hrs., with Ri $<$ 0, $\beta < 1$, the aerodynamic and heat balance flux computations were in agreement. It is not certain in any of the examples shown in Figs. 13 and 14 that the indicated differences in behaviour of temperature and wind gradient are significant in view of the uncertainties of observation.

VIII. THE CRITICAL VALUE OF RICHARDSON'S NUMBER

The wind profiles have some interesting features on the occasions of very light wind when there is radiative equilibrium in the lowest layers. The profiles for these four cases are plotted in Fig.15, and show an approach to a linear relation between u and z. The arguments of section II.ix must be kept in mind when interpreting these profiles - there was almost certainly some stopping of the anemometer cups at all heights on each occasion. The approach to a linear profile is however interesting in view

of the suggested absence of vertical mixing, as is the fact that Ri on these and no other occasions. Ri can only be estimated very approximately because of the scatter of the wind observations, but suggested values for Ri(25) are

26th November, 1948	1610 hrs.	Ri(25)= +1.4
26th November, 1948	1745 hrs.	Ri(25)= +2.1
17th June, 1949	2133 hrs.	Ri(25)= +2.5
10th September, 1949	2128 hrs.	Ri(25)= +6.5

In view of the uncertainty concerning the critical value of Ri in atmospheric flow (see e.g. Sutton, (1949, p.91) it is interesting to examine some other occasions of positive Ri. On 10th November, 1948, 1750 hrs. with Ri(25) = + 0.4 and $u < 50$ cm.sec^{-1} for $z < 50$ cm., the profile, based on four observations only, was certainly non-linear, and the convective and radiative flux changes, though small up to 25 cm, each accounted for about half the observed temperature change. On 24th November, 1948, 1755 hrs. Ri(25) was +0.25, the wind profile was normal being satisfied quite closely by $\frac{\partial u}{\partial z} \propto z^{-0.8}$ and the radiative flux change up to 25 cm. was ten times greater than the total fluz change indicated by the temperatures. Details of the flux changes for these two occasions are given in Table VII. The indications of the present observations are therefore that for Ri = +0.25 vertical turbulence is still active, for Ri= +0.4 it is probably present but not marked, whilst for Ri > +1.4 it is negligible.

IX. RECAPITULATION AND CONCLUSIONS

The main argument which we have advanced is that in most cases the classical method of Bowen, when applied to observations taken over short grass, yields the same results for the convective fluxes of sensible and latent heat as does an aerodynamic method of computation, essentially similar to that favoured by Pasquill. The results of both methods in the majority of cases can be correlated with observations of the rate of evaporation from an open tank, and in exceptional cases where the energy balance and aerodynamic methods disagree it is the results of the former which correlate in the usual way with the tank measurements. We have suggested an empirical formula, consistent with the usual treatment of problems of forced convection, for computation of the convective flux of sensible heat; the energy balance gives results more in accordance with this formula than does the aerodynamic method in cases where the two differ.

Both these methods involve the conception of the eddy diffusion coefficients, and we have pointed out the lack of direct support for this, and the difficulties introduced by the undoubtedly important advective term. Bowen's method assumes equality of eddy conductivity and eddy diffusivity, the aerodynamic method equality of eddy diffusivity and eddy viscosity, agreement of the two methods indicates equality of all three coefficients, in accordance with the assumptions of the simple mixing length theory in connection with which they were first introduced. This equality could be established directly by simultaneous observation of the three appropriate fluxes and gradients, which we have not attempted. We have however, established a strong probability that the ratio of eddy diffusivity to eddy conductivity remains constant with height within the layer investigated, from which it is a small step to the assumption of equality as in Bowen's method.

The question of change of heat flux with height has been examined using the radiation chart, and we have shown that the change of temperature of the lowest layers of air is normally the small resultant of much larger tendencies due to changes in the radiative and convective fluxes acting in opposite directions. It does however appear that in very light winds (such as are only experienced at night) the layer of air very near the surface reaches a state of radiative equilibrium.

/ Coupled

Coupled with the large values of Richardson's number on these occasions this has been taken to indicate the absence of vertical convection in the layer concerned, in spite of the comparatively large value of the convective flux, which we have suggested is connected with horizontal mixing. Such conditions are normally associated with the occurrence of radiation fog and frost, and we conclude that arguments employing the eddy coefficient conception may not be applicable to these problems. If this interpretation of the results is conceded the critical value of Richardson's number for the suppression of vertical turbulence appears to be between 0.5 and 1.5.

The most important of these conclusions appear to us to be (a) the applicability of Bowen's method to land observations, with its interest to the synoptic meteorologist tracing air mass modifications and the agricultural meteorologist computing natural evaporation; (b) the importance of direct radiation from the air in the diurnal variation of temperature and (c) the suggestion that horizontal mixing may be a controlling influence on temperature and humidity in the extreme conditions which lead to radiation frost and fog.

G.256661/JDG/4/50/40

Rutledge G.	1932	Phys. Rev. 40 p.262
Sheppard P.A.	1940 1947	J.Sci.Instrum. 17 p.218 Proc.Roy.Soc. A188 p.208
Sumner E.J.	1947	Met. Mag. 75 p.151 and p.175
Sutton O.G.	1949	Atmospheric Turbulence Methuen, London.

G.256661(a)/MKL/4/50/40

23 June 49	1432	3.0	2.4	2.8	3.6	3.3	2.6
23 June 49	1636	4.2	3.3	3.5	3.4	5.3	4.0
24 June 49	1419	4.7	4.6	4.7	7.2	4.7	5.3
1 July 49	1122	4.8	4.5	4.2	5.5	3.3	4.7
1 July 49	1428	4.3	4.0	4.1	5.9	6.3	4.6
Means		4.80	4.19	4.30	4.98	5.31	4.33

m Humidity almost constant. f indeterminate.

REFERENCES

Best A.C.	1935	Met. Office. Geophys.Mem. No.65 (Vol.7)
Bowen I.S.	1926	Phys. Rev. 27 p.779
Brunt D.	1939	Physical and Dynamical Meteorology 2nd Ed. C.U.P., London.
Deacon E.L.	1948 1949	Unpublished (Porton Tech. Rep.No.39) Q.J. Roy. Met.Soc. 75. p.89
Elsasser W.M.	1942	Harvard Met. Studies. No.6
Emmons G. and Montgomery R.B.	1947	J. Met. 4. p.206
Marvin C.F.	1912	Psychrometric Tables etc.. U.S. Weather Bureau, Washington D.C.
Nicolet M.	1948	Inst. Roy. Met. Belg. Misc. No.21
Pasquill F.	1942 1949a 1949b 1949c 1949d	Proc.Roy.Soc. A182 p.75 Q.J. Roy.Met.Soc. 75 p.239 Q.J. Roy.Met.Soc. 75 p.249 Proc.Roy.Soc. A198 p.116 Unpublished (Met. Res. Pap. 503)
Roberts J.K.	1940	Heat and Thermodynamics 3rd Ed. Blackie, London.
Robinson G.D.	1947 1950	Q.J. Roy.Met.Soc. 73 p.127 Q.J. Roy.Met.Soc. 76 p.37
Rutledge G.	1932	Phys. Rev. 40 p.262
Sheppard P.A.	1940 1947	J.Sci.Instrum. 17 p.218 Proc.Roy.Soc. A188 p.208
Sumner E.J.	1947	Met. Mag. 75 p.151 and p.175
Sutton O.G.	1949	Atmospheric Turbulence Methuen, London.

G.256661(a)/MKL/4/50/40

23 June 49	1432	3.0	2.4	2.8	3.6	3.3	2.6
23 June 49	1636	4.2	3.3	3.5	3.4	5.3	4.0
24 June 49	1419	4.7	4.6	4.7	7.2	4.7	5.3
1 July 49	1122	4.8	4.5	4.2	5.5	3.3	4.7
1 July 49	1428	4.3	4.0	4.1	5.9	6.3	4.6
Means		4.80	4.19	4.30	4.98	5.31	4.33

* Humidity almost constant. f indeterminate.

TABLE I. Magnitude of the ratio f.

1 Date	2 Time	3 (f) at z=7.5 x 10^4	4 (f) at z=13.5 x 10^4	5 (f) at z=25 x 10^4	6 (f) at z=50 x 10^4	7 (f) at z=100 x 10^4	8 (f) by super-position x 10^4
19 July 48	1415	4.6	4.9	4.9	5.5	7.2	6.0
2 Oct. 48	1110	5.2	5.1	8.2	11.1	24	6.7
¤10 Nov. 48	1510	-	-	-	-	-	-
10 Nov. 48	1750	3.8	3.2	3.1	3.0	-	2.2
11 Nov. 48	1415	15.3	11.6	10.7	10.8	6.5	12.2
24 Nov. 48	1755	1.1	1.3	1.4	1.2	1.6	1.4
26 Nov. 48	1610	2.5	2.3	2.4	2.8	4.0	2.4
26 Nov. 48	1745	1.9	2.1	2.4	2.2	4.8	2.4
3 May 49	1407	8.8	7.1	6.4	6.4	10.0	6.1
¤7 June 49	2125	-	-	-	-	-	-
15 June 49	2130	0.7	1.4	2.2	2.0	2.0	1.4
16 June 49	1620	10.2	9.9	9.4	10.3	8.3	8.8
17 June 49	2133	-	0.9	0.8	0.5	-	0.7
18 June 49	1121	4.1	3.8	3.5	3.9	3.1	3.4
20 June 49	1121	3.7	4.4	4.6	3.9	2.7	3.7
20 June 49	1410	8.1	5.5	5.4	5.4	5.1	5.9
21 June 49	1111	4.0	4.0	3.8	5.4	2.8	4.5
21 June 49	1400	7.1	4.4	4.7	4.7	7.7	3.5
21 June 49	1611	5.9	4.2	4.2	6.1	6.7	4.6
23 June 49	1103	2.5	2.4	2.4	3.9	2.9	2.6
23 June 49	1432	3.0	2.4	2.8	3.6	3.3	2.6
23 June 49	1636	4.2	3.3	3.5	3.4	5.3	4.0
24 June 49	1419	4.7	4.6	4.7	7.2	4.7	5.3
1 July 49	1122	4.8	4.5	4.2	5.5	3.3	4.7
1 July 49	1428	4.3	4.0	4.1	5.9	6.3	4.6
Means		4.80	4.19	4.30	4.98	5.31	4.33

¤ Humidity almost constant. f indeterminate.

TABLE II

1 Date	2 Time	3 Downward short wave flux$_4$ x 10^4	4 Reflectivity %	5 Downward long wave flux$_4$ x 10^4	6 Upward long wave flux$_4$ x 10^4	7 R(o)$_4$ x 10^4	8 G(o)$_4$ x 10^4	9 F(100)-F(o) x 10^6	10 R(100)-R(o) x 10^6	11 C(100)-C(o) x 10^6	12 E(100)-E(o) x 10^8
19 July 48	1415	177	16	80	135	-95 ± 9	$+5\pm3$	-10	-300	+290	-2.5
2 Oct. 48	1110	135	22	72**	111	-65 ± 11	$+10\pm3$	-1	-130	+130	+3
10 Nov. 48	1510	16	16	72	86	$+1.0\pm0.4$	$+1\pm1$	+25	+23	+2	-
10 Nov. 48	1750	-	-	72.9	78.6	$+5.7\pm0.2$	-2.2 ± 0.7	+16	+11	+5	+1.7
11 Nov. 48	1415	22	18**	76	88	-6 ± 2.5	$+3\pm1$	-5.5	+1	-6.5	-
*24 Nov. 48	1755	-	-	58.7	74.7	$+16\pm1$	-0.5 ± 0.5	+3	37	-34	0
*26 Nov. 48	1610	-	-	62.4	74.8	$+12\pm2$	-2.5 ± 1	+15	+15	0	+3
/*26 Nov. 48	1745	-	-	61.1	73.0	$+12\pm2$	-2.5 ± 0.5	+12	+7.5	+5.5	+2
3 May. 49	1407	163	20.6	70	107	-88 ± 10	$+12\pm31$	0	-105	+105	0
7 June 49	2125	-	-	71.4	87.8	$+16.5\pm0.5$	-4 ± 1	+10	+35	-25	-3.5
15 June 49	2130	-	-	74	83.5	$+9.5\pm2.5$	-3 ± 1	+20	+40	-20	+2.2
16 June 49	1620	50	20**	81	100	-21 ± 8	$+3.5\pm1.5$	-5	-55	+50	0
17 June 49	2133	-	-	76.5	82.2	$+5.7\pm2$	-3.5 ± 0.5	+2.5	+26	-24	+1
18 June 49	1121	-	-	-	110	-	-	+7	-150	+160	+0.6
20 June 49	1121	178	19.5	79	134	-91 ± 13	$+25\pm10$	-13	-300	+290	+2.1
20 June 49	1410	157	22	82	125	-79 ± 8	$+10\pm5$	-8	-205	+200	+2.5
21 June 49	1111	193	21.5	77.4	128.5	$+100\pm8$	$+10\pm5$	-10	-250	+240	-1
21 June 49	1400	163	22	86.0	136	-77 ± 8	$+13\pm6$	-10	-280	+270	+1.6
21 June 49	1611	115	23	84	116	-57 ± 7	$+11\pm5$	+8	-100	+110	-0.5
23 June 49	1103	198	21.3	79	132	-103 ± 10	$+10\pm5$	-2.5	-260	+260	-0.7
23 June 49	1432	160	22	77	121	-79 ± 9	$+10\pm5$	+13	-170	+180	+1.5
23 June 49	1636	102	24.5	77.4	113	-41 ± 7	$+10\pm3$	+5.8	-115	+120	-1
24 June 49	1419	158	21	78	135	-68 ± 8	$+10\pm5$	-1.2	-240	+240	-1
1 July 49	1122	198	20.5	82	136	-104 ± 10	$+10\pm5$	-10	-280	+270	+1
1 July 49	1428	172	20	84	130	-91 ± 9	$+20\pm10$	+4.2	-180	+180	+3.5
5 Sep. 49	2201	-	-	81.1	93.6	$+12\pm1$	-1.5 ± 0.2	-1.2	+57	-58	-1
10 Sep. 49	2128	-	-	84.6	76.1	$+8.5\pm0.3$	-5 ± 1	+9	+35	-26	-0.2
12 Sep. 49	2200	-	-	-	-	-	-	-	-	-	-
28 Sep. 49	1905	-	-	79	93	$+14\pm1.5$	-2.5 ± 0.5	+2.3	+38	-36	-0.4

Notes:- * Surface temperature below freezing point. /1 Duration of observations 10 mins. only: ** Estimated Value

TABLE III

1 Date	2 Time	3 $C(o)+\lambda E(o)$ $\times 10^4$	4 $C(o)$ $\times 10^4$	5 $E(o)$ $\times 10^6$	6 $E(o)$ mm/hr.	7 E tank mm/hr.
19 July 48	1415	90 ± 9	37	9.0	0.32	0.35
2 Oct. 48	1110	55 ± 11	21	5.7	0.20	0.12
10 Nov. 48	1510	-2 ± 1	-2	0	0	0
10 Nov. 48	1750	-3.5 ± 0.7	-2.3	-0.5	-0.018	-trace
11 Nov. 48	1415	$+3\pm3$	-1.5	+0.7	0.03	0.03
24 Nov. 48	1755	-16 ± 1	-12	-0.6	-0.02	- *
26 Nov. 48	1610	-10 ± 2	-6.4	-0.6	-0.02	- *
26 Nov. 48	1745	-10 ± 2	-6	-0.6	-0.02	- *
3 May. 49	1407	75 ± 10	31	7.5	0.27	0.32
7 June 49	2125	-12.5 ± 1	-10.5	-0.3	-0.01	0.17
15 June 49	2130	-6.5 ± 3	-10	+0.5	0.02	0.12
16 June 49	1620	17 ± 8	5.5	1.9	0.07	0.13
17 June 49	2133	-22 ± 2	-2	-0.05	-0.002	0.07
18 June 49	1121	-	-	-	-	-
20 June 49	1121	67 ± 17	34	5.5	0.20	0.12
20 June 49	1410	69 ± 9	29	6.9	0.25	0.23
21 June 49	1111	90 ± 9	48	7.7	0.28	0.17
21 June 49	1400	64 ± 10	34	4.9	0.18	0.20
21 June 49	1611	46 ± 9	22	4.0	0.14	0.37
23 June 49	1103	93 ± 11	49	5.3	0.19	0.24
23 June 49	1432	69 ± 10	42	4.5	0.16	0.36
23 June 49	1636	31 ± 8	16	2.5	0.09	0.22
24 June 49	1419	57 ± 9	25	5.4	0.19	0.30
1 July 49	1122	94 ± 11	43	8.4	0.30	0.32
1 July 49	1428	71 ± 13	33	6.2	0.23	0.40
5 Sep. 49	2201	-11 ± 1	-11	0	0	0.13
10 Sep. 49	2128	-3.5 ± 1	-2.3	-0.3	-0.01	0.07
12 Sep. 49	2200	-	-	-	-	-
28 Sep. 49	1905	-11.5 ± 1.2	-7	-0.7	-0.025	0.09

* Surface temperature below freezing point.

S 256661(3)/MKT/1/50/40

TABLE IV

1 Date	2 Time	3 Z	4 Ri	5 $0.16\ \rho z^2 \frac{\partial u}{\partial z} f \frac{\partial T}{\partial z} \times 10^6$	6 $0.16\ \rho c_p z^2 \frac{\partial u}{\partial z} \frac{\partial T}{\partial z} \times 10^4$
10 Nov. 48	1510	10	$+1.7 \times 10^{-2}$	0	-3.3
7 June 49	2125	10	$+2.7 \times 10^{-3}$	-0.42	-13
		15	$+6.0 \times 10^{-3}$	-0.22	
		20	$+6.9 \times 10^{-3}$	-0.19	
		25	$+1 \times 10^{-2}$	-0.18	
15 June 49	2130	10	$+3.3 \times 10^{-2}$	+0.57	-10
16 June 49	1620	10	-9.8×10^{-4}	+1.5	+4.1
20 June 49	1121	10	-4.3×10^{-2}	+4.1	+27
		15	-4.6×10^{-2}	+3.2	
		20	-4.0×10^{-2}	+2.7	
		25	-5.9×10^{-2}	+2.6	
20 June 49	1410	10	-1.3×10^{-2}	+4.4	19
		15	-2.5×10^{-2}	+3.7	
		20	-4.6×10^{-2}	+4.2	
		25	-8.9×10^{-2}	+3.1	
21 June 49	1111	10	-1.4×10^{-2}	+6.4	36
		15	-2.3×10^{-2}	+5.3	
		20	-3.6×10^{-2}	+4.1	
		25	-5.4×10^{-2}	+3.6	
21 June 49	1400	10	-2.7×10^{-2}	+3.1	16
		15	-3.4×10^{-2}	+3.2	
		20	-5.0×10^{-2}	+3.3	
		25	-6.1×10^{-2}	+3.6	
23 June 49	1103	10	-6.0×10^{-3}	+5.6	54
		15	-8.7×10^{-3}	+4.7	
		20	-1.4×10^{-2}	+5.0	
		25	-2.1×10^{-2}	+4.0	
23 June 49	1432	10	-2.7×10^{-3}	+5.4	52
		15	-5.3×10^{-3}	+3.8	
		20	-7.3×10^{-3}	+3.4	
		25	-1.2×10^{-2}	+3.4	
23 June 49	1636	10	-2.0×10^{-3}	+2.7	17
		15	-2.6×10^{-3}	+3.5	
		20	-3.2×10^{-3}	+4.3	
		25	-3.8×10^{-3}	+4.8	
24 June 49	1419	10	-2.6×10^{-2}	+5.8	27
		15	-3.3×10^{-2}	+4.1	
		20	-5.9×10^{-2}	+4.1	
		25	-9.0×10^{-2}	+3.7	
1 July 49	1428	10	-1.5×10^{-2}	+2.9	16
		15	-2.6×10^{-2}	+3.7	
		20	-3.2×10^{-2}	+4.2	
		25	-4.6×10^{-2}	+4.0	
5 Sep. 49	2201	10	$+3.0 \times 10^{-2}$	0	-6
28 Sep. 49	1905	10	$+3.5 \times 10^{-3}$	-0.84	-10
		15	$+4.4 \times 10^{-3}$	-0.81	
		20	$+7.6 \times 10^{-3}$	-0.65	
		25	$+1.2 \times 10^{-2}$	-0.33	

TABLE V.

1	2	3	4	5	6	7
Date	Time	Z	$F(z)-F(o)$ i.e. $-\int_o^z \rho c_p \frac{\partial T}{\partial t} dz$	$E(z)-E(o)$ i.e. $-\int_o^z \rho \frac{\partial e}{\partial t} dz$	$R(z)-R(o)$	$C(z)-C(o)$
7 Jun. 49	2125	14	$+1.1\times10^{-6}$	-5×10^{-10}	$+6.7\times10^{-6}$	-5.6×10^{-6}
		26	$+2.2\times10^{-6}$	-9×10^{-10}	$+1.1\times10^{-5}$	$+9\times10^{-6}$
		51	$+4.5\times10^{-6}$	-1.8×10^{-9}	$+2.0\times10^{-5}$	-1.5×10^{-5}
		101	$+9.6\times10^{-6}$	-3.6×10^{-9}	$+3.5\times10^{-5}$	-2.5×10^{-5}
21 Jun. 49	1400	14	-9×10^{-7}	$+3.6\times10^{-9}$	-6.9×10^{-5}	$+6.8\times10^{-5}$
		27	-2.1×10^{-6}	$+5.5\times10^{-9}$	-1.2×10^{-4}	$+1.2\times10^{-4}$
		52	-4.9×10^{-6}	$+9.7\times10^{-9}$	-1.7×10^{-4}	$+1.7\times10^{-4}$
		102	-1.1×10^{-5}	$+1.6\times10^{-8}$	-2.8×10^{-4}	$+2.7\times10^{-4}$

TABLE VI.

Date	Time	Z	$F(z)-F(o)$	$E(z)-E(o)$	$R(z)-R(o)$	$C(z)-C(o)$
26 Nov. 48	1610	13.5	$+4.5\times10^{-6}$	$+5.4\times10^{-9}$	-1×10^{-6}	$+5.5\times10^{-6}$
		26	$+8.0\times10^{-6}$	$+1.1\times10^{-8}$	$+1\times10^{-6}$	$+7.0\times10^{-6}$
		51	$+1.2\times10^{-5}$	$+1.9\times10^{-8}$	$+4\times10^{-6}$	$+8\times10^{-6}$
		101	$+1.5\times10^{-5}$	$+3.0\times10^{-8}$	$+1.5\times10^{-5}$	0
26 Nov. 48	1745	13.5	$+3\times10^{-6}$	$+4\times10^{-9}$	-4×10^{-6}	$+7\times10^{-6}$
		26	$+8\times10^{-6}$	$+1.2\times10^{-8}$	-3×10^{-6}	$+1.1\times10^{-5}$
		51	$+1.2\times10^{-5}$	$+2.3\times10^{-8}$	0	$+1.2\times10^{-5}$
		101	$+1.2\times10^{-5}$	$+2.0\times10^{-8}$	$+7\times10^{-6}$	$+5\times10^{-6}$
17 Jun. 49	2133	14	$+2.8\times10^{-6}$	$+3.1\times10^{-9}$	-2.5×10^{-6}	$+5.3\times10^{-6}$
		26	$+3.2\times10^{-6}$	$+4.3\times10^{-9}$	0	$+3.2\times10^{-6}$
		52	$+3.0\times10^{-6}$	$+5.8\times10^{-9}$	$+8\times10^{-6}$	-5×10^{-6}
		102	$+2.4\times10^{-6}$	$+1.0\times10^{-8}$	$+2.6\times10^{-5}$	-2.4×10^{-5}
10 Sep. 49	2128	14	$+3.4\times10^{-6}$	$+2.8\times10^{-8}$	0	$+3.4\times10^{-6}$
		25	$+5.7\times10^{-6}$	$+3.9\times10^{-8}$	$+7\times10^{-6}$	-1.3×10^{-6}
		50	$+8.0\times10^{-6}$	$+9\times10^{-9}$	$+1.6\times10^{-5}$	-8×10^{-6}
		101	$+9.1\times10^{-6}$	-2×10^{-9}	$+3.5\times10^{-5}$	-2.6×10^{-5}

/TABLE VII

TABLE VII.

Date	Time	Z	F(z)-F(o)	E(z)-E(o)	R(z)-R(o)	C(z)-C(o)
10 Nov. 48	1750	13.5	$+3.6\times10^{-6}$	$+4\times10^{-9}$	$+1.7\times10^{-6}$	$+2\times10^{-6}$
		26	$+8.1\times10^{-6}$	$+9\times10^{-9}$	$+4.1\times10^{-6}$	$+4\times10^{-6}$
		51	$+1.6\times10^{-5}$	$+1.7\times10^{-8}$	$+1.1\times10^{-5}$	$+5\times10^{-6}$
		101	-	-	-	-
24 Nov. 48	1755	13.5	$+6\times10^{-7}$	-	$+2.4\times10^{-6}$	-2×10^{-6}
		26	$+1.0\times10^{-6}$	-	$+1.0\times10^{-5}$	-9×10^{-6}
		51	$+1.5\times10^{-6}$	-	$+1.6\times10^{-5}$	-1.5×10^{-5}
		101	$+3.0\times10^{-6}$	-	$+3.7\times10^{-5}$	-3.4×10^{-5}

APPENDIX

Mean values of temperature, humidity and wind on the occasions investigated.

Date and Time	z cm	T °F	χ g.m^{-3}	u cm.sec^{-1}
19 July 48	0	102		
1400	5	77.77	13.09	
1430	8	77.37	12.40	
	14	76.61	12.18	
	25	75.96	12.06	287
	50	75.32	11.74	323
	100	74.84		349
	200	74.56	11.33	385
2 Oct. 48	0	83		
1055	4.5	65.07	11.66	
1125	7.5	64.29	11.13	
	13.5	63.31	10.96	
	26	62.72	10.75	
	51	62.12	10.33	
	101	61.79	10.48	
	201	61.51	10.03	
10 Nov. 48	0	47		
1455	4	47.22	7.28	
1525	5			78
	7.5	47.60	7.23	
	12			101
	13.5	47.92	7.29	
	25			116
	26	48.17	7.26	
	30			130
	50.5	48.45	7.24	
	101	48.65		
	201	48.83	7.23	
10 Nov. 48	0	36.5		
1735	4	39.04	6.18	
1805	5			26
	7	39.97	6.24	
	12			33.5
	13.5	40.89	6.41	
	26	41.31	6.47	
	27.5			40
	45			46
	51	41.84	6.53	
	101	42.48	6.64	
	201	43.33	6.85	

Date and Time	z cm	T °F	χ g.m^{-3}	u cm.sec^{-1}
11 Nov. 48	0	49.5		
1400	4	51.34	8.48	
1430	5			72
	7	51.57	8.25	
	12			88.5
	13.5	51.65	8.24	
	26	51.78	8.17	
	26.5			104
	37.5			110.5
	51	51.82	8.07	
	80			123.5
	101	51.89	8.16	126
	201	51.90	8.01	141.5
24 Nov. 48	0	30		
1740	4	34.47	5.09	
1810	5			32.0
	7	35.71	5.14	
	12.5			48.2
	13.5	36.80	5.22	
	26	37.76	5.31	
	51	38.61	5.37	
	57.5			74.6
	101	39.29	5.49	89.6
	201	40.22	5.54	107.2
26 Nov. 48	0	29.5		
1555	4	32.05	4.78	
1625	5			24
	7	33.25	4.89	
	12.5			29
	13.5	34.38	5.14	
	26	35.55	5.37	
	26.5			38
	37			38
	51	36.86	5.57	
	57.5			43
	76			43
	101	37.89	5.83	46
	201	39.92	6.09	64
26 Nov. 48	0	24.5		
1740	4	25.16	3.74	
1750	5			20
	7	26.52	3.94	
(1740	12.5			23
-1810	13.5	28.15	4.20	
for u)	26	29.61	4.42	34
	37			32
	51	31.35	4.68	
	57.5			37
	101	32.85	4.96	50
	201	34.60	5.26	82

/continued

Date and Time	z cm	T °F	χ g.m^{-3}	u cm.sec^{-1}
3 May. 49	0	76		
1352	5	63.31	10.76	240
1422	8	63.06	10.47	
	12			310
	14	62.69	10.38	
	27	62.10	10.18	429
	38			453
	52	61.34	9.77	
	57½			486
	75			500
	102	61.23	9.73	515
	202	60.84	9.57	577
7 June 49	0	50		
2110	4.5	55.13	9.29	
2140	5.5			149
	7.5	55.49	9.26	
	11.5			217
	14	55.88	9.29	
	26	56.18	9.29	
	26.5			257
	38			272
	51	56.43	9.34	
	57.5			286
	75			296
	101	56.63		301
	201	56.74	9.34	
15 June 49	0	44		
2115	5	49.98	7.80	54
2145	8	50.64	7.65	
	12			77.5
	14	51.26	7.68	
	26.5			105
	27	51.74	7.61	
	37			110
	52	52.23	7.55	
	57			120
	76.5			125
	102	52.59	7.55	131
	202	52.90	7.50	146.5
16 June 49	0	69		
1605	5	61.84	8.23	79.5
1635	8	61.58	7.86	
	12			105
	14	61.33	7.71	
	27	60.99	7.49	131
	37			136
	52	60.81	7.35	
	76.5			158.5
	102	60.59	7.31	154
	202	60.45	7.18	171.5

Date and Time	z cm	T °F	χ g.m^{-3}	u cm.sec^{-1}
17 June 49	0	42		
2118	5	45.93	7.77	
2148	8	46.66	7.55	
	12			21
	14	48.44	7.78	
	25			28
	26	49.56	7.80	
	37			30
	52	50.94	7.89	
	76			30
	102	52.23	7.90	30
	202	53.88	7.90	46
18 June 49	0	82.5		
1106	45	66.56	9.70	
1136	5			136
	7.5	65.43	8.41	
	12			183
	14	64.28	8.53	
	25			235
	26.5	62.91	8.56	
	37			238
	52	61.95	8.18	
	57			255
	76			260
	102	61.02	8.07	276
	202	60.63	7.89	295
20 June 49	0	102		
1106	5	69.04	10.49	108
1136	8	67.45	9.70	
	12			137
	14	65.87	9.29	
	25			164
	27	64.65	9.05	
	37			168
	52	63.68	8.65	
	57.5			180
	76			183
	102	62.97	8.67	191
	202	62.59	8.42	204
20 June 49	0	97.5		
1355	5	74.38	10.25	106
1425	8	73.40	9.65	
	12			140.5
	15	72.67	9.44	
	25			170.5
	27	71.53	9.05	
	37			179
	52.5	70.67	8.64	
	58			183.5
	76			192
	102	69.99	8.43	203
	202	69.59	8.23	215

/continued

Date and Time	z cm	T °F	χ g.m^{-3}	u cm.sec^{-1}
21 June 49	0	101		
1056	5	73.09	11.08	135.5
1126	8	71.71	10.42	
	12			178
	14.5	70.52	10.13	
	25			213
	27	69.13	9.75	
	37			228
	52	68.06	9.41	
	58			244
	76			250
	102	67.19	9.16	263
	202	66.70	9.05	281
21 June 49	0	106		
1345	5	77.81	11.57	126
1415	8	77.15	10.95	
	12			165
	14	75.87	10.61	
	25			194
	27	74.45	10.33	
	37			215
	52	73.39	10.05	
	58			226
	76			229
	102	72.64	10.00	239
	202	72.35	9.61	259
21 June 49	0	87		
1556	5	76.31	11.55	
1626	8	75.88	11.16	
	12			191
	145	75.21	10.96	
	25			248
	27	74.57	10.87	
	37			264
	52	74.00	10.57	
	58			274
	76			286
	102	73.54	10.58	299
	202	73.20	10.30	319
23 June 49	0	103		
1048	5	73.01	9.73	184
1118	8.5	71.96	9.34	
	12			240
	14.5	70.72	9.18	
	25.5			308
	27.5	69.34	8.98	
	37			327
	52.5	68.25	8.71	
	58.5			343
	75.5			354
	102	67.45	8.65	373
	202	66.83	8.44	397

Date and Time	z cm	T °F	χ g.m^{-3}	u cm.sec^{-1}
23 June 49	0	93		
1417	5	73.29	9.08	211
1447	8.5	72.47	8.77	
	12			282
	14.5	71.58	8.67	
	25			348
	27.5	70.58	8.48	
	37			368
	52.5	69.74	8.21	
	58			397
	76			408
	102	69.11	8.23	422
	202	68.79	7.92	454
23 June 49	0	84		
1621	4.5	70.04	9.27	
1651	5			187
	7.5	69.52	9.01	
	12			248
	14	69.01	8.93	
	25			320
	27	68.34	8.77	
	37			327
	52	67.90	8.63	
	58			352
	76			351
	102	67.56	8.96	377
	202	67.47	8.42	405
24 June 49	0	107.5		
1404	45	75.68	7.65	
1434	5			120
	7.5	74.04	7.00	
	12			158.5
	14	72.67	6.73	
	25.5			186
	27	71.33	6.22	
	37			197.5
	52	70.42	5.87	
	57.5			204
	76.5			201
	102	69.77	5.62	216
	202	69.35	5.44	229
1 July 49	0	110		
1107	5	77.61	10.04	129
1137	8	76.66		
	12			168
	14.5	75.62	9.45	
	25.5			207
	27.5	74.34	9.10	
	37			194
	52.5	73.22	8.68	
	57.5			223
	76.5			220
	102	72.52	8.54	241
	202	72.09	8.47	262

/continued

Date and Time	z cm	T °F	χ g.m^{-3}	u cm.sec^{-1}
1 July 49	0	104		
1413	5	80.71	9.61	121
1443	8	79.99	9.10	
	12			156
	14.5	79.11	8.93	
	25.5			189
	27.5	77.90	8.70	
	37			194.5
	52.5	77.08	8.28	
	57.5			209
	76.5			212
	102	76.39	8.14	223
	202	75.97	7.88	242
5 Sep. 49	0	58.5		
2146	4.5	64.25	12.57	
2216	5			86
	7	64.95	12.39	
	12			113.5
	14	65.66	12.50	
	23			128
	25	66.07	12.50	
	37.5			137
	50.5	66.45	12.48	
	53			148
	101	66.68	12.52	152.5
	201	66.67	12.54	167.5
10 Sep. 49	0	45.5		
	4.5	48.91	9.07	
	5			20
	7	49.83	8.99	
	14	51.80	9.92	
	25	53.06	10.22	27.5
	37			27.5
	50.5	54.19	10.60	
	56			33.5
	76			30.5
	101	55.15	10.89	33.5
	201	56.69	11.50	47
12 Sep. 49	0	59		
	4.5	62.18	12.77	
	5			179
	7	62.47	12.59	
	12			232
	14	62.74	12.67	
	25	63.04	12.71	
	37.5			302
	50.5	63.22	12.69	
	53			309
	76			325
	101	63.39	12.76	338
	201	63.51	12.82	373

Date and Time	z cm	T °F	χ g.m^{-3}	u cm.sec^{-1}
28 Sep. 49	0	57		
1850	5	61.25	11.78	137
1920	8.5	61.77	11.73	
	12			193
	14.5	62.21	11.79	
	23			230
	27	62.44	11.82	
	37.5			247.5
	52	62.71	11.88	258
	71			265.5
	101	62.78	11.88	276

G.256661(g)/MKL/4/50/40

FIG. 1 EXAMPLES OF WIND PROFILE.

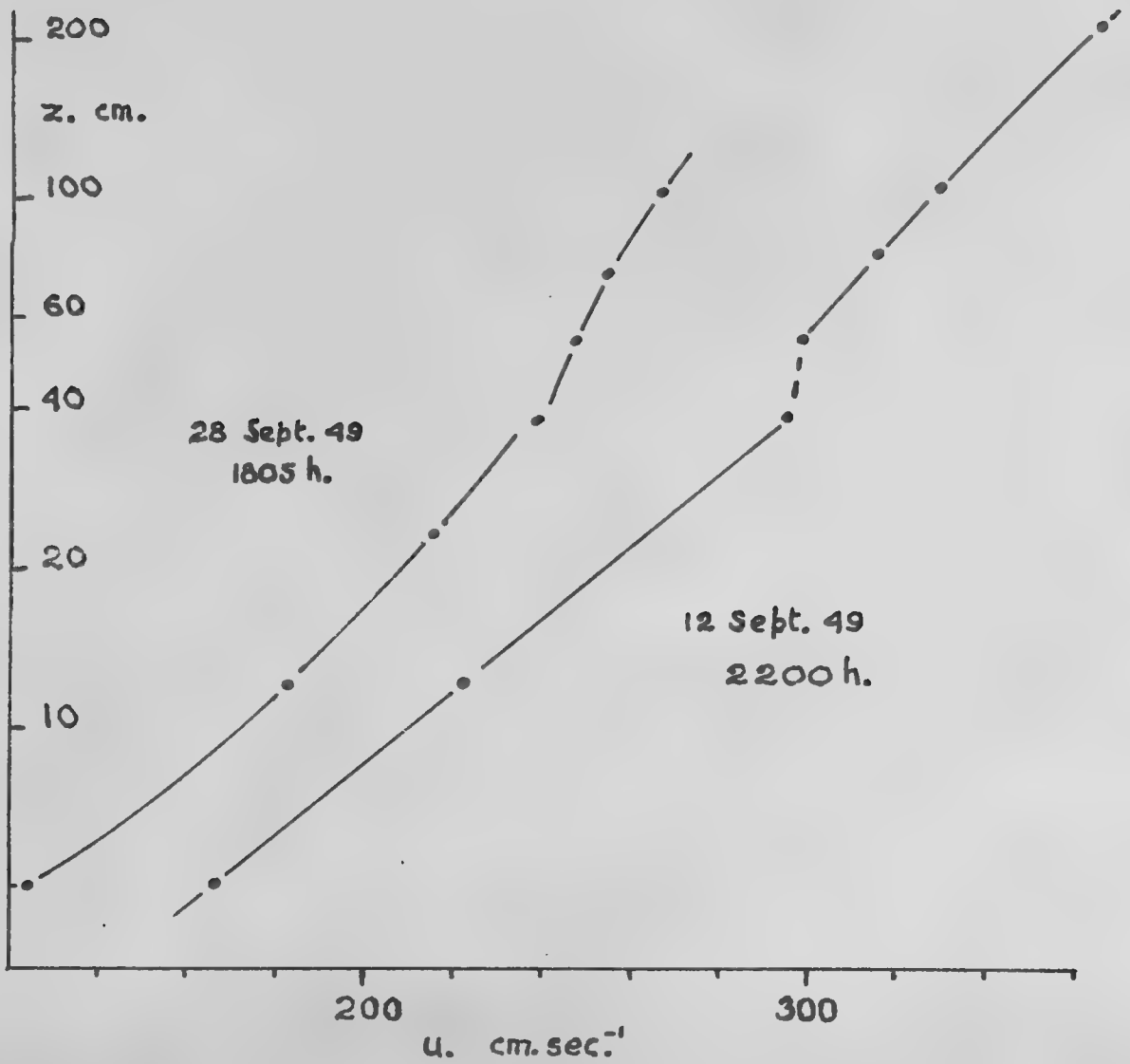

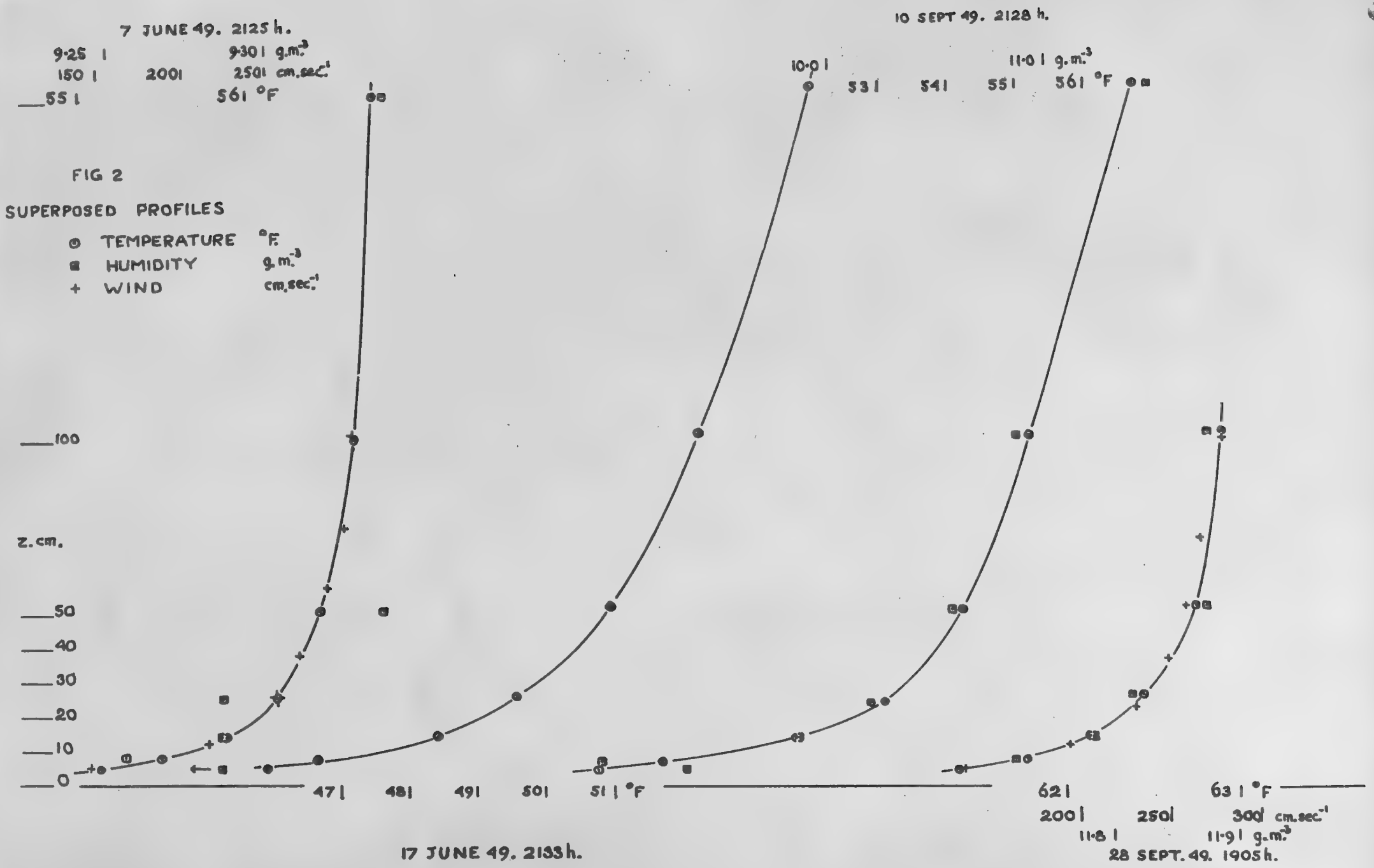
7 JUNE 49. 2125 h.
9·25 l
150 l
2001
9·301 g.m.-3
2501 cm.sec.-1
55 l
561 °F
10 SEPT 49. 2128 h.
10·0 l
11·0 l g.m.-3
531
541
551
561 °F
FIG 2
SUPERPOSED PROFILES
TEMPERATURE °F.
HUMIDITY g.m.-3
WIND cm.sec.-1
100
z.cm.
50
40
30
20
10
0
471
481
491
501
51 l °F
621
631 °F
2001
2501
3001 cm.sec.-1
11·8 l
11·91 g.m.-3
17 JUNE 49. 2133 h.
28 SEPT. 49. 1905 h.

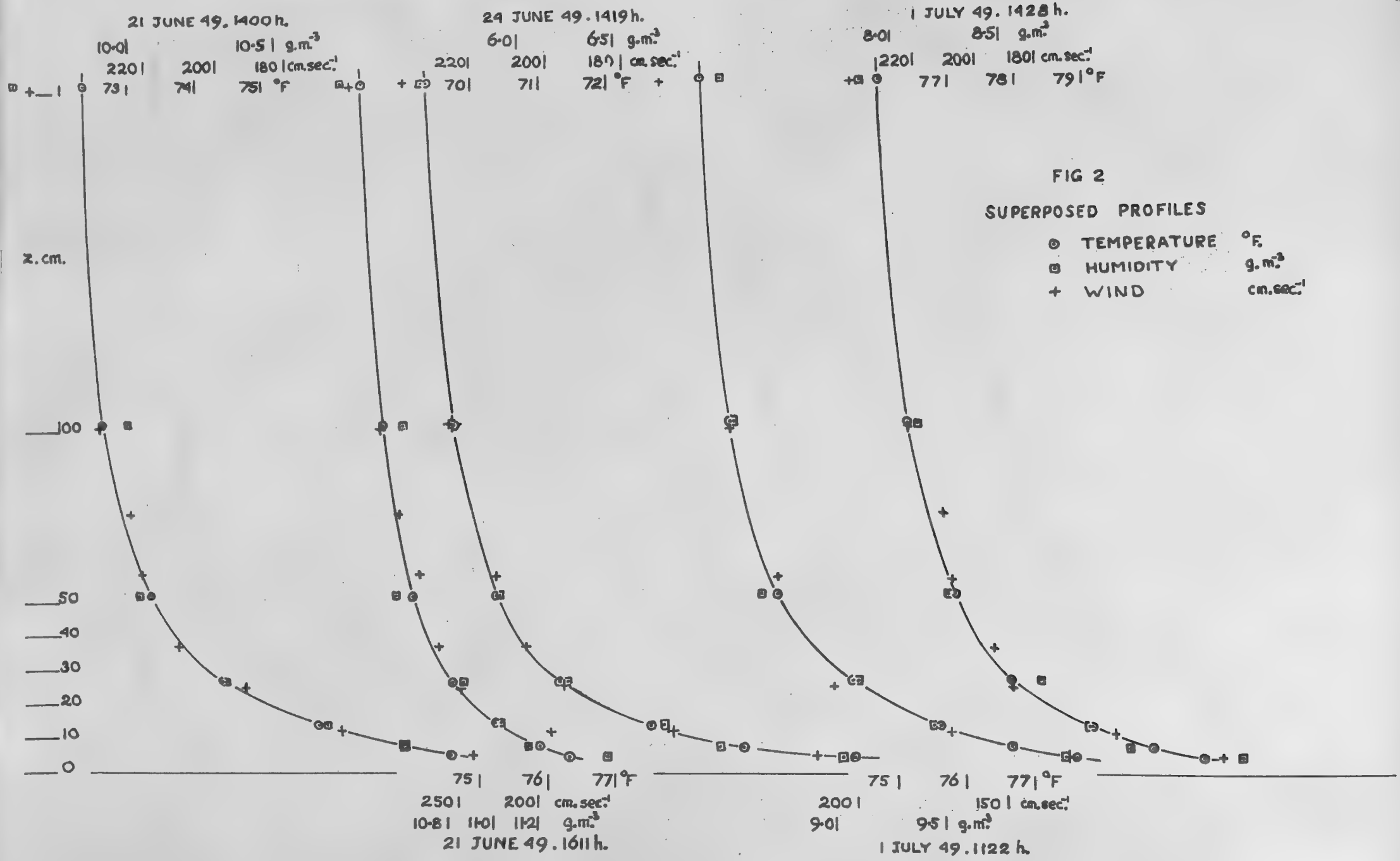
21 JUNE 49. 1400 h.
10·0 | 10·5 | g.m.⁻³
220 | 200 | 180 | cm.sec.⁻¹
73 | 74 | 75 | °F
24 JUNE 49. 1419 h.
6·0 | 6·5 | g.m.⁻³
220 | 200 | 180 | cm.sec.⁻¹
70 | 71 | 72 | °F
1 JULY 49. 1428 h.
8·0 | 8·5 | g.m.⁻³
220 | 200 | 180 | cm.sec.⁻¹
77 | 78 | 79 | °F
z. cm.
100
50
40
30
20
10
0
FIG 2
SUPERPOSED PROFILES
TEMPERATURE °F.
HUMIDITY g.m.⁻³
WIND cm.sec.⁻¹
75 | 76 | 77 | °F
250 | 200 | cm.sec.⁻¹
10·8 | 11·0 | 11·2 | g.m.⁻³
21 JUNE 49. 1611 h.
75 | 76 | 77 | °F
200 | 150 | cm.sec.⁻¹
9·0 | 9·5 | g.m.⁻³
1 JULY 49. 1122 h.

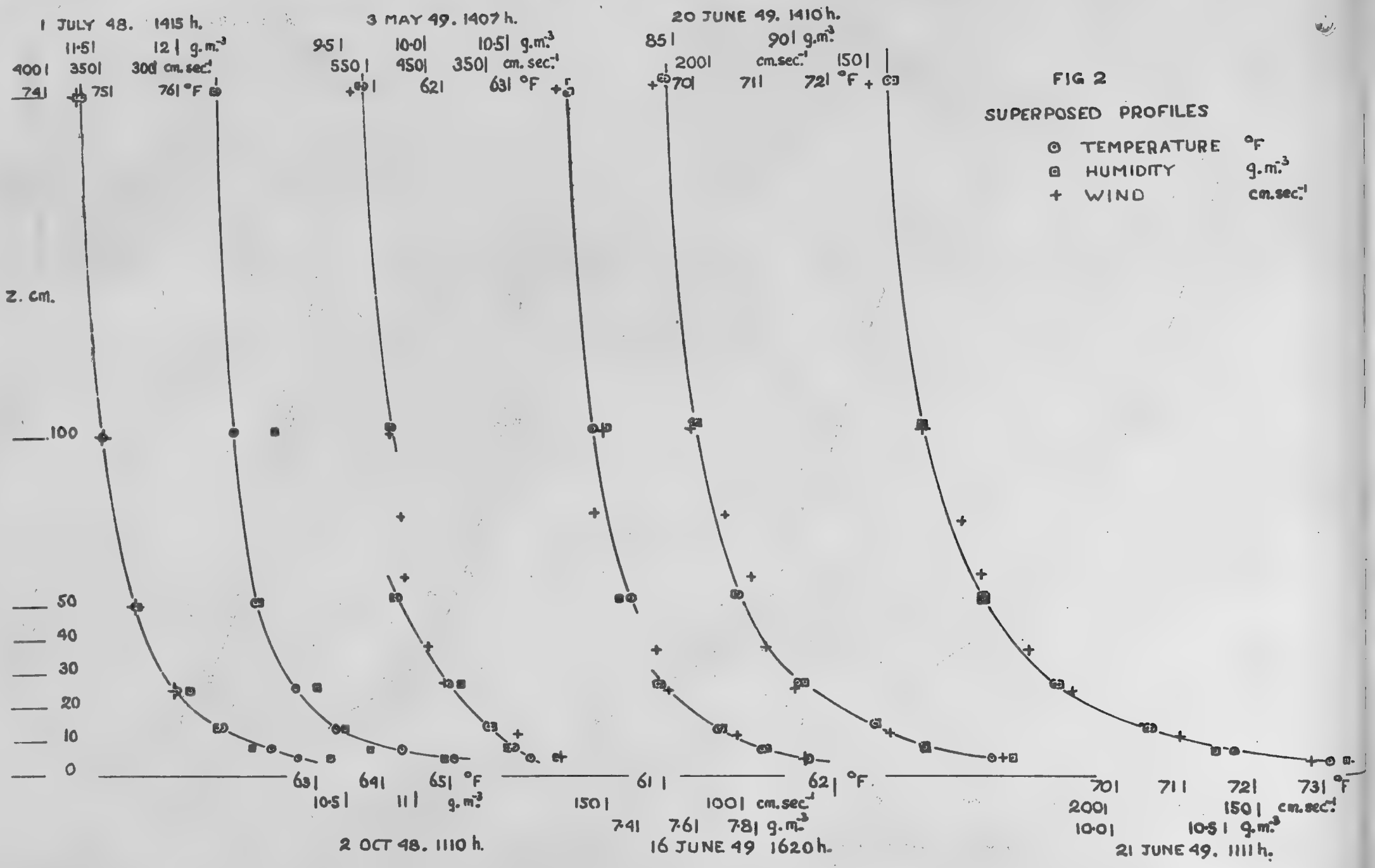

FIG 2

SUPERPOSED PROFILES

⊙ TEMPERATURE °F

⊡ HUMIDITY g.m.⁻³

\+ WIND cm.sec.⁻¹

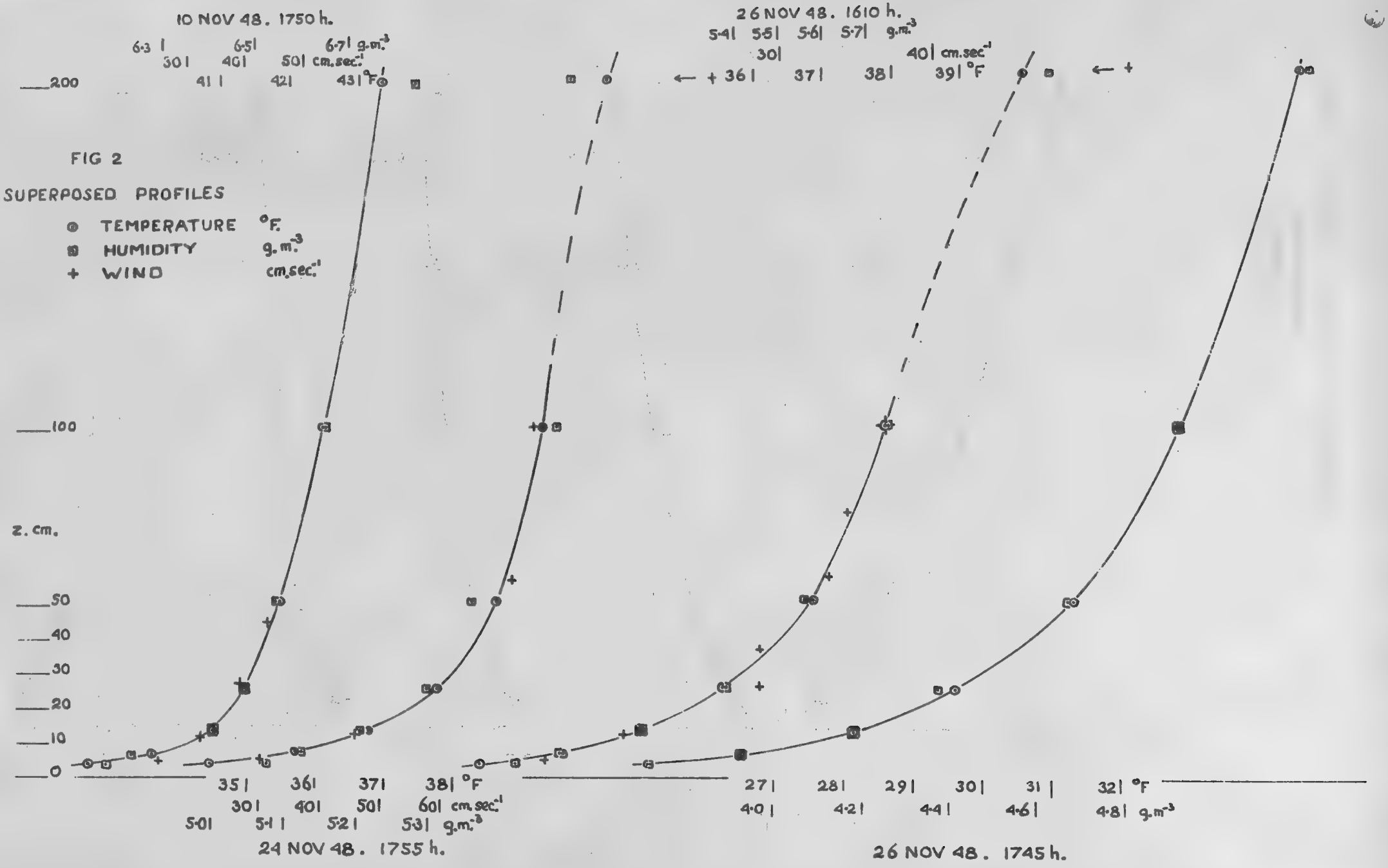

FIG 2

SUPERPOSED PROFILES

- TEMPERATURE °F.
- HUMIDITY g.m.⁻³
- WIND cm.sec.⁻¹

FIG.3 SUPERPOSED PROFILES (PASQUILL)

⊙ TEMPERATURE
⊡ HUMIDITY
\+ WIND

Fig 4. Comparison of heat balance and aerodynamic methods

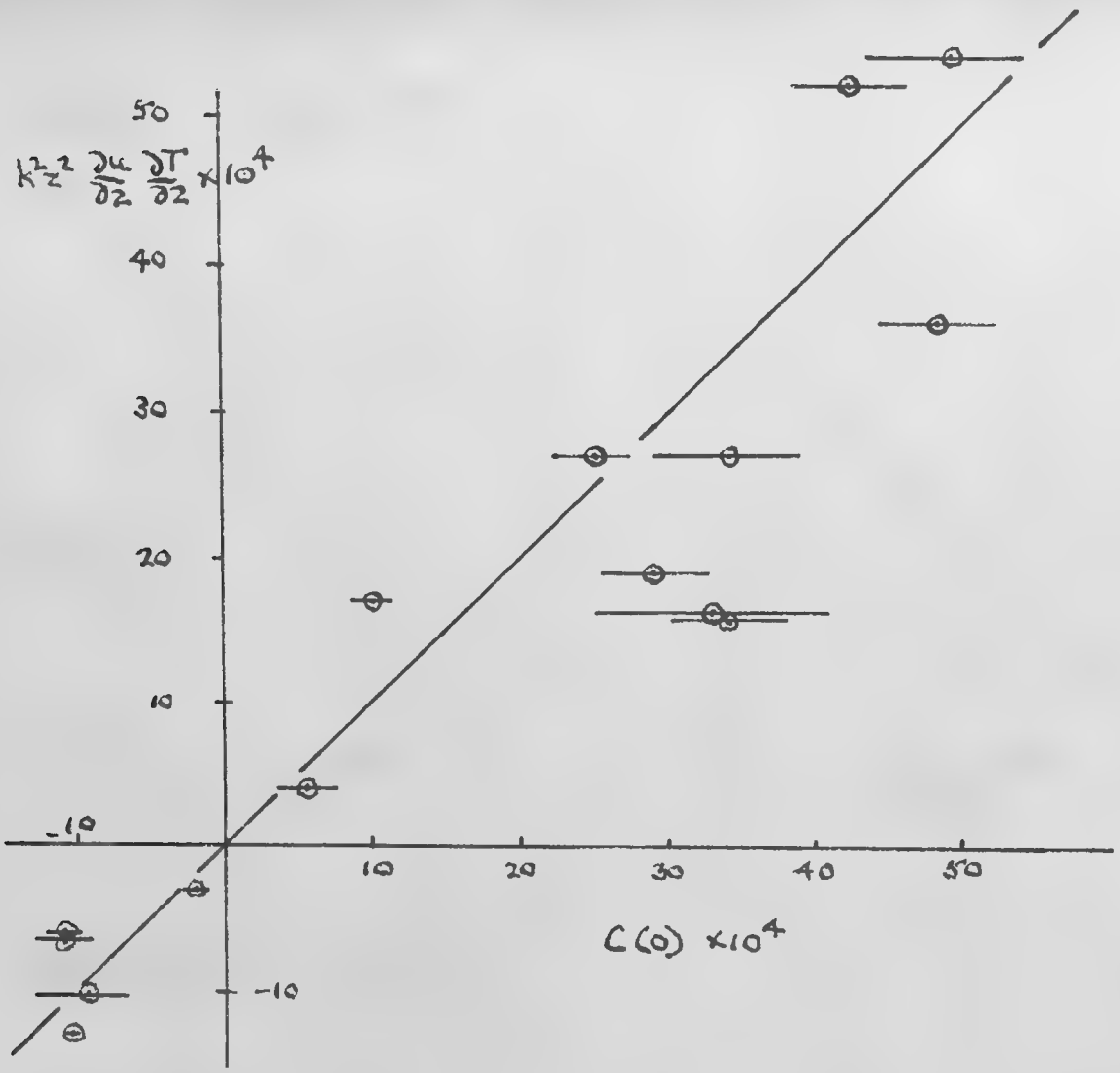

Fig 5. Comparison of heat balance and aerodynamic methods

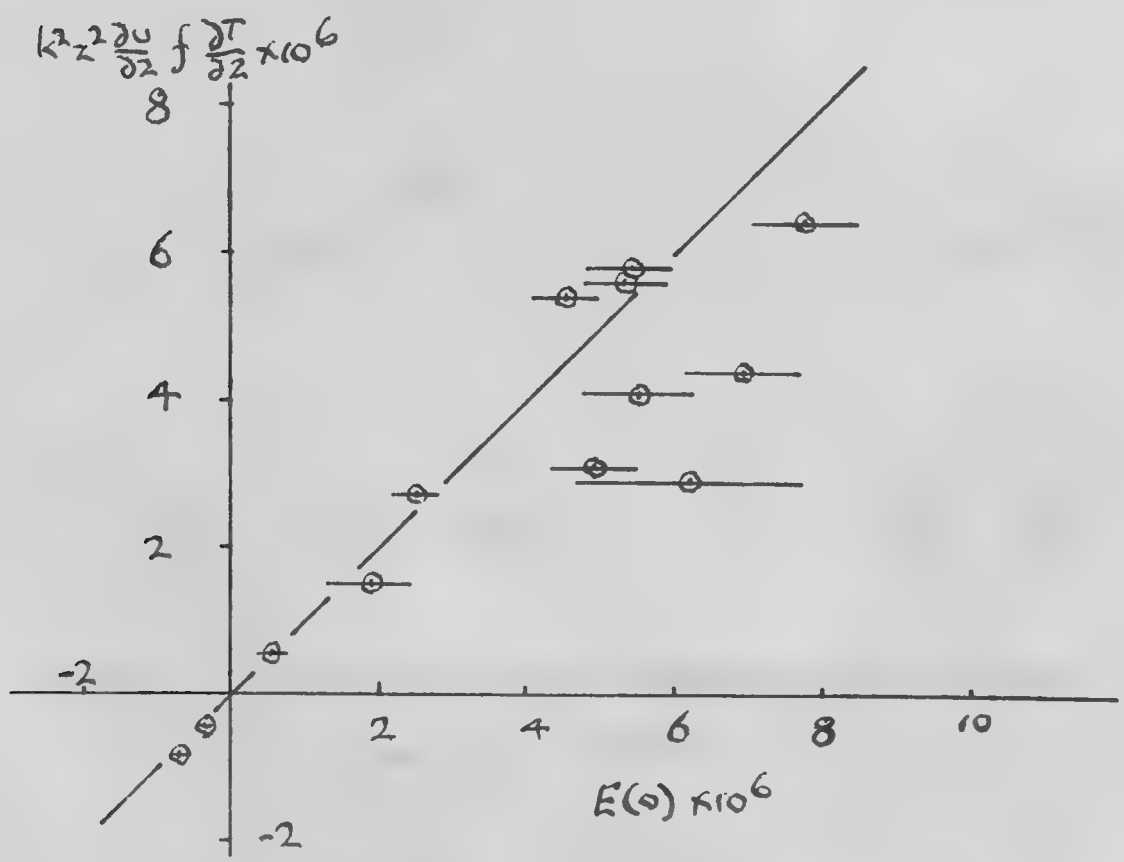

FIG. 6. Computation of Evaporation. Aerodynamic Method.
21 June 49. 1111 h.

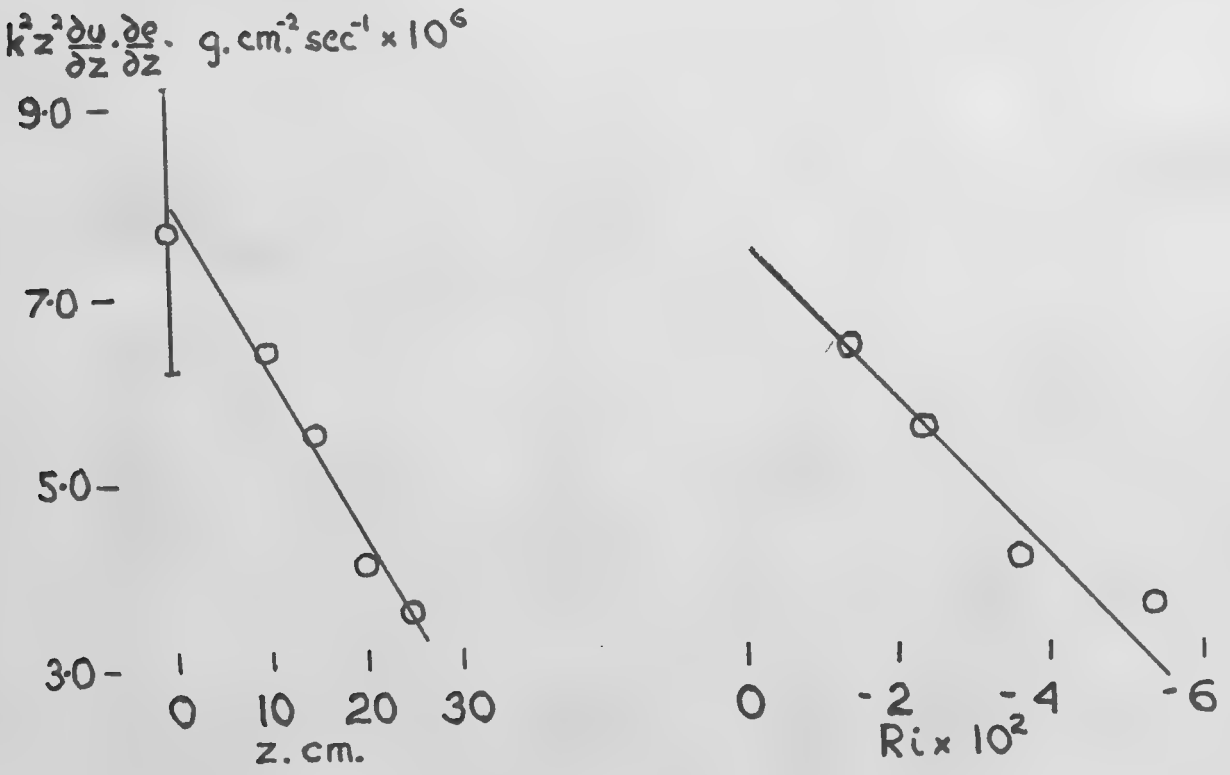

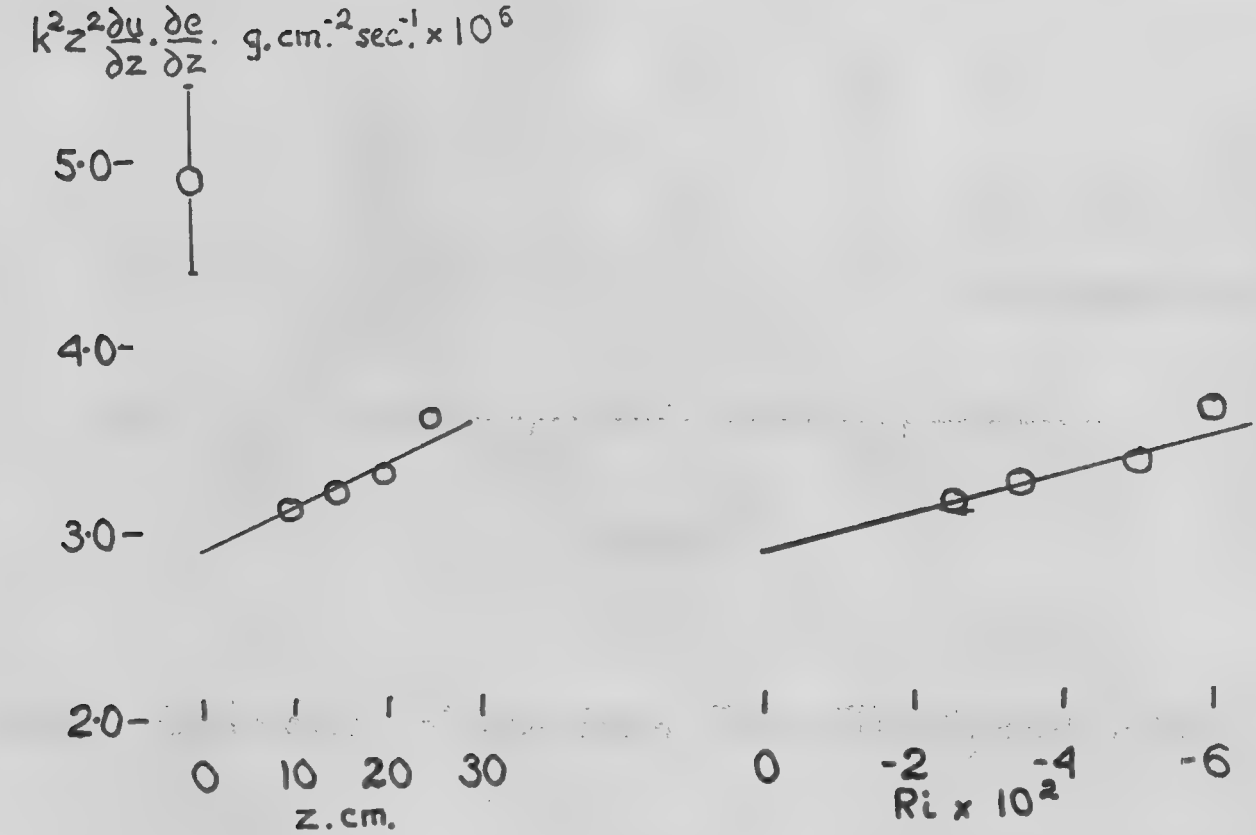

FIG. 7. Computation of Evaporation. Aerodynamic Method
21 June 49. 1428 h.

M.R.P. 547

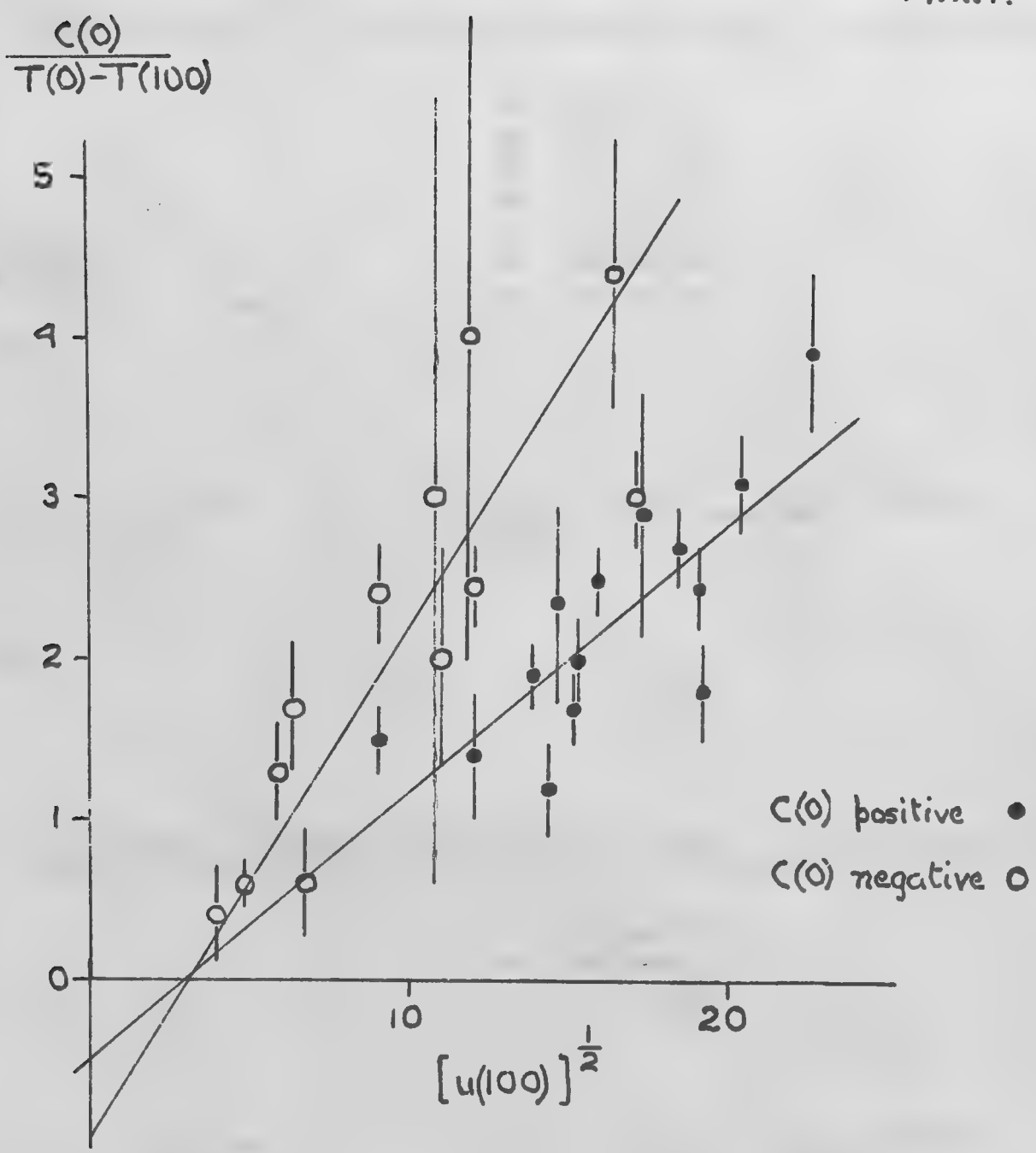

FIG.8. Estimation of C(0) from T(0), T(100), and u(100)

Fig 9. Ratio of E(o) to tank evaporation rate – grass healthy

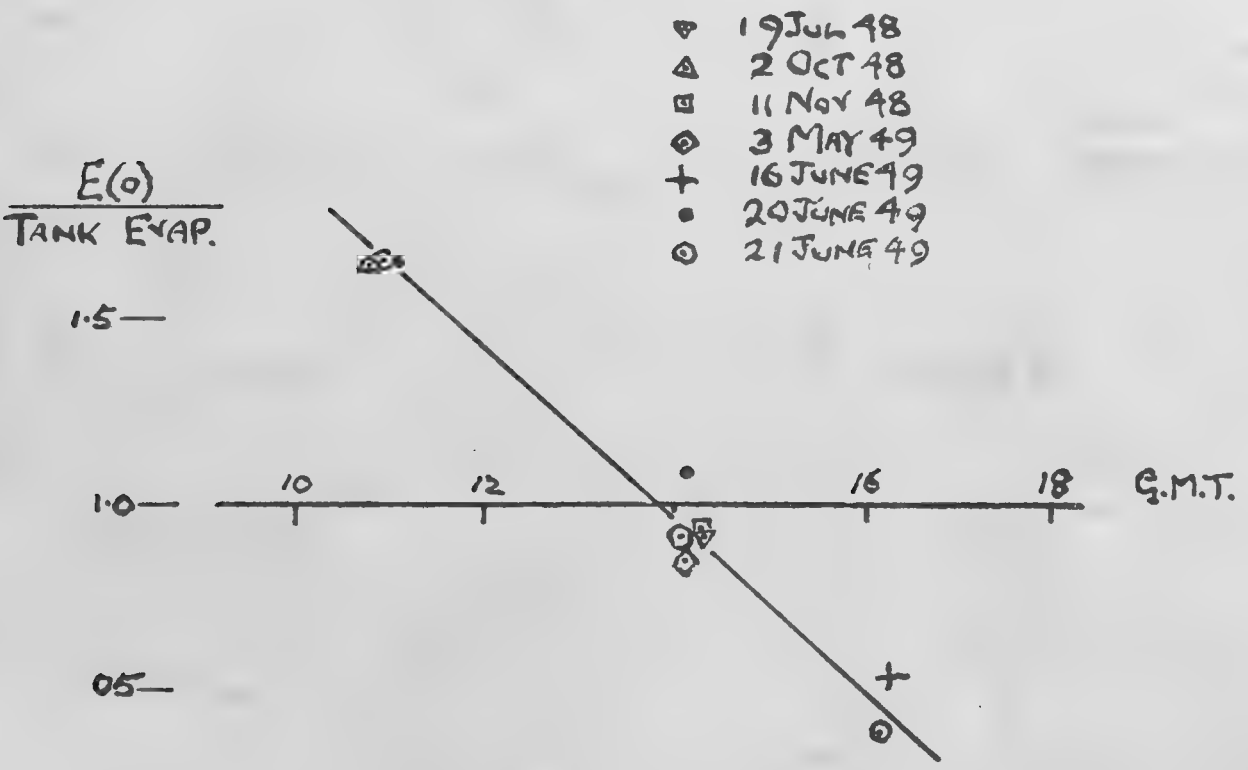

Fig 10. Ratio of E(o) to tank evaporation rate – grass brown

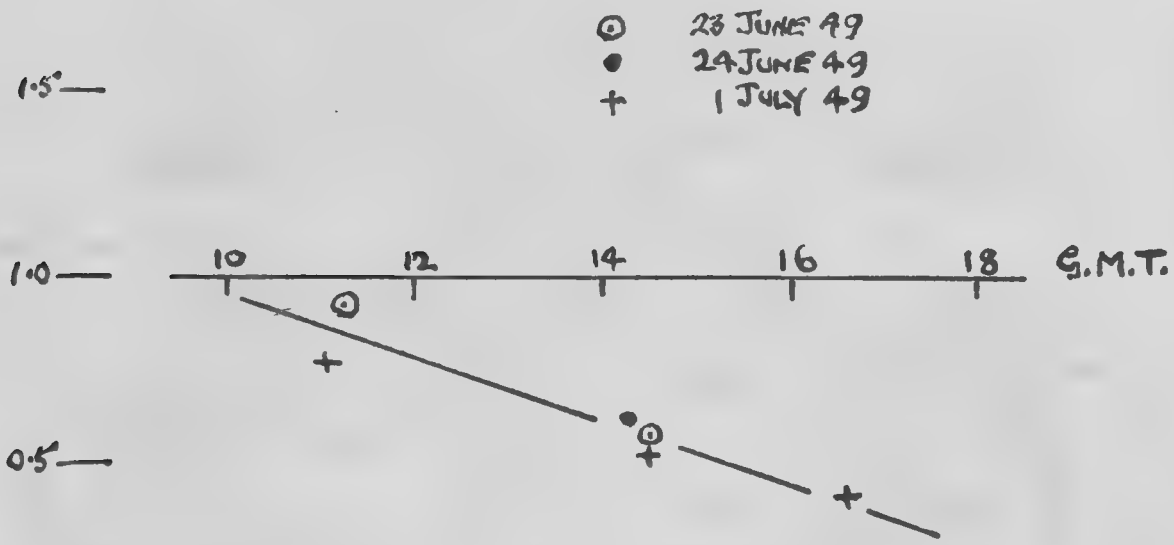

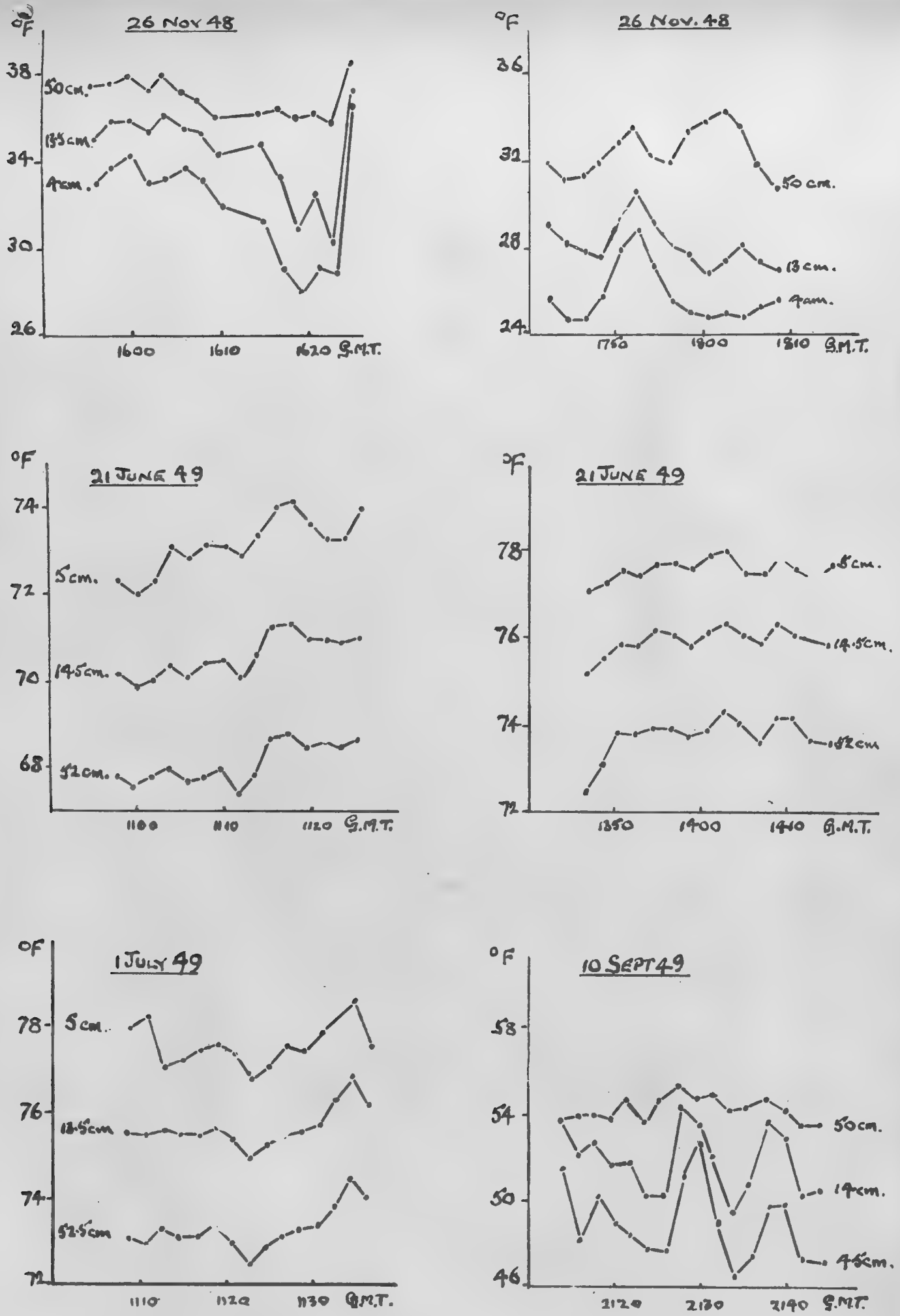

FIG. 11. EXAMPLES OF THE CHANGE OF TEMPERATURE WITH TIME

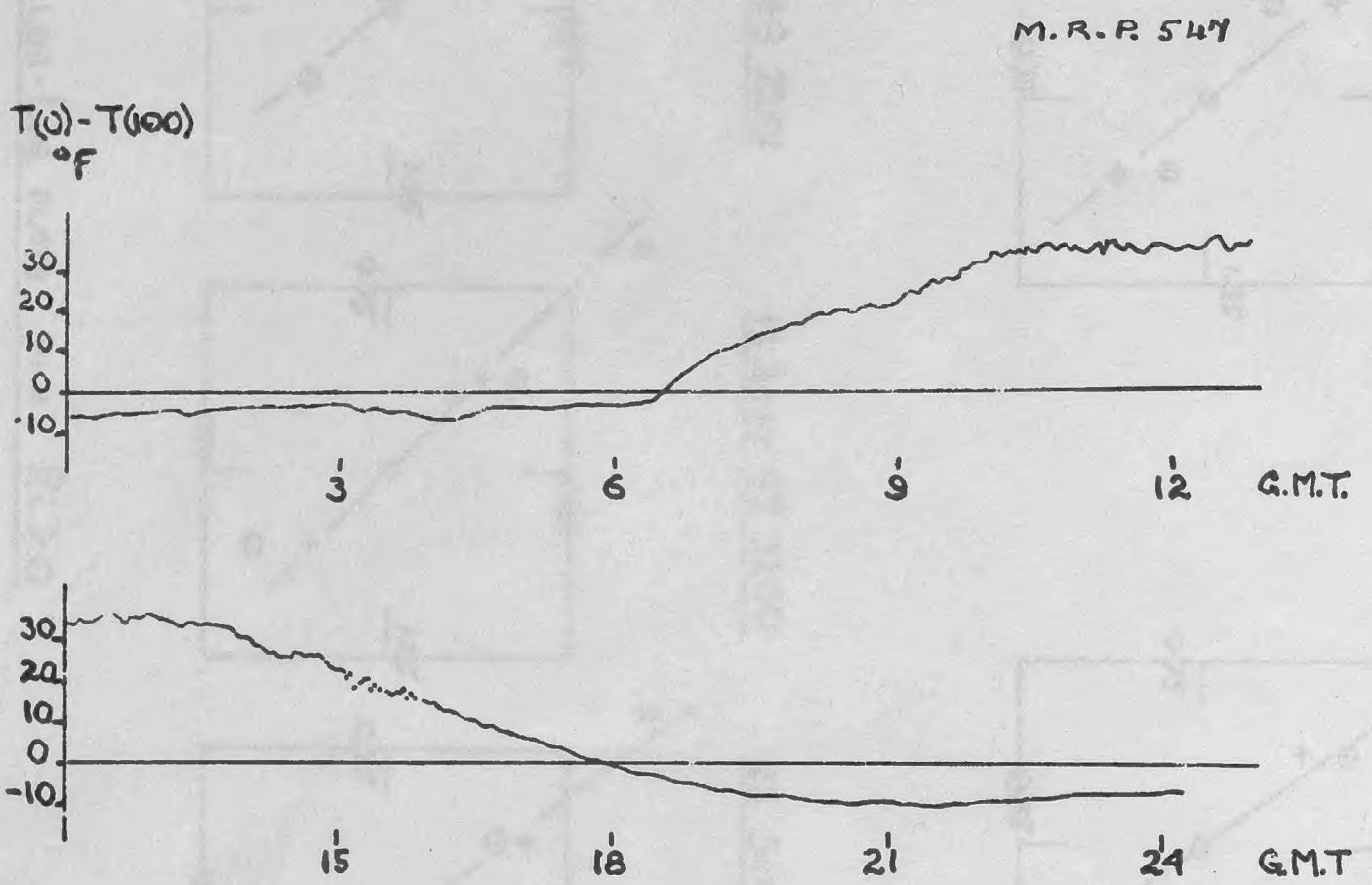

FIG. 12. Record of T(0) - T(100) 21 June 1949.

10 Nov 48 1510

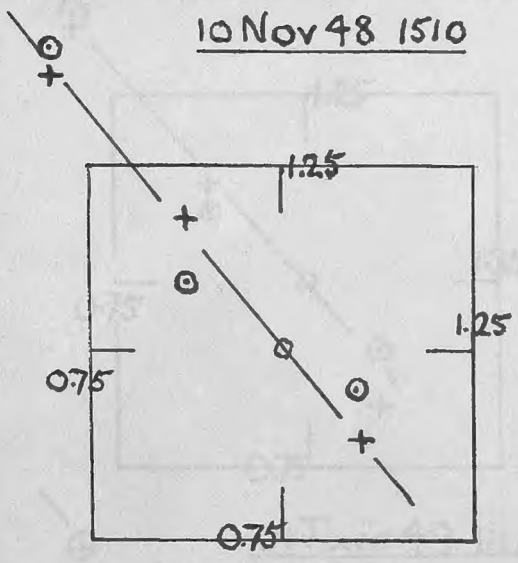

7 June 49 2125

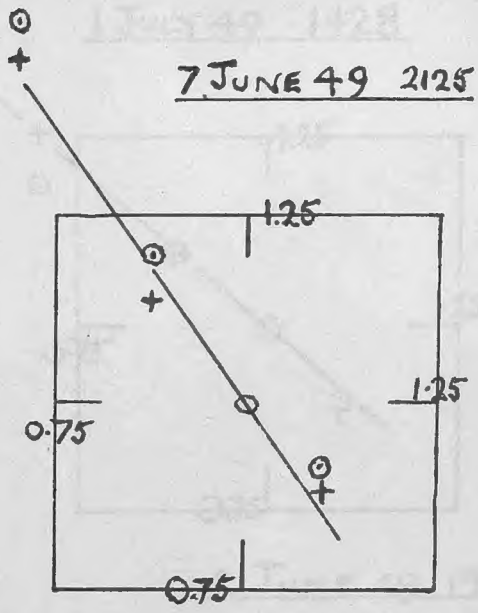

5 Sept 49 2201

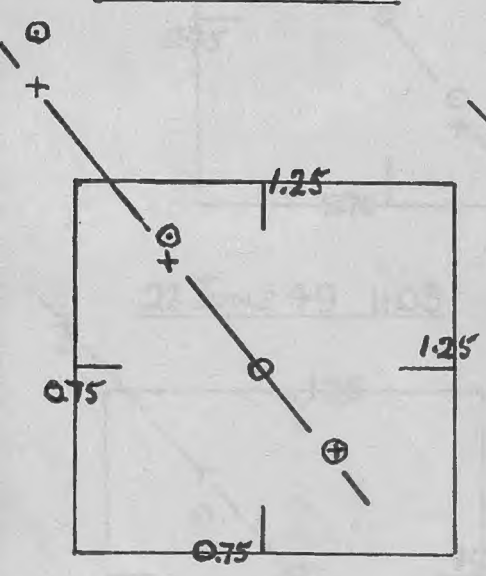

12 Sept 49 2200

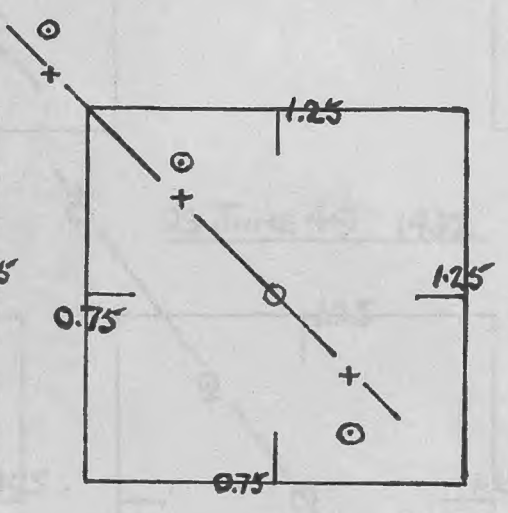

28 Sept 49 1905

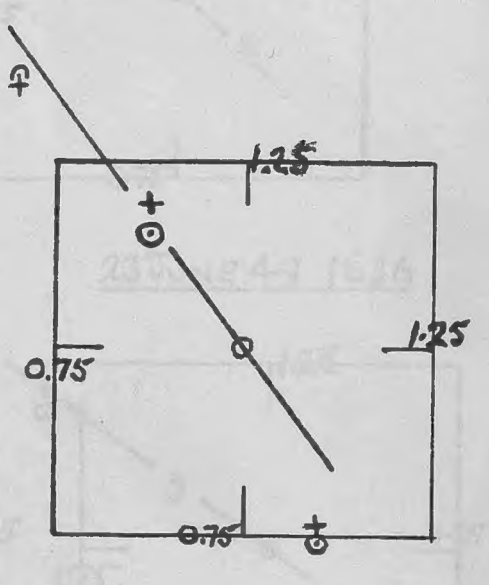

Fig 13. Log-Log plots for $Ri > 0$

Abscissae $-\text{Log } z/20$ Ordinates $+ -\text{Log } \frac{\partial u}{\partial z} / \left(\frac{\partial u}{\partial z}\right)_{20}$

$\odot -\text{Log } \frac{\partial T}{\partial z} / \left(\frac{\partial T}{\partial z}\right)_{20}$

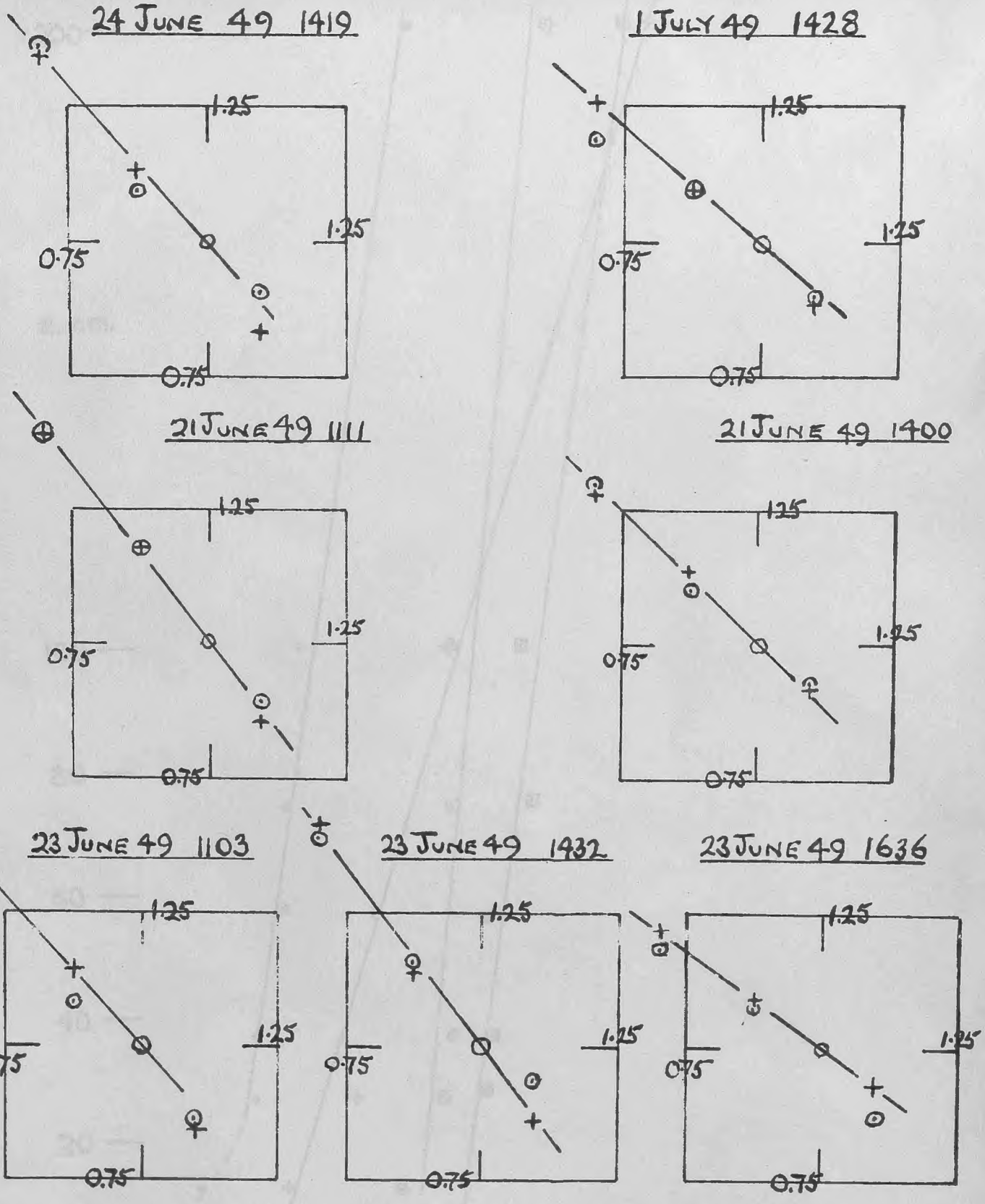

Fig 14. Log-Log plots for $Ri < 0$

Abscissae – $\log z/20$ Ordinates $+ \log \left(\frac{\partial u}{\partial z}\right) \Big/ \left(\frac{\partial u}{\partial z}\right)_{20}$

$\odot \log \left(\frac{\partial T}{\partial z}\right) \Big/ \left(\frac{\partial T}{\partial z}\right)_{20}$
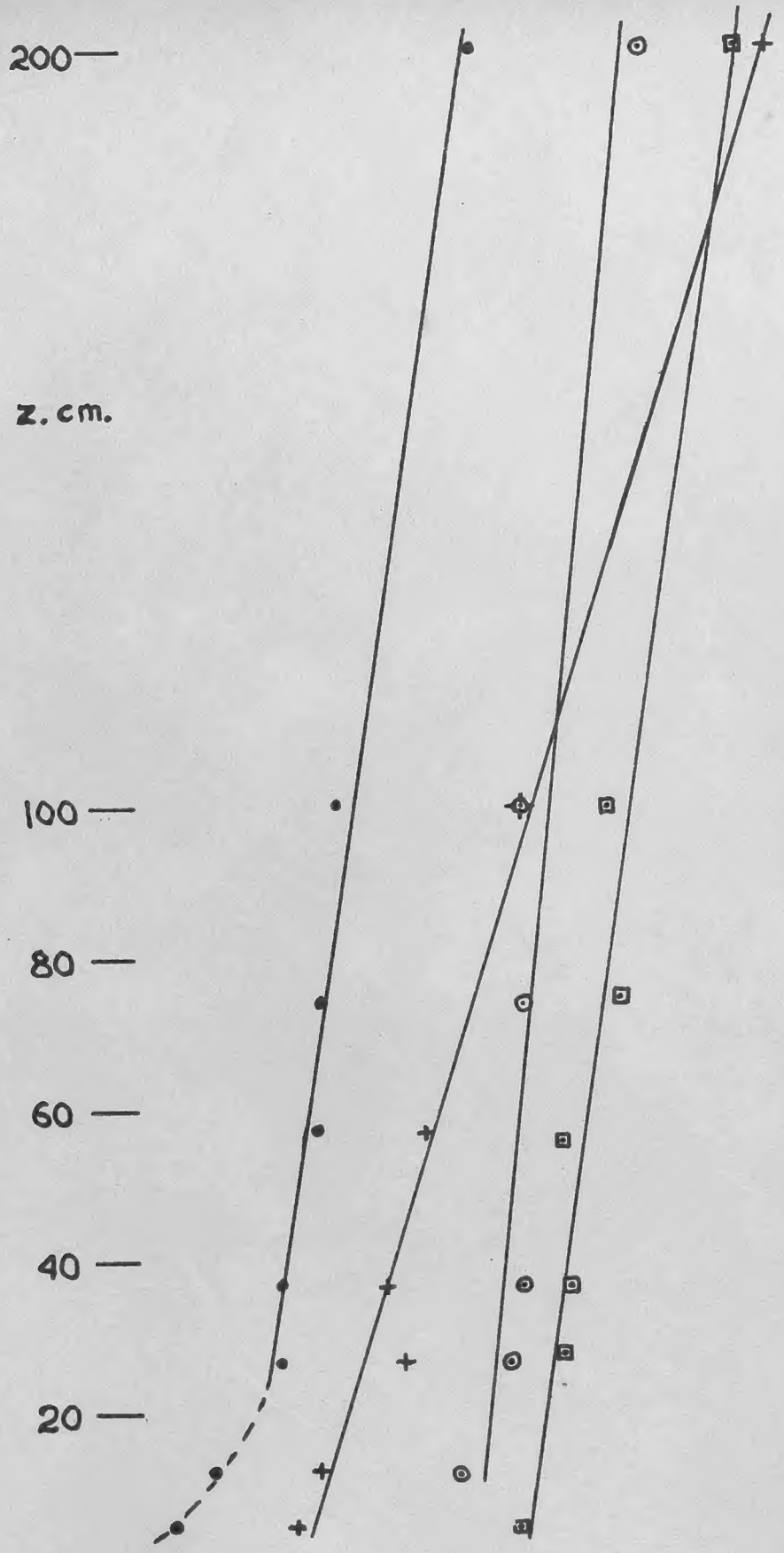
FIG. 15. Wind Profiles in Very Light Winds